

Advances in Science, Technology & Innovation
IEREK Interdisciplinary Series for Sustainable Development



Helder I. Chaminé · Maurizio Barbieri · Ozgur Kisi
Mingjie Chen · Broder J. Merkel *Editors*

Advances in Sustainable and Environmental Hydrology, Hydrogeology, Hydrochemistry and Water Resources

Proceedings of the 1st Springer Conference of the
Arabian Journal of Geosciences (CAJG-1), Tunisia 2018

Advances in Science, Technology & Innovation

IEREK Interdisciplinary Series for Sustainable Development

Editorial Board Members

Anna Laura Pisello, Department of Engineering, University of Perugia, Italy
Dean Hawkes, Cardiff University, UK
Hocine Bougdah, University for the Creative Arts, Farnham, UK
Federica Rosso, Sapienza University of Rome, Rome, Italy
Hassan Abdalla, University of East London, London, UK
Sofia-Natalia Boemi, Aristotle University of Thessaloniki, Greece
Nabil Mohareb, Beirut Arab University, Beirut, Lebanon
Saleh Mesbah Elkaffas, Arab Academy for Science, Technology, Egypt
Emmanuel Bozonnet, University of la Rochelle, La Rochelle, France
Gloria Pignatta, University of Perugia, Italy
Yasser Mahgoub, Qatar University, Qatar
Luciano De Bonis, University of Molise, Italy
Stella Kostopoulou, Regional and Tourism Development, University of Thessaloniki, Thessaloniki, Greece
Biswajeet Pradhan, Faculty of Engineering and IT, University of Technology Sydney, Sydney, Australia
Md. Abdul Mannan, Universiti Malaysia Sarawak, Malaysia
Chaham Alalouch, Sultan Qaboos University, Muscat, Oman
Iman O. Gawad, Helwan University, Egypt

Series Editor

Mourad Amer, Enrichment and Knowledge Exchange, International Experts for Research, Cairo, Egypt

Advances in Science, Technology & Innovation (ASTI) is a series of peer-reviewed books based on the best studies on emerging research that redefines existing disciplinary boundaries in science, technology and innovation (STI) in order to develop integrated concepts for sustainable development. The series is mainly based on the best research papers from various IEREK and other international conferences, and is intended to promote the creation and development of viable solutions for a sustainable future and a positive societal transformation with the help of integrated and innovative science-based approaches. Offering interdisciplinary coverage, the series presents innovative approaches and highlights how they can best support both the economic and sustainable development for the welfare of all societies. In particular, the series includes conceptual and empirical contributions from different interrelated fields of science, technology and innovation that focus on providing practical solutions to ensure food, water and energy security. It also presents new case studies offering concrete examples of how to resolve sustainable urbanization and environmental issues. The series is addressed to professionals in research and teaching, consultancies and industry, and government and international organizations. Published in collaboration with IEREK, the ASTI series will acquaint readers with essential new studies in STI for sustainable development.

More information about this series at <http://www.springer.com/series/15883>

Helder I. Chaminé • Maurizio Barbieri
Ozgur Kisi • Mingjie Chen
Broder J. Merkel
Editors

Advances in Sustainable and Environmental Hydrology, Hydrogeology, Hydrochemistry and Water Resources

Proceedings of the 1st Springer Conference
of the Arabian Journal of Geosciences
(CAJG-1), Tunisia 2018

Editors

Helder I. Chaminé
Laboratory of Cartography and Applied
Geology, School of Engineering (ISEP)
Polytechnic of Porto
Porto, Portugal

Maurizio Barbieri
Sapienza University of Rome
Rome, Italy

Mingjie Chen
Water Research Center
Sultan Qaboos University
Muscat, Oman

Broder J. Merkel
Institute for Geology
TU Bergakademie Freiberg
Freiberg, Germany

Ozgur Kisi
School of Natural Sciences and Engineering
Ilia State University
Tbilisi, Georgia

ISSN 2522-8714 ISSN 2522-8722 (electronic)
Advances in Science, Technology & Innovation
IEREK Interdisciplinary Series for Sustainable Development
ISBN 978-3-030-01571-8 ISBN 978-3-030-01572-5 (eBook)
<https://doi.org/10.1007/978-3-030-01572-5>

Library of Congress Control Number: 2018958953

© Springer Nature Switzerland AG 2019

This work is subject to copyright. All rights are reserved by the Publisher, whether the whole or part of the material is concerned, specifically the rights of translation, reprinting, reuse of illustrations, recitation, broadcasting, reproduction on microfilms or in any other physical way, and transmission or information storage and retrieval, electronic adaptation, computer software, or by similar or dissimilar methodology now known or hereafter developed.

The use of general descriptive names, registered names, trademarks, service marks, etc. in this publication does not imply, even in the absence of a specific statement, that such names are exempt from the relevant protective laws and regulations and therefore free for general use.

The publisher, the authors and the editors are safe to assume that the advice and information in this book are believed to be true and accurate at the date of publication. Neither the publisher nor the authors or the editors give a warranty, express or implied, with respect to the material contained herein or for any errors or omissions that may have been made. The publisher remains neutral with regard to jurisdictional claims in published maps and institutional affiliations.

This Springer imprint is published by the registered company Springer Nature Switzerland AG
The registered company address is: Gewerbestrasse 11, 6330 Cham, Switzerland

Preface

Water is a dynamic, finite, and vulnerable—but resilient—natural resource to be protected in an environmentally sustainable way. Water systems require a comprehensive understanding, among others, of climatology, geology, hydrogeology, hydrochemistry, hydrodynamics, and surface hydrology. In addition, the important role of variability and climate change in water systems, and hydrological cycles—particularly in times of severe weather, water scarcity and other natural disasters and hazards—must be highlighted. Furthermore, water has always had a vital significance to the entire socioeconomic sector and permanently shaped the development of civilizations through the ages.

This volume gives a general overview on current research, focusing on water issues and challenges, as well as its applications to a variety of problems worldwide—with a focus on the Middle East and Mediterranean zone and surrounding regions. Moreover, it includes a wide variety of unique contributions to environmental and hydrologic systems, and water-related research and practice. Regrettably, at present, the Mediterranean and Middle East regions have not yet been deeply investigated and assessed, compared with other regions around the world such as Europe and North America.

This volume of Proceedings is based on selected papers accepted for presentation during the 1st Springer Conference of the Arabian Journal of Geosciences (CAJG-1), Tunisia 2018. The main topics include: (i) Hydrology, Climatology and Water-Related Ecosystems; (ii) Hydrochemistry and Isotopic Hydrology; (iii) Groundwater Assessment and Management: Mapping, Exploration, Abstraction and Modelling; (iv) Water Resources Sustainability and Climate Change; (v) Hydrologic Engineering and Urban Groundwater.

This volume provides new insights into characterization, evaluation, quality, management, protection, modeling on environmental hydrology, groundwater, hydrochemistry and isotopic hydrology, and sustainable water resources studies and hydrologic engineering approaches by international researchers. So, it is possible to improve the ability to manage water resources, help the identification of potential sources of contamination, and provide potential solutions to water quality problems.

The volume will also be of interest to researchers and practitioners in the field of hydrology, hydrogeology, hydrochemistry, and water resources, as well as those engaged in environmental sciences, water technologies, and earth sciences. Graduate students and water-related professionals will also find the book to be of value for further research in water and environment.

The volume includes international case studies that illustrate how water sciences and technology can contribute to promoting a more sustainable design that respects nature and the environment. In particular, it discusses the latest advances in water sciences from diverse

backgrounds, and highlights the role of the variability and climate change in hydrological systems. Finally, it is vital that water issues be seen in the overall framework of global sustainable development while considering all the ethical aspects.

Porto, Portugal
Rome, Italy
Tbilisi, Georgia
Muscat, Oman
Freiberg, Germany
July 2018

Helder I. Chaminé
Maurizio Barbieri
Ozgur Kisi
Mingjie Chen
Broder J. Merkel

Acknowledgements

Our appreciation is extended to the authors of the papers for their hard and diligent work in producing high-quality contributions. We would like to thank the reviewers of the papers for their in-depth reviews and great efforts in improving the quality of the papers. Also, thanks are extended to Amjad Kallel who supervised and handled the evaluation process, to Sahbi Moalla who handled the submission and evaluation system for the ten conference proceedings volumes, and to the publishing staff of Springer headed by Nabil Khélifi, Senior Editor for their efforts and contributions in completing this conference proceedings volume. All the above-mentioned efforts were very important in making this book a success.

About the 1st Springer Conference of the Arabian Journal of Geosciences (CAJG-1), Tunisia 2018



The *Arabian Journal of Geosciences (AJG)* is a Springer journal publishing original articles on the entire range of Earth sciences in partnership with the Saudi Society for Geosciences. The journal focuses on, but not limited to, research themes which have regional significance to the Middle East, the Euro-Mediterranean, Africa, and Asia. The journal receives on average 2000 submissions a year and accepts around 500 papers for publication in its 24 annual issues (acceptance rate 25%). It enjoys the participation of an editorial team of 100 international associate editors who generously help in evaluating and selecting the best papers.

In 2008, Prof. Abdullah Al-Amri, in close partnership with Springer, founded the Arabian Journal of Geosciences (AJGS). In this year, the journal celebrates its tenth anniversary. On this occasion and to mark this event, the Founder and Editor-in-Chief of the AJGS Prof. Al-Amri organized in close collaboration with Springer the 1st Conference of the Arabian Journal of Geosciences (1st CAJG) in Hammamet, Tunisia, from November 12 to 15, 2018 (www.cajg.org).

The conference was an occasion to endorse the journal's long-held reputation for bringing together leading authors from the Middle East, the Euro-Mediterranean, Africa, and Asia who work in the wide-ranging fields of Earth sciences. The conference covered all cross-cutting themes of Geosciences and focused principally on the following ten tracks:

- Track 1. Climate, paleoclimate and paleoenvironmental changes
- Track 2. Geoinformatics, remote sensing, geodesy
- Track 3. Geoenvironmental engineering, geomechanics and geotechnics, geohazards
- Track 4. Geography, geoecology, geoarcheology, geotourism
- Track 5. Geophysics, seismology
- Track 6. Hydrology, hydrogeology, hydrochemistry
- Track 7. Mineralogy, geochemistry, petrology and volcanology
- Track 8. Petroleum engineering and petroleum geochemistry
- Track 9. Sedimentology, stratigraphy, palaeontology, geomorphology, pedology
- Track 10. Structural/petroleum/mining geology, geodynamics, marine geology

The dynamic four-day conference provided more than 450 attendees with opportunities to share their latest unpublished findings and learn the newest geoscience studies. The event also allowed attendees to meet and discuss with the journal's editors and reviewers.

More than 950 short contributing papers to the conference were submitted by authors from more than 70 countries. After a pre-conference peer review process by more than 500 reviewers, 700 papers were accepted. These papers were published as chapters in the conference proceedings by Springer.

The conference proceedings consist of ten edited volumes, each edited by the following group of *Arabian Journal of Geosciences* (AJGS) editors and other guest editors:

Volume 1. Patterns and Mechanisms of Climate, Paleoclimate, and Paleoenvironmental Changes from Low-Latitude Regions

Zhihua Zhang (AJGS Editor): Beijing Normal University, Beijing, China

Nabil Khélifi (AJGS Editor): Earth Sciences Editorial Department, Springer, Heidelberg, Germany

Abdelkader Mezghani (Guest Editor): Norwegian Meteorological Institute, Norway

Essam Heggy (Guest Editor): University of Southern California and Jet Propulsion Laboratory, Caltech, USA

Volume 2. Advances in Remote Sensing and Geo Informatics Applications

Hesham M. El-Askary (Guest Editor): Schmid College of Science and Technology at Chapman University, USA

Saro Lee (AJGS Editor): Korea Institute of Geoscience and Mineral Resources, Daejeon, South Korea

Essam Heggy (Guest Editor): University of Southern California and Jet Propulsion Laboratory, Caltech, USA

Biswajeet Pradhan (AJGS Editor): University of Technology Sydney, Sydney, Australia

Volume 3. Recent Advances in Geo-Environmental Engineering, Geomechanics and Geotechnics, and Geohazards

Amjad Kallel (AJGS Editor): ENIS, University of Sfax, Tunisia

Zeynal Abiddin Erguler (AJGS Editor): Dumlupinar University, Kutahya, Turkey

Zhen-Dong Cui (AJGS Editor): China University of Mining and Technology, Xuzhou, Jiangsu, China

Ali Karrech (AJGS Editor): The University of Western Australia, Australia

Murat Karakus (AJGS Editor): University of Adelaide, Australia

Pinnaduwa Kulatilake (AJGS Editor): Department of Materials Science and Engineering, The University of Arizona, USA

Sanjay Kumar Shukla (AJGS Editor): School of Engineering, Edith Cowan University, Perth, Australia

Volume 4. Exploring the Nexus of Geocology, Geography, Geoarcheology and Geotourism: Advances and Applications for Sustainable Development in Environmental Sciences and Agroforestry Research

Haroun Chenchouni (AJGS Editor): University of Tebessa, Algeria

Ezzoura Errami (Guest Editor): Chouaib Doukkali University, El Jadida, Morocco

Fernando Rocha (Guest Editor): University of Aveiro, Portugal

Luisa Sabato (AJGS Editor): Università degli Studi di Bari “Aldo Moro”, Bari, Italy

Volume 5. On Significant Applications of Geophysical Methods

Narasimman Sundararajan (AJGS Editor): Sultan Qaboos University, Muscat, Oman

Mehdi Eshagh (AJGS Editor): University West, Trollhättan, Sweden

Hakim Saibi (AJGS Editor): United Arab Emirates University, Al-Ain, Abu Dhabi, UAE

Mustapha Meghraoui (AJGS Editor): Université de Strasbourg, Strasbourg, France

Mansour Al-Garni (AJGS Editor): King Abdulaziz University, Jeddah, Saudi Arabia

Bernard Giroux (AJGS Editor): Institut national de la recherche scientifique, Québec, Canada

Volume 6. Advances in Sustainable and Environmental Hydrology, Hydrogeology, Hydrochemistry and Water Resources

Helder I. Chaminé (AJGS Editor): School of Engineering (ISEP), Polytechnic of Porto, Portugal

Maurizio Barbieri (AJGS Editor): University of Rome La Sapienza, Italy

Ozgur Kisi (AJGS Editor): Ilia State University, Tbilisi, Georgia

Mingjie Chen (AJGS Editor): Sultan Qaboos University, Muscat, Oman

Broder J. Merkel (AJGS Editor): TU Bergakademie Freiberg, Freiberg, Germany

Volume 7. Petrogenesis and Exploration of the Earth's Interior

Domenico Doronzo (AJGS Editor): Consejo Superior de Investigaciones Cientificas, Spain

Emanuela Schingaro (AJGS Editor): Università degli Studi di Bari Aldo Moro—UniBa, Italy

John S. Armstrong-Altrin (AJGS Editor): The National Autonomous University of Mexico, Mexico

Basem Zoheir (Guest Editor): Benha University, Egypt and University of Kiel, Germany

Volume 8. Advances in Petroleum Engineering and Petroleum Geochemistry

Santanu Banerjee (AJGS Editor): Indian Institute of Technology Bombay, Mumbai, India

Reza Barati (AJGS Editor): The University of Kansas, Lawrence, KS, USA

Shirish Patil (Guest Editor): Saudi Aramco and King Fahd University of Petroleum and Minerals, Dhahran, Saudi Arabia

Volume 9. Paleobiodiversity and Tectono-Sedimentary Records in the Mediterranean Tethys and Related Eastern Areas

Mabrouk Boughdiri (AJGS Editor): University of Carthage, Amilcar, Tunisia

Beatriz Bádenas (AJGS Editor): University of Zaragoza, Zaragoza, Spain

Paul Selden (AJGS Editor): University of Kansas, Lawrence, KS, USA

Etienne Jaillard (Guest Editor): University of Grenoble Alpes, France

Peter Bengtson (AJGS Editor): University of Heidelberg, Heidelberg, Germany

Bruno R. C. Granier (AJGS Editor): University of Bretagne Occidentale, Brest, France

**Volume 10. The Structural Geology Contribution to the Africa-Eurasia Geology:
Basement and Reservoir Structure, Ore Mineralisation and Tectonic Modelling**

Federico Rossetti (Guest Editor): Università Roma Tre, Roma, Italy

Ana Crespo Blanc (Guest Editor): University of Granada, Spain

Federica Riguzzi (Guest Editor): National Institute of Geophysics and Volcanology, Roma, Italy

Estelle Leroux (Guest Editor): IFREMER, Unité Géosciences Marines, Plouzané, France

Kosmas Pavlopoulos (Guest Editor): Sorbonne University Abu Dhabi, Abu Dhabi, UAE

Olivier Bellier (Guest Editor): CEREGE, Aix-en-Provence, France

Vasilios Kapsimalis (Guest Editor): Institute of Oceanography, Hellenic Centre for Marine Research, Anavyssos, Greece

About the Conference Steering Committee

General Chair



Abdullah Al-Amri: Founder and Editor-in-Chief of AJGS, King Saud University, Saudi Arabia

Conference Supervisor



Nabil Khélifi: Senior Publishing Editor, Springer Middle East and North African Program Springer, a part of Springer Nature, Heidelberg, Germany

Scientific Committee Chair

François Roure: Guest of Editorial Board of AJGS, IFP—
Energies Nouvelles, France



Walter D. Mooney: Guest of Editorial Board of AJGS, US
Geological Survey Western Region, USA

Local Organization Chair

Mabrouk Boughdiri: Associate Editor of AJGS, University of
Carthage, Amilcar, Tunisia

Evaluation Chair



Amjad Kallel: Assistant Editor of AJGS, ENIS, University of Sfax, Tunisia

Publication Chair



Biswajeet Pradhan: Associate Editor of AJGS, University of Technology Sydney, Sydney, Australia



Essam Heggy: Guest of Editorial Board of AJGS, University of Southern California and Jet Propulsion Laboratory, Caltech, USA

Program Chair

Hakim Saibi: Associate Editor/Assistant Editor of AJGS, United Arab Emirates University, Al-Ain, Abu Dhabi, UAE



Domenico Doronzo: Associate Editor/Assistant Editor of AJGS, Consejo Superior de Investigaciones Cientificas, Spain

Communication Chair

Mohamed Ksibi: Guest of Editorial Board of AJGS, ISBS, University of Sfax, Tunisia

English Language Advisory Committee

Abdelmajid Dammak: ENIS, University of Sfax, Tunisia

Chokri Khalaf: FMS, University of Sfax, Tunisia

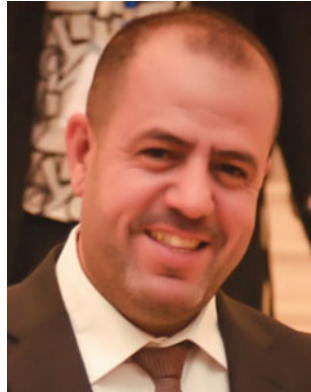
Dhouha Mabrouk: FLSHS, University of Sfax, Tunisia

Mohamed Elbahi: ENIS, University of Sfax, Tunisia

Sami Shami: ENIS, University of Sfax, Tunisia

Yasmine Basha: FLSHS, University of Sfax, Tunisia

Conference Manager



Mohamed Sahbi Moalla: Coordinator of AJGS, ISET,
University of Sfax, Tunisia

Contents

Part I Keynote

- Innovation in Process Engineering for Hydrology** 3
Enrico Drioli and Francesca Macedonio

Part II Hydrology, Climatology and Water-Related Ecosystems

- A Comparative Assessment of Meteorological Drought Indices for the Baribo Basin (Cambodia)** 9
Kimhuy Sok, Supattra Visessri, and Sokchhay Heng
- Probabilistic Precipitation Forecast in (Indonesia) Using NMME Models: Case Study on Dry Climate Region** 13
Heri Kuswanto, Dimas Rahadiyuza, and Dodo Gunawan
- Homogeneity and Trend Analysis of Rainfall and Streamflow of Seyhan Basin (Turkey)** 17
Sinan J. Hadi, Arkan J. Hadi, Kamaran S. Ismail, and Mustafa Tombul
- Mean Rainfall Variability Effects on the Hydrological Response of Medjerda High Valley (Tunisia)** 21
Sahar Abidi, Olfa Hajji, Boutheina Hannachi, and Hammadi Habaieb
- Information Gain in Rainfall-Runoff Modeling (Tunisia)** 25
Aymen Ben Jaafar and Zoubeida Bargaoui
- Hydrogeological System of Sebaou River Watershed (Northern Central Algeria): An Assessment of Rainfall-Runoff Relationship** 29
Bilel Zerouali, Mohamed Mesbah, Mohamed Chettih, Mohammed Djemai, and Zaki Abda
- New Use of Hydrograph Separation Method for Hydrological Process Identification** 33
Asma Dahak and Hamouda Boutaghane
- Modeling Processes of Water and Heat Regime Formation for Agricultural Region Area (Russia) Utilizing Satellite Data** 37
Eugene Muzylev, Anatoly Zeyliger, Zoya Startseva, Elena Volkova, Eugene Vasilenko, and Olga Ermolaeva
- Warm Season Trends of ET_a : A Case Study of Near-North Caspian Low Lands** 41
Olga Ermolaeva, Anatoly Zeyliger, Eugene Muzilev, and Zoya Startseva
- Development of Frequency Specific Flow Maps on the Sebaou Watershed in Great Kabylia in Algeria** 45
Hocine Hammoum, Karima Bouzelha, Mohammed Djemai, Malik Bouzelha, Lila Ben Si Said, and Mouloud Touat

Potentiometric Salinity Mapping of Mishrif Oilfield Waters in (Iraq's) Southern Oil Fields	49
Salih Awadh, Heba Al-Mimar, and Abdullah Al-yaseri	
A Transient Drainage Equation by Incorporating the Variable Drainable Porosity Function and the Unsaturated Zone Flow Contribution	53
Ammar Yousfi and Mohamed Mechergui	
Study of Solid Transport in Suspension in a Semi-arid Catchment: Case of Boukadir Wadi, Tipaza, Algeria	57
Omar Elahcene, Imad Eddine Bouznad, Mohamed Yacine Bendjedou, and Zohir Boulkenafet	
Temporal Variation of Specific Sediment Yield at Sidi Bel Abbas Basin, North Algeria	61
Hayet Madani Cherif and Abderezzak Bouanani	
Major and Trace Element Distribution in Suspended Particulate Matter and Sediments of the Tropical River Estuary (South Vietnam)	65
Sofia Koukina and Nikolay Lobus	
Mobility of Metallic Trace Elements in Surface Waters and Sediments: Case of the Nil Wadi (Jijel, North-East Algeria)	69
Sihem Benessam, Taha-Hocine Debieche, Souad Amieur, Amal Chine, and Smaïl Khelili	
Snowmelt Runoff Simulation During Early 21st Century Using Hydrological Modelling in the Snow-Fed Terrain of Gilgit River Basin (Pakistan)	73
Yasir Latif, Yaoming Ma, Weiqiang Ma, Muhammad Sher, and Yaseen Muhammad	
The Importance of Wetlands and Unhealthy Water Bodies in the Distribution of Malaria in Spain	77
Arturo Sousa, Leoncio García-Barrón, Mónica Aguilar-Alba, Mark Vetter, and Julia Morales	
Effects on Soil-Plant System in a Treated Wastewater Irrigated Sunflower Cultivation: Soil Chemical Characteristics, Bioaccumulation of Metals in Soil and Plants	81
Farah Bouhamed, Zaineb Bakri, and Boubaker Elleuch	
Assessment Impacts of Irrigation Using Treated Wastewater on Plants Growth, Soil Properties and Metals Accumulation in Soil and Tomato Plants	85
Zaineb Bakari, Farah Bouhamed, Nesrine Boujelben, and Boubaker Elleuch	
Phenol Formaldehyde Resin for Hydrophilic Cellulose Paper	89
Waqas Ahmed, Muhammad Sagir, M. Suleman Tahir, and Sami Ullah	
Part III Hydrochemistry and Isotopic Hydrology	
Forecasting and Mass Transport Modelling of Nitrates in the Esposende–Vila Do Conde Nitrate Vulnerable Zone (Portugal)	95
Joel Zeferino, Maria Rosário Carvalho, Tânia Ferreira, Maria Catarina Silva, Maria José Afonso, Liliana Freitas, Ana Rita Lopes, Rosário Jesus, Sofia Batista, Helder I. Chaminé, and José Martins Carvalho	
Hydrochemical Quality of the Angads Plain Groundwater (Eastern Morocco)	99
Mohammed Es-sousy, Elkhadir Gharibi, Mohammad Ghalit, Jean-Denis Taupin, and Mohsen Ben Alaya	
Physical and Chemical Characterization of the Surface Waters of Djemaa Wadi (Blida, Algeria)	103
Djaouida Bouchelouche, S. Arab, Mouna Hafiane, Imane Saal, and Abdeslem Arab	

Groundwater Quality in an Alluvial Aquifer Affected by the Anthropogenic and Natural Processes in a Rural Area, North Algeria	107
Abdelkader Bouderbala and Nacéra Hadj Mohamed	
Hydrochemical Appraisal of Groundwater in Gash River Basin, Eastern Sudan	111
Hago Ali	
Distribution of Trace Elements in the Shallow Aquifer of Guenniche (North Tunisia)	113
Nizar Troudi, Fadoua Hamzaoui, Mounira Zammouri, and Ourania Tzoraki	
Export Balance of Polybrominated Diphenyl Ethers at the Scale of the Charmoise Watershed (France)	117
Khawla Tlili, Pierre Labadie, Fabrice Alliot, Catherine Bourges, Annie Desportes, and Marc Chevreuil	
Hydrogeochemical Modeling and Isotopic Assessment of the Quaternary Aquifer at Ali al-Garbi Area in Misaan Governorate, South of Iraq	121
Hussein Ghalib, Mohsin Yaqub, and Alaa Al-Abadi	
Geochemical Classification of Groundwater System in a Rural Area of Nigeria	125
Theophilus A. Adagunodo, Rachael O. Adejumo, and Anuoluwapo M. Olanrewaju	
Contamination of Annaba bay (northeastern extremity of Algeria) by multi-pesticide residues	129
Soumeya Khaled-Khodja, Semia Cherif, and Karima Rouibah	
Complex Interactions Between Fertilizers and Subsoils Triggering Reactive Nitrogen Speciation in Lowlands	133
Micòl Mastrocicco, Nicolò Colombani, Fabio Vincenzi, and Giuseppe Castaldelli	
Hydrogeological Windows Impact on Groundwater Contamination in Moscow	137
Irina Galitskaya, Irina Pozdnyakova, Irina Kostikova, and Leonid Toms	
Impact of Pollution on the Quality of Water of Oued El Harrach (Algeria)	141
Djaouida Bouchelouche, Somia Hamil, Siham Arab, Imane Saal, Mouna Hafiane, and Abdeslem Arab	
Organic Pollutants Evolution and Degrees of Contamination of Hammam Grouz Dam Waters, North-East of Algeria	145
Badreddine Saadali, Naouel Mihoubi, Amira Ouddah, and Yasmina Bouroubi	
Impact of Reclaimed Wastewater Used for Irrigation in the Agricultural Supply Chain	149
Zaineb Bakari, Nesrine Boujelben, Nesrine Turki, Massimo Del Bubba, and Boubaker Elleuch	
The Reuse of Wastewater in the Context of Climate Change: Case of Mascara Wilaya (Algeria)	153
Benali Benzater, Anouar Hachemaoui, Abdelkader Elouissi, and Boumediene Benaricha	
Evaluation of the Contamination from Geothermal Fluids upon Waters and Soils in Alaşehir Environs, Turkey	157
Ali Bülbül, Tuğbanur Özen Balaban, and Gültekin Tarcan	

Geochemical and Isotopic Marks for Tracing Groundwater Salinization: Santiago Island, Republic of Cape Verde, Case Study	161
Paula M. Carreira, António Lobo de Pina, Alberto Mota Gomes, José Manuel Marques, and Fernando Monteiro Santos	
Application of Geochemical Tracers and Isotopic for Investigation of Recharge and Salinization of Water in the Menzel Bourguiba Aquifer, Northeast of Tunisia	165
Mohsen Ben Alaya, Safouan Ben Ammar, Jean-Denis Taupin, Mohamed Khouatmia, Raouf Jbeali, and Fetheddine Melki	
Seawater Intrusion Characterization in a Coastal Aquifer Using Geophysical and Geochemical Approach (Northeastern Tunisia)	169
Hajer Ferchichi, Boutheina Farhat, and Abdallah Ben-Mammou	
Assessment of Saline Water Intrusion in Southwest Coastal Aquifer, Bangladesh Using Visual MODFLOW	175
Tauhid Ur Rahman, Nafiz Ul Ahsan, Arman Habib, and Anjuman Ara	
Quality of Groundwater and Seawater Intrusion Along Northern Chennai Metropolitan City (India)	179
Sithu G. D. Sridhar and Muthusamy Balasubramanian	
Tracing the Evolution of Hypersaline Coastal Groundwaters in Kuwait: An Integrated Approach	185
Chidambaram Sabarathinam, Harish Bhandary, and Asim Al Khalid	
Contribution of Hydrochemical and Geoelectrical (ERT and VES) Approaches to Investigate Salinization Process of Phreatic Aquifer and Climate Change Adaptation Strategy in Arid Area: Example of Garaat Douza and Its Proximities (Mediterranean Basin)	189
Elhem Moussaoui, Abdelkader Mhamdi, Mouez Gouasmia, Ferid Dhahri, and Mohamed Soussi	
Relationship Between Hydrochemical Variation and the Seawater Intrusion Within Coastal Alluvial Aquifer of Essaouira Basin (Morocco) Using HFE-Diagram	195
Mohammed Bahir, Salah Ouhamdouch, Paula M. Carreira, and Kamel Zouari	
Use of Environmental Isotopes and Hydrochemistry to Characterize Coastal Aquifers in Semi-arid Region. Case Study of Wadi Guenniche Deep Aquifer (NE Tunisia)	199
Safouan Ben Ammar, Jean-Denis Taupin, Mohsen Ben Alaya, Kamel Zouari, Nicolas Patris, and Mohamed Khouatmia	
Multi-isotope Approach to Study the Problem of Salinity in the Coastal Aquifer of Oued Laya, Tunisia	203
Mohamed Fethi Ben Hamouda, Paula M. Carreira, José Manuel Marques, and Hans Eggenkamp	
Groundwater Evolution in the Multilayer Aquifers of the Mekelle Sedimentary Outlier (Northern Ethiopia): A Chemical and Isotopic Approach	207
Tewodros Alemayehu, Albrecht Leis, and Martin Dietzel	
Chlorine Geochemical and Isotopic ($^{37}\text{Cl}/^{35}\text{Cl}$) Signatures of CO_2-Rich Mineral Waters (N-Portugal): Revisited	211
José Manuel Marques, Hans Eggenkamp, Paula M. Carreira, and Manuel Antunes da Silva	

Relation Between Water Level Fluctuation and Variation in Fluoride Concentration in Groundwater—A Case Study from Hard Rock Aquifer of Telangana, India	215
Ankita Chatterjee, Md. Arshad, Adrien Selles, and Shakeel Ahmed	
Cesium and Uranium Radioisotopes Monitoring in Kuwait Bay Seawater	219
Aishah Alboloushi, Abdulaziz Aba, and Omar Alboloushi	
Part IV Groundwater Assessment, Modelling and Management	
Integrating Aeromagnetic and LandsatTM 8 Data for Geologic Features of Igbeti Schist Belt, Southwestern Nigeria: Implication for Groundwater Exploration	225
Nurudeen Olasunkanmi, Lukman Sunmonu, Moruffdeen Adabanija, Jimoh Ajadi, and Leke Sunday	
Remote Sensing and Geographic Information System with Geophysical Resistivity in Groundwater Investigations (West Atbara Basin–River Nile State–Sudan)	229
Ekhlas H. Ahmed, Wenbo Xu, and Basheer A. Elubid	
Radar Probing of Subsurface Moisture in Barchan Dunes	233
Giovanni Scabbia, Essam Heggy, and Abotalib Z. Abotalib	
2D ERI for Groundwater Exploration in a Crystalline Basement Terrain, Abeokuta, Southwestern Nigeria	237
Ahzegbobor P. Aizebeokhai, Adenifesimi A. Oni, and Kehinde D. Oyeyemi	
Geological-Geophysical Investigations for Hydrological Studies in a Basement Complex Terrain, Southwestern Nigeria	241
Kehinde D. Oyeyemi, Ahzegbobor P. Aizebeokhai, and Oluseun A. Sanuade	
Hydraulic Parameters Estimation Using 2D Resistivity Technique: A Case Study in Kapas Island, Malaysia	245
Nura Umar Kura, Mohammad Firuz Ramli, Ahmad Zaharin Aris, and Wan Nor Azmin Sulaiman	
Numerical Simulation of Groundwater and Surface Water Interaction and Particle Tracking Movement Due to the Effect of Pumping Abstraction of Lower Muda River	249
Mohd Khairul Nizar Shamsuddin, Wan Nor Azmin Sulaiman, Mohammad Firuz Ramli, Faradiella Mohd Kusin, and Anuar Sefie	
Estimating Groundwater Evapotranspiration in Thiaroye Aquifer (Western Senegal)	253
Ousmane Coly Diouf, Lutz Weihermüller, Mathias Diedhiou, Harry Vereecken, Seynabou Cissé Faye, Sérigne Faye, and Samba Ndao Sylla	
Geomorphological Control on Groundwater Occurrence Within the Basement Terrain of Keffi Area, North-Central Nigeria	257
Ebenezer A. Kudamnya, Aneikan E. Edet, and Azubuike S. Ekwere	
Characterization of Superficial Aquifer in Oued M'Zab (Northern Algerian Sahara)	261
Hadjira Benhedid and Mustapha Daddi Bouhoun	
Role of Kaolinisation in the Khondalitic Aquifers of Eastern Ghats (India)	265
Venkateswara Rao Bekkam	

Assessment of Vulnerability and Risk Mapping at Marsaba—Feshcha Catchment	271
Jawad Shoqeir	
Comparison of Two Methods for Groundwater Pollution Intrinsic Vulnerability Mapping in Wadi Nil (Jijel, North-East Algeria)	277
Abdelmadjid Boufekane, Hakim Saibi, and Omar Saighi	
Groundwater Risk Assessment for Shallow Aquifers within the Atankwidi Basin of (Ghana)	283
Maxwell Anim-Gyampo, Geoffrey K. Anornu, Sampson K. Agodzo, and Emmanuel K. Appiah-Adjei	
Groundwater Flow Modelling of a Multilayer Aquifer in Semi-arid Context	287
Nesrine Ghouili, Mounira Zammouri, Faten Jarraya-Horriche, Fadoua Hamzaoui-Azzaza, and José Joel Carrillo-Rivera	
Statistical Analysis of Groundwater Level Variation in Semi-arid Upper Godavari Basin	291
Pallavi Kulkarni, Sudhakar Pardeshi, and Suchitra Pardeshi	
Groundwater Pollution Index Evaluation Test Using Electrical Conductivity in a Semi-arid Quaternary Aquifer (Kousseri-Cameroon, Lake Chad Basin): Multivariate Statistical Analysis Approach	295
André Firmin Bon, Sylvain Doua Aoudou, Arouna Mbouombouo Ndam, Etienne Ambomo Bineli, and Elisabeth Dassou Fita	
Part V Water Resources Sustainability and Climate Change	
Hydrological Impacts of Climate Change in Northern Tunisia	301
Hamouda Dakhlaoui, Jan Seibert, and Kirsti Hakala	
Climate Change Impact on Future Flows in Semi-arid Environment, Case of Essaouira Basin (Morocco)	305
Salah Ouhamdouch, Mohammed Bahir, Paula M. Carreira, and Kamel Zouari	
Climate Change Effects on Groundwater Recharge in Some Subsaharian Areas	309
Maurizio Barbieri, Stefania Vitale, and Giuseppe Sappa	
Recharge Estimation of Hardrock-Alluvium Al-Fara Aquifer, Oman Using Multiple Methods	313
Azizallah Izady, Osman Abdalla, Mansoor Amerjeed, Mingjie Chen, Ali Al-Maktoumi, Anvar Kacimov, and Hilal Al-Mamari	
Groundwater Favourable Infiltration Zones on Granitic Areas (Central Portugal)	317
José Martins Carvalho, Maria José Afonso, José Teixeira, Liliana Freitas, Ana Rita Lopes, Rosário Jesus, Sofia Batista, Rosário Carvalho, and Helder I. Chaminé	
Assessment of Groundwater Potential in the Upper Tigris/Turkey Plain	321
Recep Celik	
Assessment of Turkey-Harran Basin's Groundwater Potential and Hydrogeological Properties	325
Veysel Aslan and Recep Celik	

Evaluation of the Potential for Artificial Groundwater Recharge of Crystalline Rocks Aquifer, Nuba Mountains (Sudan)	333
Dafalla Wadi, Wenbing Wu, and Abuzar Fuad	
The Impact of Urbanization Versus the Impact of the Change in Climatic Conditions on Groundwater Recharge from Precipitations: Case Study Algiers	337
Mohamed Amine Boukhemacha	
Frequency Ratio Model for Mapping Groundwater Potential Zones Using GIS and Remote Sensing; Medjerda Watershed Tunisia	341
Fatma Trabelsi, Saro Lee, Slaheddine Khlifi, and Achouak Arfaoui	
Multivariate Statistical Evaluation of Groundwater Recharge Potential in Arid Region, Southern Tunisia	347
Mohamed Haythem Msaddek, Dhekra Souissi, Yahya Mounni, Ismail Chenini, and Mahmoud Dlala	
Water Balance Estimation Under Wildfire and Restoration Scenarios in Semiarid Areas: Effects on Aquifer Recharge	351
Hassane Moutahir, Issam Touhami, Aymen Moghli, and Juan Bellot	
The Impact of the Mobilization of Water Resources in Semi-Arid Areas on Sustainable Development: The Case of Timgad Basin, Northeastern of Algeria	355
Athamena Ali, Menani Mohamed Redha, Djaiz Fouad, and Belalite Halima	
Groundwater Mounding in Fractured Fossil Aquifers in the Saharan-Arabian Desert	359
Abotalib Z. Abotalib and Essam Heggy	
A Coupled Hydrogeophysical Approach to Enhance Groundwater Resources Management in Developing Countries	363
Zakari Arétouyap, Dieudonné Bisso, Philippe Njandjock Nouck, and Jamal Asfahani	
Characterization and Origin of Some North-Eastern Algeria Thermal Waters	367
Yasmina Bouroubi-Ouadfel, Abdelkader Khiari, Corinne Le Gal La Salle, Mounira Djebbar, and Mahmoud Khaska	
Water Footprint and Governance Assessment for Sustainable Water Resource Management in Drought-Prone Barind Area, NW Bangladesh	371
Razzaqul Islam, Chowdhury S. Jahan, Quamrul H. Mazumder, Suman Miah, and Ferozur Rahaman	
Part VI Hydrologic Engineering and Urban Groundwater	
Water Quality for Irrigation Purposes in the Middle Tafna Watershed (NW, Algeria)	377
Lamia Yebdri, Fatiha Hadji, Yahia Harek, and Abbes Marok	
Statistical Multivariate Analysis Assessment of Dams' Water Quality in the North-Central Algeria	381
Somia Hamil, Djaouida Bouchelouche, Siham Arab, Nassima Doukhandji, Ghiles Smaoune, Monia Baha, and Abdeslem Arab	
Application of Water Quality Index for Surface Water Quality Assessment Boukourdane Dam, Algeria	385
Siham Arab, Djaouida Bouchelouche, Somia Hamil, and Abdeslam Arab	

Cumulative Probability and Water Quality Index (WQI) for Finding Drinking Water Suitability in a Tannery Belt (Southern India)	389
Nepal Mondal	
Bio-Evaluation of Water Quality in an Algerian Dam by the Application of Biotic Indices; Case of Ghrif Dam	393
Somia Hamil, Siham Arab, Djaouida Bouchelouche, Mounia Baha, and Abdeslem Arab	
2D Water Quality Modeling of Dam Reservoir (Case Study: Doosti Dam)	397
Saeed Reza Khodashenas, Arezoo Hasibi, Kamran Davary, and Bahman Yargholi	
Efficiency of a Neuro-Fuzzy Model Based on the Hilbert-Huang Transform for Flood Prediction	401
Zaki Abda, Mohamed Chettih, and Bilel Zerouali	
Floodline Delineation for Brandfort Area of South Africa: An Integrated Approach	405
Saheed Adeyinka Oke and George Ndhlovu	
The Effect of Urban Development on Urban Flood Runoff (Case Study: Mashhad, Iran)	409
Saeed Reza Khodashenas and Javad Azizi	
Integrated Approach to Assess the Urban Green Infrastructure Priorities (Alexandria, Egypt)	413
Mona G. Ibrahim, Bahaa Elboshy, and Wael Elham Mahmod	
Urbanization Growth Effect on Hydrological Parameters in Mega Cities	417
Ahmed Mohamed Helmi, Ahmed Mahrous, and Ashraf El. Mustafa	
Urban Hydrogeological Studies of Groundwater in Central University of Technology Bloemfontein Campus	421
Saheed Adeyinka Oke and Mpho Aloysius Matobo	
Assessment and Mapping of Proposed Dam Sites in North West Bank, Palestine Using GIS	425
Radwan El-Kelani and Abdelhaleem Khader	
Reduction in the Storage Capacity of Dokan Dam Reservoir	429
Rebwar Hasan, Ammar Ali, Anwer Hazim, Nadhir Al-Ansari, and Sven Knutsson	
Impact of Landfill Leachate Organics on the Behavior of Heavy Metals in Groundwater	433
Irina Galitskaya, Vera Putilina, Irina Kostikova, and Tatiana Yuganova	
Modeling of Toluene and Benzene Concentrations in the Groundwater of Tanjero Waste Dump Area, Kurdistan Region, Iraq	437
Aras Kareem and Omed Mustafa	
Using Chance Constrained Programming Approach for Optimal Crops Selection and Economic Profitability of Irrigation Under Hydrological Risk: The Case Study of Small Dams in Tunisia	443
Hacib El Amami, Jean R. Kompany, Taoufik Hermassi, and Nada Lellia	
Farmers' Adaptive Strategies in Face to Groundwater Depletion: A Short-Term Panacea or a Sustainable Solution? Evidences from the Center of Tunisia	447
Hacib El Amami, Taoufik Hermassi, and Nada Lellia	

About the Editors



Helder I. Chaminé is a skilled Geologist and Professor of engineering geosciences at the School of Engineering (ISEP) of the Polytechnic of Porto, with over 28 years' experience in multidisciplinary geosciences research, consultancy, and practice. He studied geological engineering and geology (B.Sc., 1990) at the Universities of Aveiro and Porto (Portugal), respectively. He received his Ph.D. in geology at the University of Porto in 2000 and spent his postdoctoral research in applied geosciences at the University of Aveiro (2001–2003). In 2011, he received his Habilitation (D.Sc.) in geosciences from Aveiro University.

Before joining academy, he worked over a decade in international projects for mining, geotechnics, and groundwater industry and/or academia related to geodynamics and regional geology, hard-rock hydrogeology and water resources, engineering geosciences and applied geomorphology, rock engineering and georesources. His research interests span over fundamental to applied fields: GIS mapping techniques for applied geology, structural geology and regional geology, engineering geosciences and rock engineering, slope geotechnics, mining geology and hydrogeomechanics, hard-rock hydrogeology, exploration hydrogeology, urban groundwater and hydromineral resources. He has interests in mining geoheritage, history of cartography, military geosciences and higher education dissemination, skills and core values.

Presently, he is Head of the Laboratory of Cartography and Applied Geology (LABCARGA|ISEP), Senior Researcher at Centre GeoBioTec|UA and Centre IDL|U. Lisbon. He is also member of the executive board of the M.Sc./B.Sc. Geotechnical and Geoenvironmental Engineering (OE+EUR-ACE Label) and of the Department of Geotechnical Engineering (ISEP). Currently, he is a board member of the Portuguese Geotechnical Society (SPG) and he used to be a board member of the APGeom—Portuguese Association of Geomorphologists (2009–2013). He was consultant and/or responsible for over 65 projects of rock engineering, applied geology, hydrogeomechanics, slope geotechnics, mining geology, exploration hydrogeology, hard-rock hydrogeology, water resources, urban groundwater and applied mapping (Mozambique, Portugal, and Spain).

He has co-authored over 195 publications in indexed journals, conference proceedings/full papers, book chapters, as well as technical and professional papers. He co-edited five conference volumes, three special volumes, one special issue for the “Environmental Earth Sciences” journal (2015, Springer). He is presently involved in editing themed issues for two journals: “Sustainable Water Resources Management” (IAH+Springer) and “Geotechnical Research” (ICE). He has a huge responsibility as a referee for several international journals. He served as invited Expert Evaluator of Bologna Geoscience programme for DGES (Portugal) and Scientific Projects Evaluation for NCST (Kazakhstan), as well as Coordinator of “Geology on Summer/Ciência Viva” programme at ISEP for geosciences dissemination. He has also been active teaching and supervising the work of many Ph.D., M.Sc., and undergraduate students.

He has been on the editorial board, among others, of Arabian Journal of Geosciences (SSG+Springer), Hydrogeology Journal (IAH+Springer), Geotechnical Research (UK), Current World Environment (India), Earth Science India (India), Revista Geotecnia (Portugal), and Geología Aplicada a la Ingeniería y al Ambiente (Argentina). Currently, he is in the organizing committee of the International Conferences “Geoethics and Groundwater Management” (IAH/IAPG, Porto, October 2019) and “Natural Hazards—Hydrological Risks” (LREC, Pico Island, Azores, May 2019).



Maurizio Barbieri has over 15 years of postgraduate experience in hydrogeochemistry. Since 2006, he has been Associate Professor of Hydrogeochemistry and Environmental Geochemistry, and before that, since 2001, hydrogeochemistry laboratory manager. He was a member of the Board of Directors at Sapienza University of Rome between 2009–2016. He is an Environmental Advisor (Hydrogeochemistry) for the International Project (2016–2019) SECOSUD II—Conservation and equitable use of biological diversity in the SADC region. The project is financed by the Italian Agency for Development Cooperation, and implemented through Eduardo Mondlane University, South African National Park and Sapienza University of Rome.

Maurizio was a scientific coordinator for the Water Unit of the International Project that provides institutional support to the management of Protected Areas in Albania, funded by the International Union for Conservation of Nature (IUCN, 2012–2014) and for the hydrogeochemical model of the Vico Lake (Lazio, Italy), funded by the Regional Agency for Environmental Protection of Lazio, Italy (2014–2016).

Currently, he is focusing on the application of the geochemistry methodologies for the characterization of environmental problems, distribution of elements and isotopes in the Earth Systems with emphasis on hydrogeology, water-rock interaction, water quality, hydrogeochemical anomalies of natural origin, hydrogeochemical surveys, Ion chromatography,

ICP-MS, water, soil and geological mapping, univariate and multivariate analysis of geochemical datasets, and isotope analyses of Sr, H, O, and B.

He has been on the editorial board of the Arabian Journal of Geosciences, Chemie der Erde, Environmental Geochemistry and Health, Euro-Mediterranean Journal for Environmental Integration, Water and Geofluids. He was a guest editor for a Water Special Issue “Isotopes in Hydrology and Hydrogeology”. Recently, he became Editor-in-Chief (Hydrogeology Section) for Geosciences.



Ozgur Kisi received his B.Sc. in Civil Engineering from the Cukurova University, Turkey (1997), his M.Sc. in Hydraulics from the Erciyes University, Turkey (1999), and his Ph.D. from Istanbul Technical University, Turkey (2003). His research fields are: Developing novel algorithms and methods towards the innovative solution of hydrologic forecasting and modeling; suspended sediment modeling; forecasting and estimating hydrological variables such as precipitation, streamflow, evaporation, evapotranspiration, groundwater, lake level; hydroinformatics; and trend analysis. He is an active participant in numerous national research projects and supervisor of several M.Sc. and Ph.D. works. He is serving as an Editorial Board Member of several reputed journals (e.g., Journal of Hydrologic Engineering (ASCE), ISH Journal of Hydraulic Engineering, Irrigation & Drainage Systems Engineering and Austin Journal of Irrigation). He has also served as a Guest Editor for Special Issues published in Hydrological Hazards in a Changing Environment-Early Warning, Forecasting, and Impact Assessment I and II (Advances in Meteorology) in 2015. He is currently serving as a Reviewer for more than 70 journals indexed in Science Citation Index (SCI) in the fields of hydrology, irrigation, water resources and hydro-informatics (e.g., ASCE Journal of Hydrologic Engineering, ASCE Journal of Irrigation and Drainage Engineering, Water Resources Research, Journal of Hydrology, Hydrological Processes, Hydrology Research, Water Resources Management, Hydrological Sciences Journal, Journal of Hydroinformatics, Water Science and Technology). He has authored more than 200 research articles and 24 discussions (Web of Science h-index = 35, Google Scholar h-index = 46; Scopus h-index 39). He is the recipient of the 2006 International Tison Award (given by the International Association of Hydrological Sciences (IAHS); URL: <http://iahs.info/About-IAHS/Competition-Events/Tison-Award/Tison-Award-winners/OKisi.do>). In 2017, he joined the AJGS as an Associate Editor responsible for evaluating submissions in the fields of hydroinformatics; hydrological modeling/evapotranspiration estimation; river flow forecasting techniques; and other fields related to hydrology.



Mingjie Chen holds a B.E. in Environmental Engineering (1997) from Tsinghua University (China), an M.Sc. in Environmental Sciences (2000) from Peking University (China), and a Ph.D. in Hydrogeology (2005) from the University of California, Santa Barbara (USA). After over 10 years of research experiences in USA, Dr. Chen joined—as a senior hydrogeologist—the Water Research Center, Sultan Qaboos University (Oman) in 2014. His research focuses on using mathematical models, numerical techniques, and high-performance computing to study fluid flow and contaminant transport in heterogeneous subsurface media. He has conducted more than 20 research projects on underground environment remediation, hydrocarbon reservoirs, CO₂ utilization and sequestration, geothermal reservoir, groundwater modeling and management. He serves as an Associate Editor for Springer Hydrogeology Journal (official journal of International Association of Hydrogeologists) and Elsevier Journal of Hydrology. He has co-published more than 25 research articles in international indexed and refereed journals. In 2014, he joined AJGS as an Associate Editor responsible for evaluating submissions in the fields of Hydrogeology, Hydrology, Contaminant Hydrology, Numerical Modeling, Uncertainty Quantification and Risk Assessment.



Broder J. Merkel studied Chemistry and Geology at the Technical University of Munich (Germany). He received his Ph.D. there in 1983 and his Habilitation in 1992 at the University of Kiel (Germany). From 1993 to 2015, he was a Full Professor of Hydrogeology and Hydrochemistry at the Technical University of Freiberg (Germany). From 1995 to 2014, he was the Director of the Institute of Geology, during 5 years he was the Dean of the Faculty of Geosciences, Geo-engineering and Mining, and from 2014 to 2017, he was Vice Rector of the Technical University of Freiberg. He initiated in 1995 the International Conference on Uranium Mining and Hydrogeology (UMH), which was held for seven times in Freiberg. He was speaker of the DFG Research Training Group and has been dealing with arid Hydrogeology, impact of mining on water, the speciation of elements and numerical modeling of groundwater flow, and chemical reactions and the reactive transport. He was co-founder of the Geoecology Bachelor and Master Program in Freiberg in 2008. In 2002, he co-founded the Scientific Diving Center at the Technical University of Freiberg and established two modules for various study programs. In 2008 he founded the international Master Program Groundwater Management. He published 155 research articles in international peer reviewed journals. In 1998 he initiated the open access Journal Freiberg Online Geoscience (FOG) as Editor. Since 2011 he is Associate Editor of Environmental Earth Sciences (EES). In 2015, he joined the AJGS as an Associate Editor responsible for evaluating submissions in the fields of Hydrogeology & Mining Geology.

Part I
Keynote

Innovation in Process Engineering for Hydrology

Enrico Drioli and Francesca Macedonio

Abstract

Currently, water demands throughout the world exceed the ability of Earth's natural hydrologic cycles to replenish adequate fresh supplies of this resource. Water must, therefore, be recycled and reused many times over the course of each period between its extraction from, and return to, those cycles. Some governments have already issued large-scale programs to recover and reuse treated municipal waste waters, rehabilitate saline and contaminated wells, desalinate brackish- and sea-water sources. In the last years, membrane operations have been assigned a key role in water reclamation schemes that are aimed at higher water quality reuse applications. In the present work, membrane operations in the field of water treatment are discussed.

Keywords

Membrane operations • Water stress • Valuable resource recovery

1 Introduction

The availability of potable water has nowadays become a worldwide problem due to the continuous growth in water demand, not balanced by an adequate recharge. Moreover, more and more often water sources are suffering from a deterioration of their quality due to the indiscriminate discharge of both domestic and industrial effluents without adequate treatments. However, in order to support increasing domestic, tourist and industrial demands and sustain growing future generations across the globe, new integrated water production, purification, distribution and reuse systems have to be considered. These systems should make possible to solve major problems such as water quantity and quality, environmental protection, reduction of energy consumption and water cost. Another important and emerging issue is the removal of new contaminants identified in water streams, such as hydrophilic organic compounds, many disinfection by-products, pharmaceutical compounds, and many different ions originating from electronic products which often end up in landfills, thus, contaminating land, water and air.

The problems of water shortage and water quality affect not only human and industrial activities, but also adequate and sustainable food production. In fact, agriculture is another sector which consumes huge amounts of water, involving about 70% of worldwide water use, increasing to over 90% in developing countries. When water resources are limited, irrigation is penalized. Moreover, another important problem is water loss. It has been estimated that around 70% of irrigation water is not returned to the surrounding water bodies and the risk that the remaining 30% may contaminate them is high [1]. Indeed, a serious drawback of irrigation is the contamination of the existing natural resources.

Furthermore, huge amounts of water are being used for cattle to satisfy the growing demand for meat around the world.

Ensuring safe, future worldwide water supply demands, today, depends on advanced and environmentally acceptable

E. Drioli (✉) · F. Macedonio
Institute on Membrane Technology, ITM-CNR, c/o University of Calabria, via P. Bucci, 17/C, I-87036 Rende, CS, Italy
e-mail: e.drioli@itm.cnr.it

E. Drioli · F. Macedonio
Department of Environmental and Chemical Engineering,
University of Calabria, Via P. Bucci, 44/A, I-87036 Rende,
CS, Italy

E. Drioli
WCU Energy Engineering Department, Hanyang University,
Room 917 9th Floor FTC Bldg., 17 Haengdang-Dong,
Seongdong-Gu, Seoul, 133-791, South Korea

E. Drioli
Center of Excellence in Desalination Technology,
King Abdulaziz University (KAU-CEDT), Jeddah, 21589,
Kingdom of Saudi Arabia

processes which would allow one to preserve water and to reduce its consumption.

Actually, sea/brackish water desalination, and wastewater treatment and reuse are well established water production processes. Water reuse is nowadays essential, and it is largely used worldwide to provide irrigation water, power plant cooling water, industrial process water, and groundwater recharge. Concerning desalination, it has become the most important source of drinking water production. Both for water reuse and for desalination, Membrane Engineering offers a possible route to a more-sustainable fresh water production. In the next sections, some of the most significant membrane unit operations involved in the areas of desalination and water treatment are discussed.

2 Membrane Operations for Water Desalination

The possibility of extracting potable water from seawater was a dream of all the populations living near seas and without access to fresh water. Currently, desalination membrane-based plants around the world are rising: the global cumulative contracted capacity, dominated by seawater reverse osmosis (SWRO), reached 99.8 million m³/day in 2017, and membrane desalination technologies account for more than 90% of all desalination plants. The success of SWRO was due to its higher recovery factor, lower investment and total water cost, and to the continuing technological advances enabling RO desalination to treat high-salinity raw water. RO applications range from the production of ultrapure water for semiconductor and pharmaceutical use, to the desalination of seawater for drinking water production and the purification of industrial wastewater. RO is capable of rejecting nearly all colloidal or dissolved matter from an aqueous solution, producing a concentrate brine and a permeate which consists of almost pure water (due to the high selectivity of the existing RO commercial membrane modules—between 99.40 and 99.80%). In order to maintain the desirable selectivity and an economically acceptable water flux, mass transfer limitations (i.e., Achilles' heel of membrane processes) have to be considered: concentration polarization and membrane fouling. For efficient SWRO processes, an adequate pre-treatment, supplying high quality feedwater is essential. Ineffective pre-treatment can lead to high rates of membrane fouling, high frequency of membrane cleanings, lower recovery rates, high operating pressure, poor product quality and reduced membrane life. Nowadays, an increasing number of plant owners are considering the use of membrane-based pre-treatments [such as microfiltration (MF) and ultrafiltration (UF)] to replace the less efficient, conventional pre-treatment systems, which do not represent

a positive barrier to colloids and suspended solids, as well as produce unsteady quality of RO feedwater. Moreover, membrane application in water pre-treatment also provides many other advantages over conventional treatment including: capability of handling wide fluctuations in raw water quality, enabling operation with a high and stable permeate flux in long term operations (even during storm events and algae blooms), small footprint, low energy consumption, production of RO feedwater of good quality; all these aspects have a direct impact on the reduction of capital and operating costs of the desalination plant.

Recently, the thermally driven membrane process—called membrane distillation (MD)—has gained popularity due to some unique benefits associated with the process, such as the possibility to concentrate the seawater till around its saturation point without any significant flux-decline, to utilize low-grade waste heat streams and/or alternative energy sources (solar, wind, or geothermal), and to reject theoretically 100% of non-volatile components [2]. Owing to these attractive benefits, MD might become one of the most interesting desalination techniques. Concentration polarization does not affect the driving force of the process significantly, and therefore, high recovery factors and high concentrations can be achieved in the operation, compared with the RO process. All the other properties of membrane systems (easy scale-up, easy remote control and automation, no chemicals, low environmental impact, high productivity/size ratio, high productivity/weight ratio, high simplicity in operation, and flexibility) are also present. Moreover, due to its characteristic to be theoretically 100% impenetrable with respect to non-volatile components (such as macromolecules, colloidal species and ions), MD can help in producing high quality water, rejecting also traces of contaminants (such as pharmaceuticals, boron, arsenic, emerging contaminants like e-waste, etc.) that cannot be easily removed with other techniques.

Another innovative membrane operation that can be used for further improving desalination processes is membrane-assisted crystallization (MCR). MCR is an extension of the MD concept which can be utilized for producing crystals and pure water from solutions and, in particular, from the RO brine streams of the desalination plants.

The studies carried out by Drioli and co-workers [3, 4] showed that the introduction of an MCR unit on NF and RO retentate streams of an integrated membrane-based seawater desalination system constituted by MF/NF/RO, increases the plant recovery factor enough to reach 92.8%. An integrated RO + Wind Aided Intensified Evaporation + MCR brackish water desalination system has been used to reduce the discharged brine to less than 0.75–0.27% of the raw water fed to the system [5]. Therefore, DCMD/MCR can not only reduce the environmental problems related to brine disposal but can also increase the technical feasibility of inland

brackish water RO with the ions contained in the concentrated streams recovered for agricultural, domestic or industrial use.

3 Membrane Operations for Wastewater Treatment and Reuse

In addition to desalination, wastewater treatment and reuse is a feasible solution and a sustainable alternative source of water that is able to face the increasing municipal, industrial, and agricultural demands. Today, the uses of reused water include the irrigation of golf courses and lawns and of edible and non-edible agricultural crops, as well as indirect potable reuse, such as groundwater recharge. Industrial reuse includes the use of water in cooling towers for boiler feed, and in the cooling cycles of power plants.

Two of the principal advantages in the use of reclaimed water are the saving of fresh water for other water uses, and the reduction in the amount of wastewater discharged to oceans and sensitive surface waters.

Both membrane and conventional activated sludge plants can be utilized for the treatment of wastewaters. In the last decades, Membrane Bioreactor (MBR), a unit combining membrane filtration with biological treatment, became an effective membrane operation for wastewater treatment and recycling. It was introduced 30 years ago and is currently considered by the European Union as one of the best available technologies (BATs) that are used to treat municipal and industrial wastewater, and one of the most effective processes to reach a high level of protection of the environment. An MBR is a compact facility that produces high quality and disinfected effluent. This implies that MBR processes can be especially suitable for the reuse and recycling of wastewater.

4 Conclusions

In the last years, membrane operations have been assigned a key role in water reclamation schemes that are aimed at higher water quality reuse applications.

The development of innovative nanostructured membrane materials—with improved properties (including selectivity and flux), appropriate module and process design, and, in general, a deeper engineering analysis—is fundamental for further boosting the efficiency of membrane technology applications. The high amount and quality of water produced from seawater and/or wastewater through membrane processes contribute to restore the hydrologic cycles for replenishing the fresh water supply.

References

1. Quist-Jensen, C.A., Macedonio, F., Drioli, E.: Membrane technology for water production in agriculture: desalination and wastewater reuse. *Desalination* **364**, 17–32 (2015)
2. Drioli, E., Ali, A., Macedonio, F.: Membrane distillation: recent developments and perspectives. *Desalination* **356**, 56–84 (2015)
3. Macedonio, F., Drioli, E.: Hydrophobic membranes for salts recovery from desalination plants. *Desalin. Water Treat.* **18**, 224–234 (2010)
4. Macedonio, F., Curcio, E., Drioli, E.: Integrated membrane systems for seawater desalination: energetic and exergetic analysis, economic evaluation, experimental study. *Desalination* **203**, 260–276 (2007)
5. Macedonio, F., Katzir, L., Geisma, N., Simone, S., Drioli, E., Gilron, J.: Wind-aided intensified evaporation (WAIV) and membrane crystallizer (MCR) integrated brackish water desalination process: advantages and drawbacks. *Desalination* **273**, 127–135 (2011)

Part II

**Hydrology, Climatology and Water-Related
Ecosystems**

A Comparative Assessment of Meteorological Drought Indices for the Baribo Basin (Cambodia)

Kimhuy Sok, Supattra Visessri, and Sokchhay Heng

Abstract

Drought is considered a looming catastrophe for socio-economic development. In recent decades, Cambodia has been affected by increased severity of drought. Since drought is a slowly evolving natural disaster, its negative impacts can be mitigated through monitoring and characterizing drought levels by assimilating data from one or several indicators into a single numerical index which is more readily usable than raw indicator data. This study performed a comparative assessment of three meteorological drought indices including Standardized Precipitation Index (SPI), Effective Drought Index (EDI), and Percent of Normal Precipitation (PNP) for the Baribo basin in Cambodia. The SPI, EDI, and PNP are generally able to be used for assessing drought severity and duration but with a slight difference in performance. The SPI is considered the best index for capturing the extreme and severe drought events, while the EDI is a cautious index for assessing drought duration. The Baribo and Kraing Ponley sub-basins located in the middle and southern parts of the entire Baribo are considered the drought-prone area.

Keywords

Drought index • SPI • EDI • PNP • Baribo basin

1 Introduction

Drought is one of the natural hazards posing a threat to lives and livelihoods in many parts of the world, including Cambodia. Increased frequency and severity of drought particularly threatens agricultural production which generates major incomes for the country. The Ministry of Environment (MoE) stated that the droughts in 1998 and 2002 were severe, causing a 20% reduction in GDP (Gross Domestic Product) in the agricultural sector. Furthermore, approximately 54% of total population suffered from water shortages [1]. The development of drought is a sequential process. This study focuses on characterizing meteorological drought as it is conceived first in the drought sequence over time. Three meteorological drought indices including Standardized Precipitation Index (SPI), Effective Drought Index (EDI), and Percent of Normal Precipitation (PNP) were selected. The selection of the indices was due mainly to minimal data requirements of rainfall and popularity in the literature. This provides an opportunity to assess the level of drought in data scarce basins such as the Baribo basin that was selected for this study. The 7155 km² Baribo basin shown in Fig. 1 is one out of eleven sub-basins in the Tonle Sap basin. The Baribo basin is divided based on the drainage areas of the main rivers into three sub-basins, namely Kraing Ponley, Bamnak, and Baribo. Forest and agriculture are the major land uses, covering 98% of the whole basin (see Fig. 1). The climate is tropical with distinct wet (May–October) and dry (November to April) seasons. The results of drought assessment using the SPI, EDI, and PNP were compared and discussed in the Results section.

2 Methods

The daily rainfall data, from 1985 to 2008, from 13 rain gauges distributed over the Baribo basin as shown in Fig. 1, were obtained from the Ministry of Water Resources and

K. Sok · S. Visessri (✉)
Chulalongkorn University, Pathumwan, Bangkok, 10330,
Thailand
e-mail: supattra.vi@chula.ac.th

S. Heng
Institute of Technology of Cambodia, P.O. Box 86 Phnom Penh,
Cambodia

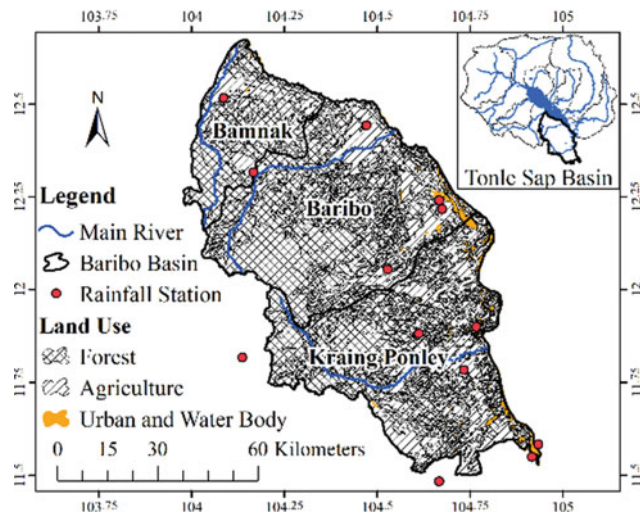


Fig. 1 The Baribo basin

Meteorology (MoWRaM). The calculation of the SPI relies on the transformation of precipitation probability distribution to a normal distribution using its mean and standard deviation. While the calculation of the SPI is simple, it cannot be performed until all daily records of rainfall data for the particular timescale are available. The EDI overcomes the weakness of SPI by considering the proportion of deviation of daily rainfall accumulation for a time period from its mean to its standard deviation. The PNP is the proportion of rainfall over a timescale to the normal precipitation. The SPI and PNP can be calculated at multiple monthly timescales. In this study, 6- and 24-month timescales (SPI6, SPI24, PNP6, and PNP24) were used to assess seasonality and trend. To compare the performance of the three indices, the EDI, which is a daily timescale index, was converted to a monthly timescale by averaging the daily values. Equations and detailed descriptions of the SPI, EDI, and PNP can be found in Guenang and Kamga [2], Byun and Wilhite [3], and Akbar et al. [4], respectively.

3 Results

3.1 Drought Severity Distribution

Referring to Morid et al. [5], drought occurs when the values of SPI, EDI, and PNP are lower than -1.0 , -0.7 , and 80.0 , respectively. Figure 2 is used here as an example of drought severity distribution analysis of the entire Baribo basin. The SPI and PNP indices show a similar pattern of the drought severity distribution at the 24-month timescale but less similarity is found at the 6-month timescale. Longer drought events were possibly found for the EDI. For example, the SPI6 and PNP6 show the drought event from June to August 1987, while the EDI suggest a longer period

continuing until December 1987. The SPI, EDI, and PNP show the longest duration of drought from September 1993 to April 1994. All the three indices can capture the long-term drought events from June 1996 to September 1999 and from September 2002 to October 2005. The values of EDI, SPI6, SPI24, PNP6, and PNP24 can be used to develop a drought severity distribution map for a drought event. When analyzing a single drought event in July 2005 as shown in Fig. 3, the SPI and PNP produced a similar pattern of drought severity distribution for both short and long timescales. However, the drought severity generated based on the SPI was more severe than the PNP. The EDI predicted the mildest level of drought severity among the test indices. There is a spatial tendency of the drought events. The Baribo and Kraing Ponley located in the middle and southern parts of the entire Baribo are considered to have higher chances of drought.

3.2 Correlation and Drought Event Analysis

The correlation coefficient (R) was used to explore the relationships between pairs of the indices. Table 1 indicates that the correlations of the EDI and the other two indices are generally low, especially at the longer time scale of 24 months. This is probably because EDI cannot sufficiently capture the trend while the other two indices can. The SPI and PNP were found to have a moderate to strong relationship with the values of R ranging from 0.33 to 1. The high R values were obtained when comparing the SPI and PNP at the same timescale, i.e. SPI24 and PNP24. This is believed to be due to similar concepts of identifying rainfall anomaly over a time period.

Table 1 also shows the percentage of drought events in each classification (wet classes not shown). The percentages of extreme drought (D3) event obtained at the 24-month timescale from the three indices are similarly low ranging from 0 to 0.4. The occurrence of D3 events at a shorter timescale (SPI6 and PNP6) is more frequent than that of the EDI. The severe drought (D2) event does not occur for the PNP24, while it does for the other indices. The moderate drought (D1) event occurs more frequently than other classes of drought. The normal (N) events for all sub-basins are mostly greater than 50% of the total events.

4 Discussion

The SPI and PNP show a similar pattern of the drought severity distribution and a high correlation. However, the SPI is considered better in capturing the extreme and severe drought events (see Fig. 3 and Table 1). The EDI has a low relationship to the SPI and PNP, but it is a cautious index for

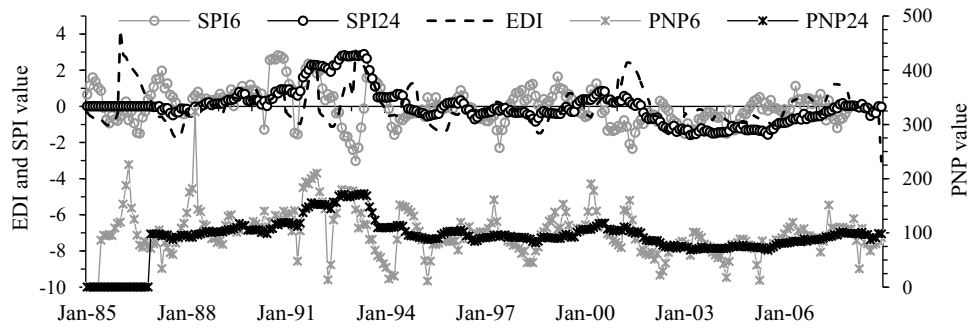


Fig. 2 Drought severity distribution for the Baribo sub-basin

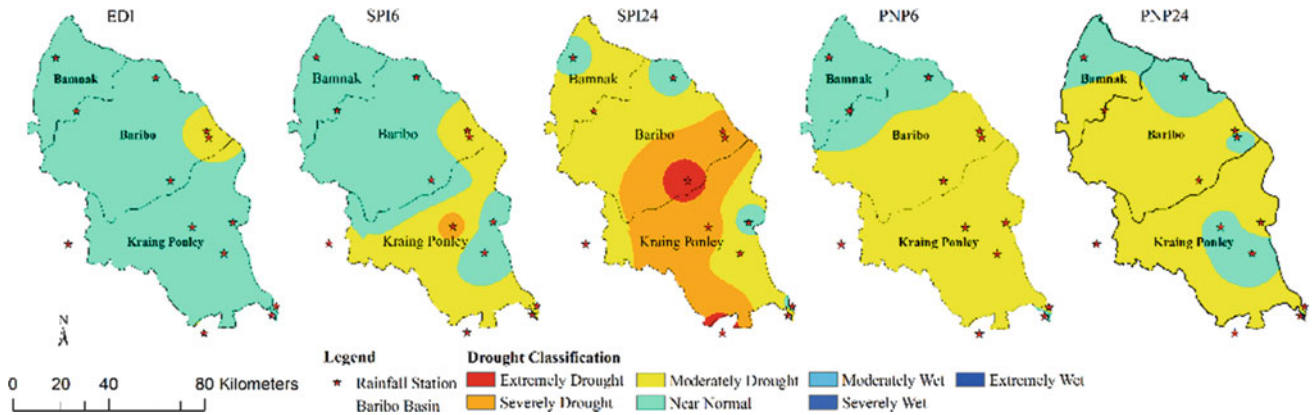


Fig. 3 Drought map for the Baribo sub-basin in July 2005

Table 1 The correlation coefficient (R) of the indices and percentage of drought events in each classification [5]

Sub-basin	Index	Correlation between pairs of drought index					% of drought events in each classification			
		EDI	SPI6	SPI24	PNP6	PNP24	N	D1	D2	D3
Kraing Ponley	EDI	1.00					56.5	19.6	2.9	0.4
Bamnak		1.00					65.2	17.4	0.7	0.4
Baribo		1.00					62.0	15.9	3.3	0.4
Kraing Ponley	SPI6	0.36	1.00				65.9	10.1	4.7	0.7
Bamnak		0.36	1.00				65.6	9.8	5.8	1.8
Baribo		0.44	1.00				71.7	9.4	2.5	2.5
Kraing Ponley	SPI24	0.16	0.48	1.00			62.1	13.6	6.1	0.0
Bamnak		0.19	0.50	1.00			65.9	13.3	3.4	0.0
Baribo		0.50	0.56	1.00			73.9	14.4	1.5	0.0
Kraing Ponley	PNP6	0.37	0.89	0.39	1.00		46.4	20.3	4.0	1.1
Bamnak		0.27	0.91	0.33	1.00		48.2	17.4	2.5	0.7
Baribo		0.41	0.93	0.52	1.00		37.7	19.6	5.4	4.3
Kraing Ponley	PNP24	0.16	0.50	0.99	0.41	1.00	71.2	7.2	0.0	0.0
Bamnak		0.19	0.54	1.00	0.55	1.00	77.7	0.4	0.0	0.0
Baribo		0.49	0.55	0.99	0.51	1.00	64.8	15.9	0.0	0.0

assessing drought duration. The three indices indicated that the drought severity tended to increase and the drought duration was prolonged in the entire Baribo basin during the recent decades.

5 Conclusions

The SPI, EDI, and PNP can be used for assessing meteorological drought in the Baribo basin. These indices showed distinct features. The SPI and PNP showed similar results and outperformed EDI in assessing drought severity and trend. However, when assessing the drought duration, EDI is recommended as it can give longer duration of drought and lead to conservative prevention. The Baribo and Kraing Ponley sub-basins are more prone to drought compared to the Bamnak sub-basin. As meteorological drought can result in agricultural and hydrological droughts, further studies

should be extended to cover the assessment of the drought indices in such categories.

References

1. Chhinh, N., Millington, A.: Drought monitoring for rice production in Cambodia. *J. Clim.* **3**(4), 792–811 (2015)
2. Guenang, G.M., Kanga, F.M.: Computation of the Standardized precipitation index (SPI) and its use to assess drought occurrences in Cameroon over recent decades. *J. Appl. Meteorol. Climatol.* **53**(10), 2310–2324 (2014)
3. Byun, H.R., Wilhite, D.A.: Objective quantification of drought severity and duration. *J. Clim.* **12**(9), 2747–2756 (1999)
4. Akbar, N., Ahmad, N., Saeedeh, M.: Comparison the suitability of SPI, PNI and DI drought index in Kahrestan watershed (Hormozgan Province/South of Iran). *J. Environ. Earth Sci.* **5**(8), 71–76 (2015)
5. Morid, S., Smakhtin, V., Moghaddasi, M.: Comparison of seven meteorological indices for drought monitoring in Iran. *Int. J. Climatol.* **26**(7), 971–985 (2006)

Probabilistic Precipitation Forecast in (Indonesia) Using NMME Models: Case Study on Dry Climate Region

Heri Kuswanto, Dimas Rahadiyuza, and Dodo Gunawan

Abstract

Reliable precipitation forecast is one of the key inputs to generate accurate and reliable hydrological forecast. This paper uses the North American Multimodel Ensemble (NMME) models to generate seasonal precipitation forecasts in Indonesia. The NMME models are verified against observed precipitation, and the analysis shows that they are biased and underdispersive. The Bayesian Model Averaging (BMA) approach was applied to calibrate the forecast for reliable prediction. East Nusa Tenggara (NTT) is chosen as the pilot study since the region has been well recognized as a dry region with the highest degree of vulnerability toward drought. The results show that the BMA improves the forecast reliability. Moreover, the Canadian Meteorological Center (CMC) models outperform the others. The map of the forecasted Standardized Precipitation Index (SPI) is validated with the observation and shows a high prediction accuracy.

Keywords

Calibration • Drought • Hydrology • NMME • Underdispersive

1 Introduction

Climate change has led to a shift in the period of seasons in Indonesia [1]. Precipitation forecast is one of the key elements to predict the beginning of the seasons. Moreover,

H. Kuswanto (✉)

Center for Earth, Disaster and Climate Change, Institut Teknologi Sepuluh Nopember (ITS), Surabaya, 60111, Indonesia
e-mail: heri_k@statistika.its.ac.id

H. Kuswanto · D. Rahadiyuza

Department of Statistics, Institut Teknologi Sepuluh Nopember (ITS), Surabaya, 60111, Indonesia

D. Gunawan

Agency for Meteorology, Climatology and Geophysics (BMKG), Jakarta, Indonesia

precipitation forecast is also useful for hydrological forecasts as the basis of flood early warning and for estimating the river flow [2, 3]. There have been many efforts carried out to improve the reliability of the precipitation forecast in Indonesia. However, most of the works focused on applying statistical models which are unable to take into account uncertainties. The North American Multi-Model Ensemble (NMME) is an ensemble forecast consisting of a collection of models generated from several climate modeling centers. Several studies found that ensemble forecast has higher accuracy in forecasting weather and climate, and allows for better characterization of prediction uncertainty [4]. The NMME models provide a global seasonal forecast, and there have been only few studies carried out to investigate the performance of NMME forecasts in Indonesia. Setiawan et al. [5] verified the NMME performance in the Sulawesi region (equatorial types) and found that NMME forecasts have a better performance on dry periods (i.e. drought prediction) than on wet periods. Another study found that the performance of the NMME models is different globally [6]. The performance of NMME models as performed in [5] cannot be generalized to be the same in all of Indonesian regions due to the fact that Indonesia has three different climate zones. This paper briefly examines the NMME performance in NTT as one of monsoonal regions (types) in Indonesia. NTT is also listed on the top priority of vulnerable regions towards drought events in Indonesia, and hence, having a reliable precipitation forecast is very important for many aspects. Furthermore, to improve the forecast reliability, the raw ensemble forecast will be calibrated using Bayesian Model Averaging to take into account the uncertainty (see [7, 8]).

2 Methods and Materials

This paper analyzes the NMME Phase-I dataset to generate the precipitation probabilistic forecast in NTT Indonesia. NTT is a dry area (short rainy season) located at 8° S–12° S latitude, and 118° E–125° E longitude (see the map at Fig. 1).



Fig. 1 Location of East Nusa Tenggara in Indonesia (marked with red color). Source google.com

The observation dataset is a satellite-based data grid with a resolution of $1^\circ \times 1^\circ$ degree. The NMME models used to build the probabilistic forecast are CanCM3 and CanCM4 from the Canadian Meteorological Centre (CMC), CCSM3 and CCSM4 from The Center for Ocean-Land-Atmosphere Studies (COLA) and CM2p1 from NOAA's Geophysical Fluid Dynamics Laboratory (GFDL). The Models are hereafter denoted as M1 to M5 consecutively. Please refer to [6] for details on the models. We examined the data spanning from January 2011 to December 2016. The observed precipitations in 2017 are used for validation. The analysis began with verifying the performance of the forecasts using ensemble plots and a rank histogram, as the basis of applying the post-processing. To apply BMA, we had to set the training window (in this case we use 12 and 24 months). The analysis in this paper is limited to 1 month lead forecast for the sake of space.

3 Results

Figure 2 shows that there is a pattern consistency between the observation and the forecasts. We see that M1 and M2 have lower biases compared to the others, while M3 and M4

Fig. 2 Ensemble plots (left panel) and rank histogram (right panel) at 8° S lat and 118° E lon for lead-1 forecast

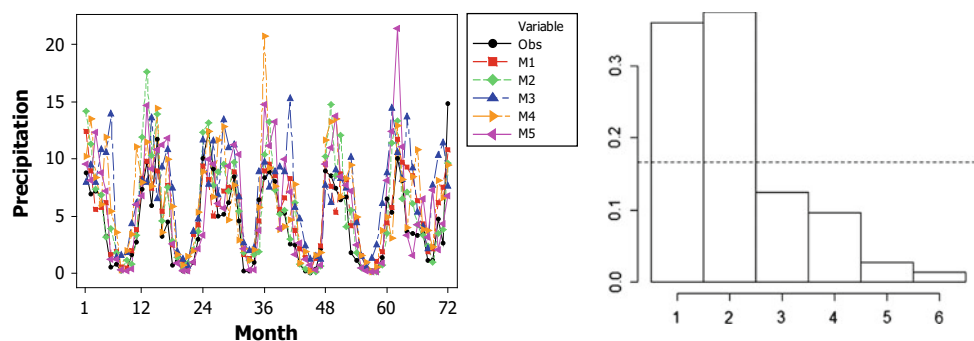


Table 1 BMA weights for each model

Training window	M1	M2	M3	M4	M5
12 months	0.062	0.4125	2.038×10^{-17}	3.83×10^{-15}	0.5243
24 months	0.243	0.4125	4.516×10^{-28}	5.95×10^{-6}	0.334

have the largest biases. The rank histogram shows that the forecasts tend to be biased (for low precipitations), while further investigation shows that lead-4 forecasts are underdispersive, as shown by a U-shape of the rank histogram. The BMA assigns the weights for each model to forecast the precipitation in November 2016 as listed in Table 1. The average of the weights for the whole periods and regions showed similar results.

The probabilistic forecasts are shown in Fig. 2 as an illustration, which clearly shows that the observations lie within the predictive intervals (indicated with dashed vertical lines). Furthermore, the point forecast bias (difference between yellow and black lines) is very small showing that the forecast accuracy is high (Fig. 3).

The forecast is transformed to SPI to create the map over NTT. The SPI map is used to monitor the climate conditions in various time scales. It is widely used in Indonesia, especially in agricultural applications (short term), as well as hydrology (long term). Figure 4 provides a sample of real and forecasted SPI in May 2017. The SPI map derived from the probabilistic forecast showed a good consistency with the observation in 2017. This means that the SPI index in a particular district was correctly predicted.

4 Discussion

The analysis above showed that the NMME forecasts are biased towards low precipitation for lead-1 forecast, which means that the raw NMME forecasts cannot predict the dry condition well. Meanwhile, the forecasts for lead-4 months are underdispersive, showing that the system produces unreliable and overconfident ensemble forecasts. The post-processing with BMA is able to improve the forecasts performance where the observations mostly fall within the

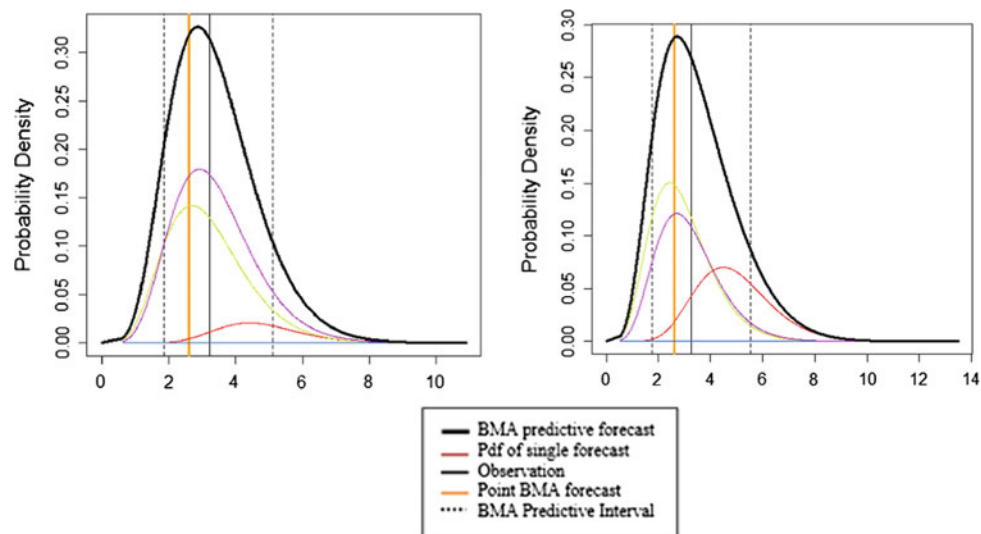


Fig. 3 PDF of precipitation forecast using BMA for the period of November 2016 at 8° S lat and 118° E lon with training window of 12 months (left) and 24 months (right)



Fig. 4 Comparison between real (left) and forecasted (right) SPI using calibrated NMME

predictive interval. The analysis showed that CMC models perform better than COLA and NOAA models. This fact is confirmed by the weight estimated with BMA, where the BMA gives more weight to the models with higher accuracy, and puts less weight for models with low accuracy. The CRPS showed that both settings of training windows have a similar performance in the sense that one outperforms another in certain cases with respect to the region and lead time forecast. Further studies need to be carried out to investigate the forecast performance (including the performance of each NMME model) on longer lead forecasts. Moreover, it will be interesting and meaningful to see whether including only good models in BMA may lead to more reliable forecasts than the forecasts with those five models.

5 Conclusions

This study examined the performance of NMME precipitation forecasts in NTT, Indonesia. The short lead forecast is biased and has been calibrated. The SPI map derived from

calibrated NMME forecasts shows a high degree of consistency with the observations. This means that the precipitation levels in some particular regions have been well predicted. Considering the fact that NTT is a dry region, having a reliable precipitation forecast is very important for many aspects such as determining the beginning of rainy seasons.

References

1. Huybers, P., Stine, A.R.: Changes in the seasonal cycle of temperature and atmospheric circulation. *J. Clim.* **25**, 7362–7380 (2012)
2. Demargne, J., Brown, J.D., Liu, Y., Seo, D.-J., Wu, L., Toth, Z., Zhu, Y.: Diagnostic verification of hydrometeorological and hydrologic ensembles. *Atmos. Sci. Lett.* **11** (2010)
3. Seo, D.-J., Herr, H.D., Schaake, J.C.: A statistical post-processor for accounting of hydrologic uncertainty in short-range ensemble streamflow prediction. *Hydrol. Earth Syst. Sci. Discuss.* **3**, 1987–2035 (2006)
4. Kirtman, B.P., Min, D., Infanti, J.M., Kinter, J.L., Paolino, D.A., et al.: The North American multimodel ensemble: phase-1

- seasonal-to-interannual prediction; phase-2 toward developing intraseasonal prediction. *Bull. Am. Meteorol. Soc.* **95**, 585–601 (2014)
5. Setiawan, M., Koesmaryono, Y., Faqih, A., Gunawan, D.: North American multi model ensemble (NMME) performance of monthly precipitation forecast over south Sulawesi, Indonesia. *IOP Conf. Ser.: Earth Environ. Sci.* **58**, 012035 (2017)
 6. Becker, E., van den Dool, H., Zhang, Q.: Predictability and forecast skill in NMME. *J. Clim.* **27**(15) (2014)
 7. Raftery, A.E., Gneiting, T., Balabdaout, F., Polakowski, M.: Using Bayesian model averaging to calibrate forecast ensembles. *Mon. Wea. Rev.* **133**, 1155–1174 (2005)
 8. Slughter, J.M., Raftery, A.E., Gneiting, T., Fraley, C.: Probabilistic quantitative precipitation forecasting using Bayesian model averaging. *Mon. Wea. Rev.* **135** (2007)

Homogeneity and Trend Analysis of Rainfall and Streamflow of Seyhan Basin (Turkey)

Sinan J. Hadi, Arkan J. Hadi, Kamaran S. Ismail, and Mustafa Tombul

Abstract

Changes in the historical rainfall and streamflow observations are important for understanding the climate change. The homogeneity of the annual and monthly times series of 9 rainfall stations and 3 streamflow gages, located at the Seyhan basin in Turkey, was examined using standard normal homogeneity test and Buishand test. The trend was studied by Mann-Kendall test, which is used for identifying the significance of the trend, and the Sen's slope estimator, which provides the magnitude of the trend. Finally, the Pettit test was also applied on the annual time series only to obtain the most probable change year. The entire time series was found as homogeneous, although several significant p values were obtained in the 0.05 but not in the 0.01 significance level. The annual trend varied from one station to another but was found to be significant in one rainfall and one streamflow station at the 0.1 significance level only. Monthly time series was found to have the most significant trend in January at 0.05 significance level. Several months have no stations with a significant trend, while others have only one station with a significant trend. The Pettit test results showed no consistent change year through all the stations, although the most frequent change year obtained was for 1981.

Keywords

Trend • Homogeneity • Mann-Kendall • Seyhan Turkey

1 Introduction

Rainfall is considered as one of the most important climatic variables in the fields of hydrology and climatology. It is also crucial in water resources management because of its critical importance in the spatial and temporal availability of water. Therefore, changes in historical rainfall observations are essential for water resources planners and climatologists. Streamflow is also extremely important in several aspects such as keeping the rivers and lakes full of water and monitoring the land change by the effect of erosion [1].

Many studies examined the trends in precipitation/rainfall around the globe. Some of these studies investigated the trends in the entire country (i.e. Turkey), and some in local scale with several stations. References [2–6] are some examples of these studies.

The objective of this study is to investigate the homogeneity and the trend of the monthly and annual rainfall and streamflow of three sub-basins located at the Seyhan basin, Turkey, using observations that extend over the period 1973–2000.

2 Materials and Methods

This study's goal is to investigate the trend in the monthly and annual rainfall and streamflow data for the period between 1973 and 2000 in 9 rainfall and 3 streamflow stations, located in three sub-basins called (coded) 1822, 1801, and 1805, as seen in Fig. 1. These three sub-basins are part of the Seyhan Basin located in the southwest of Turkey. Several stations were chosen outside the sub-basin, including all spatially correlated rainfall stations which could affect the streamflow value in addition to having a wide spatial distribution. The study area covers parts of the following provinces: Sivas, Adana, Kayseri, and Kahramanmaras. During the study period, the sub-basins are: rural, agricultural, not hydrologically disturbed, and without water storage structure.

S. J. Hadi (✉) · M. Tombul
Anadolu University, 26470 Eskisehir, Turkey
e-mail: sinan.jasirm@yahoo.com

A. J. Hadi · K. S. Ismail
Soran University, Soran, Erbil, Iraq

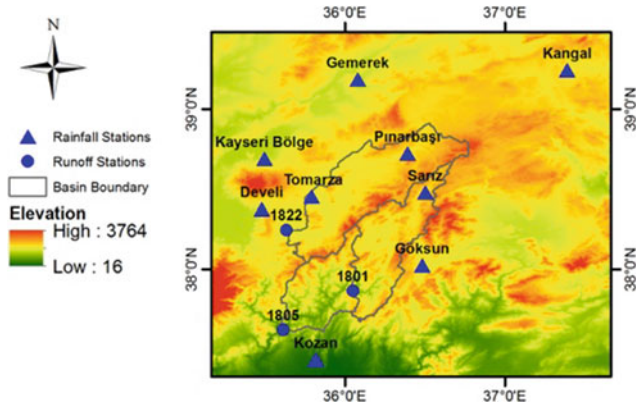


Fig. 1 Study area

Rainfall observations of 9 stations and streamflow of the 3 sub-basins' outlets were collected from the Turkish General Directory of Meteorology DMI (Devlet Meteoroloji Isleri) and General Directorate of State Hydraulic Works DSI (Devlet Su Isleri). The consistent available data for all stations are for the period 01/02/1973 to 30/09/2000. The collected data were daily totals of rainfall and streamflow.

3 Results

The p values of the homogeneity tests (i.e. Standard Normal Homogeneity Test, and Buishand Test) are listed in Table 1. The results show that the null hypotheses of the two tests cannot be rejected for a 0.01 significance level in all stations for the two temporal resolutions: Annual and monthly. For

the monthly time series, the null hypothesis—using Buis-hand test of only one rainfall station, n° 17802, and one streamflow station, n° 1805—can be rejected at 0.1 and 0.05 significance levels, respectively. For the annual series, a null hypothesis of 17162 rainfall stations using SNHT test, and of 17802 using SNHT and Buishand test, can be rejected at the significance level of 0.05. In general, the entire rainfall and streamflow stations are homogeneous, and no significant change occurred during the studied period. The most probable change year, which represents the results of the Pettit-Mann-Whitney test, showed no consistent results through all the stations. The most frequent change years are 1981 and 1988, which appear 4 and 3 times, respectively, while others have no consistent change year.

According to Table 1, the annual trend varies between the highest negative value -4.30 which is for rainfall station 17908 and the lowest negative value -0.4 which is for 17837. The only positive trend is in station 17196. Streamflow trend varies between -1.3 and -0.03 . Regardless of the magnitude of the trend mentioned earlier, only the rainfall station 17802 and streamflow station ST1805 have a significant annual trend with a 0.1 significance level.

According to Table 2 which shows the monthly trend results, January has the largest values of trend in most of the rainfall stations. Interestingly, the trend in all rainfall stations is negative, which indicates a decrease in the amount of the received rainfall in this month. The other months trend varies from negative to positive to no trend in all stations, so, no consistent pattern can be indicated.

The streamflow stations have a positive trend for two stations 1801, 1822 and negative for 1805 in January. The trend is negative through the months starting from February

Table 1 P values of homogeneity tests, SNHT: Standard normal homogeneity test, Buishand: Buishand test

	Annual		Monthly		Annual trend	
	SNHT	Buishand	SNHT	Buishand	Change year	Sen slope
17162	0.027**	0.473	0.640	0.990	1992	-0.41
17196	0.576	0.334	0.605	0.368	1985	1.78
17762	0.423	0.229	0.710	0.430	1988	-0.82
17802	0.031**	0.025**	0.187	0.075*	1981	-3.53***
17836	0.828	0.904	0.661	0.891	1983	-0.67
17837	0.519	0.931	0.497	0.988	1981	-0.40
17840	0.097	0.260	0.440	0.463	1981	-2.71
17866	0.404	0.543	0.840	0.708	1981	-4.27
17908	0.627	0.344	0.977	0.706	1988	-4.30
ST1801	0.333	0.828	0.256	0.381	1982	-0.21
ST1805	0.261	0.240	0.132	0.039**	1988	-1.30***
ST1822	0.185	0.753	0.133	0.488	1982	-0.03

* Significant at $\alpha = 0.1$, ** Significant at $\alpha = 0.05$, *** Significant at $\alpha = 0.01$ using Mann-Kendall test

Table 2 The results of the monthly trend with significance for rainfall and streamflow

Stations	January	February	March	April	May	June
17162	-1.26**	0.40	-0.39	-0.62	0.26	-0.15
17196	-0.55**	0.56	-0.35	-0.77	1.24*	0.83
17762	-1.47**	-0.57	-0.40	-0.13	0.06	0.88
17802	-1.20**	0.41	-0.30	-1.45*	-1.12	0.41
17836	-1.12**	0.33	0.17	-1.12	0.42	0.11
17837	-1.03**	0.04	0.07	-1.08	0.29	-0.17
17840	-1.44**	-0.68	-0.88	-1.08	0.14	1.20*
17866	-2.02	-1.13	-0.03	-1.03	-0.29	0.24
17908	-4.63**	0.07	-0.35	-0.73	-1.38	0.94
1801	0.22	-0.01	-0.58	-0.67	-0.42	-0.14
1805	-1.97*	-2.25	-1.79	-3.13	-2.96	-0.24
1822	0.10	-0.16	-0.20	-0.25	-0.09	-0.05
Stations	July	August	September	October	November	December
17162	-0.03	0.00	0.00	0.55	0.79	-0.10
17196	0.01	0.10	-0.07	0.58	-0.04	0.87
17762	0.25**	0.00	0.01	0.54	-0.29	-0.28
17802	0.17	0.08	-0.53	0.50	0.04	0.13
17836	0.00	0.02	-0.02	0.15	0.09	0.42
17837	-0.15	0.13	-0.28	0.28	0.51	0.81*
17840	0.33*	0.21	-0.27	0.09	0.95	-1.16
17866	-0.04	0.00	0.16	0.11	1.13	-0.61
17908	-0.09	0.40	0.58	-0.01	2.46	-0.54
1801	-0.04	-0.03	-0.04	0.00	0.06	0.22
1805	-0.29	-0.21	-0.19	-0.29	0.25	-0.37
1822	-0.02	0.00	0.04	0.07	0.12	0.12

*Significant at $\alpha = 0.1$ **Significant at $\alpha = 0.05$

till September and from February till July in the streamflow stations 1801 and 1805, respectively. The 1805 streamflow station has a positive trend only in November.

4 Conclusions

All stations were found to be, in general, homogenous and no change has occurred in the time series through the studied period, although several significant values were obtained at the 0.05 significance level. The annual trend was found as “not significant” only in one rainfall and one streamflow station, and the monthly trend was found as mostly significant in January, while other months have no or only one significant station. Pettit test was used for the identification of the most probable change year. No consistent year was found through all the stations but the most frequent change year obtained was for 1981.

References

- Hadi, S.J., Tombul, M.: Monthly streamflow forecasting using continuous wavelet and multi-gene genetic programming combination. *J. Hydrol.* (2018)
- Toros, H.: Spatio-temporal precipitation change assessments over Turkey. *Int. J. Climatol.* **32**(9), 1310–1325 (2012)
- Hadi, S.J., Tombul, M.: Long-term spatiotemporal trend analysis of precipitation and temperature over Turkey. *Meteorol. Appl.* (2018)
- Hadi, S.J., Tombul, M.: Analyzing trend and developing an empirical formula for estimating rainfall intensity: a case study Eskisehir city, Turkey. In: *International Conference on Advances in Sustainable Construction Materials & Civil Engineering Systems (ASCACES-17)*, EDP Sciences, UAE (2017)
- Türkeş, M.: Spatial and temporal analysis of annual rainfall variations in Turkey. *Int. J. Climatol.* **16**(9), 1057–1076 (1996)
- Unal, Y.S., et al.: Temporal and spatial patterns of precipitation variability for annual, wet, and dry seasons in Turkey. *Int. J. Climatol.* **32**(3), 392–405 (2012)

Mean Rainfall Variability Effects on the Hydrological Response of Medjerda High Valley (Tunisia)

Sahar Abidi, Olfa Hajji, Boutheina Hannachi, and Hammadi Habaieb

Abstract

The present study is an attempt to evaluate the spatial and temporal rainfall variability of the Medjerda High Valley on the hydrological response of the watershed. Mean time series were collected from 1980/1981 to 2014/2015 for 16 rain gauges covering the studied basin. Missing data were reconstructed using the ponderation method. Subsequently, breaks in each rainfall time series were detected by three tests: Pettitt, SNHT and Buishand's using Xlstat software. These tests and the calculation of rainfall indices reveal an alternation of wet and dry episodes with very high rainfall excesses. Spatial interpolation of rainfall was conducted on an annual, monthly, and seasonal basis by three methods: Theissen polygon, Spline, and ordinary Kriging. The predicted mean precipitation of the Medjerda High Valley was used for the hydrological study. Thus, the variation of the contributions, their relation with the rainfall and their importance to the basin were studied via the hydrological model GR2m. The flow and, consequently, the water resources constitute the hydrological response of the watershed to the rainfall impulses.

Keywords

Spatial and temporal variability • Mean rainfall • Statistical analysis • Hydrological behavior • Medjerda high valley

1 Introduction

The phenomenon of climate change is now a reality because of its impact in many domains of our life. The important task of an expert today is to call the attention of the humanity on the management of the natural resources that are subjected to disappearing, important reduction or loss in their quality. The influence of the spatial variability of rainfall on hydrological rain-flow modeling is an active research topic, as evidenced by the abundant literature published in recent years [1]. The proper understanding of rainfall pattern and its trends may help water resources development to take decisions for the developmental activities of that region [2].

The bioclimate of Tunisia varied from sub-humid (North) to Saharian (South). The precipitations, in the North of Tunisia, are very variable in time and space. The high valley of Medjerda belongs to this category where the flooding is very frequent given the relief, the climate, the river morphology, the land cover, etc.

The quantification of the various components of hydrological processes in a watershed remains a challenging topic as the hydrological system is altered by internal and external drivers. Watershed models have become essential tools to understand the behavior of a catchment under dynamic processes.

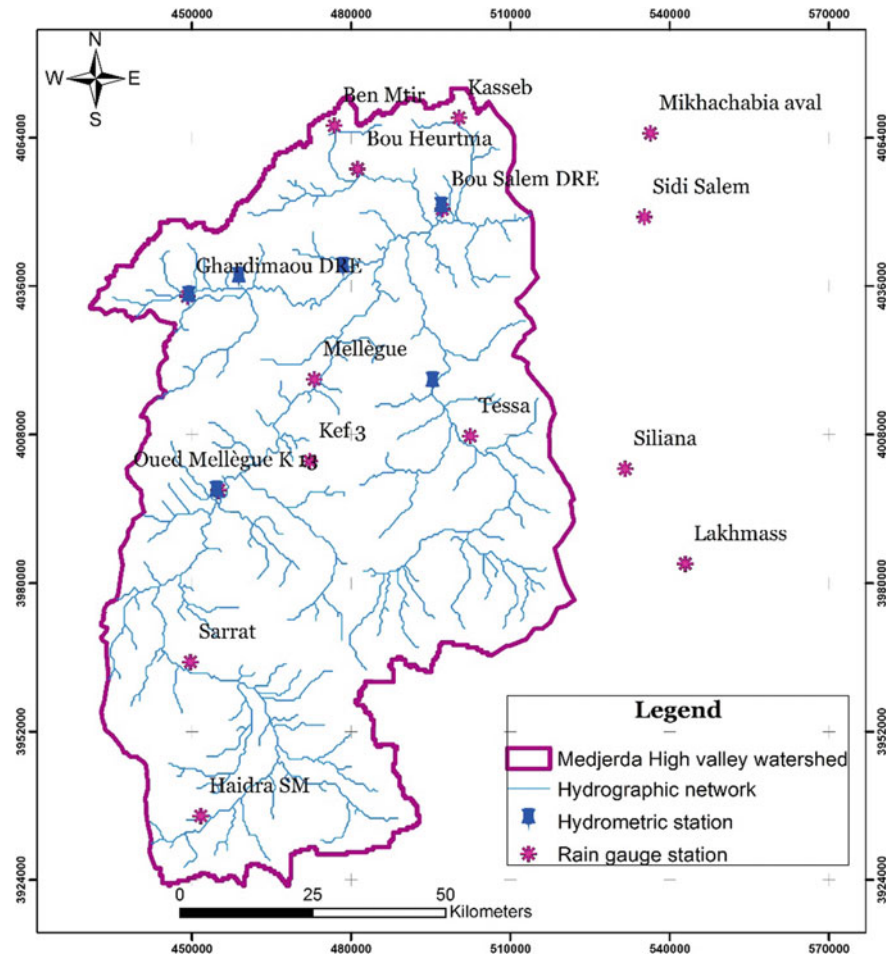
In this context, our work aims to characterize the spatial and temporal variability of rainfall and to understand the interactions between rainfall spatial and temporal resolutions, variability of catchment properties and their representation in hydrological models. To achieve this objective, we selected a simple rainfall-runoff conceptual model; GR2m. The hydro-metric collected datasets refer to Bousalem station from 1980 to 2013. The evaporation data are issued from the research of Mustapha [3]. The annual flow variation is irregular. During the period 1980 to 1983, there is an increasing of flows from 170 to 254 m³/s. The period from 2002 to 2004 is marked by three peaks, the most important is that of the 2002/2003 hydrological year (702 m³/s).

S. Abidi (✉)
Silvo-Pastoral Institute of Tabarka, 8110 Tabarka, Tunisia
e-mail: saharabidi01@gmail.com

O. Hajji · B. Hannachi
Higher School of Engineers of Medjez El Bej-Tunisia,
9070 Beja, Tunisia

H. Habaieb
Agronomy National Institute of Tunisia, 1082 Tunis, Tunisia

Fig. 1 Map location of the studied area



2 Materials and Methods

The watershed of the high valley of the Medjerda River, is located in the North-east of Tunisia. It belongs to the Tunisian High Tell. Its climate is semi-arid and it covers approximately a surface of 9238 km². It is a lengthened basin with high relief (Fig. 1).

Daily, monthly and annual rainfall data are used to investigate the spatial rainfall variability in the Medjerda High Valley. These data are derived from the observation network of 16 meteorological stations of the studied area.

Analysis of the 35-year [4] and 16-station rainfall data showed missing rainfall values that were filled by the weighted average method. The homogeneity test detected some breaks in the monthly, seasonal and annual scales. Rainfall indices were calculated to determine the dry and wet periods of the study area. Two criteria were used for different spatial interpolation methods (Theissen polygon, Ordinary Kriging and Spline). The hydrological behavior analysis was assessed by applying the GR2M model. The hydrometric collected datasets refer to Bousalem station from 1980 to 2013.

3 Results

3.1 Mean Rainfall Variation

The spatial interpolation of rainfall indicates a remarkable variability in mean rainfall with the three methods (Theissen polygon, Ordinary Kriging and Spline) (Fig. 2).

After the determination of rainfall averages by spatial interpolation using the three methods; Theissen, Ordinary Kriging and Spline, the results were evaluated using two criteria: square root of Root Mean Square Error and Mean Absolute Percent Error. It was concluded that the kriging method is the most suitable for calculating the spatial mean of rainfall. We then go on to study the hydrological regime of the upper Medjerda Valley.

3.2 Hydrologic Response Modeling

The calibration of the model is obtained with the Nash coefficient of 60%. The parameter value X1, which represents the capacity of the production tank, is 5.19.

Fig. 2 Rainfall spatial interpolation by Thiessen polygon and ordinary Kriging in annual scale

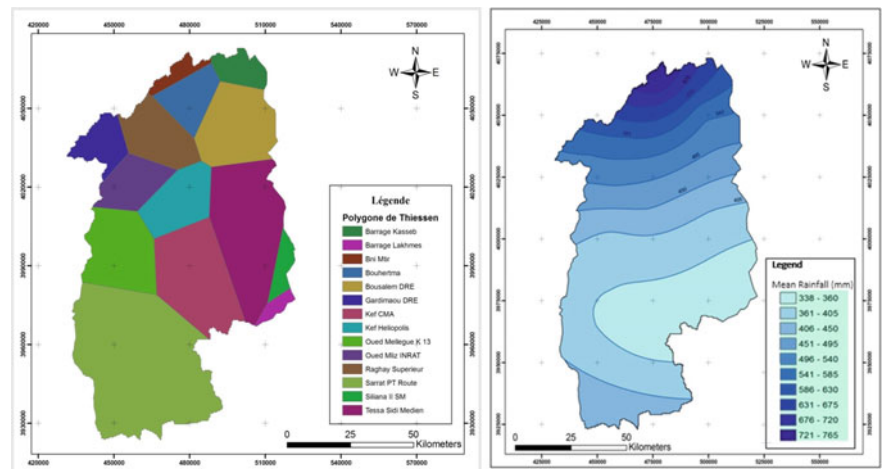
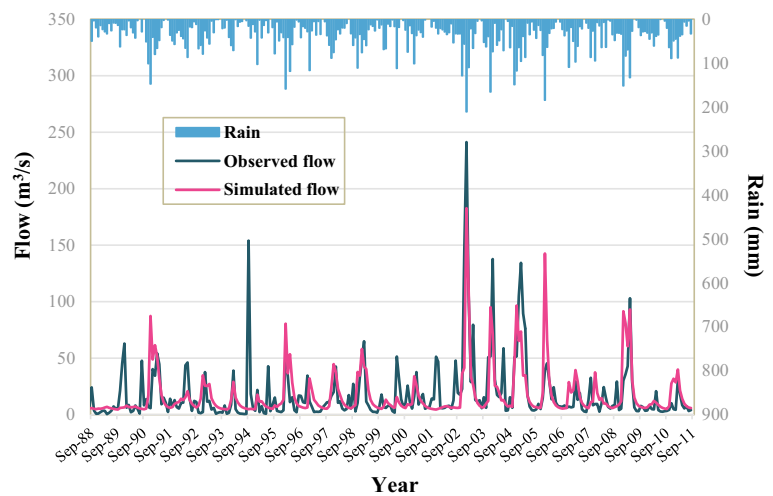


Fig. 3 Rain-flow relationship of the model simulation GR2m for the period 1984/1988



For parameter X2, a value greater than 1 represents a water gain for the basin while a value less than 1 corresponds to a loss of water. For the watershed of the Medjerda High Valley, X2 is equal to 1.38. For the validation of the model, the computation is launched by taking optimized parameters X1 and X2 during the calibration process for the period from 1988 to 2011 with a Nash coefficient of 74%. The application of the GR2M model gave satisfactory results, as optimization of the calibration parameters was obtained for Nash values above 50%. The analysis of the numerical results, namely the correlation coefficients for the monthly time steps, showed that the computed water slides have a good agreement with the water slides observed.

Thus, the graphical results of the simulated flow rates are similar to those of the observed flow rates, and for the entire basin studied. The simulation quality of the GR2M model is good. Finally, the extension of the input series, using the same calibration parameters optimized for each basin, enabled us to generate series of water inputs from the observed rainfall data (Fig. 3).

4 Discussion

The average interannual inputs oscillate from one year to another with a minimum of 165 mm³/year (1988/1989) after a rainy year of 348 mm. For an average annual rainfall of 762 mm, the maximum is 2064 mm³/year (2002/2003). The inflow peaks corresponded to large floods that took place in the catchment area of Medjerda, especially in the region of Bousalem which is located at the outlet of the high valley of the Medjerda river.

5 Conclusions

The stream flows, therefore the water resources, constitute the hydrologic response of the watersheds after the rainfall impulses. Following the hydrological study of the watershed, it is noted that the variability of inputs is strongly associated with the succession of dry and wet periods

observed over three decades. The generated water inputs can be exploited for a better water management for the upper valley watershed.

References

1. Segond, M.-L., Wheeler, H. S., Onof, C.: The significance of spatial rainfall representation for flood runoff estimation: a numerical evaluation based on the Lee catchment, UK. *J. Hydrol.* **347**, 116–131 (2007)
2. Priyan K.: Spatial and temporal variability of rainfall in Anand District of Gujarat State. *INTERNATIONAL CONFERENCE ON WATER RESOURCES, COASTAL AND OCEAN ENGINEERING (ICWRCOE'15)*, **4**, 713–720 (2015)
3. Mustapha, M.: Etude de l'évapotranspiration dans le bassin versant de Medjerda (en Tunisie): Apport de la télédétection satellitaire et des Systèmes d'Information Géographique. Thèse de Doctorat, Université de Rennes 37–39 (2015)
4. DGRE.: Hydrometric data base of Medjerda, General Direction of Water Resources of Tunisia (2016)

Information Gain in Rainfall-Runoff Modeling (Tunisia)

Aymen Ben Jaafar and Zoubeida Bargaoui

Abstract

Rainfall runoff conceptual models are used mainly to help make decisions in surface water resources and water quality management. The model calibration is an important step in selecting suitable sets of parameters. The model validation helps to demonstrate the model performance outside the calibration period, in extrapolation. Often, the calibration/validation of the model are carried out using the Generalized Split Sample Test (GSST) method. It is proposed to depict the validation analysis in view of the information gain between observed rainfall (mm day^{-1}) and runoff (mm day^{-1}). For illustration, we adopt the bucket bottom hole (BBH) model with a daily step. The model is lumped. The calibration is achieved by accepting the sets of parameters (solutions) that guarantee a relative error $<20\%$. In addition, a Nash-Sutcliffe coefficient (NSH) condition is established with $\text{NSH} > 0.75$. The evaluation of model performance in validation is based on NSH criterion at the monthly and decadal scales. The case study is the basin of the Sejnane River (376 km^2) now controlled by a dam in northern Tunisia. It is found that the period with the highest information gain between rainfall and runoff observations constitutes a good “receiver” which means a good ability to reproduce runoff data regardless of the calibration period.

Keywords

Rainfall • Runoff • NSH • Information gain • GSST

1 Introduction

The GSST method is a way to test the model in different climatic conditions, especially those in conditions non-similar to calibration periods. In previous works, the results of GSST approaches were examined considering the rainfall surplus or deficit of the validation period as well as its air temperature deviation about the mean in comparison to the calibration period [3, 5]. Here, it is proposed to depict the analysis with respect to the information gain between observed rainfall (mm day^{-1}) and runoff (mm day^{-1}) during the evaluated sub-period. In other words, the GSST test results are discussed in the light of the information gain to see whether errors in simulated runoff are correlated to the information gain of the validation period.

2 Methodology

2.1 The Hydrological Model

The model was first proposed by Kobayashi et al. [7] and modified by Bargaoui and Houcine [1]. Four parameters are estimated from the soil and basin occupation maps, i.e. soil porosity (p), soil saturation conductivity (K_s), soil retention curve parameter (B), and soil field capacity (S_{fc}). Pedo-transfer functions proposed by Saxton et al. [9] and Cosby et al. [4] are used to estimate these parameters. The three parameters are soil depth (D), resistance of vegetation to evapotranspiration (σ) and control of runoff genesis (η) and are estimated using calibration of runoff data.

2.2 Calibration Criteria

The observation period is subdivided into sub-periods of equal lengths. Every sub-period is calibrated separately. Two calibration criteria are adopted with constraints:

A. Ben Jaafar (✉) · Z. Bargaoui
Laboratoire de Modélisation en Hydraulique et Environnement,
Université Tunis El Manar, ENIT, BP 37, 1002 Tunis, Tunisia
e-mail: ayymmeeeen@hotmail.com

Z. Bargaoui
e-mail: zoubeida.bargaoui@laposte.net

- The runoff absolute relative error (AARE): $AARE < 0.2$ (Moriassi et al. [8])

$$AARE = \frac{1}{n} \sum_{j=1}^n \left| \frac{y_{jsim} - y_{jobs}}{y_{jobs}} \right| \quad (1)$$

- The runoff Nash criteria (NSH): $NSH > 0.75$ ensuring very good performance after (Moriassi et al. [8])

$$NSH = 1 - \frac{\sum_{j=1}^n (y_{jsim} - y_{jobs})^2}{\sum_{j=1}^n (y_{jobs} - y_{obsm})^2} \quad (2)$$

with n : the number of days, y_{jsim} : the daily runoff simulated for day $j = 1, n$ of the calibration period, y_{jobs} : the daily runoff observed for day $j = 1, n$ of the calibration period and y_{obsm} : the mean daily runoff observed for day j of the calibration period.

Thirty values are tested for the parameter D (from 50 to 1500 mm with a step of 50 mm). For σ , all values between 0 and 2.5 are tested with a step of 0.01 and for η all values between 0 and 1 are tested with a step of 0.01 [7]. The calibrated parameters (D , σ , η) are further adopted to simulate the model for all remaining sub-periods for model validation.

2.3 Information Gain

The information gain (IG) $I(X, Y)$ measures how much (on average) the realization of a variable X tells us about the

realization of a variable Y . It measures how much the entropy of Y (information content of Y) is reduced if we know X . Here X is the rainfall series and Y is the runoff series. $I(X, Y)$ is defined as follows Gray [6]:

$$I(X, Y) = H(X) + H(Y) - H(X, Y) \quad (3)$$

with $H(X)$ and $H(Y)$: the statistical entropy linked to, respectively, the series of rainfall and runoff, and $H(X, Y)$: the joint entropy linked to the series of rainfall and runoff. $H(X)$, $H(Y)$ and $H(X, Y)$ are obtained with non-parametric estimators.

3 Results

3.1 Data of the Case Study

The case study is the basin of the Sejnane River (376 km²). We consider a period of 15 hydrological years (1961–1962 to 1973–1975), and thirteen overlapping periods of 3 years are tested (Table 1). Data are kindly obtained from the national hydrological office (DGRE). Data are analyzed by hydrological year (i.e. from 1/9 to 31/8). Rainfall data are the average basin rainfall estimated using several rain gauges inside the basin. Runoff data are obtained using river level observations as well as up-dated rating curves (linking water levels to discharges). Sub-periods are taken with 3 years length. The rainfall interannual variability is between 1.95 and 2.77 mm day⁻¹ depending on the sub-period. As well, runoff is fluctuating between 0.5 and 0.88 mm day⁻¹ (Table 1). Two sub-periods 1972–1974 and 1973–1975 present the highest mean IG (Table 1).

Table 1 Mean rainfall and runoff per sub-period with mean information gain

Sub-period	Mean rainfall (mm day ⁻¹)	Mean runoff (mm day ⁻¹)	Mean information gain (bits)
1961–1963	2.61	0.63	144
1962–1964	2.77	0.87	142
1963–1965	2.56	0.65	144
1964–1966	2.50	0.75	145
1965–1967	2.12	0.50	148
1966–1968	1.95	0.51	149
1967–1969	2.15	0.52	146
1968–1970	2.54	0.77	144
1969–1971	2.61	0.77	145
1970–1972	2.53	0.88	148
1971–1973	2.17	0.65	151
1972–1974	2.24	0.73	153
1973–1975	2.12	0.60	153

Fig. 1 Scatter plot of respectively D (a), σ (b) and η (c) versus the NSH for each calibration period

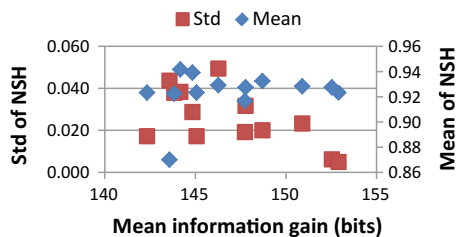
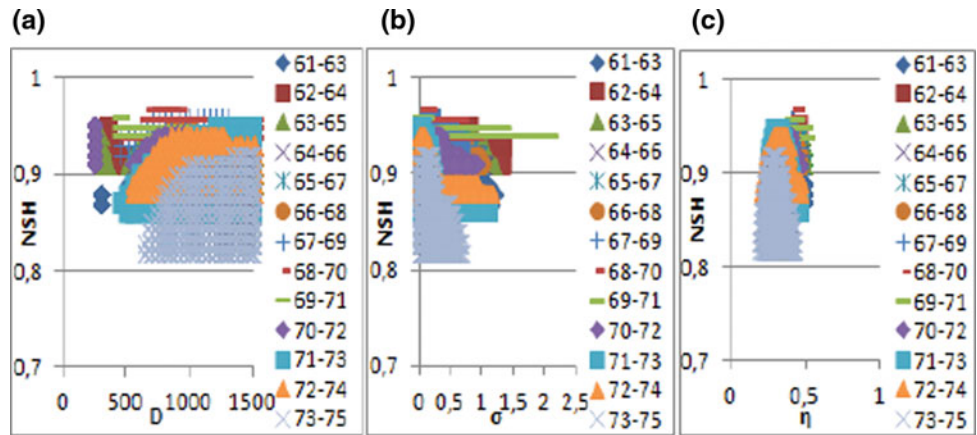


Fig. 2 Mean NSH and standard deviation of NSH versus the mean information gain by validation sub-period

3.2 Calibration Results

The equifinality [2] is observed for all the calibration periods. Figure 1 illustrates the scatter plots of calibrated D (a), σ (b) and η (c) versus the NSH for each calibration period. These solutions fulfill the conditions $AARE > 0.2$ and $NSH > 0.75$. It is seen that the parameter η is the less sensitive while D and σ are the most sensitive.

3.3 Validation Results

Figure 2 reports, per validation period, the mean and standard deviation (Std) of the NSHs. A high mean value indicates a very good performance in validation. Indeed, a low standard deviation implies high robustness towards the calibration period. It is assumed as a signature of a good receiver period.

It can be seen from Fig. 2 that the two periods with the highest mean information gain display the lowest Std(NSH) with a very good score with respect to the mean. Thus, they

exhibit the best compromise between precision and robustness.

4 Final Remarks

The final remarks that may be drawn from this study are; information gain may explain the successfulness of the transfer of the calibrated parameters from period to period. Some periods are objectively better recipients than others because they display high information gain between rainfall and runoff. As an outlook for this study, we intend to investigate other basins to validate our conclusions and to analyze the climatic and hydrological conditions behind the sub-periods with the highest information gain.

References

1. Bargaoui, Z., Houcine, A.: Sensitivity to calibration data of simulated soil moisture related drought indices. *Revue Sécheresse*. **21**(4), 1–7 (2010)
2. Beven, K.J.: A manifesto for the equifinality thesis. *J. Hydrol.* **320**, 18–36 (2006)
3. Coron, L., Andréassian, V., Perrin, C., Lerat, J., Vaze, J., Bourqui, M., Hendrickx, F.: Crash testing hydrological models in contrasted climate conditions: an experiment on 216 Australian basins. *Water Resour. Res.* **48**(5), 17p (2012)
4. Cosby, B.J., Hornberger, G.M., Clapp, R.B., Ginn, T.R.: A statistical exploration of the relationships of soil moisture characteristics to the physical properties of soils. *Water Resour. Res.* **20** (6), 682–690 (1984)
5. Dakhlaoui, H., Ruelland, D., Trambly, Y., Bargaoui, Z.: Evaluating the robustness of conceptual rainfall-runoff model under climate variability in northern Tunisia. *J. Hydrol.* **550**, 201–217 (2017)

6. Gray, R.M.: Entropy and Information Theory First Edition, Corrected. Springer, New York (2013). <https://ee.stanford.edu/~gray/it.pdf>
7. Kobayashi, T., Matsuda, S., Nagai, H., Tesima, J.: A bucket with a bottom hole (BBH) model of soil hydrology. 5p. IAHS Publ. No. 270 (2001)
8. Moriasi, D.N., Arnold, J.G., Van Liew, M.W., Bingner, R.L., Harmel, R.D., Veith, T.L.: Model evaluation guidelines for systematic quantification of accuracy in watershed simulations. *Trans. Am. Soc. Agric. Biol. Eng.* **50**(3), 885–900 (2007)
9. Saxton, K.E., Rawls, W.J., Romberger, J.S., Papendick, R.I.: Estimating generalized soil-water characteristics from texture. *Soil Soc. Am. J.* **50**, 1031–1036 (1986)

Hydrogeological System of Sebaou River Watershed (Northern Central Algeria): An Assessment of Rainfall-Runoff Relationship

Bilel Zerouali, Mohamed Mesbah, Mohamed Chettih, Mohammed Djemai, and Zaki Abda

Abstract

In this paper, the time and frequency-based methods as cross wavelet (XWT) and wavelet coherence transform (WCT) are used to search the links between rainfall and runoff of the hydrogeological systems of the Sebaou river watershed (northern central Algeria). The analysis shows a discontinuity in the linearity between rainfall and discharge that could correspond to the dry periods, storage during floods and the capacitance of the aquifer to store reserves, with the exception of some significant amplifications in some time intervals. Furthermore, human activities such as the dam construction and the smuggling of sands and rocks of the Oued (Wadi) since the year 1998 have had a significant impact on rainfall-runoff relationship, the flows decrease and the changes in the flow regime, which is more pronounced with a rupture in the annual component of 256–512 day of WCT spectrum.

Keywords

Cross wavelet • Hydrogeological • Rainfall and runoff • Human activities • Algeria

B. Zerouali (✉) · M. Chettih · Z. Abda
Research Laboratory of Water Resources, Soil and Environment,
Department of Civil Engineering, Faculty of Civil Engineering
and Architecture, Amar Telidji University, P. O. Box 37.G 03000
Laghouat, Algeria
e-mail: b.zerouali@lagh-univ.dz

M. Mesbah
LGBO Laboratory, Earth Sciences Faculty, University of Science
and Technology Houari Boumediene, BP 32, 16311 Bab Ezzouar,
Algeria

M. Djemai
Laboratory of Geomaterials, Environment and Development,
Department of Civil Engineering, Mouloud Mammeri University,
BP n°10 .RP, Hasnaoua, Tizi-Ouzou, Algeria

1 Introduction

Groundwater resources are affected by several factors such as: (1) the geological parameters (the influence of the lithology), climate change, decreasing precipitation, and rising temperatures, favouring evaporation and evapotranspiration of surface water and vegetation cover could result in lower infiltration processes of rainwater. This infiltration plays a fundamental role in groundwater recharge [1]. (2) Anthropogenic changes such as population pressure, construction and management of reservoirs and dams, the illegal logging by smuggling sand from wadis and rivers, and the huge current use of water aquifers for agriculture and industry with the installation of advanced pumping equipment, which rapidly draws the aquifer's storage, seem to be the important factors causing the significant decrease of annual flow and regulatory reserves.

The assessment of the impacts of climate and anthropogenic modifications on water resources is a major challenge, requiring a good knowledge of the external environment and hydrogeological karst structure. Knowing this deep structure is the challenge of current research, because it allows to give, or not, the green light to exploit an aquifer [2]. In this work, we applied XWT and WCT to assess the relationship between daily rainfall and discharge series by focusing on the anthropogenic modifications on the Sebaou river watershed system (northern central Algeria).

2 Materials and Methods

2.1 Study Area and Database

The watershed of the Sebaou river, located between latitudes North 36°30 and 37°00 and longitudes East 03°30 and 04°30, is representative of the Algerian Mediterranean watersheds. It extends over an area of 2500 km². In this study, the daily

rainfall and discharge series are obtained from the National Agency of Water Resources [3] of Algeria.

2.2 Cross Wavelet (XWT) and Wavelet Coherence Transform (WCT)

XWT has been developed to compare two time series in order to evaluate the similarities between them and to identify the degree of correlation through a cross-spectrum. WCT is one of the best approaches to identify the degree of correlation between two time series in the space-time frequency, where the two signals are covariant, but do not necessarily have a common high power for a spectral band selected [4].

3 Results

3.1 Rainfall-Runoff Analysis Using XWT and WCT

The spectrum XWT between daily rainfall and discharge series (Fig. 1a) do not highlight the seasonal components, except for a few isolated events temporally constituting singularities. At the annual scale, in the spectral band 256–512 days, as well as at the multiannual scale (higher than 512 day), the XWT spectra have a rather continuous component in time with strong coefficients (Fig. 1a), except for some discontinuities more marked between the years 1985 and 1995, corresponding to the dry period. This dry period has also been observed at the scale of Algeria and the Mediterranean region [5, 6].

At small scales, the WCT (Photo 1) shows scattered structures which are visible due to consecutive passages of floods. At the annual scale, the spectral band of 256–512 days indicate the most significant coherence between rainfall and

flow (Fig. 1b), but it exists in a discontinuous manner, the example of the changes in the flow regime explained by the rupture in the annual component at Oued Aissi catchment between 1998 and 2002, which has been interpreted by the construction of the Taksebt Dam. A strong coherence is also well-manifested (Photo 1) at a multiannual scale higher than 1024 days. Therefore, two main modes have been identified in the system: the wet mode with linear behaviour which probably corresponds to the annual component, and the dry mode with nonlinear behaviour which probably corresponds to the dry period and human activities [7].

In this part, the components of 2 and 4 weeks were chosen for the short-term processes. For the medium term, we chose the 26-week component and we also isolated the annual component of 52 weeks. Finally, for the long term, the 102-week component was isolated and studied using the wavelet coherence concept: the real part of the square of the wavelet coherence (Fig. 1c, d) and the phase of the coherence. For the short-term components of 2–26 weeks, there is a very poor coherence, because the real part of the coherence is very low, while the phase is different from zero, which confirms the non-linearity of the rainfall-runoff relationship (Fig. 1c, d). For the long-term component of 52–102 weeks, there is a strong coherence, because the real part of the coherence is somewhat strong, while the phase is close to zero. This confirms the quasi-linearity of the rainfall-runoff relationship for some time interval. The highest values of coherence correspond to consecutive passages of floods and rainfall.

3.2 Impacts of Human Activities

Based on several field investigations, the rainfall-runoff relationship is more influenced by illegal logging and smuggling of sand from the Wadi of the region (Photo 1). There is formation of large man-made holes on the

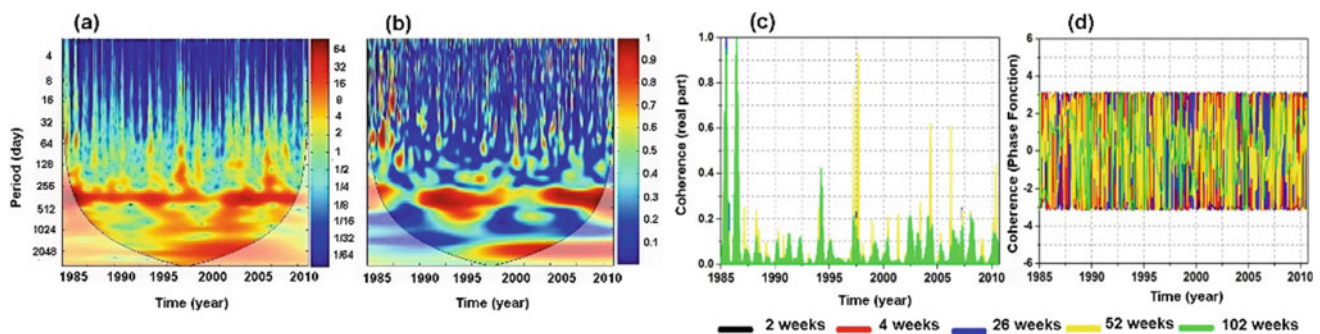


Fig. 1 a Cross wavelet spectra (XWT), b Wavelet coherence spectra (WCT) (cone of influence (COI) in which edge effects cannot be ignored), c coherence real part spectrum and d phase function spectrum

between daily rainfall and rainfall at Oued Aissi catchment for the different isolations' components of short, medium and long-term process



Photo 1 Anthropogenic (human) modifications in Oued Sebaou maritime (controlled by Baghlia station) (photos taken during a news coverage of the Algerian Television—KBC TV, web link: <https://www.youtube.com/watch?v=6EpzK1WYqtw>)

riverbanks, which modifies the nature of the minor and major bed, which influences the system flow regime and prevents very high amounts of rainfall from arriving to the gauging station, and creates measurement difficulties, which disrupts the rainfall-runoff relationship. The violations have taken place in the Wadi (Oued) of some sand quarries and bulldozers have dug up the abdomen of the Wadi and removed big amounts of sand despite the decisions of the public authority to stop operations. These offenses are currently widely debated in Algeria by the public authorities and researchers [6]. The TV Channel El-Khabar (KBC TV), in its televised report in Arabic language, also represents this problematic topic on the recurrence of such events of illegal exploitations and human modifications in the Sebaou river, the report's subtitle is: "Empire of sands" (web link: <https://www.youtube.com/watch?v=6EpzK1WYqtw>).

4 Conclusions

The cross analysis by XWT and WCT shows a discontinuity in the linearity of rainfall-runoff relationship for some karst systems of the Sebaou river. This can be explained by the replenishing of reserves, dry periods and the anthropogenic modifications, with the exception of a few peaks related to floods and rainfall sequence. Some recommendations can be made to improve the management of the basin: (1) Planning and implementation of in-depth field surveys, particularly downstream of the basin established by interventions and practical strategies for the management and control of stream-flows (water protection, protection against floods,

protection of sand and gravel against smuggling and fraud, protection of aquatic ecosystems...). (2) Publication of serious statements and decisions for limiting illegal harvesting of sediments, gravel and river rocks, and coordinating actions with other relevant fields such as land use planning, for energy and agriculture in particular. (3) Suggesting long-term rational and sustainable management solutions for wadis' development (construction of small hydraulic structures for irrigation and surface water resources mobilization...).

References

1. ONEMA Homepage: <http://www.onema.fr/eaux-souterraines-comment-suivre-les-consequences-du-changement-climatique-0>. Accessed 12 Feb 2018
2. Dörfliger, N.: Une gestion active des systèmes karstiques, pourquoi? Exemples et perspectives. CFH - Colloque Hydrogéologie et karst au travers des travaux de Michel Lepiller 17 mai (2008)
3. ANRH: The National Agency of Water Resources (ANRH) of Algeria (2013)
4. Grinsted, A., Moore, J.C., Jevrejeva, S.: Application of the cross wavelet transform and wavelet coherence to geophysical time series. *Nonlinear Process. Geophys.* **11**, 561–566 (2004)
5. Hertig, E., Trambly, Y.: Regional downscaling of Mediterranean droughts under past and future climatic conditions. *Glob. Planet. Chang.* **151**, 36–48 (2017)
6. Nouaceur, Z., Laignel, B., Turki, I.: Changements climatiques au Maghreb: vers des conditions plus humides et plus chaudes sur le littoral Algérien? *Physio-Géo. Géographie, physique, et environnement* **7**, 307–323 (2013)
7. Chinarro, D., Villarroel, J., Cuchí, J.: Wavelet analysis of fuenmayor karst spring, San Julián de Banzo, Huesca, Spain. *Environ. Earth Sci.* **65**(8), 2231–2243 (2012)

New Use of Hydrograph Separation Method for Hydrological Process Identification

Asma Dahak and Hamouda Boutaghane

Abstract

This study is a new application of the recession curve analysis with a new non-subjective method. Its objective is to construct master recession curves generated by placing, horizontally, the vertex of individual recession segments of the most suitable connection line defined by measurement points of a preceding recession segment. This proposed methodology was applied for a rural catchment with a low urban contribution, namely Madjez Ressoul, which is located in the Ain Berda region in Algeria. The results of separation always give an appropriate R^2 coefficient; they confirm the ability to calculate the recession curve coefficient k of the three processes (surface flow, subsurface flow and baseflow).

Keywords

Recession curve analysis • Hydrograph separation method • Master recession curve • Trigonometry method

1 Introduction

For a long time, the hydrological modeling has mainly been used to analyze the system behavior with physical representations of the real world. Actually, it is impossible to give a perfect representation of this real world without identifying all hydrological processes. One of the widely used techniques, which fits this objective, is to separate effective precipitation from base flow. The questions raised in this paper are: why do we need to separate base flow from precipitation? And which technique is the most recommended? [1] Asserted that the recession curve can be formed by two

(surface flow, base flow), or three (surface flow, subsurface flow, base flow) components, and taking into consideration the catchment and flood characteristics, this study is strongly aimed to select the processes contributing to a flood event by the hydrograph analysis techniques, seeing that this method had a quick development and very advanced theories.

2 Methods

The recognized function (see Eqs. (1) and (2)) of the recession curve analysis is the exponential demonstration given firstly by [1–4]. It explains that hydrographic recession modeling characterizes catchment aquifers by a quantitative parameter (K_i), that describes: water, soil, and river system as a function of storage in the natural reservoir.

$$Q_t = Q_0 \cdot K^t \quad (1)$$

$$Q_t = Q_0 \cdot e^{-\alpha t} \quad (2)$$

where: Q_t : Total discharge in the stream [m^3/s] at time T , Q_0 : Initial discharge of the recession segment, α : is recession constant. And k : is the exponential decay constant, defined as the ratio of the base flow at time t_0 : to the baseflow one day earlier. Traditionally, graphical methods have been used in hydrograph analysis, with the matching strip method, the correlating method and the tabulating method, which are typically derived from the discharge-storage relationship. These techniques are subjective procedures [5], on which the ability of each user is the key to separate processes.

The first step of this new recession curve analysis is to select the processing period by dividing the whole period of records into short fragments. Each one represents a continuous flood event. As a result of plotting, the discharge series produce groups of recession segments at varying durations, ordered from the highest to the lowest according to their vertex. The times of each recession segment are converted

A. Dahak (✉) · H. Boutaghane
Laboratory of Hydraulics and Hydraulic Constructions, Badji Mokhtar-Annaba University, P. O. Box 12 23000 Annaba, Algeria
e-mail: phd.dahak@gmail.com

Fig. 1 Event of 24/09/1973 to 29/05/1974 separated in two components

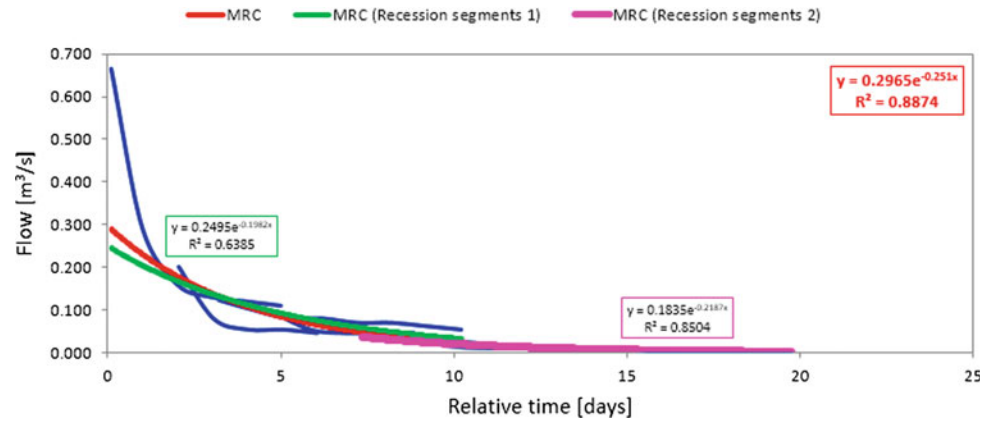
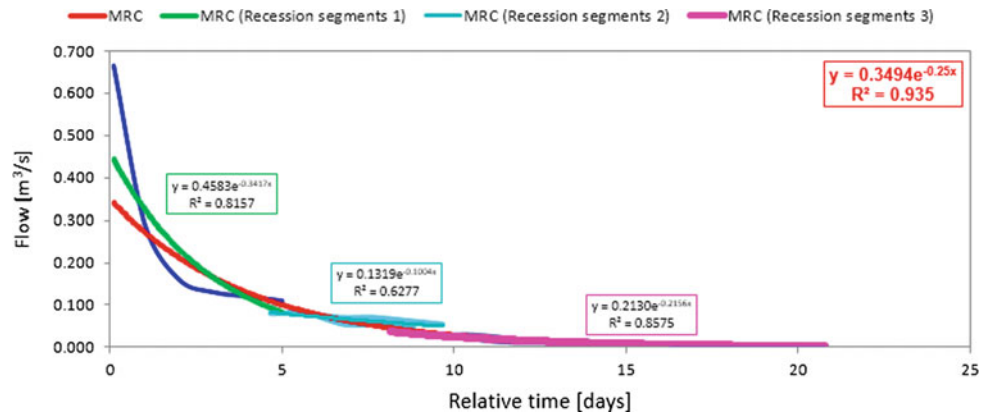


Fig. 2 Event of 24/09/1973 to 29/05/1974 separated in three components



from the absolute to the relative time beginning with zero value as the highest vertex.

The recession segments are superimposed and adjusted horizontally in an appropriate connection line given by the measurement points, until they form a single compact master recession curve MRC, interpreted with a coefficient of determination $0 < R^2 < 1$.

3 Results

Examples of this real case study from an Algerian catchment were used to test the applicability of the individual recession segments technique to separate the hydro-graph stream and identify the processes by adopting the trigonometry-based method to adjust the individual recessions. Mostly, the choice of the flood events is a subjectivity, and the overlap of the recession segments (blue lines) is done visually, but in this case the recession segments are more organized compared with other methods. The coefficient of determination R^2 is used as a best-fit selection criterion of the master recession curves MRC (red lines). The Figs. 1 and 2 down

below are two cases of separations into two (green and pink lines), or three (green, cyan and pink lines) processes.

4 Discussion

The exemplary ranges of the recession constants for the flow components, namely: surface flow $K = [0.2-0.8]$, subsurface flow $K = [0.85-0.94]$, and baseflow $k = [0.95-0.995]$ do not overlap [6]. However, high recession constants (e.g. >0.9) indicate the dominant position of the baseflow in the stream. Typical intervals of the recession coefficient k that can be replaced by the values of $e^{-\alpha}$ are organized in (Table 1).

5 Conclusions

This study is a new contribution to the modeling in Algeria. It mainly focuses on the recession curve analysis, for the purpose of identifying hydrological processes. The particular approach of separation, based on the trigonometry method, is tested on daily stream flow records between 1973

Table 1 Values of the recession coefficients

Flood event	Start	End	Two components		Three components		
			α_1	α_2	α_1	α_2	α_3
1	24/09/1973	29/05/1974	0.198	0.2187	0.341	0.100	0.215
2	23/02/1975	21/06/1975	0.126	0.1289	0.100	0.109	0.185
3	25/12/1975	17/07/1976	0.650	0.1987	0.261	0.095	0.153
4	23/10/1986	24/06/1987	0.299	0.1193	0.077	0.093	0.096
5	23/01/1992	12/02/1993	0.169	0.1274	0.299	0.093	0.031
6	01/01/1999	16/06/1999	0.213	0.0973	0.357	0.156	0.097
7	01/01/2000	23/06/2000	0.280	0.1007	0.891	0.072	0.097
8	20/01/1989	12/06/1989	0.225	0.024	0.459	0.070	0.034
9	04/11/1999	31/12/1999	0.588	0.1641	0.997	0.134	0.456
10	13/01/2001	28/05/2001	0.111	0.0434	0.41	0.051	0.044

and 2003 of an Algerian catchment. And the results confirm the ability to calculate the recession coefficient K for the three processes.

References

- Horton, R.E.: The role of infiltration in the hydrologic cycle National research council of the national academy of sciences. *Eos Trans. AGU.* **14**, 446–460 (1933)
- Boussinesq, J.: Recherches théoriques sur l'écoulement des nappes d'eau infiltrées dans le sol et sur le débit des sources. *Journal de mathématiques pures et appliquée 5e série*, tome **10**, 5–78 (1904)
- Tallaksen, L.M.: A review of baseflow recession analysis. *J Hydrol.* **165**(1–4), 349–370 (1995)
- Chapman, T.G.: Modelling stream recession flows. *Environ. Model. Softw.* **18**(8–9), 683–692 (2003)
- Sujono, J., Shikasho, S., and Hiramatsu, K.: A comparison of techniques for hydrograph recession analysis. *Hydrol Process.* **18** (3), 403–413 (2004)
- Berhail, S., Ouerdachi, L., and Boutaghane, H.: The use of the recession index as indicator for components of flow. *Energy Procedia* **18**, 741–750 (2012)

Modeling Processes of Water and Heat Regime Formation for Agricultural Region Area (Russia) Utilizing Satellite Data

Eugene Muzylev, Anatoly Zeyliger, Zoya Startseva, Elena Volkova, Eugene Vasilenko, and Olga Ermolaeva

Abstract

To assess the availability of water in a large agricultural region, the method of calculating the characteristics of water and heat regimes for vegetation seasons has been developed, using the physical-mathematical model of water and heat exchange between land surface and atmosphere (LSM, Land Surface Model), adapted to satellite data on land surface and meteorological conditions. The case study has been carried out for the part of the Central Black Earth Region (CBER) of 227,300 km², located in the European Russia, for the vegetation seasons of 2014–2016. Methods and technologies of estimating vegetation and meteorological characteristics retrieved from the measurement data of the radiometers AVHRR/NOAA, SEVIRI/Meteosat-10, and MSU-MR/Meteor-M No. 2, as well as procedures of using obtained satellite-derived estimates in the model are briefly described. The results of simulation of soil water content, evapotranspiration, and other water and heat regime characteristics for the region of interest over the above vegetation seasons are presented. The results of calculating soil surface moisture using measurement data from the scatterometer ASCAT/MetOp-B are also shown.

Keywords

Modeling • Satellite data • Soil water content • Evapotranspiration • Precipitation • Land surface temperature • Leaf area index • Vegetation cover fraction

1 Introduction

The objective of the study is to develop methods of assessing soil water content W (as an important indicator of the water availability in the agricultural region territory), evapotranspiration Ev , and other water and heat (Wt&H) regime characteristics for such regions over the vegetation season, on the basis of the physical-mathematical model of vertical Wt&H transfer in the “soil-vegetation-atmosphere” system LSM (Land Surface Model) which is suitable for using satellite-derived estimates (SDE) of vegetation and meteorological characteristics (V&MCh). The results of such investigations are especially called for arid regions with poorly developed agricultural meteorological observation network [1, 2]. Entering satellite data (SD) on V&MCh to LSM is the most important factor for the success of such modeling for similar regions [3, 4]. Satellite information is represented in the study by measurement data (MD) from scanning radiometers AVHRR/NOAA, SEVIRI/Meteosat-10, and MSU-MR/Meteor-M No. 2. Soil surface moisture (SSM) values have been estimated from scatterometer ASCAT/MetOp data. The case study has been carried out for a forest-steppe region with coordinates of 49–54 °N and 31–43 °E and an area of 227,300 km², located in the Black Earth zone of the Central Russia (CBER), including 7 districts of RF for the vegetation seasons of 2014–2016. MDs from 48 agricultural meteorological stations of the region have been used.

2 Materials and Methods

The developed LSM is designed for calculating W , Ev , vertical heat fluxes and other characteristics of Wt&H regimes, as well as the land surface (LS) temperature (LST) and the soil moisture (SM) and temperature (T) distributions over depth [3]. The basis of the LSM is the vertical soil water transfer (SWT) and heat equations for the active

E. Muzylev (✉) · Z. Startseva
Water Problem Institute of Russian Academy of Sciences,
Moscow, 119333, Russia
e-mail: muzylev@iwpr.ru

E. Volkova · E. Vasilenko
State Research Center of Space Hydrometeorology “Planeta”,
Moscow, 123242, Russia

A. Zeyliger · O. Ermolaeva
Russian State Agrarian University—MTAA, Moscow, 127550,
Russia

soil layer as well as semi-empirical formulas for calculating Ev . The LSM parameters are soil and vegetation characteristics, and the input variables are meteorological characteristics retrieved from ground observations (GO) or MD of the named sensors. Using satellite data, the estimates of the following characteristics have been obtained: precipitation Pr , three types of LST: land skin temperature T_g , air temperature at the level of the vegetation cover (taken for the vegetation temperature) T_a and efficient radiation temperature $T_{s,eff}$, as well as land surface emissivity E , normalized difference vegetation index NDVI, vegetation cover fraction B , and leaf area index LAI.

SDEs of daily, decadal and monthly sums of Pr have been obtained using the Multi Threshold Method (MTM) intended for the cloud detection and identification of its types as well as the allocation of Pr zones (PrZ) and determination of maximum Pr intensities for each pixel [5]. The values of Pr are determined from the regression equations, where MD from AVHRR (in 5 channels), SEVIRI (in 11 channels), MSU-MR (in 3 channels), and their differences are used as predictors. The accuracy of AVHRR-, SEVIRI- and MSU-MR-derived estimates of Pr has been confirmed by comparing them with each other and with ground-based (GB) data at the study region.

The estimates of LST from AVHRR and SEVIRI information have been built using previously developed methods and technologies of thematic processing measurement data obtained by these sensors [3]. Estimates of LST $T_{s,eff}$ and T_a from MSU-MR data have been obtained using the computational algorithm developed on the basis of the MTM and tested for the region of interest on AVHRR and SEVIRI data. The values of B and LAI have been determined by empirical dependencies on NDVI [3].

SSM estimates have been obtained from the MD of the scatterometer ASCAT/MetOp-B when sounding LS in the microwave range. These estimates have been converted to the top layer (0–3 cm) bulk moisture when multiplied by the porosity value.

3 Results

The assimilation of SDE of Pr , LST, LAI, and B into LSM have been made by entering them into the model, at each time step, in all nodes of the computational grid (after replacing their ground-based estimates by satellite-based ones).

The final results of the simulation are estimates of Wt&H regime characteristics of the area under study: W , Ev ,

infiltration and water fluxes in the upper 1 m soil layer and below, latent and sensible heat fluxes, as well as the three above-mentioned LST types ($T_{s,eff}$, T_a and T_g), and the SM and T distributions over depth. All simulated values are presented in the form of distributions over the area of interest. As an example, Fig. 1 shows the fields of W and their differences for the study area modeled when estimating the daily Pr sums from GB and SEVIRI- and MSU-MR-derived data for one of the dates of the vegetation season of 2016.

4 Discussion

The probability of determining PrZ from AVHRR, SEVIRI and MSU-MR data coinciding with the real ones was 75–85%. The daily and decadal Pr amounts computed from these data were in a rather good agreement with one another and with GO.

Comparison of the ground-, AVHRR-, SEVIRI- and MSU-MR-based LSTs showed that the differences between all estimates obtained for an overwhelming number of observation terms did not exceed the RMS errors of T_a , T_g and $T_{s,eff}$ estimates from AVHRR data, which were respectively, 2.3–2.7, 3.7–4.9 and 2.4–3.5 °C in the above vegetation seasons. These values can be considered as acceptable.

When the ranges of B and LAI variability constituted 0–100% and 0–10 overall, errors of their determination did not exceed 10 and 15%, respectively.

Comparisons of SSM estimates from ASCAT data with the ones simulated using GO data have shown a small difference between these estimates (about 0.05–0.10 cm³/cm³) for most of the area under study. This allows using ASCAT data in LSM when specifying the initial conditions for the vertical SMT equation as well as for calculating Ev , and then, forming the upper boundary condition for this equation.

Simulation errors of W and Ev for all variants of estimating Pr , LAI, B and LST, using all sensors for an overwhelming number of observation terms, were 10–15 and 20–25%, respectively, which corresponds to the standard accuracy of their assessment.

5 Final Remarks

The main conclusion from the obtained results is the possibility of computing, with an acceptable accuracy, spatial distributions of Ev , W and other Wt&H regime elements of a

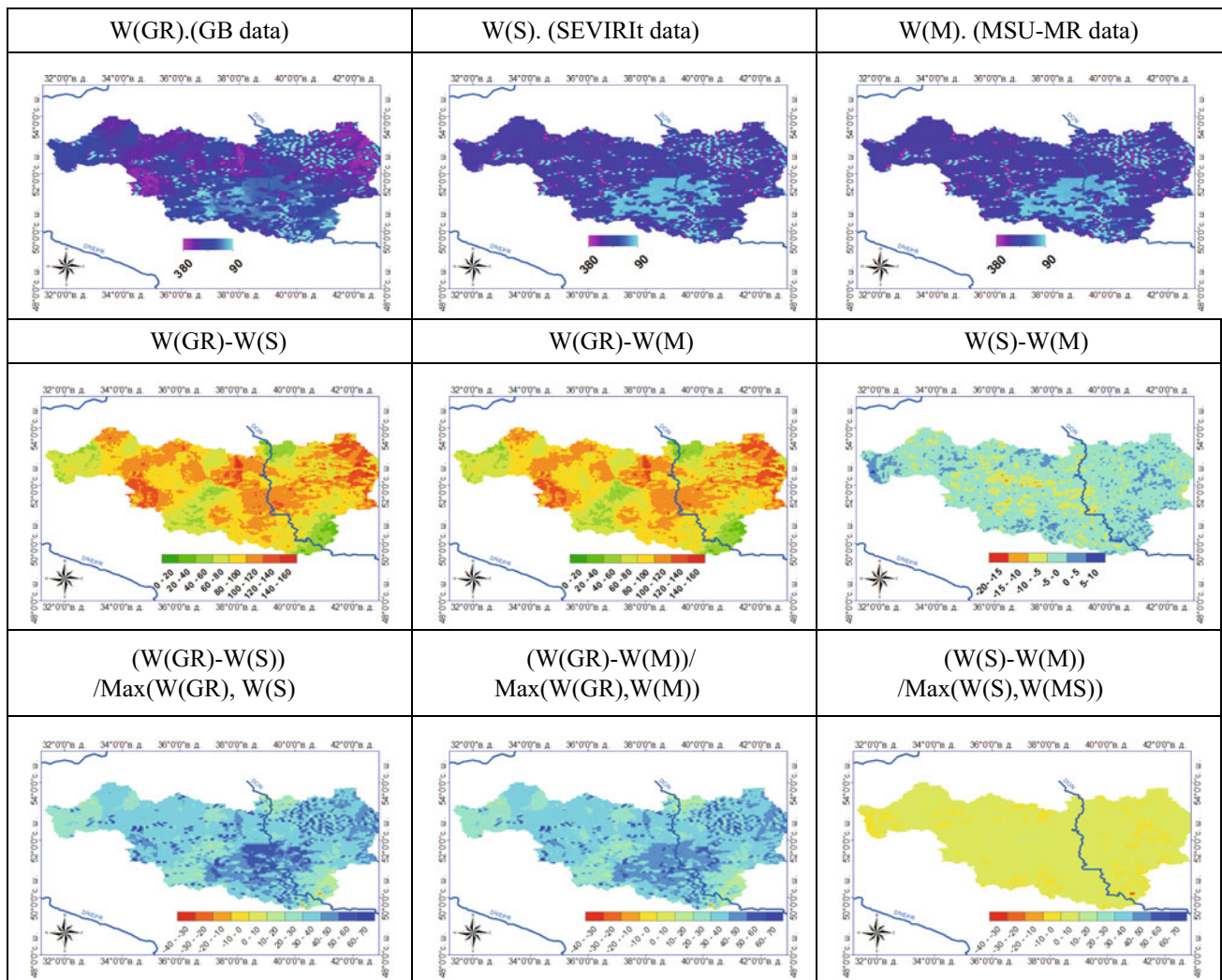


Fig. 1 Distributions over the study region area for June 18, 2016: 1st line) values of W, mm, at 1 m soil layer, modeled using a daily Pr sum: GB (W(GR)), SEVIRI- (W(S)) and MSU-MR-derived (W(M)); 2nd

line) their differences, mm, W(GR)–W(S), W(GR)–W(M), and W(S)–W(M); 3rd line) relative values of differences

vast agricultural area, by the developed model of W&H exchange between land surface and atmosphere (LSM) adapted for assimilation of SDE on V&MCh.

Acknowledgements The study was carried out within the framework of the State Programs No. AAAA-A18-118022090056-0 and No. AAAA-A18-118022290072-8 and was also supported by the Russian Foundation for Basic Research—Grant No. 16-05-01097.

References

1. Gowda, P.H., Chavez, J.L., Colaizzi, P.D., Evette, S.R., Howell, T.A., Tolk, J.A.: ET mapping for agricultural water management: present status and challenges. *Irrig. Sci.* **26**, 223–237 (2008)

2. Overgaard, J., Rosbjerg, D., Butts, M.B.: Land-surface modeling in hydrological perspective—a review. *Biogeosciences* **3**, 229–241 (2006)

3. Startseva, Z., Muzylev, E., Volkova, E., Uspensky, A., Uspensky, S.: Water and heat regimes modelling for a vast territory using remote-sensing data. *Int. J. Rem. Sens.* **35**(15), 5775–5799 (2014)

4. Chen, J.M., Chen, X., Ju, W., Geng, X.: Distributed hydrological model for mapping evapotranspiration using remote sensing inputs. *J. Hydrol.* **305**(1), 15–39 (2005)

5. Volkova, E.V.: Opredelenie summ osadkov po dannym radiometrov SEVIRI/Meteosat-9,-10 i AVHRR/NOAA dlya Evropeiskoi territorii Rossii. *Sovremennye problemy distantsionnogo zondirovaniya Zemli iz kosmosa* **11**(4), 163–177 (2014) (in Russian)

Warm Season Trends of ET_a : A Case Study of Near-North Caspian Low Lands

Olga Ermolaeva, Anatoly Zeyliger, Eugene Muzilev, and Zoya Startseva

Abstract

Actual evapotranspiration (ET_a) has a very important significance for hydrological and environmental purposes balance in arid and semi-arid areas. MOD16 product was applied to estimate seasonal ET_a trends for 2000–2009 time period, in the Pallasovsky District of Volgograd Region, South-East of the European part of Russia. The result of time series computing by Mann-Kendall test code indicated that ET_a in this study region decreased during the analyzed period. The speed value of this process gradually varies from 4.7 mm/year in the southern part with about 240 mm of annual average ET_a to 17.3 mm/year in the northern part with about 375 mm of annual average ET_a . Analysis of the seasonal spatial distribution of ET_a trend over the study region shows that it is influenced by changes of precipitation during warm seasons, and as a consequence, by land cover degradation due to farming system changes.

Keywords

Pre-North Caspian region • Evapotranspiration • Time series • Mann-Kendall test • Trend analysis • Spatial distribution

1 Introduction

Correct geanalytics of actual evapotranspiration (ET_a) data obtained by remote sensing is an important subject for numerous environmental applications, including climate

O. Ermolaeva · A. Zeyliger (✉)
Russian State Agrarian University MTA,
Timiryazevskaya str., 49, 127550 Moscow, Russia
e-mail: azeiliger@mail.ru

E. Muzilev · Z. Startseva
Water Problem Institute of Russian Academy of Sciences,
Gubkina str., 3, 119333 Moscow, Russia

changes [1], irrigation management [2], land cover change [3], etc.

In this paper, we consider the land ET_a variations in a range of a 10-year (2000–2009) period using the MOD16 product of Moderate resolution Imaging Spectroradiometer (MODIS) for the territory of the Pallasovsky District of Volgograd Region of the Russian Federation. This territory is situated in the rainfed lowlands, near the Caspian Depression, situated South-East of the European part of Russia.

The methodology used to assess the spatial distribution of ET_a trend over the study region for warm year periods (spring, summer and autumn) consists in: (1) building time series datasets for all pixels; (2) time series testing for stationary; (3) trend calculation by modified Mann-Kendall test for non-stationary time series; (4) analyzing of spatial patterns distribution. The obtained results show evidence of widespread ET_a declining linked to a precipitation rate decrease and agriculture farming changes.

2 Materials and Methods

Drylands degradation is principally manifested by the reduced biological productivity of the vegetation cover. This productivity is directly connected to ET_a , from land cover controlled by soil and vegetation parameters. In dryland environments, the multiyear changing of ET_a over a growing season is a function of vegetation water demands and water storage in root zones that depends on weather parameters like wind speed, air temperature & humidity and precipitation rate. Using a trend analysis of MOD16 time series, negative changes of ET_a can be detected and further related to negative changes of precipitation or/and land degradation.

Pallasovsky District was selected as the study region in the base of multiple information of major biodiversity disturbances, because of climatic negative variations inducing negative influence on land cover. During the last 30 years, the average temperature has increased by 2–4 °C, and the

annual precipitation has decreased by 20–40% [4]. This study region, covering an area of 12,420 km², is located in the Southeast of the European part of Russia, between the left bank of River Volga (at the distance of about 100 km) and the frontier with Kazakhstan. The spatial form of the study region territory is quite narrow, streamlined along longitude 46° 50' with distance between inmost points of about 180 km. The largest part, laying along latitude 49° 58', has a length of about 60 km. The climate of this zone varies from semi-arid to cold steppe. The mean daily temperature ranges from 25 °C in July to –5 to 7 °C in February, and the yearly average temperature is 5–8 °C. The average annual precipitation is 260 mm in the southern part and 380 mm in the northern one, with significant annual fluctuations (standard deviation is about 102 mm). Approximately, from 20 to 33 % of the total precipitation falls in the form of snow during the cold period time, while the remainder falls as rainfall throughout the rest of the year, mostly during spring and autumn.

In this study, ET_a product MOD16 (8 days temporal resolution and 1 km spatial resolution) was used, which is computed by a code based on SEBS model [5]. This model supports the spatial relationship and parameter characterizations that best describe the variations and differences in ET_a of each pixel over the land surface.

The MOD16 product tiles were cut by a mask of study region border, and after that, were used to compile the ET_a time series for each pixel of the study region area, from March to November, for the period 2000–2009. The time series of three warm seasons for all pixels over the study region were completed by summarizing ET_a in relevant time limits. A code of non-parametric, modified Mann-Kendall test was applied to estimate, in the time series, the presence of a monotonic single direction trend. The statistical significance of the trend parameters was assessed by calculating the probability of a random trend.

3 Results

The computed results of the ET_a trend were converted into maps, according to analyzed seasons. These maps show a spatial distribution of ET_a trend values (see Fig. 1). Spatial patterns presented at these maps for spring and summer seasons distinct mostly negative trends for the whole study region. For these seasons, several pixels were identified with zero trends and not a single pixel with positive trends. For autumn, negative trends are dominating in the northern part. At the same time, in the middle and southern parts, zero trends are dominating with the presence of several smaller areas with negative and positive evapotranspiration trend values.

4 Discussion

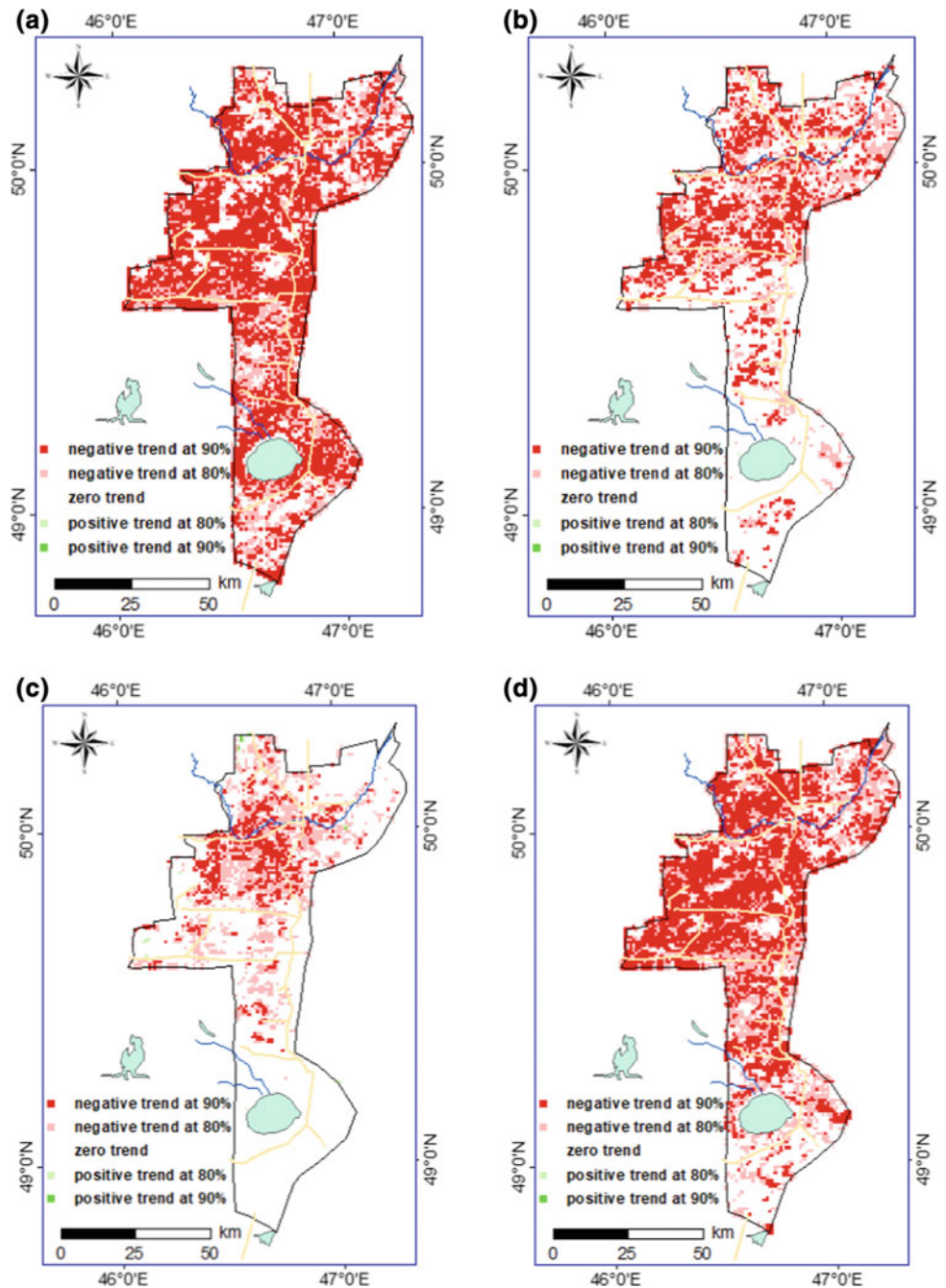
The trend analysis methodology of the time series itself has some limitations for the detection of ET_a decline [6]. Different methods applied on the same data may lead to “not similar results” [7]. The temporal aspect of a particular parameter decline is also significant. The decline occurring at the beginning or at the end of the time series was often not detected by trend analysis, while the decline beginning in the middle of the time series was typically detected [8]. Furthermore, the rate of decline affects its detectability.

Each of the three ET_a trend maps are detecting clusters of significant negative trends in the northern and middle parts during warm periods. The spatial pattern of high correlation pixels reflected locations with the strongest negative ET_a trend in the study region. The speed value of ET_a declining process gradually varies from 4.7 mm/year in the southern part, with about 240 mm of annual average ET_a, to 17.3 mm/year in the northern part, with about 375 mm of annual average ET_a. This difference was explained by additional analysis of precipitation datasets.

Depending on the year seasons, areal statistics and single season trend maps show a differentiation of the study region into two sections—first including the northern and middle parts and second including the southern part. At the first section, the spatial distribution of statistically significant negative trends has obviously not varied. At the second section, there are the same tendencies for spring and summer, but for autumn there are predominately zero trends.

At the study region, there are two meteorological stations (spaced 110 km apart) run by the Russian Hydrometeorological Centre. The first one is located in the southern part near the Elton municipality (49° 07'N, 46° 50'E) and the second one is located in the northern part near the Pallasovka municipality (50° 03'N, 46° 52'E). Datasets of precipitation measured during 2000–2009 at both meteorological stations were converted to annual averages as well as to seasonal (spring, summer and autumn) ones. The trends of these averages were analyzed by Mann-Kendall test. The value of trend of year averages for both cases was negative, but the trend declining values for the northern meteorological station were higher than the ones for the southern meteorological station. At the same time, precipitation averages of spring and summer for both cases were negative, but precipitation averages of autumn were positive with a higher trend declining value for the southern meteorological station. These results indicate a decline in effective precipitation during spring-summer and increase during autumn that has also been described in earlier regional studies [4, 7]. At the same time, results of precipitation trend analysis were used for the explanation of zero ET_a trend at the southern part of the study region during autumn.

Fig. 1 Spatial patterns of ET_a trend values over all study region territory for: **a** spring; **b** summer; **c** autumn; **d** year (from beginning of spring till end of autumn)



All of the above issues mandated caution when ET_a trends were interpreted for this study region. They should likewise do so in general applications of ET_a time series for detecting negative ET_a trends from land cover. With these considerations, it is still important to consider that trend analysis of ET_a time series is one of currently available tools to objectively monitor gradual environmental system changes through time. The obtained results also widen the scope for application of the trend analysis of ET_a time series done from remote sensing data to monitor gradual processes in a relatively small study region.

5 Conclusions

The study was focused on the Pre-North-Caspian low land located in the southeastern region of the European part of Russia. ET_a time series, derived from MOD16 for the territory of Pallasovsky District were useful in detecting negative ET_a trends, subject to some limitations. The decrease of ET_a is related to the regional climatic fluctuation as well as to the regional situation in the agricultural sector.

The dynamic behavior of ET_a from the land cover is one of the key indicators of regional assessment of environmental changes. This dynamics could be assessed at different temporal scales, like annual and seasonal.

Nowadays, remote sensing data provides a good opportunity to develop useful tools and datasets, like the spatial distributed ET_a trend required for regional environmental monitoring based on a platform of geoinformation system.

Acknowledgements Authors express their gratitude to the Russian Foundation for Basic Research for providing financial support to the project 16-05-01097.

References

- Zhang, H., Sun, J., Xiong, J.: Spatial-temporal patterns and controls of evapotranspiration across the Tibetan Plateau (2000–2012). *Adv. Meteorol.* **12** (2017). Article ID 7082606
- Yang, Y., Yang, Y., Liu, D., Nordblom, T., Wu, B., Yan, N.: Regional water balance based on remotely sensed evapotranspiration and irrigation: an assessment of the Haihe Plain, China. *Remote Sens.* **6**, 2514–2533 (2014)
- Liu, M., Tian, H., Chen, G., Ren, W., Zhang, C., Liu, J.: Effects of land-use and land-cover change on evapotranspiration and water yield in China during 1900–2000. *JAWRA J. Am. Water Resour. Assoc.* **44**, 1193–1207 (2008)
- Argaman, E., Keesstra, S., Zeiliger, A.: Monitoring the impact of surface albedo on a saline lake in SW Russia. *Land Degrad. Dev.* **23**, 398–408 (2012)
- Su, Z.: The surface energy balance system (SEBS) for estimation of turbulent heat fluxes. *Hydrol. Earth Syst. Sci.* **6**, 85–100 (2002)
- Jin, X., Guo, R., Xia, W.: Distribution of actual evapotranspiration over Qaidam Basin, an arid area in China. *Remote Sens.* **5**, 6976–6996 (2013)
- Zeiliger, A., Ermolaeva, O., Krichevtsova, A.: The results of the spatial-temporal analysis of remote sensing data sets by evaporation from the Earth's land surface MOD16 ET for 2000–2009 for the territory Pallasovsky district of the Volgograd region of the Russian Federation. In: *International Proceedings on Ekologiya. Ekonomika. Informatika*, vol. 3, pp. 35–48. Izdatelstvo Yuzhnogo Federal'nogo Universiteta, Postov-na-Donu (2015)
- Tüshaus, J., Dubovyk, O., Khamzina, A., Menz, G.: Comparison of medium spatial resolution ENVISAT-MERIS and Terra-MODIS time series for vegetation decline analysis: a case study in Central Asia. *Remote Sens.* **6**, 5238–5256 (2014)

Development of Frequency Specific Flow Maps on the Sebaou Watershed in Great Kabylia in Algeria

Hocine Hammoum, Karima Bouzelha, Mohammed Djemai, Malik Bouzelha, Lila Ben Si Said, and Mouloud Touat

Abstract

Hydrology is widely used in the design of hydraulic structures. Knowing the exact value of the specific flow of the project is a permanent preoccupation of Civil Engineers. This is why we propose in this article a set of maps giving the frequency specific flows (return periods of 10, 50, 100 years) on the Sebaou watershed in Great Kabylia (Algeria). These cards will be basic tools for design engineers to evaluate the project flow required to design a hydraulic structure such as a small dam, a sewerage network or a storm basin.

Keywords

Precipitation • Quantity of rain • Frequency specific flows • Watershed

1 Introduction

In the deterministic analysis, the hydraulic engineer uses the hydrological calculation for the flow flood assessment of the project, which is an essential parameter in the dimensioning of the hydraulic structures, such as sewerage networks, small dams, spillways and storm basins, as well as torrential correction and flood protection [1–3]. Their dimensioning is based on a given return period flood. In Algeria, we use frequencies equal to, or less than, the centennial for all hydraulic infrastructures, except for large dams that are designed for millennial or ten millennial floods. Thus, a sewerage network is calculated for a decennial precipitation frequency. A small dam is dimensioned for a return period of

twenty years or fifty years, according to its implantation site, and taking into account the risks related to the loss of human lives and material goods. As for the flood control structures (basins or storm overflows), they are designed for a return period of 50 years. This leads the design engineer to ask the following question: With which frequency specific flow should we dimension the hydraulic structure?

Several hydrological works have been carried out in Algeria and more specifically on the Sebaou watershed. Seltzer [4] drew up a rainfall map in which he defined three laws governing the distribution of rainfall in Algeria, Aissani and Laborde [5] prepared a rainfall map of northern Algeria, Medinger [6] and Samie [7] have developed the first empirical relations for estimating the flow of Algerian rivers.

The Water Resources Direction of the Tizi-Ouzou region—named DREWTO—recommends, for the design of urban water structures, taking a decennial specific flow value of about 150 l/s/ha on its territory [4]. This recommendation implies that rainfall intensities are homogeneous over this territory. Ultimately, a hydraulic structure, located in an area where the specific value is lower than that recommended by the DREWTO, would result in an over-dimensioning and consequently in an additional cost of the project. On the other hand, if the rainfall intensity is higher, it would lead to an under-dimensioning and therefore to risks on goods, and even on human lives. Sebaou watershed is poorly equipped with hydrometric stations, since only a dozen rivers are observed. On the other hand, there are 33 pluviometers distributed over the whole range of the Tizi Ouzou region. It is therefore quite logical to move towards a methodology exploiting these pluviometers. The purpose of this article is to fill this gap by proposing frequency specific flow maps of the Sebaou watershed in harmony with the hilly relief and the geographical diversity of this region. These maps will be a good tool in the hands of engineers, who will be able to dimension hydraulic structures based on the most accurate and realistic value of the frequency specific flow.

H. Hammoum (✉) · K. Bouzelha · M. Djemai · M. Bouzelha
L. Ben Si Said
Department of Civil Engineering, Mouloud Mammeri University,
15000 Tizi Ouzou, Algeria
e-mail: hammoum_hoc@yahoo.fr

M. Touat
African Geosystem Company, 16000 Algiers, Algeria

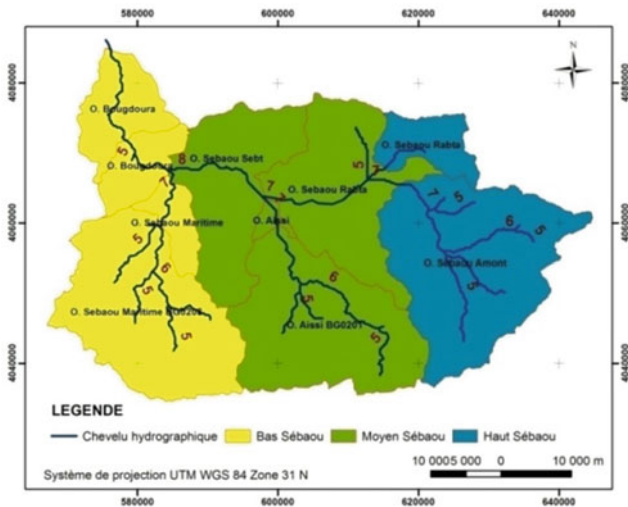


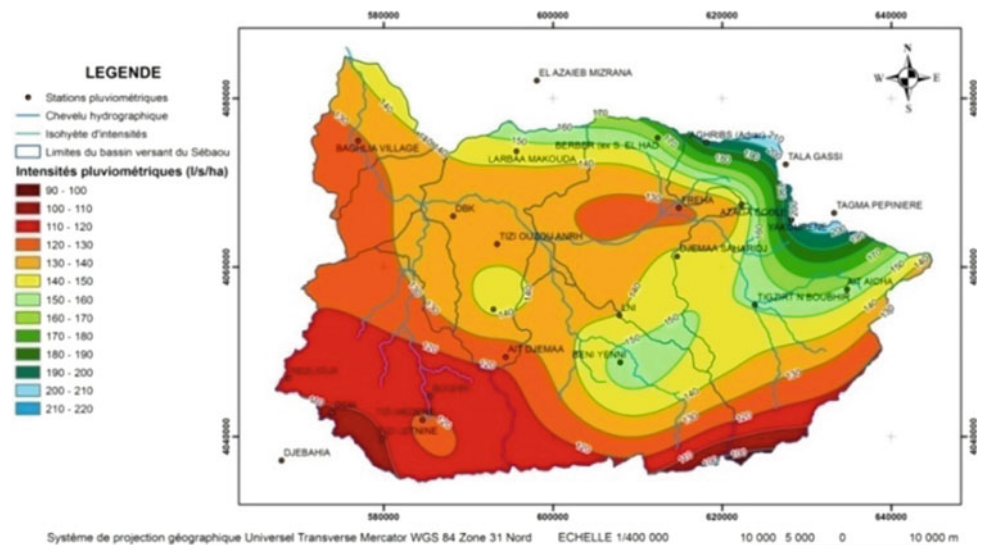
Fig. 1 Presentation of the Sebaou watershed with its three sub-basins

2 Presentation of the Study Area

The Sebaou watershed has a very extensive area of 2500 km², with a very heterogeneous relief (hills, valleys and mountains), thus causing a wide variation of the frequent rainfall intensities. This watershed is delimited in the North by the Mediterranean coastal chain, in the South by the mountain range of Djurdjura, in the East by the forests of Akfadou and Béni Ghobri, and in the West by the Sidi Ali Bounab and Bouberak mountains.

The Sebaou watershed belongs to the Algiers Soummam Hodna region, and is part of the Algiers sub-basins. It is composed of six sub-basins feeding its rivers such as Oued Sebaou upstream, Oued Rabta, Oued Aissi, Oued Sebt, Oued Bougdoura and the coastal Oued Sebaou. A Geographic Information System (GIS) was built, with the

Fig. 2 Specific flows map of decennial frequency



MapInfo© software, on topographic maps at a scale of 1/25,000°, on which the rainfall stations were implanted as georeferenced punctual objects, using the UTM projection system [8]. The Sebaou watershed can be divided into three main sub-basins, the Upper, Middle and Lower Sebaou (Fig. 1).

3 Creation of Specific Frequency Flow Maps

To develop specific frequency flows maps, we used the ArcGIS© software, which allowed us to create interactive digital maps with other programs such as Google Earth© and Global Mapper© used for the extraction of altitudes. The values of specific flows of decennial frequency (Fig. 2) vary from 130 l/s/ha at the Lower Sebaou to 150 l/s/ha at the Upper Sebaou. The minimum values (100–110 l/s/ha) are observed at the level of the Djurdjura Massif, South of the watershed.

As for the maximum values, they are observed along the Mediterranean coastal chain, at the North of the watershed, where they reach 200 l/s/ha on the heights of Aghrib. Figure 3 shows that the specific flows of a return period of 50 years vary from 150 to 170 l/s/ha from the Lower Sebaou to the Upper Sebaou. The minimum values (120–130 l/s/ha) are observed in the Djurdjura Massif. As for the maximum values, they are observed at the level of the Mediterranean coastal chain where they reach 240 l/s/ha on the heights of Aghrib.

Figure 4 shows that values of the centennial frequency specific flows vary from 160 to 220 l/s/ha from the Lower to Upper Sebaou. The minimum values of around 130 l/s/ha are observed in the Djurdjura Massif. As for the maximum values, they are observed at the level of the Mediterranean coastal chain, where they reach 260 l/s/ha on the heights of

Fig. 3 Specific flows map corresponding to a return period of 50 years

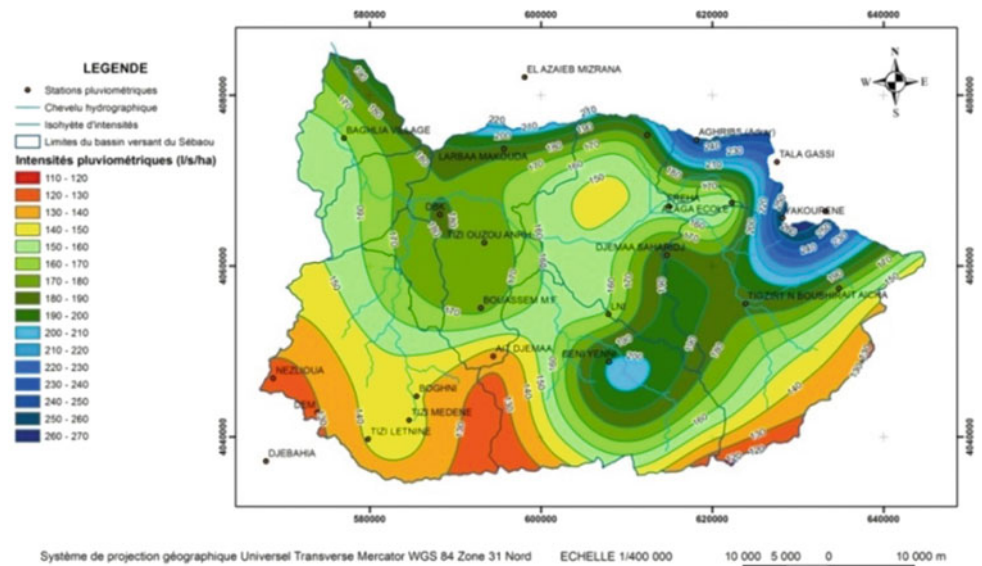
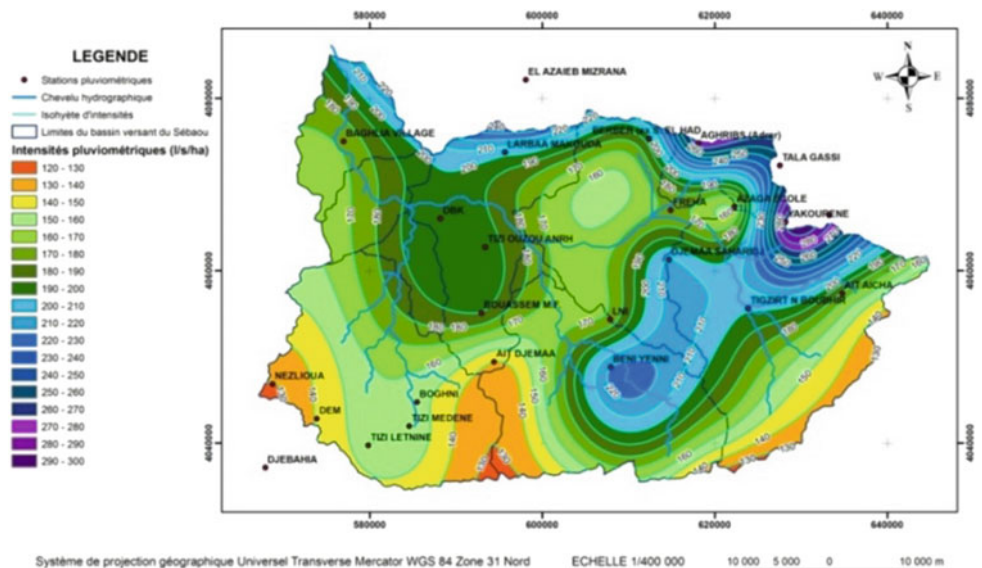


Fig. 4 Specific flows map of centennial frequency



Aghrib. The analysis of the maps reveals a clear difference between the values of the specific flow of the decennial, a return period of 50 years and the centennial frequency.

4 Conclusions

We have seen, in this study, that the accurate assessment of precipitation is a major element in management strategies. Frequency specific flow maps can be used as a decision-making tool for the design engineer, since they give the frequency flow at any point in the watershed area. The specific flows map of the decennial frequency will be useful for the dimensioning of sewerage networks, and that of the

fifty-year frequency for the design of overfalls, storm basins and small dams. We can conclude that these maps, developed in the logic of applied research, help to advance the state of knowledge of engineers working in the Great Kabylia region.

References

1. Bertrand-Krajewski, J.L.: Urban Hydrology Course, Part 2, Ed. du Seuil, Paris (1990)
2. Musy, A.: Applied Hydrology, Ed. HGA, Bucarest (1998)
3. Remeniaras, G.: The Hydrology of the Engineer. Ed. Eyrolles, Paris (1986)

4. Seltzer, P.: The Climate of Algeria. Algiers University, Algiers (1946)
5. Aissani, B., Laborde, J.P.: Rainfall Map of Northern. Project PNUD-ANRH (1993)
6. Medinger, G.: Solid transportation of Algerian oueds. An. Hydr. d'Alg. Année 1958/59. S.E.S. Alger, pp. 5–31 (1959)
7. Samie, C.: Estimation of flood flows by the formula of MM. Mallet et Gautier. An. Hydr. d'Alg. Année 1960/61. S.E.S. Algiers, pp. 5–9 (1961)
8. Hammoum, H., Bouzida, R.: Practice of GIS. Pages Bleues International, Algiers (2010)

Potentiometric Salinity Mapping of Mishrif Oilfield Waters in (Iraq's) Southern Oil Fields

Salih Awadh, Heba Al-Mimar, and Abdullah Al-yaseri

Abstract

The hydrochemistry in the Mishrif reservoir, located at the main productive oilfields at Basrah, southern Iraq, is discussed. Water chemistry coupled with boron isotopes (^{10}B , ^{11}B) were analyzed using ICP-MS and ICP-SFMS, respectively, and used to determine the subsurface fluid flow direction in the oil traps and interpret the rock-fluid interaction. The presence of boron in brine waters is useful in identifying the sources of water intrusive to oil wells. The $\delta^{11}\text{B}$ ranged between 33.7 and 35.9‰ with an average of 35.4‰ in the studied oilfields which is lower than that in the Dead Sea (39–57‰), indicating a dilution by the present seawater and injection water. The potentiometric subsurface maps were modelled and super-pressure sites that are of great importance in the oil exploration were marked to pay attention to during future drilling.

Keywords

Potential mapping • Boron isotopes • Salinity • Oilfield water

1 Introduction

The Mishrif Reservoir in the oilfields of North Rumaila (RU), South Rumaila (R), West Qurna (WQ), Zubair (ZB) and Majnoon (MJ) was investigated in southern Iraq (Fig. 1) which is an oilfield entrapping hydrocarbons in anticlinal structures of S-N axis trend.

The Mishrif Formation took place during the latest Cenomanian—Early Turonian age [1].

Fluid movement is often studied based on the values of the reservoir pressure by taking readings while ignoring the salinity role. Hydrochemistry plays a major role in controlling pressure within the oil reservoir through the on-going diagenesis processes [2]. The problem in this research is the importance of the distribution of salinity in oil exploration, especially that the Mishrif reservoir suffers from the lack of petroleum hydrochemical studies, particularly, those dealing with fluid-rock interactions.

This paper is going to discuss the role of petroleum hydrochemistry in controlling the fluid-flow direction and eventually controlling the pressure distribution in the oil reservoir in an attempt to enhance the risk assessment before drilling an oil well for further future exploration.

2 Materials and Methods

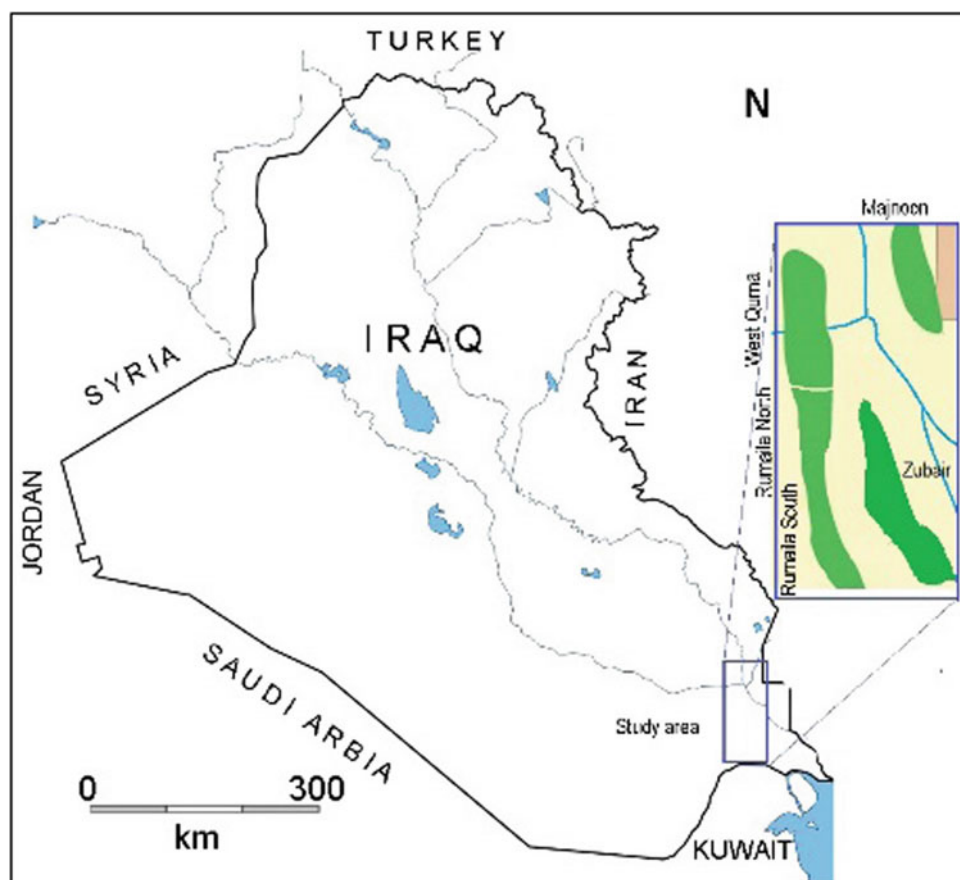
Twenty-five water samples at a depth of more than 2450 m from five oil fields (five samples from each of the R, WQ and MJ oil fields, four samples from the RU, and six samples from the ZB) were collected from the Mishrif Reservoir and studied in terms of petroleum hydrochemistry (Fig. 1). The analysis was conducted by ICP-MS technique in the laboratories of ALS, Spain. Boron isotopes (^{10}B and ^{11}B) were analyzed using ICP-SFMS and MC-ICP-MS at the laboratories of the ALS Scandinavia group, SWEDEN. The internal standard and calibration were done with NIST-SRM 951 (Boric acid). The boron stable isotope ratio is expressed in *per mil* (‰) as in Eq. (1):

$$\delta^{11}\text{B} (\text{‰}) = \frac{(^{11}\text{B}/^{10}\text{B})_{\text{Sample}} - (^{11}\text{B}/^{10}\text{B})_{\text{Standard}}}{(^{11}\text{B}/^{10}\text{B})_{\text{Standard}}} \times 10^3 \quad (1)$$

S. Awadh (✉) · H. Al-Mimar
Department of Geology, College of Science,
University of Baghdad, Baghdad, Iraq
e-mail: salihauad2000@scbaghdad.edu.iq

A. Al-yaseri
South Oil Company, Basrah, Iraq

Fig. 1 Location map shows the studied oil fields



3 Results

All oilfield waters are dominated by Na and Cl. The Na^+ , Ca^{2+} , Cl^- and SO_4^{2-} ions, originating from connate water and represent more than 90% of the total TDS; where ions descended as $\text{Na}^+ > \text{Ca}^{2+} > \text{Mg}^{2+} > \text{K}^+$ and $\text{Cl}^- > \text{SO}_4^{2-} > \text{HCO}_3^-$. The Na content is concentrated up to seven times more than seawater. The Na-chloride type is characteristic the Mishrif reservoir in all oilfields except in WQ which is defined by facies of Na-Ca-chloride type (Table 1).

The oilfield waters throughout oilfields appear almost homogeneous (Fig. 2).

A salinity-pressure model map was achieved based on the hydrochemical parameter and fluid-rock infractions.

TDS and exothermic reactions were the main factors controlling formation pressure. Increasing the temperature in the reservoir will increase the pressure and contribute to the fluid movement [3]. The high TDS in the studied oilfields (221,660 in WQ and 253,052 in MJ) ppm with a diagenesis exothermic reaction controlled the formation of pressure. The RU, R, WQ, MJ and ZB oilfields are constructed by salinity model maps shown in Fig. 3. The potentiometric maps show that the fluid moves from R (anticline center) towards the north and south (plunges) in the sense towards RU and WQ (Fig. 3a), and westward to the western limb in MJ (Fig. 3b) and then eastward (eastern limb) towards the ZB oil field (Fig. 2c). The direction of fluid movement has pointed out the low-pressure positions in the oilfields.

Table 1 Groups and families of the Mishrif reservoir oilfield water based on Schoeller's classification

Field	Anions	Cations	Group	Family
R	$\text{Cl} > \text{SO}_4 > \text{HCO}_3$	$\text{Na} > \text{Ca} > \text{Mg} > \text{K}$	Chloride	Na-Chloride
RU	$\text{Cl} > \text{SO}_4 > \text{HCO}_3$	$\text{Na} > \text{Ca} > \text{Mg} > \text{K}$	Chloride	Na-Chloride
MJ	$\text{Cl} > \text{SO}_4 > \text{HCO}_3$	$\text{Na} > \text{Ca} > \text{Mg} > \text{K}$	Chloride	Na-Chloride
ZB	$\text{Cl} > \text{SO}_4 > \text{HCO}_3$	$\text{Na} > \text{Ca} > \text{Mg} > \text{K}$	Chloride	Na-Chloride
WQ	$\text{Cl} > \text{SO}_4 > \text{HCO}_3$	$\text{Na} > \text{Ca} > \text{Mg} > \text{K}$	Chloride	Na-Ca-Chloride

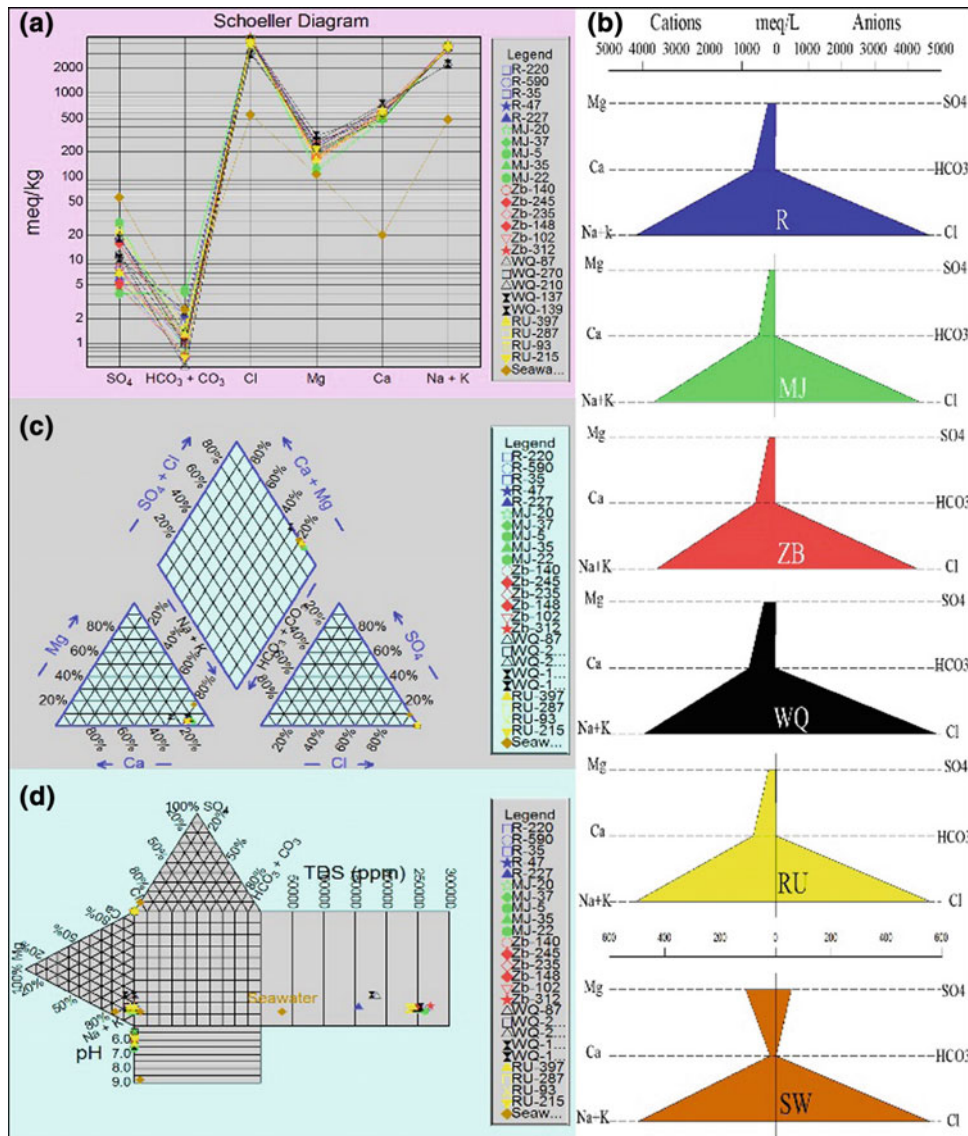


Fig. 2 Classification of the oilfield water according to Schoeller (a), Stiff (b), Piper (c) and Durov classifications (d). Symbols on stiff diagram refer to oilfield name and SW means seawater showing brine solution predominantly with sodium and chloride

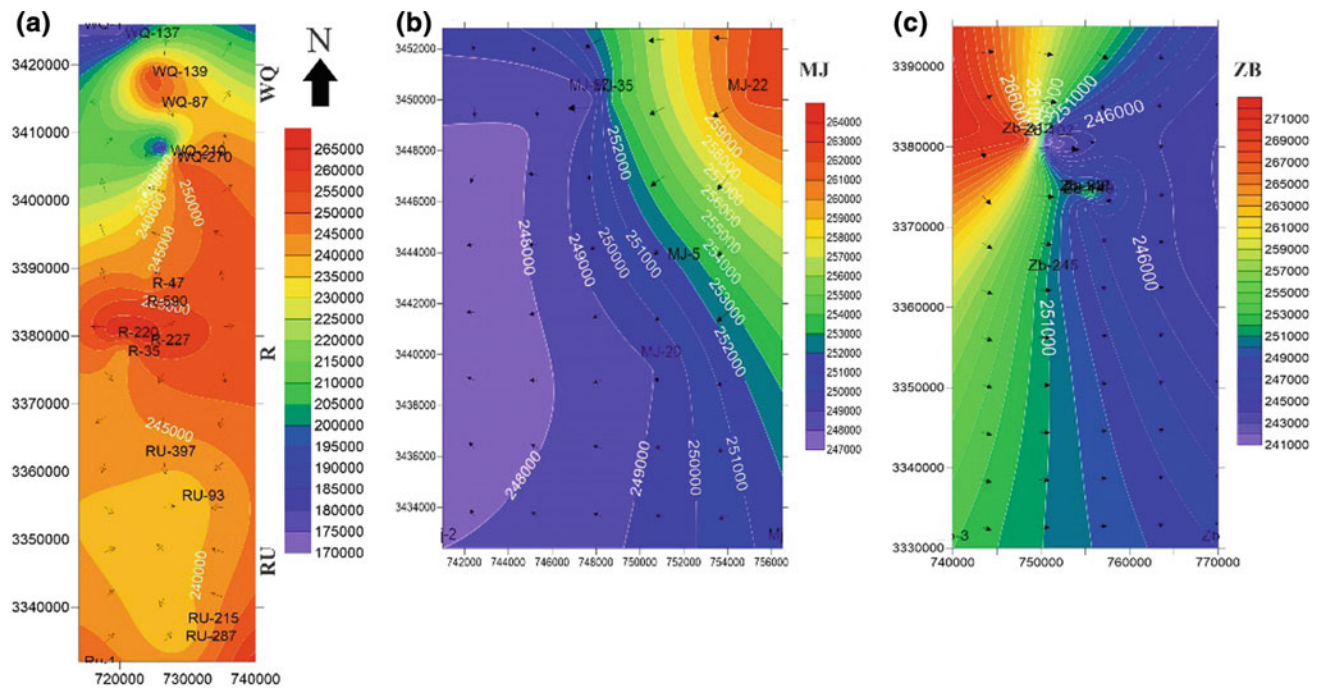


Fig. 3 Potential vector map of the West Qurna (WQ), Rumaila North (R), Rumaila South (RU), Majnoon (MJ) and Zubair (ZB) oil fields

4 Conclusions

1. Salinity and exothermic reactions are control factors of the pressure distribution in the oil reservoir.
2. Based on the potentiometric subsurface maps, the pressure values in the Mishrif reservoir in RU, R and WQ oil fields increase towards the anticline plunges, but to the western limb and eastern limb in the ZB and MJ oils fields, respectively.

References

1. Buchette, T.P.: Mishrif formation (Cenomanian-Turonian), southern Arabian Gulf: carbonate platform growth along a cratonic basin margin. In: Simo, J.A.T., Scott, R.W., Masse, J.P. (eds.) *Cretaceous Carbonate Platforms*. vol. 56, pp. 185–199. American Association of Petroleum Geologists Memoir (1993)
2. Nader, F.H., De Boever, E., Gasparrini, M., Liberati, M., Dumont, C., Ceriani, A., Morad, S., Lerat, O., Doligez, B.: Quantification of diagenesis impact on the reservoir properties of the Jurassic Arab D and C members (Offshore, U.A.E.). *Geofluids* **13**, 204–220 (2013)
3. Gurevich, A.E., Chilingar, G.V., Aminzadeh, F.: Origin of the formation fluid pressure distributions and ways of improving pressure prediction methods. *J. Pet. Sci. Eng.* **12**, 67–77 (1994)

A Transient Drainage Equation by Incorporating the Variable Drainable Porosity Function and the Unsaturated Zone Flow Contribution

Ammar Yousfi and Mohamed Mechergui

Abstract

Transient drainage equations presented earlier neglect the unsaturated flow above the water-table and assume constant drainable porosity. In this paper, a solution for the drainage problem is developed; it takes the unsaturated flow towards the drain into account and considers a variable drainable porosity. The solution is based on the spatial integration of the two-dimensional Richards Equation. The resulting integrated model is first simplified by applying Dupuit-Forchheimer (DF) theory and assuming a hydrostatic pressure distribution above the water-table, and then twice spatially integrated, yielding to a nonlinear differential equation for predicting the fall of the midway water-table height. With respect to drainage design, the developed equation, not presented before, provides a new method for designing subsurface drainage under transient conditions.

Keywords

Transient conditions • Unsaturated zone • Variable drainable porosity • Water-table • Drainage equation

1 Introduction

Transient drainage equations generally describe the relationship between the physical characteristics of the soil, depth and spacing of subsurface drains, and the fall of the water table at the mid-spacing of the drains. A number of such equations have been published, and the most popular of these include Guyon [5], Glover-Dumm [3, 4], Van Schilf-gaarde [13] and Bouwer and Van Schilf-gaarde [2]. These equations have been derived by neglecting flow in the

unsaturated zone above the water table and by assuming a constant drainable porosity [8].

The objective of this study is to develop a new transient drainage equation for predicting the fall of the midway water-table height or for computing drain spacings by reconsidering the effect of the unsaturated zone, i.e. by taking the unsaturated flow above the water-table into account and by incorporating the drainable porosity into a storage-dependent function. The theoretical development is based on the spatial integration of the two-dimensional Richards Equation [9] along with some simplified assumptions.

2 Materials and Methods

Figure 1 depicts the physical problem of subsurface drainage considered here and the parameter notation that has been adopted for this study. The drains are located at a distance D above an impervious layer with drain spacing of $2 * L$. The geometry, as described in Fig. 1, is used with the following boundary conditions: (i) a zero horizontal flux is assumed at drain mid-spacing and drain locations; (ii) a zero vertical flux is assumed at the barrier depth and at the soil surface; (iii) the tile drains are assumed to run partially full.

Before proceeding with the analysis of this problem, the assumptions used are presented as follows: (1) the problem is two-dimensional; (2) Water flux is solely in response to gradients of mechanical potential in the liquid phase; (3) hysteresis is absent, thereby restricting the analysis to drainage only; (4) the soil is homogeneous, isotropic and incompressible; (5) the fluid is homogeneous and incompressible; (6) water moves toward drains in both the saturated and unsaturated zones; and finally (7) before drainage, the initial water-table profile is assumed to be known.

Based upon the assumptions enumerated above, the water movement in the entire system can be correctly described, using the two-dimensional Richards Equation [9] expressed as follows [14]:

A. Yousfi · M. Mechergui (✉)
 Institut National Agronomique de Tunis, 43 Rue Charles Nicole
 cité El Mahrajène, 1082 Tunis, Tunisia
 e-mail: mechergui.med@inat.agrinet.tn

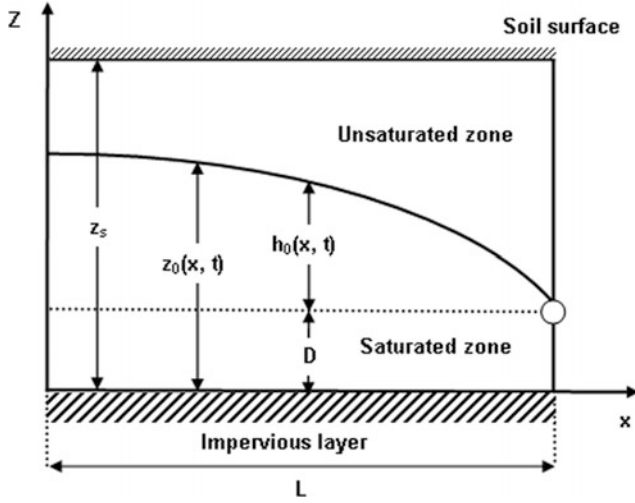


Fig. 1 Subsurface tile drainage system definition

$$\frac{\partial \theta(h)}{\partial t} = \frac{\partial}{\partial x} \left(K(h) \frac{\partial H}{\partial x} \right) + \frac{\partial}{\partial z} \left(K(h) \frac{\partial H}{\partial z} \right) \quad (1)$$

where z is the vertical coordinate (positive upward) [L], x the abscissa [L], t the time [T], θ the volumetric soil moisture content [-], $K(h)$ the hydraulic conductivity [LT^{-1}] and $H = h + z$ the total hydraulic head [L] where h is the soil water pressure head [L].

Noting that in the saturated zone $\frac{\partial \theta(h)}{\partial t} = 0$ and the hydraulic conductivity becomes saturated, Eq. (1) can therefore be simplified as:

$$\frac{\partial}{\partial x} \left(K_s \frac{\partial H}{\partial x} \right) + \frac{\partial}{\partial z} \left(K_s \frac{\partial H}{\partial z} \right) = 0 \quad (2)$$

Considering the boundary condition (ii) and integrating Eqs. (1) and (2) over the depth of the unsaturated and saturated zones, respectively, gives after applying the Leibnitz rule [15]:

$$\frac{\partial S}{\partial t} + \frac{\partial Q_{US}}{\partial x} + \frac{\partial Q_S}{\partial x} = 0 \quad (3)$$

With

$$S = \mu_0 \left(z_0 + \int_{z_0}^{z_s} \Theta(h) dz \right) \quad (4)$$

$$Q_S(x, t) = -K_s \int_0^{z_0} \frac{\partial H}{\partial x} dz \quad (5)$$

$$Q_{US} = K_s \int_{z_0}^{z_s} -K_r(h) \frac{\partial h}{\partial x} dz \quad (6)$$

where S is the total storage [L]; Q_{US} and Q_S the unsaturated horizontal flow and the saturated horizontal flow, respectively [L^2T^{-1}]; $\Theta(h) = \frac{\theta(h) - \theta_r}{\theta_s - \theta_r}$ the effective water content [-]; $\mu_0 = \theta_s - \theta_r$ the total drainable porosity [-] where θ_s and θ_r are the saturated soil moisture content [-] and the residual soil moisture content [-], respectively; K_s the saturated hydraulic conductivity [LT^{-1}]; $K_r(h)$ the relative hydraulic conductivity [-]; and z_0 the water table elevation [L].

The resulting integrated model (Eq. 2) describes the mass continuity equation in the considered drainage system and represents both unsaturated and saturated flow. This one-dimensional model, used to evaluate the shape and position of the water-table, is highly non-linear and difficult to be solved, because it requires the knowledge of the total hydraulic head distribution (H) in the saturated zone and the pressure head distribution in the unsaturated zone (h). To simplify the problem, let us introduce the following assumptions: (1) the DF assumption of essentially horizontal flow is valid in the saturated zone, which allows replacing the total hydraulic charge H by the water table elevation z_0 and (2) the pressure head distribution above the water table during drainage may be assumed nearly hydrostatic [11] so that $h = -(z - z_0)$ [6].

By applying these two assumptions to Eqs. (4), (5) and (6) and by performing some mathematical arrangements, Eq. (3) can be re-written as:

$$\begin{aligned} \mu_0 \frac{\partial}{\partial t} \left(z_0 + \int_0^{z_s - z_0} \Theta(\delta) d\delta \right) \\ = K_s \frac{\partial^2}{\partial x^2} \left\{ \frac{z_0^2}{2} - \int_0^{z_s - z_0} \int_0^\delta K_r(\eta) d\eta d\delta \right\} \end{aligned} \quad (7)$$

where δ and η (> 0) are omitted integration parameters.

The derived transient drainage model is to describe the water table elevation drawdown by considering the whole effect of the unsaturated zone (storage above the water table and the unsaturated zone flow contribution) but it requires the knowledge of the expression of the effective water content $\Theta(h)$ and the relative hydraulic conductivity $k_r(h)$.

For a drainage design purpose, the obtained equation will be hereafter spatially integrated as done by Bouarfa and Zimmer [1] to obtain a relationship between the drain

spacing, the water table height midway between drains and the tile depth.

3 Results and Discussion

To derive a transient drainage equation, the total storage $S(x, t)$ is written in a non-dimensional variable as follows:

$$S(x, t) = \mu_0 \cdot W(\varepsilon, t) \cdot \left(z_m(t) + \int_0^{z_s - z_m(t)} \Theta(\delta) d\delta \right) \quad (8)$$

where $\varepsilon = \frac{x}{L}$ the non-dimensional abscissa, L the drain mid-spacing [L], $W(\varepsilon, t)$ the non-dimensional storage and $z_m(t)$ the water table elevation at midpoint between drains [L].

Combining Eqs. (7) and (8) and integrating twice the resulting equation between drain mid-spacing ($x = 0$) and drain locations ($x = L$), yields:

$$\begin{aligned} & \mu_0 \frac{\partial}{\partial t} \left\{ C(t) \cdot \left(z_m(t) + \int_0^{z_s - z_m(t)} \Theta(\delta) d\delta \right) \right\} \\ &= -K_s \frac{\left\{ z_m^2(t) - D^2 + 2 \int_{z_s - z_m(t)}^{z_s - D} \int_0^\delta K_r(\eta) d\eta d\delta \right\}}{L^2} \end{aligned} \quad (9)$$

where $C(t)$ is the storage factor [-] such that $C(t) = 2 \int_0^1 (1 - \varepsilon) W(\varepsilon, t) d\varepsilon$.

Approximate values of C range between (0.8 and 1) as suggested by Bouwer and Van Schilfgaarde [2]. By assuming a constant C over the time and introducing the water table height ($z_m(t) - D$) above the drainage level noted $h_m(t)$ and the depth of the drain ($z_s - D$) noted h_s results in, after rearrangement:

$$\begin{aligned} & \mu_0 C \{1 - \Theta(h_s - h_m(t))\} \frac{\partial h_m(t)}{\partial t} \\ &= -K_s \frac{\left\{ h_m^2 + 2h_m D + 2 \int_{h_s - h_m}^{h_s} \int_0^\delta K_r(\eta) d\eta d\delta \right\}}{L^2} \end{aligned} \quad (10)$$

where $\mu_0 \{1 - \Theta(h_s - h_m)\}$ defined as the variable drainable porosity function, which can be obtained by taking the derivative of the total storage S with respect to z_0 [12]. The two terms on the right-hand side of the Eq. (11) represent the water-table and the unsaturated zone flow contribution, respectively.

The resulting first order non-linear differential equation provides the lowering of the water-table height midway between drains at any given time and for known drain spacing. Also, given the drop of the water table height in

time at the midpoint between two parallel drains, this equation solves for drain spacing as follows:

$$E^2 = \frac{4K_s t / C}{\int_{h_m(t)}^{h_m(0)} \left(\frac{\mu_0 \{1 - \Theta(h_s - h_m)\}}{h_m^2 + 2h_m D + 2 \int_{h_s - h_m}^{h_s} \int_0^\delta K_r(\eta) d\eta d\delta} \right) dh_m} \quad (11)$$

The derived closed-form equation, not presented before in the literature, allows computing the appropriate drain spacing E . Compared to the existing drainage theories, this equation includes the variable drainable porosity function and the unsaturated zone flow contribution. Since this equation is based on DF assumptions, the actual depth to the impervious layer (D) will be simply replaced by Houghoudt [7] equivalent depth (d) in order to correct the convergence near the drains if the drains do not reach the impervious layer [10].

If we treat the drainable porosity as a constant and we ignore the unsaturated flow above the water-table, it is noticed that the newly derived transient drainage spacing equation (Eq. 11) is equivalent to the integrated steady state equation of Houghoudt [7] obtained by Bouwer and Van Schilfgaarde [2]:

$$\frac{8K_s d}{\mu C E^2} t = \text{Log} \left(\left(\frac{h_m(0)}{h_m(t)} \right) \left(\frac{h_m(t) + 2d}{h_m(0) + 2d} \right) \right) \quad (12)$$

4 Conclusions

An attempt was made to derive a new transient drainage equation for predicting the water table drawdown at midpoint between drains or for computing drain spacings. The developed solution has the advantage over the existing drainage theories of particularly including the variable drainable porosity as a storage-dependent function and the unsaturated zone flow contribution. Further investigation should be carried out to assess the performance of the results given by the newly obtained solution under experimental laboratory and field conditions. Also, one can evaluate the influence of soil properties on the computed drain spacings.

References

1. Bouarfa, S., Zimmer, D.: Water table shapes and drain flow rates in shallow drainage systems. *J. Hydrol.* **235**, 264–275 (2000)
2. Bouwer, H., Van Schilfgaarde, J.: Simplified method for predicting fall of water-table in drained land. *Trans. ASAE.* **6**(4) 288–291, 296 (1963)
3. Dumm, L.D.: Transient flow concept in subsurface drainage: its validity and use. *Trans. Amer. Soc. Agr. Eng.* **7**(2), 142–146, 151 (1964)

4. Dumm, L.D.: New formula for determining depth and spacing of subsurface drains in irrigated lands. *Agric. Eng.* **35**, 726–730 (1954)
5. Guyon, G.: Considerations sur l'hydraulique du drainage des nappes. *Bulletin Technique du Génie Rural* No. 70, Antony, France (1967)
6. Hilberts, A.: Low-dimensional modeling of hillslope subsurface flow processes. Thesis, p. 129. Wageningen (2006)
7. Hooghoudt, S.B.: Algemeene beschouwing van het probleem van de detailontwatering en de infiltratie door middel van parallel loopende drains, greppels, slooten en kanalen. *Versl. Landbouwk. Onderz.* **14**, 46 (1940)
8. Kao, C.: Fonctionnement hydraulique des nappes superficielles de fonds de vallées en interaction avec le réseau hydrographique. Dissertation, p. 266. ENGREF, Paris (2002)
9. Richards, L.A.: Capillary conduction of liquids in porous mediums. *Physics* **1**, 318–333 (1931)
10. Ritzema H.P.: Drainage principles and applications, 2nd edn. ILRI Publication 16, Wageningen, p. 1125. The Netherlands (1994)
11. Skaggs, R.W., Tang, Y.K.: Saturated and unsaturated flow to parallel drains. *J. Irrig. Drain. Div. ASCE* **102**(IR2), 221–237 (1976)
12. Subodh, A., James, W.J., Rao, S.M.: Analytical expressions for drainable and fillable porosity of phreatic aquifers under vertical fluxes from evapotranspiration and recharge. *J. Water Resour. Res.* **48**, W11526 (2012)
13. Van Schilfgaarde, J.: Design of tile drainage for falling water tables. *J. Irrig. Drain. Div. Amer. Soc. Civ. Eng.* **89**, 1–11 (1963)
14. Todsen, M.: Numerical studies of two-dimensional saturated/unsaturated drainage models. *J. Hydrol.* **20**, 311–326 (1973)
15. Yakirevich, A., Borisov, V., Sorek, S.: A quasi three-dimensional model for flow and transport in unsaturated and saturated zones: 1. implementation of the quasi two-dimensional case. *Adv. Water Res.* **21**(8), 679–689, 1 (1997)

Study of Solid Transport in Suspension in a Semi-arid Catchment: Case of Boukadir Wadi, Tipaza, Algeria

Omar Elahcene, Imad Eddine Bouznad, Mohamed Yacine Bendjedou, and Zohir Boulkenafet

Abstract

The Mediterranean semi-arid zones are characterized by irregular rainfall patterns in time and space. A statistical approach to the quantification of solid intakes has been developed in this study. The data used are collected at the Boukadir river watershed. The observation period covers 21 years (1993–2013). Maximum values for solid transport are recorded in early fall and late spring. The average annual sediment load recorded at the outlet of the watershed of Boukadir wadi is estimated at 17,666 ton, which corresponds to a specific degradation of about $220 \text{ ton km}^{-2} \text{ year}^{-1}$. It should be noted that this value is in the range of the degradations found for some Maghrebian watersheds with similar regimes.

Keywords

Concentration • Liquid flow • Solid flow • Model • Semi-arid zone • Boukadir wadi • Algeria

1 Introduction

The most drastic consequences of basin's erosion and sediment transport are certainly the silting of dams and water pollution. Erosion and solid transport processes in the basins of Mediterranean semi-arid zones have interested a great number of hydrologists, whose studies have increased in the last ten years with the aim of understanding and explaining the mechanisms, their causes and their consequences. The studies of Demmak [1], Terfous et al. [2], Achite [3], Elahcene and Remini [4], Yles and Bouanani [5], Elahcene

et al. [6] and Megnounif et al. [7] highlighted the relationships that may apply on areas where the measures of the basin effects are rare, incomplete or non-existent.

In Algeria, sediment transport is evaluated at hydrometric stations for almost all periods of flow [8]. In this work, the hydrometric measures (water level, water discharge and suspended sediment concentration in the Mesdour station) were used for the quantification and modelling of solid transport in suspension. The approach applied on the Boukadir wadi (Algeria) is of a determinist type and uses simple regressive models whose aim is to find one or many relationships between water and sediment discharge.

2 Materials and Methods

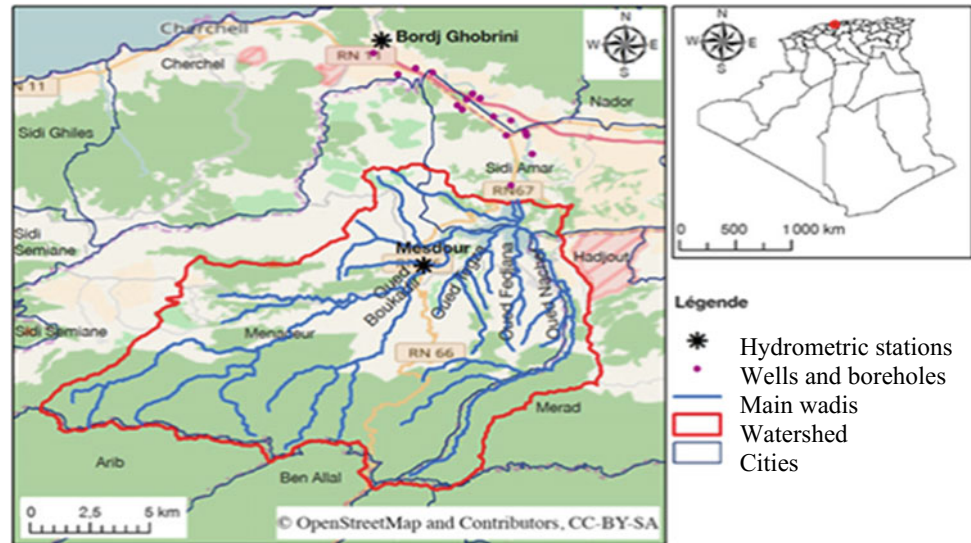
The basin of wadi Boukadir covers an area of 80.33 km^2 with a perimeter of 43.09 km. It's moderately elongated in shape (compactness coefficient $K_c = 1.53$). It is part of Algeria's coastal basin, and part of it stretches to Tipaza province (Fig. 1). The length of the equivalent rectangle to the watershed of Oued Boukadir is 16.75 km, so its width is 4,8 km. The maximum altitude is 1350 m and the minimum altitude is 112 m, hence the average altitude is 582,688 m. The average slope of the watershed of Boukadir wadi is estimated at 28.17%.

The climate of the watershed of wadi Boukadir is a semi-arid type that is wet and cold in winter, hot and dry in summer. The wettest months in the watershed of Boukadir wadi are November (97.5 mm), December (92.5 mm), January (83.13 mm) and February (82.38 mm), while the annual precipitation is between 814 and 271 mm and the inter-annual mean is 592 mm. The study was realized using the data collected during the period from 1993/94 to 2012/13 consisting of water discharge Q_1 in m^3/s and of suspended load concentration C in g/l . The data are provided by the National Agency of Water Resources in Algeria. The solid flow, Q_s (kg/s) is estimated by the product, $Q_s = C_s \times Q_1$. At the Mesdour station, we have a series of measurements of

O. Elahcene (✉) · I. E. Bouznad · Z. Boulkenafet
University of Djelfa, Djelfa, Algeria
e-mail: elahcene_o@yahoo.fr

M. Y. Bendjedou
University Center of Tindouf, Tindouf, Algeria

Fig. 1 The watershed of Boukadir wadi



372 values of water depth (H in cm), liquid flow rates (Q_l in m^3/s), concentration in suspended solids (C in g/l) and solid flow rate (Q_s in kg/s) selected for the ratio of solid flow to liquid flow. These data, used for the quantification of solid transport, were analyzed in order to determine their reliability and validity; that is to say, once measured, the solid flows are correlated with the daily fluid flow rates. The Q_s/Q_l ratio has been subjected to linear, logarithmic, polynomial, power and exponential relations. The correlation between solid flow and liquid flow is to find a relationship that links the two parameters.

3 Results

3.1 Correlation Between Solid Flow and Liquid Flow

The results are shown in Fig. 2 and in Table 1.

3.2 Calculation of Solid Transport in Suspension

To estimate the solid inputs, we used the power relationship of the complete series whose form is: $Q_s = 1.52 \times Q_l^{1.23}$ with $R = 75\%$. On the basis of this relationship, we calculated the monthly and annual A_s suspended solid feeds in tons per year, and then the specific A_{ss} degradation in tons per km^2 per year over a period of (1993/94 to 2013/2014). Specific degradation is assessed by the ratio of solid inputs to the total area of the watershed. It is given by the relation: $A_{ss} = A_s/S$, with, A_{ss} : specific solid contribution or specific degradation ($tons\ km^{-2}\ year^{-1}$), A_s : solid intake ($ton\ year^{-1}$)

and S : catchment area (km^2). The results obtained are shown in Table 2.

4 Discussion

Figure 2 shows that the cloud of points for the complete series, the seasons and the flood series is well aligned around the regression line. In general, the results obtained show that there is a good correlation between these two quantities representing the sedimentary dynamics of Boukadir wadi. This can be explained by the effectiveness of the power relationship, that is to say that the solid flow is linked to the liquid flow by the relation $Q_s = C \times Q_l$.

From Table 1, it is clear that there is a good correlation for all the studied scales. It can be concluded that the relationships of the solid flow-liquid flow correlation are respected which makes it possible to quantify and evaluate the suspended solid transport in Boukadir wadi.

Table 2 shows that the years 1995/1996, 1998/1999, 2004/2005, 2005/2006 and 2011/2012 are characterized by very strong solid contributions. This can be explained by the arrival of exceptional floods in volume and duration. In this context, we note the flood of April 1996 (339,536 ton), the flood of March 1999 (186,628 ton), the flood of March 2005 (149,344 ton), the flood of February 2006 (95,704 ton), and the flood of March 2012 (143,202 ton).

The average annual sediment load recorded at the outlet of the wadi Boukadir watershed is estimated at 17,666 ton, which corresponds to a specific degradation of $220\ ton/km^2/year$. It should be noted that this value is in the range of the degradations found for some Maghrebian watersheds.

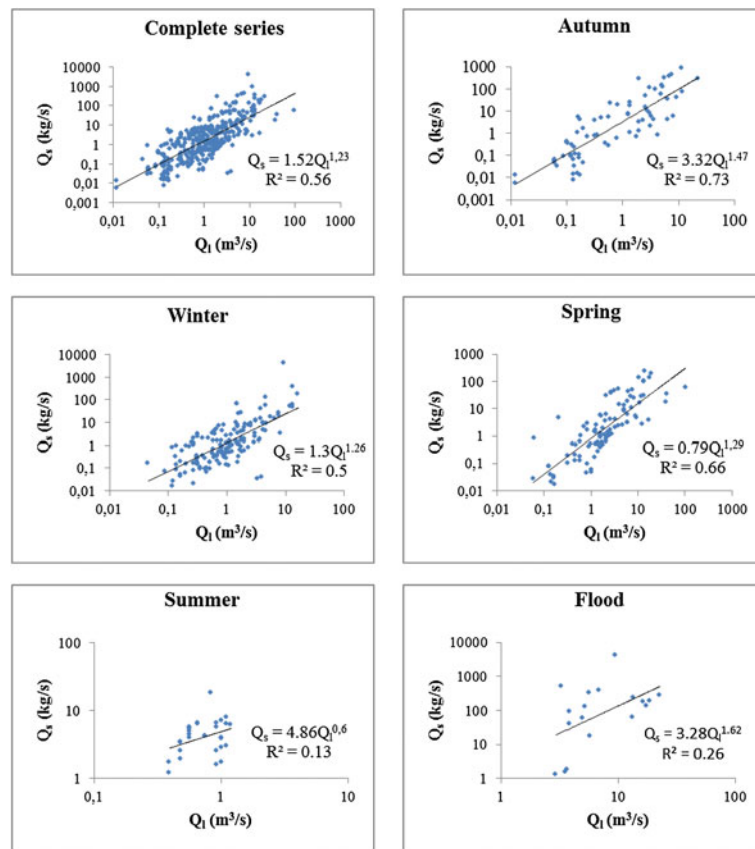


Fig. 2 Power relationship between solid flows and liquid flows at different scales in the watershed of Boukadir wadi, Mesdour station, Tipaza (1993/2013)

Table 1 Solid flow-liquid flow relationships at different scales in the watershed of Boukadir wadi (1993/2013)

Model	Series	Equations	Determination coefficient	Correlation coefficient
Power	Complete (372)	$Q_s = 1.52Q_l^{1.23}$	0.56 (56%)	0.75 (75%)
	Autumn (74)	$Q_s = 3.32Q_l^{1.47}$	0.73 (73%)	0.85 (85%)
	Winter (162)	$Q_s = 1.3Q_l^{1.26}$	0.50 (50%)	0.71 (71%)
	Spring (106)	$Q_s = 0.79Q_l^{1.29}$	0.66 (66%)	0.81 (81%)
	Summer (30)	$Q_s = 4.86Q_l^{0.6}$	0.13 (13%)	0.35 (37%)
	Flood (18)	$Q_s = 3.28Q_l^{1.62}$	0.26 (26%)	0.51 (51%)

Table 2 Annual distribution of suspended solid inputs (in tons) and specific degradations in ($ton/km^2/year$) in the watershed of Boukadir wadi, Mesdour Station, Tipaza (1993/1994 to 2013/2014)

Year	Sep.	Oct.	Nov.	Dec.	Jan.	Feb.	Mar.	Apr.	May	Jun.	Jul.	Aug.	A_s	A_{ss} ($t/km^2/y$)
													(t/y)	
93/94	22	393	1713	2224	24,431	9744	3676	6732	1220	216	0	0	4198	52
94/95	55	2022	2270	5066	72,676	12,178	148,031	9628	4303	1572	200	33	21,503	268
95/96	1330	4858	3735	5358	5250	50,153	11,697	339,536	33,987	13,117	2449	1965	39,453	491
96/97	6121	29,785	8521	4743	8438	47,760	5303	19,467	2727	689	313	0	11,156	139
97/98	0	23,004	15,262	12,842	6012	7563	6698	11,153	14,647	2789	334	0	8359	104
98/99	242	1426	13,157	9009	56,104	10,079	186,628	20,071	16,673	10,470	0	0	26,988	336

(continued)

Table 2 (continued)

Year	Sep.	Oct.	Nov.	Dec.	Jan.	Feb.	Mar.	Apr.	May	Jun.	Jul.	Aug.	A _s	A _{ss} (t/km ² /y)
													(t/y)	
99/00	0	0	5607	73,423	34,276	8195	6818	2552	1215	0	0	0	11,007	137
00/01	0	366	9465	3949	28,221	13,808	5437	12,364	2311	8	0	0	6327	79
01/02	0	0	32,640	7549	5293	6348	16,284	7605	2685	52	1361	0	6651	81
02/03	0	2861	7494	17,659	37,473	70,583	45,811	23,656	9702	3757	223	71	18,274	227
03/04	2992	71	6512	4560	14,388	5179	13,694	20,985	21,568	16,990	4133	71	9262	115
04/05	2892	648	5766	14,471	27,458	81,954	149,344	35,207	9880	4049	0	0	27,639	344
05/06	0	0	0	35,854	80,320	95,704	37,744	9181	75,493	13,197	1641	12	29,096	362
06/07	475	266	1377	24,112	5905	7733	40,469	61,247	13,425	4313	87	10	13,285	165
07/08	1563	3970	46,015	28,671	23,486	10,198	14,433	4906	2437	2230	2	0	11,326	141
08/09	41	37	1941	13,063	17,706	17,802	14,766	19,680	5948	611	2	0	7633	95
09/10	0	205	1132	12,063	32,678	61,442	67,782	27,832	14,602	5310	898	0	18,662	232
10/11	0	1212	4937	7272	5685	60,444	50,519	30,208	71,701	19,700	4560	0	21,353	266
11/12	0	96	6120	16,909	23,067	197,101	143,203	83,008	21,223	9391	706	0	41,735	520
12/13	0	199	15,857	8295	17,913	21,720	36,179	37,577	55,926	34,683	5452	0	19,483	243
13/14	1201	434	7704	847	34,408	51,413	95,835	11,496	1837	5792	163	6	17,595	219
Moy	807	3422	9392	14,664	26,723	40,338	52,398	37,814	18,262	6997	1073	103	17,666	220

5 Conclusion

This study allowed the quantification of the suspension sediment yield transported in Boukadir wadi. For this, we used the hydrometric data related to instantaneous discharge and to the suspended sediments' concentration on the right of Mesdour station, over a period of 21 years, from 1993/94 to 2012/13. During this study, we concluded that the relation is very significant (complete series), relating the sediment discharge and the water discharge in suspension: $Q_s = 1.52 \times Q_1^{1.23}$ with $R = 75\%$. The exponent b of the model found is equal to 1.23, a value close to the one found by researchers who worked in regions with a hydroclimatic regime similar to that of the site under study.

We calculated the daily suspended sediment discharge using the established relationship and we deduced the annual tonnage of suspended sediment transported in Boukadir wadi. The average annual yields of suspended sediments transported up to the basin of Bellah wadi is evaluated at 17,666 ton, which corresponds to an average specific degradation of 220 ton/km²/per year. This value is comparable to those found in basins with similar climate and hydrology in Algeria and in the Maghreb.

References

1. Demmak, A.: Contribution to the study of erosion and solid transport in northern Algeria. Thesis Doctor-Engineer, University. Paris, France, 323p (1982)
2. Terfous, A., Megnounif, A., Bouanani, A.: Study of solid transport in suspension in Oued Mouilah (North-West Algeria). *Water Sci. J.* **14**(2), 175–187 (2001)
3. Achite, M.: Statistical approach to evaluation of solid transport in the Oued Mina watershed (northwestern Algeria). *Watmed (Tunisia)* **2**, 894–899 (2002)
4. Elahcene, O., Remini, B.: Correlation between suspended matter concentration and liquid flow in the Wadi Bellah watershed (Algeria). *Eur. J. Sci. Res.* **26**(1), 139–46 (2009). ISSN 1450-216X
5. Yles, F., Bouanani, A.: Quantification and modeling of solid transport in the watershed of the Saida wadi (Algerian highlands). *Drought.* **23**(4), 289–296 (2012)
6. Elahcene, O., Terfous, A., Remini, B., Ghenaïm, A., Poulet, J.B.: Study of sedimentary dynamics in the watershed of Wadi Bellah (Algeria). *Hydrol. Sci. J.* **58**(1), 1–13 (2013)
7. Megnounif, A., Terfous, A., Ouillon, S.: Agraphical method to study suspended sediment dynamics during flood events in the wadi Sebdo, NW Algeria (1973–2004). *J. Hydrol.* **497**, 24–36 (2013)
8. Larfi, B., Remini, B.: Solid transport in the Wadi Isser watershed, impact on the siltation of the Beni Amrane dam (Algeria). *Larhyss J.* (05), 63–73 (2006). ISSN 1112-3680

Temporal Variation of Specific Sediment Yield at Sidi Bel Abbes Basin, North Algeria

Hayet Madani Cherif and Abderezzak Bouanani

Abstract

The estimation of sediment transport has aroused our interest in this work because it is a liability to the conservation of the ecological environment and the protection of hydraulic structures against siltation sediments. The adopted methodology consists in (i) studying the evolution of the suspended sediment concentrations according to the water discharge, (ii) establishing a regressive model to explain the relationship between water discharge-sediment discharge, (iii) calculating the mean annual suspended sediment load and specific suspended sediment yield in the catchment area of the plain of Sidi Bel Abbès.

Keywords

Erosion • Liquid discharge • Concentration • Modelling • Algeria

1 Introduction

Much of the work on specific degradation has been done using empirical methods to provide an actual estimation of erosion, which is usually either over- or underestimated. Several empirical formulas have been used by numerous researchers [1] and design offices [2] to quantify erosion. This first category of formulas implies explanatory parameters in the form of relationships between sediment discharge and water discharge without taking into account processes and spatial and

H. Madani Cherif (✉)

Laboratory for Rheology, Transport and Treatment of Complex Fluids (LRTTFC), Department of Hydraulics, Faculty of Architecture and Civil Engineering, University of Sciences and Technology of Oran, El- M'Naouer, PB 1505 31000 Oran, Algeria
e-mail: madcherhay@yahoo.fr

A. Bouanani

Laboratory (LPRHPM) Research N° 25, University Abu Bekr Belkaïd, PB 230 13000 Tlemcen, Algeria

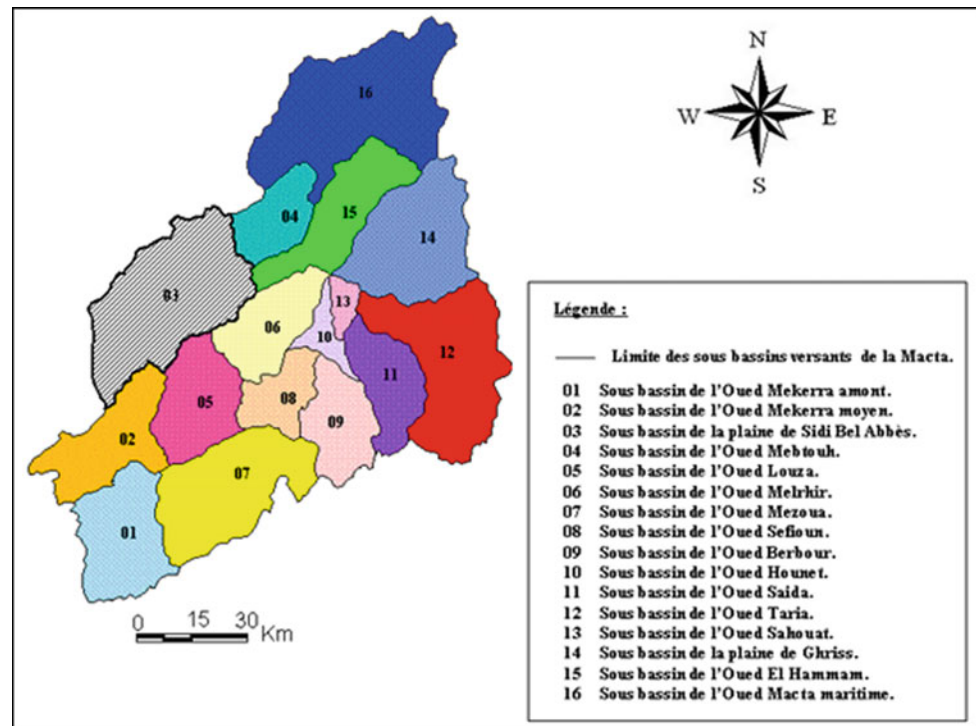
temporal recurrences that govern hydro-sedimentary functioning [3]. The proposal of general forecast models and/or specific models (specific to a given watershed) is necessary [4]. Our work falls into the second category of models, which will be used to develop a model specific to the Sidi Bel Abbès basin drained by the main wadi Mekerra river, using in situ measurements of liquid flow and instantaneous suspended sediment concentrations in order to evaluate the volume of sediments transported, to describe the hysteresis phenomenon, to analyse the evolution of sediment concentration as a function of liquid flow, and to determine the specific degradation and siltation rate in the Sarno dam. The statistical models found will also be used to fill gaps due to a lack of measurement data and to extend the existing series.

2 Data and Methodology

The Sidi Bel Abbès Basin plain occupies a very important part of the large Macta catchment area. It is limited by the El Mebtouh wadi under-basin to the North, by the Middle Mekerra wadi under-basin to the South, to the East by the Louza and Melrhir wadi under-basins, and to the West by the Oranais Coast catchment area (Fig. 1).

The basin is related to a semi-arid climatic zone with irregular rainfall, characterized by an intense autumn precipitation causing major floods, whose effects are felt in the area between Bukhnafis and the agglomeration of Sidi Bel Abbès [5]. The geographical position gives the plain of Sidi Bel Abbès the appearance of a depression filled in by Quaternary and Plio-Quaternary formations and is limited to the North and East by Miocene and Neogene, and to the South by Jurassic and Cretaceous lands. The predominance of silts, sandy clays, alluvium and terrace conglomerates on the edges of the streams, a limestone crust mainly on the edges of the limestone massifs, in the central and the northern parts of the plain, and sandstones with clayey past alternating with some dolomitic or calcareous levels in the south-west of the plain is generally noted [6].

Fig. 1 Location of Sidi Bel Abbas basin



The floods of wadi Mekerra are those which deserve the most attention in all hydrological studies in northern Algeria. These maximum floods usually occur in the second half of September or October, so in early autumn in one way or another rainfall is comparable to the worst tropical precipitations. The most effective for floods are heavy rains which can range from 20 to 190 mm/h, usually in October. This is the typical case of our wadi. Instantaneous liquid flows as well as suspended sediment concentrations were provided to us by the National Agency of hydraulic resources [7], for the periods 1987/1988 to 2006/2007.

3 Results

3.1 Statistical Modelling of Sediment Transport (Rating Curves)

To study the responses of the basin to liquid flows and suspended solids during the hydrological year, we considered it useful to group the instantaneous values (taken at the

Sidi Bel Abbas gauging station at different periods of study (1986/87 to 2006/2007) and to analyze the relationship between the liquid flow rates and the suspended solid flow rates. The exponential model is obtained which explains more than 80% of the variance (Table 1).

3.2 Assessment of Contributions

The flow of suspended matter (A_S), exported to the outlet during a time step between two samples noted ($t_j + 1 - t_j$), is calculated by the following formula:

$$A_S = \sum_{j=1}^N \frac{[(Q_{L(j+1)} \cdot C_{(j+1)}) + (Q_{Lj} \cdot C_j)]}{2} \cdot (t_{j+1} - t_j) \quad (1)$$

With: C_j and $C_{(j+1)}$; are the concentrations recorded at times t_j and t_{j+1} corresponding respectively to the liquid flows Q_{Lj} and $Q_{L(j+1)}$. The arithmetic sum of these elementary contributions during the year will constitute the annual solid contribution. Similarly, the liquid input (A_L) generating the A_S flux is calculated as follows:

Table 1 Flow relationships: Solid flow—Liquid flow

Temporal scale	Data	R ² (%)	Model
Autumn	3519	81	$Q_s = 1.7416 Q_l^{1.671}$
Winter	1148	72	$Q_s = 0.7172 Q_l^{1.958}$
Spring	1195	86	$Q_s = 0.8125 Q_l^{1.885}$
Summer	841	87	$Q_s = 4.503 Q_l^{1.482}$
All floods	8243	81	$Q_s = 1.3817 Q_l^{1.756}$

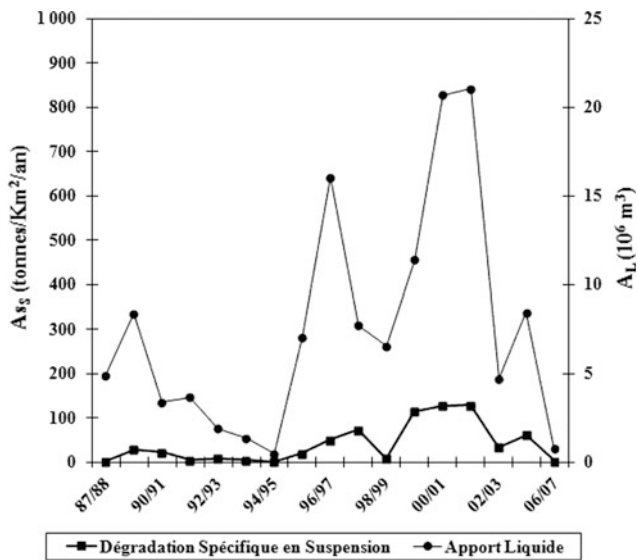


Fig. 2 Interannual variability of the specific degradation and liquid contribution

$$A_L = \sum_{j=1}^N \frac{[Q_{L(j+1)} + Q_{Lj}]}{2} \cdot (t_{j+1} - t_j) \quad (2)$$

4 Discussion

The rate of variance explained is higher in the warm season than in the cold season. After a long dry season characterized by high temperatures (summer), the rains cause the destruction of soil aggregates. The runoff triggered by these rains ensures the transport of loose particles. In addition, in summer, soils are very often bare or poorly protected.

The intra-annual and inter-annual distribution of the liquid and solid inputs thus obtained (Fig. 2) shows that the highest annual liquid input, 21 million m³, was recorded during the hydrological year 2001–2002, carrying a solid input of 387 thousand tonne of sediments, i.e. a specific degradation of 129 t/km²/year, in contrast to the other hydrological years, the solid input varies between 6000 and 300,000 tonne, representing specific degradations around 2 to 120 t/km²/year. This remains below 5000 t/km²/year, values supposed to be the maximum threshold of the solid transport rate in North Africa [8].

5 Conclusions

Sidi Bel Abbès basin is characterized by: irregular rainfall, high water levels and very high floods—which are the consequence of intensive torrential rainfall runoff—and an often-discontinuous vegetation cover. Erosion in this basin is very active because it is the result of a process of soil stripping and which admits a morphological and hydrological significance, essentially on the steep slopes and banks of the Wadi. Wadi Mekerra at Sidi Bel Abbès has an average specific degradation of about 38 tonne/km²/year, compared to the specific degradation of other wadis. Therefore, the degradation of the basin subject of our study remains with a moderate value compared to the maximum threshold of solid transport in North Africa assumed to be at 5000 tonne/km²/year [8].

References

1. Tixeront, J.: Débit solide des cours d'eau en Algérie et en Tunisie. In: General Assembly of Helsinki, 25 July–5 August 1960, IAHS Publication n° 53, 26–42 (1960)
2. Sogrèah, S.: Société Grenobloise d'études et d'applications hydrauliques, 1969. Etude générale des aires d'assainissement agricole en Algérie. Dossier, Ministère de l'agriculture et de la réforme agraire, Algérie (1969)
3. Khanchoul, K.: Quantification de l'érosion et des transports solides dans certains bassins versants de l'extrême Nord-est algérien, Thèse de Doctorat d'état en Géologie (2006)
4. Achite, M.: Methodology for the computation of normal annual yield of suspended sediments from rivers: case of the wadi Abd basin of Northern Algeria. In: Singh, V.P., Xu, Y.J. (eds.) Proceedings of the AIH 25th Anniversary Meeting & International Conference «Challenges in Coastal Hydrology and Water Quality», pp. 175–182 (2006)
5. Borsali, A.H., Bekki, A., Hasnaoui, O.: Aspect hydrologique des catastrophes naturelles: «inondation, glissement de terrains» Etude de cas : Oued Mèkerra (Sidi Bel Abbès) Communiqué du compte rendu des XXIIIème rencontres universitaires de génie civil: Risque et environnement (2005)
6. Sourisseau, B.: Etude hydrogéologique de la plaine de Sidi Bel Abbès, Ministère des Ressources Hydrauliques (1975)
7. Agence Nationale des Ressources Hydrauliques d'Oran, «Bassin versant de la MACTA», Synthèse Bibliographique inventaire des données (1996)
8. Walling, D.E.: The sediment yields of African rivers. IAHS, Publication n° 144, pp. 265–283 (1984)

Major and Trace Element Distribution in Suspended Particulate Matter and Sediments of the Tropical River Estuary (South Vietnam)

Sofia Koukina and Nikolay Lobus

Abstract

Al, Fe, Ti, Li, Zn, Pb, U, Sc, Sn, Bi, Zr, Ba, As, Sr, W, V, Co, Cu, Ni, Mo, Cr, Mn, Ba, Sn, Sb, Ag, organic (TOC) and carbonate (TIC) carbon contents in suspended particulate matter (SPM) and sediments were measured along the salinity gradient in the Cay River–Nha Trang Bay estuarine system in dry season. Most trace element contents were at natural levels. Particulate metals were characterized by the most significant loss in the frontal zone of the estuary with the highest horizontal gradients within the salinity interval of 0–8–20‰. Sedimentary metals were largely controlled by the accumulation of their most fine-grained host minerals in the sea floor depression. The calculation of the enrichment coefficient ($K_{SPM/Sed}$) revealed associations of elements with a similar geochemical behaviour. Ti, Ca, Zr, Sb and W ($K_{SPM/Sed} \ll 1$) are primarily accumulated in estuarine sediments. Co, Cu, Ni, and Mo ($K_{SPM/Sed} \gg 1$) are removed out of the estuarine zone with surface water layer SPM. Al, Fe, Mn, Li, V, Zn, Sr, Sn, Cs, Bi, Pb and U ($K_{SPM/Sed} \cong 1$) are most likely controlled by their clay host minerals abundant in both sediments and SPM.

Keywords

South China Sea • Nha Trang Bay • Trace elements • Sediments • Suspended particulate matter

1 Introduction

The Cai River–Nha Trang Bay estuarine system of the South China Sea is now exposed to multiple anthropogenic stressors such as human settlement, agriculture and aquaculture, tourism and transport [1]. Over the past two decades, several

S. Koukina (✉) · N. Lobus
Shirshov Institute of Oceanology, Russian Academy of Sciences,
Nahimovskiy pr. 36, 117997 Moscow, Russia
e-mail: skoukina@gmail.com

studies of the organic geochemistry patterns and contamination levels and trends in the Nha Trang Bay have been undertaken [1, 2]. The present work studies major and trace elements enrichment in both SPM and sediments and their potential settling into the estuary due to its salinity gradient.

2 Materials and Methods

The SPM and sediment samples were collected in July 2013 along the salinity gradient at eight locations according to standard clean techniques [1]. The elemental analysis of the samples was carried out on the TOC 5000-V-CPH Analyser (Shimadzu Co., Japan) and X-7 ICP-MS spectrometer (Thermo Scientific, USA) [1, 2].

3 Results

3.1 Major and Trace Elements in Surface SPM

The Cai River estuarine suspended particulate matter (SPM) has higher Co, Cu, Ni, As, Mo, Pb, Bi, W and U with respect to Average World River SPM (WRSPM) (Table 1). The distribution of particulate form of Al, Fe, Ti, Li, Zn, Pb, U, Sc, Sn, Bi, Zr, Ba, As, Sr, W, V and Ag followed the distribution of total suspended matter and was characterized by a maximum in the river water and then a sharp decrease seawards of element relative concentration (in $\mu\text{g l}^{-1}$) with the highest horizontal gradients within the salinity interval of 8–20‰. The absolute concentration of these elements (in $\mu\text{g g}^{-1}$ of the dry suspended particulate matter weight) was elevated in both the riverine and transitional waters (0–20‰). The distribution of particulate form of Co, Cu, Ni, Mo and Cr and, to a lesser extent, Mn, Ba, Sn, Sb and Hg is characterized by the most significant loss in the frontal zone of the estuary. Both relative (in $\mu\text{g l}^{-1}$) and absolute (in $\mu\text{g g}^{-1}$ of the dry particulate matter weight) concentrations

Table 1 Major and trace element contents in SPM and sediments (in $\mu\text{g g}^{-1}$, except for Al, Fe, Ti, Mn, Ca, organic carbon and inorganic carbon in % of dry weight)

El	SPM	Sed	$K_{\text{SPM/Sed}}$	WRSPM [3]	WRSed [3]	Pel clay [4]
Al	9.2	10.8	0.9	8.63	4.3	8.4
Fe	3.26	3.98	0.8	5.03	2.5	6.5
Ti	0.09	0.36	0.3	0.39	0.31	0.46
Mn	0.05	0.04	1.3	0.12	0.05	0.67
Ca	0.49	1.26	0.4	2.6	1.7	1.0
Li	37	47.9	0.8	35	20	57
V	88.5	89.3	1.0	120	50	120
Cr	90.2	45.8	2.0	85	50	90
Co	68.4	8.5	8.0	19	15	74
Ni	153	23.2	6.6	50	25	230
Cu	105	18.5	5.7	45	20	250
Zn	79.8	104.6	0.8	130	60	170
As	41	22.2	1.8	14	6	20
Sr	119	145	0.8	150	150	180
Zr	17.2	85.2	0.2	150	250	150
Mo	20.1	3.0	6.7	1.8	1.5	27
Ag	0.2	0.1	2.0	–	0.1	0.11
Sn	5.9	5.9	1.0	2.9	4.0	4.0
Sb	0.7	1.2	0.6	1.4	2.0	1.0
Cs	9	11.1	0.8	5.2	4.0	6.0
Ba	193	274	0.7	500	290	2300
Pb	62.7	54.4	1.2	25	15	80
Bi	7.9	9.5	0.8	0.3	0.2	0.53
U	5.7	6.6	0.9	2.4	3	2.6
W	5.3	10.4	0.5	1.4	0.4	0.42
TOC	1.30	1.36	–	–	1.4	–
TIC	0.43	1.49	–	–	0.4	–

of these elements sharply decrease with the highest horizontal gradients at the initial salinity rise (0–8‰).

3.2 Major and Trace Elements in Surface Sediments

Mean content of the major part of the studied trace elements (Li, V, Cr, Co, Ni, Cu, Zn, As, Sr, Zr, Mo, Cd, Sn, Sb, Cs, Ba and Pb) in the sediments from the Cai River estuary and Nha Trang Bay is lower than, or corresponds to, the reference values for pelagic clays and the Average World Riverbed Sediments (WRSed) (Table 1) [3, 4].

Normalized (to Al) sedimentary Fe, Ti, Li, Sc, Co, Cs, Zr, Cr, Zn, Co, Ni, Cu, Pb, Sn, V, As, U and Mo varied in relatively narrow ranges. The major part of these elements tended to increase seawards with an elevation at heightened carbonate content. Sedimentary Bi and W decreased from

river to the sea. The distribution of Sr and Ca and, to a lesser extent, of Mn and Ba was largely controlled by the total inorganic carbon content in the sediments.

3.3 Element Distribution Between Particulate and Sedimentary Phases

The enrichment factor ($K_{\text{SPM/Sed}}$) calculated as a ratio of mean element contents in particulate matter and sediments revealed associations of elements that are characterized by a similar geochemical behavior (Table 1). Ti, Ca, Zr, Sb and W ($K_{\text{SPM/Sed}} \ll 1$) are primarily accumulated in estuarine sediments. Co, Cu, Ni, and Mo ($K_{\text{SPM/Sed}} \gg 1$) are removed out of the estuarine zone with surface water layer suspended particulate matter. Al, Fe, Mn, Li, V, Zn, Sr, Sn, Cs, Bi, Pb and U ($K_{\text{SPM/Sed}} \cong 1$) are most likely controlled by the clay host minerals abundant in both sediments and suspended

particulate matter. Along the salinity gradient, $K_{SPM/Sed}$ decreased from river to the sea for most of the elements that were studied.

4 Discussion

In the stratified Cai River estuary, the coarsest river material enriched in detrital minerals is deposited where the river flow velocity decreases sharply, influenced by the dam. The most significant losses of suspended elements occurred in the frontal to transitional zone of the estuary (0–20‰) by an intensive sedimentation of dissolved and suspended river material. However, the significant part of the particulate trace elements may be carried out seawards with the surface water layer. In the marine part of the estuary, most of the fine-grained material of surface water layer enriched in clay minerals, carbonates and trace metals is deposited. The particulate organic matter of terrigenous and/or planktonogenous origin may contribute to trace element accumulation in SPM in the bay. Calculation of the enrichment coefficient $K_{SPM/Sed}$ supports accumulation of Ti, Ca, Zr, Sb and W ($K_{SPM/Sed} \ll 1$) in the estuary in the sedimentary phase. On the contrary, Co, Cu, Ni, and Mo ($K_{SPM/Sed} \gg 1$) are removed out of the estuarine zone in the particulate phase with surface water layer.

The observed distribution of the normalized trace element contents in sediments reflects the association with and/or the inclusion of Fe, Ti, Li and most trace elements in the lattices of clay minerals that constitute the bulk of the fine-grained sedimentary material accumulated in the sea floor depression in the bay [1]. Some elements (Bi and W) may be associated with the coarsest river material enriched in detrital minerals which is mostly deposited in the riverine part of the estuary. Carbonate carbon is a major carrier for Ca, Sr, Ba and Mn, while organic carbon showed no affinity to the other major or trace elements that were studied.

5 Conclusions

The major part of the studied trace elements was at natural levels. The particulate major and trace elements were characterized by a massive removal from the water column in the frontal to transitional zone (0–20‰) of the estuary. Sedimentary metals were largely controlled by the accumulation of their fine-grained aluminosilicate host minerals in the bay (32–36‰). The calculation of the enrichment coefficient ($K_{SPM/Sed}$) revealed associations of elements that are characterized by a similar geochemical behavior. Ti, Ca, Zr, Sb and W ($K_{SPM/Sed} \ll 1$) are primarily accumulated in estuarine sediments. Co, Cu, Ni, and Mo ($K_{SPM/Sed} \gg 1$) are removed out of the estuarine zone with surface water layer SPM. Al, Fe, Mn, Li, V, Zn, Sr, Sn, Cs, Bi, Pb and U ($K_{SPM/Sed} \cong 1$) are most likely controlled by their clay host minerals abundant in both sediments and suspended particulate matter.

This research was performed in the framework of the state assignment IO RAS (theme No. 0149-2018-0005).

References

1. Koukina, S.E., Lobus, N.V., Peresykin, V.I., Dara, O.M., Smurov, A.V.: Abundance, distribution and bioavailability of major and trace elements in surface sediments from the Cai River estuary and Nha Trang Bay (South China Sea, Vietnam). *Estuar. Coast. Shelf Sci.* **198**, 450–460 (2017)
2. Lobus, N.V., Peresykin, V.I., Shulga, N.A., Drozdova, A.N., Gusev, E.S.: Dissolved, particulate, and sedimentary organic matter in the Cai River basin (Nha Trang Bay of the South China Sea). *Oceanology* **55**(3), 339–346 (2015)
3. Savenko, V.S.: Chemical composition of World River's suspended matter. GEOS, Moscow (2006)
4. Li, Y.H.: Distribution patterns of the elements in the ocean. *Geochim. Cosmochim. Acta* **55**, 3223–3240 (1991)

Mobility of Metallic Trace Elements in Surface Waters and Sediments: Case of the Nil Wadi (Jijel, North-East Algeria)

Siheem Benessam, Taha-Hocine Debieche, Souad Amieur, Amal Chine, and Smaïl Khelili

Abstract

The Metallic Trace Elements (MTEs) occur in the waters and sediments of wadis with low concentrations. Their mobility is controlled by several physico-chemical parameters (Eh, pH and dissolved oxygen). To determine the effect of these factors on the concentration and mobility of metallic trace elements (Cd, Cr, Cu, Fe, Pb and Zn), bimonthly monitoring of physico-chemical parameters was conducted during the period from November 2013 to January 2015. The results obtained show that the MTEs are very influenced by the variations of the pH and Eh. Under natural conditions, neutral to basic pH and oxidizing medium, only lead is present in waters with high values, indicating its solubility in water and its release of sediments. Other MTEs have high concentrations in sediments, indicating their adsorption and/or chemical precipitation trapping qualities. The spatial monitoring of these MTEs shows the effect of the confluence of the wadi with its tributaries on the variation of its concentrations.

Keywords

Chemistry • Water • Sediment • Metallic trace elements • Nil wadi • Algeria

S. Benessam · T.-H. Debieche (✉) · S. Amieur · A. Chine
 Laboratory of Geological Engineering, Research Team of Water and Environment, Faculty of Nature and Life Sciences, University of Mohamed Seddik Benyahia—Jijel, B.P. 98 Ouled Aissa, 18000 Jijel, Algeria
 e-mail: debieche@yahoo.fr

S. Benessam
 Department of Chemistry, Faculty of Exact Sciences and Computer Science, University of Mohamed Seddik Benyahia—Jijel, B.P. 98 Ouled Aissa, 18000 Jijel, Algeria

S. Khelili
 Laboratory of Pharmaceutical Chemistry, Pharmacology and Ecotoxicology, Faculty of Exact Sciences and Computer Science, University of Mohamed Seddik Benyahia—Jijel, B.P. 98 Ouled Aissa, 18000 Jijel, Algeria

1 Introduction

The physicochemical composition of natural waters is mainly related to the geological nature. The anthropogenic discharges (urban, industrial and agricultural) modify these waters considerably, especially when the rejections have not been previously treated.

Several researches in the world [1, 6, 7] and in Algeria [2, 3, 5] have been carried out on this subject and showed the effect of anthropic activities on the quality of water (superficial and underground).

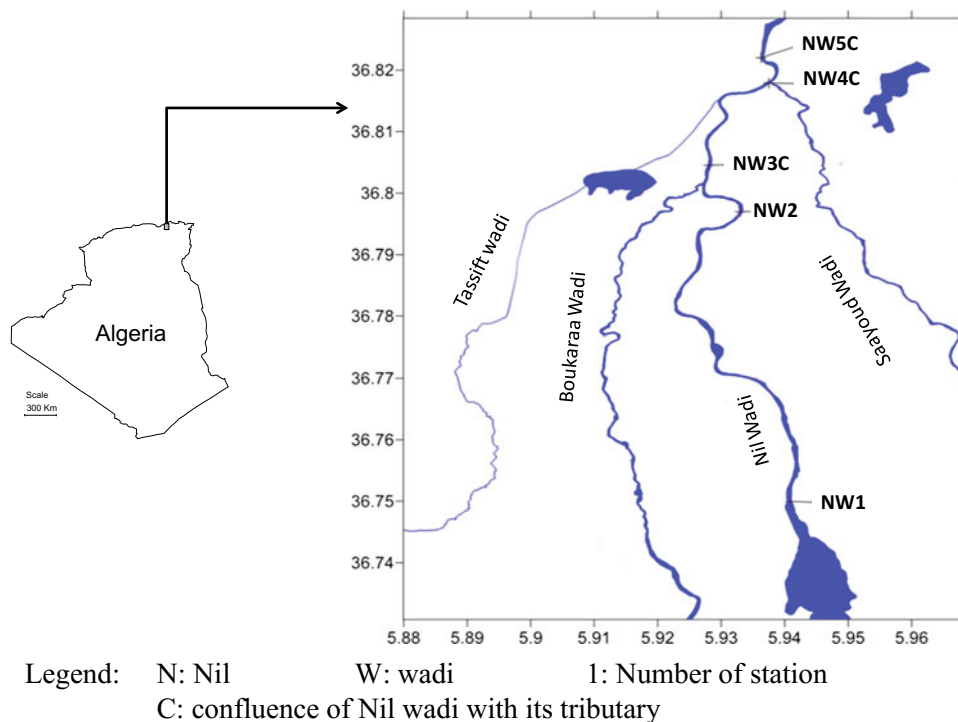
Since 2000, the Nil wadi region has witnessed significant demographic, agricultural and industrial growth. This has resulted in an increase in water demand and discharges. In order to determine the effect of these on the water quality of the Nil wadi, this research work was conducted. Its objectives are to determine the concentrations of metallic trace elements (Cd, Cr, Cu, Fe, Pb and Zn) in waters and sediments of the Nil wadi and their mobility as a function of physicochemical conditions.

2 Materials and Methods

Five sampling stations were chosen to carry out the spatial monitoring of metallic trace elements in the Nil wadi. The first point was positioned upstream of the plain to determine the initial state of the wadi, and the others before and after the confluence of the main Nil wadi with its three tributaries (Fig. 1).

Four physico-chemical parameters (T, pH, Eh, conductivity) were measured in situ using the multiparameter 350i (WTW). The samples taken are kept at a temperature of 4 °C away from light. The analyzes of the metallic trace elements (Cd, Cr, Cu, Fe, Pb and Zn) were made in the laboratory using the SHIMADZUAA-6200 atomic absorption spectrometer (AAS) with the exception of the iron which has been analyzed by an ODYSSEY spectrophotometer.

Fig. 1 Positioning of the sampling stations



The choice of these ETMs is related to the availability of measuring devices of these elements in the laboratory.

3 Results

3.1 Spatial Evolution of Physicochemical Parameters

The MTEs evolution shows high initial concentrations at the NW1 station, indicating a contribution of these from the catchment area of the Nil Wadi water. The confluence of the Nil Wadi with its tributaries shows: an increase in concentrations of copper and lead after its confluence with the Boukaraa wadi, an increase of zinc and copper and a decrease in lead after its confluence with the Tassift wadi, an increase in zinc and copper and a decrease in lead and cadmium after its confluence with the Saayoud wadi.

This evolution shows that the origin of the MTEs in the Nil Wadi is related to the geological nature of the catchment area of the Nil Wadi as well as to anthropic inputs.

To compare our results, we used the Water Quality Assessment System for Watercourses (SEQ-Water) [8], because there is no Algerian directive for surface water. The cadmium, Copper and lead have concentrations higher than the standard (consecutively 0.00037, 0.0025 and

0.01 mg/L). Zinc has concentrations below the standard (0.052 mg/L) but chromium has concentrations below the standard (0.07 mg/L) in stations NW1,2,3C and higher in stations NW4C,5C. For iron, there is no value within the standard.

3.2 Water–Sediment Exchange of Metallic Trace Elements

The analysis of the water-sediment relation is present in Fig. 2.

The average concentrations of the 5 metallic trace elements (cadmium, lead, copper, zinc and chromium) show that lead concentrations in water and sediments are comparable, indicating the possibility of ion exchange between sediments and water. On the other hand, the other metallic trace elements have high concentrations in the sediments compared to the water, which can indicate that these chemical elements tend to be adsorbed by the sediments of the wadi bed [4].

The spatial evolution of MTEs in sediments shows a decrease in concentration from upstream towards downstream for all MTEs, with the exception of cadmium increasing downstream, which may indicate an anthropogenic origin.

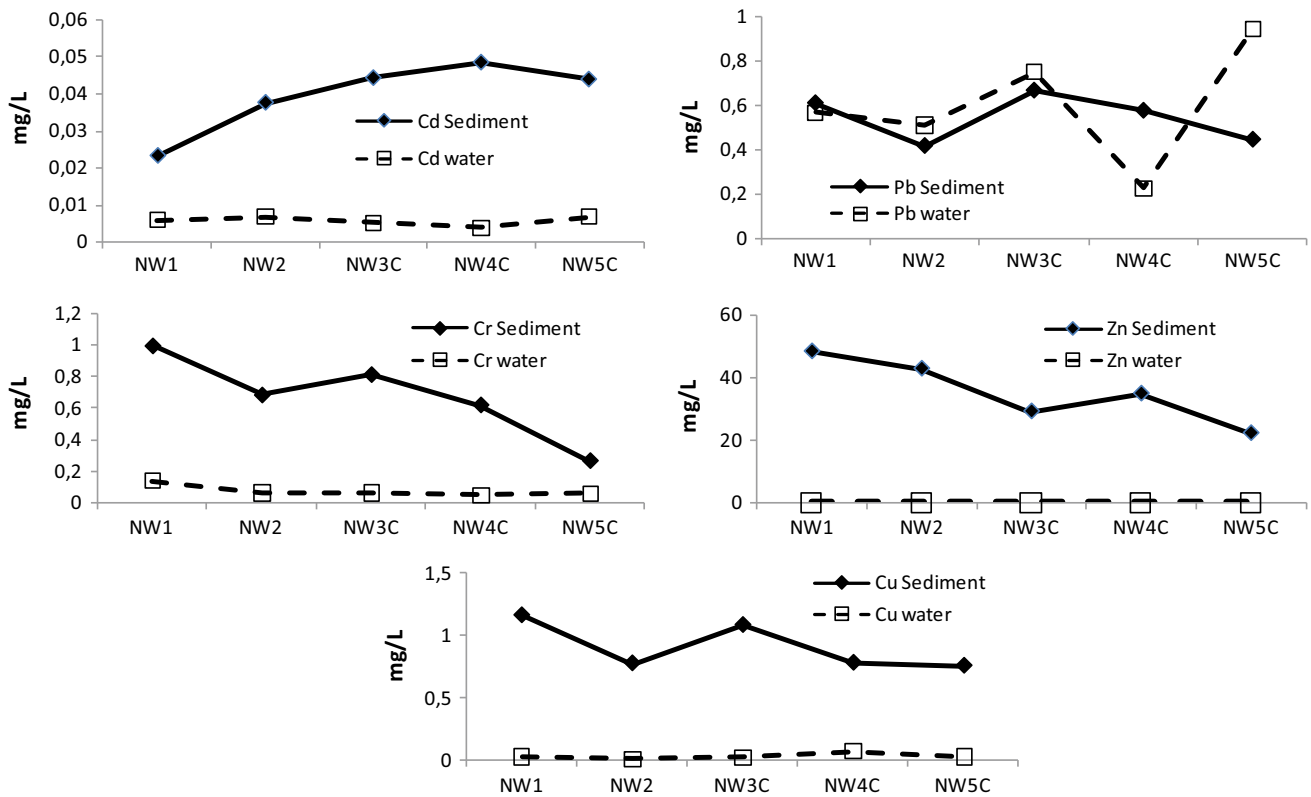


Fig. 2 Water-sediment exchange of metallic trace elements

4 Conclusions

This study shows the presence of MTEs (Cd, Cr, Cu, Fe, Pb and Zn) in the Nil Wadi waters and sediments with concentrations that exceed the surface water standard (SEQ-Water) for lead, Copper and cadmium. It also shows the effect of physicochemical conditions (pH and Eh) on MTE mobility and ion exchange between water and sediments.

References

1. Baran, N., Mouvet, C., Négrel, Ph: Hydrodynamic and geochemical constraints on pesticide concentrations in the groundwater of an agricultural catchment (Brévilles, France). *Environ. Pollut.* **148**, 729–738 (2007)
2. Benrabah, S., Bousnoubra, H., Kherici, N., Cote, M.: Characterization of the water quality of West Kebir Wadi (North-East Algeria). *Rev. Sci. Technol. Synthèse* **26**, 30–39 (2013)
3. Bougherira, N., Hani, A., Djabri, L., Toumi, F., Chaffai, H., Haied, N., Nechem, D., Sedrati, N.: Impact of urban and industrial waste water on surface and groundwater, in the region of Annaba (Algérie). *Energy Proc.* **50**, 692–701 (2014)
4. Burmol, A., Duro, L., Grive, M.: Recommendation for the modeling of trace metal transfers in soils and groundwater. Methodological guide. INERIS, 119p (2006)
5. Debieche, T.H., Mania, J., Mudry, J.: Species and mobility of phosphorus and nitrogen in a wadi-aquifer relationship. *J. Afr. Earth Sc.* **37**, 47–57 (2003)
6. Duh, J.D., Shandas, V., Chang, H., George, L.A.: Rates of urbanization and the resiliency of air and water quality. *Sci. Total Environ.* **400**(1–3), 238–256 (2008)
7. Jarvie, H.P., Neal, C., Withers, P.J.A., Robinson, A., Salter, N.: Nutrient water quality of the Wye catchment, UK: exploring patterns and fluxes using the environment agency data archives. *Hydrol. Earth Syst. Sci.* **7**(5), 722–743 (2003)
8. MEDD and Water Agencies.: Water quality assessment system for watercourses (SEQ-Eau), Evaluation Grid version 2, 40p (2003)

Snowmelt Runoff Simulation During Early 21st Century Using Hydrological Modelling in the Snow-Fed Terrain of Gilgit River Basin (Pakistan)

Yasir Latif, Yaoming Ma, Weiqiang Ma, Muhammad Sher, and Yaseen Muhammad

Abstract

The indispensable water supply of major reservoirs in Pakistan, essentially depends on meltwater runoff, mainly generating from the Upper Indus Basin (UIB). The present study includes snowmelt runoff simulation within Gilgit River, basin a sub basin of UIB. Snowmelt runoff model (SRM) incorporated with MODIS remote sensing snow cover products, was selected to simulate the daily discharges and to calculate the contribution of snowmelt impact on the discharge within Gilgit River basin, during the early 21st century (first decade). Our results revealed a Nash–Sutcliffe efficiency (NSE) as R^2 (0.81) and average volume difference as D_V (−0.51) in observed and simulated flow. Almost 9.2% of the total basin area is covered by glacier and permanent ice cover which contributes to the river runoff during summer. We also noted that the observed efficiency of the model becomes uncertain during high flow months such as June, July and August, such ambiguity during summer was attributed to glacier-melt runoff, which generates in August by the melting of glaciers.

Y. Latif (✉) · Y. Ma · W. Ma
Key Laboratory of Tibetan Environment Changes and Land Surface Processes, Institute of Tibetan Plateau Research, Chinese Academy of Sciences, Beijing, 100101, China
e-mail: yasir.latif@uaf.edu.pk

Y. Ma
CAS Center for Excellence in Tibetan Plateau Earth Sciences, Chinese Academy of Sciences, Beijing, 100101, China

Y. Latif · Y. Ma · W. Ma
University of Chinese Academy of Sciences, Beijing, 100049, China

M. Sher
Institute of International Rivers and ECO-Security, Yunnan University, Kunming, China

Y. Latif
University of Agriculture Faisalabad, Faisalabad, Pakistan

Y. Muhammad
Centre for Integrated Mountain Research, University of the Punjab, Lahore, Pakistan

Keywords

Runoff · Gilgit river basin · Climate change · MODIS snow cover products · SRM

1 Introduction

The objective of the present study is to evaluate the current climate change impacts on river flows regarding temperature, precipitation and stream flows, using (Snowmelt Runoff Model) over the Gilgit river basin in the light of recently collected data. The average daily precipitation and mean temperature at the Gilgit observatory, and the stream flows data observed at Gilgit River were collected through Pakistan Metrological Department (PMD) and Water and Power Development Authority (WAPDA), respectively. Previous hydrological modelling studies [2, 5, 6, 7, 13] were based on the variability and uncertainties in the modelling, while some of them were biased due to some reasons, such as over and under estimation of area and precipitation, snow melt rates, temperature lapse rate and being restricted to few years' data only [8]. The SRM is designed to simulate river flows in the snow-fed basins, when this model is used in such a basin, covered by glaciers and permanent ice sheets, the model's accuracy would become questionable due to the glacier's contribution to runoff. According to Hasson et al. [3], around 15–80% of Gilgit basin area was covered with snow during 2001–2012. We considered this area as a constant fraction to estimate error-free runoff for the Gilgit river basin. The major reason for considering a persistent glaciers cover, is that the Moderate Resolution Imaging Spectroradiometer (MODIS) does not capture most of the glacier cover, mainly the lower and debris cover part due to low albedo. Also, the glacier area changes very slowly with respect to time, and the error in frequent (daily/monthly) glacier cover area change may exceed the actual change in glacier cover area. These results can be used for local and regional planning of water resources sections and will be

helpful enough for policy makers to select optimum strategies related to water management.

2 Materials and Methods

One of the broadly applicable models to simulate and forecast daily stream flows in the high-altitude catchments is the (Snowmelt Runoff Model) designed by Martinec [10]. Previously, it has been applied to evaluate the effect of climate change in the Hunza River Basin [13]. They also reported that SRM can be used efficiently in the snow and glacier fed catchments of UIB. The MODIS snow products are provided as a sequence of products, commencing with a swath product, developing through a spatio-temporal transformation to an eight-day global gridded product [5]. Snow cover products derived from MODIS are based on two bands i.e. band 4 (Green) (0.545–0.565 μm) and band 6 (infrared) (1.628–1.652 μm). The Normalized Difference Snow Index (NDSI) is calculated by these two bands as

$$\text{NDSI} = (\text{Band4} - \text{Band6}) / (\text{Band4} + \text{Band6})$$

3 Results

We have calculated the snow-covered area (SCA) for the Gilgit River basin and revealed that the accumulation of seasonal snow starts in the month of September of a year, reaches its maximum level in March of the following year, and continues to recess from April of that year (Fig. 1). By the end of July, most of the seasonal snow covers melt away. We also observed the snow cover trend, which seemed to be stable or marginally increasing during (Apr–Sep) for the period of the early 21st century. We have shown trends of precipitation and temperature within the Gilgit basin in

Fig. 1 Cumulative depletion curves (CDC) values during (2001–2015) in GRB

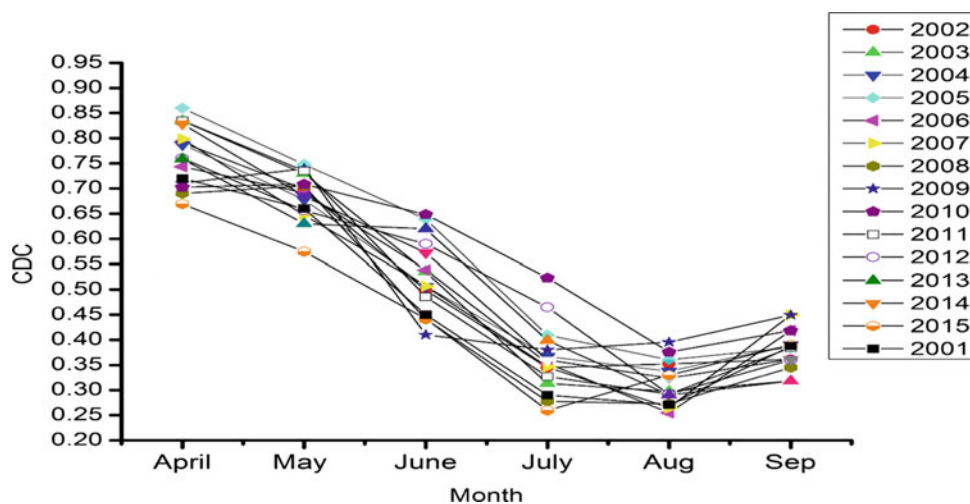


Fig. 2. Yasin and Ushkore stations, being in the high-altitude region, showed maximum precipitation and minimum temperature, amongst all of the stations, annually and seasonally. Maximum monthly precipitation was recorded during April (45 mm) and followed by December (37 mm) during (2001–2012). Similarly, maximum annual and summer precipitation for all of the stations was recorded for the year 2010, as for winter maximum precipitation, it was recorded during 2009.

We have applied SRM zone wise within the GRB for 12 hydrological years during the extreme discharge period (Apr–Sep) as shown in Fig. 3. Our Nash-Sutcliffe Efficiency (NSE) coefficient value ranged above 0.80 except in the years 2007 and 2008.

4 Discussion

- (1) Increasing snow cover within the Gilgit basin might be attributed to increasing winter precipitation as discussed by [11, 9] at the Gilgit station during 1961–2013. Similar findings of increasing snow cover trends during summer were revealed by Tahir et al. [14] during (2001–2010) within the Hunza basin. Recently, [4] reported a decreasing snow cover within all UIB sub-basins, except for the Gilgit basin during (2001–2012). These results are completely consistent with our increasing snow cover trends for the same region. The snow cover is directly linked with the snow amount as discussed by Hasson et al. [3]. They established a smooth relationship with the slope and snow accumulation. They also suggested that the high slopes of the Gilgit basin exhibit less accumulation, because new snow cannot stay longer at such a steeper angle. Our results are partially in line with such a supposition, because the mountains of the Gigit basin are not as high

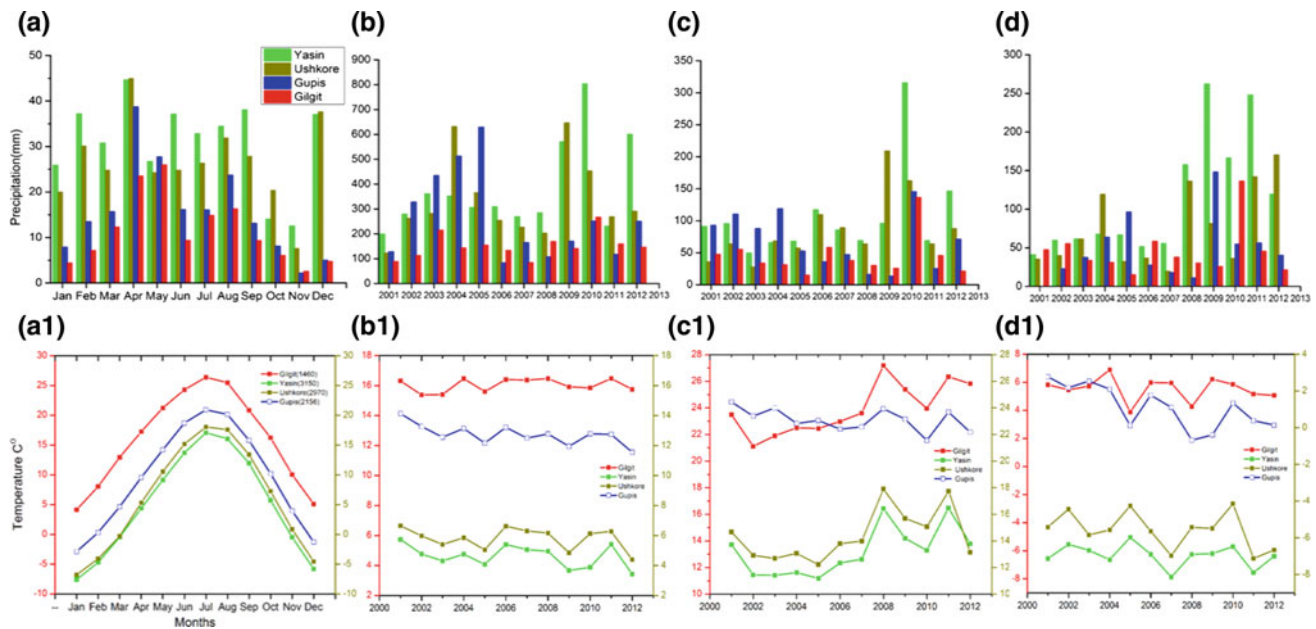


Fig. 2 Precipitation and Temperature of climatic stations in the Gilgit River Basin: **a** monthly, **b** annual, **c** summer, **d** winter, **a1** monthly mean, **b1** annual mean, **c1** summer mean, **d1** winter mean

as the Hunza basin ones. So, the increasing snow cover might be attributed to the increasing precipitation [11].

- (2) The calculation of snow and glacier contribution is the most important part of the model application within a snow fed basin. The flows are generated during (June–Sep) from the glaciers and snow packs, including seasonal snow, perennial snow and ice covers. The discharge within the Gilgit river basin is mainly attributed to snowmelt, followed by glacier melt and rainfall [1]. Our findings are consistent with the results of these authors, because we also noted the same contribution of discharge essentially depending upon snowmelt followed by glacier melt and rainfall.
- (3) We have noted that, during three years 2006, 2007 and 2008, flows during May were quite higher as compared to the rest of the year. Therefore, the NS coefficient was lower and curves could not be matched correctly. Despite these high discharges during May, the model performed quite better and efficiency remained acceptable. The underestimation of high summer discharge leads to the possibility of glacier melt contribution to flow as compared to snowmelt. During summer, precipitation of the catchment does not cause high flows resulting in peaks but temperature goes suddenly higher resulting in more snow and glacier melt. Due to this reason, the model becomes less efficient. During early April and May, the NS was higher and we observed less over and underestimation of flow. The efficiency of the model will become questionable, when an abrupt change occurs during the melt season, especially in the

month of May. The seasonal snow at an elevation less than 3500 m starts melting in May causing high flows, although the second pulse generated during June due to withdrawing of 0°C isotherm over high altitudinal zones [12]. We have also noted that each year multiple peaks generate during summer.

5 Conclusion

We noted, for the month of August and September, that the simulated flows were highly efficient. We have also observed that the model's efficiency largely depends upon the snow cover data as basic inputs, and it is likely to be less affected by the precipitation as discussed by Tahir et al. [13]. The snow cover over the Gilgit basin has increased slightly during the early 21st century. Our results showed an increasing trend of flows at the Gilgit River in the future. Therefore, the water policy should be planned according to this distressing situation and much larger capacity dams and reservoirs will be needed in future for flood control and hydropower production. The available larger capacity dams in Pakistan (Tarbela and Mangla) have already been affected by silt accumulation and are unable to provide storage and electricity according to the current requirement. The further improvement of SRM needs an extended knowledge of glaciers, field observations and glacier mass balance studies. Our knowledge of glacier and snow cover dynamics over UIB requires extensive field data and surplus of snow depth

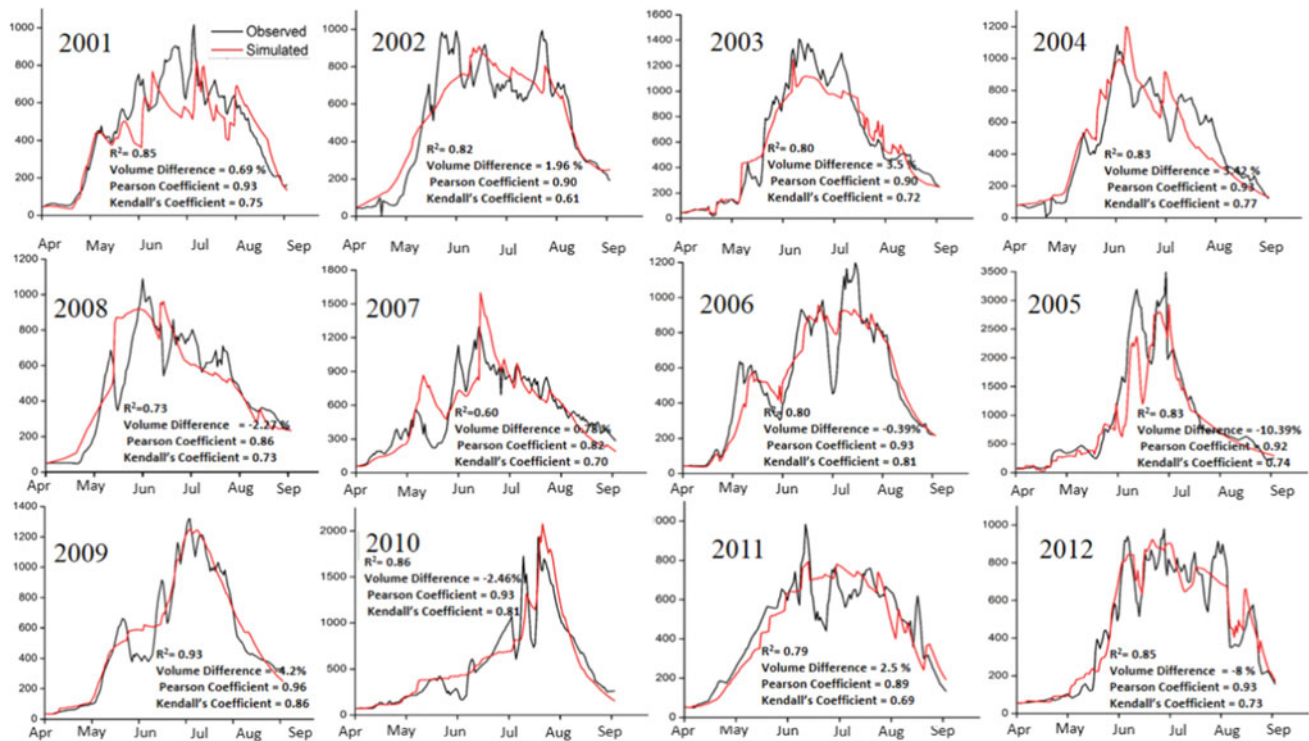


Fig. 3 Hydrographs showing Observed (gauged) and measured (model) discharge during 2001–2012

data at high altitudes in order to completely understand the hydrology of this region. Particularly, the Temperature Lapse Rate (TLR) is highly sensitive for the model's accuracy. TLR could be recorded precisely by installing temperature data loggers in the high-altitude region to get more detailed results in monthly or hourly temperature variation with respect to height.

References

- Adnan, M., Nabi, G., Saleem, P., Ashraf, A.: Snowmelt runoff prediction under changing climate in the Himalayan cryosphere: a case of Gilgit River Basin. *Geosci. Front.* **8**, 941–947 (2016)
- Butt, M., Bilal, M.: Application of snowmelt runoff model for water resource management. *Hydrological Process* **25**, 3735–3747 (2011)
- Hasson, S., Lucarini, V., Khan, M., Petitta, M., Bolch, T., Gioli, G.: Early 21st century Snow cover state over 5 the western river basins of the Indus River system. *Hydrol. Earth Syst. Sci.* **18**, 4077–4100 (2014). <https://doi.org/10.5194/hess-18-4077-2014>
- Hasson, S., Böhner, J., Lucarini, V.: Prevailing climatic trends and runoff response from Hindukush–Karakoram–Himalaya, upper Indus basin. *Earth Syst. Dyn. Discuss.* **6**, 579–653 (2015)
- Immerzeel, W., Droogers, P., De Jong, S.M., Bierkens, M.F.P.: Large-scale monitoring of snow cover and runoff simulation in Himalayan river basins using remote sensing. *Remote Sens. Environ.* **113**, 40–49 (2009)
- Immerzeel, W.W., Van Beek, L.P.H., Bierkens, M.F.P.: Climate change will affect the Asian water towers. *Science* **328**, 1382–1385 (2010)
- Immerzeel, W.W., Pellicciotti, F., Bierkens, M.F.P.: Rising river flows throughout the twenty-first century in two Himalayan glacierized watersheds. *Nat. Geosci.* **6**, 742–745 (2013)
- Khan, A.: Hydrological modelling and their biases: constraints in policy making and sustainable water resources development under changing climate in the Hindukush-Karakoram-Himalayas. Brief for GSDR (2015)
- Latif, Y., Yaoming, M. and Yaseen, M.: Spatial analysis of precipitation time series. *Theor. Appl. Climatol.* **131**, 761–775 (2016). <https://doi.org/10.1007/s00704-016-2007-3>
- Martinez, J.: Snowmelt-Runoff model for stream flow forecasts. *Nord. Hydrol.* **6**, 145–154 (1975)
- Minora, U., Bocchiola, D., D'Agata C., Maragno, D., Mayer, C., Lambrecht, A., Mosconi, B., Vuillermoz, E., Senese, A., Compostella, C., Smiraglia, C., and Diolaiuti, G.: 2001–2010 glacier changes in the Central Karakoram National Park: a contribution to evaluate the magnitude and rate of the “Karakoram anomaly”. *Cryosphere Discuss.* **7**, 2891–2941(2013)
- Mukhopadhyaya, B., Khan, A.: Rising river flows and glacial mass balance in central Karakoram. *J. Hydrol.* **513**, 192–203 (2014)
- Tahir, A., Chevallier, P., Arnaud, Y., Neppel, L., Ahmad, B.: Modeling snowmelt-runoff under climate change scenarios in the Hunza River basin, Karakoram Range, Northern Pakistan. *J. Hydrol.* **409**, 104–111 (2011)
- Tahir, A.A., Chevallier, P., Arnaud, Y., Ashraf, M., & Bhatti, M.T.: Snow cover trend and hydrological characteristics of the Astore River basin (Western Himalayas) and its comparison to the Hunza basin (Karakoram region). *Sci Total Environ.* **505**, 748–761 (2015)

The Importance of Wetlands and Unhealthy Water Bodies in the Distribution of Malaria in Spain

Arturo Sousa, Leoncio García-Barrón, Mónica Aguilar-Alba, Mark Vetter, and Julia Morales

Abstract

Malaria is one of the infectious diseases with the highest number of cases worldwide. It has always been linked to aquatic environments, since these can be a necessary reservoir for the anophelines that transmit the disease. This study analyses the role that unhealthy water bodies have played, since the early 20th century, in the most endemic and/or prevalent foci of malaria in Spain. Western Andalusia was the region with the largest surface of unhealthy water bodies and wetlands. The desiccation of much of the continental waters contributed to its eradication.

Keywords

Malaria foci • Water bodies • Wetlands • Spain • Spatial analysis

1 Introduction

Aquatic environments constitute, in many cases, an essential reservoir for the reproduction of female mosquitoes of the genus *Anopheles*. These vectors can transmit, through their sting, the parasite *Plasmodium*, which is responsible for malaria. Some studies [1] link the decrease of malaria in the United Kingdom, in the late 19th century, to the reduction of wetlands. In the particular case of Spain, autochthonous malaria was officially declared eradicated by the World Health Organization in 1964 [2].

The aim of this interdisciplinary study was to analyze the data from different sources to generate a global perspective of the importance that unhealthy water bodies had, in the prevalence and/or endemicity of malaria in Spain, in the early 20th century. Nowadays, autochthonous malaria is being fought in countries where it is still endemic, and experts are discussing the risk of the re-emergence of this disease (especially that of introduced malaria), associated with large demographic movements and climate change [3].

2 Materials and Methods

Malaria is a notifiable infectious disease. Therefore, in the Documentary Archives of the Spanish Statistical Institute (INEbase), there are files with annual reports for the whole of Spain from the year 1900 with data about the number of deaths and people infected, separated by province [4]. Moreover, the yearbooks INEbase 1915 and INEbase 1917 provide information, at the regional level, about the disease and other economic and environmental variables. These data are from the advance-summary of statistical data about paludism in 1913 and 1916, in Spain, which were published in the environmental health inspection yearbooks of 1915 and 1917 (Spanish Directorate General of Agriculture). These two yearbooks clarify that paludism “foci” surface refers to waterlogged terrains that need to be sanitized to

A. Sousa · J. Morales (✉)
Department of Plant Biology and Ecology,
University of Seville, 41012 Seville, Spain
e-mail: jmorales@us.es

A. Sousa
e-mail: asousa@us.es

L. García-Barrón
Department of Applied Physics II, University of Seville,
41012 Seville, Spain
e-mail: leoncio@us.es

M. Aguilar-Alba
Department of Physical Geography and AGR,
University of Seville, 41004 Seville, Spain
e-mail: malba@us.es

M. Vetter
Geovisualization, Würzburg University of Applied Sciences,
97070 Würzburg, Germany
e-mail: mark.vetter@fhws.de

prevent them from becoming contagious foci. These terrains exclude those foci constituted by rice fields, hemp ponds, river banks and channeled streams, and road and railroad ditches.

3 Results and Discussion

The authors conducted a comparative analysis of the spatial distribution of unhealthy water bodies and the mortality by autochthonous malaria, in Spain, in the early 20th century. To this end, the surface occupied by unhealthy water bodies in the Spanish regions (average of the years 1913 and 1916) and the provincial distribution of mortality in 1916 by cases of autochthonous malaria, were represented in a map of Spain (see Fig. 1b).

In 1916, the total paludic surface of the Spanish territory, occupied by different types of unhealthy water bodies, was 313,200 ha, distributed in 1518 municipalities. In this sense, it must be highlighted that Fig. 1a includes potentially unhealthy water bodies but not anthropic accumulations of water (rice fields, ditches, channeled streams, river banks, etc.). The most immediate consequence of this was that 301,360 people infected and 2192 deceased by malaria were reported in 1916 in all of Spain. The regions with the largest surface occupied by unhealthy waters with malaria in 1916 were Western Andalusia (214,692 ha), followed, by far, by La Mancha (58,188 ha). Between 1913 and 1916, in Western Andalusia and La Mancha, unhealthy water bodies

varied less than 6.5%. On the other hand, the reduction in Levante was 90.5%.

Figure 2 represents the surface occupied by paludic foci and the percentage of municipalities of each region with cases of autochthonous malaria.

In 1916, most of the unhealthy water bodies of Spain were located in Western Andalusia. More specifically, these represented 76.9% of the total (214,692 ha), followed by the region of La Mancha (18.6%). The remaining surface of these unhealthy waters was distributed among the rest of the Spanish regions (4.5%, see Fig. 2a). This is consistent with the distribution of municipalities with cases of paludism in the different Spanish regions for the same year. In percentages, Western Andalusia presented, in 1913 and 1916, respectively 58.4 and 61.8% of its municipalities with malaria, and La Mancha did so with 51.4 and 53.1% for the same two years (see Fig. 2b). On the other hand, Levante—which had sharply decreased the surface occupied by paludic foci between 1913 and 1916—presented a reduction, for these two years, of 43.7–25.2% of its municipalities with malaria.

The differentiated behavior of Extremadura could be related to poorer hygienic-sanitary conditions than the rest of Spain, especially in the north of Badajoz [4]. This seems to be confirmed by a higher mortality rate for a morbidity rate that is equivalent to other regions of Spain. However, the region of Levante shows a higher morbidity rate than expected for its unhealthy water surface. This may be due to the fact that in the southeast of Spain, there were two vectors

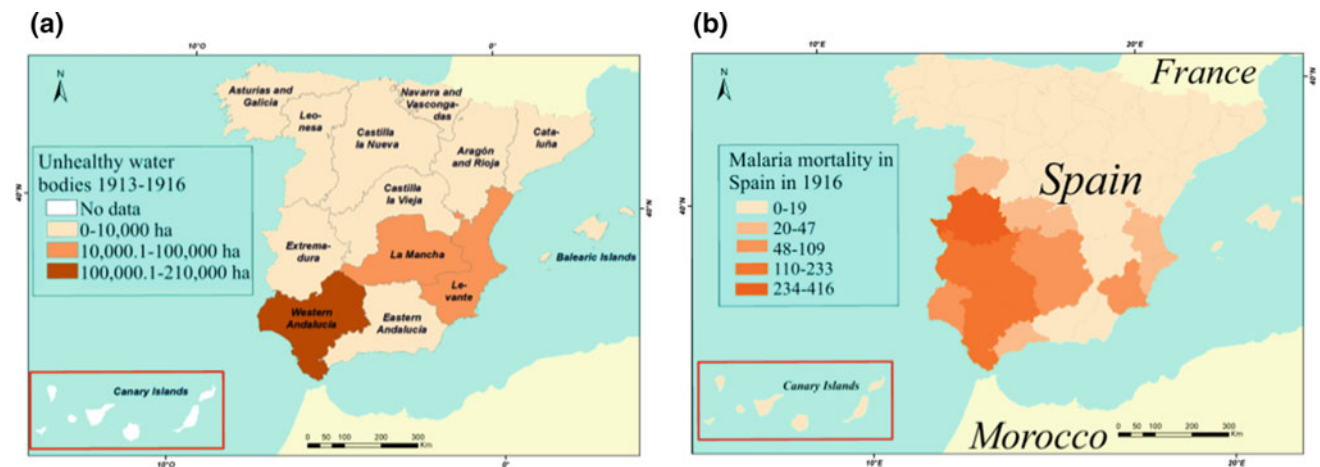


Fig. 1 a Spatial distribution of unhealthy water bodies by Spanish regions, associated with the transmission of malaria in 1913–1916 (excluding the Canary Islands). b Number of deaths by autochthonous malaria in all the provinces of Spain in 1916

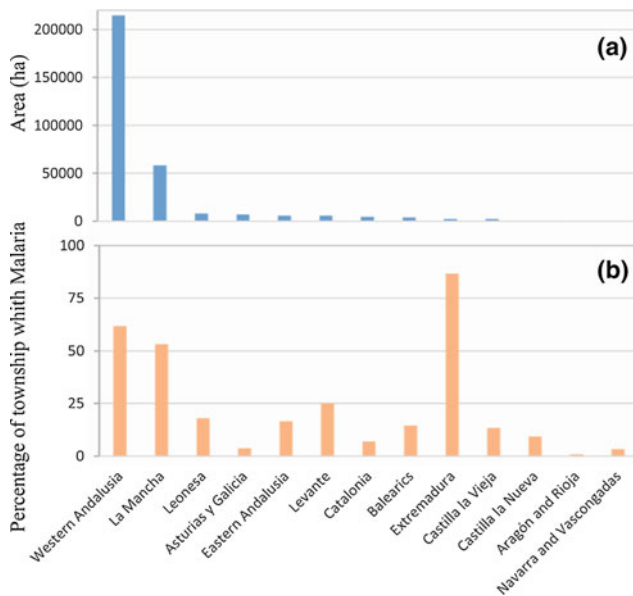


Fig. 2 **a** Distribution of the total surface in hectares of unhealthy water bodies with malaria in 1916, excluding the Canary Islands. **b** Percentages of municipalities in the Spanish regions with cases of malaria in 1916 with respect to the total number of municipalities of each region

capable of transmitting the disease (*Anopheles atroparvus* and *Anopheles labranchiae*).

In the region of Western Andalusia, in 1916, 63,664 people affected and 706 dead by malaria were detected. From that date, the desiccation of large areas infected by malaria caused the remission of the disease. In the mid 1950s, the southwest of Andalusia (especially Seville, Huelva and Cadiz) was the Spanish region with a higher number of cases of malaria. In order to solve that, from the mid 1940s, an ambitious plan to desiccate the wetlands was implemented, which consisted basically in planting *Eucalyptus globulus* Labill and *E. camaldulensis* Dehnh in the current Doñana Natural Park. This desiccation coincides with a dramatic decrease in morbidity in ten years (from 10,074 cases in 1952 to 24 in 1961), although it caused the

disappearance of continental aquatic environments of great biodiversity value [5].

4 Final Remarks

The distribution of main malaria foci in Spain, during the 20th century, was linked to the presence of unhealthy water bodies and aquatic environments, since these are suitable for the development of the mosquito species that transmit the disease. This was especially relevant in Western Andalusia, La Mancha and Levante. Other factors that influenced this distribution were the presence of *Anopheles labranchiae* (as well as *A. atroparvus*) in some regions like Levante. Finally, the socioeconomic conditions of areas such as Extremadura, at the beginning of the 20th century, explain a higher mortality rate.

References

1. Kuhn, K.G., Campbell, D.H., Armstrong, B., Davies, C.R.: Malaria in Britain: past, present, and future. *Proc. Natl. Acad. Sci. U. S. A.* **19**, 9997–10001 (2003)
2. Díaz, J., Ballester, F., López-Vélez, R.: Impacts on human health. In: Moreno, J. M., Aguiló, E., Alonso, S., Cobelas, M. Á., Anadón, R., Ballester, F. (eds.) *A Preliminary Assessment of the Impacts in Spain due to Effects of Climate Change*, pp. 699–741. Ministry of the Environment, Madrid (2005)
3. Sainz-Elipe, S., Latorre, J.M., Escosa, R., Masià, M., Fuentes, M. V., Mas-Coma, S., Bargues, M.D.: Malaria resurgence risk in southern Europe: Climate assessment in an historically endemic area of rice fields at the Mediterranean shore of Spain. *Malar. J.* **9** (2010). <https://doi.org/10.1186/1475-2875-9-221>
4. Sousa, A., García-Barrón, L., Vetter, M., Morales, J.: The historical distribution of main malaria foci in Spain as related to water bodies. *Int. J. Environ. Res. Public Health* **11**(8), 7896–7917 (2014)
5. Sousa, A., Morales, J., García-Barrón, L., Garcia-Murillo, P.: Changes in the *Erica ciliaris* Loeffl. ex L. peat bogs of Southwestern Europe from the 17th to the 20th centuries AD. *Holocene* **23**(2), 255–269 (2013)

Effects on Soil-Plant System in a Treated Wastewater Irrigated Sunflower Cultivation: Soil Chemical Characteristics, Bioaccumulation of Metals in Soil and Plants

Farah Bouhamed, ZaineB Bakri, and Boubaker Elleuch

Abstract

The use of wastewater in agriculture is a good way for countries where water resources are facing quantity and quality problems. The goal is to study the effect of treated wastewater irrigation on the physico-chemical characteristics and soil geochemistry amended and unamended on one hand, and to follow the bioaccumulation of heavy metals in soils and sunflowers on the other hand. Wastewater and by-products of Sfax wastewater treatment plants and Agareb wastewater treatment plants are widely used for irrigation. The geochemical analysis of these waters shows enrichment in nutrients (nitrogen and phosphorus) and reveals high levels of exchangeable bases. Compost and sewage sludge brought organic matter and nutrients to the substrates, these elements are essential for the growth and the conservation of plant life. Maximum sunflower development was found in the presence of sewage sludge and following irrigation with Agareb treated wastewater (82 cm in length and 479 $\mu\text{g/g}$ MF soluble sugar in plant tissues). The experimental results also show that the addition of sludge, with small quantities of metals from treated wastewater, to the substrate resulted in a decrease of the exchangeable amounts of these metals. This reduction is probably due to their strong immobilization.

Keywords

Wastewater • Heavy metal • Soil • Irrigation
Phytostabilisation

1 Introduction

The exploitation of fresh water has made a remarkable progress. Water resources will also become rarer if current water management and water demand figures are maintained.

F. Bouhamed · Z. Bakri (✉) · B. Elleuch
Sfax University, 3029 Sfax, Tunisia
e-mail: bakari.zaineB@gmail.com

An important strategic goal of water policy is therefore to efficiently reduce the use of fresh water. The use of treated wastewater in agricultural irrigation is an important possibility for achieving this objective [1]. Therefore, Tunisia has formulated the national aim of increasing the use of wastewater in agriculture to 50%.

That's why, in this work, we study the effect of wastewater from two stations, Sfax and Agareb, on sunflower growing in different samples using soil mixed with compost or with sewage sludge and soil only.

2 Materials and Methods

Different water samples are taken from the Agareb and Sfax wastewater treatment stations.

The parameters measured were: pH, electrical conductivity (EC), SS, sodium (Na^+), potassium (K^+), calcium (Ca^{2+}), magnesium (Mg^{2+}), chemical oxygen demand (COD), biological oxygen demand over five days (BOD_5), bicarbonates (HCO_3), Nutrients (phosphates $\text{PO}_4\text{-P}$, sulphates, ammonium-nitrogen $\text{NH}_4\text{-N}$, nitrate-nitrogen $\text{NO}_3\text{-N}$) and chlorides [2], and heavy metals. The experiment was laid out in a greenhouse, with three types of irrigation water: Sfax treated wastewater (STWW), Agareb treated wastewater (ATWW) and potable water (PW).

Three series of experimental pots (17 cm) were used for planting sunflowers: some pots contained soil mixed with compost, some contained contain soil with sludge and others contained only soil. Heavy metal content is determined in the soil and in the plants at the end of the cultivation as well as in the chlorophyll, soluble sugar.

3 Results

3.1 Characteristics of Treated Wastewater

Some parameters slightly exceeded the guidelines (Tunisian or FAO standards), especially in Sfax treated effluents (Fe,

Cr, Pb, Zn), which can be related to the existing industrial activities in this region. According to the physico-chemical parameters mentioned in Table 1, treated effluents are full of nutrients (nitrogen phosphorus, potassium) and organic matter—which promotes the development of plants—since they act as fertilizers, hence, their supply with irrigation is favorable for plant nutrition.

3.2 Accumulation of Metals in the Different Organs of the Plant of Sunflower

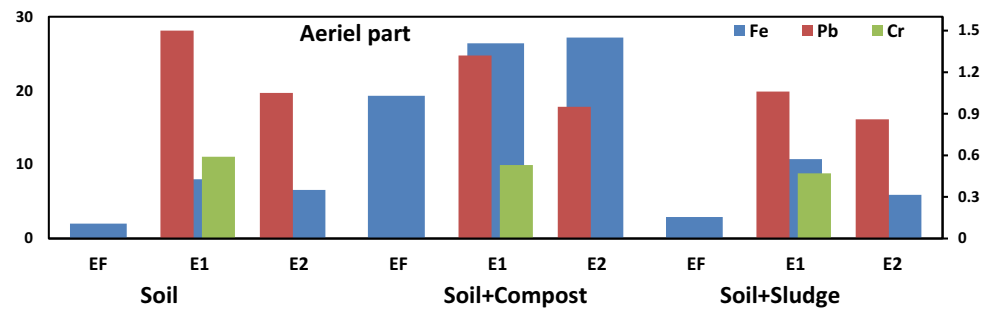
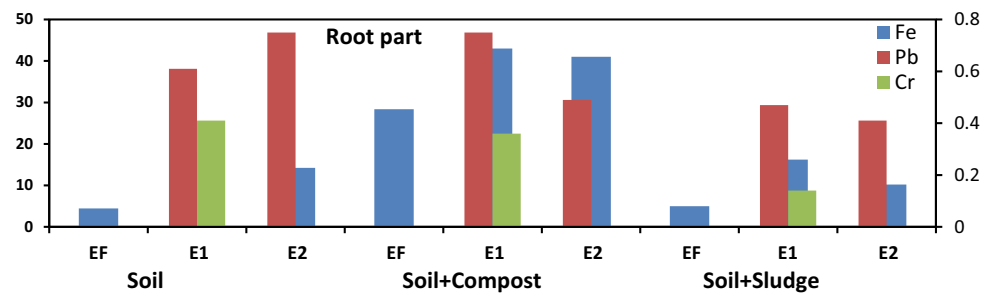
The comparison of the contents of Cr and Pb ions shows an enrichment of the root part with the aerial part of the plant at the level of the different substrates used, whereas the Fe levels are less important in the roots than in the aerial part (Figs. 1 and 2).

4 Discussion

The results obtained show that there is a migration of iron, chromium and lead to the various organs of the sunflower plant. These contents decrease in the substrates amended by sludge. Indeed, Chlopecka and Adriano (1996a, b) observed a reduction in the accumulation of Zn, Cd and Pb by maize and barley, following phytostabilization experiments on contaminated soils and in our cases irrigated by waters containing Pb and Cr contents. Then, they highlighted the important role played by the dissolution of hydroxylapatite, added as a stable phase to these soils. The sludge used in the stabilizer is effective in reducing the levels of these bioavailable elements and can be used as a stabilizer for the micropollutants of ores present in substrates irrigated with TWW. However, according to these results, irrigation with treated wastewater can be considered as a fertilizer since

Table 1 Water quality analysis of potable water (PW), Sfax treated wastewater (STWW) and Agareb treated wastewater (ATWW)

Parameters	PW	STWW	ATWW	Norms Tunisian standards
pH	7.11	6.54	6.9	6.5–8.5
CE (ms/cm)	–	7.65	3.08	7
MES (mg/l)	–	30	280	30
DCO (mg/l)	–	106.97	92.97	90
DBO ₅ (mg/l)	–	37.03	48	30
P _i (mg/l)	Nd	14.45	10.3	–
NO ₃ (mg/l)	3.9	8.02	26	–
Cl [–] (mg/l)	257	720	540	2000
SO ₄ (mg/l)	251	603	500	–
Na ⁺ (mg/l)	161	2816.5	393	–
K ⁺ (mg/l)	5	175	180	–
Mg ²⁺ (mg/l)	27	280	163	–
Ca ²⁺ (mg/l)	100	241.65	183.8	–
NH ₄ (mg/l)	–	66.3	35	–
HCO ₃ (mg/l)	130	239.8	438.3	–
Cu ²⁺ (mg/l)	<0.01	0.24	Nd	0.5
Fe ²⁺ (mg/l)	<0.013	6.58	2.22	5
Mn ²⁺ (mg/l)	<0.08	Nd	Nd	0.5
Zn ²⁺ (mg/l)	<0.003	5.77	0.59	5
Cd ²⁺ (mg/l)	Nd	Nd	Nd	0.01
Cr ³⁺ (mg/l)	Nd	2.06	Nd	0.1
Pb ²⁺ (mg/l)	Nd	2.82	1.17	1

Fig. 1 Accumulation of metals in the aerial part**Fig. 2** Accumulation of metals in the root part

there is no harmful effect after their use. The high input of nutrients such as phosphorus, nitrogen and potassium [3] by the Agareb treated wastewater with sewage sludge stabilizing effect [4] gives higher yields. This study shows that sludge from the treatment plants, used as a stabilizing agent, is effective in reducing the levels of these bioavailable elements, and can thus be used as a stabilizing amendment for mineral micropollutants present in substrates irrigated by TWW.

5 Conclusions

Treated wastewater irrigation improves crop yields compared to fresh water because of their high nutrient and organic nutrient content, which acts mainly on the quantitative aspect of all the tested plants provided that they undergo prior adequate treatment to reduce their pollutant load for reuse for agricultural purposes. However, based on the nutrient requirements of sunflower plants and their development in the different types of irrigated and control

substrates, it can be inferred that the use of soil amendments such as sludge as a by-product of treated wastewater can be an alternative to mineral fertilization and also act as a stabilizer for the exertion of trace metal elements and major elements which can be toxic to the plant if given at high doses.

References

1. Pedrero, F., Kalavrouziotis, I., Alarcon, J.J., Koukoulakis, P., Asano, T.: Use of treated municipal wastewater in irrigated agriculture—review of some practices in Spain and Greece. *J. Agric. Water Manage.* **97**, 1233–1241 (2010)
2. Bakari, Z., Boujelben, N., Bouhamed, F., Kallel, M., Elleuch, B.: Effects of Treated Wastewater Irrigation of Sfax, Agareb and Mahres Stations on Olive Plants. Springer Nature, Berlin (2018)
3. Bedbabis, S., Ben Rouina, B., Boukhris, M., Ferrara, G.: Effect of irrigation with treated wastewater on soil chemical properties and infiltration rate. *J. Environ. Manage.* **133**, 45–50 (2014)
4. Ghosh, M., Singh, S.P.: A review on phytoremediation of heavy metals and utilization of its byproducts. *Appl. Ecol. Environ. Res.* **3**, 1–18 (2005)

Assessment Impacts of Irrigation Using Treated Wastewater on Plants Growth, Soil Properties and Metals Accumulation in Soil and Tomato Plants

Zaineb Bakari, Farah Bouhamed, Nesrine Boujelben, and Boubaker Elleuch

Abstract

The objective is to study the impact of treated wastewater on the physico-chemical parameters of soil and amended soil with compost or sewage sludge, their effects on plant development as well as the accumulation of heavy metals in cultivated plants. The study was conducted using the wastewaters of the Sfax North treatment plant and the Agareb treatment plant. Experiments were undertaken to evaluate the phytotoxicity of metals present in treated wastewater: the implementation is carried out in a greenhouse under controlled conditions, with a regular monitoring of plant morphology, physiology and followed by physico-chemical soil parameters. Sewage sludge and compost resulted in the addition of micronutrients and organic matter in the soil parameters which are considered important for the development and maintenance of a vegetative cover. Following these experiments, optimum tomato plants growth is observed in substrates amended with sewage sludge and irrigated by the Agareb treated wastewater (122 cm). The most interesting observation is the importance of the contribution of sewage sludge that minimizes the phytotoxicity of the effluent.

Keywords

Wastewater • Heavy metal • Soil • Irrigation
Phytostabilisation

1 Introduction

Agriculture is characterized by a high-water demand, since about 70% of worldwide freshwater (FW) withdrawals is used for agricultural irrigation [1]. On the other hand, limited FW availability is a problem of increasing concern and FW

resources will become insufficient to sustain agricultural irrigation, due mainly to climate-related conditions. It is, therefore, of paramount importance to increase water availability for agriculture to overcome the problem of water scarcity, which limits the country's economic growth. In the last decades, a growing attention has been devoted to the search of alternative sources of water for agriculture, also in view of saving high-quality waters for human consumption [2]. The TW reuse for irrigation could be an efficient tool to reduce water shortage. However, the TW reuse is currently far from being fully realized, due to several barriers, such as potential risks of the reuse of improperly treated wastewater. The presence, in TW, of residual concentrations of priority, and/or emerging heavy metal of high concern for the environment and human health, represents without doubt one of the most important barriers in TW reuse.

2 Methods

Waters used for irrigation were either freshwater or secondary treated effluents that were sampled at the outlet of municipal waste water treatment plants of the north of Sfax and of Agareb. The treated wastewater (STW) and (ATW) was characterized as follows: pH, Biological Oxygen Demand (BOD₅), Chemical Oxygen Demand (COD), Total Organic Carbon (TOC), Total Carbon (TC), Inorganic Carbon (IC), Total Solids (TS), Total Suspended Solids (TSS) [3] and Color. The experiment was laid out in a greenhouse environment, with two types of irrigation water: Sfax treated wastewater (STWW), Agareb treated wastewater (ATWW) and potable water (PW).

Each type of substratum was irrigated with potable water (PW) with Sfax treated wastewater or Agareb treated wastewater.

Young sunflower plants were cultivated into pots containing soil mixed with sewage sludge, soil mixed with compost or only soil. Heavy metal contents were determined

Z. Bakari (✉) · F. Bouhamed · N. Boujelben · B. Elleuch
Sfax University, 3029 Sfax, Tunisia
e-mail: bakari.zaine@gmail.com

in the soil and in the plants at the end of the cultivation as well as in the chlorophyll, soluble sugar.

3 Results

3.1 Characteristics of Treated Wastewater

Colloid organic matter and biodegradable dissolved matter were removed using secondary treatment by aerobic biological processes. Table 1 summarizes the quality of different treated wastewaters from the plants of Sfax (STWW) and of Agareb (ATWW).

3.2 Accumulation of Trace Elements and Trace Metals in Plants

The physico-chemical analysis of the plant shows that the concentrations of Fe, Cr in the aerial and root parts of tomatoes irrigated by the EUTs are the highest compared with the same parts in plants irrigated with fresh water. For the sludge-amended substrate, Fe, Cr and Pb levels in the root parts of the plants are less important compared to plants

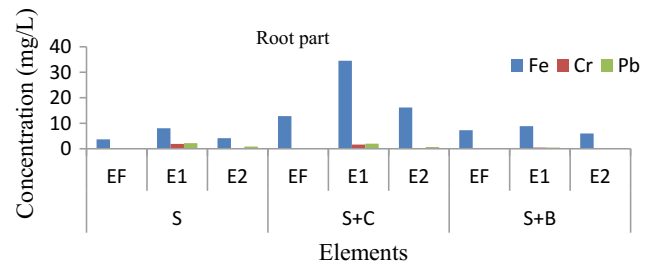


Fig. 1 Accumulation of trace elements and trace metals in plants

grown on substrates amended by compost. These levels increase more and more with the application of the EUTs of the Sfax North station, this is explained by the stabilizing role of the sludge used (Fig. 1).

4 Discussion

The different treated wastewaters showed an alkaline pH. Some parameters, such as lead ions (Pb) and biochemical oxygen demand (BOD), have exceeded the guideline of reuse of treated wastewater in irrigation (NT 106.03). However, the treated effluents have promoted the soil

Table 1 Physico-chemical characteristics of potable water and Sfax and Agareb treated wastewaters

Parameters	PW	STWW	ATWW	Tunisian Norms
pH	7.11	6.54	6.9	6.5–8.5
CE (ms/cm)	–	7.65	3.08	7
MES (mg/l)	–	30	280	30
DCO (mg/l)	–	106.97	92.97	90
DBO ₅ (mg/l)	–	37.03	48	30
P _i (mg/l)	Nd	14.45	10.3	–
NO ₃ (mg/l)	3.9	8.02	26	–
Cl ⁻ (mg/l)	257	720	540	2000
SO ₄ (mg/l)	251	603	500	–
Na ⁺ (mg/l)	161	2816.5	393	–
K ⁺ (mg/l)	5	175	180	–
Mg ²⁺ (mg/l)	27	280	163	–
Ca ²⁺ (mg/l)	100	241.65	183.8	–
NH ₄ (mg/l)	–	66.3	35	–
HCO ₃ (mg/l)	130	239.8	438.3	–
Cu ²⁺ (mg/l)	<0.01	0.24	Nd	0.5
Fe ²⁺ (mg/l)	<0.013	6.58	2.22	5
Mn ²⁺ (mg/l)	<0.08	Nd	Nd	0.5
Zn ²⁺ (mg/l)	<0.003	5.77	0.59	5
Cd ²⁺ (mg/l)	Nd	Nd	Nd	0.01
Cr ³⁺ (mg/l)	Nd	2.06	Nd	0.1
Pb ²⁺ (mg/l)	Nd	2.82	1.17	1

fertility and the plant development through their contribution of nutrients such as potassium, phosphorus and nitrate. The higher levels of chromium, lead and iron found in the substrates irrigated with the TWWs, is particularly related to the high levels of these elements in these TWWs.

The amendments mentioned above reduced the absorption and the availability of metals and metalloids in plants by the formation of insoluble complexes using these elements [4] (Fig. 1).

The low concentrations found in this work may be due to the alkaline pH of the used substrates, which support the uptake of heavy metals by soil elements and the apparition of insoluble organic complexes or the precipitation of metal carbonates [5]. In our work, better growth is observed for tomatoes grown in soils amended with sewage sludge and irrigated by the ATW. These results are explained by the sludge role of stabilizers for the excess of bioavailable elements.

5 Conclusions

Based on analyses performed on plants and soils during this study, the efficacy of irrigation using TWW in planting tomato may be confirmed, which reduces the use of freshwater.

The microbiological effect of irrigation using treated wastewater on fruits and their composition can be examined.

References

1. European Environment Agency: <http://www.eea.europa.eu/articles/water-for-agriculture>
2. Yang, H. et al.: *Environ. Sci. Technol.* **37**, 3048–3054 (2003)
3. Ramírez-Sosa, D.R., Castillo-Borges, E.R., Méndez-Novelo, R.I., Sauri-Riancho, M.R., Barceló-Quintal, M., Marrufo-Gómez, J.M.: Determination of organic compounds in landfill leachates treated by Fenton–Adsorption, *Waste Manage.* **33**(2), 390–395 (2013)
4. Hussain, S I.: Irrigation of crops with sewage effluent: implications and movement of lead and chromium as affected by soil texture, lime, gypsum and organic matter, thèse de doctorat, Département des sciences du sol, Faisalabad, Université de l’agriculture, p. 190 (2000)
5. Smith, C.J., Hopmans, P., Cook, F.J.: Accumulation of Cr, Pb, Cu, Ni, Zn and Cd in soil following irrigation with treated urban effluent in Australia. *Environ. Pollt.* **94**, 241–246 (1996)

Phenol Formaldehyde Resin for Hydrophilic Cellulose Paper

Waqas Ahmed, Muhammad Sagir, M. Suleman Tahir, and Sami Ullah

Abstract

Phenol formaldehyde resin is a thermosetting plastic which has been used for various applications. The important factor of its versatile use is its thermal stability, resistance to chemical attack and water resistance—which protect it from micro-organism attacks. The hydrophobic nature of phenol formaldehyde makes Kraft paper waterproof upon drying. This property decreases the cooling efficiency of cooling pads. Therefore, it is required to make phenol formaldehyde resin unaffected by the hydrophilic nature of paper. In the present work, phenol formaldehyde is being used to impregnate Kraft paper to make evaporative cooling pads. For this purpose, phenolic resin was synthesized with inorganic additives, at specific ratios and degree of polymerization, which allowed the paper to absorb water when it was impregnated with diluted resin. During the drying process, by evaporation of some volatile elements in phenolic resin, pores are created in the paper which allows it to absorb water. Solid contents of the synthesized samples were also determined. The coating on paper was examined after different time intervals to observe the solubility of the coated resin in water, which ensures the long-term protection of pads from microorganism attacks.

chemical resistance in its cured form. This is produced by the reaction of phenol (hydroxyl benzene) and formaldehyde by using a specific catalyst [1–3].

Phenol formaldehyde resin was the first completely synthetic polymer. It was the first thermosetting plastic discovered in early 20th century [4]. In the first decade of the 20th century, Bakelite, trademarked phenolic plastics and revolutionized the market for molded and laminated parts for use in electrical equipment [5, 6]. Being more stable in heating environments and moisture resistant, it was widely used in molding and in laminated products [7–9]. Phenol formaldehyde is basically used as a binder to strengthen paper and as an antiseptic material which protects the paper from microorganism attacks for longer periods. When it is cured in the fibers of the paper, it can protect it from water dissociation and microorganism activity [10, 11]. When cellulosic fiber was exposed to water, it was broken, thus, a salt which can provide mechanical strength to the fibers for a longer time is required. Generally, increasing the mechanical strength of cellulosic paper decreases its absorption ability [12]. Wet strength is the ability of fiber which determines how long it can sustain water without breakage [13]. Phenol formaldehyde is the suitable agent to enhance the mechanical strength without disturbing its absorbing ability.

In the present work, the resol resin is being used as a salt for mixing with cellulosic fibers to enhance their wet strength without disturbing their water absorption ability. The solid content of the phenolic resin, free phenol, free formaldehyde contents were also determined.

1 Introduction

Phenol formaldehyde (PF) resins are synthetic polymers obtained from the reaction of phenol with formaldehyde. It is a high-performance and very stable thermosetting polymer with high mechanical properties and high temperature and

2 Sample Preparation and Experimentations

1000 g of formaldehyde was dissolved in water by the ratio of 37% formaldehyde in water. The solution was heated and stirred continuously until all the powder was dissolved in water. The resin was synthesized by taking ratios of phenol to formaldehyde as (1:1.6) and the physical properties of the sample were observed.

W. Ahmed · M. Sagir (✉) · M. S. Tahir
Department of Chemical Engineering, University of Gujrat,
Jalalpur Jattan Road, Gujrat, 50700, Punjab, Pakistan
e-mail: m.sagir@uog.edu.pk

S. Ullah
Department of Mechanical Engineering, University of Gujrat,
Jalalpur Jattan Road, Gujrat, 50700, Punjab, Pakistan

1 kg of liquefied phenol was mixed in 1.5 kg of the formaldehyde-water solution and it was stirred to mix the phenol into formaldehyde homogeneously. Then, a strong base (NaOH) was added in water to maintain the pH of the solution between 8 and 9. Next, the mixture was heated up to 'X' degrees centigrade so that the reaction is triggered. The mixture was continuously stirred at 90 rpm. The reaction proceeded until the desired conversion was achieved and the solid contents of the product came out to be 50–55%. The product was cooled down at room temperature under continuous stirring. A specific hardener and additives like acid slurry and soluble carbonates were added in the solution when the reaction was completed. FTIR spectroscopy was used to determine the existence of free formaldehyde in the resin. Table 1 illustrates the molar ratios, reaction time, pH and free formaldehyde contents.

A total of seven samples were synthesized. The synthesized resin was applied onto cellulosic paper to study its effect on paper properties [14, 15]. It was noticed that the synthesized resins with additives increased the mechanical strength of paper without changing its water absorbing quality. The 4th synthesized sample showed the good properties, lowering the free formaldehyde contents up to 3.15% and solid content up to 55%.

3 Results and Discussion

By performing different experiments with varying ratios of phenol to formaldehyde, checking at different values of pH and reaction temperatures, we determined the suitable condition for our application. Table 2 presents the specification of synthesized Phenol formaldehyde resin.

These are specific parameters which are important to consider during the manufacturing of phenolic chemical, especially for evaporative cooling pads. The solubility factor is very important as it is required to dilute the solution with water. Therefore, an appropriate amount of resin impregnated in the paper was necessary. The solubility of resin is the function of pH of prepared resin. The thermal decomposition temperature shows the extent of its applications and expresses the thermal stability of resin. The temperature should not increase above 230 °C; otherwise, the strength of coated paper starts to decrease. When the storage temperature is higher than room temperature, shelf life starts to decrease with increasing temperature. Temperature above 30 °C for the storage of resin is highly risky and it will decrease the shelf life of phenol formaldehyde resin to the least limit.

Table 1 Different samples of the phenolic resin prepared by varying reactants ratio i.e. phenol to formaldehyde ratio

Synthesis	Molar ratio phenol: form.	Time (min.)	pH	Free formaldehyde (%)
Synthesis 1	1:1.6	62	8	3.35
Synthesis 2	1:1.5	50	9	3.15
Synthesis 3	1:1.8	25	7	8.85
Synthesis 4	1:1.8	62	8	2.76
Synthesis 5	1:1.9	65	8	5.77
Synthesis 6	1:2.0	70	8	3.75
Synthesis 7	1:1.3	50	10	3.25

Table 2 Specifications of prepared phenol formaldehyde resin

Property	Value
Curing temperature	130 °C
Solid contents	52–58%
PH value	8–10
Viscosity	30–40 cp
Free phenol	0.5–1.5%
Di-hydroxymethyl phenol	0.4%
Thermal decomposition temp.	230 °C and more
Methylene	0.2%
Free formaldehyde	0.1–0.3%

3.1 Comparison of Pure and Coated Paper

Comparison of pure paper water absorption and the absorption of impregnated paper is expressed in Figs. 1 and 2. From Fig. 1, shows the absorption axis and the distance covered by water, in pure paper, in an upward direction in a specific time. In the beginning, water penetrates vigorously and later the rate gradually decreases. Paper gradually absorbs water as time moves on, this shows the high wet ability of paper and its readiness to absorb water without deformation.

Figure 2 shows that there is negligible change in the wet strength of paper after it is coated with phenolic resin. Hence, this shows that phenolic resin did not change the wet ability of paper by making it waterproof [16]. That's why phenolic resin was selected to provide mechanical strength to paper and to protect the paper from bacterial attacks, which increased the shelf life of evaporative cooling pads. From Fig. 2, it is confirmed that the coating with phenolic resin has an ignorable effect on the absorption quality and it may enhance mechanical strength.

3.2 FTIR Spectroscopy Results

The result presented in Fig. 3 shows that the concentration of free phenol formaldehyde is the direct function of temperature and pH of the reaction. As the pH value of the mixture increased, the conversion of phenol increased and the amount of free phenol decreased. FTIR analysis is important to adjust the quality of resol according to our

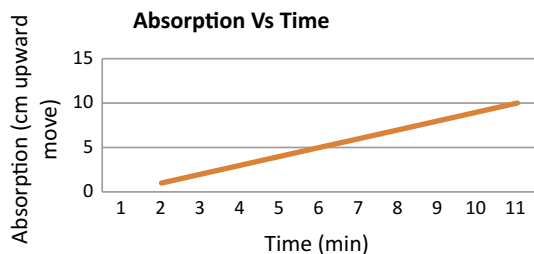


Fig. 1 Absorption versus time curve for pure paper

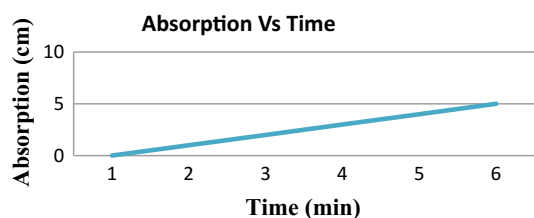


Fig. 2 Absorption versus time curve for impregnated paper

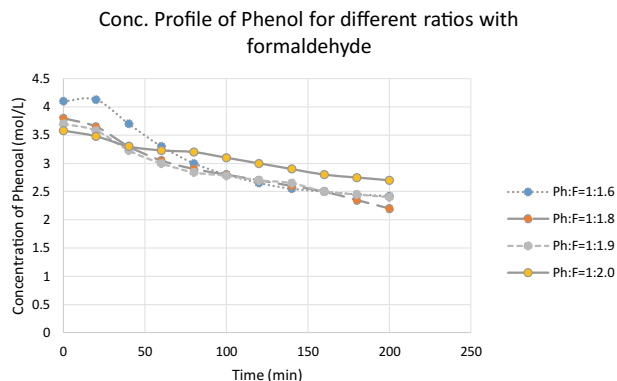


Fig. 3 Concentration profile of formaldehyde at different molar ratios during synthesis of PF resin

requirement. The free phenol concentration up to 0.5–0.8% is suitable for the formation of resol to use in Kraft paper. Also, the existence of free formaldehyde in resol plays an important role in the solubility of resol in water. Therefore, these two parameters are adjusted according to a requirement by using FTIR techniques. Similar is the case with free phenol during the reaction.

4 Conclusion

Phenol formaldehyde was successfully synthesized and applied on Kraft paper. It improved the mechanical strength of fibers and protected them from micro-organism attacks. The use of phenolic resin to provide mechanical strength to fibers of cellulose paper and to protect them from micro-organism attacks without disturbing their hydrophilic property confirmed that coating with phenolic resin has an ignorable effect on the absorption quality and it may enhance mechanical strength. The 4th synthesized sample showed good properties, lowering the free formaldehyde contents up to 3.15% and the solid content up to 55%.

Acknowledgements I would like to acknowledge the University of Gujrat for research assistance, Dr. Muhammad Sagir for his guidance and my Research Master Rana Javaid Anwar for his guidance throughout my practical research career, my best friend Aqeel Ahmed who supported me throughout my work.

References

- Pizzi, A., Ibeh, C.C.: Phenol–formaldehydes. In: Dodiuk, H., Goodman, S.H. (eds.) Handbook of Thermoset Plastics, 3rd edn., pp. 13–44. William Andrew Publishing, Boston (2014)
- Fink, J.K.: Phenol/formaldehyde resins. In: Fink, J.K. (ed) Reactive Polymers Fundamentals and Applications, 2nd edn., pp. 155–177. William Andrew Publishing, Oxford (2013)
- Dabbagh, H.A., Shahraki, M.: Mesoporous nano rod-like γ -alumina synthesis using phenol–formaldehyde resin as a template. *Microporous Mesoporous Mater.* **175**, 8–15 (2013)

4. Handique, J.G., Baruah, J.B.: Polyphenolic compounds: an overview. *React. Funct. Polym.* **52**(3), 163–188 (2002)
5. Pilato, L.: *Phenolic Resins: A Century of Progress*. Springer, Berlin (2010)
6. Ullah, S., Bustam, M.A., Nadeem, M., Naz, M.Y., Tan, W.L., Shariff, A.M.: Synthesis and thermal degradation studies of melamine formaldehyde resins. *Scientific World J.* **6** (2014) (Article ID 940502)
7. Liu, C., Li, K., Li, H., Zhang, S., Zhang, Y.: The effect of zirconium incorporation on the thermal stability and carbonized product of phenol–formaldehyde resin. *Polym. Degrad. Stab.* **102**, 180–185 (2014)
8. Burmistr, M., Boiko, V., Lipko, E., Gerasimenko, K., Gomza, Y. P., Vesnin, R., Chernyayev, A., Ananchenko, B., Kovalenko, V.: Antifriction and construction materials based on modified phenol-formaldehyde resins reinforced with mineral and synthetic fibrous fillers. *Mech. Compos. Mater.* **50**(2), 213–222 (2014)
9. Ullah, S., Bustam, M.A., Ahmad, F., Nadeem, M., Naz, M.Y., Sagir, M., Shariff, A.M.: Synthesis and characterization of melamine formaldehyde resins for decorative paper applications. *J. Chin. Chem. Soc.* **62**, 182–190 (2015)
10. Lenghaus, K., Qiao, G.G., Solomon, D.H.: The effect of formaldehyde to phenol ratio on the curing and carbonisation behaviour of resole resins. *Polymer* **42**(8), 3355–3362 (2001)
11. Ganeshram, V., Achudhan, M.: Synthesis and characterization of phenol formaldehyde resin as a binder used for coated abrasives. *Indian J. Sci. Technol.* **6**(6), 4814–4823 (2013)
12. Alamri, H., Low, I.M.: Mechanical properties and water absorption behaviour of recycled cellulose fibre reinforced epoxy composites. *Polym. Test.* **31**(5), 620–628 (2012)
13. Azwa, Z., Yousif, B., Manalo, A., Karunasena, W.: A review on the degradability of polymeric composites based on natural fibres. *Mater. Des.* **47**, 424–442 (2013)
14. Fernández-Costas, C., Gouveia, S., Sanromán, M., Moldes, D.: Structural characterization of Kraft lignins from different spent cooking liquors by 1D and 2D Nuclear Magnetic Resonance spectroscopy. *Biomass Bioenerg.* **63**, 156–166 (2014)
15. Obi Reddy, K., Uma Maheswari, C., Shukla, M., Muzenda, E.: Preparation, chemical composition, characterization, and properties of Napier grass paper sheets. *Sep. Sci. Technol.* **49**(10), 1527–1534 (2014)
16. Figueiredo, A.B., Evtuguin, D.V., Monteiro, J., Cardoso, E.F., Mena, P.C., Cruz, P.: Structure–surface property relationships of kraft papers: implication on impregnation with phenol–formaldehyde resin. *Ind. Eng. Chem. Res.* **50**(5), 2883–2890 (2011)

Part III

Hydrochemistry and Isotopic Hydrology

Forecasting and Mass Transport Modelling of Nitrates in the Esposende–Vila Do Conde Nitrate Vulnerable Zone (Portugal)

Joel Zeferino, Maria Rosário Carvalho, Tânia Ferreira, Maria Catarina Silva, Maria José Afonso, Líliliana Freitas, Ana Rita Lopes, Rosário Jesus, Sofia Batista, Helder I. Chaminé, and José Martins Carvalho

Abstract

Esposende–Vila do Conde, a nitrate-vulnerable zone, in the littoral north of Portugal, is contaminated by nitrates of an agricultural origin. Measures have been implemented to reduce that contamination. The effectiveness of the measures was evaluated, predicting the time required for the groundwater body reach the quality standard, i.e., less than 50 mg/L for dissolved nitrates. Two methodologies were used, groundwater flow and nitrates transport modelling, and predictive analysis of time series. The transient simulation of nitrate transport shows that the minimization measures imposed in the NVZ are being effective. However, the persistence of concentrations above 50 mg/L in some areas is notorious even in the next 24 years. The forecasting points out to a recovery period of ten years if current agricultural practices are maintained. The prediction of NO₃ concentration based on forecasting methodology may not be applicable in the long run because it is a punctual analysis, not taking into consideration the contaminant dispersion dependent on the aquifer characteristics.

Keywords

Groundwater • Nitrates • Numerical modelling
FEFLOW • Forecasting

1 Introduction and Regional Framework

European Directive 91/676/EEC of 12 December, 1991, (Nitrate Directive, ND) has the objectives to reduce water pollution caused or induced by nitrates from agricultural sources and define nitrate-vulnerable zones (NVZ) to prevent the spread of such pollution, where minimization measures must be applied. The prediction of the time required for the reduction of aquifers contamination is important to evaluate the effectiveness of the minimization measures. Mass transport modelling has been shown as a fundamental tool in predicting hydraulic heads and dispersion of contaminants in aquifers. On the other hand, the predictive analysis of time series has long been known as a useful forecasting tool. To evaluate the real effect of the measures, the time required for the groundwater body to reach the objective within ND was estimated and the environmental objective was defined by the Water Framework Directive (Directive 2000/60/CE; WFD), which is 50 mg/L for dissolved nitrates.

Esposende–Vila do Conde NVZ is located on the north-western coast of Portugal. Its aquifers are unconfined and develop in very fractured granitic and metasedimentary rocks, essentially schist and greywacke. Above these units, are marine and wind terraces dependent on river systems and coastal environments (e.g., [1, 3]). The average productivity for alluvial deposits, alluviums and terraces is 2 L/s, while igneous and metamorphic rocks have a low permeability and yield generally lower than 3 L/s [2]. The natural recharge occurs through direct infiltration of precipitation, between 70 and 141 mm/year [2], or by infiltration from surface water bodies. The natural discharge of the system occurs in springs on the slope bases, on the bottom of the valleys and mainly into the ocean.

Groundwater shows contamination by nitrates of agricultural origin due essentially to the abusive use of nitrogen fertilizers and application of livestock effluents on soils. In 2003, a program of measures was implemented.

J. Zeferino · M. R. Carvalho (✉) · T. Ferreira · M. C. Silva
IDL and Department of Geology, Faculty of Sciences, University
of Lisbon, Lisbon, Portugal
e-mail: mdrcarvalho@fc.ul.pt

M. J. Afonso · L. Freitas · H. I. Chaminé · J. M. Carvalho
Laboratory of Cartography and Applied Geology (LABCARGA),
DEG, School of Engineering (ISEP), Polytechnic of Porto, Porto,
Portugal

A. R. Lopes · R. Jesus · S. Batista
APA—Portuguese Environment Agency, Lisbon, Portugal

M. J. Afonso · H. I. Chaminé · J. M. Carvalho
Centre GeoBioTecUA, Aveiro, Portugal

These measures included, among others, the limitation for animal manure placement in the soil with a maximum value of 170 kg N/ha. Despite the imposed measures, in 2010, 70% of the groundwater had NO_3 concentrations above 50 mg/L, with a maximum value of 484 mg/L in 2006.

2 Materials and Methods

In order to predict the time required for groundwater to reach the environmental objectives, flow and nitrates transport modelling and predictive analysis of time series were performed.

The FEFLOW software (DHI) was used for modelling the aquifers. The aquifers were simulated in 3D, using a finite element mesh and one unconfined layer with 25 m of thickness. The recharge and hydraulic conductivity of the layer were fully calibrated by inverse calibration, according to the available piezometric observations and the lithology of the aquifers. For this purpose, FEPEST was used, an adaptation of automatic calibration software PEST.

The land uses were grouped in 5 main classes with different NO_3 mass input for mass transport simulations: agricultural areas with temporary crops (15.5 kg/ha/year), agricultural areas with permanent crops (8.37 kg/ha/year), heterogeneous agricultural areas (11.94 kg/ha/year), permanent pastures (4.65 kg/ha/year) and forest areas (6.2 kg/ha/year, due to animal manure deposition).

The forecast analysis to predict the future NO_3 concentration was based on time series of the highest nitrate value measured in groundwater, semi-annually between 2003 and 2015, and the application of Exponential Smoothing (ETS) algorithm.

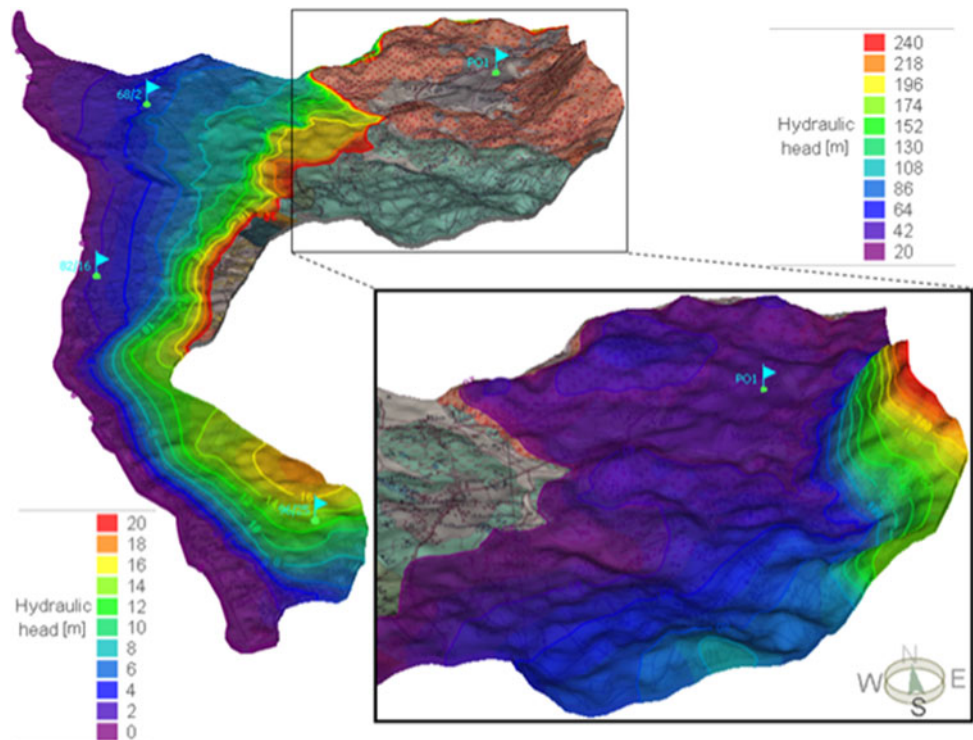
3 Results and Discussion

3.1 Groundwater Flow and Mass Transport Modelling (FEFLOW)

Figure 1 shows the obtained hydraulic head in the aquifers, ranging from 240 m, in the highest granitic areas, to 0 m at the sea level. The modelled area is delimited to the north by the Cávado River, to the West by the Atlantic Ocean, and to the South by the Ave River. The Ocean occupies the entire western border, where a head of 0 m was imposed. For the river borders, the heads were defined as function of the slope of the river bed. In general, the groundwater flows from west and northwest towards the Atlantic Ocean.

The reference situation of the nitrate concentration was obtained by kriging 22 quality control points from SNIRH (National Water Resource Information System) monitoring data in 2016. The average value for NO_3 in groundwater is 74.88 mg/L, reaching a maximum of 191 mg/L. According to the agricultural loads from each soil occupation type, a total input of 94 tons of nitrate affects the groundwater body

Fig. 1 Simulated hydraulic head in the aquifers



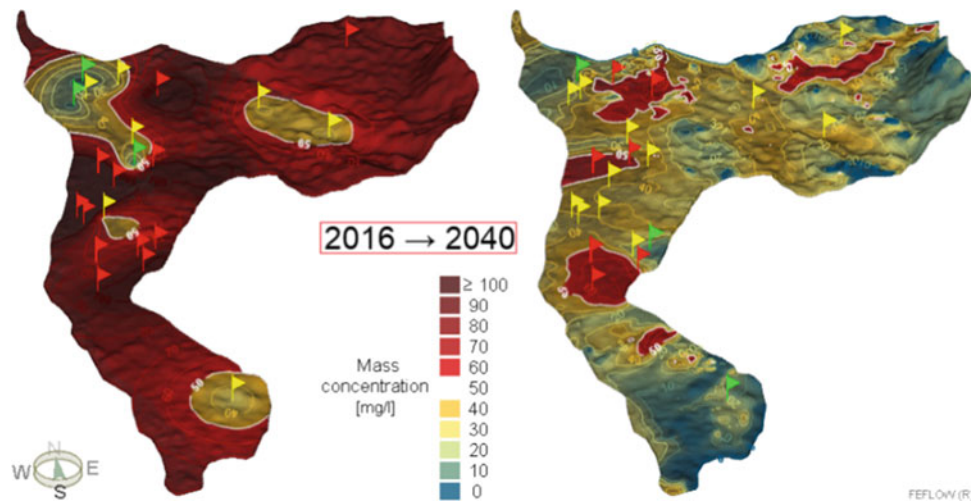


Fig. 2 Initial conditions and nitrate concentration at the end of simulation (2040)

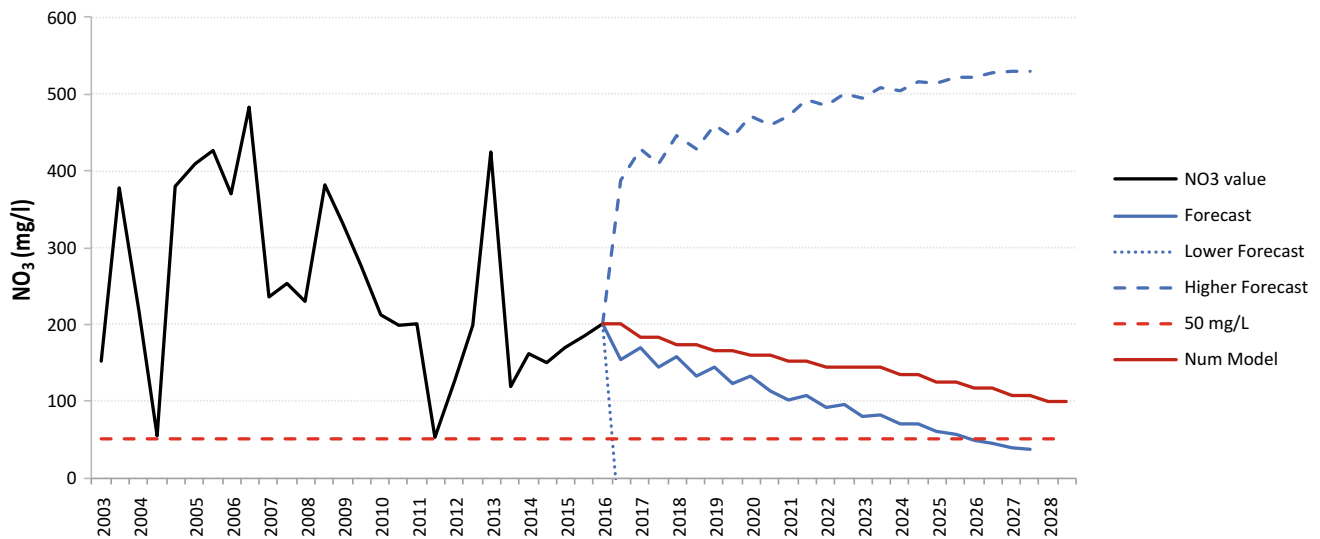


Fig. 3 Forecasting of the nitrate concentration in the groundwater body

every year. The simulations were carried out for a period of 24 years, ending in 2040.

The transient simulation of nitrate transport shows that over time, NO_3 concentrations are decreasing, pointing out that the minimization measures imposed in the NVZ are being effective (Fig. 2). However, the persistence of concentrations above 50 mg/L in some areas is notorious, even after 24 years.

3.2 Forecasting and Predictive Analysis

The NVZ forecast model points to the year 2028 as the year in which the WFD environmental objectives are achieved. The forecast obtained considering the confidence intervals

(95%) seems unrealistic, considering that, in the best scenario, the objectives were reached in 2017, would never be achieved in the worst scenario (Fig. 3).

4 Final Remarks

The analysis of these results must consider that the numerical modeling uses loads of NO_3 based on the land uses, which may not be respected by the farmers. The prediction of the evolution of NO_3 based on forecasting methodology may not be applicable in the long run, because it is a punctual analysis that does not take into consideration the dispersion of the contaminant dependent on the aquifer characteristics.

References

1. Almeida, C., Mendonça, J.J.L., Jesus, M.R., Gomes, A.J.: *Sistemas Aquíferos de Portugal Continental*. Centro de Geologia da Faculdade de Ciências de Lisboa e Instituto da Água, Lisboa (2000)
2. APA—Agência Portuguesa do Ambiente: *Plano de Gestão da Região Hidrográfica do Cávado, Ave e Leça (RH2)*. Relatório Técnico. Parte 2 – Caracterização e Diagnóstico. Agência Portuguesa do Ambiente, Lisboa. (2016)
3. Pedrosa, M.Y., Brites, J.A., Pereira, A.P.: *Nota explicativa da carta das fontes e do risco de contaminação da região de Entre-Douro-e-Minho*. Folhas Norte e Sul, escala 1/100000. Instituto Geológico e Mineiro, Lisboa (2002)

Hydrochemical Quality of the Angads Plain Groundwater (Eastern Morocco)

Mohammed Es-sousy, Elkhadir Gharibi, Mohammad Ghalit, Jean-Denis Taupin, and Mohsen Ben Alaya

Abstract

The Angads plain aquifer system, composed of a phreatic groundwater and a deep confined aquifer, currently shows that some sites are contaminated with nitrates. These sites are located downstream of the eputation plant of Oujda. The current contamination affects almost 70% of the water collected in the study area, south of the groundwater aquifer. This situation may worsen if a policy of irrigating a large area by the treated wastewater is adopted.

Keywords

Angads • Morocco • Groundwater • Nitrates • Irrigation

1 Introduction

The aquifer system of Angads plain is potentially threatened by overexploitation. Its salinity is increasing, especially in phreatic groundwater, due to pollution from farming activities—linked to the excessive use of fertilizers—and to industrial and urban pollution. The vulnerability of groundwater to pollution concerns the unsaturated zone [1] and the saturated zone [2]. The plain of Angads (460 km²) located in the north of the city of Oujda, is limited to the south by the chain of Horst, to the north by the chain of Bni

Znassen, to the west by Megrez Jbel and to the east by the Algerian-Moroccan border. The aquifer system of Angads is a “transboundary aquifer”. It extends on the plains of Angads and Maghnia. The aquifer system is characterized by a flexure (Wadi Isly) separating the northern part of Angads (200 km²) from its southern part (260 km²). This complex system is composed of a phreatic groundwater and a deep confined aquifer [3]. A wide sampling was carried out in 2015–16 which allowed to obtain the spatial distributions of physico-chemical characteristics of the major and trace elements in the two aquifers. We have detected areas marked by contamination. In 2017, the reuse of treated wastewater by the water treatment plant of Oujda started in this area for the irrigation of the Ecological Park (25 ha) in Oujda zone. Another project, at a larger scale, is in progress, concerning the irrigation of agricultural land (1500 ha) over the prefecture of Oujda Angads.

The objective of this study is to follow the evolution of the physico-chemical characteristics in the aquifer system after the reuse of treated wastewater for irrigation.

2 Materials and Method

The area studied (393 km²) is a component of the aquifer of Angads. It is located in north-eastern Morocco, close to the Algerian-Moroccan border ((X = 612,600, Y = 3,830,800) and (X = 580,500, Y = 3,860,000)). It is limited to the northern by the mountain range of Beni Snassen. In the western part, it is close to Megrez and Harraza reliefs and Bou Houria. In the southwest, its border is the Jebel Hamra. To the east, the Angads aquifer continues in Algeria towards the Marnia lowland (Fig. 1). This groundwater system is situated in a lesser watershed which is undergoing by a fault network defining graben subvertical [4]. The geology of the reservoir is composed of a fractured basaltic volcano-sedimentary which connects from a hydraulics point of view the deep aquifer of Jebel Hamra and the groundwater of Angads [5].

M. Es-sousy · E. Gharibi (✉) · M. Ghalit
Department of Chemistry, Faculty of Sciences, Laboratory of Solid Minerals and Analytical Chemistry, Oujda, Morocco
e-mail: gharibi_elkhadir@yahoo.fr

J.-D. Taupin
Hydrosciences, UMR 5569 (IRD, CNRS, UM), Montpellier, France

M. Ben Alaya
National Institute of Research and Physical-Chemical Analysis (INRAP), Technopole, Sidi Thabet, 2020 Ariana, Tunisia

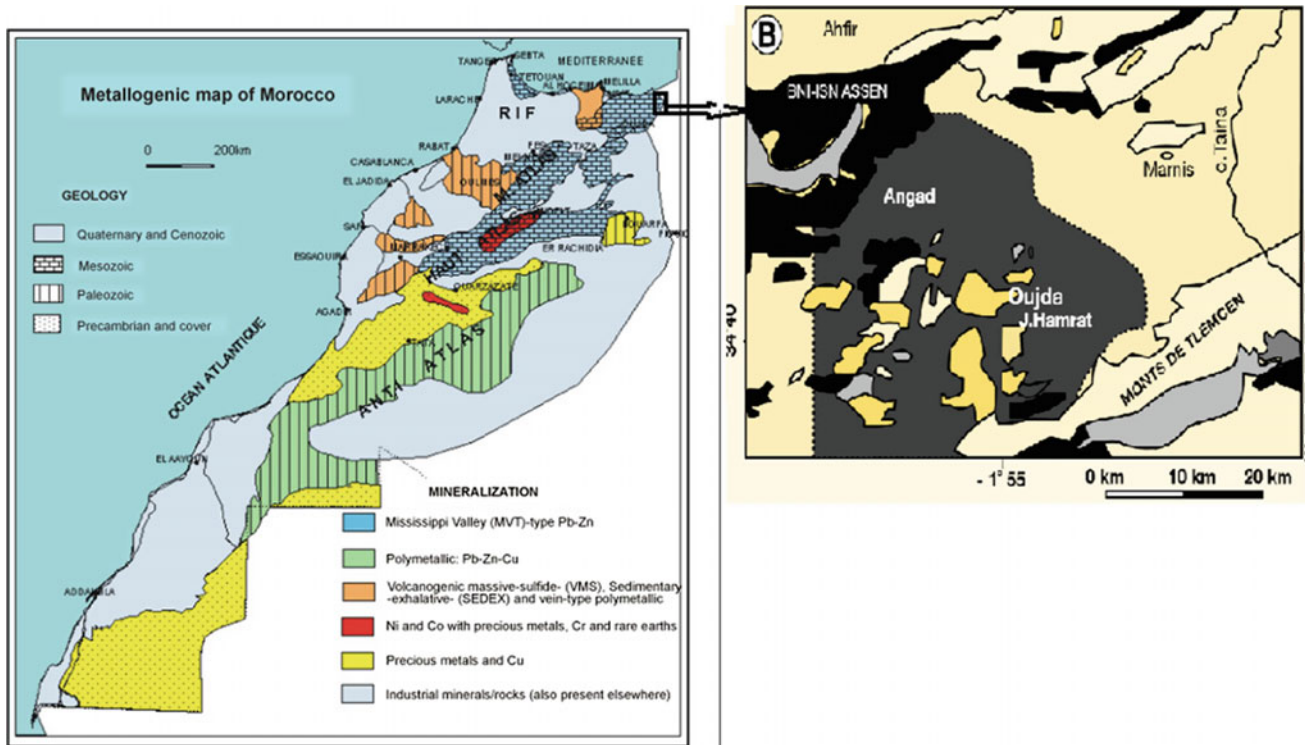


Fig. 1 Location of the Angads plain

Table 1 Hydrochemical facies

	South area	North area	Deep aquifer
Na-Cl (%)	19.57	52.00	36.36
Ca-Cl (%)	30.43	28.00	18.18
Ca-HCO ₃ (%)	4.35	8.00	36.36
Mg-Cl (%)	17.39	8.00	
Mg-HCO ₃ (%)	8.70	4.00	
Na-HCO ₃ (%)	4.35		
	r(CE-Cl) = 0.90	r(CE-Cl) = 0.986	r(CE-Cl) = 0.998
	R(CE, SO ₄) = 0.55	R(CE, SO ₄) = 0.65	R(CE, SO ₄) = 0.36

The permeability of this geological formation ranges between 10^{-4} and 10^{-3} m/s [3].

This study zone is defined by a continental semi-arid climate with a dry season and a temperate winter. The groundwater's steady variations, linked to rainfall variations, show a dephasing between 6 and 11 months [6]. The sampling was carried out over a period of four months, from 15 Dec, 2015, to 20 April, 2016, 86 ground-water samples have been sampled throughout the Angads plain, 46 samples in the southern zone, 25 in the northern zone, 15 in the confined aquifer.

The analysis has been made by the methods described by Rodier [7].

3 Results

3.1 Piper Diagram

The electrical conductivity (EC) of water collected from the northern zone varies from 510 to 5260 with an average of 2236 $\mu\text{S}/\text{cm}$; the EC of the waters of the Southern Zone (711–5830, average = 2310) and of the deep water (1470–5260, average = 2710 $\mu\text{S}/\text{cm}$).

The correlation between the Cl^- ions, SO_4^{2-} and the electrical conductivity depends on the area of the debit. Table 1 gives the correlation factors. We note that when the

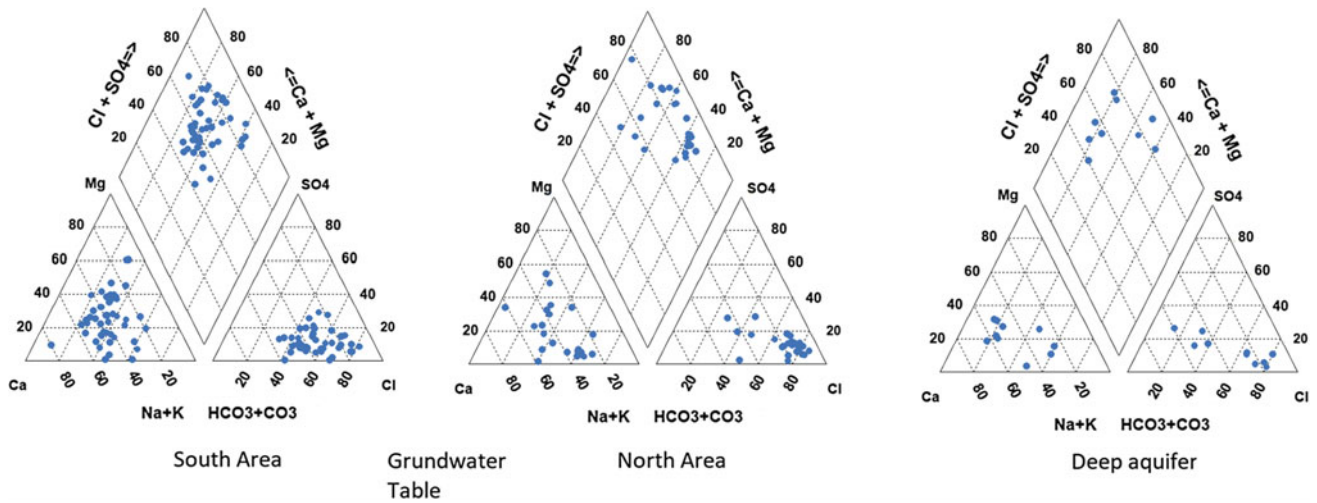


Fig. 2 Piper diagram

CE-SO₄²⁻ correlation increases, the CE-Cl⁻ correlation decreases.

Table 1 shows a bicarbonate facies predominant in the deep aquifer. By contrast to the Groundwater table, the chloride facies is predominant (Fig. 2). The origin of the ions SO₄²⁻ in the water table may be due to deposit evaporites.

3.2 Concentration of Nitrates

The concentration of nitrates is given by Fig. 3. The most polluted part of the phreatic groundwater ([NO₃⁻] > 50 mg/L) [8] is in the southern area, downstream of the wastewater treatment plant.

4 Conclusions

The phreatic groundwater of the Angads plain, in the Oriental part of Morocco, presents a significant vulnerability to contamination because of agricultural and urban activities. The low recharge of the aquifer, the arid climate and the geological limestone structure make this water table level, currently partially reached, likely to be totally polluted. More than 70% of the samples collected in the southern zone downstream of the wastewater treatment plant show a nitrates rate greater than 50 mg/L, above the allowable limit for drinking water recommended by the WHO. The forthcoming study will highlight the impact of using treated wastewater for irrigation in this area.

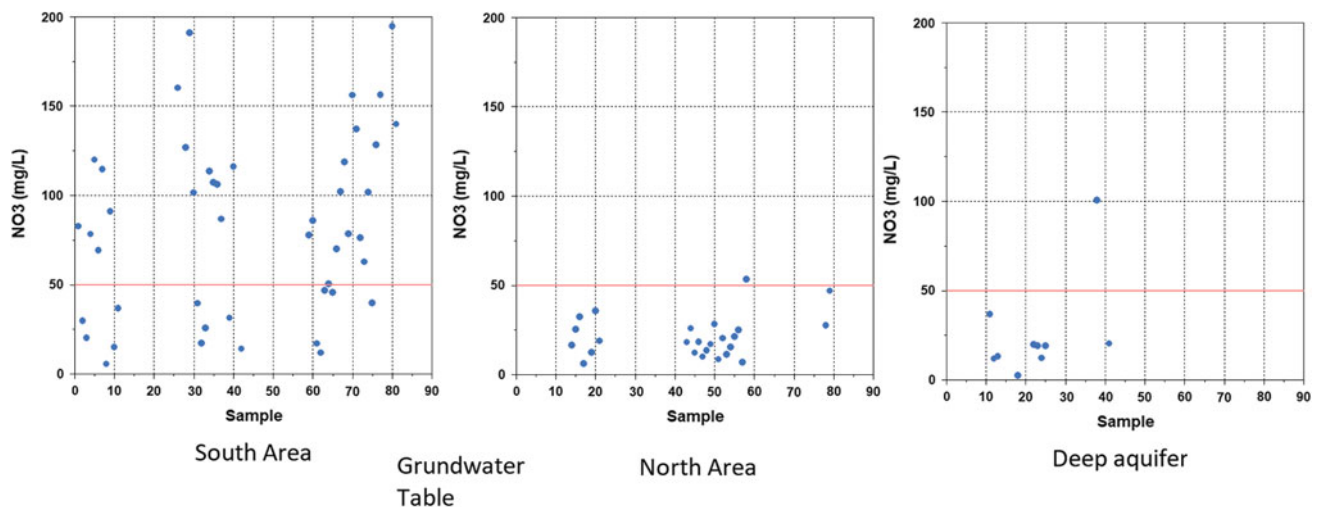


Fig. 3 Concentration of nitrates

References

1. Margat, J.: Vulnérabilité des nappes d'eau souterraine à la pollution: bases de la cartographie. BRGM Publication (1968)
2. Gogu, R.C., Dassargues, A.: Current trends and future challenges in groundwater vulnerability assessment using overlay and index methods. *Environ. Geol.* **39**(6), 549–559 (2000)
3. Quang Trac, N., Simonot, M.: Le couloir Taourirt-Oujda in Ressource en eau du Maroc **1**, 279–287 (1971)
4. Lahrach, A.: Caractérisation du réservoir Liasique profond du Maroc oriental et étude hydrogéologique, modélisation et pollution de la nappe phréatique des Angads. Thèse de doctorat, Université Sidi Mohammed Ben Abdellah. Maroc, Fès-Saïss (1999)
5. Mortier, F., Quang Trac, N., Sadek, M.: Hydrogeology of the volcanic rock formations of North-East Morocco in hydrology of fractured rocks. In: Proceedings of the Dubrovnik Symposium, pp. 327–333. IASH-UNESCO, Ceuterick, Belgium (1967)
6. Amharref, M., Bouchnan, R., Bernoussi, A. S.: Extension of DRASTIC approach for dynamic vulnerability assessment in fissured area: application to the Angad aquifer (Morocco). In: Hydrogeological and Environmental Investigations in Karst Systems, pp. 407–414. Springer, Heidelberg (2015)
7. Rodier, J., Legube, B., Merlet, N.: L'Analyse de L'eau. Dunod, Paris (2009)
8. WHO.: Guidelines for Drinking-Water Quality. World Health Organization, **216**, 303–304 (2011)

Physical and Chemical Characterization of the Surface Waters of Djemaa Wadi (Blida, Algeria)

Djaouida Bouchelouche, S. Arab, Mouna Hafiane, Imane Saal, and Abdeslem Arab

Abstract

Oued Djemaa is the largest tributary that feeds El Harrach wadi. It comes from Atlas Blidéen (the Tablat Mountains); its catchment area covers an area of 225 km². The waters of this wadi show a strong alkalinity and a strong mineralization. The upstream waters are well oxygenated compared to the downstream waters. High values of nutrient salts were observed mainly at stations located near agricultural lands. Chlorides exceed 600 mg/l at downstream. The water situation of Wadi Djemaa is poor in the downstream part, the biological oxygen demand (BOD₅) reaches a maximum of 255 mg/l and the chemical oxygen demand (COD) exceeds 350 mg/l level of the S4 (Larbaâ city).

Keywords

Surface water • Physical quality • Chemical quality

1 Introduction

The exponential development of industrialization and urbanization generates sub-stances of various kinds in the environment. These compounds often end up in the aquatic environment, which acts as the final receptacle for a number of anthropogenic pollutants. River valleys have thus become collectors of substances of various origins, transporting waste to the marine littoral which accumulates in the bays. The study area unfortunately suffers from this situation.

D. Bouchelouche (✉) · S. Arab · M. Hafiane
I. Saal · A. Arab
LaDyBio, FSB, USTHB, LP 32, El Alia, Bab Ezzouar,
Algiers, Algeria
e-mail: bouchelouche_djaouida@hotmail.com

S. Arab
G&G, FST/GAT—USTHB, Bab Ezzouar, Algeria

Discards have emptied the stream of its fauna in its lower part. The consequences on the aquatic fauna are clear. The main objective of this work is to study the physical and chemical characteristics of the water to know the concrete situation of the water quality in this wadi and to characterize the sources of pollution in this region, to be able to halt the degradation of these aquatic environments

2 Materials and Methods

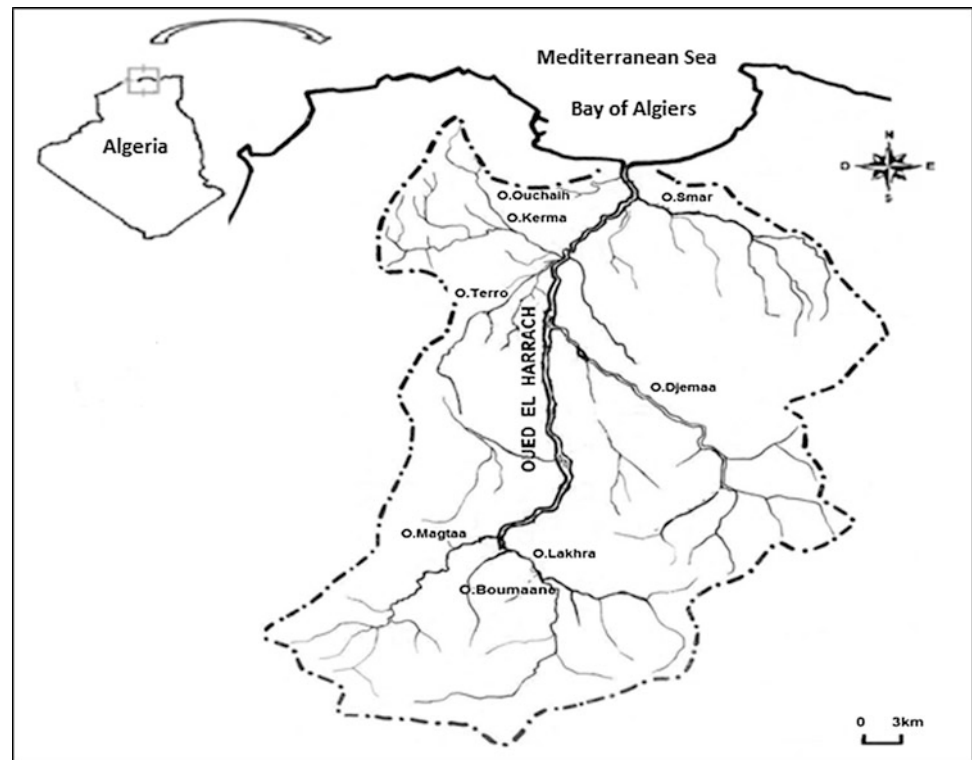
Seasonal sampling was conducted from April 2016 to March 2017. Four stations were selected along the Wadi (Fig. 1). Temperature of the water (°C), pH, dissolved oxygen and conductivity (µs/cm) were measured in situ by a Multi Field Analyzer Multi 340-i Set WTW. The other parameters (chlorides, calcium, nutrient salts (nitrates, nitrites, phosphorus), BOD₅ and COD) were determined at the laboratory by volumetric, titrimetric, gravimetric methods, etc. (expressed in mg/l according to Rodier's protocol [2]).

3 Results and Discussion

The results of the parameters studied are mentioned in Fig. 2.

The profiles of the spatial variation of the parameters measured on all the stations of the wadi do not show a great variation; generally, the concentrations are high along the wadi (Kruskal Wallis test, $p > 0.05$). On the other hand, the temporal evolution of these parameters shows that there is a remarkable fluctuation during the study period of the following parameters: phosphorus, nitrates, nitrites, Calcium, dissolved oxygen. A minimum water temperature of 9.25 °C

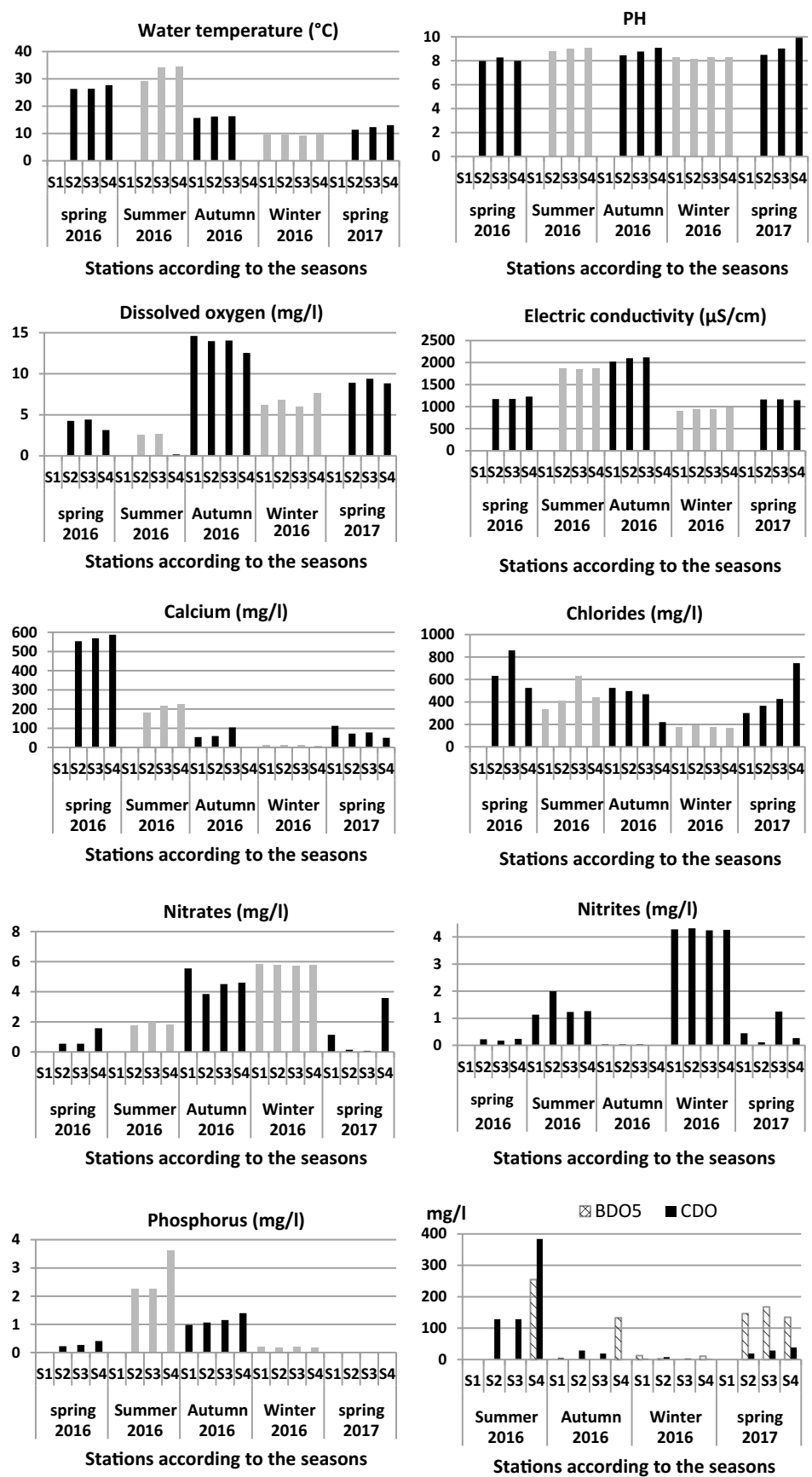
Fig. 1 Geographical location of the study area



is recorded at S3 in winter. A maximum of 34.5 °C is recorded at S4 in summer. The pH of the water ranges from 7.98 (S2) to 9.93 (S4) indicating medium to high water alkalinity. This strong alkalinity at S4 is reflected by the nature of the lands crossed by the waters, as well as the external contributions of the city of Larbaâ. The temporal evolution of the dissolved oxygen along the wadi shows that the oxygen contents follow a very marked variation (Kruskal Wallis test, $P < 0.05$). The recorded concentrations vary between 0.17 mg/l, in summer, and 14.62 mg/l in autumn. Conductivity values range from 901 $\mu\text{s}/\text{cm}$ to 2120 $\mu\text{m}/\text{cm}$, reflecting a high mineralization, which is explained by [4] the mineral composition of domestic wastewater to which is added the geological nature of the lands crossed. Calcium has a temporal variation (Kruskal Wallis test, $P < 0.05$), it reaches a minimum of 8.02 mg/l in winter; this is caused by the effect of dilution caused by heavy rainfall. A maximum of 587.52 mg/l is recorded in spring; this is probably due to the evaporation of the waters causing a high concentration of these ions and the geological limestone nature of the lands traversed by the wadi. Chloride concentrations are high at all stations and throughout the study period they range from

170.4 mg/l at S4, in winter, to 859.4 mg/l at S3 in spring. These high concentrations are due not only to the geological nature of the lands traversed by the wadi but also to intensive urban and industrial pollution in this region. The domestic and industrial discharges of the city of Larbaâ are poured into the wadi, adding to the intense washing of cars in this region and the use of detergents. Nitrates and nitrites exhibit a temporal variation. The levels of nitrates and nitrites are high in winter; this is probably due to the abundant leaching of these ions in the soils of agricultural fields in the vicinity of the wadi. According to [1], the presence of nitrates and nitrites in water-courses is related to the leaching of agricultural soils. Phosphorus has a significant temporal variation. Phosphorus results range from 0.02 mg/l, in spring, to 3.6 mg/l in summer. Its high levels of phosphorus observed during the summer can be explained by the phenomenon of evaporation, concentration, release of phosphorus trapped in large quantities in the sediments and excessive intake of pollutants in the wastewater [3] of the city of Larbaâ. The water quality of Wadi Djemaa is poor, the BOD5 reaches a maximum of 255 mg/l and the COD exceeds 350 mg/l in summer at the level of S4 station (Larbaâ city).

Fig. 2 Physical and chemical parameters measured in Djemaa Wadi



4 Conclusions

Upstream (S1 and S2), the quality of the water is affected by the washing of the vehicles throughout the year, in addition to the transformation of the wadi into swimming pools. The water quality downstream of its two stations decreases markedly due to the increase in human encroachment. Stations 3 and 4 located downstream from the city of Larbaa receive domestic and industrial discharges from this city without any prior treatment, and the wadi has become a real receptacle of these discharges.

References

1. Igbiosa, E.O., Okoh, A.I.: Impact of discharge wastewater effluents on the physico-chemical qualities of a receiving watershed in a typical rural community. *Int. J. Environ. Sci. Tech.* **6**(2), 175–182 (2009)
2. Rodier, J.: *L'analyse de l'eau*. 9ème Edition, 1530p (2005)
3. Sharpley, A.N.: phosphorus loss from an agricultural watershed as a function of storm size. *J. Environ. Qual.* **37**, 362–368 (2008)
4. Williams, W.D.: Anthropogenic salinisation of inland waters. *Hydrobiologia* **466**, 329–337 (2001)

Groundwater Quality in an Alluvial Aquifer Affected by the Anthropogenic and Natural Processes in a Rural Area, North Algeria

Abdelkader Bouderbala and Nacéra Hadj Mohamed

Abstract

The impact of individual septic tank effluent on groundwater quality was investigated in the rural area of the Ain Soltane municipality. The septic tank is a solution for the pre-treatment of sewage. It ensures the partial liquefaction of concentrated pollutants in wastewater and the retention of solids and floating waste. The alluvial gravel aquifer of the Cheliff Plain is especially susceptible to microbial contamination due to the significant number of septic tanks and the high quantity of pre-treated wastewater passing toward the groundwater which may transport bacteria and contaminants over large distances. Geological investigations established the presence of limestone carapace, and stones with high thickness and good permeability, which forms an unconfined aquifer in the area. Groundwater quality monitoring showed a significant degree of an organic pollution in the majority of wells, with very high concentrations of sulfate and chloride exceeding 450 and 250 mg/L, respectively. It also showed the presence of bacterial germs in the groundwater whose origin are fecal, so these monitoring wells are contaminated and are unfit for drinking in this area. The presence of these pathogen germs poses a major problem for public health. This study has identified the effects of septic tank effluent on groundwater quality in Ain Soltane area.

Keywords

Groundwater quality • Septic tank effluent
Ain soltane • Bacteria germs • Septic tank
Algeria

1 Introduction

Numerous diseases influencing the world's population are connected to the contamination of surface water or/and groundwater by untreated domestic and industrial wastewater. Without treatment, this wastewater can cause health problems and natural environment risks due to its toxic chemical components and to pathogenic microorganism loads (microscopic organisms, viruses, parasites, etc.). Bacteria are organisms that have the capacity to travel through soil matrix. Moreover, numerous sicknesses are caused by bacteria such as diarrhoea, dysentery, cholera, and typhoid fever.

The threat to public health due to the transmission of pathogenic bacterial organisms from the sewage system to groundwater has been accounted for around the world [3, 4]. Septic tanks are built to treat human wastewater, and to attenuate organic matter and microorganisms. They are placed at the highest point of the saturation zone at few meters, which can purify water due to the unsaturated zone of soil, and they can in some cases attenuate nitrogen, but they are ineffective at attenuating pathogens, organic matter, and phosphorus. They constitute permanent dangers to both human and animal health and even to the soil and plants, if they are poorly built.

The traditional septic tanks located in the study area were realized in the same way as the infiltration basins, with infiltrations at the bottom and the sides of these basins constitute a real problem for the contamination of groundwater.

In this investigation, samples from thirty-three wells situated in a rural agglomeration in the alluvial aquifer of Upper Cheliff were analyzed for physico-chemical and biological parameters. The objective of this work is to see the effect of the septic tank effluent on the groundwater quality, and to check the role of an unsaturated zone as a natural system of purification of wastewater.

A. Bouderbala (✉) · N. Hadj Mohamed
Department of Earth Sciences, University of Khemis Miliana,
Ain Defla, Algeria
e-mail: bouderbala.aek@gmail.com

2 Study Area

The Upper Cheliff plain covers an area of 375 km². It is confined between the massif of Zaccar and the Ouarsenis chain. It is characterized by a Mediterranean semi-arid climate. The study area is located in a rural agglomeration, south of the Ain Soltane province. The provinces have sewage networks with a discharge in Wadi Cheliff river, due to the absence of wastewater treatment plants, whereas the rural agglomerations use individual septic tanks for the discharge of wastewater, which represents an ecological issue that is confronting the plain, due to its impact on superficial and groundwater resources.

This rural agglomeration of about 10,000 inhabitants, spread over an area of about 3000 ha, is located in the south

of the commune of Ain Soltane, and does not have any drinking or sewerage networks. The population use private wells for drinking supplies and septic tanks for discharging wastewater.

The alluvial aquifer of Upper Cheliff is mainly formed by alluvial deposits, including pebbles, gravels, sands and clay formations; with a thickness that can reach 150 m (Fig. 1).

It is a confined aquifer, covered by clay on the surface, with a thickness of more than 5 m, while the Mio-Pliocene formations can reach 200 m of thickness.

The Mio-plio-quaternary formations have been considered as a multi-layer aquifer system. The hydraulic continuity between these formations suggests a continuity in one part of the area, and a separation via clay lenses in the other

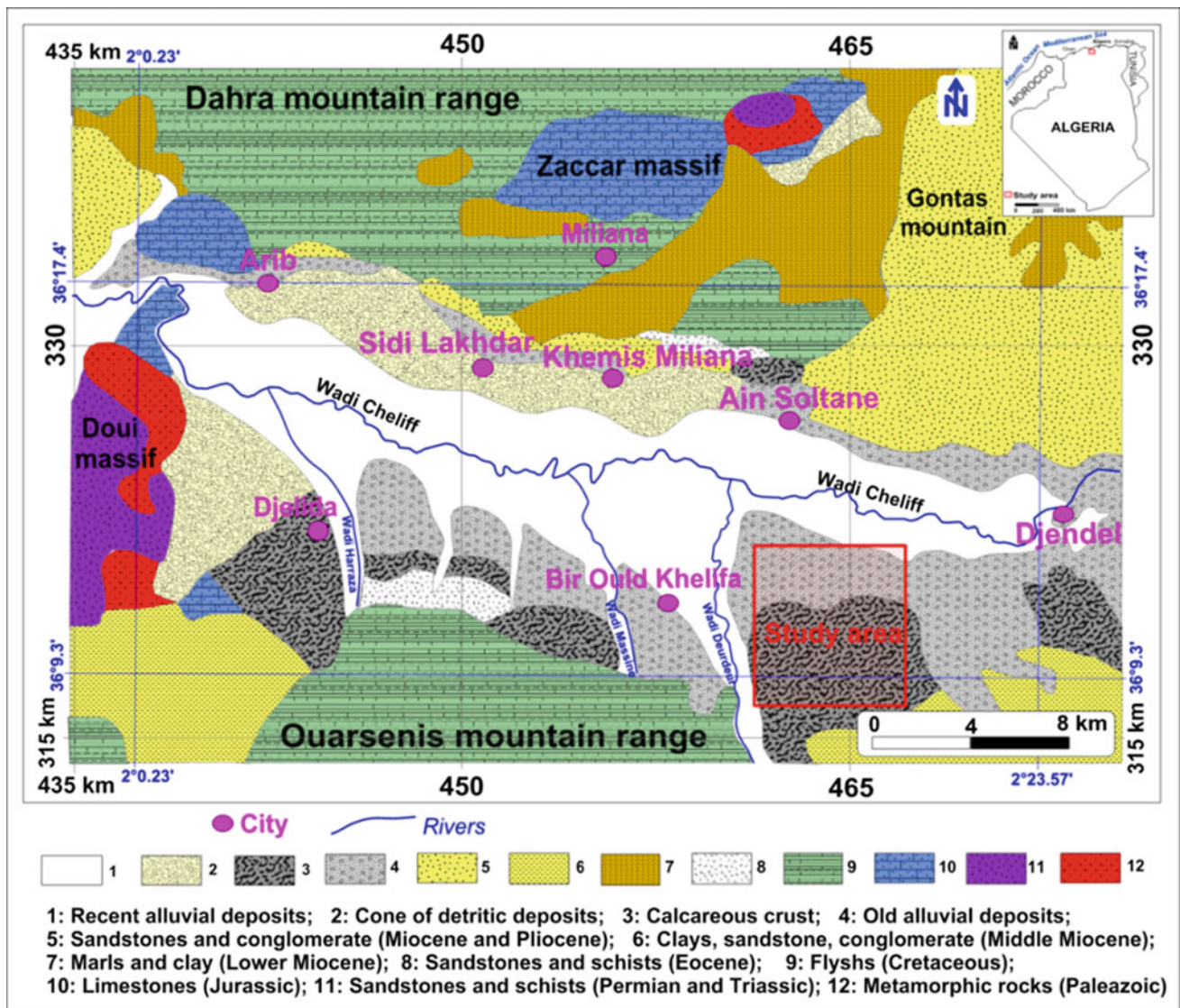


Fig. 1 Geological situation of the study area

part of the area. In this study, we are only involved in the quaternary alluvial aquifer.

The groundwater of this aquifer flows from the northern and southern parts of the plain towards the centre, where the predominant drainage axis is positioned, and which coincides with Wadi Cheliff. The main flow is from East to West.

The depth of groundwater measurements varies from 5 m in the West sector (near Djendel) to 30 m in the East sector (near Arib and Djelida), with an average depth of 10 m in the central part of the plain [1].

The pollution of groundwater in the region may originate from domestic, agricultural, or industrial activities. The only significant recharge source of the aquifer is the effective infiltration of irrigation water. The movement of large volumes of groundwater (quality of recharge) through the highly permeable alluvial aquifer, while rapidly diluting chemical contaminants, will allow the transport of micro-organisms from the septic tank effluent over large distances.

3 Results

The analysis of 33 groundwater samples shows that the pH is ranging from 6.8 to 7.3 with an average value of 7.1, indicating a slightly alkaline condition. It is attributed to the anthropogenic activities and comes from wastewater, disposal, and use of fertilizers in agriculture. The dissolved oxygen concentrations of groundwater show values less than 5 mg/L. The limited dissolved oxygen data indicate an anaerobic condition (<5.0 mg/L). However, the electric conductivity (EC) ranged from 1915 to 3730 $\mu\text{S}/\text{cm}$, with an average of 2627 $\mu\text{S}/\text{cm}$, which exceeds the standard limit of EC in drinking water of 1500 $\mu\text{S}/\text{cm}$ [5]. The groundwater in the study area is classified as brackish water.

The high values of EC are probably due to anthropogenic activities, and to geological weathering conditions, giving higher concentrations of dissolved minerals. The high values of EC ($\text{EC} > 1500 \mu\text{S}/\text{cm}$) reveal an enrichment of salts in groundwater. The total hardness (TH) varies from 53.2 to 146.8 °F indicating that the groundwater belongs to the very hard category ($\text{TH} > 53 \text{ }^\circ\text{F}$). Total dissolved solids (TDS) in groundwater samples ranged from 927 to 2087 mg/L, with an average of 1364.4 mg/L, indicating that the majority of samples fall within the quality of water not desirable for drinking.

Among cations, the concentrations of Ca^{2+} , Mg^{2+} , Na^+ and K^+ range from 156 to 348 mg/L, 34 to 143.3 mg/L, and from 94 to 195 mg/L, respectively. Similarly, the concentrations of anions Cl^- , SO_4^{2-} , HCO_3^- and NO_3^- vary from 295.2 to 736.5 mg/L, 97.8–615.8 mg/L, 183 to 286.7 mg/L and from 5 to 40 mg/L, respectively (Fig. 2). The origin of Ca^{2+} and Mg^{2+} , in groundwater comes mainly from the dissolution of the calcareous crust of the quaternary. High levels of calcium in drinkable water have some negative health effects; they promote vascular degeneration (arteriosclerosis) and osseous degenerative disease (osteoarthritis) [2]. The majority of the samples have high concentrations of Ca^{2+} (more than 54%) as compared to the WHO standards. Sodium is also present in most rocks and soils, as well as in many foods and human intakes. The contents of Na^+ also increase if the residence time in groundwater increases. In the study area, the concentrations of Na^+ are less than 200 mg/L, which is the limit recommended by WHO. In general, groundwater rarely has potassium levels more than 10 mg/L. Potassium results from the alteration of silicate formations (gneiss and schist), and from the dissolution of chemical fertilizers (intensive fertilization used in agricultural activities, NPK). It can also result from domestic and industrial

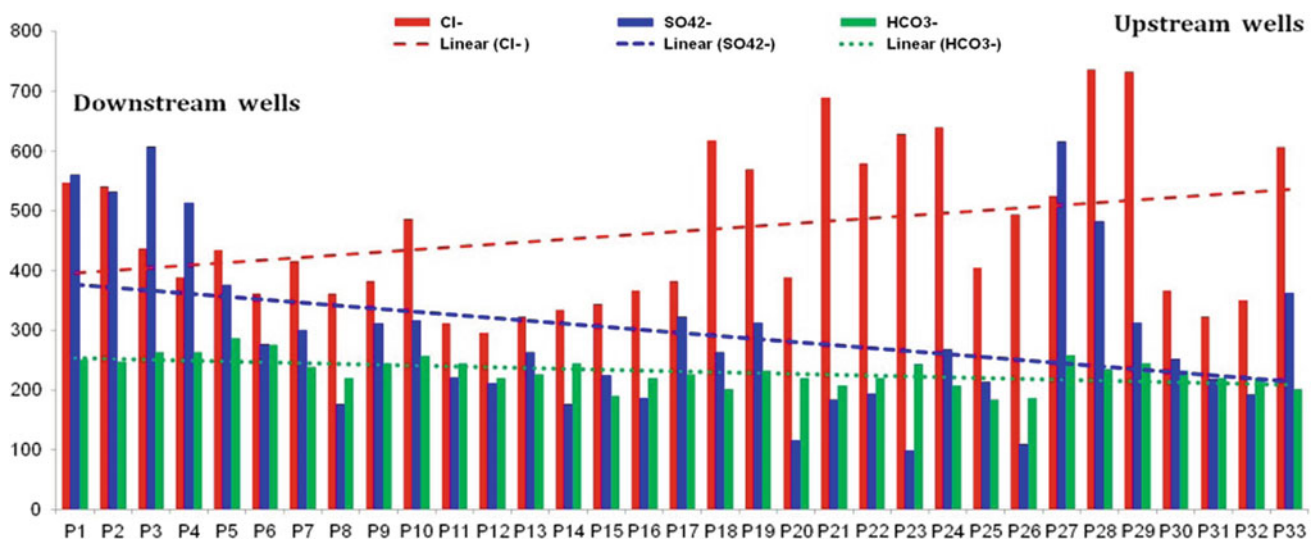


Fig. 2 Evolution of Cl^- , SO_4^{2-} and HCO_3^- from the upstream to downstream of the plain

discharge [1]. In the study area, all samples have concentrations less than 10 mg/L.

The excess of Cl^- in groundwater (100%) may be linked to the anthropogenic effect, with a high probability of the impact of wastewater coming from traditional septic tanks used by inhabitants in this rural area. The excess of SO_4^{2-} concentrations of groundwater in the majority of samples (more than 57%) in this area is probably due to the effect of the use of fertilizers in agriculture and the dissolution of gypsum observed in the Marls substratum. But the largest part of the high sulfates levels comes from untreated wastewater, coming from traditional septic tanks. The higher levels of sulfates can cause health hazards, particularly gastrointestinal problems. The concentrations of NO_3^- indicate values from 5 to 40 mg/L in this part of the plain, due to the use of fertilizers in agricultural activities. The high values have been observed in the southern part of the study area, where the depth of the water table is very low. The high HCO_3^- concentrations are mainly derived from the dissolution of carbonate minerals, and from CO_2 present in the atmosphere and in the soil above the water table. It can be due to the occurrence of oxidation of the organic matter of the soil layers at the emerging land [1].

4 Conclusion

The hydro chemical analysis showed the poor groundwater quality, due to the existence of pollution in the area, resulting from the excess of the contents of chlorides,

sulfates, calcium and nitrates. This pollution can have two origins, one natural and the other anthropogenic.

The bacteriological analysis of groundwater shows high concentrations of total coliforms, faecal coliforms and faecal streptococci, which confirms the contamination of groundwater by domestic wastewater discharge. The septic tanks, make nonpoint pollution via the infiltration of contaminants such as pathogenic bacteria, nutrients, and organic matter. It is due to the lower depths of the water table in the unconfined part of the aquifer in the study area, which represents a high risk for groundwater contamination.

References

1. Bouderbala, A., Gharbi, B.: Hydrogeochemical characterization and groundwater quality assessment in the intensive agricultural zone of the upper Cheliff plain, Algeria. *Environ. Earth Sci.* **76**(21), 744 (2017)
2. Bouderbala, A.: Assessment of water quality index for the groundwater in the upper Cheliff plain, Algeria. *J. Geol. Soc. India* **90**(3), 347–356 (2017)
3. Pandey, P.K., Kass, P.H., Soupier, M.L., Biswas, S., Singh, V.P.: Contamination of water resources by pathogenic bacteria. *AMB Express* **4**(1), 51 (2014)
4. Reay, W.G.: Septic tank impacts on ground water quality and nearshore sediment nutrient flux. *Groundwater* **42**(7), 1079–1089 (2004)
5. WHO: Guidelines for Drinkingwater Quality, 2nd edn. WHO, Geneva (2008)

Hydrochemical Appraisal of Groundwater in Gash River Basin, Eastern Sudan

Hago Ali

Abstract

The main goal of the present study is to evaluate the groundwater quality in Gash River Basin, Eastern Sudan. Groundwater is the main source in the area for all purposes: drinking, industrial as well as agricultural. Twenty-seven groundwater samples from agricultural farms in and around Kassala town were analyzed for their major ion concentrations. The TDS content of the collected samples ranged from 245.9 to 869.20 mg/l, whereas the EC values were below the maximum permissible limit of 1400 $\mu\text{S}/\text{cm}$ prescribed by WHO for drinking water. The cation and anion concentrations were in the following order: $\text{Ca}^{2+} > \text{Na}^+ > \text{Mg}^{2+} > \text{K}^+$ and $\text{HCO}_3^- > \text{Cl}^- > \text{SO}_4^{2-} > \text{NO}_3^-$. The main groundwater types identified are Ca–(Mg)– HCO_3 and Na– HCO_3 types. The samples fall in the water–rock interaction zone on the Gibb’s plot. Carbonates dissolution, silicates weathering and ion exchange are the major chemical processes controlling the groundwater chemistry in the study area. The groundwater in the area is suitable for irrigation in terms of sodium adsorption ratio SAR and residual sodium carbonate RSC, both of which are below the permissible limit, 10 and 1.25, respectively.

Keywords

Hydrochemical appraisal • Groundwater quality
Water-rock interaction • Gash river • Eastern Sudan

1 Introduction

The River Gash is an intermitted stream that originates in the highlands of Eritrea and flows northwest across the flat plain and ends as an inland fan delta, which is the most important

agricultural land in the area [1]. The study area is bounded by longitudes $36^\circ 20'$ and $36^\circ 35'E$ and latitudes $15^\circ 10'$ and $15^\circ 25'N$. It is characterized by a semiarid climate with two main seasons: hot and dusty summer from April to October, with a maximum temperature exceeding 45°C , and a cold season, from November to March, with a mean temperature of 25°C . The rainy season extends from July to the end of September, with an annual average rainfall in Kassala town of about 350 mm. The main geological units are the Pre-Cambrian basement complex and the alluvial deposits. The basement rocks comprise meta-sediments intruded by scattered outcrops of granitic composition [3].

2 Materials and Methods

Groundwater samples from 27 boreholes were analyzed for major ion chemistry. The total depth of the wells ranges from 25 to 30 m. The samples were collected in polyethylene bottles of 1-l capacity. Prior to their filling with sampled water, the plastic bottles were rinsed to minimize the chance of any contamination. The samples were preserved and analyzed using techniques of the standard methods from American Public Health Association [2]. Hydrogen ion concentration (pH), total dissolved solids (TDSs) and electrical conductivity (EC) were determined in situ by using a pH-meter, a portable EC-meter and a TDS-meter (Hanna Instruments, Michigan, USA). The sodium (Na^+), potassium (K^+), magnesium (Mg^{2+}) and calcium (Ca^{2+}) ions were determined by the atomic absorption spectrophotometer (AAS). Bicarbonate (HCO_3^-) and chloride (Cl^-) were analyzed by volumetric methods. Sulfate (SO_4^{2-}) was estimated by colorimetric and turbidimetric methods. Nitrate (NO_3^-) was measured by ionic chromatography.

H. Ali (✉)

Faculty of Petroleum and Minerals, Al Neelain University,
Khartoum, P.O. Box 12702 Sudan
e-mail: hagoali@gmail.com

3 Results and Final Remarks

For domestic use, in terms of hardness, the groundwater is hard to moderate. Regarding TDS values, the groundwater is fresh. Sodium, Chloride, Sulphate and Nitrate ions are within the WHO and Sudanese Standards of permissible limits.

For irrigation purposes; the suitability of groundwater is as follows: SAR is low (<10), Sodium percent is generally from good to excellent, Residual Sodium Carbonate is suitable, Magnesium hazard is suitable, and permeability index is 75%, i.e. suitable.

Mechanisms and processes governing water-rock interaction are mainly: carbonate dissolution, ion exchange and silicate weathering.

The dominated groundwater facies are Ca-HCO₃ groundwater and Na-HCO₃ types.

References

1. Ali, H.: Quantification of groundwater recharge in the Midstream Area-Gash River Basin using the water table fluctuation method. *Al Neelain J. Geosci.* **1**, Khartoum-Sudan (2017)
2. APHA: Standard methods for the examination of water and wastewater, 19th edn. Am. Publ. Health Assoc., Washington DC (1995)
3. Elsheikh, A.E.M., Zeinelabdein, K.A.E., Elobeid, S.A.: Groundwater budget for the upper and middle parts of the River Gash Basin. *Arab. J. Geosci.* **4**(3-4), 567-574 (2010)

Distribution of Trace Elements in the Shallow Aquifer of Guenniche (North Tunisia)

Nizar Troudi, Fadoua Hamzaoui, Mounira Zammouri, and Ourania Tzoraki

Abstract

This paper examines the trace elements level in the shallow groundwater of the Guenniche plain (North Tunisia) and its suitability for drinking water use in comparison with national (NT 2013) and international (WHO 2006) standards. Samples collected from twenty (20) wells and ten (10) streams in May 2016 were analyzed for the most common trace elements contents (arsenic, cadmium, chromium, copper, iron, manganese, mercury, selenium and zinc). Cadmium (1.14–6.11 µg/l) and mercury (0.06–2.89 µg/l) showed higher values in surface water in comparison to the groundwater (0.06–5.43 µg/l for Cd and 0.04–1.91 for Hg µg/l). The severely polluted wells, located in the El Alia region in the border of Wadi El Malah, are considered to impose high human health risk. The irrational use of pesticides, the uncontrolled waste disposal and the untreated industrial wastewater effluents directly into the streams are strongly associated with the deterioration of the water quality of surface and groundwater of Guenniche plain.

Keywords

Plain of guenniche • Shallow groundwater
Pollution • Trace elements

and agricultural activities. Topographically, the plain of Guenniche is a basin opened towards the lake of Bizerte [1]. The major settlements are El Alia and Menzel Jemil. The population increase from 58,967 residents in 1984 to 74,299 residents in 2014 [2] drove rapid urbanization and caused severe environmental problems [3]. The industrialization, the irrational use of fertilizers and pesticides, and the untreated wastewater discharge into the aquatic environment disturbed the ecosystem balance and generated pollutants that can affect the physicochemical and biological quality of the receiving aquatic environments [4]. The plain of Guenniche presents an important industrial area, with various activities such as metal industry, food-processing industry, steel industry, oil refinery, textile industry, building materials, etc. The possible sources of pollution are the untreated wastewater, the drainage of the waste disposal sites due to the lack of adequate sanitation and waste collection network for many cities such as El Alia, El Khetmine, etc., and the various industrial and agricultural activities taking place in the Guenniche plain and in the neighboring towns [5]. The objective of this work is to assess the concentrations of the most common trace elements in the Guenniche shallow aquifer, used for irrigation and drinking water supply, and to detect possible human health risk by its use.

1 Introduction

The plain of Guenniche (130 km²) is located in the northeast of Tunisia (35° 10', 37° 15'N, 9° 66' 10"E), in the South of Bizerte, which is largely known for the various industrial

N. Troudi (✉) · F. Hamzaoui · M. Zammouri
Faculty of Sciences of Tunis, University of Tunis El Manar,
Tunis, Tunisia
e-mail: nizar.troudi@fst.utm.tn

O. Tzoraki
Department of Marine Sciences, University of the Aegean,
Mytilene, Greece

2 Materials and Methods

2.1 Description of the Study Area

The Guenniche plain is characterized by a semi-arid climate, with heavy rains and floods of rivers occurring generally in winter seasons, and with hot summer seasons and a strong evaporation. The mean rainfall is 600 mm/year while the annual potential evaporation is 1140 mm [6]. The major area is covered by quaternary sediments with secondary and tertiary formations outcrops in its boundaries. It contains a phreatic aquifer, which consists of heterogeneous and lenticular environments, Quaternary detrital formations with a

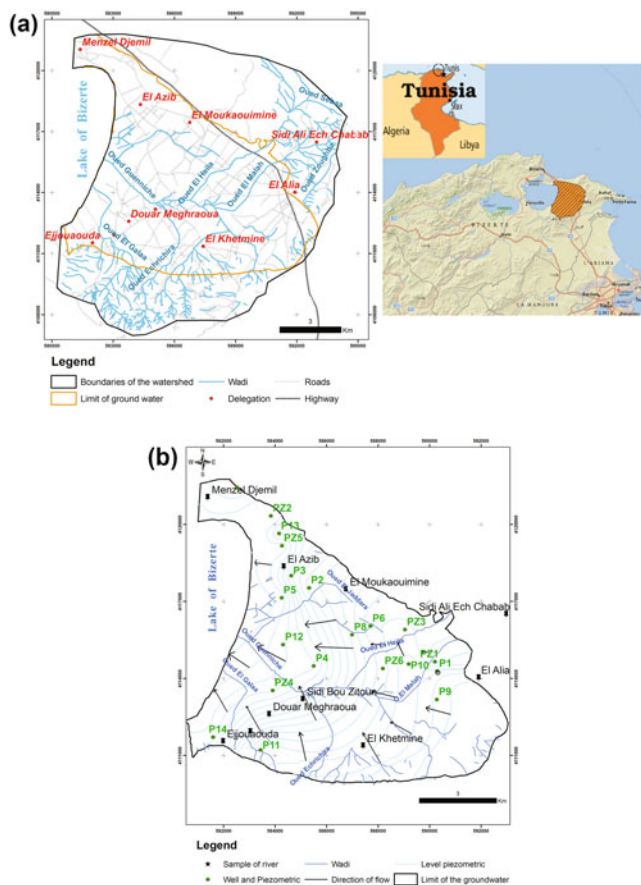


Fig. 1 a Location of the study area. b Hydrographic network, location of water sampling campaign and piezometric level in 2015

thickness varying between 50 and 100 m [1]. The phreatic aquifer is exploited by the local farmers through shallow wells with depths varying from a few meters in the plain center to 50 m at its borders. The plain is crossed by several ephemeral streams (wadis) such as wadi El Malah, wadi Guenniche, wadi Nechrine, wadi Hela, wadi El Jaddara, wadi Echrichira and wadi El Galaa (Fig. 1a). The most important one is wadi Guenniche. These streams contribute to the aquifer recharge in the plain upstream while they drain the aquifer in the downstream. The piezometric map in 2015 (Fig. 1b) shows that the groundwater flow direction is mainly Southeast-Northwest. The leakage to the Lake of Bizerte is the main natural outlet of the aquifer.

2.2 Description of the Experimental Protocol

During the sampling campaign conducted in May 2016, twenty (20) samples were collected from the shallow groundwater wells and ten (10) from the ephemeral streams. The physicochemical parameters, which are the potential of hydrogen (pH), temperature (T°), and electric Conductivity (EC) were measured in situ using a portable field kit.

For laboratory trace element analysis, samples were collected into a 125 ml polyethylene bottle. Special care was taken to avoid contamination during sampling for dissolved trace elements. Before sample collection, the bottle was rinsed at least three times with groundwater filtered through 0.45 mm mixed cellulose ester membrane (Advantec MFS, USA) directly. Each sample was immediately acidified to $\text{pH} < 2$ with ultrapure nitric acid (Fluka, Buchs, Switzerland) and then stored at approximately 4°C (in an icebox) before analysis. The samples of Guenniche plain were analyzed at the Gdir El Golla laboratory of the national company of exploitation and distribution of drinking water (SONEDE) and all concentrations of the trace elements were determined by the atomic absorption spectrometry (Flame or Oven: AAS 240 FS Varian). Three methods are used with this measuring device. The Atomic Absorption Spectrometry flame mode is used for the analysis of the Iron (Fe), the Manganese (Mn), the Copper (Cu), the Zinc (Zn), the Selenium (Se) and the Cadmium (Cd). The hydride mode of atomic absorption spectrometry is used for the Mercury (Hg) and the Arsenic (As). The third mode of Atomic Absorption Spectrometry is used to detect Chromium (Cr).

3 Results and Discussion

Results of the analytical determination of the groundwater samples of the Guenniche plain are shown in Table 1.

Conductivity is a parameter which informs about the zones of mixture or infiltration [7]. The average conductivity of the Guenniche plain was found to be 3.75 mS/cm in the groundwater and 4.33 mS/cm in the rivers. The temperature, on the one hand, plays an important role in the solubility and the dissolution of dissolved salts, and on the other hand, influences the electric conductivity and the water pH [7]. In the shallow groundwater of Guenniche plain, the temperature varies between 19.10 and 21.90 $^\circ\text{C}$, and in the streams between 21.3 and 25.8 $^\circ\text{C}$ (Table 1). The pH characterizes a large number of physicochemical equilibrium and depends on multiple factors which originate from water. This parameter determines the acidity, alkalinity and neutrality of the solutions [7]. The pH varied between 6.8 and 7.72 in the groundwater of Guenniche, and between 7.07 and 7.98 in the streams. Iron, manganese, copper, and zinc concentrations are lower than the national (TN) [8] and international standards (WHO) [9] (Table 1). In addition, the Fe values are close to the standard value in some wells. The average Fe value is 107.4 $\mu\text{g/l}$ in streams, and 73.6 $\mu\text{g/l}$ in groundwater. The Fe increase in the Guenniche plain is probably due to the presence of ironworks in the West of the study area, the oil refinery in the northern part, and many factories in the zone of El Alia. In streams, two sampling areas have higher Hg values than the standard value of 1 $\mu\text{g/l}$, according to the

Table 1 Maximum (Max), Minimum (Min), Mean, Standard deviation for groundwater (20 samples) and streams (10 samples) of Guenniche plain, and national (NT) [8] and international (WHO) [9] standard for drinking water

The measuring elements	Groundwater				River				Standard	
	Max	Min	Mean	Standard deviation	Max	Min	Mean	Standard deviation	WHO (2006)	NT (2013)
EC (mS/cm)	7.32	0.64	3.75	1.85	6.54	2.38	4.33	1.35	–	–
T (°C)	21.90	19.10	20.90	0.88	25.8	21.3	24.31	1.51	25	25
pH	7.72	6.80	7.21	0.26	7.98	7.07	7.50	0.37	6.5–9.5	6.5–8.5
Manganese (µg/l)	20.17	0.12	4.51	5.78	22.89	0.43	1.11	0.58	40	50
Iron (µg/l)	188.3	10.2	73.6	54.1	191.1	57.1	107.4	29.3	–	200
Copper (mg/l)	0.88	0.00	0.08	0.20	1.98	0.01	0.72	0.64	2	2
Zinc (mg/l)	0.41	0.01	0.06	0.09	1.13	0.08	0.62	0.42	3	5
Mercury (µg/l)	1.91	0.04	0.75	0.47	2.89	0.06	1.11	0.97	6	1
Arsenic (µg/l)	8.55	0.05	3.16	2.60	10.98	0.01	3.80	4.65	10	10
Chromium (µg/l)	6.62	0.00	1.40	1.88	5.71	1.01	4.11	1.73	50	50
Cadmium (µg/l)	5.43	0.06	1.69	1.85	6.11	1.14	3.16	1.75	3	5
Selenium (µg/l)	4.92	0.31	2.38	1.45	9.87	1.57	5.07	3.17	10	10

national standard (TN) [8] which is associated to the high Hg concentrations in the seven groundwater wells close to these streams. Considering the international standard (WHO) [9] that sets the limit value of Hg at 6 µg/l (Table 1), all water samples are considered to have permitted values. Hg presence is linked to industrial waste and wastewater discharge in the study area. Regarding Zn, the national standard (TN) [8] fixed the limit at 5 µg/l. Two groundwater and two surface water samples show Hg values which exceed this limit. In contrast, considering the international standard (WHO) [9], which sets the limit value to 3 µg/l, five groundwater and five surface water samples are found to exceed this limit. The Cd is a relatively rare metal in nature. Its presence in water is linked to the industrial and household waste disposed into the rivers, especially in wadi El Malah. Plastics, engine oils, batteries, thermal stability products, pesticides and wastewater discharges contribute to the increase of this element. Its presence in the rivers affects the wells (Fig. 2) that are close to these wadis (Wadi El Maleh and Guenniche). The arsenic is low in the groundwater compared to both standards WHO [9] and TN [8] (10 µg/l), but the element is present in some streams, specifically in the region of El Alia, where its values are moderately equal to, or exceed, the limit. This is reflected in the presence in the wells P1, P10 and PZ1 of the groundwater with values close to the recommended limit. For chromium and selenium, all recorded values are lower in comparison to the national and international standards for both water sources (Table 1).

The direction of surface water flow is from East to West (Fig. 1b). All the wadis (Wadi El Malah, Wadi El Hella, Wadi El Chrechira) are connected to the Guenniche Wadi, which is the main collector of the hydrographic network; these Wadis are considered polluted [1]. This pollution appears to be the result of intense agricultural activities, livestock waste, as well as untreated sewer discharges from the settlements located in the neighborhoods of this Wadi (El Alia, El Khietmine and Maghrawa) and which are, in their majority, not connected to the sewerage network [5], precisely the small villages. The uncontrolled disposal of household waste is intense in all the wadis' courses. All these sources of pollution explain the high values of some trace elements (cadmium and mercury) in some samples of shallow groundwater (Fig. 2). Moreover, the phreatic aquifer is mainly recharged by the infiltration of the surface runoff of the rivers. The nature of the soils, generally permeable in study area, facilitates the infiltration of surface water [1] and subsequently the infiltration of water polluted with toxic minerals. Indeed, the intensity of groundwater pollution depends on the type of soil and the pollutant dose [10]. In addition, the excessive use of pesticides may cause the pollution of groundwater in the Guenniche plain where agricultural activities are intense. Compared to the national standard (NT) [8], the wells P1, P2, P4, P9, P10, P14, PZ1, PZ4 and PZ6 (Fig. 2) have high values in mercury and/or cadmium. These wells are not recommended to be used for drinking water supply. The use of the wells P1, P2, P4, P6,

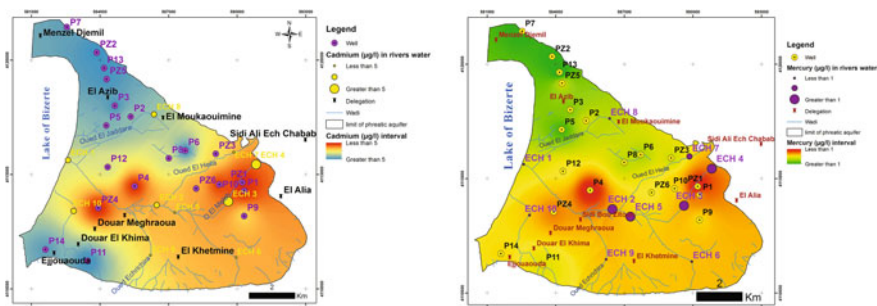


Fig. 2 The spatial distribution of. **a** Cadmium ($\mu\text{g/l}$). **b** Mercury ($\mu\text{g/l}$) in the shallow aquifer of the plain of Guenniche

P9, PZ4 and PZ1 (Fig. 2) which have a high value of cadmium presents a high risk to the human health.

4 Conclusions

Three trace elements were found to pollute the Wadi El Malah and Wadi Guenniche and this pollution is reflected in the wells that are adjacent to it. Cadmium and mercury values exceed the national standard and international WHO standard in some wells. The uncontrolled release can be dangerous to human health, as it may cause a change in the quality of soil and water in particular. Agricultural activities, uncontrolled discharges, and sewage are all contributing to the pollution of river waters, and thus, to the pollution of groundwater through the infiltration of water in the plain of Guenniche, specifically in the El Alia area. To overcome this problem and to protect the water resources of the plain of Guenniche, regarding the presence of trace elements, it is necessary to inhibit the direct urban and industrial discharges into the rivers, avoid the massive use of chemical fertilizers and pesticides on sites known for their high vulnerability and high permeability, and compensate by techniques and ecological matters that contribute to the conservation of the environment.

References

- Hammami, J., Kouzana, L., Farhat, B., Ben Mammou A, Waterloo, M., Ghabri, D.: Approaches for evaluating the groundwater suitability for domestic and agricultural uses in guenniche plain, northern Tunisia. *J. Hydraul. Eng.* 38–51. <https://doi.org/10.17265/2332-8215/2016.01.005> (2016)
- INS.: Institut National de la Statistique, Recensement général de la population et du logement (2014)
- MCKinney, M.L.: Urbanization, biodiversity and conservation. *BioScience* **52**(10), 883–890. <https://doi.org/10.1641/0006-3568052> [0883:UBAC]2.0.CO;2 (2002)
- DGEQV.: “Direction Générale de l’Environnement et de la Qualité de la Vie”—Etude sur la dépollution industrielle dans le bassin versant du lac de Bizerte. Min. Agric., p. 200. Tunisie (2003)
- Garali, A., Ouakad, M., Gueddari, M.: Bilans hydrologiques de la lagune de Bizerte (nord-est de la Tunisie). *Rev. Sci. Eau* **22**(4), 525–534 (2009). <https://doi.org/10.7202/038329ar>. Tunisie
- INM.: “Institut National de la météorologie” Données climatologique de la plaine de Guenniche (2010–2016)
- Dussart, B.: *Limnologie: Etude des eaux continentales*. Gauthier-Villars, Ed., Paris (1966)
- NT.: Norme tunisienne NT 09-14, relative a la qualite des eaux de boisson (2013)
- WHO.: *Guidelines for drinking-water quality, Vol.1, Recommendations*. – 3rd ed. World Health Organization, Geneva. www.who.int/water_sanitation_health. (ISBN 978 92 4 154761 1) (2006)
- Bermond, R., Vuichaard, R.: *Les paramètres de la qualité des eaux*. Documentation Française, p. 179. Paris (1973)

Export Balance of Polybrominated Diphenyl Ethers at the Scale of the Charmoise Watershed (France)

Khawla Tlili, Pierre Labadie, Fabrice Alliot, Catherine Bourges, Annie Desportes, and Marc Chevreuil

Abstract

Fire sources in indoor spaces keep increasing, especially because of the growing number of electrical and electronic equipment uses. To reduce the risks of fire, several chemicals, called flame retardants (FRs), are used particularly in brominated compounds (BFRs). Polybrominated biphenylethers (PBDEs) are widely used in industry to prevent fires. These compounds are part of the composition in many consumer products (textiles, electronics, plastics...) in order to reduce their flammability. They have a pronounced structural similarity with thyroid hormones and they are strongly suspected for being responsible of endocrine disruption processes. The pathways of PBDEs to surface waters are multiple: atmospheric inputs, releases of Waste Water Treatment Plant (WWTP), urban storm-water discharge (USD), leaching or erosion of contaminated soils (atmospheric route or following urban sludge amendments). To identify the relative importance of each source of inputs in PBDE at the level of a peri-urban elemental catchment area, a flow assessment was carried out at the level of the basin of the Charmoise, France.

Keywords

PBDEs • Bulk deposition • Flux • Surface water • Sewage sludge

1 Introduction

The technological advances of recent decades have made human societies fervent consumers of new industrial products which contain xenobiotic compounds such as polybrominated biphenylethers (PBDEs). PBDEs are brominated Flame Retardants added to consumer products to help slow the spread of fire. It is due to their persistence, bioaccumulation ability and toxicity properties, that PBDEs have gradually been subject to use restrictions within the European Union. Surface water receives and carries many organic micropollutants such as PBDEs, particularly in urban areas. In dry weather, treated wastewater discharges are the primary source of PBDEs to surface water [10]. On the other hand, in rainy weather, rivers can also be contaminated by PBDEs via urban storm water discharges [11], the overflow of unit sewer networks [4] and atmospheric deposition (especially wet deposition, [12]). PBDE surface water contamination is still largely unknown; moreover, in France, several questions concerning the origin of PBDEs and their levels in hydrographic networks remain unanswered. This study aims to determine the relative PBDE inputs to the surface water, by performing a mass balance at the level of an elementary watershed.

2 Materials and Methods

The Charmoise River (7.5 km) is a tributary of the Rémarde, which is itself a tributary of the Orge River. It receives the discharge of the Fontenay-les-Briis WWTP that collects domestic effluents and the rainwater from the town of Fontenay-les-Briis by the unitary network. In this study, the samples were taken on a monthly basis over a period of three months (November 2010–January 2011). 3.5 L of unfiltered surface water (upstream/downstream1 and downstream 2 from the discharge of WWTP) and a total bulk deposition were collected. This volume was reduced to 500 mL in the

K. Tlili (✉)

Faculty of Sciences of Bizerte, 7021 Jarzouna, Tunisia
e-mail: khawlatlili@hotmail.com

P. Labadie

UMR 5805 EPOC, Equipe LPTC, 33405 Talence, France

F. Alliot · C. Bourges · A. Desportes · M. Chevreuil
Laboratoire Hydrologie et Environnement EPHE,

UMR 7619 METIS, Université Pierre et Marie Curie,
75252 Paris Cedex 05, France

case of wastewater (inlet/outlet from Fontenay-les-Briis WWTP). During this campaign, a soil sample was also collected near the Charmoise River, as well as dry sewage sludge produced by the Fontenay-les-Briis WWTP.

In the case of bulk deposition, surface and wastewater, a liquid-liquid extraction was performed on unfiltered water samples. The sewage sludge (1 g) and soil samples (1 g) were extracted by ultrasonication [7]. Extracts were first purified through florisil cartridges and were then further cleaned-up through a multilayer column as described by [7]. PBDE analysis was achieved using an Agilent 7890 A gas chromatograph coupled to an Agilent 7000 B triple quadrupole mass spectrometer (GC-MS/MS; Agilent, Massy, France) as described by [7].

3 Results

3.1 Level of PBDE Contamination

In the wastewater at the entrance of the WWTP, the mean concentration is equal to $14.23 \pm 2.7 \text{ ng L}^{-1}$ for Σ tri-hepta BDE and $50.0 \pm 28.0 \text{ ng L}^{-1}$ for BDE-209 (Fig. 1).

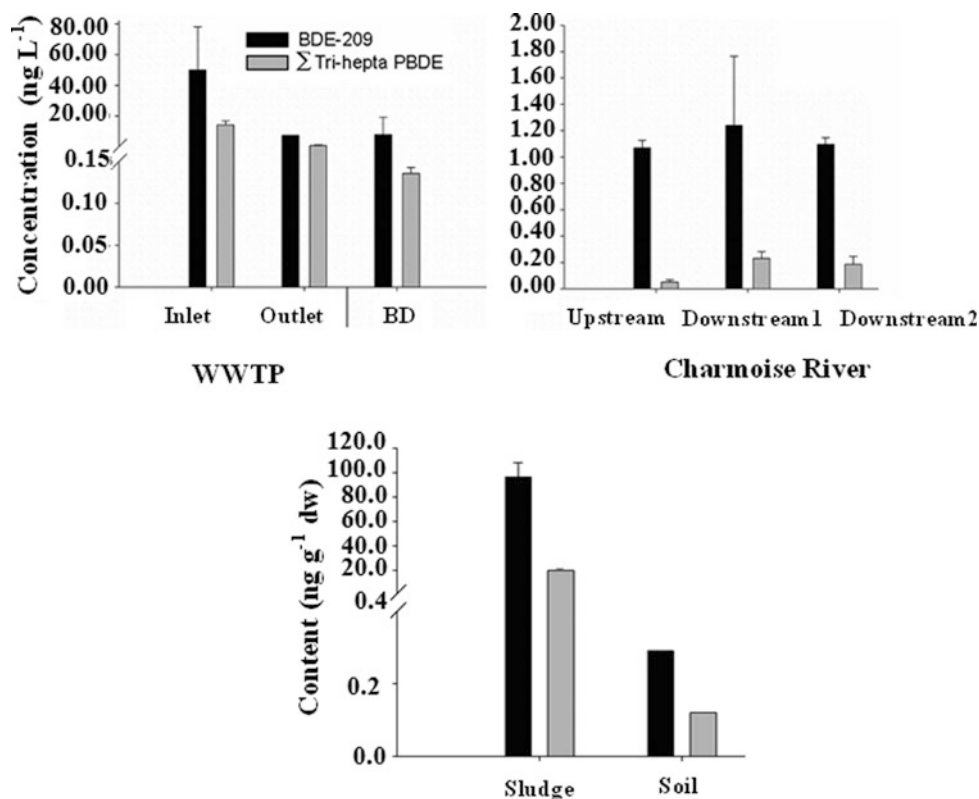
The concentrations observed at the output of WWTP are approximately 7–19 times lower: $0.75 \pm 0.10 \text{ ng L}^{-1}$ for the Σ tri-hepta BDE and $7.45 \pm 0.06 \text{ ng L}^{-1}$ for the BDE-209.

For bulk deposition, the mean concentrations of Σ tri-hepta BDE and BDE-209 are 0.14 ± 0.01 and $8.0 \pm 11.2 \text{ ng L}^{-1}$, respectively (Fig. 1). An increase in PBDE concentrations in the upstream-downstream of the WWTP discharge was observed. The average of Σ tri-hepta-BDE concentrations upstream and downstream of the WWTP discharge are respectively 0.05 ± 0.02 and $0.23 \pm 0.05 \text{ ng L}^{-1}$. The mean BDE-209 upstream concentration ($1.07 \pm 0.06 \text{ ng L}^{-1}$) is also below its mean concentration determined in immediately downstream of the WWTP release ($1.24 \pm 0.53 \text{ ng L}^{-1}$). Contamination levels of Σ tri-hepta BDEs and BDE-209 in the sewage sludge of the Fontenay-les-Briis WWTP are respectively equal to 19.86 ± 0.34 and 96.50 ± 11 , $54 \text{ ng g}^{-1} \text{ dw}$ (i.e. $116 \pm 12 \text{ ng g}^{-1} \text{ dw}$ of Σ tri-deca BDEs). The levels determined in the soil near the La Charmoise River (Σ tri-hepta BDEs: $0.11 \text{ ng g}^{-1} \text{ dw}$ and BDE-209: $0.29 \text{ ng g}^{-1} \text{ dw}$, Fig. 1) are below those determined for an amended soil at Giremoutiers (Σ tri-hepta BDEs: $0.27 \text{ ng g}^{-1} \text{ dw}$ and BDE-209: $0.72 \text{ ng g}^{-1} \text{ dw}$) [9].

3.2 Balance of Flows

The average flow at the inlet and outlet of the WWTP ($\sim 460 \text{ m}^3 \text{ d}^{-1}$) was used to estimate PBDE fluxes. Besides,

Fig. 1 PBDE Concentrations in unfiltered water (ng L^{-1} , $n = 3$) at inlet/outlet WWTP, in bulk deposition (BD), water of the Charmoise River, sewage sludge (ng g^{-1} dry weight: dw, $n = 3$) and the soil ($n = 1$)



the flow of PBDEs associated with sludge production was determined by the average amount of sludge produced daily in dry matter (88 kg). The average flow of Σ tri-deca BDE in the unfiltered water at the entrance to the WWTP is $0.039 \pm 0.025 \text{ g d}^{-1}$. They (i.e. PBDEs) are 10 times lower in the effluents ($0.004 \pm 0.002 \text{ g d}^{-1}$). The PBDE fluxes observed at the different sampling points are as follows, upstream: $0.006 \pm 0.005 \text{ g d}^{-1}$, downstream immediate: $0.009 \pm 0.008 \text{ g d}^{-1}$ and downstream distant: $0.008 \pm 0.007 \text{ g d}^{-1}$ the discharge of WWTP.

4 Discussion

The increase in PBDE concentrations in the upstream-downstream of the WWTP discharge, confirms the initial hypothesis that the WWTP Fontenay-les-Briis is a source of PBDEs for the Charmoise River, this is in line with what was reported for other WWTPs [1, 2, 10]. The decrease of PBDE concentrations from downstream 1 to downstream 2 could result from (i) the incomplete homogenization of the discharge input to a lower level or (ii) sedimentation of larger particles in water column. PBDEs are highly hydrophobic and preferentially associated with particles in aqueous matrices, and are thus, concentrated in sludge during wastewater treatment [8]. Otherwise, Σ 8 PBDE contents are higher (186–781 ng g^{-1} dw, for 11 WWTPs, [6]) than those determined by this study but remained in the same order of magnitude.

The molecular profile of PBDEs in soil and bulk deposition revealed the absence of a significant difference ($p > 0.05$, Mann-Whitney). A similar result has been reported by [5]. This probably suggests that the atmosphere could be a source of PBDE inputs to the soil. For sewage sludge, the flows of Σ tri-deca BDE are equal to $0.011 \pm 0.001 \text{ g d}^{-1}$. This value is also much lower than that determined for Σ 41PBDE in sewage sludge produced by the Palo Alto WWTP in USA (0.06 kg d^{-1} , [10]). The flows of Σ tri-deca BDE in sludge taken from 31 WWTPs in Spain range from 0.6 to 17.8 g d^{-1} [3]. These values far exceed those determined in this work. Regardless of the spatial scale considered (agricultural plots or catchment area), the atmospheric inputs of PBDE are 14–26 times greater than the contributions by application of urban sludge. For both PBDEs and other compounds, atmospheric deposition is an important source of soil contaminants. However, urban sludge inputs are a known source of contamination of the amended plots. Because of its predominance in the set of abiotic matrices, the contributions in BDE-209 are much higher than in those of other PBDEs; regardless of the source considered (atmospheric or associated with the application of sludge).

The total PBDE intake, in the Charmoise watershed, is approximately 105 g/year. The annual PBDE intake from BD would be the main source of PBDE entry into the environment (100 g). As mentioned above, the application of sewage sludge on agricultural plots is also a diffuse source of PBDEs (4 g), which constitutes an indirect PBDE source to the Charmoise River. Treated wastewater discharges represent only 1% of the total annual. At the outlet of the Charmoise watershed, the annual flux of PBDEs (3 g) represents only 3% of the total annual contributions. This suggests (i) a sequestration of PBDEs in the soils and sediments of the basin and/or (ii) a degradation of PBDEs (biological or photolytic) in all compartments of the studied ecosystem.

5 Conclusions

The supply of wastewater purified by the WWTP Fontenay-les-Briis is a point source of PBDE inputs to the Charmoise River; nevertheless, they represent only a relatively minor source of contamination. The PBDE inputs to the watershed are mainly due to two diffuse sources: firstly, the atmospheric deposition and secondly, the sewage sludge amendments of the agricultural plots.

Thus, rainwater runoff on the amended agricultural plots, coupled with the presence of high levels of PBDEs in sewage sludge, represents another potential route of PBDE introduction into the aquatic environment, even though the flows exported to the outlet of the Orge River remain low in terms of total inputs. These exports would thus be mainly conditioned by hydrological and hydrological conditions.

References

1. Anderson, T.D., MacRae, J.D.: Polybrominated diphenyl ethers in fish and wastewater samples from an area of the Penobscot River in Central Maine. *Chemosphere* **62**(1), 1153–1160 (2006)
2. De Boer, J., Wester, P.G., van der Horst, A., Leonards, P.E.G.: Polybrominated diphenyl ethers in influents, suspended particulate matter, sediments, sewage treatment plant and effluents and biota from the Netherlands. *Environ. Pollut.* **122**(1), 63–74 (2003)
3. De la Torre, A., Sverko, E., Alae, M., Martínez, A.M.: Concentrations and sources of Dechlorane Plus in sewage sludge. *Chemosphere* **82**(5), 692–697 (2011)
4. Gasperi, J., Garnaud, S., Rocher, V., Moilleron, R.: Priority pollutants in surface waters and settleable particles within a densely urbanised area: case study of Paris (France). *Sci. Total Environ.* **407**(8), 2900–2908 (2009)
5. Hayakawa, K., Takatsuki, H., Watanabe, I., Sakai, S.I.: Polybrominated diphenyl ethers (PBDEs), polybrominated dibenzo-p-dioxins/dibenzofurans (PBDD/Fs) and monobromo-polychlorinated dibenzo-p-dioxins/dibenzofurans (MoBPXDD/Fs) in the atmosphere and bulk deposition in Kyoto, Japan. *Chemosphere* **57**(5), 343–356 (2004)

6. Knoth, W., Mann, W., Meyer, R., Nebhuth, J.: Polybrominated diphenyl ether in sewage sludge in Germany. *Chemosphere* **67**(9), 1831–1837 (2007)
7. Labadie, P., Tlili, K., Alliot, F., Bourges, C., Desportes, A., Chevreuil, M.: Development of analytical procedures for trace-level determination of polybrominated diphenyl ethers and tetrabromobisphenol a in river water and sediment. *Anal. Bioanal. Chem.* **396**(2), 865–875 (2010)
8. Langford, K.H., Scrimshaw, M.D., Birkett, J.W., Lester, J.N.: The partitioning of alkylphenolic surfactants and polybrominated diphenyl ether flame retardants in activated sludge batch tests. *Chemosphere* **61**(9), 1221–1230 (2005)
9. Moreau-Guigon, E., Labadie, P., Gaspéri, J., Blanchard, M., Cladière, M., Teil, M.-J., Tlili, K., Desportes, A., Bourges, C., Alliot, F., Lorgeoux, C., Chevreuil, M.: Diffusion de perturbateurs endocriniens par le compartiment atmosphérique et les amendements agricoles, contamination des sols et transferts, pp. 1–13 (2007–2010)
10. North, K.D.: Tracking polybrominated diphenyl ether releases in a wastewater treatment plant effluent, Palo Alto, California. *Environ. Sci. Technol.* **38**(17), 4484–4488 (2004)
11. Oram, J.J., McKee, L.J., Werme, C.E., Connor, M.S., Oros, D.R., Grace, R., Rodigari, F.: A mass budget of polybrominated diphenyl ethers in San Francisco Bay, California. *Environ. Int.* **34**(8), 1137–1147 (2008)
12. Ter Schure, A.F.H., Larsson, P., Agrell, C., Boon, J.P.: Atmospheric transport of polybrominated diphenyl ethers and polychlorinated biphenyls to the Baltic Sea. *Environ. Sci. Technol.* **38**(5), 1282–1287 (2004)

Hydrogeochemical Modeling and Isotopic Assessment of the Quaternary Aquifer at Ali al-Garbi Area in Misaan Governorate, South of Iraq

Hussein Ghalib, Mohsin Yaqub, and Alaa Al-Abadi

Abstract

Geochemical modeling and environmental isotopes were used to determine the hydrogeochemical evolution and the main factors controlling the groundwater chemistry in Misaan, South of Iraq. All available $\delta^{18}\text{O}$ and $\delta^2\text{H}$ data for the study area are plotted along the Global Meteoric Water Line (G-MWL) and Mediterranean Meteoric Water Line (M-MWL), indicating a meteoric origin of all waters. The groundwater samples were exposed to evaporation before entering the aquifer. Tritium values of groundwater are between 0.8 and 1.2 TU. These are estimated as modern and pre-modern (older than about 50 years). The geochemical modeling results show that the dissolution of dolomite, gypsum, halite, siderite, the cation exchange of $\text{Ca}^{2+}/\text{Na}^+$, and the precipitation of calcite, sylvite and hematite are the main chemical reactions in the first period (dry period), whereas there are no specific reactions that can be shown in the second period (wet period). The inverse geochemical modeling shows that the main reaction controlling the groundwater quality is the Dedolomitization process (dolomite dissolution driven by anhydrite dissolution and calcite precipitation).

Keywords

Geochemical modeling • Environmental isotopes • Groundwater geochemical evolution • Iraq

1 Introduction

In recent years, there have been increasing concerns about the reduction in discharge and the degradation of the water quality of the Euphrates, Tigris and Shatt Arab Rivers in

H. Ghalib (✉) · M. Yaqub · A. Al-Abadi
 Department of Geology, College of Science, University of Basra,
 Basra, Iraq
 e-mail: hbggeo@gmail.com

Iraq, thus increasing the need for serious investigations of the availability and quality of groundwater resources in the region. In arid regions, groundwater is a significant part of the total water resource to determine the safe yield of an aquifer. Reliable estimates of groundwater recharge are needed for a sustainable management of groundwater resources [1, 2].

Water scarcity is now emerging as the most detrimental environmental issue afflicting the population of the Middle East. This is especially true in the south of Iraq, particularly after the emergence of drought conditions in the country [3].

The main objectives of this research were to apply the isotopic composition, stable and radioactive isotopes of the water and:

- (1) compare the isotopic composition of water resources in Misaan area with that of global meteoric water line (GMWL) and Mediterranean meteoric water line (MMWL);
- (2) use the tritium concentration in groundwater as an indicator of groundwater age by comparison with historical records of elevated tritium levels in precipitation; and
- (3) use major ions and the isotopic composition ($\delta^2\text{H}$, $\delta^{18}\text{O}$) as environmental tracers to investigate the stream-aquifer connectivity in the study area.

2 Materials and Methods

Figure 1 shows the all selected samples and the locational map in the study area. The Chemical analysis of groundwater for two periods measured the concentrations of major cation (Ca^{+2} , Mg^{+2} , Na^+ , K^+) and anion (Cl^- , SO_4^{2-} , NO_3^- , HCO_3^-), total dissolved salts (TDS), and electrical conductivity (EC) Table 1. The current study has been conducted to determine groundwater evolution and quality by considering the physicochemical groundwater quality variables such as

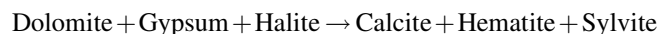
EC, pH, TDS, Ca^{2+} , Mg^{2+} , Na^+ , K^+ , Cl^- , HCO_3^- , SO_4^{2-} and CO_3^{2-} . The analyses (stable isotopes) were conducted at the Laboratory of Stable Isotopes in Davis at the University of California in the US. Isotopic ratios were measured using an IRMS. The tritium analyses were done at the Isotope Laboratory in the Ministry of Science and Technology, Iraq (Baghdad) by using LWSIA (Liquid Water Stable Isotope Analyzer). The isotopic composition of the water samples ranges from -3.83 to -1.65‰ for $\delta^{18}\text{O}$ versus V-SMOW (with an average of -3.05‰), and the $\delta^2\text{H}$ values vary between -14.9 and -3.9‰ versus V-SMOW (with an average of -10.5‰) (Fig. 1).

3 Results

Twenty samples of groundwater wells were selected to evaluate the hydrogeochemical evolution and isotopic composition for groundwater of the studied area (see Fig. 2). The hydrogeochemical characteristics of the study area for groundwater were determined by the Piper diagram and the Scholler. According to these diagrams, the chemical composition of groundwater in most wells of the study area was dominated by the Ca– SO_4 over the two study periods, while a few wells have shown an Na– SO_4 or Mg– SO_4 dominance. Hydrogeochemical spatial variation in groundwater shows an increase in concentration of salinity with a flow direction of groundwater in the study area (see Fig. 2). According to geochemical modeling calculations, ionic contents of groundwater differ according to dissolution and precipitation of carbonate and sulphate minerals.

NETPATH software was used for the calculations of the geochemical models. Dolomite and gypsum were the

predominant reactions along with calcite precipitation (d-dolomitization).



The isotopic composition of the water samples ranges from -3.83 to -1.65‰ for $\delta^{18}\text{O}$ versus V-SMOW (with an average of -3.05‰), and the $\delta^2\text{H}$ values vary between -14.9 and -3.9‰ versus V-SMOW (with an average of -10.5‰) (Fig. 3). According to the stable isotope data $\delta^{18}\text{O}$ and $\delta^2\text{H}$, most wells of groundwater are of meteoric origin and are exposed to evaporation. The isotopic composition allows the possibility to identify a hydraulic connection between the two types of water [4]. Local Meteoric Water Line (L-MWL) is close to GMWL (see Fig. 3), this indicates that the climate of the study area is affected by Arab Gulf climate.

4 Conclusions

Calculations of saturation indices of mineral phases indicate that there are changes in these values in the study area for two periods (dry and wet). Major minerals such as calcite, dolomite, gypsum and sylvite show significant spatial and temporal changes but no significant change in other minerals. Also, the calculations show us the precipitation and dissolution processes of minerals in the study area. The situation during the wet period shows a significant difference as compared to the dry period in December. Generally, the results of the applied geochemical models are the dominant geochemical process of dolomitization involving dolomite, gypsum and halite dissolution, and the calcite precipitation

Table 1 Chemical analysis for two periods of the study area

Dry period					Wet period				
Parameter	Units	Min	Max	Ave	Parameter	Units	Min	Max	Ave
EC	($\mu\text{s}/\text{cm}$)	619	7660	4302.3	EC	($\mu\text{s}/\text{cm}$)	610	4938	3287.9
TDS	mg/l	400	5800	3048	TDS	mg/l	400	3900	2479.7
pH		6.2	6.7	6.4	pH		5.89	6.99	6.79
T	($^{\circ}\text{C}$)	27	30	28.6	T	($^{\circ}\text{C}$)	20.6	26.3	23.71
Na^+	mg/l	25	1135	482.6	Na^+	mg/l	114	1240	821.35
K^+	mg/l	3	52.5	16	K^+	mg/l	1.5	29	9.92
Ca^{+2}	mg/l	104	1100	738.8	Ca^{+2}	mg/l	100	960	601.76
Mg^{+2}	mg/l	10	550	298.8	Mg^{+2}	mg/l	10	450	219.59
Cl^-	mg/l	70	1372	934.6	Cl^-	mg/l	56	1180	818.53
SO_4^{-2}	mg/l	300	3050	2070.1	SO_4^{-2}	mg/l	300	2850	1647.6
NO_3^-	mg/l	1.9	30.59	11.2	NO_3^-	mg/l	1	27	10.54
HCO_3^-	mg/l	40	204	126.4	HCO_3^-	mg/l	30	200	115.44
Fe^{+2}	mg/l	0.23	0.86	0.5	Fe^{+2}	mg/l	0.09	0.73	0.44

Fig. 1 Location of the study area

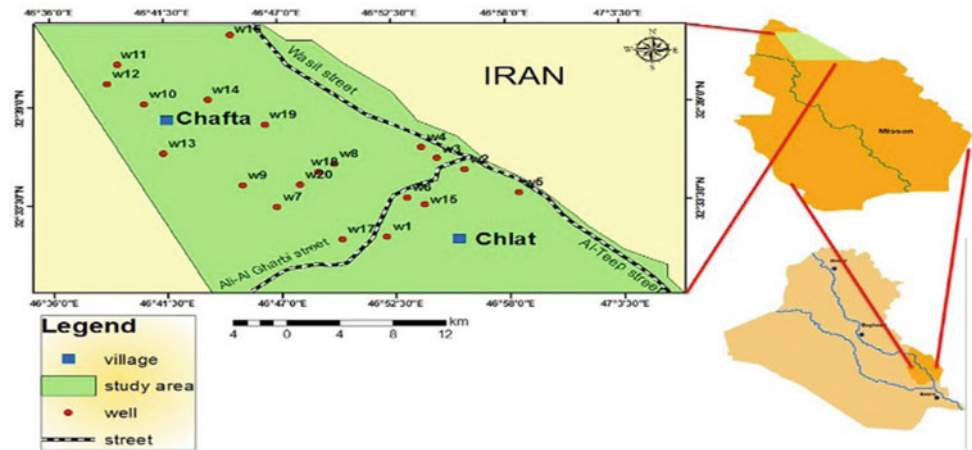


Fig. 2 TDS distribution of groundwater

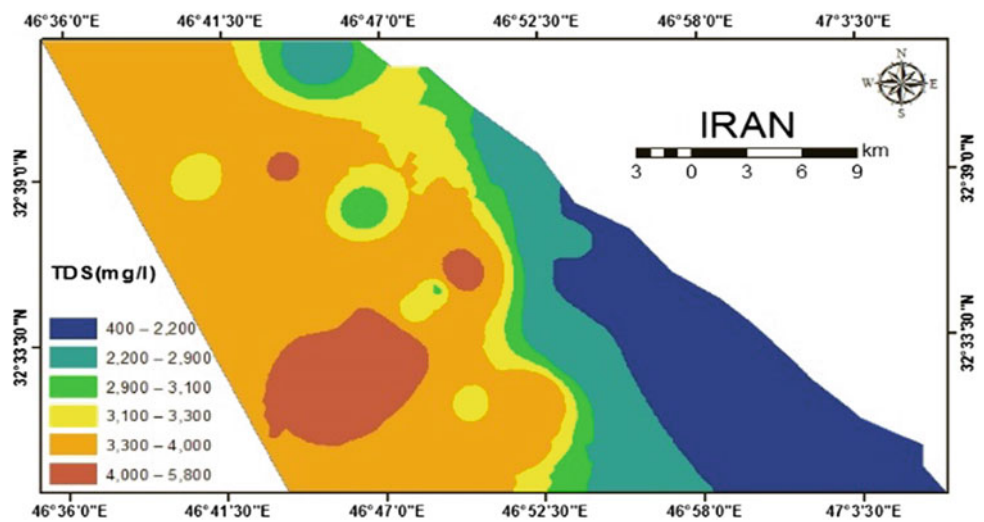
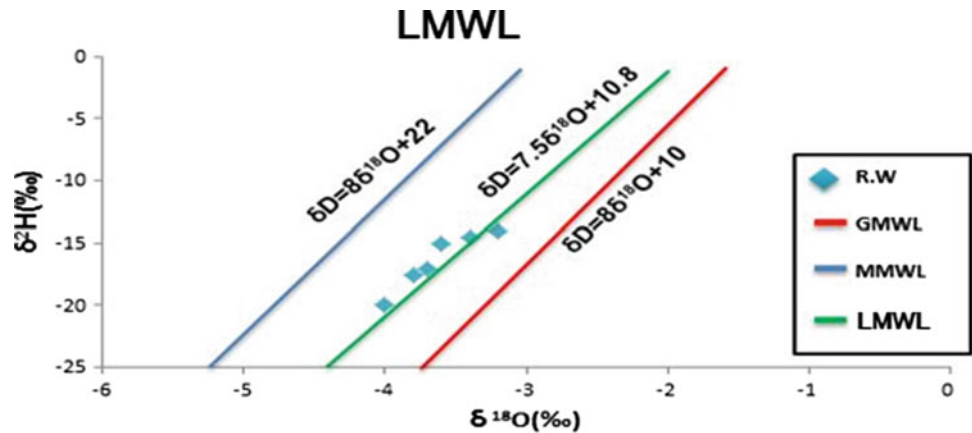


Fig. 3 LMWL for Missan (Ali Al-Gharbi) during the observation periods December 2015 and January, February 2016



of groundwater in the study area. The stable isotopes for all samples of groundwater are located between GMWL and MMWL, this indicates that these samples are a mixture of two types. Local meteoric water line (LMWL) is close to GMWL and away from MMWL, this indicates that the

climate of the study area is affected by the Arab Gulf climate. Based on the stable isotope compositions and radioactive isotope (^3H), most of the Missan group aquifer groundwater is considered to be sub-modern—recharged prior to 1952, during the last three to four decades.

References

1. Bowen, G.J.: The online isotopes in precipitation calculator, version 2.2. <http://www.waterisotopes.org> (2010)
2. Clark, I.D., Fritz, P.: Environmental Isotopes in Hydrogeology, p. 320. CRC Press, Florida (1997)
3. Ghalib, H.B.: Groundwater Chemistry Evaluation for Drinking and Irrigation Utilities in East Wassit province, Central Iraq. *Applied Water Science* (2017)
4. Ghalib, H.B., Sogut, A.R.: Environmental Isotopic Characterization of Groundwater and Surface Water in Northeast Missan Province, South Iraq. *ACGS Acta. Geol. Sin. Engl. Edn.* **88**, 1227–1238 (2014)

Geochemical Classification of Groundwater System in a Rural Area of Nigeria

Theophilus A. Adagunodo, Rachael O. Adejumo,
and Anuoluwapo M. Olanrewaju

Abstract

The characteristics of the groundwater system in Iresa-Apa, Oyo state, Nigeria, were studied using the Piper linear approach. Twenty-four water samples were randomly collected to cover the area of study. The analyzed cations from the samples are Mg^{2+} , Na^+ , K^+ , and Ca^{2+} , while the anions are CO_3^{2-} , HCO_3^- , SO_4^{2-} , and Cl^- . The three hydrochemical facies identified are Ca–Mg–Na, Ca–Mg–Na– SO_4 , and Na–K–Cl– SO_4 types. The similarities in the observed water types suggest that almost the same geochemical processes are controlling the cation-anion reaction of the groundwater system in the study area.

Keywords

Geochemical • Groundwater classification
Hydrochemical facies • Iresa-Apa • Cations and anions

1 Introduction

The geochemical characteristics of groundwater could give an insight into the subsurface rocks and the groundwater system relationships which influence its quality. The aim of this work is to explain the basic chemical characteristics of groundwater in Iresa-Apa, SW Nigeria and their effect on its quality.

The study was conducted in Iresa-Apa, Oyo state, Nigeria (Fig. 1). The study area has good road networks that linkup with the neighboring communities. The residents are into

agricultural practices. The study area is located on one of the basement complex rocks in Nigeria [8], with gneiss, quartzite and biotite being the major rocks. The hydrogeological setting of the study area is classified as PreCambrian basement rock [4], which houses groundwater within the weathered rocks and/or fractured bedrocks [3].

2 Materials and Method

Samples from twenty-four (24) dug well, with the depths varying from 10 to 12 m, were randomly collected in Iresa-Apa, Oyo state, Nigeria, using polyethylene bottles. The sample collection procedures were in line with Selvakumar et al. [11], Ganiyu et al. [7] and Narsimha et al. [9] methods for water analysis, while the cationic and anionic analyses were carried out as recommended by APHA [6]. The chemical constituents of the water samples were carried out at the Water Supply and Sanitation Project Laboratory, Ibadan. The atomic absorption spectrophotometric method was used for the analyses of the cations; namely magnesium, sodium, potassium and calcium. The titrimetric method was used for the analyses of carbonate and bicarbonate ions (alkalinity tests), the spectrophotometric method was used for sulphate analysis, while the silver nitrate titrimetric method was used for the chloride analysis. The Piper analysis was used to classify the hydrochemical facies of the study area from the obtained geochemical results.

3 Results and Discussion

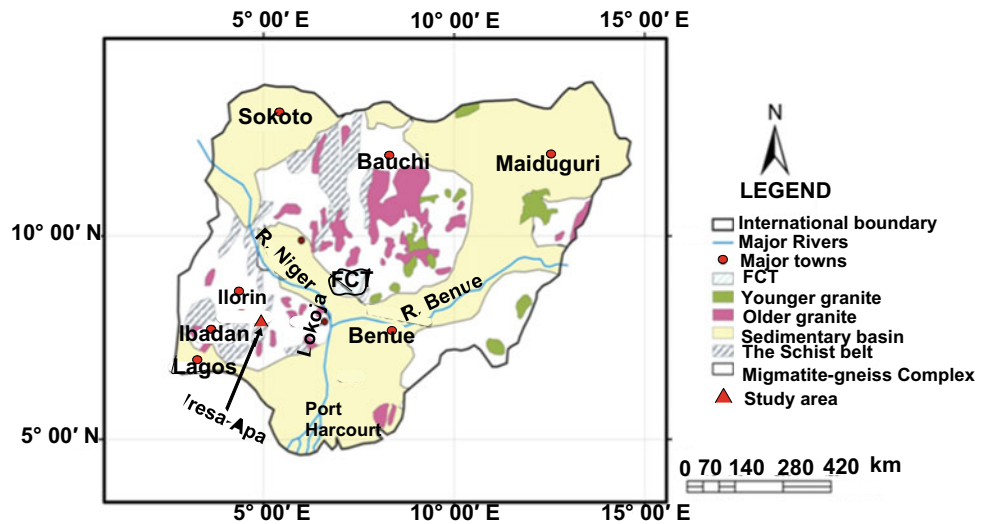
The geochemical results obtained from the study area showed that magnesium (Mg^{2+}) ranged from 1.96 to 21.56 mg/l, sodium (Na^+) ranged from 0 to 18.0 mg/l, potassium (K^+) ranged from 0 to 10 mg/l, calcium (Ca^{2+}) ranged from 16.80 to 75.20 mg/l, carbonate ion (CO_3^{2-}) ranged from 15.0 to 98.0 mg/l, bicarbonate ion (HCO_3^-)

T. A. Adagunodo (✉)
Department of Physics, Covenant University, Ota, Nigeria
e-mail: taadagunodo@yahoo.com

R. O. Adejumo
Independent Geologist, Osogbo, Osun State, Nigeria

A. M. Olanrewaju
Department of Mathematics, Covenant University, Ota, Nigeria

Fig. 1 The study area and the Nigerian geology (Adapted and modified from [5])



ranged from 18.0 to 117.6 mg/l, sulphate (SO_4^{2-}) ranged from 0 to 19.0 mg/l and chloride (Cl^-) ranged from 4.0 to 42.0 mg/l.

The Piper diagram (Fig. 2) used in this work is a graphic representation method of the percentage equivalence (where mg/l is converted to meq/l). For this study, three main water types were identified as follows:

1. Ca–Mg–Na water type: This is characterized as a water type with relatively high calcium hardness when compared with total hardness. This, in effect, means that there are more ions than the available alkaline earth metal ions (Ca^{2+} and Mg^{2+}) in equivalent concentrations. Consequently, the excess ions then react with the alkali metal ions in the solution (usually Na^+) through the cation exchange process to enrich the water with sodium ions. The chemical weathering processes, which result in the

dissolution of sodium rich materials in the water, as well as soaps and detergents washed in from the adjoining streams may be responsible for the cation exchange reaction.

- Ca–Mg–Na– SO_4 water type: This is similar to the first water type (Ca–Mg–Na) experience in the study area. The first two water types both result from cation exchange processes, the only difference being that SO_4^{2-} is the dominant anion. The source of SO_4^{2-} in the water can be narrowed down to the final oxidation stages of sulphides, sulphites and the sulphates organic matters and in most cases as a product of pollution from domestic and fertilizer leaching. The sources of SO_4^{2-} in the water sample in the study area can be linked to the decomposition and dissolution of waste material within the dumpsites and possibly from dissolved SO_2 in rain water, as a result of the combustion of fossil fuels associated with vehicles.
- Na–K–Cl– SO_4 water type: The presence of sodium and potassium might be from clay material, while Chloride results from sewage effluents into the surrounding drainage system. In general, groundwater samples from the area are chemically Ca–(Mg)–Na–Cl type. The chemical character of the water is controlled by the aqueous concentration of bicarbonate, calcium, magnesium and chloride, on the basis of the abundant mean concentration.

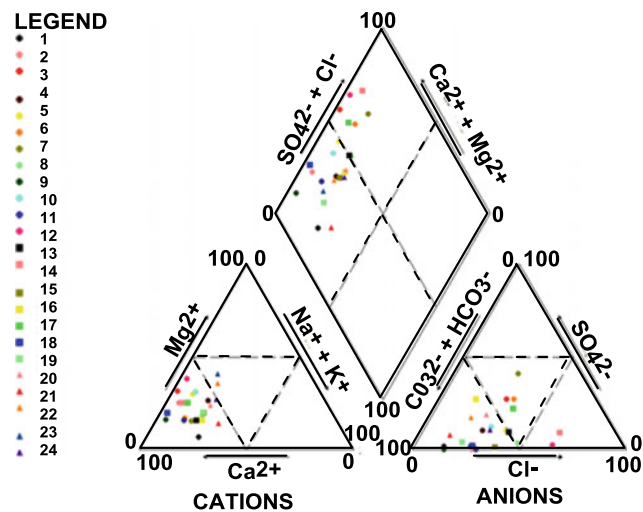


Fig. 2 Geochemical classification of the groundwater in Iresa-Apa

Based on the results of this study, it was revealed that groundwater contaminations are from geogenic (weathering processes) and anthropogenic sources. Nevertheless, the global standards as set by WHO [12] revealed that the groundwater system in the study area is fit for agricultural practices but that it would require treatment before it can be fit for domestic usages.

4 Conclusion

The trilinear diagram has been used for the classification of hydrochemical facies scheme of the groundwater system in Iresa-Apa. The plot gives the hydrochemical facies classification or the type of water that occurs in the study area. The similarities in water types suggest that similar geochemical processes are probably controlling the major ion chemistry in Iresa-Apa. This is in agreement with the pattern of water chemistry in Basement Complex: a water system that is controlled by lithology and precipitation [10]. Periodic evaluation is recommended for domestic usability of groundwater in the study area.

Acknowledgements We appreciate the conference support received from Covenant University, Nigeria.

References

1. Adagunodo, T.A.: Groundwater Pollution and Control: An Overview. Chapter 1 in Book: Groundwater Contamination: Performance, Limitations and Impacts, pp. 1–135. ISBN: 978-1-153611-017-3; 978-1-53611-003-6. Editor: Anna L. Powell © 2017 Nova Science Publishers, Inc. pp. 1–12 (2017a)
2. Adagunodo, T.A.: Groundwater Contamination: Performance, Effects, Limitations and Control. Chapter 3 in Book: Groundwater Contamination: Performance, Limitations and Impacts, pp. 1–135. ISBN: 978-1-153611-017-3; 978-1-53611-003-6. Editor: Anna L. Powell © 2017 Nova Science Publishers, Inc. pp. 33–64 (2017b)
3. Adagunodo, T.A., Akinloye, M.K., Sunmonu, L.A., Aizebeokhai, A.P., Oyeyemi, K.D., Abodunrin, F.O.: Groundwater exploration in Aaba residential area of Akure, Nigeria. *Front. Earth Sci.* **6**, 66 (2018). <https://doi.org/10.3389/feart.2018.00066>
4. Adagunodo, T.A., Sunmonu, L.A., Ojoawo, A., Oladejo, O.P., Olafisoye, E.R.: The hydro geophysical investigation of Oyo State industrial estate Ogbomosho, Southwestern Nigeria using vertical electrical soundings. *Res. J. Appl. Sci. Eng. Technol.* **5**(5), 1816–1829 (2013)
5. Adejumo, R.O., Adagunodo, T.A., Bility, H., Lukman, A.F., Isibor, P.O.: Physicochemical constituents of groundwater and its quality in crystalline bedrock, Nigeria. *Int. J. Civ. Eng. Technol.* **9** (8), 887–903 (2018)
6. APHA: Standard Methods for the Examination of Water and Wastewater. American Public Health Association, Washington DC (1998)
7. Ganiyu, S.A., Badmus, B.S., Olurin, O.T., Ojekunle, Z.O.: Evaluation of seasonal variation of water quality using multivariate statistical analysis and irrigation parameter indices in Ajakanga area, Ibadan, Nigeria. *Appl. Water Sci.* **8**, 35 (2018)
8. Maxwell, O., Wagiran, H., Ibrahim, N., Lee, S.K., Soheil, S.: Comparison of ^{238}U , ^{232}Th , and ^{40}K in different layers of subsurface structures in Dei-Dei and Kubwa, Abuja Northcentral Nigeria. *Radia. Phys. Chem.* **91**, 70–80 (2013)
9. Narsimha, A., Venkatayogi, S., Geeta, S.: Hydrogeochemical data on groundwater quality with special emphasis on fluoride enrichment in Menneru River Basin (MRB), Telangana state, South India. *Data Brief* **17**, 339–346 (2018)
10. Offodile, M.E.: The occurrence and exploitation of groundwater in Nigeria Basement rocks. *Journal of Mining and Geology* **20**, 131–146 (1983)
11. Selvakumar, S., Chandrasekar, N., Kumar, G.: Hydrogeochemical characteristics and groundwater contamination in the rapid urban development areas of Coimbatore, India. *Water Resour. Ind.* **17**, 26–33 (2017)
12. WHO: Guidelines for Drinking-Water Quality. First Addendum to 3rd edn. Recommendations. World Health Organization, Geneva (2004)

Contamination of Annaba bay (northeastern extremity of Algeria) by multi-pesticide residues

Soumeya Khaled-Khodja, Semia Cherif, and Karima Rouibah

Abstract

Annaba Bay is the ultimate receiver of innumerable chemical substances issued from various anthropogenic activities. These telluric releases could have biocidal properties. In order to preserve the quality of the coastal waters and to limit these flows that are dangerous for the marine environment, seasonal monitoring of water quality of the two main wadis has been carried out. The results show that Bouhamra wadi is mainly polluted by organochlorine and organophosphate insecticides, herbicides and fungicides. While the Seybouse wadi is affected mainly by organophosphate insecticides, herbicides and fungicides. The quality of the wadis is very poor with respect to organochlorine, organophosphate insecticides and herbicides. Acceptable quality is attributed to water with respect to fungicides.

Keywords

Multi-pesticide residues • Organic pollution • Surface water • Bouhamra and Seybouse • Annaba Bay

1 Introduction

Phytosanitary products, or pesticides, are widely used in the sectors of crop protection, gardening and industry. Due to their toxicity and ecotoxicity, they are the subject of particular concern both in terms of public health, and for the preservation of waters and environment [1]. They are widely used in Algerian agriculture and Algeria is also a producer of plant protection products and fertilizers [2]. Given the dangers of these xenobiotics for public health and the natural environment [3–6], they should be used with great caution.

The aim of this research is the evaluation of water quality from two wadis which receive all the anthropogenic discharges from the city. As a result, they are the main source of contamination of Annaba Bay by organic micropollutants and particularly pesticide residues.

2 Materials and Methods

Bouhamra wadi collects, essentially, the domestic wastewater of more than 100,000 inhabitants of the western plain of the city. In addition, it receives domestic effluents from three lift stations, numerous wastewater connections and minor effluents from the Fertial, phosphate fertilizer complex. As such, it is one of the major sources of wastewater input into Annaba gulf.

The Seybouse wadi is the biggest wadi in Algeria, with an average annual flow of $11.5 \text{ m}^3 \cdot \text{s}^{-1}$. It comes from the Tell mountain and ends in the Mediterranean Sea into the coastline of Annaba city. Its lowland is the site of intensive industrial and farming activities. All discharges from agriculture and industries end in the Seybouse wadi, without prior treatment.

Seasonal sampling was conducted during 2009-2010. Water samples were collected in 1L glass bottles free of contamination. In the laboratory, the samples were frozen at $-20 \text{ }^\circ\text{C}$ until analysis. The determination of the multi

S. Khaled-Khodja (✉)

Laboratory of Geological Engineering, Team:
Water-Environment, University of Jijel, BP 98,
18000 Ouled Aissa Jijel, Algeria
e-mail: khaledkhodjasoum@gmail.com

S. Cherif

Research Unit Chemistry of Materials and the Environment,
UR11ES25, ISSBAT, University of Tunis El Manar,
1006 Tunis, Tunisia

K. Rouibah

Department of Process Engineering, University of Jijel,
BP 98, 18000 Ouled Aissa Jijel, Algeria

pesticide residues was carried out by gas chromatography coupled to a mass spectrometer (GC/MS). An Agilent 6890N GC connected to an Agilent 5975 MS was used (Agilent technologies, USA). The GC-MS was equipped with Agilent 7683B autosampler and split/splitless injector with electronic pressure control. The column used was a capillary column (HP-5MS, 30 m, 0.25 mm i.d., 0.25 μm , Agilent J&W GC columns). Analysis was performed in the selected ion monitoring mode (SIM) based on the use of one target and two or three qualifier ions.

The standards used for the assessment of raw water quality are: French system for quality assessment of water streams (SEQ-Eau) recommended by water agencies for raw waters [9] and the circular of 7 May 2007 DCE/23 defining « standards of provisional environmental quality (NQE_p) » for surface French waters [10].

3 Results

3.1 Organochlorine insecticides

Fifteen organochlorine pesticides were dosed by GC/MS, only two were detected in wadis' waters (Table 1). Their concentrations range from 0.005 $\mu\text{g.L}^{-1}$ to 0.062 $\mu\text{g.L}^{-1}$.

Two organochlorine insecticides were detected during the autumn and winter periods in Bouhamra (Table 1). Lindane is highly concentrated compared to the limits recommended by SEQ-Eau and NQE_p. Bouhamra is contaminated by lindane, and its water presents a poor biological potential. In Seybouse, lindane concentration is below standard.

3.2 Organophosphate insecticides

Twelve organophosphate insecticides were tested, two were detected in both wadis: Dichlorvos and malathion (Table 2).

Both were found in Bouhamra during autumn. Their concentrations, far exceed the limits set by the NQE_p. Bouhamra has a poor biological potential with regard to these insecticides. In Seybouse, malathion was detected during autumn, its concentration is high and exceeds the NQE_p limit. Waters have a poor biological potential.

The two wadis are relatively altered by organophosphate insecticides but the Bouhamra contains the highest concentrations.

3.3 Herbicides

Twenty herbicides were detected in the waters. Four of those were detected in Bouhamra (Table 3). Only 2,4-D greatly exceeds SEQ-Eau limit and attributes poor suitability for biological life to waters. Many herbicides were found in Seybouse but only two far exceed the SEQ-Eau limits, namely dinoterb and 2,4-D. Water is classified as poor for aquatic life.

3.4 Fungicides

Five fungicides were found in Bouhamra: azoxystrobin, carbendazim, flusilazole, propamocarb HCl and propiconazole (Table 4). Only carbendazim content greatly exceeds the SEQ-Eau limit. The wadi is mainly contaminated by carbendazim. The water presents a passable aptitude to biology.

Only azoxystrobin has been detected during the winter season in Seybouse. Two fungicides (carbendazim and propamocarb HCl) were found during the summer season. The carbendazim concentration is higher than the SEQ-Eau limit. Water presents passable quality for biological life.

Table 1 Organochlorine insecticides found in water of both wadis (oct 09: october 2009; feb 10: february 2010; number in bold: exceed the norm)

Organochlorine Insecticides ($\mu\text{g.L}^{-1}$)	Bohamra wadi				Seybouse wadi			
	oct 09	feb 10	may 10	august 10	oct 09	feb 10	may 10	august 10
Alpha-HCH	<0.005	0.005	<0.005	<0.005	<0.005	<0.005	<0.005	<0.005
Lindane	0.062	<0.005	<0.005	<0.005	0.007	<0.005	<0.005	<0.005

Table 2 Organophosphorus insecticides found in the water of both wadis

Organophosphorus Insecticides ($\mu\text{g.L}^{-1}$)	Bohamra wadi				Seybouse wadi			
	oct 09	feb 10	may 10	august 10	oct 09	feb 10	may 10	august 10
Dichlorvos	0.084	< 0.01	< 0.01	< 0.01	< 0.01	< 0.01	< 0.01	< 0.01
Malathion	0.018	< 0.01	< 0.01	< 0.01	0.015	< 0.01	< 0.01	< 0.01

Table 3 Herbicides found in the water of both wadis

Herbicides ($\mu\text{g.L}^{-1}$)	Bouhamra wadi				Seybouse wadi			
	oct 09	feb 10	may 10	august 10	oct 09	feb 10	may 10	august 10
Bromacil	<0.009	<0.009	<0.009	<0.009	0.022	<0.009	<0.009	0.022
Dicamba	0.027	<0.025	<0.025	<0.025	<0.025	<0.025	<0.025	<0.025
Dichlorprop	<0.002	0.007	<0.002	<0.002	<0.002	<0.002	<0.002	<0.002
Dinoterb	<0.002	<0.002	<0.002	<0.002	0.013	<0.002	<0.002	<0.002
Diuron	<0.003	<0.003	<0.003	<0.003	0.009	<0.003	0.003	0.010
2,4-D	0.027	<0.008	0.029	<0.008	0.027	<0.008	0.075	<0.008
Flazasulfuron	<0.002	<0.002	0.008	<0.002	<0.002	<0.002	0.008	<0.002
Fluroxypyr	<0.006	<0.006	<0.006	<0.006	<0.006	0.006	0.011	<0.006
Iodosulfuron-methyl-sodium	<0.002	<0.002	<0.002	<0.002	<0.002	<0.002	<0.002	0.032
Isoproturon	0.003	<0.002	<0.002	<0.002	<0.002	<0.002	<0.002	<0.002
Lenacil	<0.02	<0.02	<0.02	<0.02	<0.02	<0.02	0.021	<0.02
Linuron	<0.003	0.004	<0.003	<0.003	<0.003	<0.003	<0.003	<0.003
Mésosulfuron-methyl	<0.003	<0.003	0.013	0.054	<0.003	<0.003	0.007	0.010
Mesotrione	<0.01	<0.01	0.039	<0.01	<0.01	<0.01	<0.01	<0.01
Metoxuron	<0.002	<0.002	<0.002	<0.002	<0.002	<0.002	0.005	<0.002
Metribuzin	<0.005	<0.005	<0.005	<0.005	<0.005	<0.005	0.038	<0.005
Metobromuron	<0.003	0.004	<0.003	<0.003	<0.003	<0.003	<0.003	<0.003
Nicosulfuron	<0.01	<0.01	0.019	<0.01	<0.01	<0.01	0.024	<0.01
Propyzamide	0.005	<0.005	<0.005	<0.005	<0.005	<0.005	<0.005	<0.005
Terbutryn	<0.002	<0.002	<0.002	<0.002	0.005	<0.002	0.004	<0.002

Table 4 Fungicides found in water of both wadis during the four seasons

Fungicides ($\mu\text{g.L}^{-1}$)	Bouhamra wadi				Seybouse wadi			
	oct 09	feb 10	may 10	august 10	oct 09	feb 10	may 10	august 10
Azoxystrobin	<0.005	0.013	<0.005	<0.005	<0.005	0.013	<0.005	<0.005
Carbendazim	0.025	<0.002	0.007	0.046	<0.002	<0.002	0.005	0.024
Flusilazole	<0.01	<0.01	0.032	<0.01	<0.01	<0.01	<0.01	<0.01
Metalaxyl	<0.005	<0.005	<0.005	<0.005	<0.005	<0.005	0.017	<0.005
Propamocarb HCl	<0.002	<0.002	<0.002	0.016	<0.002	<0.002	<0.002	0.008
Propiconazole	0.008	<0.005	<0.005	<0.005	<0.005	<0.005	0.011	<0.005

4 Conclusions

According to these results, Bouhamra wadi seems to be relatively more polluted than Seybouse wadi. Their waters are altered respectively by organophosphate and organochlorine insecticides, herbicides and fungicides.

According to the adopted standards (SEQ-Eau and the NQEp), the waters of the two wadis have a poor biological aptitude regarding organochlorine (lindane) and organophosphate insecticides (Dichlorvos and malathion),

but also regarding two herbicides 2,4-D and dinoterb. The suitability of water for biology, by the alterations in water quality by micropollutants like pesticides was calibrated on the results of ecotoxicity tests carried out on at least 3 trophic levels (algae / plants, invertebrates, fish). This will result in a significant loss of many species that are sensitive to pollution and *ipso facto* a reduction in biodiversity. The carbendazim content, a fungicide, is greater than the limit recommended by SEQ-Eau, in the two wadis, and gives these waters a moderate aptitude for biology. This state of degradation will be reflected by the disappearance of many aquatic species.

References

1. Conseil Général de la Sarthe: Teneurs en pesticides des eaux souterraines et superficielles en Sarthe, données 2002-2007. Santé Environnement-DDASS de la Sarthe, France (2009)
2. Khaled-Khodja, S. Le glyphosate est largement utilisé dans les cultures maraîchères en Algérie. *Journal National Liberté* (article de presse) (2017).
3. Briand, O., Seux, R., Millet, M., Clément, M.: Influence de la pluviométrie sur la contamination de l'atmosphère et des eaux de pluies par les pesticides. *Revue des Sciences de l'Eau* **15**(4), 767–787 (2002)
4. Ferrand, M., Lequenne, D., Manneville, V., Jannot, P., Lorez, C.: Apport de la spatialisation des données en analyse multidimensionnelle pour évaluer l'impact des activités agricoles sur la teneur en nitrates des eaux. *Revue MODULAD*, Numéro **39**, 81–94 (2009)
5. Bordjiba, O., Ketif, A. Effet de trois pesticides (Hexaconazole, Bromuconazole et Fluazifop-p-butyl) sur quelques métabolites physio-biochimiques du blé dur : *Triticum durum*. *Desf. European Journal of Scientific Research*, Vol. 36 N°. 2, 260-268 (2009).
6. Garric, J. La contamination des eaux superficielle par les produits phytosanitaires, les effets sur le milieu aquatique. hal-00461015, 55-64 (2010).
7. Ministère de l'Aménagement du Territoire et de l'Environnement: Rapport sur l'état et l'avenir de l'environnement. ONEDD, Algérie (2002)
8. Derradji, F., Kherici, N., Romeo, M., Caruba, R.: Aptitude des eaux de la vallée de la Sey bouse à l'irrigation (Nord-est algérien). *Sècheresse* **15**(4), 353–360 (2004)
9. Agences française de l'Eau. SEQ-Eau: Système d'évaluation de la qualité de l'eau des cours d'eau (version 2), <http://www.observatoire-eau-bretagne.fr/Ressources-etdocumentation/> Documents-de-planification/Systeme-devaluation-de-la-qualite-de-l-eau-des-cours-d-eau- SEQ-Eau (2003)
10. Rodier, J., Legube, B., Merlet, N.: L'analyse de l'eau, 9th edn. Dunod, Paris (2009)

Complex Interactions Between Fertilizers and Subsoils Triggering Reactive Nitrogen Speciation in Lowlands

Micòl Mastrocicco, Nicolò Colombani, Fabio Vincenzi, and Giuseppe Castaldelli

Abstract

The present research was performed in the Ferrara Province (Italy), an intensively cropped low-lying landscape covering 2636 km², situated in the southern portion of the Po River valley. The foremost used fertilizer in this zone is synthetic urea which is known to induce nitrate leaching towards the unconfined aquifer. Approximately 800 soil samples, distributed throughout the most representative soil types of the area, were collected from the ploughed layer (0–50 cm below ground) and subsoils (50–100 cm below ground) in 2010. Soil samples were analyzed for: soil porosity, dry bulk density, soil water content, ammonium, nitrate and nitrite. A subset was also analyzed for: urea, soil pH, total organic carbon, and total and organic nitrogen. Scatter diagrams showed an accumulation of ammonium in peaty subsoils, whereas in drained sandy soils ammonium was, in general, very low. The most acidic peaty subsoils were characterized by high ammonium concentrations (20–70 mM-N/kg of dry soil), while the peaty soils amended with poultry chicken manure showed the lowest ammonium concentrations. Instead, the largest accumulation of NO₃⁻ was observed in sandy and loamy subsoils (10–27 mM-N/kg of dry soil), where the deep water table and neutral-alkaline soils pH delivered the best conditions for nitrification.

Keywords

Nitrate • Ammonium • Peat • Soil organic carbon • Agricultural practices

1 Introduction

Excess soil reactive nitrogen due to fertilization, like nitrate (NO₃⁻) and ammonium (NH₄⁺), can induce adverse environmental impacts and the watershed scale [1]. In particular, the presence of dissolved organic carbon (DOC) is frequently thought to be the major limiting factor for denitrification [2]. In comparison with nitrogen (N), fewer studies have been done to measure organic C in the field and under different management practices, such as tillage or fertilization practices [3–5]. To assess the role of different fertilization practices on the reactive nitrogen speciation in subsoils, soil samples were collected in different soils of the terminal part of the Po River plain. Here, soils were intensively fertilized with synthetic urea (CO(NH₂)₂) and poultry chicken manure.

2 Materials and Methods

A distributed network of 790 soil samples were collected to assess the reactive nitrogen speciation in both top and subsoils. Boreholes were performed with an Ejielkamp Agri-search auger apparatus. Soils samples were collected from the ploughed layer (0–50 cm below ground), here called topsoil, and from the deeper soil horizons, here called subsoil (50–100 cm below ground), in 2010. The soil samples were collected in cultivated plots, in which crop kind and rotation, irrigation quantity and applied fertilizers were known. The soil samples' sites were chosen using soil's characteristics, here grouped in: Sandy soils, Loamy soils, Clayey soils and Peaty soils.

Soil porosity and dry bulk density were measured gravimetrically, using water saturated soil samples of 100 cm³, then oven dried at 105 °C for 24 h.

M. Mastrocicco
University of Campania “Luigi Vanvitelli”, 81100 Caserta, Italy

N. Colombani (✉) · F. Vincenzi · G. Castaldelli
University of Ferrara, 44121 Ferrara, Italy
e-mail: clo@unife.it

Soil concentrations of NO_3^- and NO_2^- were quantified by ion chromatography, using an ICS-1000 Dionex. Soil concentrations of $\text{CO}(\text{NH}_2)_2$ and NH_4^+ were quantified using a double beam Jasco V-550 UV/VIS spectrophotometer. SOM and organic N concentrations were quantified with an Elemental Analyser, Carlo Erba Instrumentation.

3 Results

3.1 Reactive Nitrogen Speciation of Topsoils and Subsoils

Figure 1 shows the main speciation of reactive nitrogen in both topsoils and subsoils of the province of Ferrara, differentiated by soil type. The maximum NO_3^- concentrations of topsoils were present in the Peaty and Sandy soils, while maximum NH_4^+ concentrations were present in the Loamy and Sandy soils. The maximum NO_3^- and NH_4^+ concentrations of subsoils were present in the Peaty and Sandy soils.

4 Discussion

Figure 1 has shown that, in the topsoil, there was not a clear trend of prevailing redox environments, with both the NO_3^-

and NH_4^+ species concomitantly present in the soil samples, regardless of the soil type. This is not surprising, since the different agricultural practices, such as, crop rotation, fertilization timing and type usually led to the coexistence of redox species representative of both reducing and oxidative environments.

On the other hand, the right panel of Fig. 1 shows that, in subsoils, the reactive nitrogen speciation has distinct patterns, with a hyperbolic behavior of NO_3^- and NH_4^+ better distinguishing the prevailing redox conditions present at the sites. This is due to limited atmospheric oxygen exchange with the subsoils' environments, leading to reducing conditions, where the organic carbon is in excess, like in Peaty soils, but also where organic fertilizers are employed. Here, the most common organic fertilizer is poultry chicken manure, which, especially in Sandy soils, increases the NH_4^+ content over NO_3^- , and thus, limiting the mobility of the reactive nitrogen. In addition, the Peaty subsoils characterized by acidic conditions showed the highest NH_4^+ concentrations (20–70 mM-N/kg of dry soil), while the Peaty soils amended with poultry chicken manure showed the lowest NH_4^+ concentrations. Conversely, the largest accumulation of NO_3^- was observed in Sandy and Loamy subsoils not amended with poultry chicken manure (10–27 mM-N/kg of dry soil), where the water table was, in general, deeper than 2 m and

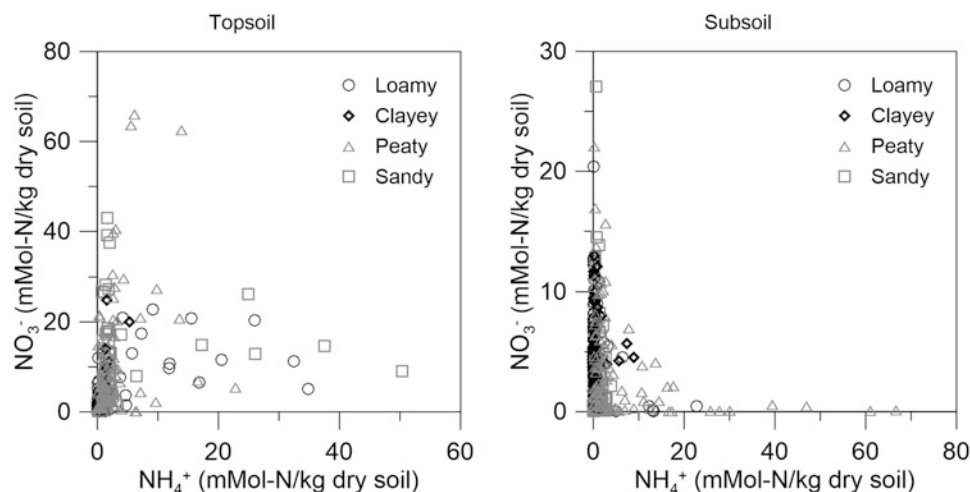


Fig. 1 Soil NO_3^- and NH_4^+ concentrations in topsoils (left panel) and subsoils (right panel) for the different soil types present in the province of Ferrara

the neutral-alkaline soils pH provided the best conditions for nitrification.

5 Conclusions

This study has shown that the speciation of reactive nitrogen in the main redox sensitive species NO_3^- and NH_4^+ is well distinguishable in subsoils, irrespectively from the soil type, while a complex interaction between fertilization timing and type, atmospheric oxygen, crop rotation and soil type largely limit a clear distinction in the tillage layer. The organic carbon availability largely controls the speciation of reactive nitrogen, triggering reducing conditions in relatively isolated environments, like the studied lowland subsoils. The finding shown here can be widely applicable to lowland soils located in deltaic environments under temperate sub-humid climates.

References

1. Galloway, J.N., Townsend, A.R., Erisman, J.W., Bekunda, M., Cai, Z., Freney, J.R., Martinelli, L.A., Seitzinger, S.P., Sutton, M.A.: Transformation of the nitrogen cycle: recent trends, questions, and potential solutions. *Science* **320**, 889–892 (2008)
2. Taylor, P.G., Townsend, A.R.: Stoichiometric control of organic carbon–nitrate relationships from soils to the sea. *Nature* **464**, 1178–1181 (2010)
3. Cantero-Martínez, C., Plaza-Bonilla, D., Angás, P., Álvaro-Fuentes, J.: Best management practices of tillage and nitrogen fertilization in Mediterranean rainfed conditions: combining field and modelling approaches. *Eur. J. Agron.* **79**, 119–130 (2016)
4. Kolář, L., Vaněk, V., Kužel, S., Peterka, J., Borová-Batt, J., Pezlarová, J.: Relationships between quality and quantity of soil labile fraction of the soil carbon in Cambisols after liming during a 5-year period. *Plant Soil Environ.* **57**(5), 193–200 (2011)
5. Castaldelli, G., Colombani, N., Vincenzi, F., Mastrocicco, M.: Linking dissolved organic carbon, acetate and denitrification in agricultural soils. *Environ. Earth Sci.* **68**(4), 939–945 (2013)

Hydrogeological Windows Impact on Groundwater Contamination in Moscow

Irina Galitskaya, Irina Pozdnyakova, Irina Kostikova, and Leonid Toms

Abstract

This paper presents the results of assessing the hydrogeological windows' impact on the Podol'sko-Myachkovskii aquifer contamination in Moscow as the most important reserve source of drinking water supply. Groundwater contamination in these territories can occur due to rapid mixing of contaminated groundwater of the overlying above-Jurassic aquifer and pure groundwater of the Podolsko-Myachkovskii aquifer. The study consisted in the analysis of the water chemistry data of these aquifers; the choice of the elements—indicators of groundwater contamination; the analysis of the indicators' distribution schemes and comparison with the boundaries of hydrogeological windows. The research results testified to the significantly elevated concentrations of contamination indicators in the Podolsko-Myachkovskii aquifer at the sites of hydrogeological windows allocated within the specific geostructural and hydrogeological conditions.

Keywords

Hydrogeological windows • Groundwater contamination • Hydrogeological condition • Aquifer vulnerability

1 Introduction

Significant anthropogenic contamination of groundwater is one of the most pressing problems that our world is facing today. Particular attention is paid to the study of groundwater contamination in the territories of hydrogeological windows location, where “contaminants can penetrate rapidly from near-surface into deeper aquifers in the areas

where continuity of separating low-permeability deposits is disturbed and their permeability is relatively high” [1, 2]. The aim of our study, carried out within the framework of the project of the Russian Foundation for Basic Research, is to assess the impact of the hydrogeological windows on the contamination of the Podol'sko-Myachkovskii aquifer in Carboniferous deposits as the most important reserve source of drinking water supply in Moscow. This aquifer is the most vulnerable to contamination in the sites of hydrogeological windows where the transport of contaminants can occur from overlying the above-Jurassic aquifer. As a result of water abstraction and drainage from the underground workings, the groundwater levels in all Carboniferous aquifers are significantly reduced and are everywhere set below the levels of the above-Jurassic aquifer. Thus, there are hydrodynamic prerequisites for the penetration of contaminants from the above-Jurassic aquifer into the Podol'sko-Myachkovskii aquifer. In this article are presented and discussed the results obtained in the first stage of research. At this stage, the main tasks were the research of the spatial distribution of contaminants' concentrations in the overlying and the exploitable aquifers, the choice of the elements—indicators of the contamination—and then the construction of schemes on the basis of combining the schemes of the indicators' concentration and the map of the boundaries of hydrogeological windows.

2 Materials and Methods

This study consisted in the collection and synthesis of the groundwater chemistry data of the exploitable aquifer and also the overlying aquifer; the choice of elements—indicators of groundwater contamination on the basis of the study of the groundwater chemistry in the overlying aquifer; the construction and analysis of the elements'/indicators' distribution schemes in the exploitable aquifer and the comparison with the boundaries of hydrogeological windows. Groundwater samples were collected from monitoring 52

I. Galitskaya (✉) · I. Pozdnyakova · I. Kostikova · L. Toms
Institute of Environmental Geoscience, Russian Academy of Science, Moscow, 101000, Russia
e-mail: galgeoenv@mail.ru

wells in the above-Jurassic aquifer and 210 wells in the Podol'sko-Myachkovskii aquifer. When constructing the schemes of the indicators' distribution, the software package, "Surfer", was used and the most acceptable result (for a given sampling network) was obtained by the Kriging method. During the data interpolation by kriging, the exponential theoretical variogram model was used. A more detailed comparison of the experimental variograms with the theoretical ones was carried out in the second stage of the research and these results have not been considered in this article.

3 Results and Discussion

Indicators of contamination can be the components of a primarily technogenic origin—ammonium, nitrates, oil products, phenols, surfactants, as well as chloride ion and sodium, significantly higher concentrations of which, compared to the background, also have anthropogenic genesis (the application of anti-icing products). As the main indicator of contamination, it is advisable to use chloride ion, which, unlike other components, is not sorbed by rocks, practically does not undergo physical and chemical transformations, and is characterized by a fairly stable character of the concentration change in the study area. Other components of technogenic genesis—oil products, phenols, surfactants, and nitrogen compounds, can be used as additional indicators, as well as for elucidating the possibility of using the chemical composition of groundwater as

hydrogeochemical sign of the hydrogeological windows. The results of the study showed that the change of the natural hydrogeochemical situation in the exploited aquifer due to the impact of technogenesis is insignificant. Hydrocarbonate and sulfate-hydrocarbonate types of groundwater were formed due to the water-rock interactions in the natural conditions. The impact of technogenic processes led to the formation of chloride-hydrocarbonate groundwater in some sites, but in general the area of their distribution is insignificant. In comparison with the overlying aquifer, the concentration of technogenic components in the exploited groundwater are much lower (Table 1).

The higher concentrations of the indicators of contamination such as chloride ion, nitrate ion, oil products, and ammonium ions in the exploitable aquifer are found in the sites of hydrogeological windows location in the Moskva River valley and also in the valleys of its tributaries. The most significant values of indicators' concentrations are restricted to the sites of the hydrogeological windows of the first and second orders: chloride ion, up to 293; sulphate ion, up to 440.0; nitrate ion, up to 37.2; oil products, up to 0.113; and ammonium, up to 183. The vertical filtration time for the windows of the first order is less than 400 days (survival time of pathogenic microorganisms in groundwater) and for the windows of the second order, it is less than 1000 days (the petroleum products' half-life due to biodegradation). The influence of hydrogeological windows on the exploitable groundwater contamination can be seen the most clearly in the scheme of chloride ion distribution (Fig. 1).

Table 1 Concentration of chemical substances in overlying and exploitable aquifers

Element	Concentration, mg/L in overlying above-Jurassic aquifer	Concentration, mg/L in exploitable Podol'sko-Myachkovskii aquifer
Chloride	0.5–12259	<0.05–293.0
Sulfate	0.1–748.9	<0.01–440.0
Nitrate	0.04–83.85	<0.01–37.2
Sodium	0.2–7778	4.4–1069.0
Ammonium	0.05–236	<0.05–183.0
Calcium	0.5–1900	3.2–250.5
Magnesium	0.27–350	0.01–141.0
Oil products	0.005–53.0	<0.005–113.0
Iron	0.1–1693	<0.01–14.2
Manganese	0.001–22.9	<0.01–1.02

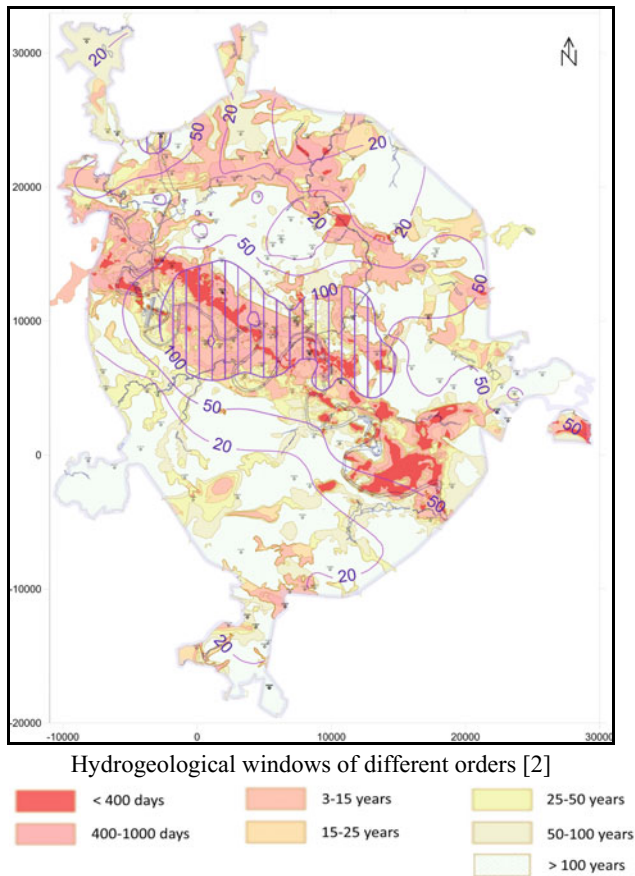


Fig. 1 The concentration of chloride ion in exploitable groundwater, mg/L

4 Conclusions

The results of this study lead to the conclusion that the hydrogeological windows can affect the groundwater chemistry in the exploitable Podolsko-Myachkovskii

aquifer, especially in the sites of the hydrogeological windows of the first and second orders. Further studies, some of which are already underway, include: (1) obtaining more detailed spatial estimation using models from the kriging family; (2) selection of the test sites with different types of the hydrogeological windows, simulation of geofiltration and gemigration for the clarification the mechanisms of the transfer of the contaminants and the ways of their entering into the wells; (3) development of a methodical approach to the assessment of the risk of groundwater contamination in the sites of the hydrogeological windows and the risk maps construction; (4) determination of the features of the influence of the hydrogeological windows on the groundwater quality change.

Acknowledgements The research was financially supported by the project of the Russian Foundation for Basic Research (RFBR) № 17-05-01016.

References

1. Pozdniakova, I.A., Kozhevnikova, I.A., Kostikova, I.A., Toms, L.S.: Groundwater interaction assessment based on the large-scale mapping of geological and hydrogeological conditions in Moscow. *Water Resour.* **40**(7), 695–705 (2013)
2. Pozdnyakova, I.A., Galitskaya, I.V., Mironov, O.K., Kostikova, I.A., Dorozhko, A.L., Batrak, G.I., Matveeva, L.A., Fesel, K.I.: Identification of hydrogeological windows based on large-scale mapping of the geological and hydrogeological conditions in Moscow. *Water Resour.* **43**(7), 1012–1022 (2016)

Impact of Pollution on the Quality of Water of Oued El Harrach (Algeria)

Djaouida Bouchelouche, Somia Hamil, Siham Arab, Imane Saal, Mouna Hafiane, and Abdeslem Arab

Abstract

El Harrach wadi is one of the largest wadis that cross the plain of Mitidja. The current state of the wadi is calamitous, and its influence on the Algerian coast is disastrous since it became an open sewer; this wadi poisons the lives of local residents and has become a real problem for the whole commune of El Harrach and one of the factors degrading the water quality of the Bay of Algiers. In altitude, the pressures on the Oued El Harrach come mainly from the agricultural activity. At low altitude, these pressures are the result of human activity; they may be the result of population growth, the rapid expansion of urban areas, the development of agricultural activities and industrialization. Water quality is poor in all downstream stations. In summer, in the H9 station (Baba Ali town) where the degree of pollution is very high, the BOD₅ exceeded the limit, reaching a maximum of 238 mg/l. The results of the COD also indicate that the water quality is bad. The COD reaches a maximum of 407 mg/l, in summer at the H11 station (City of Baba Ali).

Keywords

Pollution • Wadi • Physical chemistry • Water quality

1 Introduction

The pollution of rivers in the industrialized regions has reached a new and worrying level, with the appearance of pesticides, discharges of industrial or urban origins that saturate the self-purification capabilities of the waters or have proved non-degradable. River valleys have thus become collectors of original substances, transporting to the seashore with waste that accumulates in the bays. The example of El Harrach Wadi is edifying. It has become a real sewer, carrying annually, in the form of suspended solids and soluble products, tons of organochlorine waste, hydrocarbons and heavy metals dumped in the regions of Baba Ali, El Harrach and Oued Smar by companies that are located all along the wadi. Industrial discharges drained the stream of its fauna in the lower part of its mouth. The current state of Oued El Harrach is calamitous, and its influence on the Algerian coast is disastrous since it has become an open sewer. This wadi poisons the lives of local residents and has become a real problem for the whole municipality of El-Harrach and one of the factors degrading the quality of the water in the Bay of Algiers. The main objective of this study is to evaluate the impact of pollution on the water quality of this wadi by physicochemical parameters. This wadi is supposed to be a barometer of the urban environment and the ecological status of the Wilaya of Algiers.

2 Materials and Methods

Seasonal sampling was conducted from April 2016 to March 2017. Thirteen stations were selected along the Wadi. The temperature of the water (°C), the hydrogen potential, the dissolved oxygen (mg/l), the conductivity (µs/cm) and the salinity (PSU) are measured in situ by a Multi Field Analyzer Multi 340-i Set WTW. The speed water measurement is carried out using a float. The other parameters, chlorides, calcium, nutrient salts (nitrates, nitrites, phosphates),

D. Bouchelouche (✉) · S. Hamil · S. Arab · I. Saal
M. Hafiane · A. Arab
LaDyBio, FSB, USTHB, LP 32 El Alia, Bab Ezzouar,
Algiers, Algeria
e-mail: bouchelouche_djaouida@hotmail.com

S. Hamil
L.E.B.A., ENS Kouba, Kouba, Algeria

S. Arab
G&G, FST/GAT—USTHB, Bab Ezzouar, Algeria

suspended Matter, chlorides, BOD₅ and COD are determined at the laboratory level by volumetric, titrimetric, gravimetric methods, etc. expressed in mg/l according to Rodier's protocol [7].

3 Results

The mean and standard deviation of water environmental parameters measured in El Harrach wadi are shown in Table 1.

4 Discussion

The values, recorded throughout our study, show that there is a seasonal variation (ANOVA, $P < 0.0001$): the temperature reaches its maximum in summer (34.5 °C) at station S2, the minimum (9.6 °C) is recorded in winter at the S8 station. According to [2], the temperature depends on the altitude, the distance from the source, the hydrological regime and the season. The waters of the wadi vary between weak and strong alkalinity. The results indicate that pH values range from a minimum of 7.17 to H13 in summer, and a maximum of 10.67 to H4 in spring. The pH has temporal and spatial stability (ANOVA, $P > 0.05$). According to [5], the pH of rivers depends on the geological nature of the world. The values of the conductivity, know an important variation spatiotemporal (ANOVA, $P < 0.05$). These conductivity values are very important at the H5 station (downstream of the thermal station Hammam Melouen) in autumn (5130 $\mu\text{S}/\text{cm}$), this is probably explained by the infiltrations and discharges of the thermal station. The low value is recorded at the H2 (oued Lakhra) station in autumn (334 $\mu\text{S}/\text{cm}$). The measured values of the salinity range from 0 PSU at stations S1 and S4 to 2.7 PSU at station S5. The downstream stations are the most mineralized; these values are probably related to the nature of the lands crossed and the mineral composition of urban and industrial wastewater [3, 8]. The results show a spatiotemporal variation (ANOVA, $P < 0.05$): the levels of SM reach a minimum of 0 mg/l at the upstream stations S1, S2 and S3 in spring, and a maximum of 179 mg/l at S12 (Oued Kerma) in winter and 206 mg/l at S13 (Gué de Constantine) in spring. These values are probably due to the leaching of the land after a strong flood (the terrain is essentially limono-sableus). The SM is based on the nature of the land crossed, the season and the rainfall. The speed of the water has a remarkable spatiotemporal variation (ANOVA, $P < 0.0001$): it reaches a minimum of 16.68 cm/s at S8 in autumn, this is due to the rarity of the precipitations and the decrease of flow. A maximum of 158.18 cm/s is recorded at S8 in winter, this is due to the importance of the precipitations which cause a remarkable rise of flow and consequently the increase of the flow velocity.

The spatial variation of the flow velocity at the El Harrach wadi shows that the waters of the upstream and piedmont stations flow rapidly in relation to the downstream stations, this is probably due to the importance of the slope in this part of the stream. The flow velocity of the water depends mainly on flow and slope [1]. The stations of the upstream and middle courses of the wadi are well-oxygenated with a maximum value of 10.01 mg/l recorded at S2 (Oued Lakhra) in spring. This spatial variation of oxygenation (ANOVA, $P < 0.0001$), is due to the importance of the slope, which causes an increase in the agitation of the water and promotes its natural ventilation. The low levels are recorded in the downstream part with a minimum value of 0.01 mg/l at S13 (town of Gué de Constantine) in autumn, this is probably due to the presence of organic matter following urban and industrial spills in the wadi without any prior treatment. A significant difference in nitrate concentrations was recorded during the study period (ANOVA, $P < 0.0001$). Nitrate concentrations range from a low of 0.017 mg/l in spring to a high of 6.8 mg/l in winter. These high concentrations are probably due to the leaching of agricultural land by heavy winter precipitation. Stable nitrate concentrations were recorded along the wadi (ANOVA, $P > 0.05$). Spatial stability of nitrite was recorded along the wadi (ANOVA, $P > 0.05$). A significant difference in nitrite concentrations was recorded during the study period (ANOVA, $P < 0.0001$), the recorded nitrite values range from a low of 0.001 mg/l in spring to a high of 5.027 in winter; these high concentrations are likely due to leaching of the terrain after a severe flood. Their presence indicates a critical state of organic pollution [4]. Phosphorus results show that there is a temporal variation. The maximum value is observed during summer with 3.6 mg/l. This can be explained by the phenomenon of evaporation and excessive concentration of pollutants contained in wastewater [6], while the minimum value is recorded in spring with 0.002 mg/l. Spatial stability of phosphorus was recorded along the wadi (ANOVA, $P > 0.05$). Calcium concentrations exhibit spatial stability (ANOVA < 0.05), and a significant temporal variation (ANOVA, $P < 0.0001$). The minimum concentration of calcium salts is obtained in winter with 4.008 mg/l, this is due to the dilution phenomenon. As for the maximum, it is obtained in summer with 597.99 mg/l. These concentrations are high during this season, following evaporation, and in addition to the calcareous geological nature of the lands crossed [6]. Spatiotemporal variation in chloride concentrations was recorded (ANOVA, $P < 0.05$). Chloride concentrations range from 105 mg/l at S1 in winter to 866.2 mg/l at S5 in autumn. Excessive chlorides content is very often the index of a particular urban or industrial pollution that is confirmed with our site of study where we find many industrial units and urban discharges. A spatiotemporal variation of BOD₅ has been recorded. The water situation in El Harrach Wadi is poor in all downstream stations with a

Table 1 Environmental factors measured at the El Harrach Wadi

Stations	T° (water)	pH	Cond (µS/cm)	Sal (PSU)	SM (mg/l)	VC (cm/s)	O ₂ d (mg/l)	NO ₃ ⁻ (mg/l)	NO ₂ ⁻ (mg/l)	Ca ²⁺ (mg/l)	Cl ⁻ (mg/l)	PO ₄ ³⁻ (mg/l)	BOD ₅ (mg/l)	COD (mg/l)
S1	19.07 ± 8.7	9.04 ± 0.58	841.6 ± 241.11	0.38 ± 0.23	7.7 ± 10.33	71.28 ± 34.27	7.81 ± 6	3 ± 3.03	1.18 ± 1.79	151.53 ± 121.58	142.27 ± 30.49	0.78 ± 0.95	0 ± 0	38.21 ± 55.96
S2	18.63 ± 9.53	8.89 ± 0.34	931.8 ± 362.99	0.45 ± 0.11	8.68 ± 12.93	77.66 ± 42.77	6.4 ± 3.49	2.83 ± 2.9	1.17 ± 1.79	114.79 ± 119.57	126.85 ± 73.76	0.8 ± 0.93	2 ± 4.47	37.82 ± 51.45
S3	18.09 ± 7.56	9.15 ± 0.9	968.8 ± 371.87	0.45 ± 0.09	7.24 ± 9.97	58.59 ± 18.76	7.57 ± 5.24	2.44 ± 2.44	1.22 ± 1.78	249.3 ± 233.23	219.27 ± 116.99	0.78 ± 0.95	1.8 ± 4.02	68.74 ± 80.4
S4	18.62 ± 8.48	9.56 ± 0.97	702.4 ± 344.9	0.22 ± 0.19	3.66 ± 3.1	66.66 ± 42.23	7.01 ± 4.06	2.63 ± 2.48	1.25 ± 1.91	178.6 ± 203.69	266.01 ± 228.41	0.79 ± 0.93	0.54 ± 1.21	41.66 ± 56.44
S5	19.3 ± 8.98	9.01 ± 0.62	2218.4 ± 1682.17	1.08 ± 0.93	6.13 ± 4.08	88.96 ± 37.53	9.72 ± 9.11	2.17 ± 2.26	1.32 ± 1.7	168 ± 170.07	530.61 ± 233.49	0.81 ± 0.96	0 ± 0	70.08 ± 76.21
S6	18.5 ± 7.26	8.49 ± 0.33	1730.2 ± 985.96	0.78 ± 0.54	7.04 ± 6.71	42.98 ± 15.45	7.02 ± 5.69	1.91 ± 2.26	1.37 ± 1.79	200.8 ± 237.48	471.58 ± 312.55	0.95 ± 0.96	3.24 ± 5.63	66.82 ± 74.82
S7	19.06 ± 9.17	8.64 ± 0.34	1383.4 ± 424.21	0.6 ± 0.18	9.98 ± 8.4	46.36 ± 12.09	7.3 ± 3.87	1.91 ± 2.24	1.39 ± 1.76	145.21 ± 95.68	431.48 ± 207.17	0.9 ± 0.89	0.82 ± 1.83	52.22 ± 64.59
S8	18.64 ± 9.12	9.08 ± 0.56	1755 ± 1058.54	0.8 ± 0.5	11.42 ± 9.24	82.08 ± 65.28	9.11 ± 6.48	2.01 ± 2.13	1.7 ± 1.75	140.22 ± 108.91	268.96 ± 161.11	0.84 ± 0.94	0 ± 0	77.95 ± 100.75
S9	18.39 ± 8.18	9.07 ± 0.37	1684.6 ± 781.74	0.76 ± 0.38	13.59 ± 13.23	58.19 ± 23.74	5.7 ± 2.68	2.02 ± 2.37	1.37 ± 1.84	141.27 ± 129.06	341.02 ± 137.17	1.13 ± 1.49	48.6 ± 105.9	169.34 ± 125.84
S10	18.17 ± 7.71	9.37 ± 0.77	1472.4 ± 480.89	0.66 ± 0.19	19.51 ± 16.16	73.06 ± 26.3	5.8 ± 3.7	2.08 ± 2.49	1.3 ± 1.76	173.37 ± 178.4	298.4 ± 116.9	1.14 ± 1.47	24 ± 33.35	144.38 ± 118.32
S11	16.84 ± 4.91	8.81 ± 1.01	1736.4 ± 139.95	0.76 ± 0.11	14.8 ± 10.25	47.65 ± 13.39	1.09 ± 1.44	1.97 ± 2.44	1.64 ± 2.04	251.11 ± 190.83	307.04 ± 73	1.68 ± 1.3	61 ± 45	212.07 ± 148.94
S12	17.36 ± 4.54	7.84 ± 0.48	1482.8 ± 73.98	0.62 ± 0.13	76.31 ± 71.33	51.35 ± 30.16	2.3 ± 2.62	2.21 ± 2.62	1.75 ± 1.59	166.32 ± 220.49	34.14 ± 322.92	1.51 ± 1.16	23.2 ± 25.63	128.64 ± 89.44
S13	16.82 ± 5.62	7.81 ± 0.49	1436.4 ± 224.19	0.61 ± 0.09	74.38 ± 93.08	42.85 ± 13.97	0.89 ± 1.42	2.31 ± 2.39	1.36 ± 1.79	198.57 ± 189.65	259.67 ± 123.42	1.17 ± 1.19	48.34 ± 75.21	174.34 ± 150.95

T° water: water temperature (°C), Cond.: Electric conductivity (µS/cm), Sal.: Salinity (PSU), SM.: Suspended matter (mg/l), V.C.: current velocity (cm/s), O₂d: Dissolved oxygen (mg/l), BOD₅: Biological oxygen demand (mg/l), COD.: Chemical oxygen demand (mg/l)

maximum of BOD₅ of 238 mg/l at S9 (City of Baba Ali) in summer, where the degree of pollution is very high (urban effluents, agricultural leaching, industrial discharges). The results of the COD also indicate that the water quality is bad. COD reaches a maximum of 407 mg/l in summer at S11 (Baba Ali town).

5 Conclusions

The stations upstream of El Harrach Wadi (S1, S2, S3, S4) are characterized by a rapid flow and a good oxygenation of water. They are rich in nitrates due to their proximity to agricultural lands. The stations of the medium section (S5, S6, S7 and S8) are characterized by a rather strong mineralization, this comes from the location of these stations downstream of the spa of Hammam Melouene whose effluents are added to the domestic discharges. The downstream stations (S9, S10, S11, S12 and S13) are characterized by pollutant parameters (BOD₅, COD and SM), since the waters of these stations are threatened by agricultural, domestic and industrial discharges.

References

1. Aberle, J., Smart, G.M.: The influence of roughness structure on flow resistance on steep slopes. *J. Hydraul. Res.* **41**(3), 259–269 (2003)
2. David, M.: River water temperature in the United Kingdom: changes over the 20th century and possible changes over the 21st century. *Prog. Phys. Geogr.* **39**(1), 68–92 (2015)
3. McCartney, M., Scott, C., Ensink, J., Jiang, B., Biggs, T.: Salinity implications of wastewater irrigation in the Musi river catchment in India. *Cey. J. Sci. (Bio. Sci.)* **37**(1), 49–59 (2008)
4. Neal, C., Jarvie, H.P., Howarth, S.M., Whitehead, P.G., Williams, R.J., Neal, M., Harrow, M., Wickham, H.: The water quality of the River Kennet: initial observations on a lowland chalk stream impacted by sewage inputs and phosphorus remediation. *Sci. Total Environ.* **251–252**, 477–495 (2000)
5. Nelson, M.L., Rhoades, C.C., Dwire, K.A.: Influence of bedrock geology on water chemistry of slope wetlands and headwater streams in the southern Rocky Mountains. *Wetlands* **31**, 251–261 (2011)
6. Rodier, J., Legube, B., Merlet N.: *L'analyse de l'eau*. Ed. Dunod. 78–1368 (2009)
7. Rodier, J.: *L'analyse de l'eau*. Eaux naturelles. Eaux résiduaires. L'eau de mer. Chimie. Physico-chimie. Bactériologie. 8ème Edition. DUNOD.1383p (1996)
8. Williams, W.D.: Anthropogenic salinisation of inland waters. *Hydrobiologia* **466**, 329–337 (2001)

Organic Pollutants Evolution and Degrees of Contamination of Hammam Grouz Dam Waters, North-East of Algeria

Badreddine Saadali, Naouel Mihoubi, Amira Ouddah, and Yasmina Bouroubi

Abstract

The construction of Hammam Grouz dam allowed to store the quantities of runoff water inside the Haut Rhumel watershed extended over 1130 km². The dam is destined to supply drinking water. The territory of the watershed has witnessed an expansion of the human activity—with its ensuing socioeconomic accessories—which was followed by an irrational dumping of various toxic substances which have been accumulating downstream. The dam's waters are contaminated by organic pollutants due to domestic, agricultural and industrial discharges stemming from anthropogenic activities within the watershed. These organic pollutants will be leached by the rainwater and transported by the streams to the dam. The objective of this work is to study the evolution of some organic parameters analyzed during the years 2016 and 2017, based on the standards recommended by the WHO, and to identify the degree of contamination of dam waters using the methods of the OPI and IHE for December and July of 2015, 2016 and 2017. The results obtained show high concentrations of the analyzed parameters, with an increase recorded during 2017, indicating high organic water pollution. The degree of pollution, according to OPI and IHE, is moderate to high for the dam waters.

Keywords

Hammam Grouz • Anthropogenic • Rhumel WHO • Watershed

1 Introduction

Water is essential for life and for human survival [4]. Rivers are one of the sources used for water supply for various purposes [1]. Various types of organic pollutants have appeared in the water due to the increase of human activities causing a serious threat to human beings and the environment [2].

The study area is located in the north-east of Algeria, about 30 km south-west of Constantine city. It corresponds to geographical coordinates 36° 14' 50" N latitude, and 06° 16' 49" E longitude (see Fig. 1). The dam is made of normal weight concrete of a height above the foundation of 49.5 m, and a restraint that extends over a flood area of nearly 500 ha [3]. Human activities exercised inside the watershed (infrastructure, agriculture, industry) will have negative consequences on the dam waters by the subtracted wastes rich in pollutants which will accumulate downstream the dam.

2 Materials and Methods

The physicochemical and organic parameters, given by Hydric Resources National Agency (ANRH), allow to perceive and estimate the pollution levels of dam waters.

The recommended parameters: Biological Oxygen Demand (BOD₅), Chemical Oxygen Demand (COD), Organic Matter (OM), Nitrites (NO₂⁻), Ammonium (NH₄⁺) and Phosphate (PO₄³⁻) were treated. On the one hand, we studied the growth of these parameters for the months of 2016 and 2017 using Microsoft Excel by adapting the standards recommended by the World Health Organization (WHO). On the other hand, we have adopted the methods (Leclercq) of the organic pollution index (OPI) and the Institute of Hygiene and Epidemiology (IHE) for choosing the months of July and December of the years 2015, 2016 and 2017. The classification of the parameters is mentioned

B. Saadali (✉) · A. Ouddah · Y. Bouroubi
Larbi Ben M'hidi University, 04000 Oum El Bouaghi, Algeria
e-mail: saadali.badreddine@univ-ueb.dz

N. Mihoubi
Mentouri University, 25000 Constantine, Algeria

Fig. 1 Geographical location of the study area



according to five classes of colors corresponding to the pollution degrees (see Table 1). These methods consist in distributing the pollutants' values in five classes and in determining, from these obtained measurements, the corresponding class number for each parameter in order to make an average (see Tables 2 and 3).

3 Results

3.1 Evolution of Organic Pollutants

Two representative curves obtained for each processed parameter evolve during the twelve months of each of the years 2016 and 2017. These values are positioned according to five colors corresponding to the degrees of pollution (see Fig. 2).

For the BOD₅, the values are outside the norms and indicate concentrations between 5 and 10 mg/l. For COD, OM, NH₄⁺, PO₄³⁻ and NO₂⁻, the concentrations are higher and exceed even the recommended standards.

3.2 Degrees of Pollution

We calculated the averages for each method (see Table 4) and positioned them compared to the color grid indicated in Table 1.

For the OPI, the value is inferior to 3 in July illustrated by the orange color and increases in December (2015) and July (2016), but it does not exceed 3.25, represented by the yellow color. As of December (2016) and July (2017), the values decrease, referring again to the orange color, reaching the value of 1.75 in December (2017) indicated by the red color.

4 Discussion

The dam's waters are contaminated by organic pollutants of anthropogenic origin. For BOD₅, the water is moderately polluted. COD, OM, NH₄⁺, NO₂⁻ and PO₄³⁻ show elevated concentrations, indicating a high to very high pollution.

According to the methods of the IPO and the IHE (see Table 4), the degree of pollution of the dam waters is increasing, indicating a moderate to high pollution.

Table 1 Grid of water pollution degrees

	No	Low	Moderate	High	Very high
Organic pollution degree	5–4.6	4.5–4	3.9–3	2.9–2	1.9–1

Table 2 Interval of OPI parameters classes

Parameters classes	BOD ₅ (mg-O ₂ /l)	NH ₄ ⁺ (mg-N/l)	NO ₂ ⁻ (µg-N/l)	PO ₄ ³⁻ (µg-N/l)
5	<2	<0.1	<5	<15
4	2–5	0.1–0.9	6–10	16–75
3	5.1–10	1–2.4	11–50	76–250
2	10.1–15	2.5–6	51–150	251–900
1	>15	>6	>150	>900

Table 3 Interval of IHE parameters classes

Parameters classes	BOD ₅ (mg-O ₂ /l)	COD (mg-O ₂ /l)	NH ₄ ⁺ (mg-N/l)	Dissolved O ₂ (%)	P ₂ O ₅ (µg-N/l)	PO ₄ ³⁻ (µg-N/l)
5	≤ 1	≤ 5	≤ 0.05	90–110	≤ 50	≤ 50
4	1.1–3	5.1–10	0.06–0.5	70–89	51–100	51–100
3	3.1–5	10.1–20	0.51–1	50–69	101–200	101–200
2	5.1–10	20.1–50	1.01–2	30–49	201–400	201–400
1	>10	>50	>2	<30	>400	>400

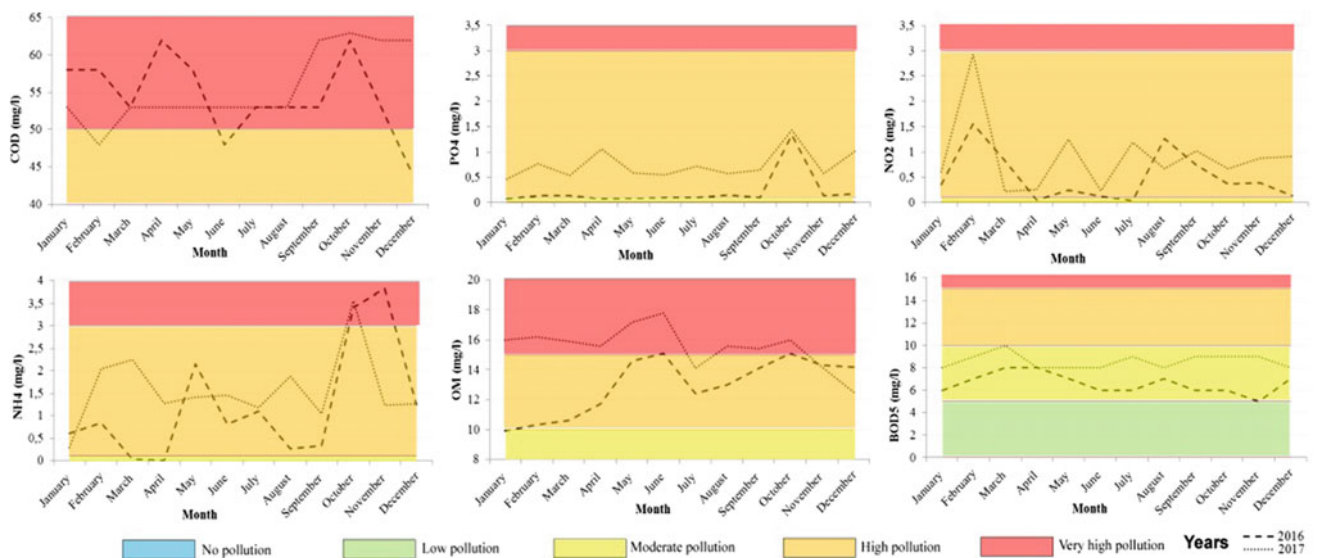


Fig. 2 Evolution of organic parameters in dam waters

Table 4 The deduced averages of the pollution indexes

	2015		2016		2017	
	July	December	July	December	July	December
OPI	2.75	3.00	3.25	2.75	2.00	1.75
IHE	3.33	3.33	3.33	2.83	2.33	2.33

5 Conclusions

We conclude that the waters of the Hammam Grouz dam are loaded with nutrients resulting from the wastes of anthropogenic activities exercised inside the watershed.

These nutrients, in high concentrations, pollute the water and could cause the appearance of eutrophication and dangerous diseases for its users.

References

1. Falah, F., Haghizadeh, A.: Hydrochemical evaluation of river water quality—a case study: Horroud River. *Appl. Water Sci.* **7**(8), 4725–4733 (2017)
2. Khadhar, S., Achouri, D., Chekirben, A., Mlayah, A., Azibi, R., Charef, A.: Assessment of organic pollutants (PAH and PCB) in surface water: sediments and shallow groundwater of Grombalia watershed in northeast of Tunisia. *Arab. J. Geosci.* **11**(109), 11:34 (2018)
3. Mihoubi, N., Mebarki, A.: Haut-Rhumel basin: hydrogeological context and water leakage from the Hammam Grouz dam. *Sci. Technol.* **45**, 131–140 (2017)
4. Prasanth, S.V.S., Magesh, N.S., Jitheshlal, K.V., Chandrasekar, N., Gangadhar, K.: Evaluation of groundwater quality and its suitability for drinking and agricultural use in the coastal stretch of Alappuzha District, Kerala, India. *Appl. Water Sci.* **2**(3), 165–175 (2012)

Impact of Reclaimed Wastewater Used for Irrigation in the Agricultural Supply Chain

Zaineb Bakari, Nesrine Boujelben, Nesrine Turki, Massimo Del Bubba, and Boubaker Elleuch

Abstract

The purpose of this work is to evaluate the impacts of strawberry crop irrigation with treated wastewater (TWW) as compared to fresh water (FW) irrigation on crops productivity. Different dilutions of TWW from urban and mixed urban-industrial origins were used for the irrigation of strawberry in pots. This crop was selected as a fruit model species for its high economic value in the countries involved in the project, and due to the high water-content of this fruit, it is presumably vulnerable to the presence of residual organic micropollutants dissolved in reused TWW. Chemical contamination indicators—polychlorinated biphenyls (PCBs), polycyclic aromatic hydrocarbons (PAHs), ethoxylatedalkylphenols (APnEOs) and alkylphenols (APs)—were studied.

Keywords

Treated wastewater • Irrigation • Strawberry
Organic compounds • Impact

1 Introduction

A high volume of wastewater is produced by the urban sector following the increase in fresh household waste. Indeed, the reuse of treated wastewater in agriculture has become a necessity, especially where freshwater is deficient [1]. In this work, the impact of irrigation of strawberries by treated wastewater will be analyzed.

2 Methods

Irrigation water sources were either fresh water or secondary treated effluents that were sampled at the outlet of municipal wastewater treatment plant in the north of Sfax. The Sfax treated wastewater (STWW) has been characterized by the presence of (i) basic quality parameters (pH, COD, electrical conductivity, N and P species, Na^+ , K^+ , Cl^- , SO_4 , Ca^{2+} , Mg^{2+}). TWW was analyzed to evaluate the presence of residual PAHs, PCBs, PFAAs, APs and APnEOs. TWW was analyzed weekly, during the whole irrigation period (about three months from January to March 2018), using GC-MS for the determination of PCBs and PAHs [2] and on-line SPE coupled to liquid chromatography and MS for PFAAs, APnEOs and APs [3, 4]. Target tests were extracted from strawberry fruits following a procedure appositely developed and optimized. The extraction was performed following the QuE-ChERS approach [5]. This approach adopted by Rossini et al. [5] is described briefly by adding 1 gr of freeze-dried strawberries into a 50 mL centrifuge tube and 5 mL of acidic water. The mixture was then hand-shaken for 15 s and vortex-mixed for 1 min, and 10 mL of CH_3CN were added. After a further step of hand-shaking (15 s) and vortex mixing (1 min), 2 g of NaCl and 2 g of MgSO_4 were added, and the obtained mixture underwent additional hand-shaking and vortex-mixing processes. The tube was centrifuged at 3500 rpm for 5 min [5]. Accordingly, the QuEChERS extraction lasted about 10 min. The CH_3CN supernatant phase, obtained from the QuEChERS extraction, was transferred to a 15 mL centrifuge tube containing 12.5 mg of C_{18} , and 75 mg of MgSO_4 per mL of extract. The tube was hand-shaken for 15 s and vortex-mixed for 1 min, followed by centrifugation at 3500 rpm for 2 min, 1 mL of CH_3CN supernatant phase was made up to 10 mL with acidic water in a centrifuge tube and transferred to a 2 mL glass vial for LC-MS/MS analysis. Accordingly, the clean-up procedure lasted about 5 min. Analysis by LC-MS/MS was done according to the same instrumental conditions of water

Z. Bakari (✉) · N. Boujelben · N. Turki · B. Elleuch
Sfax University, 3029 Sfax, Tunisia
e-mail: bakari.zaineb@gmail.com

M. Del Bubba
Florence University, 3-50019 Sesto Fiorentino, Italy

analysis [3, 4]. For the analysis of PCBs and PAHs, a different QuEChERS procedure was developed, using CH₂Cl₂ as an extraction solvent and primary secondary amine as a dispersive SPE agent.

3 Results

3.1 Characteristics of Sfax Treated Wastewater

Physico-chemical characteristics of the treated wastewater are presented in Table 1. The treated wastewater remained alkaline.

Concerning the organic pollutant load, the monitoring parameters (COD, BOD₅, MES...) indicated values that exceed the Tunisian and FAO standards for the reuse of treated wastewater in agriculture [6]. Nitrates, phosphate and potassium, which are essential nutrients for fertilizing the soil and plant growth, are found in large quantities in the Sfax treated wastewater, hence, their supply by irrigation is appropriate for plant nutrition (Table 2).

3.2 Organic Compounds Found in Raw Wastewaters and in Strawberries

4 Discussion

The methods developed and optimized for the evaluation of residual contamination by organic micropollutants were applied for the determination and quantification of PAHs, PCBs, PFAAs, APnEOs and APs in strawberry samples irrigated with different kinds of treated wastewater and tap water, as control. Target analytes were not detected in any of the analyzed samples, notwithstanding the high method sensitivity. As an example, perfluorooctane sulfonic acids (PFOS) were determined in TWW at mean concentrations in the ranges of <0.08–0.7 ng/L. Considering the volumes of water applied to strawberry cultivation (1750 L) and strawberry yields (211–272 g dry weight, depending on the TWW used) obtained during the experiments, it is possible to calculate the maximum levels of PFOA and PFOS expected in strawberries due to the transfer from TWWs. These values resulted in the ranges of <0.5–6.0 ng/g d.w., for PFOS that are two-three magnitude orders higher than the corresponding method detection limits (10 pg/g d.w.). Accordingly, the concentration values which are lower than the detection limits should be considered as an actual absence of transfer from TWWs to strawberries.

Table 1 Physico-chemical characteristics of Sfax treated wastewater (STW)

Parameter	pH	CE (ms /cm)	MES (mgL ⁻¹)	DCO (mgL ⁻¹)	DBO ₅ (mgL ⁻¹)	P _t (mgL ⁻¹)	NO ₃ ⁻ (mgL ⁻¹)	Cl (mg L ⁻¹)	SO ₄ (mg L ⁻¹)	Na ⁺ (mg L ⁻¹)	K ⁺ (mg L ⁻¹)	Mg ²⁺ (mgL ⁻¹)	Ca ²⁺ (mg L ⁻¹)	NH ₄ ⁺ (mg L ⁻¹)
STW	6.56	5.3	30	106.9	37	14.4	8	720	603	2816.5	175	280	241.6	66.3

Table 2 PFAAs, APnEOs and APs in the TWW effluents (ng/L) used for irrigation and corresponding maximum expected contaminations in strawberries (ng/g d.w.)

Compounds	STWW	Strawberries
4-t-OP	1500	1345
4-T-OP ₂ EO	51	27.64
4-t- OP ₃ EO	10	12.02
4-t-OP ₄ EO	7	6.51
4-t- OP ₅ EO	4	8.87
4-t- OP ₆ EO	<0.045	3.24
4-t- OP ₇ EO	9	10.38
4-t- OP ₈ EO	<0.045	0.06
NP	1245	1100
NP ₂ EO	697	789
NP ₃ EO	167	153.6
NP ₄ EO	34	37.42
NP ₅ EO	61	13.98
NP ₆ EO	21	119
4-NP ₇ EO	98	42.75
4-NP ₈ EO	124	179
PFBus	1.01	7.2
PFPeA	33.57	231
PFHxS	<0.02	0.15
PFNA	10	68.5
PFOS	0.8	5.94
PFNA	8.97	57

5 Conclusions

The results indicate that the use of TWW for strawberry irrigation does not imply the transfer of chemical contamination from TWWs to fruits, at least regarding the concentration levels of the classes of micropollutants herein investigated. In this regard, it should be, however, considered that the analyses object covers a wide range of physicochemical characteristics (e.g. solubility and octanol-water partition properties), which makes this investigation more informative than that specifically linked to target compounds.

Future researches are necessary in order to investigate the fate of more polar micropollutants (e.g. pharmaceuticals), as well as other fruit species, characterized by very different water and lipid percentages in the fruit compared to strawberry.

References

- Pedrero, F., Kalavrouziotis, I., Alarcon, J.J., Koukoulakis, P., Asano, T.: Use of treated municipal wastewater in irrigated agriculture—review of some practices in Spain and Greece. *J. Agric. Water Manag.* **97**, 1233–1241 (2010)
- USEPA.: Standard method 3535, revision 1 (2007)
- Ciofi, L., et al.: *Anal. Bioanal. Chem.* **408**, 3331–3347 (2016)
- Ciofi, L., et al.: *Talanta* **176**, 412–421 (2018)
- Rossini, D., Ciofi, L., Ancillotti, C., Checchini, L., Bruzzoniti, M. C., Rivoira, L., Fibbi, D., Orlandini, S., Del Bubba, M.: Innovative combination of QuEChERS extraction with on-line solid-phase extract purification and preconcentration, followed by liquid chromatography-tandem mass spectrometry for the determination of non-steroidal antiinflammatory drugs and their metabolites in sewage sludge. *Anal. Chim. Acta* (2016)
- FAO: Agriculture et rareté de l'eau: une approche programmatique pour l'efficacité de l'utilisation de l'eau et la productivité agricole. COAG/2007/7, Rome, p. 15 (2007)

The Reuse of Wastewater in the Context of Climate Change: Case of Mascara Wilaya (Algeria)

Benali Benzater, Anouar Hachemaoui, Abdelkader Elouissi, and Boumediene Benaricha

Abstract

According to the United Nations World Water Development Report 2017, wastewater, which is an untapped resource, effluents from domestic discharges into Algeria are discharging:

- A volume of collected sewage of 1570×10^6 m³/year.
- Only 275×10^6 m³/year of wastewater are treated (17%)
- Of the 17% purified, only 7% are used in irrigation (19.3×10^6 m³/year).

This work, conducted in the 18 sewage treatment plants of the Wilaya of Mascara, provides quantitative and qualitative results, which can be exploited by decision-makers in the water resources sector.

Keywords

Climate change • Lagooning • Reuse of wastewater • PCA • Mascara • Algeria

1 Introduction

Agriculture consumes 70% of the world's water needs. The industry's water is growing and is expected to reach 80% by 2030. The use of treated wastewater, for the time being largely unexploited, could indeed be one of the solutions to ease the tensions on the water resources which will not fail to worsen with the global warming [1, 3–5, 8].

The Mascara Wilaya, located in northwestern Algeria, which is experiencing water stress due to rainfall deficit and overexploitation of groundwater, has adopted the strategy for the reuse of treated wastewater from different wastewater treatment plants for irrigation. This vision is reliable to mitigate the lack of water [6].

2 Methods and Materials

The area concerned by this study is the Wilaya of Mascara, located in the north-west of Algeria, longitude between -0.5° West and 0.91° East, and latitude between 35° and 35.8° North (Fig. 1).

Mascara is an agricultural area where groundwater is the main resource used to irrigate crops. It includes three (03) agricultural spatial units [1]: the plain of Ghriss, the irrigated area of Habra and the perimeter of Sig. The reuse of treated wastewater in irrigation remains an absolute alternative to conventional water.

The Wilaya of Mascara has the following underground aquifers:

- The Ghriss Plain is an independent hydrogeological identity, formed by a superposition of four layers: superficial or phreatic nappe, the lacustrine limestone nappe, the Tighennif sand and sandstone nappe, and the dolomitic limestone nappe.
- The Oggaz water table located west of Mascara.

B. Benzater (✉) · A. Elouissi · B. Benricha
Laboratoire de Recherche sur les Systèmes Biologiques et la Géomatique (L.R.S.B.G.), Faculté des Sciences de la Nature et de la Vie, Université de Mascara, Route de Mamounia, 29000 Mascara, Algeria
e-mail: benzaterbenali@gmail.com

A. Elouissi
e-mail: elaek@yahoo.fr

B. Benricha
e-mail: benarichab@yahoo.fr

A. Hachemaoui
Direction Des Ressources En Eau et de L'Environnement de La Wilaya de Mascara, Mascara, Algeria
e-mail: a_hachemaoui@hotmail.com

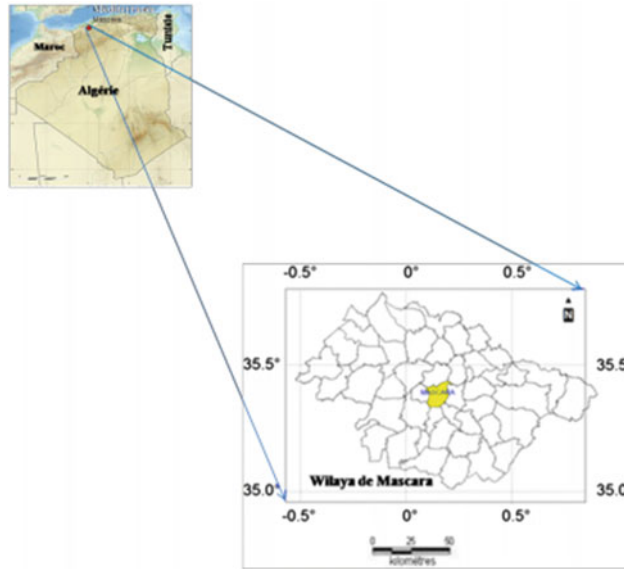


Fig. 1 Location map of the study area

3 Results

Samples of effluents from waste discharges were taken over a period of 12 months of 2017 at the entry (E) and exit (S) of the 18 operational treatment plants across the Mascara wilaya (ONA Mascara 2017).

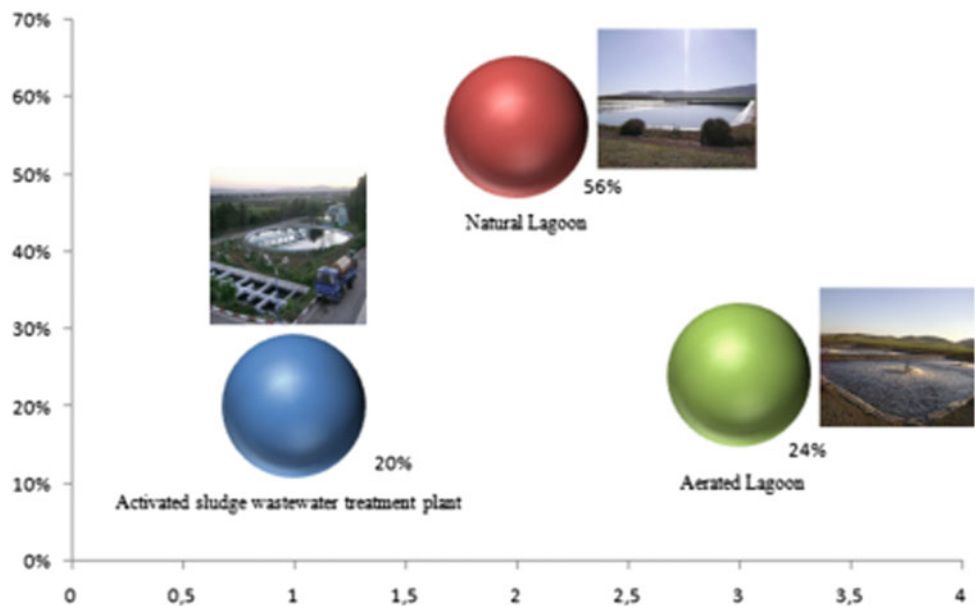
The studied parameters were pH, BOD5, COD and Suspended Matter (SM). They represent pollution indices. On the basis of these indices, we can qualify and quantify water

pollution and choose the appropriate process for the depollution of these waters.

3.1 Quantitative Analysis

According to the Oranie River Basin Agency (ABH) [7] (Fig. 2), the most widely used wastewater treatment process in western Algeria is natural lagooning (56%).

Fig. 2 Types of purification processes used in the West (ABH)



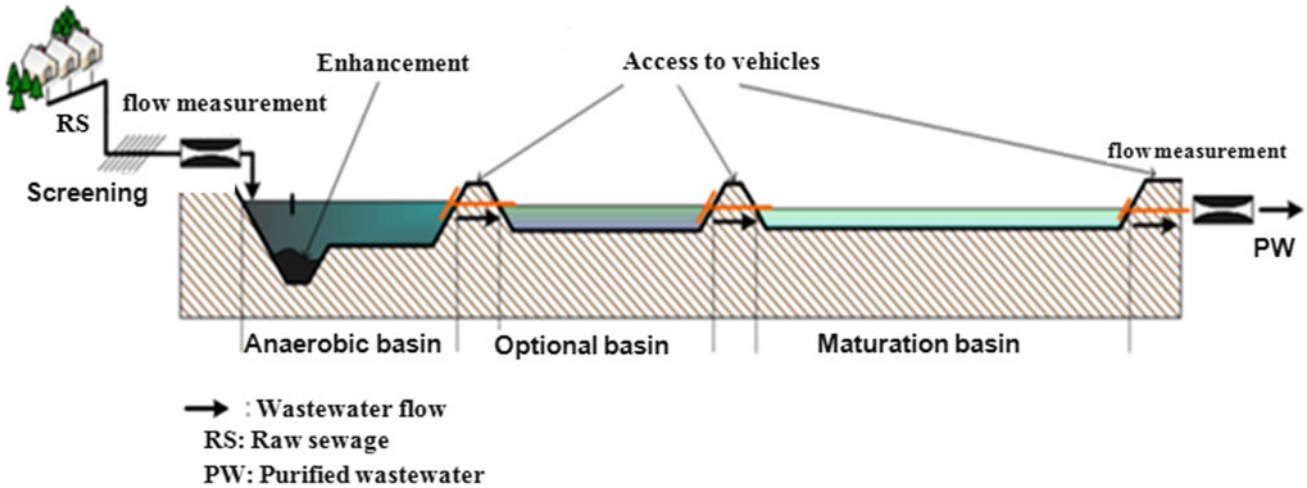


Fig. 3 Natural lagooning

According to ABH [7], out of 18 operational treatment plants at the level of the Wilaya of Mascara, 13 are natural lagooning stations (72%).

3.2 Qualitative Analysis

Natural lagooning is a simple process that requires large areas (an average of 4–5 ha for a station) according to the population equivalent (Eq/inhab).

In natural lagooning, the purification process is carried out on the basis of a simple principle (Fig. 3).

3.2.1 Principal Component Analysis (PCA)

Using the projection of the variables on the two axes (Fig. 4), which represent 74.81% of the information, we form three regional groups (SM_E with BOD5_E), (COD_E with BOD5_S) and (SM_S with COD_S).

In Fig. 4, the 1st factor of the projection plan is dominated by the variables COD_E and BOD5_S. The 2nd factor represents the variables SM_E and BOD5_E which oppose the variables SM_S and COD_S.

Figure 5 shows the projection of the treatment plants on the F1 × F2 plan. The position of the stations on axis 1 shows that the Mascara, Mohammadia and Bouhanifia

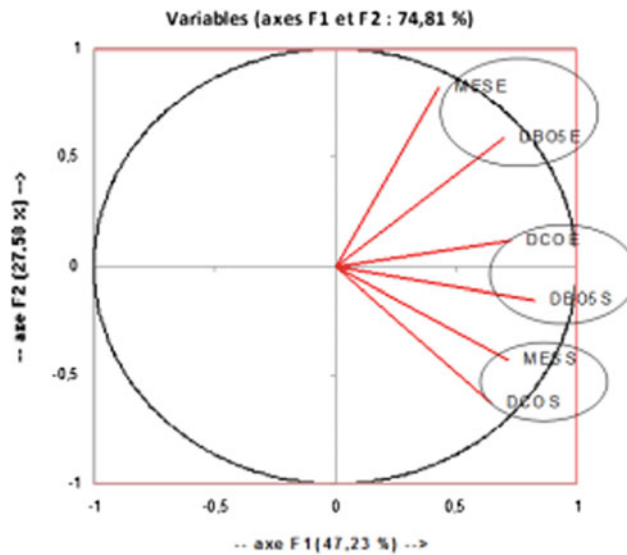
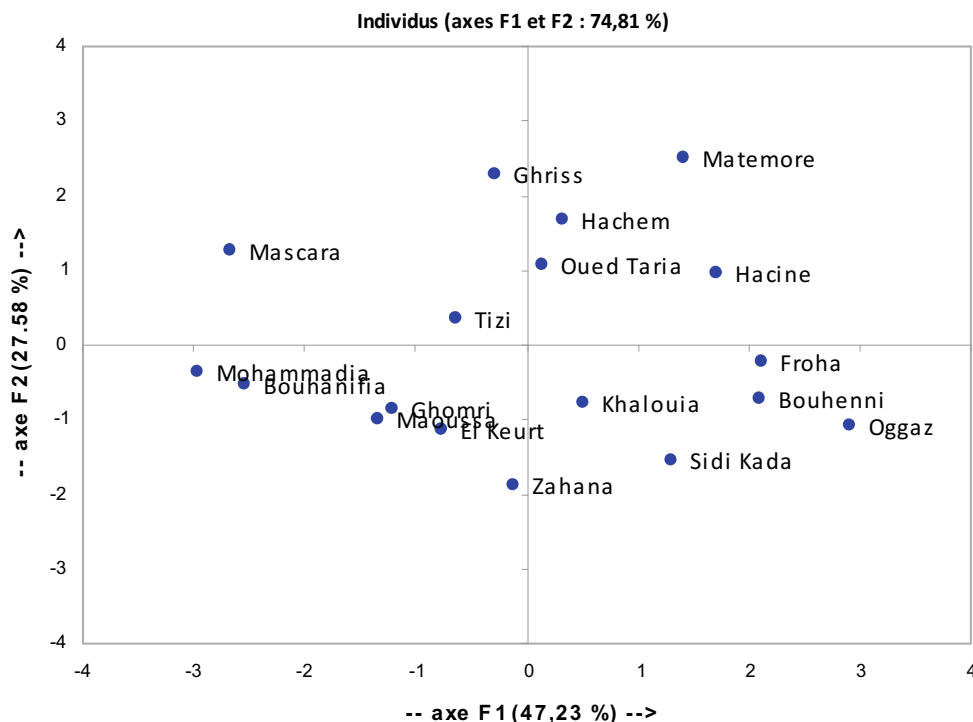


Fig. 4 Projections of the variables on the 2 axes

Fig. 5 Projection of stations on the F1 × F2 plan



stations have the lowest values of pollution. These stations are respectively activated sludge and aerated lagoons.

The position of the Zahana, Sidi Kada and Oggaz stations on axis 2 indicates that they have the highest values of COD and BOD₅ at the exit point, which requires a more rigorous control.

4 Conclusion

The quantitative analysis yielded 7.75 hm³/y of treated wastewater which will irrigate 2580 ha (8% of water requirements). The PCA qualitative analysis of the pollution parameters allowed us to define the best yields of the 18 stations with the appropriate type of purification.

References

1. Benaricha, B., Elouissi, A.: Physico-chemical characterization of effluent from the effluent treatment plant using activated sludge from Saida city (Algeria) and evaluation of the pollution degree. *J. Chem. Pharm. Res* **7**(9), 749–763 (2015)
2. BRL: Etude du réaménagement hydroagricole des périmètre de Habra et Sig. Direction des Ressources en Eau de la Wilaya de Mascara (2004)
3. Exall, K.: A review a water reuse and recycling with reference to Canadian practice and potential: 2 applications—review article. *Water Qual. Res. J.* **39**(1), 13–28 (2004)
4. Hannachi, A., Gharzouli, R., Djellouli, T.Y.: Gestion et valorisation des eaux usées en Algérie. *Larhyss J.* **19**, 51–62 (2014)
5. Lazarova, V., Brissaud, F.: Intérêts, bénéfices et contraintes de la réutilisation des eaux usées en France. *L'eau, l'industrie, les nuisances*, n **299**, 29–39 (2007)
6. Remini, B.: La problématique de l'eau en Algérie du nord. *Larhyss J.* **8**, 27–46 (2010)
7. FAO: Groundwater management in Algeria. Food and Agriculture Organization of the United Nations Rome (2009)
8. Drouiche, N., Ghaffour, N., Naceur, M. W., Lounici H., Drouiche, M.: Towards sustainable water management in Algeria. *Desalination Water Treat.* **50**(1–3), 272–284 (2012)

Evaluation of the Contamination from Geothermal Fluids upon Waters and Soils in Alaşehir Environs, Turkey

Ali Bülbül, Tuğbanur Özen Balaban, and Gültekin Tarcan

Abstract

The thermal and mineral waters, with high mineral contents from the geothermal fields of Alaşehir, Turkey, and which are discharged onto the ground surface, can cause contamination in surface water, in ground water, and in soil. Because of the fact that the water resources of the region are used for drinking and irrigational purposes, the evaluation of water quality is perfected in this study. Additionally, the surface soil samples are analyzed for their boron, arsenic and other contaminating substances to depict the measurement of the contamination. The results acquired from the analysis of the water samples suggest that some of the components (particularly B, and As) in some of the samples exceed the drinking-water limits. Also, some of the soil samples collected near the geothermal fields are contaminated with B, As, S, Hg, and other contaminants sourced from geothermal fluids, in a moderate to extreme degree. Further, contaminants in soil and water are expected to enlarge in the future unless effective sewage collection and treatment are present in the geothermal fields. This paper discusses the geochemical evaluations of the availability of B, As, and other contaminants derived from the geothermal activities within soil and water in Alaşehir and its environs. Proper re-injection of the thermal and mineral waters into the geothermal reservoirs is the best way to dispose of the geothermal fluids and cope with contamination problems.

Keywords

Water contamination • Soil contamination • Geothermal fluids • B and As • Geochemical evaluation

1 Introduction

Alaşehir town is located in Western Anatolia, Turkey, with a population of 105,644 in 65 villages. It was known as Philadelphia in antiquity and the middle ages (Fig. 1). Alaşehir and Gediz grabens are two of the important areas because of dried Sultana raisins in the world. There are small industries such as leather, ceramics and metal works, several factories, many fruit and vegetable gardens, and greenhouses in the study area. Additionally, the regions have geothermal potential due to the favorable geological conditions sourced from young tectonic activities.

Geothermal energy is one of the most important renewable energy sources for electric power generation in the Alaşehir graben. Geothermal fields were geographically divided into six main groups; (1) Alaşehir, (2) Piyadeler, (3) Horzumsazdere, (4) Kavaklıdere, (5) Göbekli and (6) Acıdere (Fig. 1). Thermal and mineral waters had mostly issued from natural springs and lots of wells during the sampling period of this study, in the years 2007–2009. The aims of this study are to investigate concentration of harmful element contaminants and to describe geothermal activities' effects on waters and agricultural soil in the study area.

2 Geological and Hydrogeological Setting

The study area is located in the eastern part of the Gediz graben, which is also known as Alaşehir graben. In this study, a hydrogeological map of the field was prepared by using combined geological units, which are divided into three distinct formations as Menderes Massif rocks, Neogene continental sediments, and Quaternary alluvium (Fig. 1).

A. Bülbül (✉)

Department of Geological Engineering, Pamukkale University,
35160 Denizli, Turkey
e-mail: abulbul@pau.edu.tr

T. Ö. Balaban

Central Research Labs, Izmir Katip Çelebi University, 35620
Çigli, Izmir, Turkey

G. Tarcan

Department of Geological Engineering, Dokuz Eylül University,
35370 Izmir, Turkey

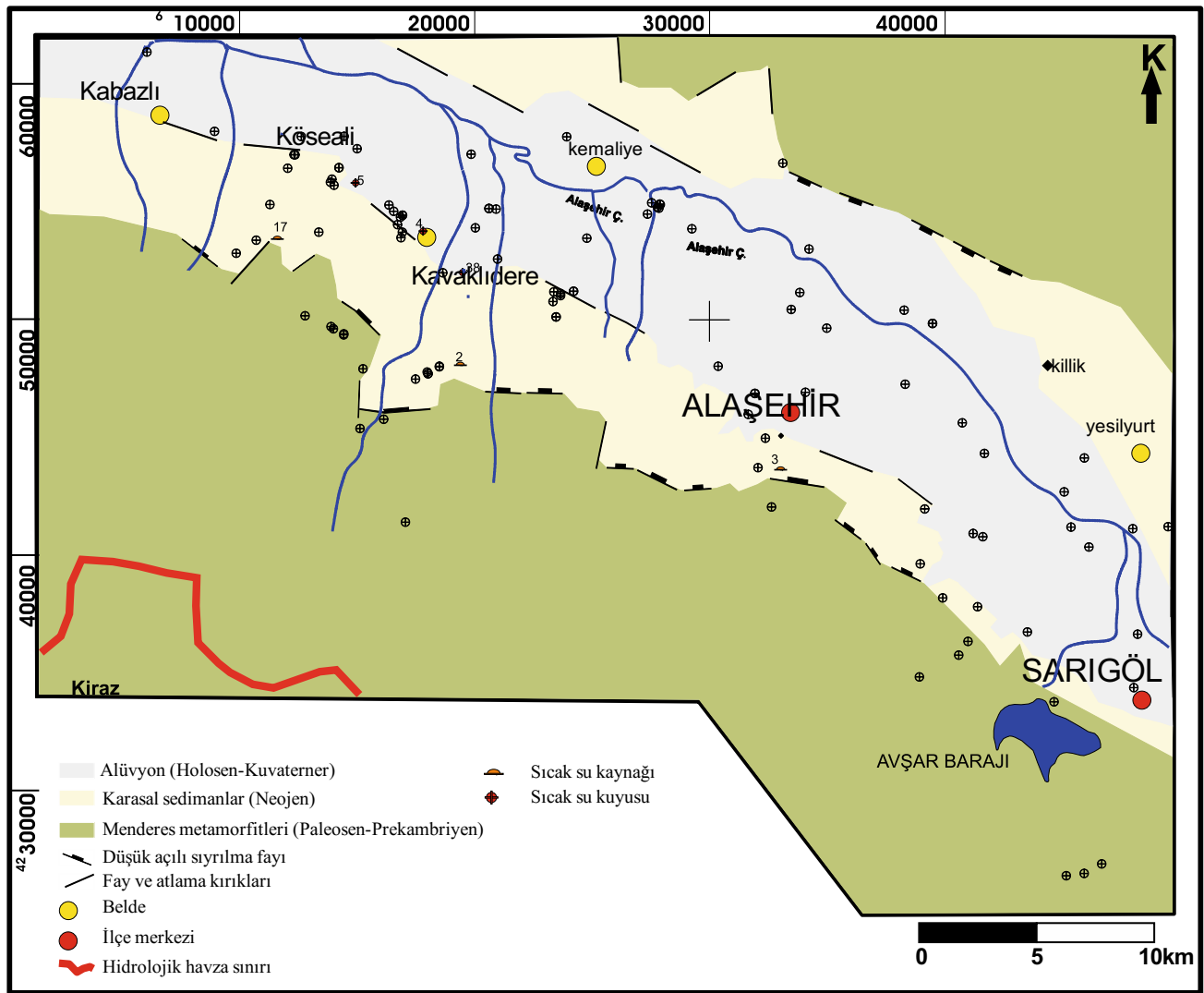


Fig. 1 Geological map of the study area and location of sample points [1]

Meteoric waters percolate through the faults, cracks, and fissures, and karstic voids are heated at least 1100 m depth in the reservoirs and are then moved up to the surface along the faults (Fig. 2).

Fractured rocks, such as gneiss, quartz schist, granodiorite, and karstic marbles of Menderes Massif are reservoirs of the geothermal systems. Since the clayey levels of the Neogene continental sediments are relatively impermeable, they act as the system cap rock. Since mica schist levels of the Menderes Massif rocks are also relatively impermeable, they act as the second system cap rocks as well as basement rocks. Heat source may be a magmatic intrusion close to the surface via the young faults [2]. The Early Miocene aged granodiorite intrusion in the area is too old to be the heat source of the geothermal systems. It must have cooled and lost heat due to the conductive cooling up to now. So, high geothermal gradient sourced graben tectonics is more

appropriate to explain the heat source of the geothermal systems. As seen in Fig. 2, most of the cold reservoirs and surface waters and agricultural soils are situated in the flow path of the thermal and mineral waters of the geothermal systems. Therefore, surface and groundwaters, and soil may be contaminated by mixing with the geothermal fluids.

3 Results

3.1 Water Contamination

Water samples from 106 sources were collected for chemical analyses in the area. The chemistry of deep circulated geothermal waters (wells AK-1, AK-2, Tariş, KG-1, and Sazdere springs) can be clearly differentiated from the other waters and they reflect the Na-HCO₃ type. Some of the

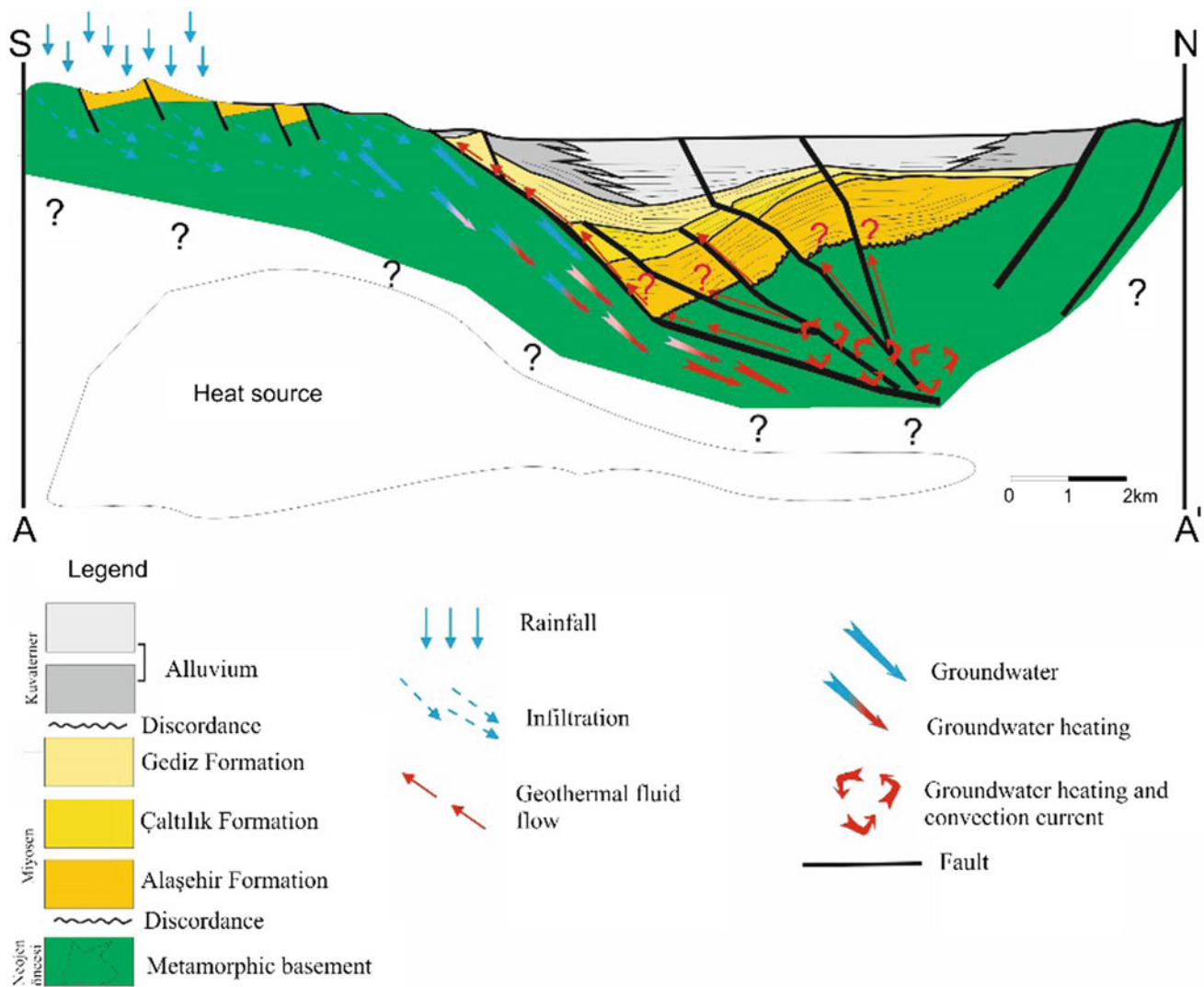


Fig. 2 Hydrogeological model of the geothermal system in the study area [3]

thermal and mineral waters (Alaşehir spa, Sarıkız mineral water, etc.) have shown Na–Ca–HCO₃ or Mg–Na–HCO₃ type and they have probably been shallow circulated. The chemistries of the other thermal and mineral waters, ground waters, and surface waters are mostly close to each other [2]. Dominant anion for all the waters is HCO₃. However, dominant cations are variable. The chemistry of thermal and mineral waters is mostly dominated by sodium (926–1894 ppm), potassium (12–13.5 ppm) and partly magnesium (63–624 ppm) (Table 1). They also have high concentrations of boron (1.21–124.14 ppm) and conductivity (2710–7780 μS/cm) and sometimes sulfate (258–4254 ppm), arsenic, iron and barium (Table 1). In the ground waters and surface waters Ca, Mg, and HCO₃ are prevalent; sulfate, sodium, potassium, boron and arsenic are in excess in some cases.

3.2 Soil Contamination

A total of 56 soil samples (agricultural soil and stream sediments) were collected from the Alaşehir environs to assess the existent distribution of contaminants deriving from the fields of the thermal and mineral waters. Chemical analyses of soils from the surroundings of Alaşehir environs show that % Na, As (ppm), Cu (ppm), Ni (ppm) and Hg (ppm) levels of some samples exceed the maximum acceptable limits given in Turkish Soil Pollution Control Regulation [4]. Samples 27, 28, 43, and 44 have high quantity contaminants, particularly for B, S, Ni, and Hg, due to the fact that they are directly affected from geothermal fluids. As expected, all the concentrations of the contaminants in soils increase near the locations of geothermal fluids and decrease with increasing distance from geothermal fields.

Table 1 Pollution index (PI) values for the soil samples from the study area

Samp. No	PI	No	PI	Samp. No	PI	Samp. No	PI
1	2.25	15	0.34	29	1.58	43	3.69
2	1.71	16	0.95	30	0.69	44	4.84
3	5.42	17	0.97	31	0.51	45	0.89
4	10.86	18	0.37	32	1.11	46	0.78
5	5.13	19	0.74	33	4.44	47	1.00
6	3.77	20	0.55	34	0.78	48	1.87
7	1.79	21	0.43	35	0.82	49	1.88
8	3.74	22	0.56	36	0.85	50	0.23
9	0.33	23	0.52	37	0.71	51	0.75
10	0.61	24	0.48	38	4.00	52	0.31
11	0.37	25	0.43	39	2.93	53	0.46
12	0.45	26	2.04	40	4.01	54	0.28
13	0.62	27	12.29	41	0.93	55	0.59
14	0.72	28	7.66	42	2.15	56	0.54

Bold characters show PI values above 1.0 indicate that the soils might be contaminated by geothermal fluids or another anthropogenic input

The pollution index value (PI), which was proposed [5] is one of the factors for contamination assessment in soils. The equation used for this study is as follows:

$$PI = [(As/20) + (Cd/1) + (Cu/50) + (Hg/1) + (Pb/50) + (Zn/150) + (Ni/30) + (Cr/100) + (B/20) + (Co/20) + (Ba/200) + (S/2)]/12$$

PI values above 1.0 for this study are evaluated that the soils might be contaminated by geothermal fluids and/or any anthropogenic inputs like agricultural chemicals. PIs range between 0.33 (sample 9) and 12.50 (sample 27) for soil samples from the Alaşehir environs (Table 1). PIs of almost half of the soil samples are above one and correspond to contamination by the effects of geothermal fluids.

4 Conclusions

Geothermal fluids may also be drained into the Alaşehir River via brooks by the effects of precipitation. These can cause contamination of soils and surface waters, as well as groundwaters. Concentrations of the contaminants in waters and soils increase with the decreasing distance from geothermal fields to sampling locations. All of these threaten the agricultural production and human health in the Alaşehir environs.

Water contamination areas coincide with the soil contamination areas around Alaşehir environs. All the areas showing contamination are located in nearby the geothermal fields. To cope with contamination problems for waters and soils, geothermal fluids should be properly re-injected into the geothermal reservoirs and/or a proper fluid collecting and treatment system must be established in the geothermal fields.

References

- Bülbül, A., Özen, T., Tarcan, G.: Hydrogeochemical and hydrogeological investigations of thermal waters in the Alaşehir-Kavaklıdere area (Manisa-Turkey). *Afr. J. Biotech.* **10**(75), 17223–17240 (2011)
- Bülbül, A.: Hydrogeological and hydrogeochemical investigation of hot and cold water systems of Alaşehir (Manisa). Ph.D. Thesis, Dokuz Eylül University, Institute of Sciences, İzmir, Turkey (in Turkish) (2009)
- Tarcan, G., Gemici, Ü., Aksoy, N.: Hydrogeological and geochemical assessments of the Gediz Graben geothermal areas, western Anatolia, Turkey. *Environ. Geol.* **47**, 523–534 (2005)
- TSPCR: Turkish Soil Pollution Control Regulation by Turkish Ministry of Environment and Forestry, Official Journal No. 25687, p. 9 (2005)
- Nishida, H., Miyai, M., Tada, F., Suzuki, S.: Computation of the index of pollution caused by heavy metals in river sediment. *Environ. Pollut. Ser. B, Chem. Phys.* **4**(4), 241–248 (1982)



Geochemical and Isotopic Marks for Tracing Groundwater Salinization: Santiago Island, Republic of Cape Verde, Case Study

Paula M. Carreira, António Lobo de Pina, Alberto Mota Gomes, José Manuel Marques, and Fernando Monteiro Santos

Abstract

In Santiago Island, the overexploitation of coastal aquifers and pollution are among the main problems related to groundwater resources assessment and management. The national water authorities are dealing with brackish groundwater for agriculture and human supply in numerous parts of the Island, as it is the only type of water available. Solutes and environmental isotope obtained in different aquifer systems were used in the identification/sources of groundwater resources degradation. Chemical and isotope analyses were carried out in groundwater samples in order to understand the role of anthropogenic activities and the main origin of salts in the groundwater units. The results obtained indicate water-rock interaction mechanisms as the major process responsible for the groundwater quality (mainly Ca–HCO₃-type), reflecting the lithological composition of the Island's geological formations. The geochemistry, together with the isotopic data, gives essential information on groundwater recharge, as well as on the identification of salinization mechanisms (e.g., seawater intrusion, salt dissolution, and marine aerosols). The isotopic pattern presented by part of the groundwater samples can be related to direct infiltration of irrigation

waters undergoing significant evaporation, during the dry periods. Carbon-14 determinations (six boreholes) indicate an apparent groundwater ages between 1.3 and 3.1 ka BP.

Keywords

Semi-arid region • Stable isotopes • ¹⁴C groundwater dating • Salinization origin • Republic of Cape Verde

1 Introduction

In arid and semi-arid regions, surface water is either seasonal or non-existent and groundwater becomes the only dependable source of water supply. Water scarcity problems (e.g., saltwater intrusion) can lead to damages of coastal aquifers. This issue is one of the natural hazards that have a vast and enormous impact on agriculture-based societies and on urban development. Santiago Island is characterized by scarce hydrological resources, low and irregular precipitation, varying between 190 and 320 mm/year, respectively, at low levels and in the highest mountains of Pico da Antónia or Serra Malagueta (Fig. 1). Under a semi-arid to arid climate, Santiago Island shows unpredictable and erratic rainfall periods, which leads to prolonged drought periods.

The main geological formations found in the island have a volcanic origin, composed mainly by a volcano-stratigraphic sequence, used as the basic support for hydrological and hydrogeological resources research. The main units (Fig. 1) with strong hydrogeological significance are the following: (i) the Base Unit mainly composed by the Eruptive Complex (CA), Flamengos formation ($\rho\lambda$) and the Orgãos formation (CB); (ii) the Eruptive Complex of Pico da Antónia (PA) and Assomada formation (A) (iii) the Monte das Vacas formation (MV) and (iv) recent Quaternary sedimentary formations (a) [1]. The aim of this research was to find responses to some hydrogeological questions such as the origin and mechanisms of groundwater mineralization

P. M. Carreira (✉)

Centro de Ciências e Tecnologias Nucleares, Instituto Superior Técnico, (C2TN/IST), Universidade de Lisboa, Estrada Nacional 10, km 139,7, 2695-066 Bobadela LRS, Portugal
e-mail: carreira@ctn.tecnico.ulisboa.pt

A. Lobo de Pina · A. M. Gomes
Faculdade de Ciências e Tecnologia, Universidade de Cabo Verde, Campus do Palmarejo, Praia, Santiago, Republic of Cabo Verde

J. M. Marques
Centro de Recursos Naturais e Ambiente, Instituto Superior Técnico (CERENA/IST), Universidade de Lisboa, Av. Rovisco Pais, 1049-001 Lisbon, Portugal

F. M. Santos
Universidade de Lisboa - DEGGE-IDL, Campo Grande Ed. C8, 1749-016 Lisbon, Portugal

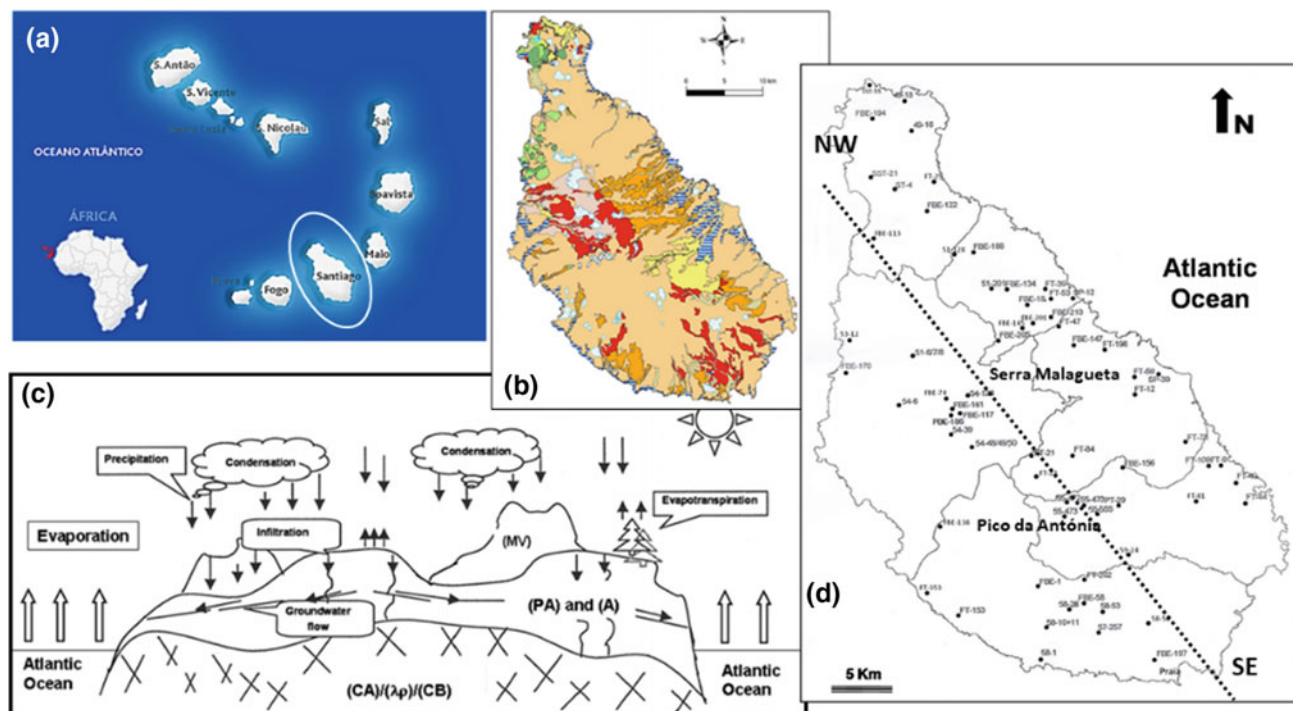


Fig. 1 a Santiago Island location; b Santiago Island geological map [1]; c schematic NW–SE, hydrogeological conceptual model of Santiago Island (adapted from [1]); d location of the sampling points

and mean residence time within these systems using environmental isotopes and geochemical approaches.

2 Results and Discussion

The mean temperature of the groundwater samples is approximately 25.4 °C, ranging from 22 to 29 °C. The electrical conductivity varies between 130 and almost 10,000 $\mu\text{S}/\text{cm}$. Groundwater samples collected in the central part of Santiago Island, such as Pico da Antónia or Serra Malagueta, belong to the Na–HCO₃ type, pointing to the influence of the volcanic terrains. Groundwaters with highest salt content are found near the coastline, mostly in valleys known for being the busiest agricultural areas on the island, with excessive pumping of the aquifer systems [1], revealing the effects of the saltwater intrusion phenomenon and/or marine aerosol influence (Fig. 2).

Based on the isotopic composition of the water samples (Fig. 3), two groups of groundwater samples are recognized: the first includes the groundwaters samples collected in the eastern part of Santiago Island (near the coastline), while the second group is mainly represented by groundwater samples ascribed to high-altitude places and located in the western part of the island. The mean stable isotope content ($\delta^{18}\text{O}$; $\delta^2\text{H}$) of the groundwater systems in Santiago Island is $-3.80 \pm 0.53\text{‰}$ and $-26.6 \pm 5.8\text{‰}$ versus V-SMOW

respectively for ^{18}O and ^2H . The isotopic data suggest that all groundwaters are meteoric waters and most of them were not subjected to previous evaporation before recharge. The recharge seems to occur by direct infiltration of rainfall in the most permeable geological formations of the island. Nevertheless, the contribution of irrigation waters undergoing significant evaporation, during the dry periods, cannot be excluded.

Tritium content was measured in all of the groundwater samples; the values obtained vary between 0 and 3 ± 0.6 TU. Most of the groundwater samples without ^3H (higher residence time) are located near the coastline, supporting the hypothesis formulated of longer flow paths. No correlation was found either between the sampling altitudes of waters and the ^3H concentrations or with the groundwater mineralization.

^{14}C analyses were carried out in six selected boreholes located in different areas of the island. The ^{14}C concentration obtained varies between 73.2 ± 0.4 and 95.72 ± 0.4 pmC. Applying the equation proposed by [2] the apparent carbon-14 age of the groundwater was calculated, using the carbon-13 values for groundwater age correction, and assuming C4 plants photosynthetic cycle (maize and sugar cane) and also C3 plants (banana plantations). The apparent ages vary between 1.3 and 3.1 ka BP (using C4 plants for age correction), and modern apparent ^{14}C ages assuming $\delta^{13}\text{C}_{\text{C3}}$ values for groundwater age calculations/correction.

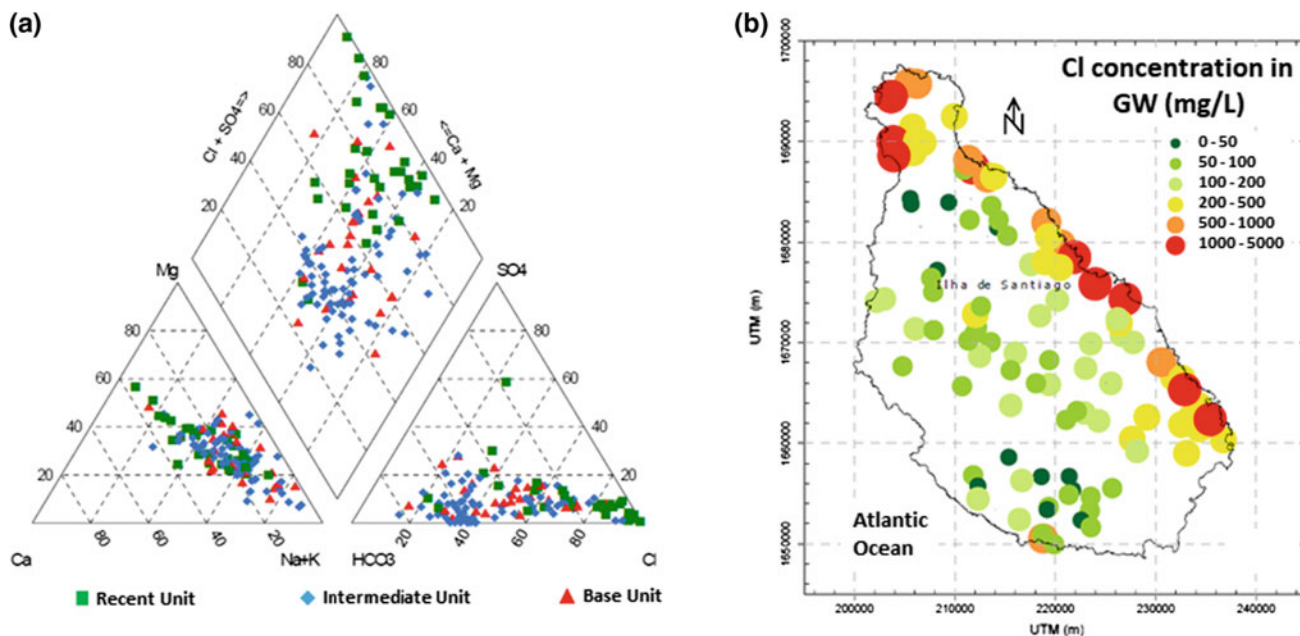


Fig. 2 a Piper diagram. b Cl concentration in groundwater samples of Santiago Island. Adapted from [1]

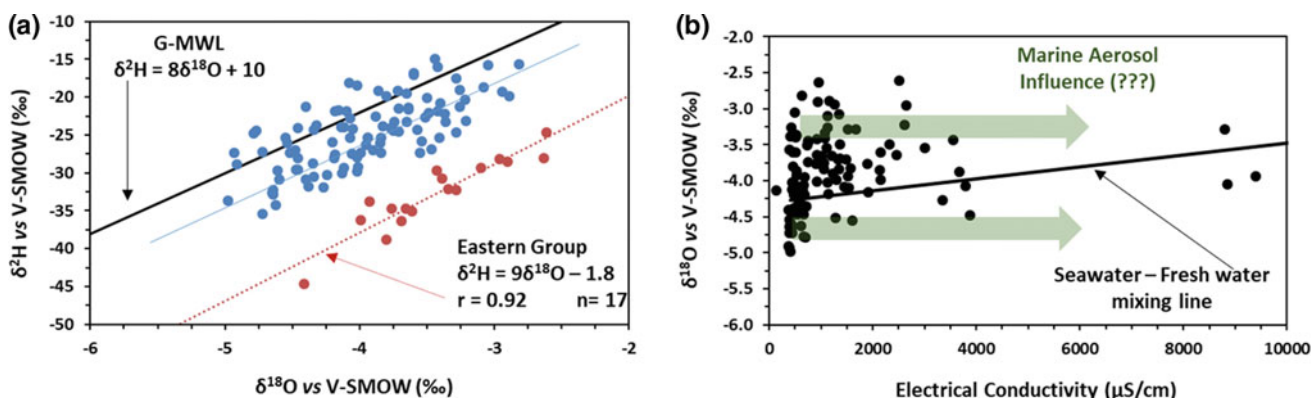


Fig. 3 a $\delta^{18}\text{O}$ versus $\delta^2\text{H}$, the blue line stands for the isotopic composition trend of the second group. b Electrical conductivity versus $\delta^{18}\text{O}$ content; two mineralization mechanisms can be responsible for the groundwater salinization

3 Final Remarks

The major challenge in this study was to distinguish saline water of different origins and groundwater of different ages. The results point out to the fact that the extent of seawater intrusion into the land and the influence of marine aerosol appear to be moving forward. Considering only C4 plants (original vegetation on the Island), the presence of old groundwater reduce/exclude, in those areas, the human interference in the water mineralization. Old seawater intrusion can be considered as one source of groundwater

salinization. Furthermore, the constant exploitation for human supply and by the farmers (e.g., banana plantations) will lead to the degradation of these resources. Moreover, one possible explanation for the existence of the eastern group is infiltration/recharge under different climatic conditions (existence of a palaeoclimatic effect).

Acknowledgements This work was developed in the scope of the project HYDROARID (POCI/CTE/GEX/55399/2004) funded by FCT and FEDER. C²TN/IST author acknowledge the FCT support through the UID/Multi/04349/2013 project; CERENA/IST acknowledge the FCT support through the UID/ECI/04028/2013 project.

References

1. Lobo de Pina, A.F.: Hydrochemistry and quality in the groundwater of Santiago Island–Cabo Verde. Ph.D. Thesis, University of Aveiro, Portugal (in Portuguese) (2009)
2. Salem, O., Visser, J.M., Deay, M., Gofiantini, R.: Groundwater flow patterns in western Lybian Arab Jamahitiya evaluated from isotope data. In: *Arid Zone Hydrology: Investigations with Isotope Techniques*, IAEA. Vienna, pp. 165–179 (1980)

Application of Geochemical Tracers and Isotopic for Investigation of Recharge and Salinization of Water in the Menzel Bourguiba Aquifer, Northeast of Tunisia

Mohsen Ben Alaya, Safouan Ben Ammar, Jean-Denis Taupin, Mohamed Khouatmia, Raouf Jbeali, and Fetheddine Melki

Abstract

In order to better understand the hydrogeological functioning of the Menzel Bourguiba aquifer system (NE Tunisia), chemical and isotopic (^{18}O , ^2H) analyses of water are carried out. This work highlights the fact that the water of this aquifer system is highly modified by geochemical interactions: cationic exchange and precipitation/dissolution phenomena. By using isotopic tools, it was shown that the water of this aquifer system has been recently recharged by direct infiltration from the boundary and in the valley of wadis.

Keywords

Aquifer system • Natural tracers • Isotopes • Menzel Bourguiba plain • NE Tunisia

1 Introduction

The salinity of water resources has been studied intensively during the past decades, and in particular in Northern Tunisia [1]. Indeed, understanding the recharge modes and processes that control the evolution of saline water in the aquifers over the years remains an academic challenge with

important practical implications for water resource evaluation and management.

In Menzel Bourguiba basin (Fig. 1), located in the north-eastern part of Tunisia, agriculture and industry are the primary economic activities. The Menzel Bourguiba hydrological basin covers approximately 57 km², of which 50 km² lie over the plain. The plain hosts a large number of wells and boreholes with depths varying from a few meters to nearly 120 m. Most of these wells and boreholes, which tap into a multilayered unconfined aquifer (Fig. 1), penetrate the Plio-Quaternary conglomerate sands and sandstones and supply water for irrigation. Some of the wells are used for drinking water, and only few for industry, and approximately 90% of the water is used for irrigation. The over-pumping of the aquifer system of Menzel Bourguiba has resulted in a water level decrease ranging from 0.2 to 0.8 m/year during the past three decades. The water quality is highly variable and, in some areas, reaches high salinity levels exceeding 3 g/L. Determination of recharge modes and evaluation of the mechanisms that cause the degradation of the groundwater quality in the Menzel Bourguiba basin are the focus of this paper.

2 Methods

Twenty-five groundwater samples from Quaternary and Pliocene aquifers were sampled in September–October 2016 from pumping wells and boreholes. Several analyses of: water temperature (18.7–23 °C), pH (6.58–7.63), electrical and conductivity (EC) (0.87–4.61 mS/cm) were carried out on-site. All samples were filtered directly in situ through 0.45 µm membrane filters, stored in high-density polyethylene bottles of 250 ml, and kept at 4 °C. Stable isotope composition of water samples was analyzed at the Laboratory LAMA of HydroSciences Montpellier. Major chemistry and trace elements were determined by several methods in INRAP geochemistry laboratory (Titration, Ion Chromatography, flame photometry and inductively coupled plasma–optical emission spectrometry—ICP-OES).

M. B. Alaya (✉) · R. Jbeali
National Institute of Research and Physical-Chemical Analysis (INRAP), Technopole, 2020 Sidi Thabet, Ariana, Tunisia
e-mail: benalaya.mohsen@gmail.com

S. B. Ammar
Carthage University, 2035 Tunis, Tunisia

J.-D. Taupin
Hydrosciences, UMR 5569 (IRD, CNRS, UM), Montpellier, France

M. Khouatmia
CNSTN, Sidi Thabet, Tunis, Tunisia

F. Melki
Tunis-El Manar University, 1060 Tunis, Tunisia

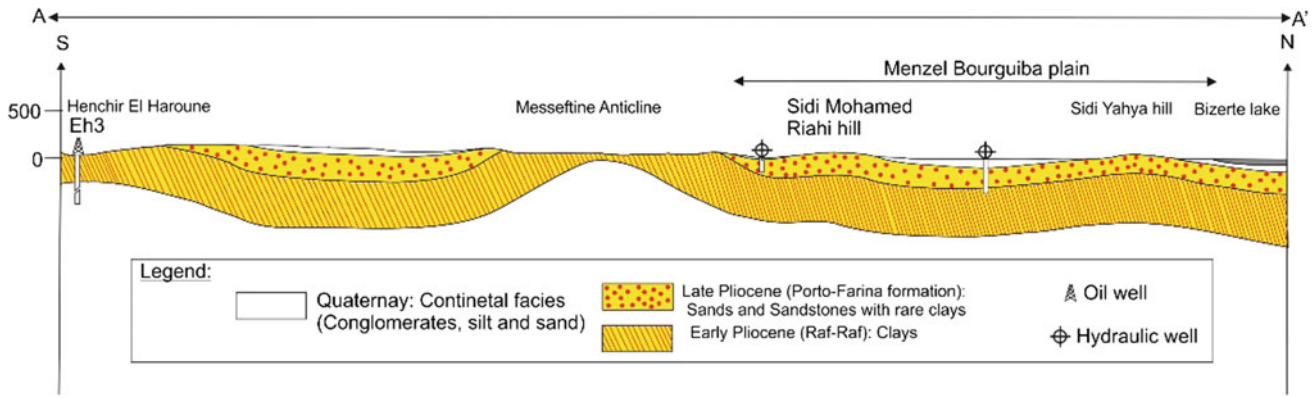


Fig. 1 Hydrogeological cross section in the study area

3 Results

Water levels in the aquifer of Menzel Bourguiba were measured at 17 monitoring wells during September–October 2016, and a map of the water table is shown (see Fig. 2a). The altitude of the water table ranges from lake levels along the Ichkeul and Bizerte lakes to almost 55 m in the southern part of the study area. A good correlation exists between topography and water levels in the study area. Recharge occurs primarily through permeable formation outcrops in Jebels Zaarour and Kef Ennsour. The general direction of groundwater flow is from J. Zaarour and J. Kef Ennsour foothill zone towards the Ichkeul and Bizerte lakes which are the natural discharge area. The hydraulic gradient of groundwater flow in the Quaternary aquifer ranges from 0.6 to 1.2‰ in the downstream zone and 2.2 to 3.4‰ in the upstream zone.

Groundwater salinity, represented by the TDS values, shows a large range of variation from 0.87 g/L to almost

3.5 g/L. This variation conforms partially with the main groundwater flow directions (see Fig. 2b), indicating that the groundwater salinity is somewhat controlled by the residence time in the aquifer. Indeed, relatively low TDS values which characterize the south-western band of the study area reveal the dilution of the groundwater by the recharge coming from the basin border highlands. However, high salinities appear in the central and northern parts of the basin which relatively disturbs the evolution of the mineralization in the direction of the groundwater flow. This sudden increase of groundwater salinity is expected since the central part of the study area is marked by the development of land use activities.

The results of chemical analyses indicate enrichment in Cl^- relative to SO_4^{2-} , except for some samples which are depleted in Cl^- with respect to SO_4^{2-} ions. Consequently, most of the Menzel Bourguiba groundwater samples show similar water types: $\text{SO}_4\text{-Cl-Ca}$ and Cl-Na (mainly in the deep part of the aquifer). A net enrichment in Cl^- , SO_4^{2-} and Na^+ is explained by evaporite mineral dissolutions

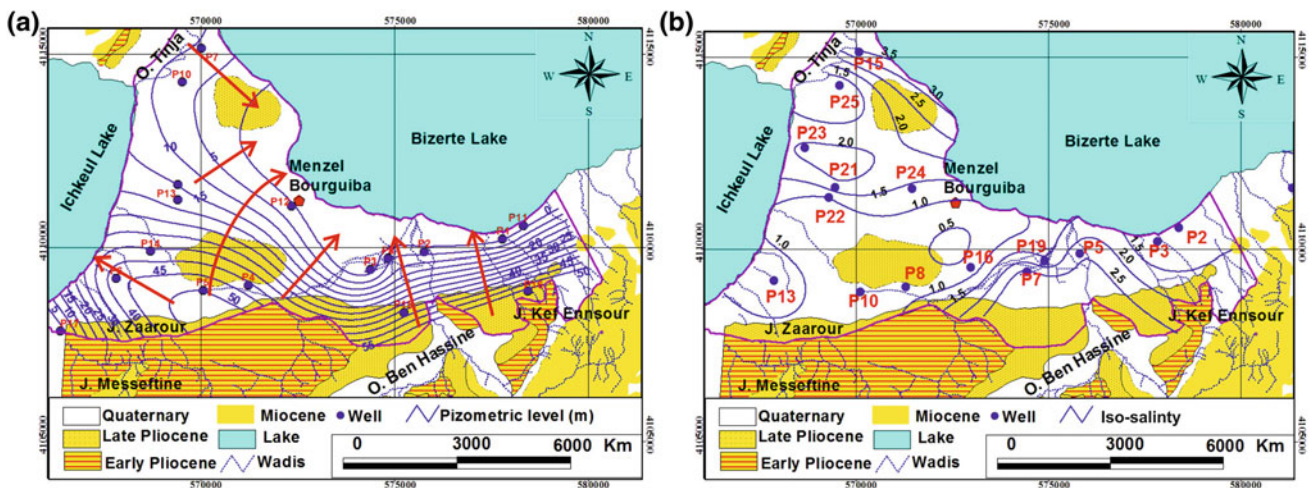


Fig. 2 Piezometric (a) and salinity (b) maps of the phreatic aquifer of Menzel Bourguiba

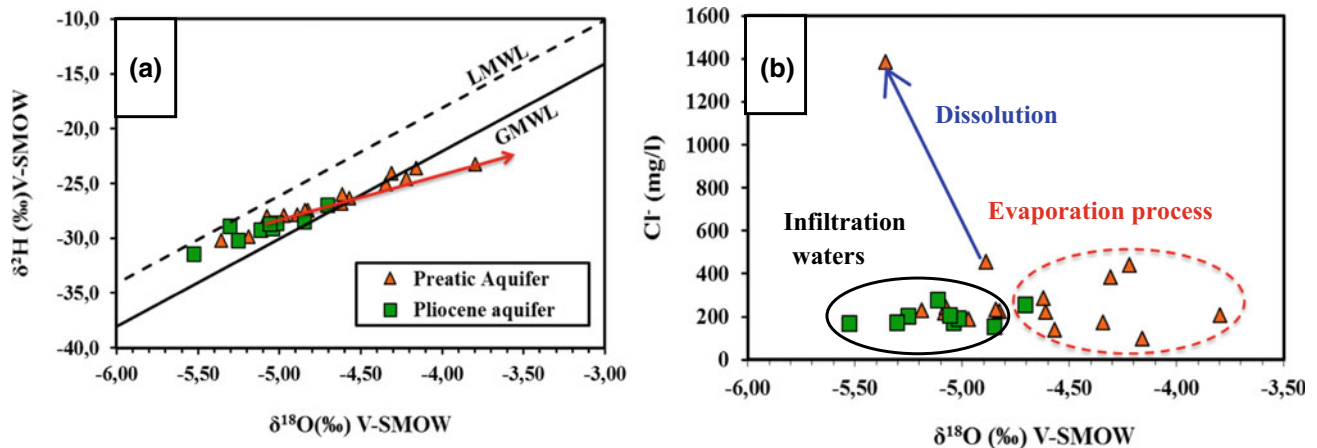


Fig. 3 a Stable isotope composition and b $\delta^{18}\text{O}$ - Cl^- relationship for of phreatic and Pliocene groundwaters

($-6.52 \leq \text{SI}_{\text{halite}} \leq -5.79$, $-1.68 \leq \text{SI}_{\text{gypsum and anhydrite}} \leq 1.59$) and reverse cation exchange with clays ($1.2 \leq \text{Na}^+/\text{Cl}^- \leq 2.27$). High NO_3^- concentrations characterize the study area with values ranging between 74 and 288.5 mg/L, indicating excessive use of synthetic fertilizers in this intensively cultivated area and a recharge by irrigation water return.

Stable isotope composition of water samples from all wells and boreholes collected in the groundwater system of Menzel Bourguiba suggests the presence of recently recharged water (Fig. 3a). Oxygen-18 and deuterium values in this area range, respectively, from -5.18 to -4.70 ‰ versus V-SMOW and from -31.2 to -23.2 ‰ versus V-SMOW. The mean isotopic values are, respectively, -4.84 and -27.5 ‰ V-SMOW for $\delta^{18}\text{O}$ and $\delta^2\text{H}$, close to values found in precipitations ($\delta^{18}\text{O} = -5.00$ ‰ and $\delta^2\text{H} = 28.6$ ‰) [2] in the humid season suggesting the groundwater is linked to current rainfall origin.

The importance of recent water infiltration, dissolution of evaporites (halite, anhydrite and/or gypsum) and evaporation process, as the main processes responsible for the variation in salinity of groundwaters, is depicted in the $\delta^{18}\text{O}$ versus Cl^- diagram (see Fig. 3b). Different trends, indicating different origins of groundwater salinity, are observed in this diagram (see Fig. 3b). The first trend indicates the presence of a young local component including enriched waters with lower chloride concentrations. These diluted groundwaters have a concentration of Cl^- ranging between 155 and 278.4 mg/L and $\delta^{18}\text{O}$ varying between -5.53 and -4.85 ‰. The second trend shows the enrichment of the stable isotopic compositions due to the evaporation process of surface irrigation water before infiltration. Indeed, evaporation appears to be an important process contributing to groundwater salinization. The third trend shows a well-defined dissolution process.

4 Conclusions

The results of this study show that the analysis of hydrochemical data, coupled with environmental isotopes, can help elucidate the hydrologic and geologic factors controlling water chemistry in Menzel Bourguiba basin. The chemical facies of waters are $\text{SO}_4\text{-Cl-Ca}$ and Cl-Na which are in relation with (I) their interaction with the geological formations of the basin (various evaporites), (II) cation exchange and (III) evaporation. This evaporation occurs in the upper part of the unsaturated zone during infiltration, especially for some phreatic aquifer samples. Stable isotope signature contents of groundwater provide evidence for recent groundwater recharge and return flow from irrigation. Obviously, continued water utilization in the central part of Menzel Bourguiba basin and near the outlet (Ichkeul and Bizerte Lakes) of the aquifer system would further increase the depletion of the water resources and degradation of groundwater quality. These factors should be taken into consideration in future water management plans.

References

1. Ben Ammar, S., Taupin, J.D., Zouari, K., and Khoutmia, M.: Identifying recharge and salinization sources of groundwater in the Oussja Ghar el Melah plain (northeast Tunisia) using geochemical tools and environmental isotopes. *Environ. Earth Sci.* **75**(7), 606 (2016). <https://doi.org/10.1007/s12665-016-5431-x>
2. Mannai, K.: Interprétation climatique de la variabilité isotopique (^{18}O et ^2H) des précipitations dans le Nord-Est Tunisien (région de Bizerte). Master's report. Université de Tunis-el Manar (2016)

Seawater Intrusion Characterization in a Coastal Aquifer Using Geophysical and Geochemical Approach (Northeastern Tunisia)

Hajer Ferchichi, Boutheina Farhat, and Abdallah Ben-Mammou

Abstract

The shallow aquifers in the Mediterranean coastal areas are potential groundwater resources for many purposes. Groundwater from sands and sandstone deposits in the Medjerda lower valley aquifer (Northeastern Tunisia) represents a source which is characterized by high saline variations with Total Dissolved Solids (TDS) levels up to (19,000 mg/l) and with high Cl^- (>4000 mg/l) and Na^+ (>3000 mg/l) contents near the coastline, indicating the saline nature of the groundwater. This study consisting in an integrated geophysical approach (using Vertical Electrical Sounding (VES)) and hydrochemical analyses (60 groundwater samples) to circumscribe seawater intrusion phenomena. Several VES results were utilized using Schlumberger configurations with AB/2 « $\rho_a = f(AB/2)$ » varying from 1 to 200 m. The low resistivity (<5 Ω m), as saline water intruded up, extended over several km inland within the eastern parts of the study area. Mapping of TDS, Cl^- , Na^+ and iso-resistivity using GIS tools and electrical pseudo-sections revealed the extent of the seawater intrusion inland and the presence of direct cation exchange linked to seawater intrusion and dissolution processes associated with cation exchange. Finally, we demonstrate that these results may be used to enhance the management of the groundwater resources in the Medjerda lower valley aquifer in a complex terrain.

Keywords

Saltwater intrusion • Geophysical investigation
Geochemical • Groundwater • NE Tunisia

1 Introduction

Currently, the growing need for fresh-water supplies in the coastal aquifers is rapidly increasing due to the steady population growth and intensive economic activity. However, this resource is especially susceptible to deterioration owing to its closeness to the seawater, in addition to the excessive water needs that accompany higher population densities and agricultural activities. The Medjerda lower valley shallow aquifer, located in the Northeast of Tunisia, is exposed to the problem of marine intrusion affecting most of the Mediterranean littoral areas. Several studies dealt with this problem worldwide such as Pulido-leboeuf [2], Samsudin et al. [5]; Montety et al. [2], Zghibi et al. [6]; etc. The investigation of the thickness and geometry of the subsurface systems, is a special procedure to develop all the susceptible information from geological data, drilling, and exploitation boreholes. In order to investigate these parameters, the electrical resistivity values have been successfully applied and mapped. Nevertheless, indirect geophysical methods (like electrical resistivity profiles) and Schlumberger VES surveys generate continuous data throughout several profiles.

The geochemical investigation shows that, in the MLV aquifer, the resistivity is conditioned by the chloride and sodium content, together with the piezometric depression near the coastline in the main aquifer of the region.

The principal objective of this study is to furnish a precise geological reconstruction. This reconstruction performs a fundamental tool to suggest a new framework of susceptibility to the possible appearance near the surface. To this end, electrical resistivity profiles, seismic profiles, geochemical field mapping and lithological observations have been carried out.

H. Ferchichi (✉) · B. Farhat · A. Ben-Mammou
Department of Geology, Mineral Resources and Environment
Laboratory (LRME), Faculty of Sciences of Tunis,
University of Tunis El Manar, 2092 Tunis, Tunisia
e-mail: hajerferchi@gmail.com

H. Ferchichi
Isotope Hydrology and Geochemistry Unit, CNSTN, UMTN,
Technopark of Sidi Thabet, 2020 Sidi Thabet, Tunisia

2 Materials and Methods

The MLV area is part of a large coastal plain covering an area extent of about 1090 km² (Fig. 1). The Mediterranean Sea forms the eastern limit. The north and the south are occupied by several hills. For the topography, two different climate environments are found: a coastal environment with marine influence, and a semi-continental mountain environment. The deltaic basin benefits from both the runoff of the watershed and the underground flow of the surrounding geological structures, which have given to the reservoir a vast synclinal basin [1]. From lithology and structural configuration, carbonate sediments (Jurassic and Cretaceous) and sandstones (Mio-Pliocene) of hills bordering the Utique Domain and the Mabtouha plain (potential aquifer) may contribute to the supply of the aquifer in the upstream part (Fig. 1).

3 Results and Discussion

A total of 60 groundwater samples were collected in the MLVA during December 2015 and analyzed for chemical parameters using standard procedures. The results obtained from the chemical analyses are summarized in Table 1.

3.1 Geochemical Results

The chemical results from the field measurements in the LVM aquifer are summarized in Table 1. All the chemical parameters show very wide ranges and important standard deviations. The Electrical Conductivity (EC) ranged from 1.4 to 29.2 mS/cm (EC seawater = 66.8 mS/cm) and pH values ranged from 6.9 to 8.8 (mean 7.3) indicating slightly acidic to slightly alkaline waters [4]. The TDS variation is

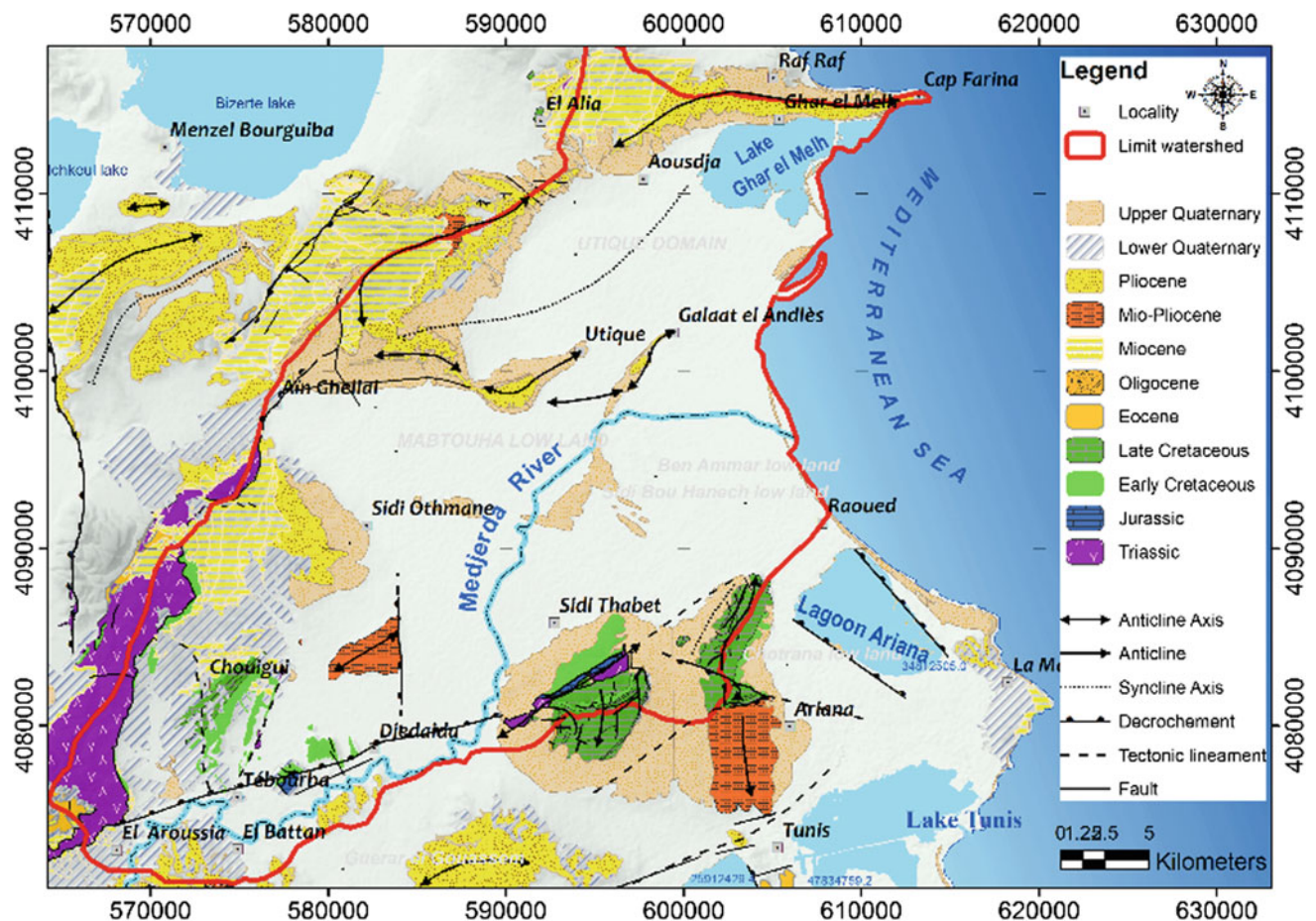


Fig. 1 Geological map of the MLVA

Table 1 The results obtained from the chemical analyses are summarized

Colonne 1	Valid N	Mean	Median	Minimum	Maximum	Variance	Std.Dev.	Coef.Var.
TDS	59	3477.19	2592.00	1005.00	19,254.00	8,583,136.09	2929.70	84.25
Ca ²⁺	59	267.94	220.00	44.00	1610.00	55,999.06	236.64	88.32
Mg ²⁺	59	126.72	93.84	27.36	825.60	13,554.16	116.42	91.88
Na ⁺	59	710.31	480.70	142.60	3698.40	447,150.78	668.69	94.14
K ⁺	59	42.36	12.87	1.95	795.60	11,845.56	108.84	256.95
SO ₄ ²⁻	59	773.20	541.48	90.00	5756.88	758,959.49	871.18	112.67
Cl ⁻	59	1026.67	723.28	255.14	5968.00	940,928.31	970.01	94.48
NO ₃ ⁻	59	73.53	60.25	4.83	596.00	8313.27	91.18	124.00
HCO ₃ ⁻	59	446.13	446.40	1.00	806.00	20,707.52	143.90	32.26
F ⁻	59	4.92	3.84	0.23	52.63	45.83	6.77	137.50
Br ⁻	59	4.59	3.20	0.23	38.50	27.81	5.27	115.01
IS Anhydrite	59	-1.08	-1.04	-2.18	0.14	0.19	0.44	-40.55
IS Aragonite	59	0.35	0.34	-0.43	1.62	0.15	0.39	112.88
IS Calcite	59	0.49	0.48	-0.29	1.77	0.15	0.39	80.07
IS Dolomite	59	1.02	1.04	-0.40	3.84	0.55	0.74	72.68
IS Gypsum	59	-0.86	-0.82	-1.96	0.36	0.19	0.44	-50.84
IS Halite	59	-5.06	-5.12	-6.06	-3.47	0.32	0.57	-11.26

within 1005 mg/l and 19,254 mg/l with a mean value of about 3477.18 mg/l. All of them are classified as brackish ($1000 \text{ mg/l} \leq \text{TDS} \leq 10,000 \text{ mg/l}$) except for the samples 26, 27 and 29 which are saline (near the coast) (Fig. 2).

3.2 Geophysical Results

Vertical Electrical Sounding (VES) surveys were carried out at 100 locations using Schlumberger configurations with $AB/2 \llbracket \rho_a = f(AB/2) \rrbracket$ varying from 1 to 200 m. The interpretation of the vertical electrical soundings (VESs) is a quantitative method for the identification of aquifers. It allows the determination of the distribution of the resistivity of the subsurface at several depths and to know the thicknesses of the saturated zones in order to draw conclusions on the hydrogeology of the region. In this study, we will characterize the potential aquifer deposits based on their physical characteristics. The curves of the electrical soundings perform the evolution of the apparent resistivity as a function of $AB/2$; the interpretation makes it possible to calculate the thicknesses and resistivity of the different layers traversed by the current. These curves will provide not only details of the lithology but also the initial assessment of the quality of the water, and also the porosity and the permeability of the aquifer's formations. The interpretation of the lithological logs of the boreholes as well as the electrical results will highlight the lateral and vertical extension of the Plio-Quaternary deeper aquifer along the study area.

Located in the North of J. Naheli, this borehole reveals the distinction of the following sets: 3 m resistivity soil with $32 \Omega \text{ m}$; 6 m dry clay sands with $25 \Omega \text{ m}$; 43 m of saturated clay sands with $14 \Omega \text{ m}$. This Quaternary horizon is probably an aquifer extending between 9 and 52 m; a conductive soil to marls up to 75 m with low resistivity values $7.5 \Omega \text{ m}$. These marls rest on a layer of up to 100 m containing marly Cretaceous limestones with a resistivity of about $20.5 \Omega \text{ m}$, representing the electric substratum (Fig. 3).

The AB section (Fig. 4) with an N-S direction shows subsurface-resistant anomalies attributed to the dry Pliocene terrain. These anomalies correspond to the Utic fault that affects the subsurface and can be attributed to the marine intrusion extending over the few first meters in the basement. Between the resistance level and the conductivity level, there is the presence of a mean resistivity horizon forming a synclinal basin that can be a source of freshwater.

Towards the South, we display a lateral change of facies and the delimitation of this aquifer horizon by several faults that can indicate their hydrogeological role. In the J. Ammar, we note the presence of another horizon aquifer lain in a carbonate formation attributed to the Cretaceous.

– CD Cross section

The CD section is located according to an E-O direction profile. It highlights the geological faults already observed by the previous geological studies.

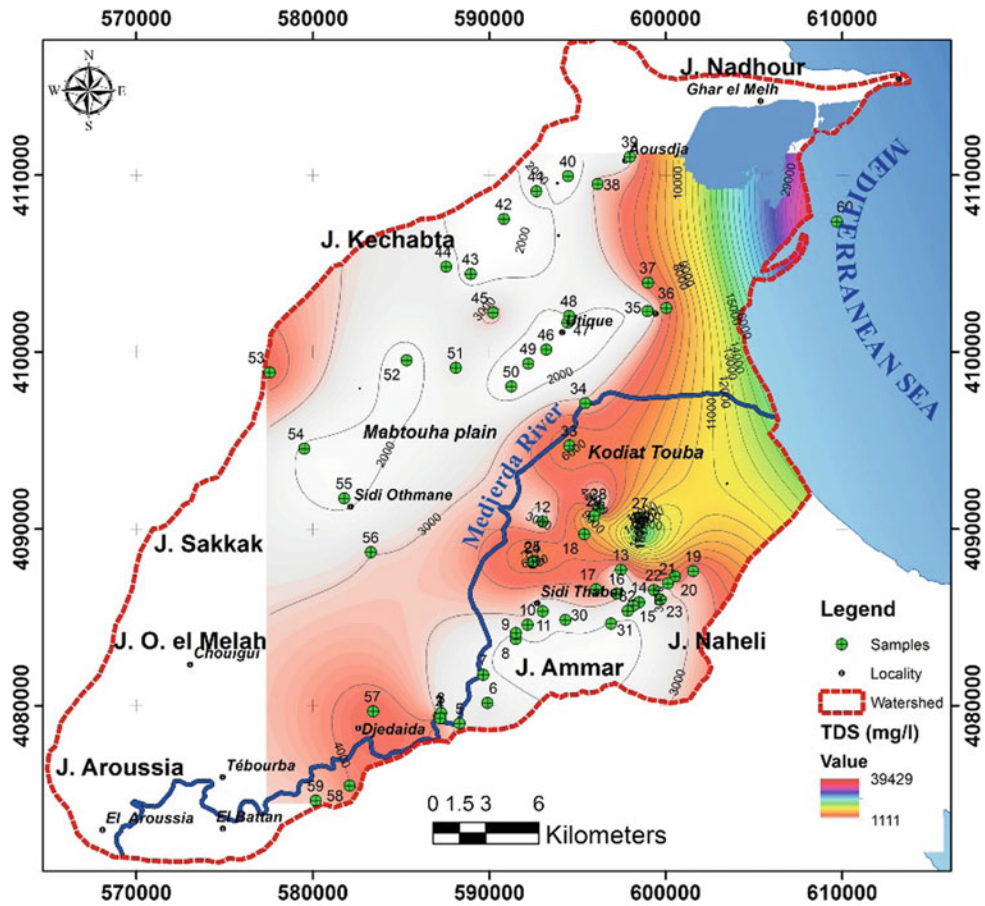


Fig. 2 Map of TDS content (December 2015)

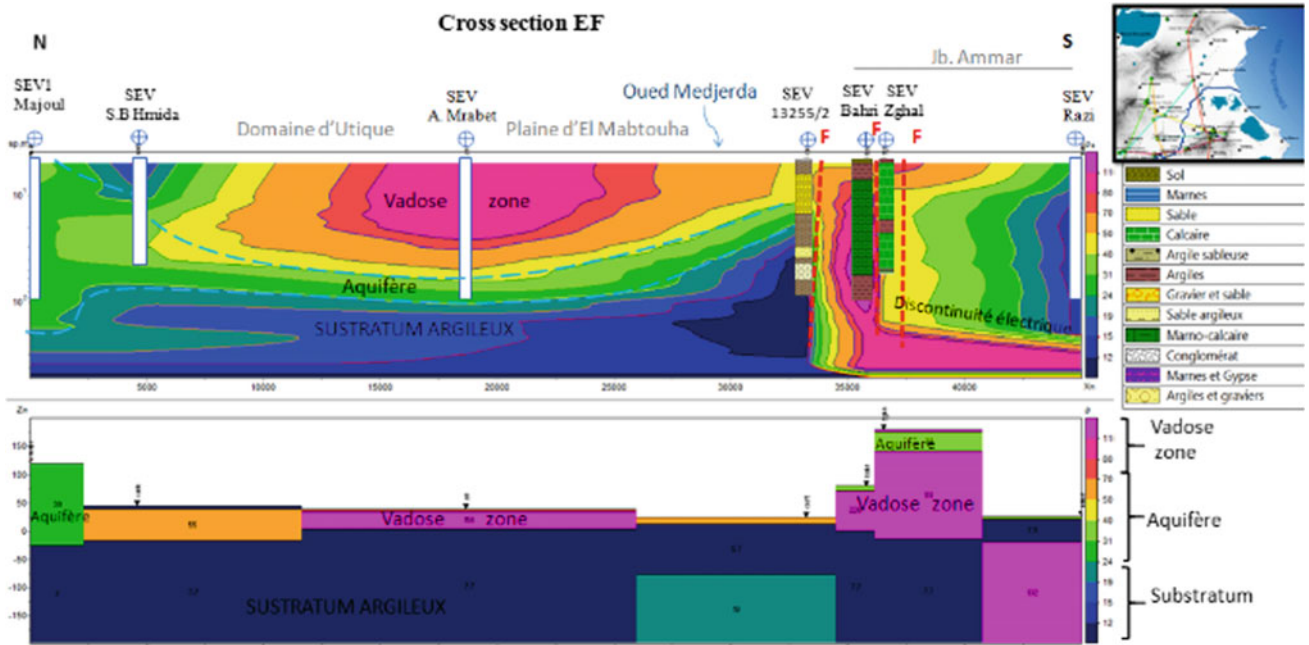


Fig. 3 Pseudo-section AB and localisation of lithological logs

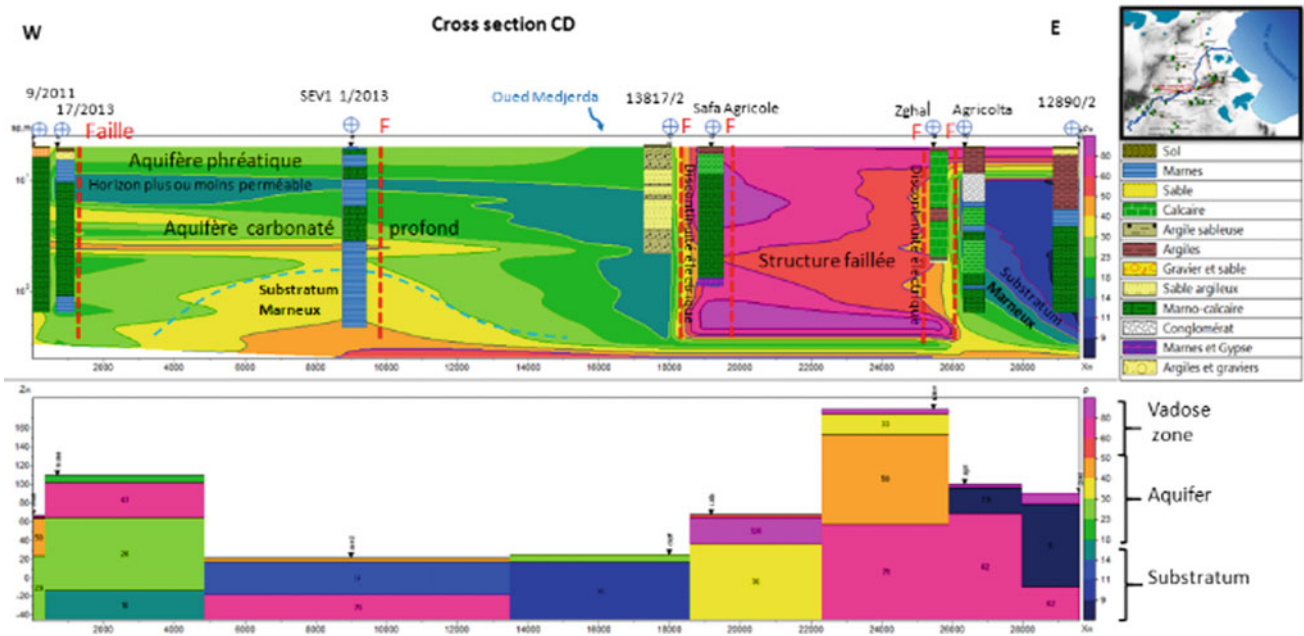


Fig. 4 Pseudo-section CD and localization of lithological logs

Towards the west, the locality of the CD cross section is near the shoreline. The lithology of the shallow aquifer is mainly sandy and sandy-loam with detrital soils attributed to the Quaternary. The deeper discontinuous aquifer's horizons are hosted in carbonate soils attributed to the Cretaceous. They are deposited on a marly impermeable substratum attributed to the lower Cretaceous. These aquifer levels are thicker in the upstream part of the Medjerda River. Laterally, towards the east, (in the region of J. Ammar and J. Naheli), the subsurface is occupied by high resistant anomalies, precisely by electrical discontinuities. The aquifer's horizons are then limited by a faulted subsurface structure.

4 Conclusions

The high total dissolved solids (TDS), chloride, and sodium contents in the study area have induced us to perform the geophysical investigation to characterize elevated salinity areas through the use of several lithological data from boreholes to establish the nature of subsurface geological formations. Based on a combined analysis of geophysical, hydro-chemical and geostatistical data, the present study was performed to help estimate the extent of seawater intrusion. This geophysical study, accomplished by geoelectric methods, allowed the recognition of the geometrical configuration of the subsurface and semi-deep aquifers of the MLV

system. This approach also highlighted the extent of marine intrusion at the eastern shore of the MLV.

References

1. Ammar, B.: Etude de l'environnement de Tunis et de sa région en relation avec l'art de l'ingénieur en génie civil. PhD. Dissertation. Univ. Sci. Tech, Languedoc, 296 (1989)
2. Montety, V.D., Radakovitch, O., Vallet-Coulomb, C., Blavoux, B., Hermitte, D., Valles, V.: Origin of groundwater salinity and hydrogeochemical processes in a confined coastal aquifer, case of the Rhône delta (Southern France). *Appl. Geochem.* **23**, 2337–2349 (2008). <https://doi.org/10.1016/j.apgeochem.2008.03.011>
3. Pulido-Leboeuf, P.: Seawater intrusion and associated processes in a small coastal complex aquifer (Castell de Ferro, Spain). *Appl. Geochem.* **19**, 1517–1527 (2004). <https://doi.org/10.1016/j.apgeochem.2004.02.004>
4. Richter, B.C., Kreitler, C.W.: Identification of Sources of Ground-Water Salinization using Geochemical Techniques. U.S. Environmental Protection (1991). <https://doi.org/10.2113/11.2.107>
5. Samsudin, A.R., Haryono, A., Hamzah, U., Rafek, A.G.: Salinity mapping of coastal groundwater aquifers using hydrogeochemical and geophysical methods: a case study from north Kelantan, Malaysia. *Environ. Geol. J.* 1737–1743 (2008). <https://doi.org/10.1007/s00254-007-1124-9>
6. Zghibi, A., Tarhouni, J., Zouhri, L.: Assessment of seawater intrusion and nitrate contamination on the groundwater quality in the Korba coastal plain of Cap-Bon (North-east of Tunisia). *J. Afr. Earth Sc.* **87**, 1–12 (2013). <https://doi.org/10.1016/j.jafrearsci.2013.07.009>

Assessment of Saline Water Intrusion in Southwest Coastal Aquifer, Bangladesh Using Visual MODFLOW

Tauhid Ur Rahman, Nafiz Ul Ahsan, Arman Habib, and Anjuman Ara

Abstract

Saltwater intrusion through the coastal rivers is threatening the groundwater aquifers of the southwest coast of Bangladesh. This paper comprises the simulation and assessment of groundwater movement and salinity transportation in the southwest coastal aquifer of Bangladesh. A groundwater model was developed, through the porous medium of the aquifer for a range of existing and possible future conditions. This groundwater model was developed by comprising the model setup and flow properties, and by assigning boundary conditions. The development model was accomplished using GIS, Surfer 13 and Visual MODFLOW Flex. After developing the numerical model for a time period of 10 years, the concentration of salinity in groundwater was found to have increased at a very slow rate due to the intrusion of saline water from the river water.

Keywords

Coastal aquifer • Salinity intrusion • Visual MODFLOW • Solute transport

1 Introduction

Access to fresh water in coastal areas is of great importance since any development and evolution activity will largely depend upon the availability of water to meet domestic and agricultural needs and other requirements [1, 2]. The climate-induced stresses on the south-western coast of Bangladesh are immense (Fig. 1). The people living in coastal areas have not only been facing the burden of coastal flooding but they are also at risks of saline water contamination in the fresh water sources. The projected changes in

climate are likely to bring adverse effects on human health, the majority of which will fall disproportionately on poorer populations. With the consequence of climate change, salinity intrusion will gradually extend towards inland water and soil [3].

Tidal flood occurs in Satkhira, Khulna, Bagerhat, Pir-ozpur, Jhalukhati, Barisal, Patuakhali, Chittagong and Cox's Bazar district, covering a total of 65% of the coastal area.

A numerical model was developed showing the dynamics of groundwater in the coastal aquifer of Bangladesh. The model considered the simulation of both groundwater flow and the infiltration of saltwater into the aquifer. The model helped to understand and to assess the salinity intrusion in the coastal aquifer.

2 Materials and Methods

To define the geology of the upper aquifer, data was taken from the bore log of Bangladesh Water Development Board from January 2000 to December 2015. Using this limited data, the geological layer for the model was defined. In the study area, the elevations of the layer are defined as top and bottom of the model layer. In Visual MODFLOW Flex, we used varying layer elevations which were defined from Surface data objects. Surface data objects were imported from Surfer GRID. In this study, four surfaces (from Surfer GRID files) were imported and then utilized to define the layer elevations.

The ground water flow profile was created using Visual MODFLOW-2015 [4–6] and the transportation of salinity contamination using MT3DMS. The developed model covered the entire study area with grid cells sized 40×40 .

The model setup includes identification of the model domain, the river line that would be included in the model, identification of pumping stations, identification of geological layers and their hydraulic properties, identification of boundary conditions, land use and preparation of various hydro-meteorological input data, identification of head

Tauhid UrRahman (✉) · Nafiz UIAhsan · A. Habib · A. Ara
Climate Change Lab, Dept of Civil Engineering, Military Institute of Science and Technology, MIST, Dhaka, 1216, Bangladesh
e-mail: tauhid_cee@yahoo.com

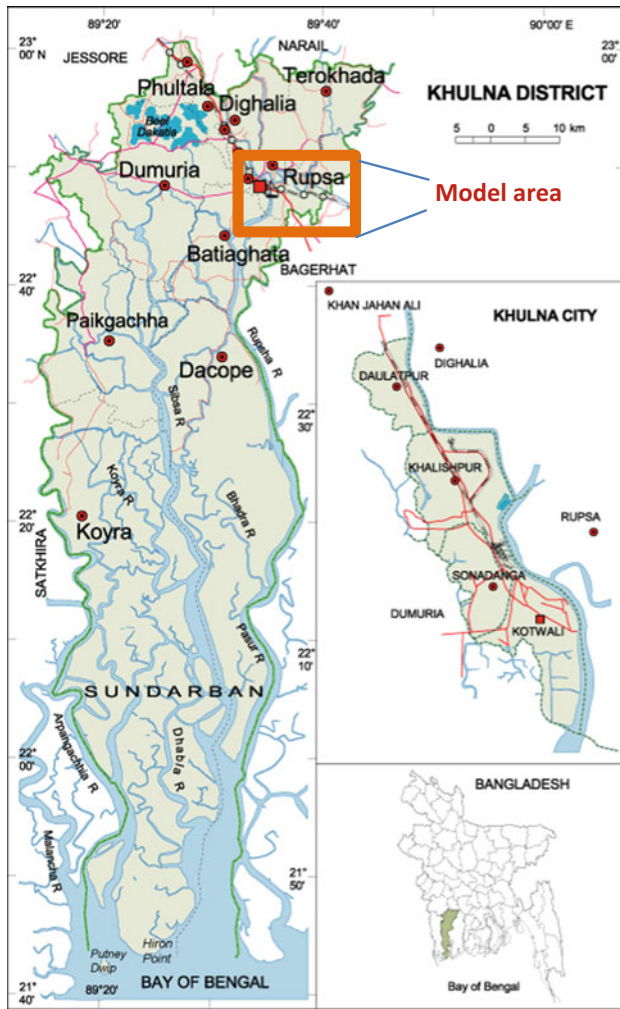


Fig. 1 Location map of Khulna city and its surrounding river, model area and Bangladesh [7]. Source wikimapia.org

observation stations and concentration of observation stations.

All the time steps, including control and computational control parameters for overland flow (OL), unsaturated zone (UZ) and saturated zone (SZ), were used for the entire simulation period. Input data including the value of conductivity, storage, and initial heads property for individual grid cells were considered for running the flow model.

To predict the contamination during transport, input data such as recharge value of salinity into groundwater for each grid cell was considered. For this study, a constant value property zone was used since this is simple and straight forward and can be used for all properties of the model supported by Visual MODFLOW [3]. Model properties were adopted by assembling grid cells sharing the same property

values into “property zones”. Each property zone contains a unique set of property values, and is represented by a different grid cell color. Multiple distinct layers were considered. These layers were separated from each other and indicated different conductivity values ranging between 6 and 8 m/day. The model was assigned by the conductivity in X direction as K_x , and conductivity in Y direction as K_y , with a value of 3.05 and 0.55 m/day, respectively.

3 Results

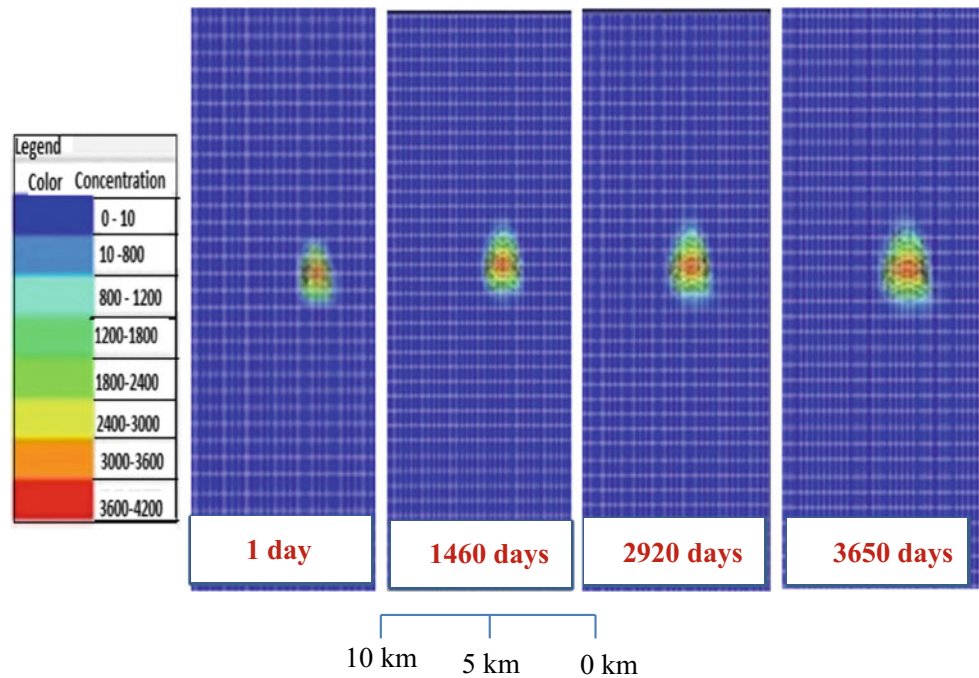
The concentration contours were plotted for the first transport output time (in this case the first transport output time is 1 day). In order to see the concentration results, the time step was increased one by one and the last input time was 3650 days (10 years), and the salinity concentrations of the model output can be observed in Fig. 2. After 1 day, the salinity plume of around 2000 ppm was observed within a smaller portion of the affected aquifer.

With the progress of time, the concentration of surface water salinity increased after 365 days. A salinity of 3000 ppm was observed as comparatively bigger than what was for one day in the earlier case. After 2920 days, the salinity of 3500 ppm was observed as slightly larger than what was observed during 365 days. Finally, after 3650 days, the salinity of 3600 ppm and more was observed for the affected aquifer. Interestingly, the salinity was found to be confined in a particular aquifer which is closer to the Bhairab River of the Khulna district. Other aquifers were not found to be affected as much. This was probably due to the effect of the utilization of limited data set.

4 Discussion and Conclusions

Through this model, the vulnerability of salinity intrusion into groundwater was assessed. After 10 years, salinity contamination was identified as “not very significant”, but we should be careful enough to prevent future saltwater intrusion into the aquifers. As groundwater is one of the main sources of drinking water, steps need to be taken in order to stop this vulnerability. To alleviate the harmful effect of salinity intrusion, groundwater recharge will have to be increased at a higher level and obstacles that impede the infiltration of rain water will have to be reduced. However, this study suggested that, in the future, there may be a potential risk of salinity intrusion in the coastal aquifers.

Fig. 2 Model simulation showing the salinity intrusion after 1 day, 1460 days, 2920 days and 3650 days



References

1. Ajami, H., Meixner, T., Maddock, T., Hogan, J.F.: Impact of land-surface elevation and riparian evapotranspiration seasonality on groundwater budget in MODFLOW models. *Hydrogeol. J.* **19**, 1181–1188 (2011)
2. Zamri, W., Ismail, Y., Bahaa-eldin, E.A.R.: Simulation of horizontal well performance using Visual MODFLOW. *Environ Earth Sci.* **68**, 1119–1126 (2013)
3. Shi, W., Zeng, W., Chen, B.: Application of visual MODFLOW to assess the sewage plant accident pool leakage impact on groundwater in the Guanting reservoir area of Beijing. *Front Earth Sci. China* **4**(3), 320–325 (2010)
4. Khadri S.F.R., Pande C.P.: Ground water flow modeling for calibrating steady state using MODFLOW software: a case study of Mahesh River basin, India. *Earth Syst. Environ.* **2**(39), (2016)
5. Haque, M. Al Mamunul, Jahan C. S., Mazumder Q. H., Nawaz S. M. S, Mirdha G. C., Mamud P. And Adham M. I.: Hydrogeological condition and assessment of groundwater resource using visual modflow modeling, Rajshahi City aquifer, Bangladesh. *J. Geol. Soc. India* **79**, 77–84 (2012)
6. Dowlatabadi S. Zomorodian S.M.A.: Conjunctive simulation of surface water and groundwater using SWAT and MODFLOW in Firoozabad watershed. *KSCE J. Civil Eng.* **20**(1), 485–496 (2016)
7. Khulna city Geology Map: www.wikimapia.org. Accessed 11 June 2018

Quality of Groundwater and Seawater Intrusion Along Northern Chennai Metropolitan City (India)

Sithu G. D. Sridhar and Muthusamy Balasubramanian

Abstract

Fifty-five groundwater samples were collected during each monsoon season representing the pre-monsoon and post monsoon seasons for four consecutive years from 2014 to 2018 to assess the groundwater quality. As the study area represents a coastal aquifer, seawater intrusion studies were also carried out in the northern region of Chennai Metropolitan City, Tamil Nadu, India. They were analyzed to establish the physical and chemical characteristics, such as pH, EC, TDS, Ca^+ , Mg^+ , Na^+ , K^+ , Cl^- , HCO_3^- , SO_4 and NO_3 . Chennai Metro city experienced more than 40 cm of rainfall within two days due to a cloudburst during December 2015 and its effect is being reported.

Keywords

Chennai metropolitan city • Coastal aquifer • Physico-chemical characteristics • Quality of groundwater and seawater intrusion

1 Introduction

The quality of groundwater in coastal regions is generally affected by natural processes such as saline water intrusion, evaporation and interaction of groundwater with hard rock formations [1]. The study area covers the northern region of Chennai Metropolitan City, which has a coastal aquifer constituted mainly of alluvium and basement rock Charnockite. The region extends from Ennore to Santhome, from north to south, and comes under the Thiruvallur district of Tamil Nadu. To the east is Bay of Bengal and to the west is part of Chennai Metropolitan City where the thickly populated residential areas are common. It covers an area of

S. G. D. Sridhar (✉) · M. Balasubramanian
Department of Applied Geology, University of Madras,
Chennai, India
e-mail: sgd_sri@yahoo.co.in

250 km² that falls between 13° 4'N and 13° 12'N latitude and from 80° 16'E to 80° 24'E" longitude, as shown in Fig. 1, where sample locations are indicated within the river and water ways.

2 Materials and Methods

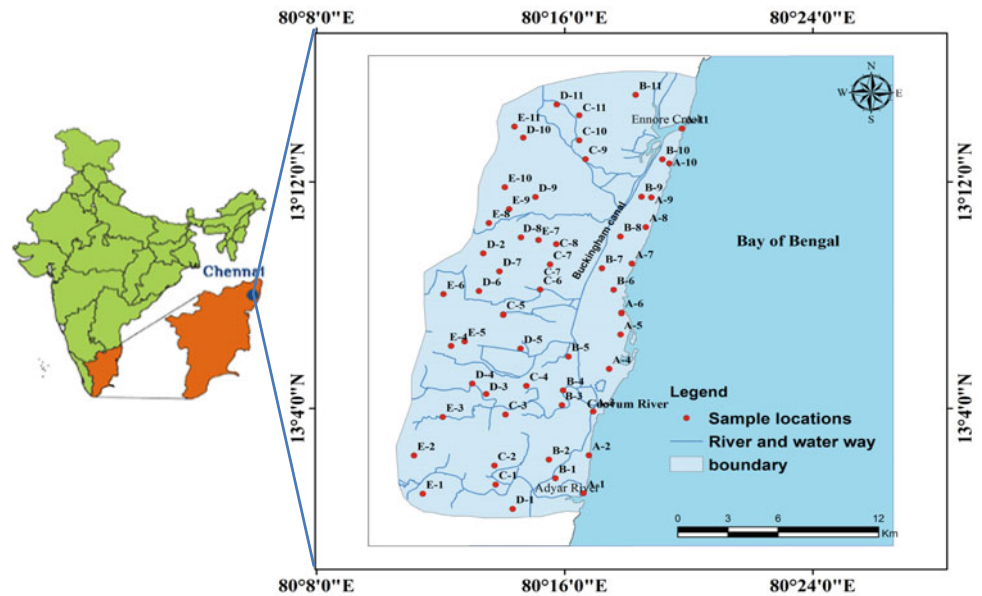
One liter of water sample was collected at 55 locations in polyethylene bottles from various bore wells and dug wells from the same aquifer. The pH, temperature, electrical conductance (EC), and total dissolved solids (TDSs) were measured in situ using a portable kit. Major cations like calcium, magnesium, potassium and sodium, and major anions like sulphate, nitrate and chloride were analyzed by Ion Chromatography in the laboratory. Bicarbonate were analyzed by the titration method. The analytical procedures followed are as per the American Public Health Association [2]. The base map of the study area was prepared using the Survey of India toposheets 66 D/1 and 66 D/5 and was digitized using surfer 9.0 software.

3 Results and Discussion

3.1 Physico-Chemical Parameters

The minimum, maximum and average values for different parameters of the eight seasons are presented in Table 1. From the table, it is evident that the groundwater has been alkaline in nature for the past four years, irrespective the seasons. TDS decreases during post-monsoon compared to the pre-monsoon season during the reported number of years. TH decreases during post-monsoon compared to pre-monsoon season, except for the post-monsoon season of January 2016; and the same trend can be seen for Ca, Mg, Na, K, and SO_4 . The cloud burst, that brought more than 40 cm of precipitation within 48 h during December 2015, is attributed to the increase in the concentration of these

Fig. 1 Study area with sample locations



parameters during January 2016. There is no significant variation in HCO_3^- and NO_3^- during the reported 4 years.

The permissible limit of pH for drinking purposes is from 6.5 to 8.5 [3]. pH is considered as an indicator of overall productivity that causes habitat diversity [4]. In the study area, high conductivity [3] was observed in most of the groundwater samples and this may be attributed to high sodium and chloride content in groundwater as the study area is a coastal plain, where saline water mixes with fresh water in terms of seawater intrusion. In the northeastern part of the study area, the higher values [3] of TDS are due to seawater intrusion from the nearby coastal area and the influence of brackish water of Buckingham canal that parallels the coast. Due to the heavy rainfall during December 2015 (cloud burst), most of the locations had recharging from rainwater such that the TDS lowers during post-monsoon (January 2016). Due to the official constraints, Uranium in groundwater samples is analyzed during the pre-monsoon season of the year 2017 and post-monsoon season of the year 2018. The uranium concentration in the study area ranges from 0.6 to 68 ppb with an average of 10 ppb during the pre-monsoon season and it varies in post monsoon from 0.14 to 108 ppb with an average of 14 ppb. Only at one location, the U concentration is more than the permissible limit of 60 ppb prescribed by Atomic Energy Regulation Board of India during both pre- and post-monsoon seasons and it is attributed to the waste disposal of the shipping yard.

3.2 Chadha's Plot

The diagram proposed by Chadha [5] has been used in this study to interpret the hydrogeochemical processes occurring in the study area. The same procedure was successfully applied [6] along coastal aquifers to determine the evolution of two different hydrogeochemical processes. The cations are converted into their milli-equivalent percentages between alkaline earths ($\text{Ca}^{2+} + \text{Mg}^{2+}$) and alkali metals ($\text{Na}^+ + \text{K}^+$) and are plotted on the X axis and the anions are converted into the milli-equivalent percentages between weak acid ($\text{CO}_3 + \text{HCO}_3^-$) and strong acid ($\text{Cl}^- + \text{SO}_4^{2-}$) and are plotted on the Y axis. The hydrochemical processes suggested [5] are indicated in each of the four quadrants of the graph.

- The majority of about 54% (June 2014), 10% (June 2015), 31% (June 2016) and 36% (June 2017) of the groundwater samples of the study area fall in (Ca–Mg–Cl) type reverse ion-exchange waters during pre-monsoon season. About 46% (June 2014), 90% (June 2015), 70% (June 2016) and 58% (June 2017) of the samples fall in the (Na–Cl) type end members waters (sea water) during pre-monsoon, respectively.
- The majority of about 52% (January 2015), 54% (January 2016) and 12% (January 2018) of the groundwater samples of the study area fall in (Ca–Mg–Cl) type reverse ion-exchange waters during the post-monsoon

Table 1 Minimum and maximum of the physico-chemical parameters

	pH	EC ($\mu\text{S/cm}$)	(mg/l)										U (ppb)	
			TDS	TH	Ca	Mg	Na	K	HCO ₃	Cl	SO ₄	NO ₃		
<i>Pre-monsoon June 2014</i>														
Min	6.6	664	425	130	34	11	49	6	160	77	10	4	–	
Max	8.2	34,700	21,514	9508	2540	768	3850	135	560	11,050	134	44	–	
Avg	7.1	3679	2318	893	253	63	422	25	328	957	47	23	–	
<i>Post monsoon January 2015</i>														–
Min	6.7	822	526	225	22	15	55	2	110	120	4	4	–	
Max	8.0	15,660	9709	3761	960	331	1700	192	732	5194	223	81	–	
Avg	7.6	2680	1697	591	140	58	294	36	387	655	39	22	–	
<i>Pre-monsoon June 2015</i>														–
Min	6.5	546	349	90	12	7	55	8	67	102	14	12	–	
Max	8.2	19,562	12,520	4139	1080	350	2778	138	653	7229	122	130	–	
Avg	7.1	2717	1739	401	84	46	383	26	240	711	41	28	–	
<i>Post monsoon January 2016</i>														–
Min	6.5	396	253	82	13	12	46	2	85	98	30	0	–	
Max	8.2	8200	5248	2139	423	298	1422	128	580	2688	563	193	–	
Avg	7.2	2276	1457	614	121	76	327	25	304	546	182	66	–	
<i>Pre-monsoon June 2016</i>														–
Min	7.1	625	400	108	12	19	112	17	42	98	50	10	–	
Max	8.2	10,313	6600	2714	460	380	1368	118	640	2170	541	238	–	
Avg	7.8	2503	1602	652	127	82	375	44	346	492	219	58	–	
<i>Post monsoon January 2017</i>														–
Min	7.0	684	438	119	24	10	78	6	122	88	22	15	–	
Max	8.1	10,391	6650	391	100	54	658	95	750	986	487	133	–	
Avg	7.5	2151	1376	209	46	23	288	29	384	321	83	53	–	
<i>Pre-monsoon June 2017</i>														–
Min	6.4	1017	651	56	16	4	16	5	110	54	52	8	0.6	
Max	8.5	6434	4118	1205	321	143	1021	91	576	1987	929	321	68.61	
Avg	7.5	2815	1802	586	137	60	359	29	350	464	366	55	10.04	
<i>Post monsoon January 2018</i>														–
Min	7.1	923	591	161	29	13	57	6	160	88	13	6	< DL	
Max	8.8	3877	2481	1175	258	129	694	66	767	875	331	150	108	
Avg	7.8	2072	1326	370	87	37	290	22	399	362	96	43	7	

season. About 48% (January 2015), 46% (January 2016), 29% (January 2017) and 54% (January 2018) of the samples fall in the (Na–Cl) type end members waters (sea water) during the post-monsoon season, respectively. 20% (January 2017) and 9% (January 2018) of the samples fall in the (Na–HCO₃) type. 5% (January 2018) of the samples fall in the recharge water zone.

It is explained that Field 1 indicates recharging water, Field 2 indicates reverse ion-exchange waters, Field 3

indicates Na⁺–Cl[–] waters, and Field 4 Na⁺–HCO₃ waters (Fig. 2).

3.3 Na⁺/Cl[–] Molar Ratio

Sea water intrusion has been evaluated by studying a series of ionic ratios, specifically the Na/Cl molar ratio [7]. Conservative seawater–fresh water mixing is expected to show a linear increase in Na and Cl [7]. Groundwater ratio values are below the seawater ratio of 0.86, which indicates that

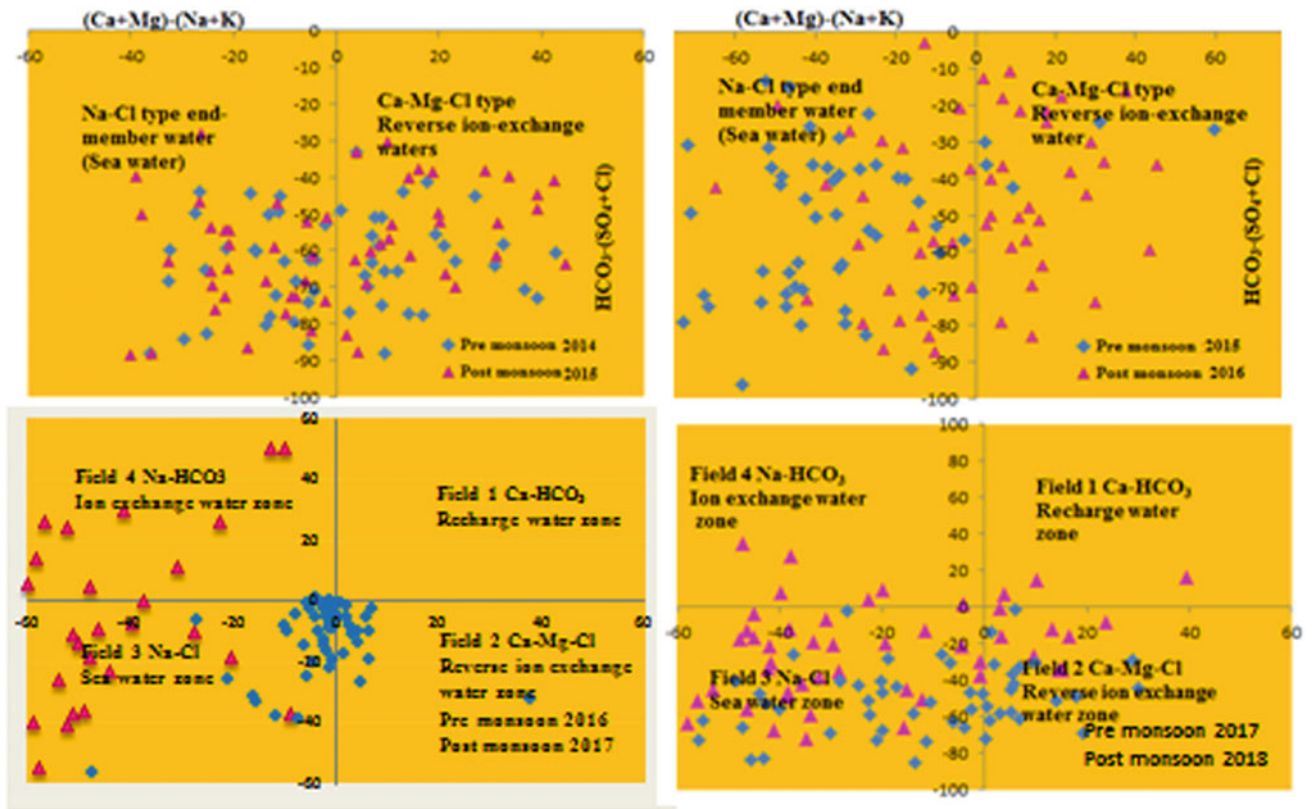


Fig. 2 Chadha's plot

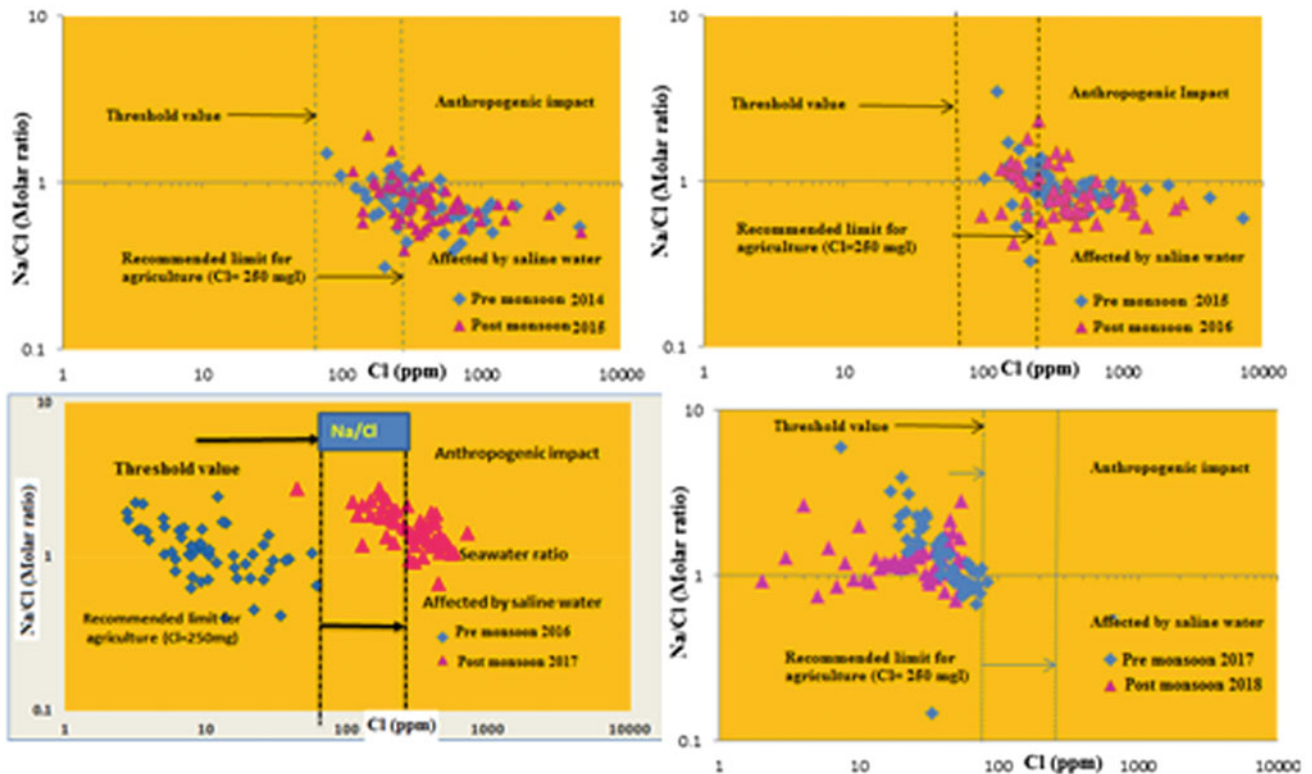


Fig. 3 Na^+/Cl^- molar ratio

fresh groundwater was contaminated with saline waters. The threshold value of Cl^- concentration is 63 mg/l. Moles ratios of Na^+/Cl^- versus Cl^- concentrations indicate that groundwater ratio values fall close to the seawater ratio (0.86) which indicates that the fresh groundwater was contaminated with saline waters.

For the study area, the Na^+/Cl^- molar ratio ranges from 0.3 to 1.5 during June 2014; from 0.39 to 1.94 during January 2015; from 0.33 to 3.5 during June 2015; from 0.41 to 2.35 during January 2016; from 0.4 to 2.4 during June 2016; from 0.6 to 2.7 during January 2017; from 0.14 to 6.02 during June 2017; and from 0.7 to 2.8 during January 2018. The Na/Cl ratio indicates that most of the groundwater is being affected by seawater intrusion due to the over-exploitation of groundwater during pre-monsoon season and a few samples show recharge from precipitation during post monsoon seasons in the study area. Maximum values close to the seawater ratio indicate recent simple mixing of groundwater with seawater. Very high Na/Cl ratios may be indicative of anthropogenic contamination, like fertilizers [8], as shown in Fig. 3.

4 Conclusions

The groundwater of the study area is alkaline in nature. TDS decreases during the post-monsoon season compared to pre-monsoon season during the reported number of years. TH decreases during post-monsoon compared to pre-monsoon season, except for the post-monsoon season of January 2016, and the same trend can be seen for Ca, Mg, Na, K, and SO_4 . The cloud burst that brought more than 40 cm of precipitation within 48 h during December 2015 is being attributed to the increase in concentration of these parameters during January 2016. There is no significant variation in HCO_3^- and NO_3^- during the reported 4 years. Only at one location, the U concentration is more than the permissible limit of 60 ppb prescribed by the Atomic Energy

Regulation Board of India during both pre- and post-monsoon seasons and it is attributed to the waste disposal of the shipping yard. According to Chadha's plot, Field 3 ($\text{Na}^+ - \text{Cl}^-$) waters are typical of seawater mixing and are mostly constrained to the coastal areas that are attributed to over-exploitation of groundwater due to urbanization, with a thickly populated field area. The Na/Cl ratio indicates that most of the groundwater is being affected by seawater intrusion due to an over exploitation of groundwater during the pre-monsoon season and a few samples show recharge from precipitation during post-monsoon seasons in the study area.

References

1. Srinivasamoorthy, K., Vasanthavigar, M., Chidambaram, S., Anandhan, P., Sharma V.S.: Characterization of groundwater chemistry in an eastern coastal area of Cuddalore District, Tamilnadu. *J. Geol. Soc. Ind.* **08**, 549–558 (2011)
2. APHA: American Public Health Association: Standard Methods for the Examination of Water and Wastewater, 19th edn. Washington, DC (1998)
3. BIS: Bureau of Indian Standards: Specifications for Drinking Water, New Delhi (2012)
4. Minns, C.: Factors affecting fish species richness in Ontario lakes. *Trans. Am. Fish. Soc.* **76**, 332–333 (1989)
5. Chadha, D.K.: A proposed new diagram for geochemical classification of natural waters and interpretation of chemical data. *Hydrogeol. J.* **7**(5), 431–439 (1999)
6. Vandenbohede, A., Lebbe, L., Adams, R., Cosyns, E., Durinck, P.A.U.L., Zwaenepoel, A.: Hydrogeological study for improved nature restoration in dune-Kleyne Vlakte case study, Belgium. *J. Environ. Mang.* **91**(11), 2385–2395 (2010)
7. Vengosh, A., Gill, J., Davisson, M.L., Hudson, B.: A multi-isotope (B, Sr, O, H and C) and age dating (^3He and ^{14}C) study of groundwater from Salinas valley, 3-H-California: hydrochemistry, dynamics and contamination processes. *Water Resour. Res.* **38**, 9–17 (2002)
8. Jones, B.F., Vengosh, A., Rosenthal, E., Yechieli, Y.: Geochemical investigations of Seawater intrusion in coastal aquifers—concepts, methods and practices, pp. 51–71. Springer, The Netherlands (1999)

Tracing the Evolution of Hypersaline Coastal Groundwaters in Kuwait: An Integrated Approach

Chidambaram Sabarathinam, Harish Bhandary, and Asim Al Khalid

Abstract

Hypersaline (HS) coastal groundwaters along the Kuwaiti shoreline were identified by collecting samples along the Kuwait Bay and along the open sea coast. Out of the 28 collected samples, 9 samples were considered as hypersaline considering the salinity of the Kuwaiti sea water. They were mostly of Na–Cl facies and the ratios of the different elements to Cl were studied to determine their source and nature. Few HS samples were acidic, and it was observed that these samples have representation of sulfides. The PHREEQC model reveals that the pO_2 values in the acidic samples were lesser. The mole values of $CaSO_4$ and the saturation states of Anhydrite and Gypsum were higher in these samples. The model was also attempted for temperature variations and it showed variations in pH, Ionic Strength and Saturation states. The statistical analysis of these HS waters reveals that the impact of desalination rejects, waste water and urban sewage, variation in water level of the aquifers and occurrence of H_2S gas governs the hypersaline nature of the groundwaters along the coast.

Keywords

Ion ratios • Geochemical modeling • Acidic pH • Statistical analysis

1 Introduction

Hypersaline (HS) groundwater in the MENA region is reported in Nile delta aquifer [1], Iran [2], Israel [3], Kuwait [4] and in the Dead sea aquifer [5]. Reports have also identified the acidic nature of hypersaline groundwaters in the Dead sea aquifer. This was also inferred to be a function

of H_2S oxidation in relation to pH, temperature and ionic strength. The occurrence of H_2S in the groundwaters of Kuwait City has also been reported. But this paper tries to address the HS evolution using PHREEQC modeling and statistical techniques apart from ion ratios. It also tries to understand the acidic HS waters and their variation with respect to change in temperature.

2 Study Area and Methodology

The study area lies between $47^\circ 40' 8.47''$ to $48^\circ 44' 5.584''$ E and $28^\circ 32' 11.590''$ to $29^\circ 45' 18.493''$ N, with a coast line length of 500 km including all islands. The shoreline of Kuwait extends for about 195 km including 40 km of bay. The average annual rainfall is about 110 mm/year and the evaporation is 3000 mm/year. There are two major groups of aquifers: the Kuwait group and the Hasa group. In these groups, Dibdibbah and the Ghar formation of the Kuwait group, along with Dammam formation of the Hasa group, form potential aquifers. Despite the local presence of clay lenses that may act as aquitards and the variation in the degree of karstification within the Dammam formation, which affects the vertical hydraulic conductivity, the two aquifers are hydraulically connected. Jahra, Riqqa, Um-Al-Haiman & Sulaibya are the four main municipal wastewater treatment plants, and it is reported that Kuwait generates about 600,000 m^3/d of wastewater. The highest volume is discharged in Doha, followed by Az-Zour and then Sabiya.

Twenty-eight groundwater samples were collected along the coast from wells of 20 m in depth from the northeastern part to the southern boundary of Kuwait along the coast line. The collected groundwater samples were filtered and analyzed for EC and pH by electrodes, TDS by evaporation method, major cations and anions (Na, K, Ca, Mg, Cl, SO_4 , NO_3 , Br, PO_4) using ion chromatograph, sulphide by titration and trace metals were analyzed using Agilent ICP-OES following the USPE. These laboratory analyses were carried out in the WRC laboratory of KISR (ISO 9001:2008

C. Sabarathinam (✉) · H. Bhandary · A. A. Khalid
WRC, Kuwait Institute for Scientific Research, Safat, Kuwait
e-mail: csabarathinam@kisir.edu.kw

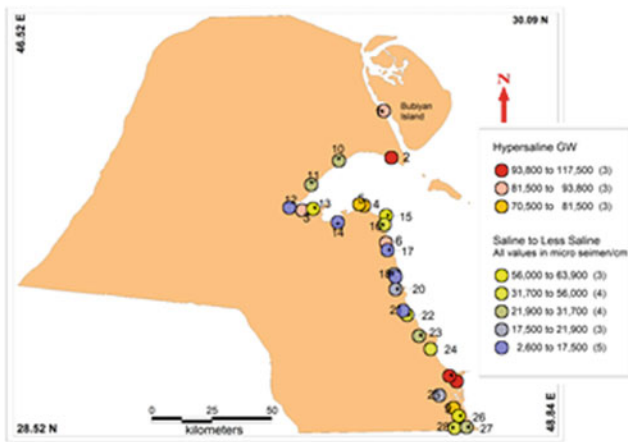


Fig. 1 Sampling location along with their EC values ranges of both HS and SLS samples

certified) and standard methods have been adopted to analyze the water quality parameters in the laboratory.

3 Results and Discussion

The samples showed that EC ranged from 117,500 to 2650 $\mu\text{S}/\text{cm}$ (Fig. 1), the sea water of the region was reported to be at a range of 62,500–65,000 $\mu\text{S}/\text{cm}$, the

highest values were reported in the samples collected from Kuwait bay. Considering the EC of the sea water, 9 samples above 70,000 $\mu\text{S}/\text{cm}$ were considered as hypersaline (HS) for the study. The samples number 1–9 are hypersaline and the rest are considered as saline to less saline (SLS). Comparing the average values of the samples (Table 1), NO_3 , PO_4 and Mn are higher in the SLS samples. The Piper facies show that the SLS samples are Na–Ca–Cl type and HS samples are Na–Cl type. It is interesting to note that few samples of the HS category have acidic pH (samples number 4, 5, 6 and 7).

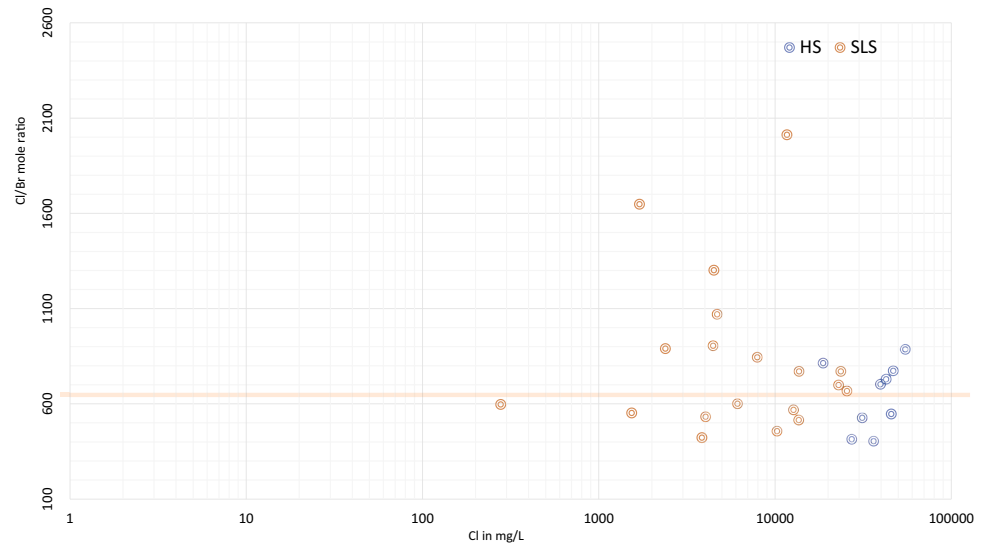
Cl/Br shows that there is representation of three groups of HS samples, less than sea water composition (sample 9), close to sea water composition, and higher than sea water composition (Considered as HS). Furthermore, there are groups in HS samples category representing desalination sites (1, 2, 3 and 8), high bromides (4, 5, 6 and 7) affected by H_2S and a lower Cl/Br value than sea water. It is interesting to note that groundwater near the desalination plants is represented by similar ratios of Cl/Br, without much variation (Fig. 2).

The Saturation Index (SI) of the sulfate minerals like Anhydrite and Gypsum, showed an increase in SI values with respect to Cl values, in general, and that of Carbonate minerals (Calcite Aragonite, Dolomite and Magnesite) was inferred to be governed by pCO_2 values. The SI values of

Table 1 Maximum, Minimum, Average and Stdev of HS and SLS samples, All values are in mg/L except EC in $\mu\text{S}/\text{cm}$, Rn in pci and pH

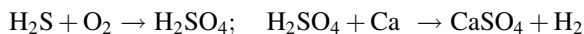
	Hypersaline				Saline to less Saline			
	Max	Min	Avg	Stdev	Max	Min	Average	Stdev
EC	117,500.00	70,500.00	86,455.56	15,419.96	63,900.00	2650.00	27,934.74	17,572.85
pH	7.34	6.30	6.93	0.35	7.96	6.81	7.28	0.32
TDS	98,692.00	50,266.00	65,828.44	15,768.40	45,112.00	1649.00	19,284.63	12,437.27
HCO_3	240.00	38.80	124.12	56.97	203.00	58.10	117.39	39.52
Na	24,595.00	10,836.00	19,436.67	5266.32	13,703.00	449.00	5073.21	4122.06
K	1147.00	366.00	688.33	267.63	618.00	11.00	173.32	171.11
Ca	3836.00	990.00	2119.11	932.60	1909.00	72.00	935.00	503.15
Mg	2845.00	1097.00	2037.11	745.21	1673.00	78.74	643.20	480.31
SO_4	5854.00	2207.00	4043.11	1586.67	3837.00	623.19	2622.12	1002.97
Cl	54,813.00	18,764.00	38,148.78	11,060.32	25,604.00	278.00	9252.79	7814.10
Br	202.40	51.97	140.02	42.32	86.47	1.05	30.01	27.04
PO_4	0.58	0.03	0.13	0.21	0.96	0.03	0.23	0.26
NO_3	85.00	19.22	63.56	25.74	709.93	8.36	126.05	159.21
S^2	16.00	<0.1	8.60		<0.1	<0.1	<0.1	
Fe	0.39	0.00	0.08	0.12	0.12	0.00	0.03	0.04
B	8.06	2.91	5.03	1.69	3.87	1.22	2.14	0.72
Li	1.13	0.10	0.47	0.36	0.90	0.03	0.30	0.26
Mn	0.52	0.00	0.11	0.16	2.72	0.00	0.19	0.62
Sr	26.59	7.28	13.88	5.74	19.30	1.26	7.47	4.34
Va	0.11	0.00	0.04	0.03	0.11	0.01	0.03	0.03
Rn	211.00	0.00	51.48	63.48	146.00	0.00	46.08	49.21

Fig. 2 Inferences from Cl/Br mole ratios of both HS and SLS samples with Cl in mg/L



Halite increase with the increase in Cl values as it has a direct relation with the composition of Halite. Furthermore, it was inferred that the SI of Halite was undersaturated even at the highest Cl value (54,813 mg/L). It was observed that the HS samples 4, 5, 6 and 7 were acidic to near neutral despite higher EC values, indicating the available free H⁺ ion in these samples which resulted in the reduction of pH. These samples also showed the representation sulfide in analysis. Later, the H⁺ and OH⁻ ion concentration in moles for the HS samples were calculated by PHREEQC interactive (using Phreeqc database) and later the moles of CaOH⁺, Fe(OH)₂⁺, Fe(OH)₃, Fe(OH)₄⁻, KOH, LiOH, MgOH⁺, MnOH⁺, NaOH, SrOH⁺, Fe₂(OH)₂⁴⁺ and Fe₃(OH)₄⁵⁺ were calculated. The results showed that in all the acidic samples, the sum of these listed hydroxides was observed to be lesser. It was inferred that the CaSO₄ had higher values in the acidic samples (Fig. 3).

This is due to the fact that affinity of Sulfate to Ca²⁺ is higher than that of Carbonates. The comparison of the Sulfate Saturation states of HS samples with that of pH shows that, at lesser pH, the Saturation states of the acidic HS samples are higher than other HS samples and vice versa in the carbonate minerals. It was also confirmed with the fact that, at lower pO₂ values, acidic HS samples show higher mole CaSO₄ values and an acidic nature.



These samples also show that the Ca values are higher than the Mg values, indicating that Sea water incursion is not the major governing factor. The temperature variation in time step for the HS samples was attempted by PHREEQC model to know its impact on the chemical composition of the groundwater samples. It was inferred that there is a

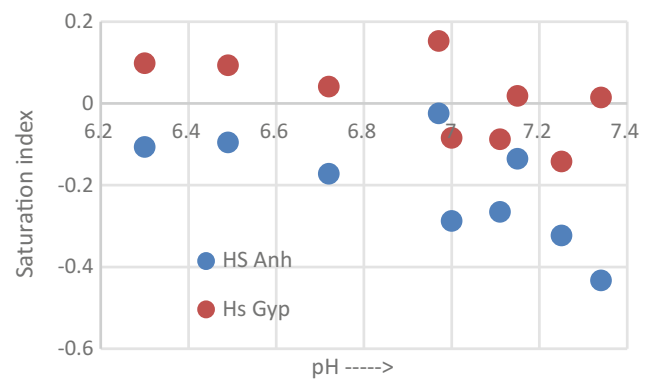


Fig. 3 Saturation index of sulfate minerals in HS samples

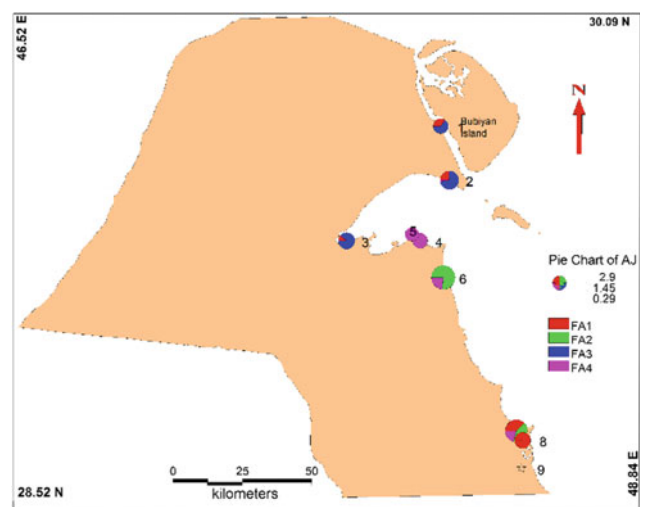


Fig. 4 Factor Score representation with respect to samples of HS

significant variation in the ionic strength and the pH of the samples with the increase in temperature.

The PCA analysis of the HS samples shows that four factors were extracted from the data set with 91% of TDV (FA1-39.6%; FA2-27.7%; FA3-13.39% and FA4-10.3%). The association of elements of the first factor indicates the impact of desalination rejects. The second factor is governed by waste water and urban sewage at samples 6 and 7 (Fig. 4). The third factor is governed by the variation in the water level of the aquifers, resulting in the release of V into the environment and this is observed in the samples around the bay 1, 2 and 3. The last factor was identified as the influence of H₂S gas in the locations 4, 5, 6 and 7. The PCA analysis shows that 3 factors are represented in samples 2 and 7 and that no significant factors act in location 9.

4 Conclusions

The HS groundwater contains lesser NO₃, PO₄ and Mn than SLS water. They are chiefly governed by the proximity to desalination plants, domestic sewage and the oxidation of H₂S. It is also inferred that multiple processes may also act at the sample location to increase the salinity as observed in samples 2 and 7. But the major source of hypersaline water is attributed to desalination rejects. Furthermore, the acidic nature of the HS water was inferred to be due to the

oxidation of H₂S and the combination of the released sulfate with Ca²⁺. This results in the increase of H⁺ in water and reduces the pH but increases the mole concentration of CaSO₄ as well as the saturation states of sulfate minerals in these waters. The modeling attempted by the batch reactions varying the temperatures has revealed significant changes in pH and ionic strength of the groundwaters.

References

1. van Engelen, J., Oude Essink, G.H., Kooi, H., Bierkens, M.F.: On the origins of hypersaline groundwater in the Nile Delta Aquifer. *J. Hydrol.* **560**, 301–317 (2017)
2. Mehr, S.S., Moghaddam, A.A., Field, M.S.: Hydrogeological and geochemical evidence for the origin of brackish groundwater in the Shabestar plain aquifer, northwest Iran. *Sustain. Water Resour. Manag.* 1–24 (2017) <https://doi.org/10.1007/s40899-017-0192-6>
3. Vengosh, A., Spivack, A.J., Artzi, Y., Ayalon, A.: Geochemical and boron, strontium, and oxygen isotopic constraints on the origin of the salinity in groundwater from the Mediterranean coast of Israel. *Water Resour. Res.* **35**(6), 1877–1894 (1999)
4. Bhandary, H., Sabarathinam, C., Al-Khalid, A.: Occurrence of hypersaline groundwater along the coastal aquifers of Kuwait. *Desalination* **436**, 15–27 (2018)
5. Avrahamov, N., Antler, G., Yechieli, Y., Gavrieli, I., Joye, S.B., Saxton, M., Sivan, O.: Anaerobic oxidation of methane by sulfate in hypersaline groundwater of the Dead Sea aquifer. *Geobiology* **12**(6), 511–528 (2014)

Contribution of Hydrochemical and Geoelectrical (ERT and VES) Approaches to Investigate Salinization Process of Phreatic Aquifer and Climate Change Adaptation Strategy in Arid Area: Example of Garaat Douza and Its Proximities (Mediterranean Basin)

Elhem Moussaoui, Abdelkader Mhamdi, Mouez Gouasmia, Ferid Dhahri, and Mohamed Soussi

Abstract

The geophysical, hydrogeochemical and climatological investigations of the plio-quadernary aquifer, in Garaat Douza (Moulares-Redayef Mining Basin, Southwestern Tunisia), enabled us to identify the origin and the extension of salinization in time and space. Thus, the hydrogeological study has revealed a piezometric draw-down, showing the insufficiency of the natural recharge of the aquifer due to the low rainfall events and the increasing use of groundwater. The hydrochemical study has shown that the high salinities are recorded at the level of Garaat Douza (outlet of the aquifer). The geophysical study (ERT and VES) has revealed that the surveyed area is characterized by the presence of two zones with different resistivities. The first zone is near the outlet, and generally has very low resistivity values (less than 3 Ω m) revealing the presence of salt-water, whereas in the second zone (far from the outlet), the resistivity values are higher than 100 Ω m, testifying for the presence of water with a better quality than the previous one.

Keywords

Plio-quadernary aquifer • Garaat Douza • Salinization • Hydrogeochemical study • Geophysical study

E. Moussaoui · A. Mhamdi (✉) · M. Gouasmia · F. Dhahri
Département des Sciences de la Terre, Faculté des Sciences de Gafsa, Université de Gafsa, Campus universitaire Sid Ahmed Zarroug, 212, Gafsa, Tunisia
e-mail: mhamdi_abdelkader@yahoo.fr

E. Moussaoui · A. Mhamdi · M. Gouasmia · M. Soussi
Faculté des Sciences de Tunis, UR11ES15: Environnement sédimentaires, Systèmes pétroliers et caractérisation des réservoirs, Université de Tunis El Manar, Tunis, Tunisia

1 Introduction

The current situation of the water resources and their uses in Tunisia, presents stakes which are common to many areas of the Mediterranean basin [1]. Especially in Southwestern Tunisia, the problems related to water access by populations are very frequent, when modest rainfall and arid climate are combined with the deficiency of natural water resources [2]. Therefore, the Douara-Chenoufia region, located in the Moulares-Redayef Mining Basin (Northwest of Gafsa region), has experienced a significant increase in agricultural activities, causing an increased demand for water resources in this region, which has led to a qualitative deterioration of these waters.

The main aim of the present work is to determine the salinization extent in the plio-quadernary aquifer of Garaat Douza and its proximities (Douara-Chenoufia region).

2 Materials and Methods

The empirical part of this work was conducted in September 2017, in Douara-Chenoufia region and it was carried out within the framework of this paper (the geoelectrical investigation and the hydrogeochemical results have only depended on the concerned team's effort and no external source has been adapted). Thereby, several studies and methods were selected for this investigation, of which the most important ones are the ERT and VES methods.

Electrical resistivity tomography method (ERT): Three ERT lines were placed in the surveyed area using the Wenner array to determine the salinization extent. The data are presented in 2D geophysical images with modeled electrical resistivity values. The equipment used is Syscal Pro and additional accessories (12 V batterie, SD card and RES2DINV inversion software).

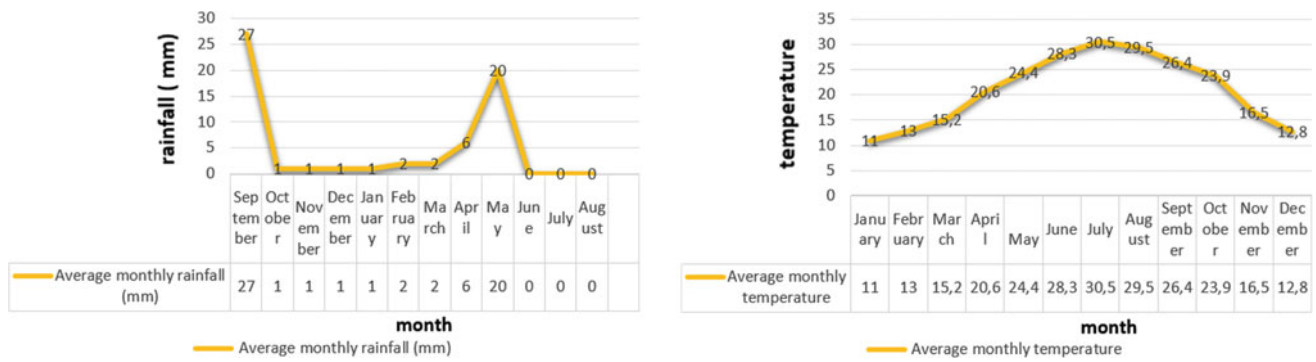
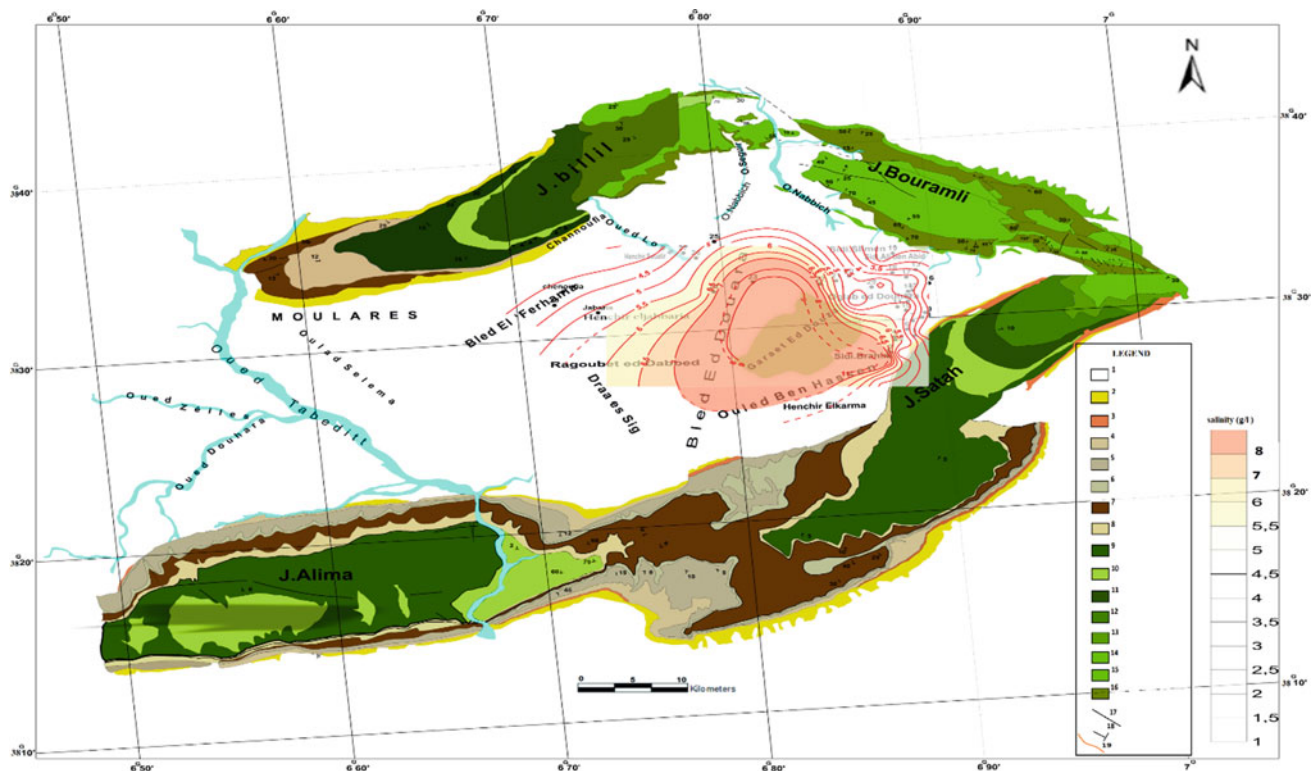


Fig. 2 Average monthly rainfall and temperature of Douara-Chenoufia region (2016)



1. Plio-quaternary, 2. Miocene, 3. Oligocene, 4. Lutetian-Priabonian, 5. Ypresian-Lutetian, 6. Ypresian, 7. Upper Paleocene, 8. Lower Paleocene, 9. Upper Maastrichtian, 10. Upper Campanian-Maastrichtian, 11. Lower Campanian, 12. Coniacian, 13. Turonian, 14. Upper Cenomanian-Lower Turonian, 15. Cenomanian, 16. Upper Albian, 17. Fault, 18. Dip, 19. Salinity lines.

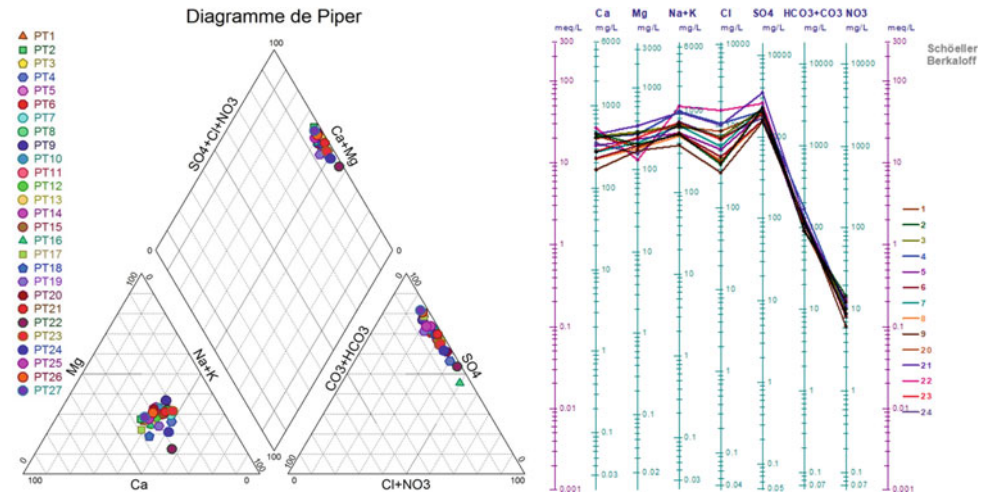
Fig. 3 Groundwater salinity map of Garaat Douza (2017)

values for aragonite (-0.01, 0.61) and calcite (0.14, 0.75) are very close to zero indicating the equilibrium state of water relative to these minerals. However, the saturation index values for dolomite (0.52, 1.72) are much higher than zero, suggesting a supersaturation state of water relative to this mineral.

According to Piper and Schoeller—Berkaloff diagrams (Fig. 4), that salinity is generated by the dissolution of chloride, calcium, sodium and sulphate minerals. In addition,

the mineralization origin studies have shown a good correlation between sodium/ Σ cations ($R_{Na}^2 = 0.9$), calcium/ Σ cations ($R_{Ca}^2 = 0.8$), sulphate/ Σ anions ($R_{SO4}^2 = 0.9$) and chloride/ Σ anions ($R_{Cl}^2 = 0.8$), indicating that salinity is due to the dissolution of evaporites, whilst the bicarbonate (HCO_3) shows a bad correlation with Σ anions ($R_{HCO3}^2 = 0.2$), proving that water salinization in the plio-quaternary aquifer of Garaat Douza has never been controlled by carbonate minerals.

Fig. 4 Piper and Schoeller—Berkaloff diagrams



3.3 Geophysical Investigation

A total of 25 geophysical vertical electrical soundings and three tomographic profiles (Fig. 5) have shown that the surveyed area is characterized by the presence of two zones with different resistivities, the first zone is near the outlet and generally has very low resistivity values (less than 3 Ω m) revealing the presence of salt-water, whereas in the second zone (far from the outlet) the resistivity values are higher than 100 Ω m, testifying for the presence of water with a better quality than the previous one.

The calibration of electrical soundings with boreholes (Channoufia borehole depth is 197 m, Douara borehole depth is 558 m; surface wells depth around Garaat Douza varies between 30 and 80 m) and the achievement of geo-electrical cross sections allowed to understand the geometry and the structure (synclinal structure) of the plio-quaternary aquifer in Garaat Douza (Fig. 5).

4 Discussion

The combination of the different climatological, hydrogeological, hydrochemical and geophysical tools in the study of the salinity problems in the plio-quaternary aquifer of Garaat Douza, enabled us to identify the origin and the processes responsible for water mineralization.

Furthermore, in the Northern part (J. Billil J. Bouramli and J. Satah), and by the effect of the dissolution of the evaporitic formations in runoff water (lessivage) caused by water rock interaction, the water receives a high concentration of Cl^- , Na^+ , SO_4^{2-} , Ca^{2+} . Thereafter, the water that reaches Garaat Douza outlet evaporates, while forming salt crystals. During water precipitation, the salt crystals dissolve in water. So, the aquifer receives some natural contamination on several parts of the aquifer under the effect of the infiltration of salt water from the surface.

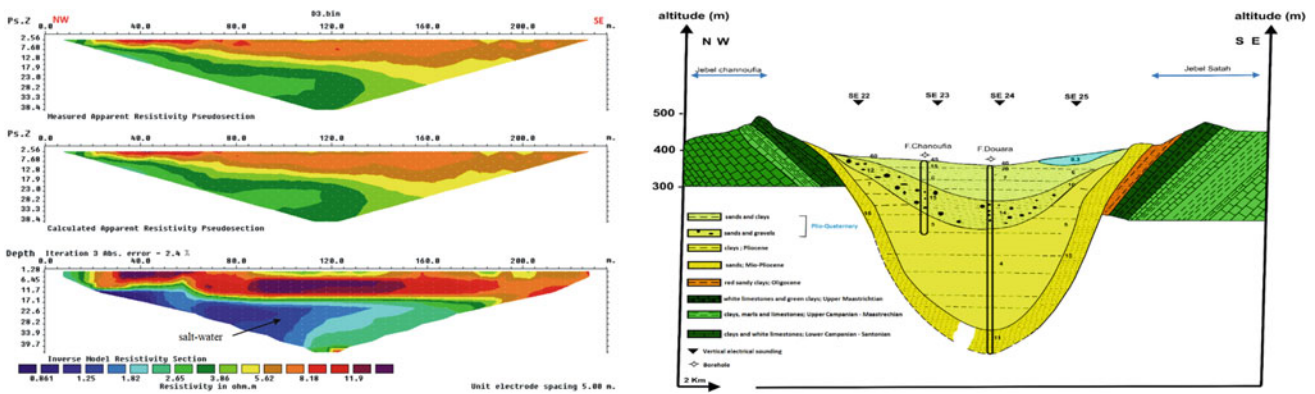


Fig. 5 The most representative pseudo-section and geoelectrical cross section

5 Conclusions

The climatological study has shown that Douara-Chenoufia region is characterized by an arid climate and a modest rainfall. The hydrogeological study has revealed a piezometric drawdown. Moreover, the hydrochemical analysis of major elements has indicated, that the mineralization of the plio-quaternary aquifer is due to the dissolution of evaporites, and that the high salinities (8.9 g/l) are recorded at the outlet of the aquifer. Furthermore, the geophysical approach has shown the presence of two main areas. The first area is located near the outlet of the aquifer, characterized mainly by a low electrical resistivity (salt-water), while the second area is located far from the outlet, generally characterized by high electrical resistivity (pure water).

On the basis of the results of this research, it can be concluded that the increased demand for water resources of

the plio-quaternary aquifer (especially in the upstream part), and the insufficiency of natural recharge of this aquifer, would cause a spread of contamination (salinization) and an inevitable possibility of changing water flow direction, which led us to suggest challenging strategies such as, the use of artificial groundwater recharge and the establishment of desalination plants (desalination of salt water).

References

1. Romagny, B., Cudennec, C.: Considérations physiques et sociales pour l'identification des territoires pertinents dans le Sud-Est tunisien. OpenEdition, Développement durable et territoires, (Dossier 6), 23p (2006)
2. Malik, N., Slim, N.: Effects of Urbanization on Groundwater Quality in the Gafsa Town (Southwestern Tunisia) Desalination and Water Treatment. Taylor & Francis Online, 10–12 (2014)

Relationship Between Hydrochemical Variation and the Seawater Intrusion Within Coastal Alluvial Aquifer of Essaouira Basin (Morocco) Using HFE-Diagram

Mohammed Bahir, Salah Ouhamdouch, Paula M. Carreira, and Kamel Zouari

Abstract

The determination of the relationship between hydrochemical variation and seawater intrusion within the coastal alluvial aquifer of the Essaouira basin (Morocco) was the main objective of this investigation. In order to achieve this objective, the Hydrochemical Facies Evolution Diagram (HFE-D) was used. The obtained results show that the hydrochemical variations of groundwater from the coastal alluvial aquifer of Essaouira basin can be interpreted in terms of intrusion of seawater and bases exchange phenomenon. However, the exploitation of the HFE-D diagram results can lead to a better management of the aquifer by identifying areas affected by the marine intrusion.

Keywords

Essaouira basin • Seawater intrusion • Hydrochemical variation • HFE-Diagram

1 Introduction

In coastal basins, groundwater salinization is generally associated with the effects of anthropogenic activities, climatic conditions, and seawater intrusion. Also, the intrinsic properties of aquifers and external factors such as the climate can mitigate or aggravate these problems. The percentage of

seawater present and the participation of secondary processes, such as bases exchange, are major factors that control the chemical composition of aquifer groundwater [1]. To better understand the relationship between hydrochemical variations and the seawater intrusion into a coastal aquifer, the hydrochemical facies evolution diagram (HFE-D), recently published by [2], was used. The aquifer used as an example here is the Plio-Quaternary alluvial aquifer of Essaouira basin which is part of the semi-arid zones of Morocco with an average rainfall of 300 mm year⁻¹ (Fig. 1b) and a temperature of 20 °C [3 and 4]. It is limited to the north by the Ksoub wadi, to the south by the Tidzi wadi, to the east by the Tidzi diapir and to the west by the Atlantic Ocean (Fig. 1a).

2 Methodology

A total of 104 samples were collected from the alluvial aquifer during 1990, 1995, 2009 and 2015 for chemical determinations and used to determine the relationship between hydrochemical variations and the seawater intrusion within the Plio-Quaternary aquifer of Essaouira basin. The physical parameters (temperature, pH, electrical conductivity) were measured in situ, and the major chemical parameters (Ca, Mg, Na, K, Cl, HCO₃, SO₄, and NO₃) were determined at the Faculty of Science Semlalia of Marrakech.

3 Results and Discussion

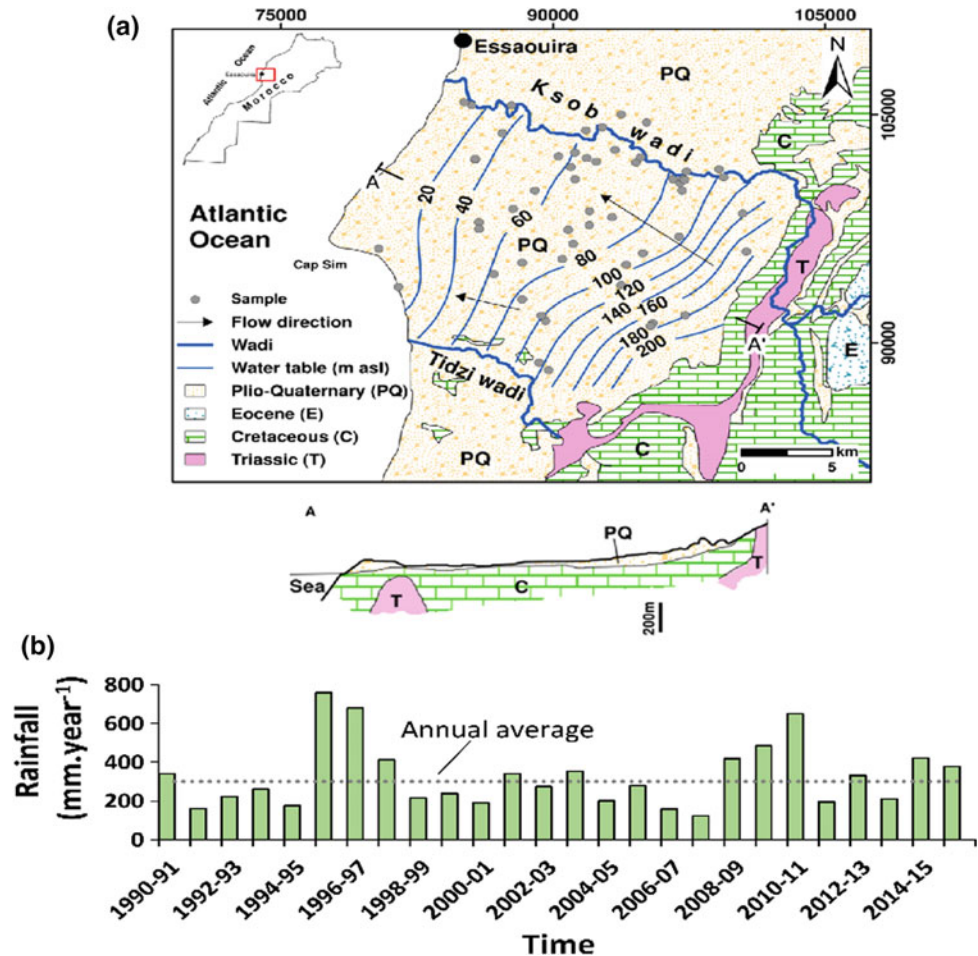
In 1990, more than 66% of the samples were located in the intrusion stage with Na-Cl facies (Fig. 2). This can be attributed to insufficient recharge for direct base exchange reactions to occur and reach the Na-HCO₃ facies in the freshening phase. This is confirmed by the dominance of SW + i₄ sub-stages (52%) (Table 1). But this does not exclude that the aquifer tries to return to the equilibrium state which is manifested by the location of certain points in the f₂ sub-stage with a percentage of 24%.

M. Bahir · S. Ouhamdouch (✉)
LGE-ENS, ENS, Université Cadi Ayyad, 40000 Marrakech,
Morocco
e-mail: salah.ouhamdouch@edu.uca.ma

P. M. Carreira
Centro de Ciências e Tecnologias Nucleares, Instituto Superior
Técnico (C2TN/IST), Universidade de Lisboa, Estrada Nacional
10, km 139,7, 2695-066 Bobadela LRS, Portugal

K. Zouari
LRAE, Ecole Nationale d'Ingénieurs de Sfax, Université de Sfax,
BP W3038, Sfax, Tunisia

Fig. 1 a Location and geological map of study area and b annual precipitation



For 1995, more than 62% of the samples are located in the intrusion domain with a MixNa-Cl facies (Fig. 2). While some other points are located in the stage of freshening and reach the facies MixNa-HCO₃ and Na-HCO₃ characterizing fresh water. Table 1 shows an evolution of the sub-stage i_1 (3%) towards the sub-stages $Fw + i_4$ (38%). This suggests that the aquifer is still governed by the intrusion phase following the insufficiency of recharge. The same situation was observed in 2015, with the appearance of the second MixCa-Cl facies. This may be due to the reverse exchange processes triggered by the intrusion of seawater. This suggestion is corroborated by the dominance of i_3 (49%) and $Sw + i_4$ (3%) sub-stages (Table 1).

With the exception of a single sample, the remaining samples, representing the 2009 campaign, are located in the stage of freshening. This can be explained by a significant recharge confirmed by the dominance of the f_1 sub-stage (56%) compared to the $Sw + i_4$ sub-stages (38%).

However, the exploitation of the results obtained leads to the conclusion that the coastal alluvial aquifer of Essaouira basin is threatened by marine intrusion due to climatic variability and over-exploitation resulting from a demographic

pressure. This corroborates the results obtained by [5] in 2012, based on the Durov diagram and the results obtained by [6] in 2017 with the application of hydrogeochemical and isotopic approach.

4 Conclusions

The seawater intrusion is a phenomenon that occurs in many coastal aquifers around the world. The hydrochemical facies evolution diagram (HFE-D) is a diagram that allows a good understanding of the variations in the state of a coastal aquifer as well as the evolution of the marine intrusion. It also makes it possible to differentiate the water having undergone a marine intrusion from the fresh water, and it makes it possible to recognize the recharge zones of the aquifer. The application of this diagram on the coastal alluvial aquifer of Essaouira basin has shown that this aquifer is dominated by the marine intrusion stage compared to the freshening stage. This can be explained by the scarcity of rainfall that eventually results in insufficient recharge of the aquifer. However, the exploitation of the HFE-D diagram

Fig. 2 Representation of water samples on a HFE-Diagram

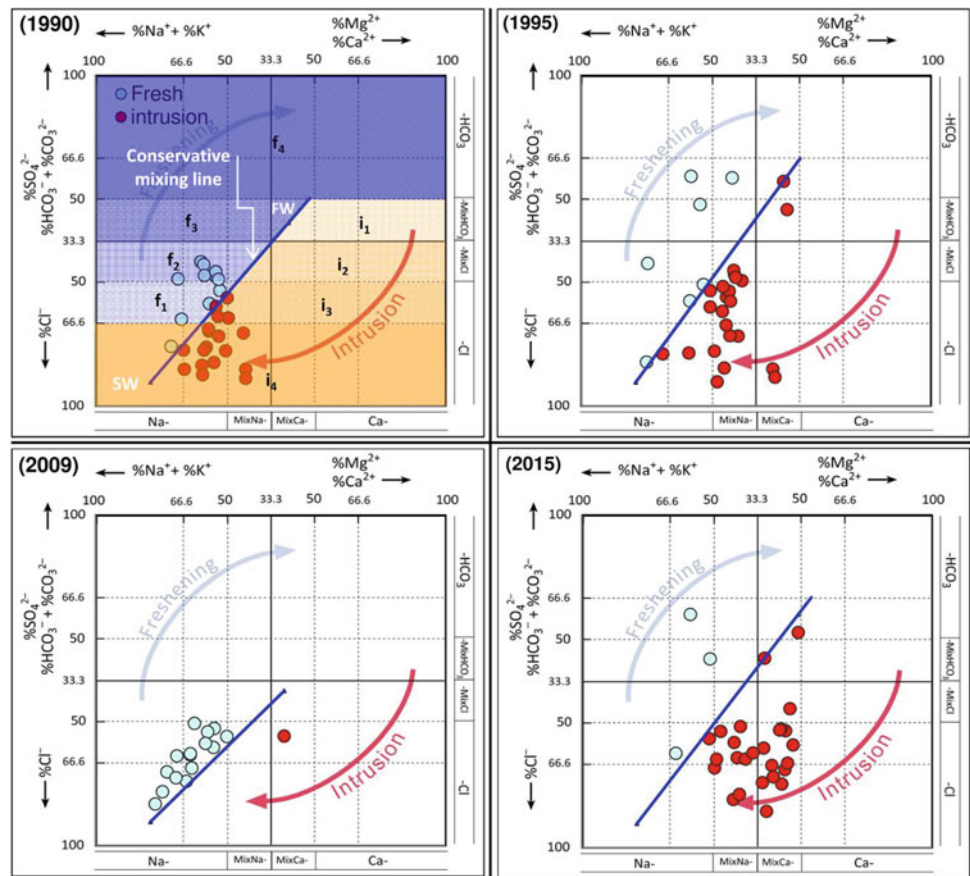


Table 1 Distribution of sub-stages in freshening and intrusion phases for each sample

	Freshening (%)				Intrusion (%)			
	Fw + f ₄	f ₃	f ₂	f ₁	i ₁	i ₂	i ₃	Sw + i ₄
1990	0	0	24	10	0	0	14	52
1995	10	3	3	7	3	13	23	38
2009	0	0	0	56	0	0	6	38
2015	7	3	0	3	3	3	49	32

results can lead to a better management of the aquifer by determining the areas affected by seawater intrusion.

References

- De Montety, V.: Origin of groundwater salinity and hydrogeochemical processes in a confined coastal aquifer: case of the Rhône delta (Southern France). *Applied Geochem.* **23**, 2337–2349 (2008)
- Giménez-Forcada, E.: Dynamic of seawater interface using hydrochemical facies evolution diagram (HFE-D). *Groundwater* **48**(2), 212–216 (2010)
- Bahir, M.: Ressources hydriques du bassin synclinal d’Essaouira (Maroc). *Estudios Geologicos* **56**, 185–195 (2000)
- Ouhamdouch S.: Climate Change impact on future rainfall and temperature in semi-arid areas (Essaouira Basin, Morocco). *Environ. Process.* **4**(4), 975–990 (2017)
- Bahir M.: Hydro-geochemical behaviour of two coastal aquifers under severe climatic and human constraints: comparative study between Essaouira basin in Morocco and Jeffara basin in Tunisia. *Int. J. Hydrol. Sci. Technol.* **2**(1), 75–100 (2012)
- Ouhamdouch, S.: Geochemical and isotopic tools to deciphering the origin of mineralization of the coastal aquifer of Essaouira basin, Morocco. *Procedia Earth Planet. Sci.* **17**, 73–76 (2017)

Use of Environmental Isotopes and Hydrochemistry to Characterize Coastal Aquifers in Semi-arid Region. Case Study of Wadi Guenniche Deep Aquifer (NE Tunisia)

Safouan Ben Ammar, Jean-Denis Taupin, Mohsen Ben Alaya, Kamel Zouari, Nicolas Patris, and Mohamed Khouatmia

Abstract

This study presents the first results from the multicriteria approach using geochemical and isotopic tools to understand the origin, geochemical evolution and renewability of deep groundwater in Wadi Guenniche basin, north-eastern Tunisia. The study area is a coastal plain that plays an important regional socio-economic role, as the groundwater resources are the most important source for agricultural and drinking supply. Geochemical and isotopic (^{18}O , ^2H) data show that the water-rock interaction and cation-exchange process are the major geochemical mechanisms controlling hydrochemical evolution of groundwater. Isotope data (Oxygene-18, deuterium and tritium) point out recent recharge by atmospheric precipitations. Samples from deeper boreholes (300 m) characterized by low ^{18}O and ^3H contents suggest older recharge under different climatic conditions.

Keywords

Coastal aquifer • Geochemistry • Isotopes • Recharge • NE Tunisia

1 Introduction

The basin of Wadi Guenniche (130 km²) is a coastal plain situated in the northeastern part of Tunisia (Fig. 1). It is a complex and highly compartmentalized synclinal structure, forming a part of the subsident structure, located between Bizerte and Ichkeul lagoons [3]. Quaternary alluvial formations lodge the phreatic aquifer characterized by heterogeneous and lenticular detrital sequences, and deeper Pliocene layers formed by sand and sandstone host the deep aquifer between 75 and 300 m in depth. Studies concerning water resources in this basin are rare. They have only focused on an electrical prospection leading to the hydrogeological modeling of the phreatic aquifer. The purposes of this study are: (1) better understanding of groundwater recharge mechanism using environmental isotopes (^{18}O , ^2H and ^3H) in conjunction with geochemical data; (2) assessing salinization sources of deep groundwater; and (3) estimating its residence time.

2 Methods

Twenty-nine boreholes covering the whole basin were sampled between March and April 2013 (Fig. 1). Temperature, pH and Electric Conductivity (EC) were measured in situ. Major chemical elements were analysed using ion chromatography (Dionex DX120) and atomic absorption. The stable isotope contents (^{18}O and ^2H) were performed by a laser spectroscopy liquid-water isotope analyzer (LGR LT-100—Los Gatos Research) according to the recommendations of the International Atomic Energy Agency [1], with an analytical error of 0.2‰ and 1‰ for ^{18}O and ^2H , respectively. Tritium values were determined by liquid scintillation method after the enrichment of thirteen samples. Results were presented as tritium units (TU) with a precision of 0.3 TU.

S. Ben Ammar (✉)
ISTEUB, University of Carthage, La Chargaia II, Tunis, Tunisia
e-mail: safouan_ammam@yahoo.fr

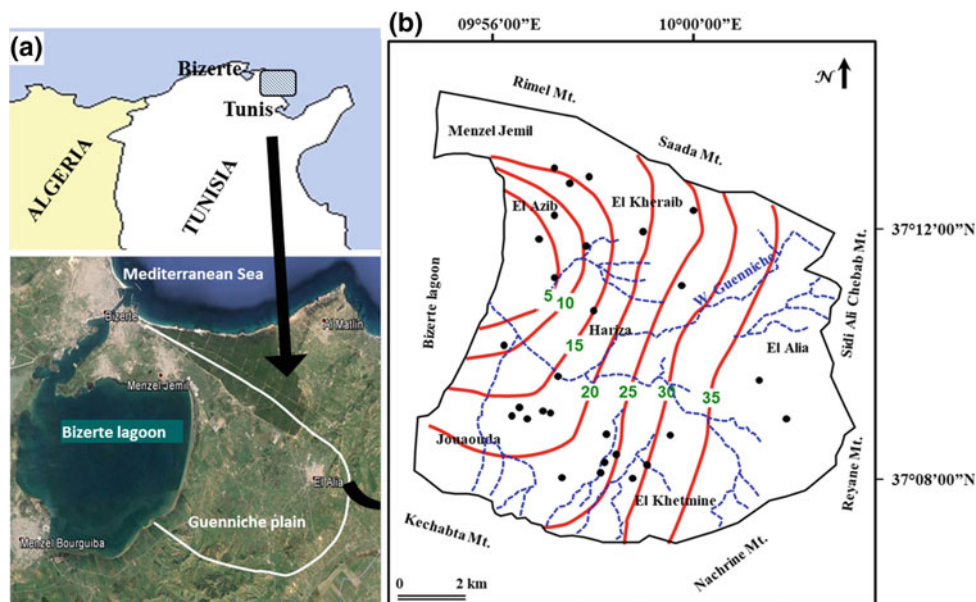
J.-D. Taupin · N. Patris
UMR 5569 (IRD, CNRS, UM), Montpellier, France

M. Ben Alaya
LMU, INRAP Pôle Technologique Sidi Thabet, Sidi Thabet, Tunisia

S. Ben Ammar · K. Zouari
LRAE, ENI Sfax, Univ. Sfax route de Soukra, Sfax, Tunisia

M. Khouatmia
CNSTN, Sidi Thabet, Tunis, Tunisia

Fig. 1 Situation of the study area (a) and location of sampled boreholes with piezometric contour map (b)



3 Results and Discussion

The piezometric map established from borehole records (Fig. 1) shows that the groundwater flow is from the SE to NW, where it discharges to the Bizerte lagoon (Fig. 1). Piezometric levels vary between 35 m in the eastern part of the plain to 5 m in the downstream part around the Bizerte lagoon. Deep groundwater resources are estimated as $12.7 \text{ Mm}^3 \text{ year}^{-1}$ and actual abstraction is about $8.16 \text{ Mm}^3 \text{ year}^{-1}$ with 233 boreholes. Groundwater use is shared between domestic (28%) and agricultural use (72%).

Measured TDS values indicate good quality of groundwater in major parts of the basin. TDS values vary between 0.3 and 3.8 g L^{-1} . The lowest values ($<1 \text{ g L}^{-1}$) characterize the northern half of the basin, near the foot of the surrounding mountains, whereas, the highest values ($1 < \text{TDS} < 3.8 \text{ g L}^{-1}$) are recorded in the southern part of the plain as well as the lower zone of Hariza (Fig. 1). The dominant facies is of mixed and Na-Cl types (Fig. 2) in

some areas of the plain. Variations of the chemical facies of groundwater can be explained by: (i) frequent lateral variations of lithological facies of the aquifer (Pliocene formation becomes finer and clayey in the downstream part of the basin); (ii) relative prolonged contact between water and rock resulting from long residence time of groundwater in the aquifer; (iii) the presence of base exchange phenomena with the clay minerals present in the different aquifer levels.

The $\text{Ca}^{2+} + \text{Mg}^{2+}$ versus $\text{SO}_4^{2-} + \text{HCO}_3^-$ diagram (Fig. 2) shows that the cation exchange (explained by a slope of 1 [4]) is not the only process controlling the composition of groundwater. For most samples, the Ca^{2+} and Mg^{2+} are in excess with respect to $\text{SO}_4^{2-} + \text{HCO}_3^-$ indicating the dissolution of carbonate (calcite, dolomite and aragonite) and evaporate minerals (gypsum and anhydrite). High Ca^{2+} and SO_4^{2-} contents can be related to the dissolution of gypsum and anhydrite as indicated by saturation indexes (SI) varying between -2.5 and -0.5 for all samples. Similarly, the dissolution of carbonate minerals ($-0.5 \leq \text{IS} \leq 0.5$) is believed to be responsible for high levels of calcium and bicarbonates in the groundwater.

Fig. 2 Piper diagram (a) and correlation between ($\text{HCO}_3^- + \text{SO}_4^{2-}$) and ($\text{Ca}^{2+} + \text{Mg}^{2+}$) (b)

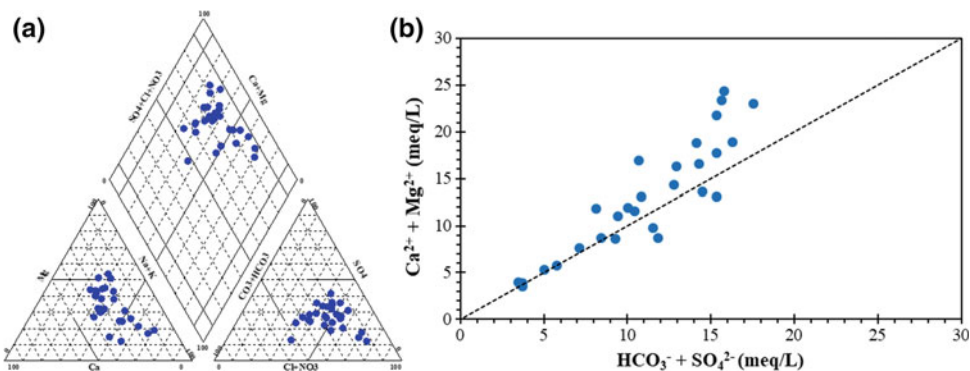
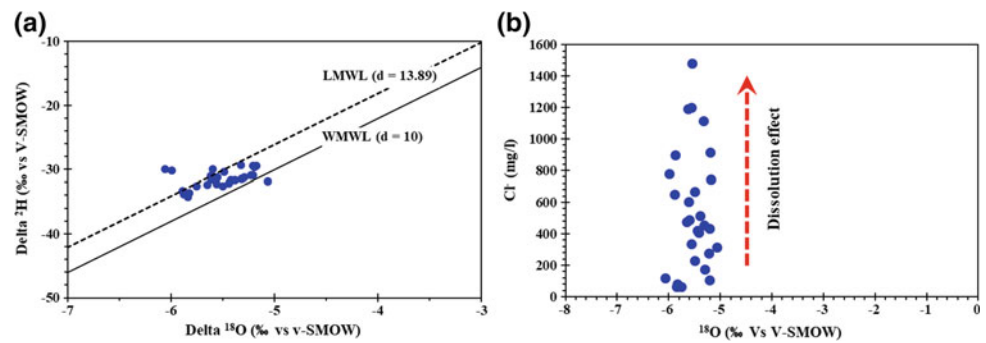


Fig. 3 ^{18}O versus ^2H (a) and ^{18}O versus Cl^- diagrams (b)



Isotopic contents of sampled boreholes were ranging from -6.06 to -5.06‰ versus V-SMOW for $\delta^{18}\text{O}$ and from -34.29 to -29.44‰ versus V-SMOW for $\delta^2\text{H}$. The mean values are respectively -5.52 and -31.49‰ versus V-SMOW for $\delta^{18}\text{O}$ and $\delta^2\text{H}$. On the $\delta^{18}\text{O}/\delta^2\text{H}$ diagram (Fig. 3), all samples form a single group, that is situated between the world meteoric water line (WMWL, $d = 10$) and the local meteoric water line (LMWL, $d = 13.89$) of Bizerte indicating that the dominant isotope signature of Guenniche deep groundwater is quite similar to that of actual rain water. Because of this similarity, the isotope signature of groundwater can be interpreted as indicative of recent recharge of the aquifer from rain water by direct infiltration in the outcropping area of Pliocene formations on surrounding mountains of the plain. The $^{18}\text{O}/\text{Cl}^-$ diagram indicates that groundwater geochemistry is controlled by water-rock interaction phenomena and that groundwater is not affected by the evaporative effect in the unsaturated zone (Fig. 3).

Tritium values are ranging from below detection to 4.81 TU. High contents (>2 TU) obtained for samples, from the upstream area near the piedmonts of mountains, are similar to the weighted mean value of tritium content in precipitation and advocate for a recent groundwater renewal during or after the era of nuclear testing in the 1950s and 1960s [2]. Samples from boreholes with a depth of about 300 m are characterized by low tritium contents less than 1 TU and more depleted water in ^{18}O . This is related to an older recharge time.

4 Conclusions

The first dual geochemical and isotopic investigation conducted in Guenniche improves our understanding of the hydrogeological framework and hydrologic conditions in the

deep aquifer system. The study shows that groundwater salinity is strongly influenced by the lithological nature of aquifer formations which shows frequent lateral variations. The main phenomenon controlling the salinity of the groundwater seems to be the dissolution of evaporate and carbonate minerals. Isotope analyses confirm recent recharge post-nuclear of the aquifer. Low tritium values characterizing some samples from the deeper aquifer suggest ancient recharge prior to the nuclear period and occurring under different climate conditions.

Acknowledgements The study is a part of the Tunisian-French scientific action supported by a collaboration contact between ISTEUB (Univ. Carthage) and HSM (IRD).

References

1. Aggarwal, P.K., Araguas-Araguas, L., Groning, M., Kulkarni, K.M., Kurtas, T., Newman, B.D., Tanweer, A.: Laser Spectroscopic Analysis of Liquid Water Samples for Stable Hydrogen and Oxygen Isotopes, IAEA, p. 49 (2009)
2. Clark, I., Fritz, P.: Environmental Isotopes in Hydrogeology. CRC Press, Boca Raton (1997)
3. Melki, F., Zouaghi, T., Harrab, S., Casas Sainz, A., Bedir, M., Zargouni, F.: Structuring and evolution of Neogene transcurrent basins in the Tellian foreland domain, north-eastern Tunisia. *J. Geodyn.* **52**, 57–69 (2011)
4. Vengosh, A., Spivack, A.J., Artzi, Y., Ayalon, A.: Geochemical and Boron, strontium and oxygen isotopic and geochemical constraints for the origin of the salinity in groundwater from the Mediterranean coast of Israel. *Water Resour. Res.* **35**, 1877–1894 (1999)

Multi-isotope Approach to Study the Problem of Salinity in the Coastal Aquifer of Oued Laya, Tunisia

Mohamed Fethi Ben Hamouda, Paula M. Carreira,
José Manuel Marques, and Hans Eggenkamp

Abstract

Geochemical and both stable ($\delta^2\text{H}$, $\delta^{18}\text{O}$ and $\delta^{37}\text{Cl}$) and radioactive (^3H) isotopic determinations were applied to identify the main processes involved in the increased salinization of groundwater in the Mio-Pliocene aquifer of Oued Laya, located in the eastern coast of Sousse, Tunisia. Geochemical results indicate water-rock interaction, including dissolution of evaporitic minerals, as the major process responsible for groundwater salinity. In addition, seawater intrusion is also responsible for the groundwater mineralization in this region, resulting in Cl-Na-type groundwaters and degradation of groundwater quality. The geochemical and isotopic composition of the groundwater reflects the lithological composition of the subsurface geology, the presence of salt basins (“sebkhas”), and ion exchange processes between the groundwater and clays.

Keywords

Geochemistry • Salinization • Coastal aquifers
Isotopes • Tunisia

1 Introduction

The high salinity can originate from a variety of sources, natural or anthropogenic, such as dissolution of halite and gypsum, concentration by evaporation, seawater intrusion, pollution, etc. The Oued Laya coastal aquifer system is no exception. It is located in a coastal saline wetland along the Mediterranean Sea, surrounding the city of Sousse. This water resource is mainly characterized by poor quality groundwaters with high salinity compared with surrounding aquifers.

This study aims to characterize the geochemistry of the poorly known Oued Laya aquifer system and to elucidate the different geochemical processes responsible for groundwater mineralization. Ionic ratios, such as Na/Cl and Br/Cl, and isotopic data ($\delta^{18}\text{O}$, $\delta^2\text{H}$, $\delta^{37}\text{Cl}$ and ^3H) have been used to identify different sources of salinity in coastal zones [1] and will be applied to the Oued Laya aquifer system in this study.

The Oued Laya aquifer system consists of two main reservoirs: a shallow one, with a thickness between 30 and 60 m and consisting of Mio-Pliocene sandstone formations with interbedded gypsum lenses; the second one, between 100 and 250 m, is a confined aquifer made of Miocene loamy sands. The Miocene aquifer is separated from Mio-Pliocene aquifer by a thick layer of clays, approximately 20 m thick, which is sufficiently impermeable and continuous to ensure a hydraulic head for the deep aquifer. The shallow groundwater aquifer has a flow direction from inland towards the coast (W-E or SW-NE).

2 Materials and Methods

Groundwater was collected in 29 sampling points in the study area for the identification of major elements, stable isotopes ^2H and ^{18}O and Tritium during a field campaign carried out in 2011. The chemical analyses of the water

M. F. Ben Hamouda (✉)
UMTN/LSTE, Isotope Hydrology and Geochemistry Unit,
CNSTN, 2020 Ariana, Tunisia
e-mail: f_benhamouda@yahoo.fr

P. M. Carreira
Centro de Ciências e Tecnologias Nucleares, Instituto Superior
Técnico (C2TN/IST), Universidade de Lisboa, Estrada Nacional
10, km 139,7, 2695-066 Bobadela LRS, Portugal

J. M. Marques
Centro de Recursos Naturais e Ambiente, (CERENA/IST),
1049-001 Lisbon, Portugal

H. Eggenkamp
FB Geowissenschaften, Math.-Natur. Fakultät, Univ. Tübingen,
72074 Tübingen, Germany

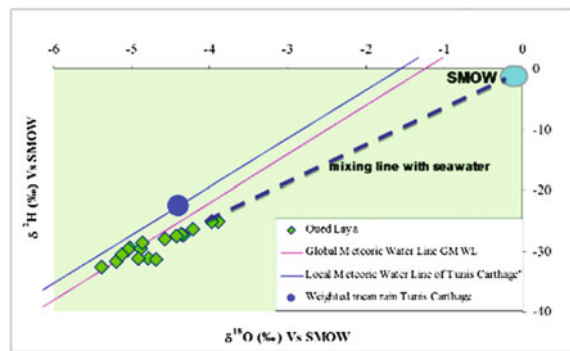


Fig. 1 Plot of $\delta^2\text{H}$ Vs. $\delta^{18}\text{O}$ ‰ (V-SMOW)

samples were performed at the Isotope Hydrology and Geochemistry Unit at the CNSTN (Centre National des Sciences et Technologies Nucléaires), Tunisia. Major cations (Ca, Mg, Na, and K) were analyzed in filtered samples using an atomic absorption spectrometer with a furnace, and major anions (Cl , SO_4 and NO_3) were analyzed in filtered samples using a Dionex DX 120 ion chromatograph. The electrical charge balance between major anions and cations is $> \pm 5\%$ in most samples. Isotope analysis of the water samples (^2H and ^{18}O) were performed by the LSCE (Laboratoire des Sciences du Climat et de l'Environnement, CEA), France. Tritium (^3H) was measured by the ITN at the Isotope Hydrology Laboratory, Lisbon, Portugal.

3 Results

3.1 Na/Cl and Br/Cl Relationship

Chlorine is strongly correlated with sodium for the majority of the shallow groundwater samples ($r = 0.88$). The positive correlation between Na and Cl with a molar ratio close to one indicates a contribution of halite dissolution to groundwater mineralization. The Na/Cl ratio obtained in the groundwater samples suggests that the predominance of sodium and chlorine cannot be explained only by seawater intrusion, even for samples taken near the coast line, since the Na^+/Cl^- molar relationship differs significantly from that of the Mediterranean ($\text{Na}/\text{Cl SW} = 0.86$) [2]. The enrichment in the sodium content is observed in some of the most mineralized groundwater samples and also in part of the water samples with lower salinity. This correlation shows two parallel trend lines, one reflecting the 1:1 ratio of halite dissolution and another one with Na/Cl higher than the marine ratio reflecting an input of sodium to the system, which could be related to water-rock interaction and ion exchange (Na–Ca). Ion exchange processes involve transfers

of mass between solid matter and the solution and is very common in deltaic areas where clay minerals and organic matter are abundant.

The Br^-/Cl^- relationship is an important hydrological tool in order to identify the possibility of seawater intrusion since it is relatively constant (1.5×10^{-3}) in seawater due to the extremely long residence time in the oceanic masses [1, 2]. In the Mio-Pliocene aquifer, the Br^-/Cl^- relationship is not distinctive with more than two thirds of the shallow groundwater points within a range of 20% from the seawater ratio. This proximity can be explained both by continental waters mixing with seawater and an influence of the marine spray on the infiltrated rainwaters. The shallow groundwater points ascribed to Br^-/Cl^- ratios away from the seawater dilution line are related to sampling sites located outside of the likely seawater intrusion area.

3.2 $\delta^{18}\text{O}$ and $\delta^2\text{H}$ Isotopic Signatures

Plots of $\delta^{18}\text{O}$ versus $\delta^2\text{H}$ (Fig. 1) and Cl^- versus $\delta^{18}\text{O}$ for the Mio-Pliocene aquifer of Oued Laya show that the isotopic composition ($\delta^{18}\text{O}$) in the groundwater can be divided in two groups. In the first one, the composition of $\delta^{18}\text{O}$ varies between -3.8 and -4.91% . This group represents water enriched in ^{18}O and ^2H along the mixing line of seawater, indicating a probable marine source. The other samples in this group are located between the global meteoric water line (GMWL) and the local water line (LMWL) of Tunis Carthage. The contribution of the present-day precipitation to the recharge is the most probable. The second group is composed by wells with water showing $\delta^{18}\text{O}$ values ranging between -5.39 to -4.91% . These values are relatively different from the weighted average mean of the precipitation water of the Tunis Carthage station (-4.4%). Considering this isotopic difference of about 1% (mean values) in the oxygen-18 content, another explanation which must be added to characterize the groundwater system. Geographic and altitude changes in the region were negligible, so other climatic conditions during recharge, which are very different from modern day, are needed to explain the depletion found in the groundwater system. Studies performed in groundwater from the United Kingdom and from western and central Europe recharged during the last glaciation are also depleted in both ^{18}O and ^2H in comparison with modern precipitation in the region [3] due to the colder climate during recharge. The Mio-Pliocene aquifer of Oued Laya shows signs of an isotopic fingerprint characteristic of old water that was probably recharged during the last glacial maximum. On the other hand, plotting the isotopic composition (^{18}O) as a function of Cl^- shows some indication of mixing between fresh

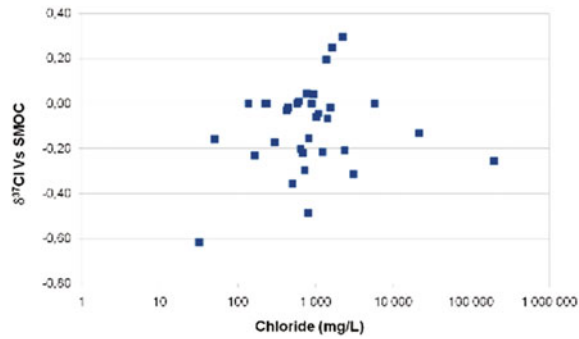


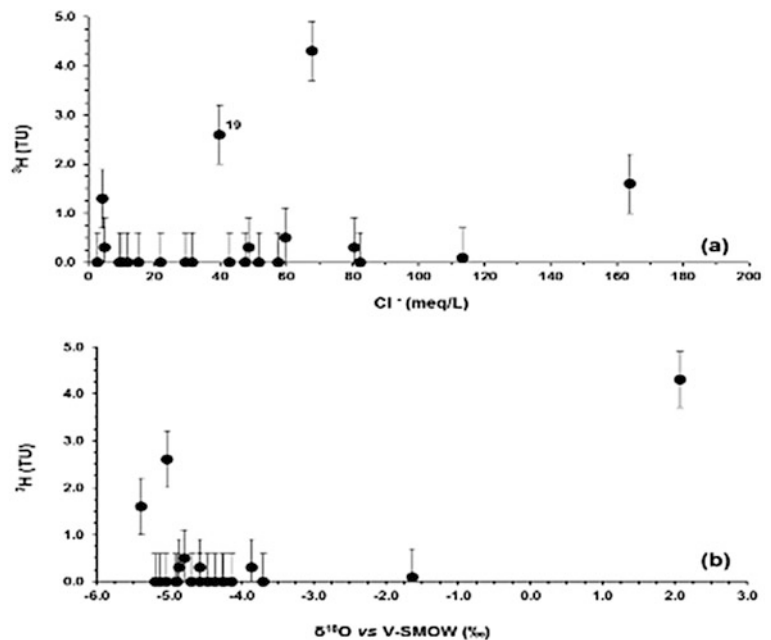
Fig. 2 Plot of ^{37}Cl ‰ (SMOC) Vs. Cl^-

groundwater and seawater. An isotopic shift is observed in the plot showing some isotopic enrichment in the groundwater samples towards a seawater composition, so a marine origin of salinity cannot be excluded. Furthermore, one possible explanation for the enrichment detected in the other points that present “heavy isotopic content” and lower mineralization is groundwater evaporation in the borehole or previous to infiltration, although problems during the sample collection cannot be left out.

3.3 Chlorine Isotopes

The Cl isotope variation in the aquifer is large and $\delta^{37}\text{Cl}$ values range from -0.6 to $+0.3$ ‰ vs. SMOC (Fig. 2). The

Fig. 3 ^3H Vs. Cl^- a and ^3H Vs. ^{18}O b diagrams



variation depends on the location of the wells. In the eastern part of the aquifer, they show a limited range (between -0.3 and 0 ‰), while inland they show the full range of values. The data indicate that the Cl isotope composition close to the coast is influenced by the presence of seawater, whereas inland, it is more influenced by physical and chemical processes such as diffusion and ion-exchange.

3.4 Tritium

Tritium is known as an indicator of recent groundwater recharge. Most groundwater samples have ^3H content close to zero and the chloride is quite variable, which indicates that we are dealing with actual-day salinization. The fact that most samples have low tritium levels (in most of the samples lower than 2.0 TU), and the presence of a clay fraction in the aquifer matrix leads us to conclude that the residence time of the recharge water promotes the dissolution of evaporite minerals and the ion exchange processes. The relation between $^3\text{H}-\text{Cl}^-$ and $^3\text{H}-\delta^{18}\text{O}$ (Fig. 3) indicates that the origin of the high mineralization is due to recent saltwater intrusion [4]. Merging the analysis of these three parameters allowed us to formulate the hypothesis of evaporite minerals dissolution as a main mechanism responsible for the increase of salinization in the groundwater system.

4 Conclusions

The results of geochemical and isotopic analysis have shown that water mineralization seems to have been acquired by a dissolution of minerals in the aquifer system, especially halite and gypsum. Ion exchange processes likely play an important role in the groundwater mineralization. The contamination of the Mio-Pliocene shallow aquifer by mixing with seawater is probable and the stable isotopes data support the hypothesis of mixing with seawater.

The high mineralization of water coming from saltwater intrusion is located in the northeastern part of the aquifer. The absence of correlation is typical of the dissolution processes of evaporite minerals (halite and/or gypsum) substantiated by an increase in the content of sodium and calcium. This process is supported by the existence in the region of salt basins (“sebkhas”) and the interbedded formations of gypsum in the sandy-clay formations. The fact that most samples have low tritium levels and the presence

of a clay fraction in the aquifer matrix leads us to conclude that the residence time of the recharge water is relatively high which favours the dissolution processes of evaporite minerals and the ion exchange processes.

References

1. Jones, B.F., Vengosh, A., Rosenthal, E., Yechieli, Y.: Geochemical investigations. In: Bear, J., et al. (eds.) *Seawater Intrusion in Coastal aquifers*, pp. 51–71. Kluwer Academic Publisher, Dordrecht (1999)
2. Vengosh, A.: Salinization and Saline Environments, Reference Module in Earth Systems and Environmental Sciences, *Treatise on Geochemistry*. 2nd ed., vol 11, 325–378 (2014)
3. Negrel, P., Petelet-Giraud, E.: Isotopes in groundwater as indicators of climate changes. *Trends Anal. Chem.* **30**, 1279–1290 (2011)
4. Ben Hamouda, M.F., et al.: Understanding the origin of salinization of the Plio-Quaternary eastern coastal aquifer of Cap Bon (Tunisia) using geochemical and isotope investigations. *Environ. Earth Sci.* (63), 889–901 (2011)

Groundwater Evolution in the Multilayer Aquifers of the Mekelle Sedimentary Outlier (Northern Ethiopia): A Chemical and Isotopic Approach

Tewodros Alemayehu, Albrecht Leis, and Martin Dietzel

Abstract

The study aims to evaluate groundwater geochemistry characterization of multilayer aquifers of the Sedimentary Rock in Mekelle Outlier in order to gain knowledge on the dominant geochemical processes and water quality status. Groundwater samples were collected and analyzed for major ion chemistry and stable isotopes ($\delta^2\text{H}$ and $\delta^{18}\text{O}$). The findings reveal that the sources of ions into the groundwater are controlled by the duration of the water-rock interaction in confined and semi-confined aquifers. The chemical facies of the water evolve from Ca-HCO_3 to Ca-SO_4 along the flow direction. The stable isotope of $\delta^2\text{H}$ versus $\delta^{18}\text{O}$ signifies a source of local meteoric water. The isotopic signature of few samples depicts the effect of the evaporation process prior to infiltration.

Keywords

Geochemical processes • Groundwater • Mekelle • Sedimentary rocks • Stable isotopes

1 Introduction

The Mesozoic Sedimentary Sequence, from which most groundwater in the investigated area is abstracted, has a much wider distribution in the Mekelle Outlier. Aynalem and Elala sub-basins are multi-layered aquifers at the center of the outlier. Locally, the basins are an important aquifer system and meet a significant portion of water demand of

T. Alemayehu (✉)
Mekelle University, P. O. Box 231 Mekelle, Ethiopia
e-mail: tewodros.ale@gmail.com

A. Leis
JR-AquaConSol, Steyrergasse 21, 8010 Graz, Austria

M. Dietzel
Graz University of Technology, Rechbauerstrasse 12,
8010 Graz, Austria

Mekelle town. However, following many years of groundwater extraction, the issues of water quantity and quality have become a public concern.

It is evident that the differences in baseline groundwater chemistry reflect the complex interlayering of shale, limestone, and marl units [1]. As the chemical compositions of groundwater are controlled by many interrelated processes, understanding geochemical processes affecting the water quality is essential. To this effect, the geochemical evolution of the Aynalem and Elala aquifer system is not distinctly established. This study provides an insight on the origin of the chemical composition of groundwater and the controlling geochemical processes to detect groundwater quality deterioration.

2 Study Area and Methods

The study area is characterized by a semi-arid climate zone with an average monthly temperature ranging from 15.6 to 20.7 °C and a mean annual rainfall of 671 mm. It occupies a central portion of the Mekelle basin where Agulae Shale and Antalo Limestone formations are widely exposed. Both are composed of intercalation of shale, limestone and marl; however, the Antalo formation is dominated by massive fractured limestone [2]. These sedimentary sequences are later intruded by younger dolerite in the form of sills and dykes.

Because of the interbedded fractured limestone and shale beds, groundwater occurs in different water-bearing formations of varying lithologies. The multi-layered aquifers of the study area are represented by more productive deeper limestone and shale intercalation owing to the presence of secondary porosity [2]. At places, groundwater occurs under semi-confined conditions due to the vertical alternative layering of the low hydraulic conductivity of shale. The deep fractured limestone of Aynalem main aquifer is also hydraulically connected to upper Elala aquifer [1].

Groundwater samples were collected from active pumping wells from both aquifers (Aynalem and Elala sub-basins). Field parameters, including pH, electrical conductivity (EC), Total Dissolved Solid (TDS), temperature and total alkalinity (i.e. HCO_3^-) were recorded during sampling. Concentrations of major cations and trace elements were analyzed by ICP-OES. Anions were measured by ion chromatography.

Samples for the stable isotopes of water ($^{18}\text{O}/^{16}\text{O}$ and D/H) were collected in HDPE bottles. The oxygen isotopic composition of the water was measured by the $\text{CO}_2\text{-H}_2\text{O}$ equilibrium fully automated technique, coupled to a Finnigan DELTAplus mass spectrometer. The isotopes of hydrogen were measured using a continuous flow Finnigan DELTAplus XP mass spectrometer coupled to HEKAtech high-temperature oven by chromium reduction.

3 Results

3.1 Geochemical Characterization of the Groundwater

The groundwater samples were plotted on a Piper diagram (Fig. 1) to understand the processes controlling the groundwater chemistry. The hydrochemical facies are characterized by the dominance of Ca-HCO_3 and Ca-SO_4 , in groundwater from Aynalem and Elala basins, respectively. The average TDS concentrations of the samples from Aynalem and Elala sub-basins are 924 mg/l and 1874 mg/l, respectively.

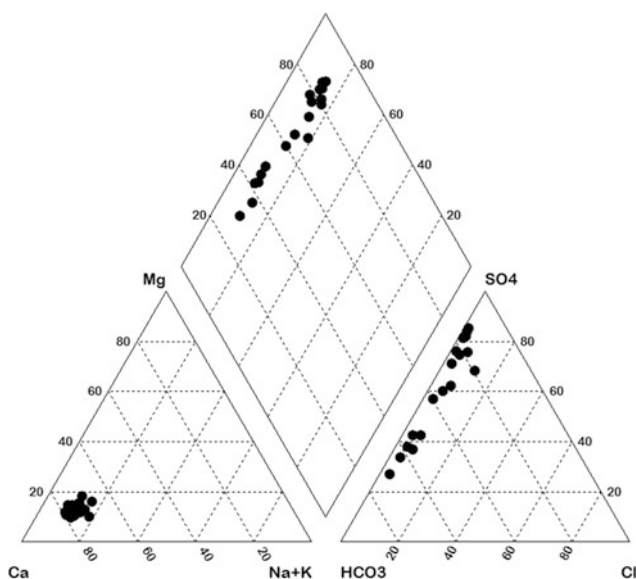


Fig. 1 Piper diagram of the analyzed groundwater samples

The Ca-CO_3 waters are typical of fresh water indicating the recharge zones. The TDS in this sub-basin is mostly less than 1000 mg/l. The shift to SO_4^{2-} water type is associated with higher TDS ranging from 1400 to 2066 mg/l. The increase in TDS is associated with increasing of Ca^{2+} , Mg^{2+} , Na^+ , HCO_3^- and SO_4^{2-} contents, an indication of prolonged water-rock interactions.

3.2 Stable Isotopes of $\delta^2\text{H}$ and $\delta^{18}\text{O}$

The $\delta^2\text{H}$ and $\delta^{18}\text{O}$ values of the groundwater range from -10.1 to -1.4‰ and -3.4 to -1.6‰ , with an average of -5.8 and -2.7‰ , respectively. Most of the samples plot close to meteoric water line of Addis Ababa (LMWL) and Global Meteoric Water Line (GMWL) showing recharge of local precipitation (Fig. 2). Few values are slightly enriched relative to the LMWL, suggesting limited direct infiltration. In confined and semi-confined aquifer systems where vertical groundwater flow is limited, secondary isotope fractionation due to evaporation is apparent.

The isotopic compositions of Ca-HCO_3 and Ca-SO_4 water type are isotopically different. Recharge in the carbonate aquifer is likely to take place at the contact zones of the dolerite intrusions through faults/fractures.

4 Discussion

Stable isotope and chemical data for the carbonate-dominated aquifer show distinct groundwater types of Ca-HCO_3 fresh water and a higher-mineralized Ca-SO_4 . The spatial distribution of hydrochemical facies infers the carbonate and

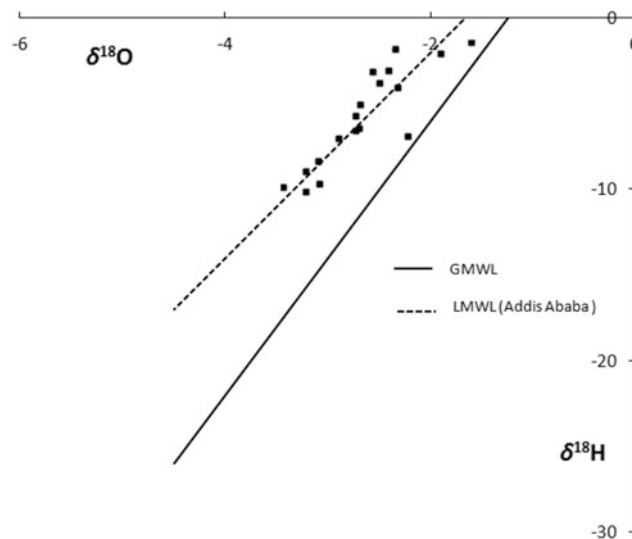


Fig. 2 $\delta^2\text{H}$ versus $\delta^{18}\text{O}$ plot of groundwater samples

gypsum dissolution. Nevertheless, dissolution is not the only factor, as the residence time of the water within the aquifer determines the concentrations of dissolved ions. At places, the short residence time in the fractured aquifers leads to lower dissolved ions. It is found that high permeabilities in the carbonate aquifer allow a rapid recharge and circulation of groundwater that result in low dissolution and low concentration of ions [3]. At the contact zones between sedimentary rocks and the dolerite dikes, water percolates fast along interconnected fractures [4]. The dissolved ions are expected to increase significantly with depth in the area where vertical groundwater flow is limited [1]. The occurrence and flow of groundwater in the upper sedimentary section are low because of the shale-dominated lithology [4]. Consequently, groundwater that occurs under confined and semi-confined conditions, along the bedding planes and in weathered zones, is often characterized by a better water quality.

The results are consistent with isotope data of $\delta^2\text{H}$ and $\delta^{18}\text{O}$. While confined and semi-confined aquifers are exposed to evaporation, deeper groundwater gets locally recharged through the deep-seated fractures [4].

5 Conclusions

The results indicate that the chemical composition of groundwater is controlled not only by the water-rock interaction of the aquifers, but also by the resident time. It is

noted that groundwaters recharged mainly along the fracture zones, exhibiting relatively lower dissolved ions, whereas the presence of shale-dominated lithology increases mineralization. The degree of hydrochemical evolution is largely determined by the residence time of the water within the aquifer. The isotopic compositions of $\delta^2\text{H}$ and $\delta^{18}\text{O}$ depict local precipitation as a source for groundwater and the heavier isotope implies the effect of secondary fractionation by evaporation prior to infiltration.

References

1. Gebreyohannes, T.: Regional groundwater flow modeling of the Geba basin, northern Ethiopia. Ph.D. Thesis, Vrije Universiteit, Brussel Belgium (2009)
2. Gebreyohannes, T., Smedt, F., Walraevens, K., Gebresilassie, S., Hussien, A., Hagos, M., Amare, A., Deckers, J., Gebrehiwot, K.: Regional groundwater flow modeling of the Geba basin, northern Ethiopia. *Hydrogeol. J.* **25**(3), 639–655 (2017)
3. Hailu, H.: Hydrogeochemistry of groundwater in Mekelle and its surrounding area. Master Thesis, Addis Ababa University, Ethiopia (2010)
4. Girmay, E., Ayenew, T., Kebede, S., Alene, M., Wöhnlich, S., Wisotzky, F.: Conceptual groundwater flow model of the Mekelle Paleozoic-Mesozoic sedimentary outlier and surroundings (northern Ethiopia) using environmental isotopes and dissolved ions. *Hydrogeol. J.* **23**(4), 649–672 (2015)

Chlorine Geochemical and Isotopic ($^{37}\text{Cl}/^{35}\text{Cl}$) Signatures of CO_2 -Rich Mineral Waters (N-Portugal): Revisited

José Manuel Marques, Hans Eggenkamp, Paula M. Carreira, and Manuel Antunes da Silva

Abstract

The CO_2 -rich mineral waters from Vilarelho da Raia, Chaves, Vidago and Pedras Salgadas region (N-Portugal) were analyzed for $^{37}\text{Cl}/^{35}\text{Cl}$, Cl and other major elements. Local rain and shallow cold dilute waters were also studied. The main objective of this study was to use Cl geochemical signatures together with Cl isotope geochemistry to improve our knowledge on the origin of Cl in the hot ($\approx 76^\circ\text{C}$) and cold ($\approx 16^\circ\text{C}$) $\text{Na-HCO}_3\text{-CO}_2$ -rich mineral waters that discharge in the region. Chlorine, a good tracer of water-rock interaction, presents a strong correlation with sodium (dominant cation) indicating that Cl^- present in the mineral waters originates from water-granitic rock interaction. $\delta^{37}\text{Cl}$ isotope signatures indicate that i) $^{37}\text{Cl}/^{35}\text{Cl}$ in the studied mineral waters can also be explained by water-granitic rock interaction and ii) the contribution of a deep-seated (upper-mantle) Cl component should not be excluded.

Keywords

Geochemistry • Isotopes • Sources of Cl • CO_2 -rich mineral waters • N-Portugal

J. M. Marques (✉)

Centro de Recursos Naturais e Ambiente, Instituto Superior Técnico (CERENA/IST), Universidade de Lisboa, Av. Rovisco Pais, 1049-001 Lisbon, Portugal
e-mail: jose.marques@tecnico.ulisboa.pt

H. Eggenkamp

FB Geowissenschaften, Mathematisch-Naturwissenschaftliche Fakultät, Universität Tübingen, Wilhelmstraße 56, 72074 Tübingen, Germany

P. M. Carreira

Centro de Ciências e Tecnologias Nucleares, Instituto Superior Técnico (C2TN/IST), Universidade de Lisboa, Estrada Nacional 10, km 139,7, 2695-066 Bobadela LRS, Portugal

M. Antunes da Silva

Super Bock Group, Apartado 1044, 4466-955 S. Mamede da Infesta, Portugal

1 Introduction

Chlorine has two stable isotopes with the following abundances: $^{35}\text{Cl} = 75.53\%$ and $^{37}\text{Cl} = 24.47\%$. The $^{37}\text{Cl}/^{35}\text{Cl}$ ratio is expressed in the δ notation ($\delta^{37}\text{Cl}$) as per mil (‰) relative to SMOC—Standard Mean Ocean Chlorine (e.g., [1, 2]). Chloride is found in small amounts (1000–10,000 ppm) in some silicate and phosphate minerals, usually found in different minerals from the granitic rocks, including biotite, amphibole and apatite (e.g., [3]).

The CO_2 -rich mineral waters from the Vilarelho da Raia, Chaves, Vidago and Pedras Salgadas region, N-Portugal (Fig. 1), have been widely studied (e.g., [4, 5]), indicating an upper mantle source for the CO_2 . The aim of this study is to enhance the role of chlorine geochemical and isotopic signatures as important tools to identify the source of Cl in these hot and cold CO_2 -rich mineral waters.

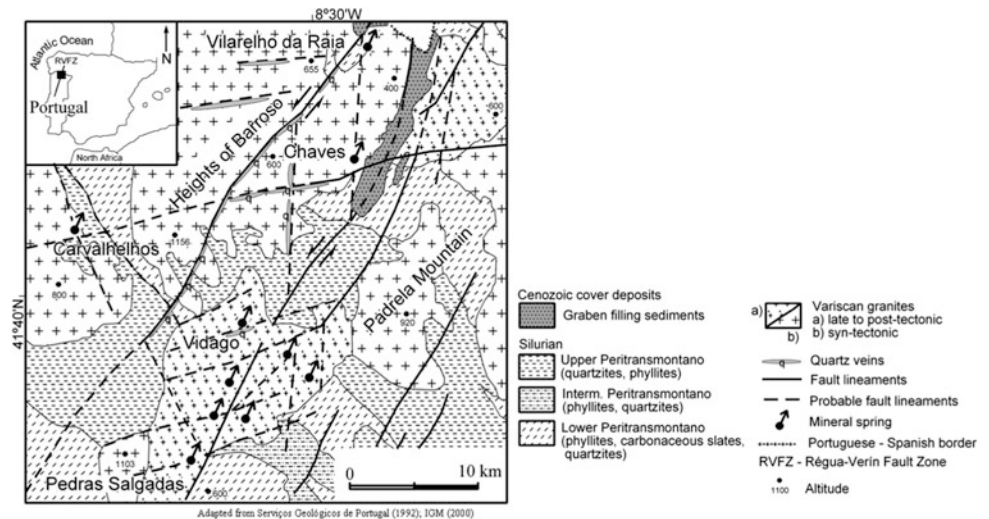
2 Geological and Tectonic Background

The study region, situated in the Central-Iberian Zone of the Hesperic Massif [5], is dominated by the Chaves depression, a graben whose axis is oriented NNE-SSW [4] (Fig. 1). The geology is mainly composed by Hercynian granites and Silurian metasediments—quartzites, phyllites and carbonaceous slates (e.g., [4–6]).

3 Results

The studied mineral waters belong to the bicarbonate-sodium type ($\text{HCO}_3^- > \text{Cl}^- > \text{SO}_4^{2-}$ and $\text{Ca}^{2+} > \text{Mg}^{2+}$) [7]. The $^{37}\text{Cl}/^{35}\text{Cl}$ ratios (vs. SMOC) were determined, by mass spectrometry, at the Geochemistry Department of Utrecht University following the methodology described by [2, 5]. The spectrum of $\delta^{37}\text{Cl}$ values in the studied CO_2 -rich mineral waters (between -0.31 and $+0.31$ ‰) is reasonably similar to

Fig. 1 Schematic geological map of the Vilarelho da Raia-Pedras Salgadas region. Adapted from [5]



the $\delta^{37}\text{Cl}$ values found in the regional shallow cold dilute groundwaters ($-0.32\text{‰} < \delta^{37}\text{Cl} < +0.49\text{‰}$). With respect to rainwaters, it should be noted that the Cl concentrations are very low (2.2 mg/L and 3.6 mg/L in Pedras Salgadas and Vidago areas, respectively), which makes it difficult to determine the $^{37}\text{Cl}/^{35}\text{Cl}$ ratios.

4 Discussion

The mineralization of the CO_2 -rich mineral waters is strongly controlled by HCO_3^- and Na^+ , indicating that water-rock interaction is dominated by the hydrolysis of the Na-plagioclases of the granitic rocks [4, 5] (see Fig. 2). By observing Fig. 2, we can formulate the hypothesis that Cl^- present in the mineral waters is also the result of water-rock interaction, since the increase in Na^+ concentration in the mineral waters is accompanied by an increase of Cl^- .

In a first approximation, $\delta^{37}\text{Cl}$ of the studied mineral waters can be explained by a water-rock interaction in a granite-dominated environment, where biotite (as well as

other minerals with chlorine) usually shows variable $\delta^{37}\text{Cl}$ values (see [9]). Nevertheless, in the case of Vidago mineral waters, it is possible to delineate a slight tendency of depletion in heavy isotopes associated with an increase in chlorine concentration (represented by the dashed line of Fig. 3). This trend seems to indicate a possible deep-seated (upper mantle) source for Cl.

As concluded by [10], there is a good correlation between CO_2 and Cl^- content in Vidago CO_2 -rich mineral waters.

5 Concluding Remarks

In the present study, a special emphasis was put on Cl chemical and isotopic signatures in mineral waters. The Cl^- concentrations and the $\delta^{37}\text{Cl}$ values ascribed to the studied CO_2 -rich mineral waters indicate two possible origins for the Cl^- : water-granitic rock interaction and/or a deep-seated (upper mantle) source. This study heightens the fact that chlorine geochemical and isotopic signatures of groundwaters should be faced as powerful hydrogeological tools to

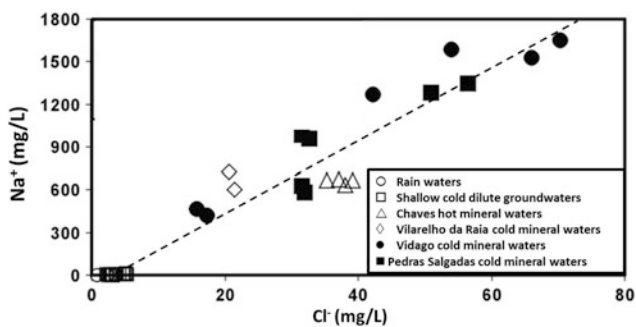


Fig. 2 Cl^- versus Na^+ diagram ascribed to the studied waters. The dashed line stands for a concentration trend from the dilute groundwaters to the high mineralized waters. Data from [5, 8]

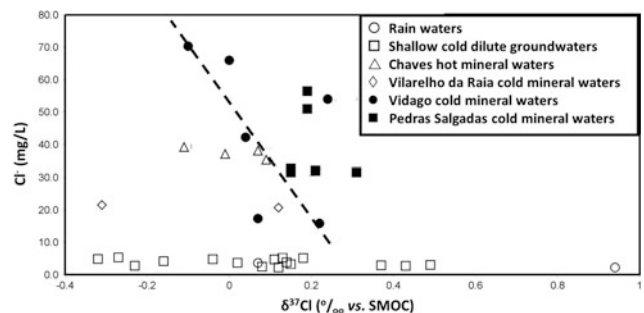


Fig. 3 Cl as a function of the $\delta^{37}\text{Cl}$ values for the waters under study. Data from [5, 8]

assess the source of salinity of deep groundwaters percolating granitic rocks.

Acknowledgements This work was funded by the PRAXIS Project “FLUMIRE” under the Contract No. C/CTE/11004/98. CERENA/IST acknowledges the FCT (the Portuguese Science and Technology Foundation) support through the UID/ECI/04028/2013 Project and C²TN/IST author gratefully acknowledge the FCT support through the UID/Multi/04349/2013 Project.

References

1. Kaufmann, R.S. Chlorine in ground water: Stable isotope distribution. PhD thesis, The University of Arizona, Tucson (1984)
2. Eggenkamp, H.G.M.: The Geochemistry of Stable Chlorine and Bromine Isotopes. Springer, Berlin (2014)
3. Kamineni, D.C.: Halogen-bearing minerals in plutonic rocks: A possible source of chlorine in saline groundwater in the Canadian Shield. In: Fritz, P., Frape, S.K. (eds.) Saline Water and Gases in Crystalline Rocks, vol. 33, pp. 69–80. Geological Association of Canada Special Paper (1987)
4. Aires-Barros, L., Marques, J.M., Graça, R.C., Matias, M.J., Weijden, C.H. van Der, Kreulen, R., Eggenkamp, H.G.M.: Hot and cold CO₂-rich mineral waters in Chaves geo-thermal area (Northern Portugal). *Geothermics* **27**(1), 89–107 (1998)
5. Marques, J.M., Andrade, M., Carreira, P.M., Eggenkamp, H.G.M., Graça, R.C., Aires-Barros, L., Antunes da Silva, M.: Chemical and isotopic signatures of HCO₃/Na/CO₂-rich geofluids, North Portugal. *Geofluids* **6**, 273–287 (2006)
6. Portugal Ferreira, M., Sousa Oliveira, A., Trota, A.N.: Chaves geothermal pole. Geological Survey, I and II. Joule I Program, DGXII, CEE. UTAD—Universidade de Trás-os-Montes e Alto Douro, Internal Report (1992)
7. Eggenkamp, H.G.M., Marques, J.M.: A comparison of mineral water classification techniques: occurrence and distribution of different water types in Portugal (including Madeira and the Azores). *J. Geochem. Explor.* **132**, 125–139 (2013)
8. Andrade, M.P.L.: Isotopic geochemistry and thermomineral waters. Contribution of Sr (87Sr/86Sr) and Cl (37Cl/35Cl) isotopes to the elaboration of circulation models. The case of some CO₂-rich waters from N Portugal. Dissertation, MSc Thesis, Technical University of Lisbon, Instituto Superior Técnico (in Portuguese with English abstract) (2003)
9. Frape, S.K., Bryant, G., Durance, P., Ropchan, J.C., Doupe, J., Blomquist, R., Nissinen, P., Kaija, J.: The source of stable chlorine isotopic signatures in groundwaters from crystalline shielded rocks. In: Arehart, G.B., Hulston, J.R. (eds.) Water-Rock Interaction, pp. 223–226. Balkema, Rotterdam (1998)
10. Torgal, M.C.L.: Modelação Estatística das Águas Gasocarbónicas de Vidago e Pedras Salgadas. Dissertation for the Master’s Degree in Georesources. Instituto Superior Técnico. Universidade Técnica de Lisboa (in Portuguese with English abstract) (2000)

Relation Between Water Level Fluctuation and Variation in Fluoride Concentration in Groundwater—A Case Study from Hard Rock Aquifer of Telangana, India

Ankita Chatterjee, Md. Arshad, Adrien Selles, and Shakeel Ahmed

Abstract

In this study, groundwater level and fluoride data of fifteen years (from 2003 to 2017) have been used to identify the influence of water level and its fluctuation on the variation of fluoride (F^-) concentration in groundwater. For this purpose, five locations have been chosen along the groundwater flow direction and amongst these locations, two locations are situated at or near the recharge area, having F^- concentration below 1.5 mg/l (most of the time), two other locations are situated around the discharge area, having F^- concentration above 1.5 mg/l (most of the time). At the transitional location between recharge and discharge, F^- concentration went above or below 1.5 mg/l in a proportional way. The time series plot of the water level and F^- concentration at each location show that the addition of freshwater during monsoon generally dilutes F concentration in groundwater. The positive relation between water level fluctuation and fluctuation in F^- concentration also reflects that fluoride release in groundwater is mostly due to water-rock interaction. The average fluctuation in F^- concentration increases along the flow line, which reflects more water-rock interaction in the discharge area than in the recharge area. The points in the discharge area showed the highest water level fluctuation, fluctuation in F^- concentration and the highest hydraulic conductivity.

Keywords

Fluoride • Water level • Fluctuation • Telangana

1 Introduction

Several studies have documented the general characteristics of fluoride in groundwater, like the fluoridated area must have the presence of crystalline basement rocks/volcanic bedrocks that contain most of the fluoride-containing minerals. Fluoride comes to groundwater through an anion exchange or the dissolution of minerals. The fluoride accumulation further promoted by calcium (Ca^{2+}) deficient sodium (Na^+)—bicarbonate (HCO_3^-) type groundwater, long residence time of groundwater, strong evapotranspiration in a semi-arid/arid climate [1, 4, 7]. But very few studies have documented [2] the influence of hydraulic properties (water level, hydraulic conductivity) on the behavior of fluoride in groundwater. Therefore, this study is conducted only for fifteen years water level and F^- concentration data to understand the effect of water level fluctuation on fluoride occurrence and its behaviour in the aquifer. Hydraulic conductivity of the aquifer is also considered to get an idea about the fracture network and its influence on F^- concentration.

2 Methodology

The study area (Maheshwaram watershed) is situated in the Ranga Reddy district of Telangana, at a distance of about 35 km from Hyderabad. The watershed has an area of 53 km². The study area is situated between longitude 78° 24' 30"E–78° 29' 00"E and latitude 17° 06' 20"N–17° 11' 00"N. The laminated saprolite and the fissured layer together form the two-tier aquifer system in this region and they coexist almost in the entire area [6]. The methodologies of groundwater level and sample collection from the field

A. Chatterjee (✉) · S. Ahmed

Academy of Scientific and Innovative Research (AcSIR),
CSIR-National Geophysical Research Institute, Hyderabad,
500007, India

e-mail: ankitachatterjee2589@gmail.com

Md.Arshad

CSIR-National Geophysical Research Institute, Hyderabad,
500007, India

A. Selles

IFCGR, NGRI-BRGM, D3E/NRE, Hyderabad, India

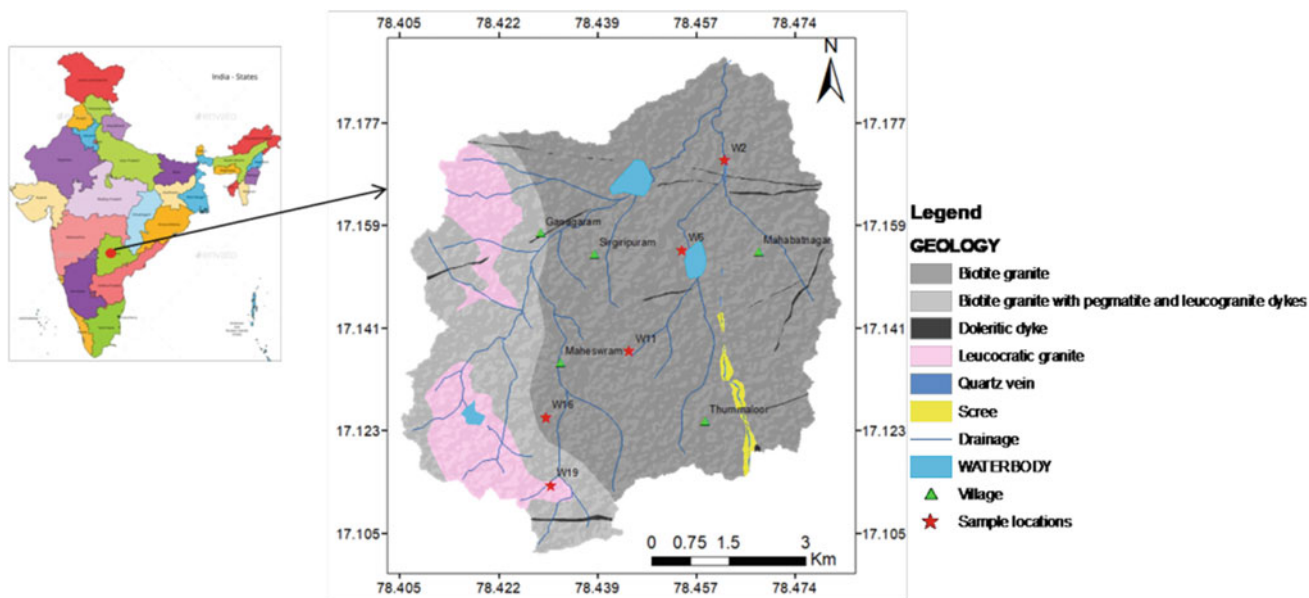


Fig. 1 The study area along with its geology and sample locations

and the analysis of groundwater samples for fluoride are discussed in detail in Chatterjee et al. [3]. Hydraulic conductivities (in meter/second) are obtained by a slug test in the study area [5]. The graphs were prepared in Microsoft excel 2007 (Fig. 1).

3 Results

It is seen from the graph (Fig. 2) that F^- concentration was either 1.5 or below 1.5 mg/l most of the time, at locations W19 and W16 (located around the recharge area or at a high elevation). Whereas, at locations W6 and W2 (located around the discharge area or at a low elevation), most of the time, F^- concentrations were above 1.5 mg/l. However, the location W11, which falls in between the recharge and discharge area, has F^- concentration below or above 1.5 mg/l in a proportional way. The water level ranges from 5 to 30 m, 5 to 27 m and 7 to 24 m at locations W19 and W16, W6 and W2, and W11, respectively, within the time period of 2003–2017. The water level fluctuation, Δh (difference between pre and post-monsoon water level) and the fluctuation of F^- concentration, ΔF (difference between pre and post-monsoon water level) were plotted (Fig. 3) to understand the influence of increase or decrease of water level on F^- concentration. Most of the samples show a positive relation between Δh and ΔF , which indicates that fluoride is released into groundwater

through the rock-water interaction and it generally decreases due to the dilution after the increase of water level.

Moreover, the relations between the hydraulic conductivity (K) of the aquifer, the average Δh and average ΔF (Table 1) show that, near the discharge area, K values are high with higher Δh and ΔF values. This reflects the fact that, if fracture connectivity is good, then during monsoon there will be high recharge into the aquifer which leads to high Δh (as groundwater usage depends on availability) and high recharge dilutes fluoride concentration in groundwater which leads to high ΔF .

4 Conclusions

This study has used groundwater level and fluoride concentration data, and showed that, in this study area, high water level fluctuation is related to high fluctuation in fluoride concentration. However, these high fluctuations are occurring at the discharge area of the watershed, where water gets more time to interact with rocks. Hence, this results in high fluoride in groundwater. Therefore, it can be concluded that high water level fluctuation, high fluctuation in fluoride concentration and high fluoride content are mutually dependent. The discharge area of this watershed needs more attention regarding drinking water sources. Decision makers and planners may implement an alternate drinking water

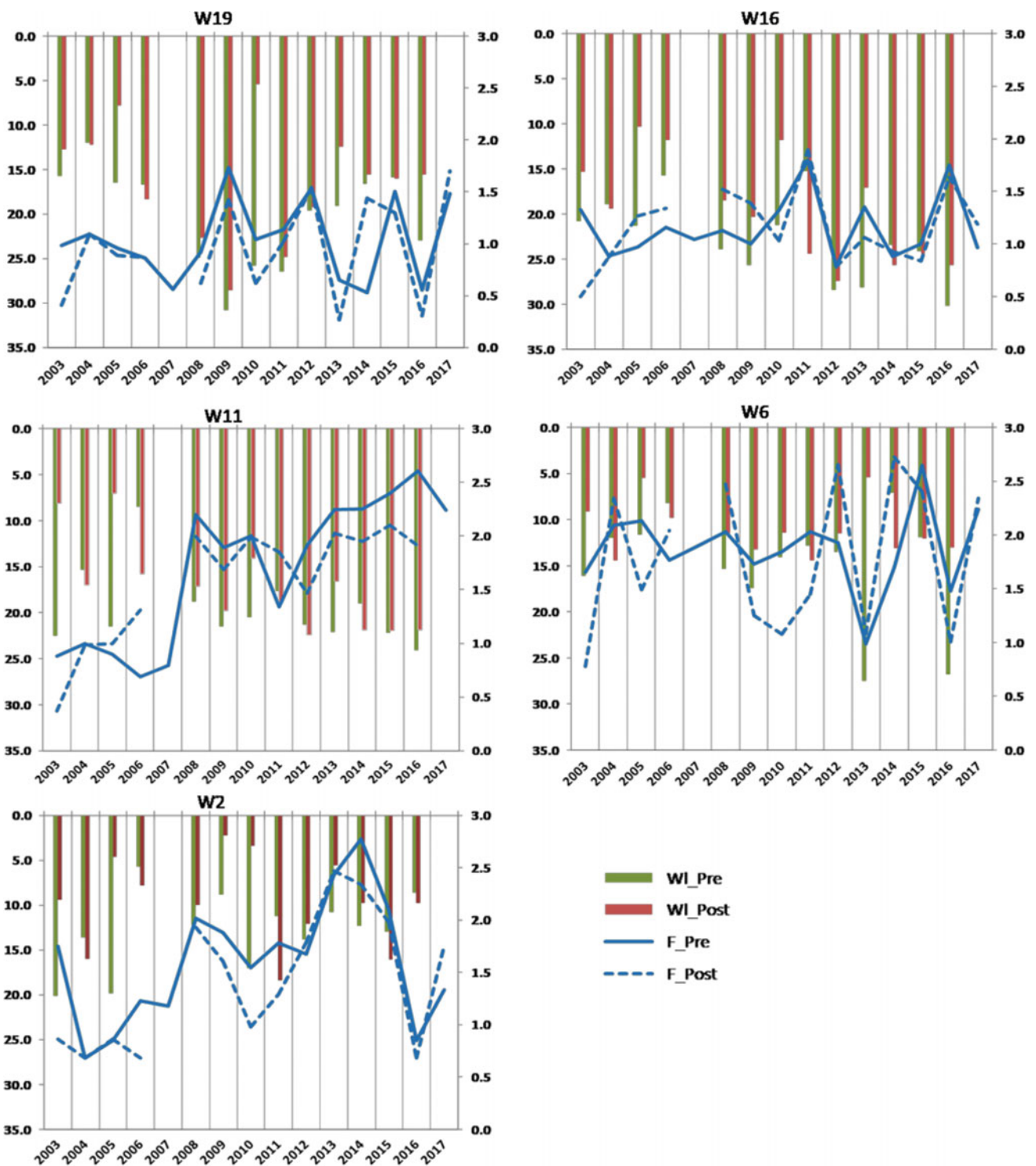


Fig. 2 Time series plot of water level (m) represented along the left y- axis, fluoride concentration (mg/l) represented along right y-axis. Time is given in year along the x-axis. From left to right of the figure represents flow direction

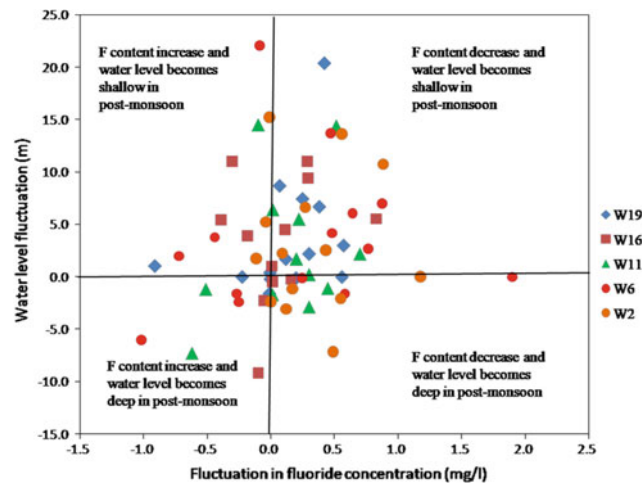


Fig. 3 Relationship between water level fluctuation and fluctuation in fluoride concentration at five locations

Table 1 Table showing relationship amongst hydraulic conductivity (K), water level fluctuation and fluctuation in F concentration

Location	Elevation	K(M/S)	Average Δh	Average ΔF
W19	654	0.313	3	0.29
W16	647	0.432	4.5	0.29
W11	641	0.169	2.8	0.38
W6	614	2.243	6	0.62
W2	601	1.334	5.2	0.39

source for the villagers around the discharge area, as this region has high fluoride content most of the time.

References

1. Apambire, W.B., Boyle, D.R., Michel, F.A.: Geochemistry, genesis, and health implications of fluoriferous groundwaters in the upper regions of Ghana. *Environ. Geol.* **33**(1), 13–24 (1997)
2. Brindha, K., Jagadeshan, G., Kalpana, L., Elango L.: Fluoride in weathered rock aquifers of southern India: managed aquifer recharge for mitigation. *Environ. Sci. Pollut. Res.* **23**(9), 8302–8316 (2016)
3. Chatterjee, A., Sarah, S., Sreedevi, P. D., Selles, A., Ahmed, S.: Demarcation of fluoride vulnerability zones in granitic aquifer, semi-arid region, Telengana, India. *Arab. J. Geosci.* **10**(24), 558 (2017)
4. Handa, B.K.: Geochemistry and genesis of fluoride-containing ground waters in India. *Ground Water* **13**(3), 275–281 (1975)
5. Maréchal, J.C., Dewandel, B., Subrahmanyam, K.: Use of hydraulic tests at different scales to characterize fracture network properties in the weathered-fractured layer of a hard rock aquifer. *Water Resour. Res.* **40**:11 (2004)
6. Maréchal, J.C., Dewandel, B., Ahmed, S., Galeazzi, L., Zaidi, F.K.: Combined estimation of specific yield and natural recharge in a semi-arid groundwater basin with irrigated agriculture. *J. Hydrol.* **329**(1), 281–293(2006)
7. Saxena, V., Ahmed, S.: Dissolution of fluoride in groundwater: a water-rock interaction study. *Environ. Geol.* **40**(9), 1084–1087 (2001)

Cesium and Uranium Radioisotopes Monitoring in Kuwait Bay Seawater

Aishah Alboloushi, Abdulaziz Aba, and Omar Alboloushi

Abstract

Both people and the environment are continuously exposed to sources of radioactivity. Continuous monitoring of the concentration of natural and anthropogenic radioisotopes is of the utmost importance in the estimation of an individual's received dose. In order to evaluate the radiological safety of locally sourced desalinated water and seafood, the activity concentrations of Cesium-137 (^{137}Cs), Uranium-234 (^{234}U), and Uranium-238 (^{238}U) in Kuwait Bay seawater were measured. Ten 25-L seawater samples were collected from Kuwait Bay and underwent radiochemical analysis. ^{137}Cs levels in the samples were determined by the Ammonium Molybdenum Phosphate (AMP) co-precipitation method, followed by gamma spectrometry measurement. ^{234}U and ^{238}U levels were determined by a radiochemical separation using anion exchange chromatography, followed by an alpha spectrometry measurement. The levels of ^{137}Cs , ^{234}U , and ^{238}U in Kuwait Bay are considered low and comparable to other regional marine water levels. These low levels do not pose a radiological hazard of locally sourced desalinated water and seafood consumption. The ratio of $^{234}\text{U}/^{238}\text{U}$ was also calculated in order to investigate the impact of any anthropogenic sources. These data can be considered a baseline reference for any future comparative analysis, especially since some Gulf countries are initiating their first nuclear reactors within the next few years.

Keywords

Radioisotopes • ^{137}Cs , ^{234}U , ^{238}U • AMP co-precipitation • Gamma spectrometry • Anion exchange • Alpha spectrometry • Radiological hazard • $^{234}\text{U}/^{238}\text{U}$ ratio

1 Introduction

The continuous monitoring of the concentration of radionuclides in Kuwait Bay plays a major role in maintaining the radiological safety of the surrounding areas. Knowing the levels of radioactivity present in Kuwait Bay is of particular importance with regard to safety of locally sourced seafood and desalinated water. Establishment of rapid and reliable radiochemical analysis techniques has become a global demand for the protection of public health. Hazards can be classified as chemical or radiological toxicity if the individual is exposed from a moderate to a high level of radiation. ^{234}U and ^{238}U , classified as highly toxic, are naturally existing radioisotopes in the earth's crust with a half-life of 246,000 and 4.47 billion years sequentially. Radioactive uranium decays into a range of daughter isotopes through alpha, beta, and gamma emissions; therefore, it is hazardous to public health if people are exposed to it through food and water [1]. ^{137}Cs is a common product of the fission of ^{235}U in nuclear reactors. It is classified as a mildly toxic element, and it can pose a significant persistent hazard due to its intermediate half-life of 30 years and its single gamma photon with energy of 661.6 keV. ^{137}Cs is an electropositive alkaline metal that can contaminate large volumes of water after nuclear accidents, such as in the Chernobyl disaster [2]. In this study, baseline data of ^{137}Cs , ^{234}U , and ^{238}U in seawater from Kuwait Bay are presented. These data can be considered a baseline reference with a significant importance, especially that Saudi Arabia and UAE have considered activating their own nuclear reactors within the next few years.

A. Alboloushi (✉) · A. Aba · O. Alboloushi
Kuwait Institute for Scientific Research, P.O. Box 24885 Safat,
13109, Kuwait
e-mail: aboloushi@kisir.edu.kw

2 Methods

^{137}Cs analysis is achieved by the adsorption of cesium onto AMP (2 g/L) and adding some known amounts of stable cesium as a carrier, which is CsCl (10 ml of 25 mg/ml solution). Cs-AMP, separated from the sample by gravitational settling and centrifuge of four hours; and then, the precipitation is measured by gamma spectrometry. Determination of ^{234}U and ^{238}U by radiochemistry method includes adsorption of uranium onto 9-N Hydrochloric acid anion exchanger. The known amount of ^{232}U (200 mBq) is added as a radiotracer at the beginning of mineralization. Uranium is directly extracted from 0.5-N Hydrochloric acid-Hydroxyl ammonium chloride solution. Alpha source is prepared by NdF_3 co-precipitation method using 0.1 μm propylene 25 mm diameter resolve filter. The prepared alpha source is counted using alpha spectrometry.

3 Results

The obtained results of ^{137}Cs radioactivity and the associated uncertainty (\pm) in seawater samples are shown in Table 1.

The obtained results of ^{234}U and ^{238}U radioactivity, associated uncertainty (\pm) and $^{234}\text{U}/^{238}\text{U}$ ratio in seawater samples are shown in Table 2.

4 Discussion

According to Table 1, the concentration of ^{137}Cs in seawater varied between 1.0 and 1.51 mBq/L with an average value of 1.24 mBq/L. This range of ^{137}Cs concentration is

comparable to that obtained in the gulf, Arabian Sea, and North Indian Ocean areas (1.6 Bq/m³) [3]. These values can be considered low compared with the recent ^{137}Cs average concentration measured in the Western North Pacific, one year after the Fukushima nuclear accident occurred in March 2011 (3.39 Bq/L) [4]. Obviously, the low data of ^{137}Cs monitored in Kuwait Bay can be attributed to the absence of nuclear applications and incidents in the region.

The concentrations of ^{234}U and ^{238}U in Kuwait Bay seawater are presented in Table 2. Both activity concentrations of ^{234}U and ^{238}U varied from 39 to 50 mBq/L, which are considered relatively low. The obtained results of the uranium concentrations are comparable to the average content in seawater (42 mBq/L ^{238}U) [5]. In addition, the reported concentrations of uranium in eastern Mediterranean seawater were 44 to 68 mBq/L in Lebanon [6], and 36.9–44.5 mBq/L in Syria [7]. The ratio of ^{234}U to ^{238}U in Kuwait Bay seawater is calculated to investigate if there is any natural or anthropogenic variation between both radioisotopes that will lead to a radioactive disequilibrium. The $^{234}\text{U}/^{238}\text{U}$ ratio was found to be more than the unity (1.07 ± 0.017) due to the radionuclide recoil process during alpha decay of ^{238}U [8]. The $^{234}\text{U}/^{238}\text{U}$ ratio is compatible with the $^{234}\text{U}/^{238}\text{U}$ ratio found in Western North Pacific before the Fukushima accident (1.09 ± 0.05) [9]. Conclusively, the near unity value of the $^{234}\text{U}/^{238}\text{U}$ ratio in Kuwait Bay seawater indicates the radioactive equilibrium of Uranium and excludes the release of any anthropogenic uranium sources in Kuwait Bay.

To ensure the quality of the analytical results, the certified reference material, IAEA-Irish Seawater-443, was repeatedly analyzed along with the samples. The obtained results of $^{234}\text{U}/^{238}\text{U}$ ratio in the reference material was 1.1 ± 0.005 which is in agreement with the certified value (1.12 ± 0.005).

Table 1 ^{137}Cs activity concentration (mBq/L)

Sample	^{137}Cs	\pm
1	1.01	0.04
2	1.29	0.05
3	1.36	0.05
4	1.18	0.05
5	1.51	0.06
6	1.31	0.05
7	1.05	0.04
8	1.23	0.05
9	1.23	0.05
10	1.2	0.05

Table 2 ^{234}U , ^{238}U activity concentration (mBq/L) and $^{234}\text{U}/^{238}\text{U}$ ratio

Sample	^{238}U	\pm	^{234}U	\pm	$^{234}\text{U}/^{238}\text{U}$	\pm
1	50	4	48	4.6	0.96	0.016
2	44	3.5	47	3.7	1.07	0.016
3	41	2.4	43	2.6	1.05	0.013
4	42	2.9	48	3.3	1.14	0.007
5	48	3.8	50	4	1.04	0.0095
6	48	3.6	44	4.1	0.91	0.013
7	47	2	48	4.5	1.02	0.014
8	42	4	49	3.1	1.17	0.011
9	40	3.3	43	2.6	1.08	0.013
10	39	4.1	45	3.9	1.15	0.04

5 Conclusions

^{137}Cs , ^{234}U , and ^{238}U activity concentrations in Kuwaiti Bay seawater are considered low and comparable to the regional marine environment. The calculated $^{234}\text{U}/^{238}\text{U}$ ratio confirms that the impact of the anthropogenic sources is neglected. These findings confirm the radiation stability of Kuwait Bay seawater, which reflects radiological safety of locally sourced desalinated water and seafood consumption. These experimentally determined levels of ^{137}Cs , ^{234}U , and ^{238}U will be very beneficial for the radiation monitoring program of the marine environment.

References

- Carter, M.W., Burns, P.: Radiotoxicity Hazard Classification—The Basis and Development of a New List, 2nd version. Australian Government Publishing Service, Australia (1993)
- <https://pubchem.ncbi.nlm.nih.gov/compound/5486527>, last accessed 26/04/2018
- Al-Qaradawi, I., Abdel-Moati, M., Al-Yafei, M.: Radioactivity levels in the marine environment along the Exclusive Economic Zone (EEZ) of Qatar. *Marine Pollut. Bull.* **90**(1–2), 323–329 (2015)
- Men, W., Jianhua, H., Wang, F.: Radioactive status of seawater in the northwest Pacific more than one year after the Fukushima nuclear accident. *Sci. Rep.* **5**, 7757 (2015)
- Monty, C.: UNSCEAR report 2000: sources and effects of ionizing radiation. *J. Radiol. Protect.* **21**(1) (2001)
- http://www.iaea.org/inis/collection/NCLCollectionStore/_Public/45/006/45006761.pdf. Last accessed 24 April 2018
- Mamish, S., Al-Masri, M.S., Durgham, H.: Radioactivity in three species of eastern Mediterranean jellyfish. *J. Environ. Radioactivity* **149**, 1–7 (2015)
- Chabaux, F., Riotte, J., Clauer, N.: Isotopic tracing of the dissolved U fluxes of Himalayan rivers: implications for present and past U budgets of the Ganges–Brahmaputra system. *Geochim. Cosmochim. Acta* **65**(19), 3201–3217 (2001)
- Miyake, Y., Sugimura, Y., Uchida, T.: Ratio $\text{U}^{234}/\text{U}^{238}$ and the uranium concentration in seawater in the western North Pacific. *J. Geophys. Res.* **71** (1966)

Part IV
Groundwater Assessment, Modelling and
Management



Integrating Aeromagnetic and LandsatTM 8 Data for Geologic Features of Igbeti Schist Belt, Southwestern Nigeria: Implication for Groundwater Exploration

Nurudeen Olasunkanmi, Lukman Sunmonu, Moruffdeen Adabanija, Jimoh Ajadi, and Leke Sunday

Abstract

In an attempt to establish the geologic structures in connection with the assessment of groundwater resources within Igbeti crystalline basement complex terrain, Landsat 8 and aeromagnetic data were analysed using various sub-menus of Geographic Information System (GIS) and 2D Fast Fourier transform filters, respectively. Visual and automated models of the landform types and relief, the range of color composition of the Landsat 8 data controlled by the climato-morphogenic processes and alternating positive and negative magnetic anomalies revealed the contrasting lithologic units in the basement rock of the area. Lithologic contacts were developed with a vertical gradient while the linear features decipher the fracture orientation in concordance with a northeast-southwest low gradient trend. The associated groundwater flow direction revealed catchment in the northern, north-western and southern parts of the area and indicated low run off, more infiltration time and better recharge potential for these regions, while zones of high degree indicated otherwise. The hydrology potential for groundwater development in the area should be targeted at geologic deformation.

Keywords

Geologic structures • Groundwater resources • Crystalline basement complex • Landsat 8 • Aeromagnetic

1 Introduction

Igbeti is a sub-urban area in the hard rock terrain of southwestern Nigeria (Fig. 1), generally classified as a poor groundwater potential zone [5, 9] due to its lack of primary porosities and permeability needed to make a good aquifer. Its dwellers do not have access to pipe-borne water supply as a result of economic water shortage; where the government cannot provide the necessary infrastructure to exploit water from rivers and aquifers. They, therefore, rely on shallow hand-dug wells with invariably low yield and susceptibility to pollution. Therefore, for meaningful groundwater exploration surveys in these terrains, the focus is anticipated largely towards delineating geologic structures (such as fractures, faults and weathered parent rocks), which create secondary porosities that may make crystalline rock formations aquiferous and, hence, exploitable as suggested in [1, 4].

2 Materials and Methods

2.1 Data Set

Landsat8 image (Path/Row-191/054) of 15 m resolution and aeromagnetic data of sub-nanotesla resolution scale were obtained from MapMart© and Nigeria Geological Survey Agency (NGSA), respectively. The Landsat image was captured on 4th February, 2014, using the Operational Land Imager (OLI) sensor at 10:03:33 am while the azimuth of the sun was 130.8° and the solar elevation angle at 52.14°, while the aeromagnetic data is part of the acquired dataset of total

N. Olasunkanmi (✉)
Physics and Materials Science Department, Kwara State
University, Malete, Nigeria
e-mail: nurudeen.olasunkanmi@kwasu.edu.ng

L. Sunmonu
Pure and Applied Physics Department, Ladoké Akintola
University of Technology, Ogbomosho, Nigeria

M. Adabanija
Earth Science Department, Ladoké Akintola University of
Technology, Ogbomosho, Nigeria

J. Ajadi
Geology and Mineral Science Department, Kwara State
University, Malete, Nigeria

L. Sunday
Geoscience Research Unit, West African Geo-Mining Systems,
Lagos, Nigeria

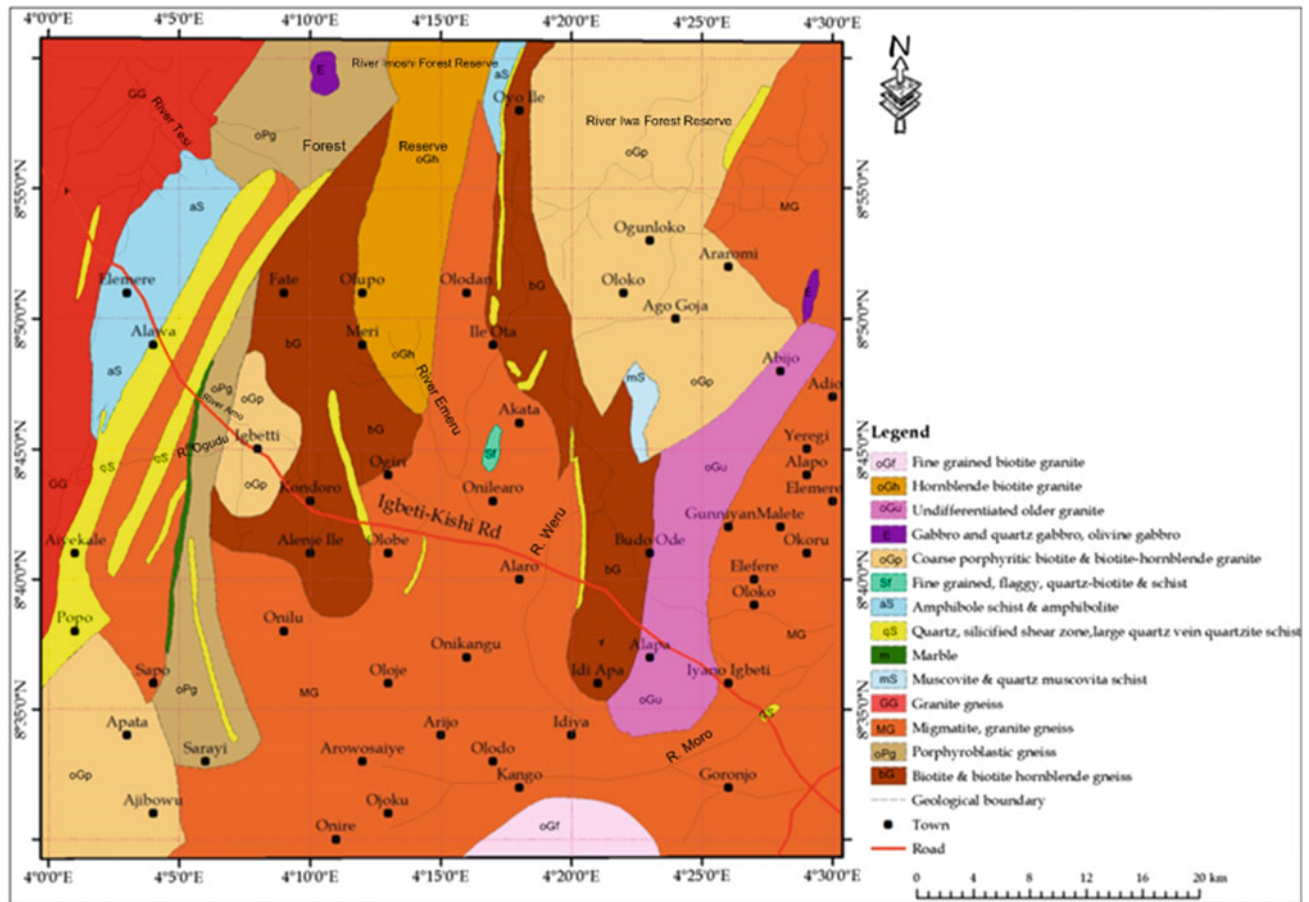


Fig. 1 Geological map of the area showing the major geological components

field magnetic intensity for Nigeria Geological Survey Agency (NGSA) between 2003 and 2009.

2.2 Data Processing

Elevation model (DEM) was digitally manipulated to produce thematic layers that include land-use, topography, slope maps and drainage network systems. Principal component analysis (PCA) and band combination were applied to the Landsat 8 data. The aeromagnetic data was de-cultured, leveled and corrected for international Geomagnetic Reference Field (IGRF) in concordance with [7]. The complex information provided on the TMI map was simplified using reduction to magnetic equator (RTE) as covered in [3]. Then, to improve the data quality that reveals the edges of rocks and structures, a vertical derivative VDR map was developed using the approach of [6].

3 Results

Morphology, roughness and texture relating to each lithology in the enhanced FCC-741 color and RTE residual magnetic anomalies (RMA) within a range of 338.3–208.0 nT are as shown in Fig. 2. The linear features are conspicuous as regions of low magnetic gradient on vertical derivative (VDR) map (Fig. 3a) which were traced on Fig. 3b. Slope map and single band D8 model showing surface and groundwater flow are depicted in Fig. 4.

4 Discussion

The range of color composition of the Landsat image (Fig. 2a) indicated contrasting lithologic units in the basement rock of the area, as corroborated by alternating positive and negative magnetic anomalies, which range between

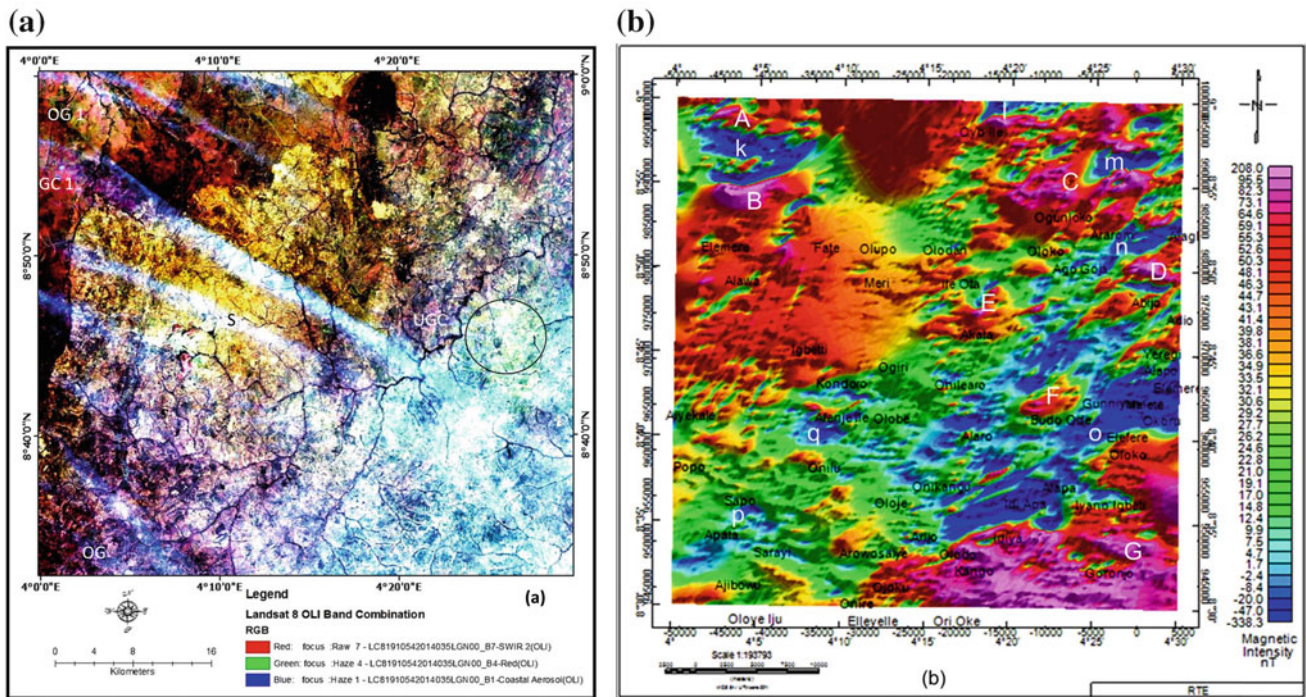


Fig. 2 a Landsat 8 and b RTE-residual magnetic anomaly maps

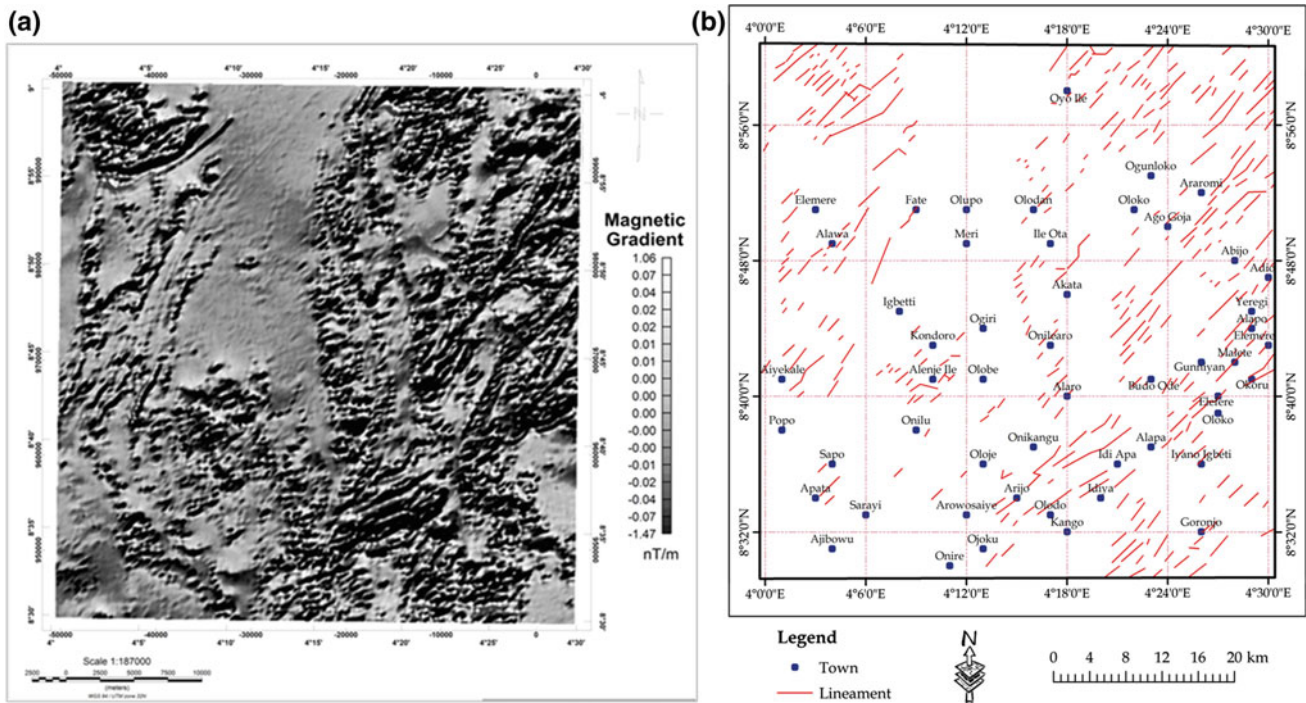


Fig. 3 Structural a VDR and; b lineament maps

-338.3 and 208.0 nT. The low magnetic anomalies coincide with the intrusion of older granitoids (OG) and/or rocks of lower content of ferromagnetic minerals viz, undifferentiated older granite and biotite granite (UGC), while the high

anomalies correspond to the gneiss complex (GC) rocks, which are traversed by intermediate and low magnetic linear features (S). The intermediate magnetic anomaly signatures are interpreted as fractures and/or sheared zone associated

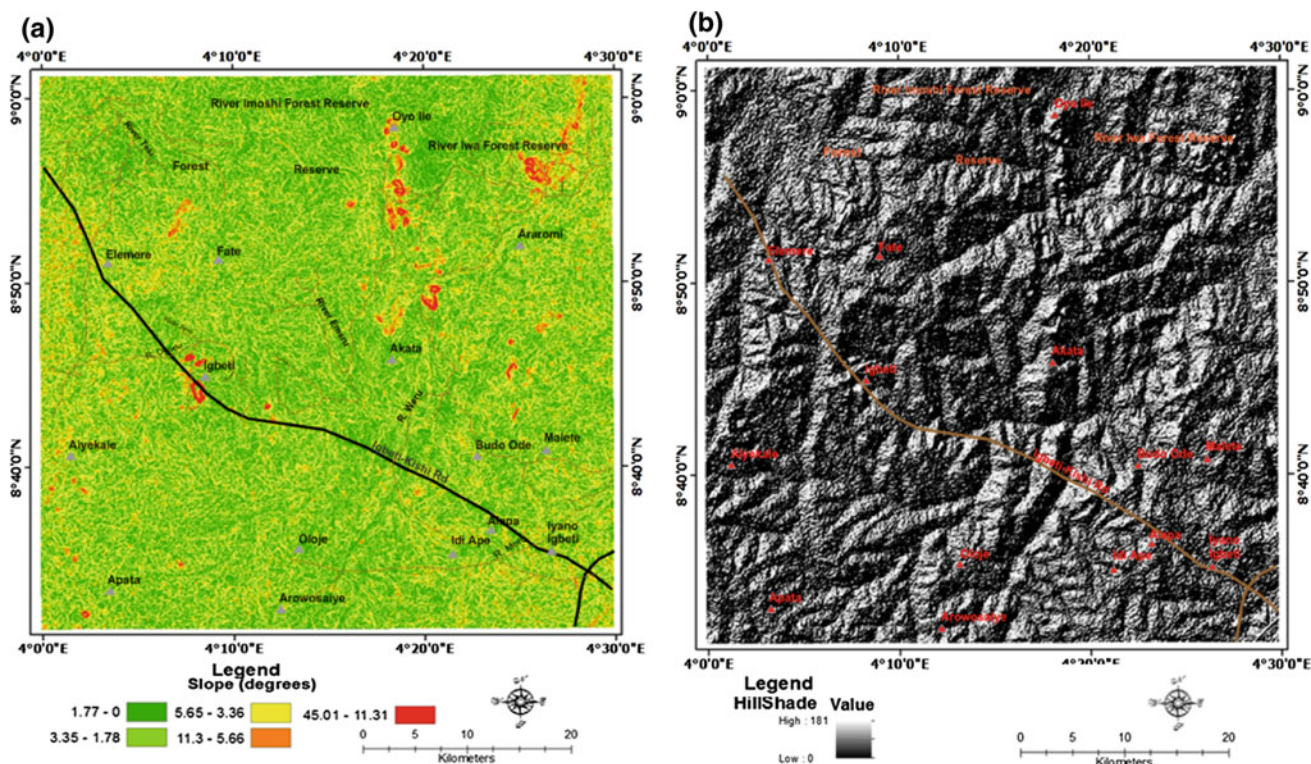


Fig. 4 a Slope and; b D8 drainage maps

with depletion of magnetite [8], and in concordance with predominantly NE–SW trending lineaments, which provided more information on the regional deformation and suggested relict imprints associated with Pan African orogeny [2]. The northeast–south trending low gradient (within 0° – 11.3° ; Fig. 4a) coincides with the fracture trend and drainage direction (Fig. 4b), which attributes to catchment in the northern, northwestern and southern parts of the area.

5 Conclusions

The geomorphology and geologic structures obtained from high resolution Landsat 8 and aeromagnetic data of Igbeti and its environs have deciphered its groundwater prospect. The high degree of fracturing within a low gradient region in the northeastern, north-central and western parts of the area indicates low run-off and better aquifer recharge potential, while zones of high gradient may experience otherwise. The hydrology potential for groundwater development in the area should be targeted at geologic deformation.

References

- Adabanija, M.A., Afolabi, A.O., Olatunbosun, A.T., Kolawole, L. L.: Integrated approach to investigation of occurrence and quality of groundwater in Ogbomosho North, Southwestern Nigeria. *Environ. Earth Sci.* **73**, 139–162 (2015)
- Burke, K.C., Dewey, J.F.: Orogeny in Africa. In: Dessauvage, T.F., Whiteman, A.J. (eds.) *Africa Geology*, pp. 583–608. University of Ibadan Press, Ibadan (1972)
- Foss, C.: Magnetic data enhancement and depth estimation. In: Gupta, H.K.: *Encyclopedia of Solid Earth Geophysics*. Springer Science + Business Media B.V, Berlin (2011)
- Jones, M.J.: The weathered zone aquifers of the basement complex areas of Africa. *Quarter. J. Engineer. Geol.* **18**, 35–46 (1985)
- Nag, S.K.: Application of remote sensing and GIS in groundwater exploration. In: Ahmed, S., Jayakumar, R., Salih, A. (eds.) *Groundwater Dynamics in Hard Rock Aquifer*. Springer, Dordrecht (2008)
- Paananen, M.: Complete lineament interpretation of the Oikiluoto region. Posiva, 2013-02 ISBN 978-951-652-234-3 (2013)
- Patterson, N.R., Reeves, C.V.: Effects of the equatorial electrojet on aeromagnetic data acquisition. *J. Int. Geophys.* **55** (1985)
- Telford, W.M., Geldart, L.P., Sheriff, R.E., Keys, D.A.: *Applied Geophysics*. Cambridge University Press, Cambridge (1990)
- UNESCO.: Groundwater in hard rocks, Project 8.6 of the International Hydrological Programme. Studies and Reports in Hydrology 33, New York, p. 228 (1984)

Remote Sensing and Geographic Information System with Geophysical Resistivity in Groundwater Investigations (West Atbara Basin–River Nile State–Sudan)

Ekhlas H. Ahmed, Wenbo Xu, and Basheer A. Elubid

Abstract

Remote Sensing (RS) data have been widely used in combination with Geographic Information System (GIS) in groundwater resource management. Thus, (GIS) and (RS) integration tools with Geophysical resistivity are proposed to define the groundwater potential zone in the study area. Remotely sensed data of the Landsat 7 ETM+ have been used in this study. Different digital image processing techniques were applied to the satellite images to reveal the geological and hydrological aspects. The Geophysical method used in this study is electrical resistivity Vertical Electrical Sounding (VES), in this case, Schlumberger electrode array was applied. Thirty-four VESs have been conducted in the study area. The interpretation of studied data showed that the area consists of three main aquifer types: Sandstone aquifer (the best one), alluvial deposits (of minor importance) and weathered basement complex aquifer (of lesser concern).

Keywords

Remote sensing • GIS • Geology • Geophysics • Groundwater

E. H. Ahmed (✉) · W. Xu

School of Resources and Environment, University of Electronic Science and Technology of China, Chengdu, 611731, Sichuan, China

e-mail: ekhlasgeo81@yahoo.com

E. H. Ahmed

Ministry of Minerals, Geological Research Authority of Sudan, Khartoum, Sudan

B. A. Elubid

School of Geoscience and Environmental Engineering, Southwest Jiaotong University, High-Tech Zone, Chengdu, 611756, Sichuan, People's Republic of China

B. A. Elubid

Faculty of Petroleum and Minerals, Department of Hydrogeology, Al Neelain University, Khartoum, Sudan

1 Introduction

Remote Sensing data have been widely used in combination with Geographic Information System in groundwater resource management [7]. Groundwater is considered a significant source of water supply for both human consumption and irrigation. About 80% of the inhabitants of Sudan depend on groundwater for their living most of the year [8]. In the northern part of the country, rain rarely falls and the country is mainly desert [4, 9]. This study came as a result of modern information technologies of the RS and GIS linked with Geophysical Resistivity data. Many studies have been conducted around the Atbara basin. The British Geological Survey [3, 10] investigated the source of aquifers' recharge in the lower Atbara River. The geology and structural evolution of the area around the Nile River between Atbara and Abidiya was studied by Ali et al. [1], El Khidir [5] considered the applications of remote sensing and GIS in geological mapping, prospecting for mineral deposits and groundwater in Berber sheet, Northern Sudan. The geological map of the study area had been made based on the Geological map of Sudan, scale 1:2000,000 of the Geological Research Authority of Sudan, GRAS [6], which has been used as raster format with Landsat ETM+ satellite image, while the vector format is the produced geological maps layer such as road, river, settlement and drainage layers.

2 Materials and Methods

2.1 Location and Geology

The study area lies in the Nile River State, between longitudes (35.80° and 34.51°E) and latitudes (17.66° and 16.66°N), Fig. 1. The geological situation of the study area is mainly basement complex (Precambrian Cambrian), Cretaceous sedimentary formation, Olegosin and surface deposits in the

ascending chronological order. The basement complex consists mostly of crystalline rocks categorized by high foliated gneiss outcropping on the western bank of the Nile about 20 km west of the Nile River at the Atbara area and there are some marble outcrops in the area covering some square kilometers [2]. Where the sedimentary rocks of varied lithology and textural grades are cropping out in some localities in the study area, dissected by seasonal streams (e.g., Wadi el Hudi and Wadi el Mukabrab) and this geological unit is associated with a minor unit called Hudi Chert.

3 Results

The Vertical Electrical Sounding (VES) measurements using Schlumberger array were conducted to acquire information about the vertical lithological variations and aquifer depths. A number of 34 VESs had been collected in this study. These VESs have been linked into five profiles, each profile is more than 400 meters in length. The interpretation has been done by using the inversion technique through RES2DINV. Ver.4.08-2018 software to understand the sub-surface lithology, Fig. 2.

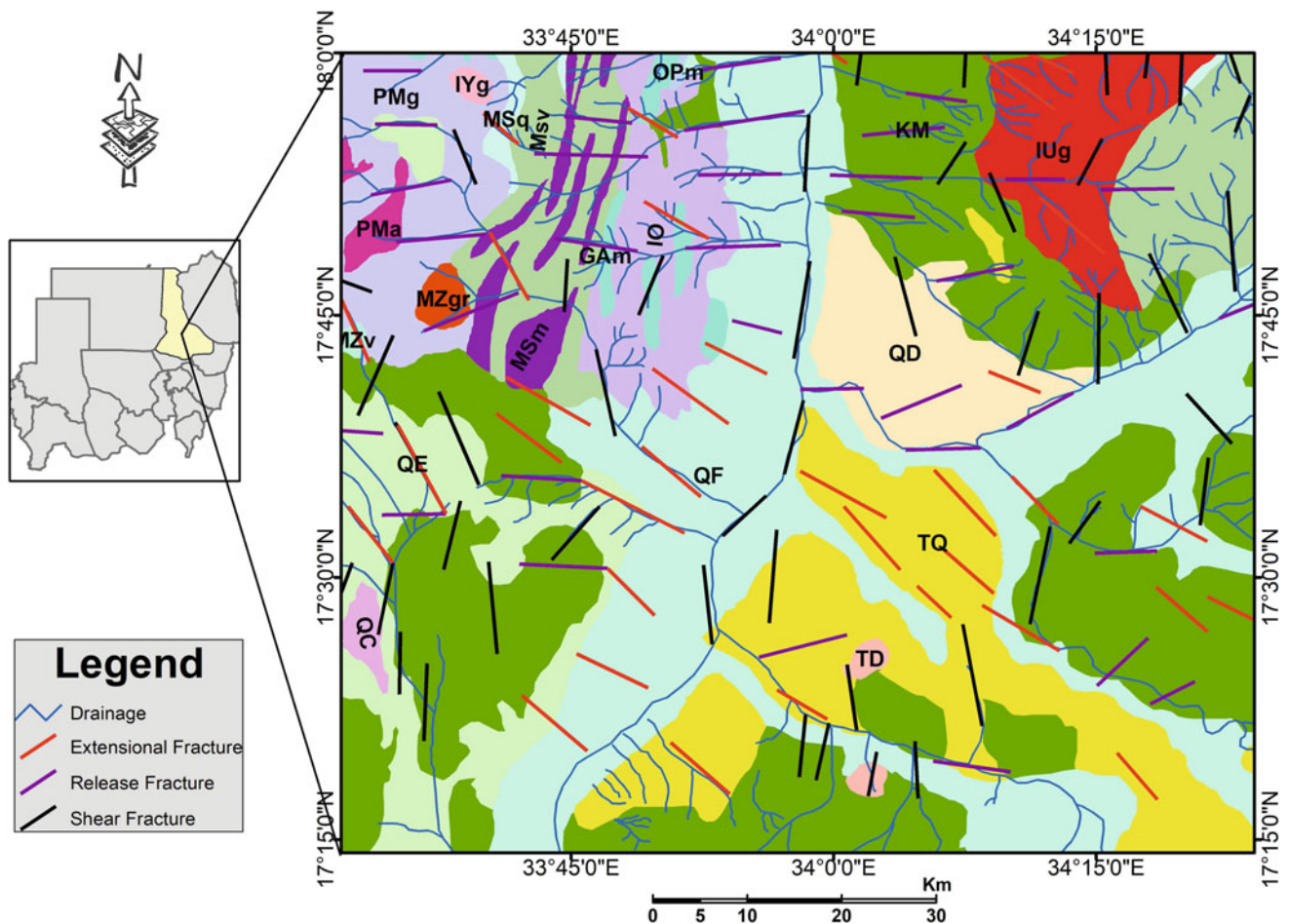


Fig. 1 Location map of the study area and regional geological map of River Nile State modified after [6]. QF: recent alluvial and Wadi deposits, QE: colluvium, sand sheets and amalgamated dunes, QD: older alluviums, raised terraces, younger gravel and sand plains, QC: lacustrine deposits, alluvial fans, dunes and dune fields, TQ: Umm Ruaba Formation: gravel, sand, silt and clay, TD: undifferentiated territory sandstone, Hudi chert, KM: fluvialite sandstone, lacustrine siltstone and mudstone, IYg: Younger granite intrusions, MZgr:

mesozoic intrusive (granitic intrusions), MZv: mesozoic volcanic (acidic volcanic and pyroclastic), IUg: undifferentiated Syn-Late orogenic Granit Intrusions, IO: older granite intrusions, Msv: volcano-sedimentary greenschist assemblage, MSm: meta-sediments: marble, MSq: eta-sediments: Quartzite, OPm: ophiolite: Mafic oceanic upper sequence, Gam: amphibolite (roots of the arc-assemblage), PMg: gneiss (middle proterozoic remobilized continental basement), PMa: amphibolite (Middle Proterozoic remobilized continental)

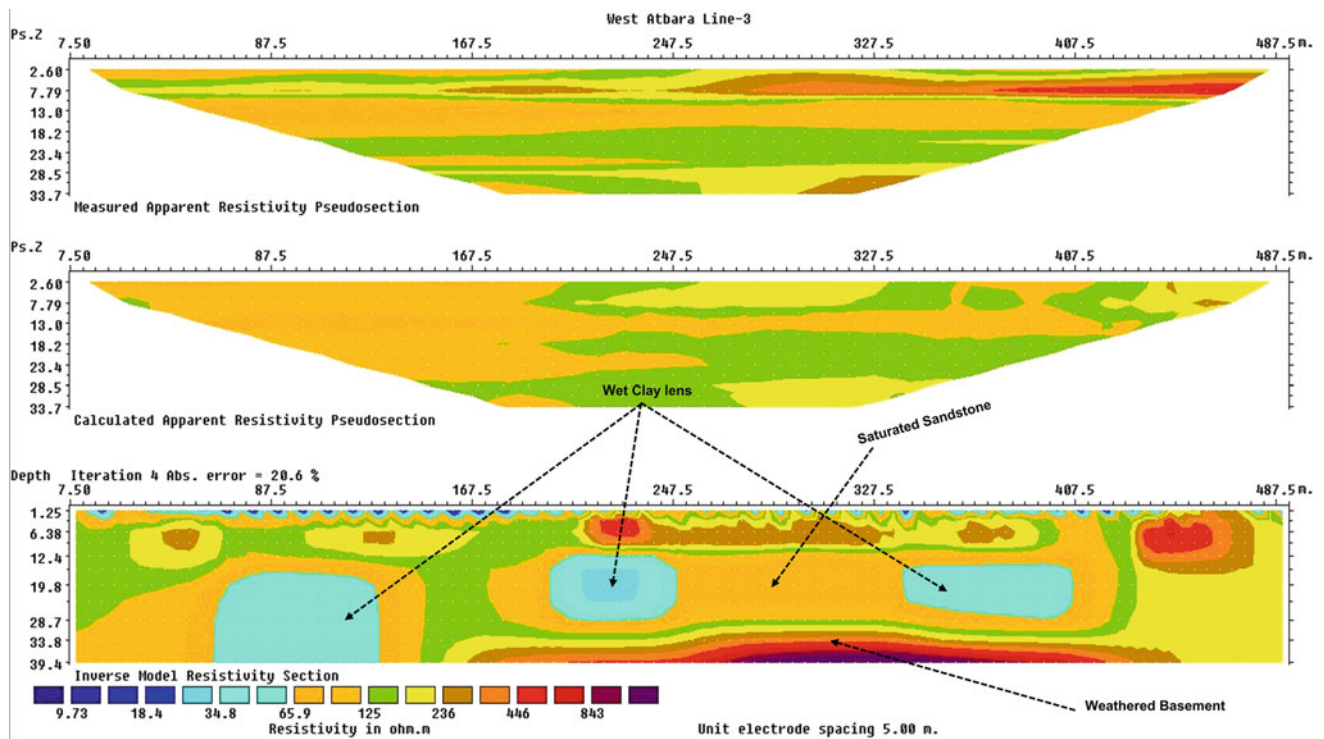


Fig. 2 The result of inversion model of profile 3

With VES configuration, accurate resistivity can be measured up to a depth of 30 m. Most data plotting is characterized by a low resistivity value indicating the existence of conductive material interpreted as wet clay layers, while the moderate amounts are interpreted as saturated sandstone and the high values as weathered Basement.

4 Discussion

The use of RS allows determining the significant lineaments' directions; these are in order of importance as follows: NE-SW (Extensional Fractures), E-W (Release Fractures) and rarely N-S (Shear Fractures), respectively, Fig. 1. In this study, many geological aspects have been used to clarify the final output in the proposed site; enhancement of satellite data using different processing manipulations for the production of a geological map based on visual interpretation of satellite data and other maps.

5 Conclusions

The resistivity image for five meters electrode spacing, Fig. 2, shows that the topsoil layer's resistivity ranges from 9.7 to 236 Ω m, with a thickness of about 4 m. At depth below 4 m, a medium resistivity of 34–65 indicates wet Clay lenses,

and 65–135 shows saturated Sandstone layers with thickness greater than 20 m. A high resistivity zone $> 443 \Omega$ m observed in the image is interpreted as weathered basement.

The applications of GIS and RS are incorporated with Geophysical Resistivity to study the potentiality of groundwater in the area west of Atbara, which has helped to locate potential water-bearing zones.

The interpretation of resistivity data showed that; the area consists of three main aquifer types: (1) Sandstone aquifer is the best one. (2) Alluvial deposits (of minor importance) and (3) Weathered basement complex aquifer (of lesser concern).

The Regional Geological Map around the study area has been modified after [6]. Also, the Lineaments map in the study area has been created by using RS and GIS techniques.

References

1. Ali, E.A., El Khidir, S.O., Babikir, I.A.A., Abdelrahman, E.M.: Landsat ETM+ 7 digital image processing techniques for lithological and structural lineament enhancement: case study around Abidiya area, Sudan. *Open Remote Sensing J.* **5** (2012)
2. Abdelatif, B.: Detection of bacteriological pollution of groundwater in Shendi-atbara Basin, River Nile State, Sudan. *J. Appl. Sci.* **4** (11), 1458–1462 (2008)
3. Edmunds, W., Darling, W., Kinniburgh, D.: Estimation of aquifer recharge using geochemical techniques. Final report of the Lower Atbara River Basin Project (1987)

4. El Gamri, T., Saeed, A.B., Abdalla, A.: Rainfall of the Sudan: characteristics and prediction. *Arts J.* **27**, 18–35 (2009)
5. El Khidir, S.: Remote sensing and GIS applications in geological mapping, prospecting for minerals deposits and groundwater Berber Sheet Area, Northern Sudan. Ph. D., Al Neelain University, Khartoum, Sudan
6. GRAS.: The Geological Research Authority of Sudan, 2004. Geological map of the Sudan, scale 1:2000, 000, Khartoum
7. Jha, M.K., Chowdary, V., Chowdhury, A.: Groundwater assessment in Salboni Block, West Bengal (India) using remote sensing, geographical information system and multi-criteria decision analysis techniques. *Hydrogeol. J.* **18**, 1713–1728 (2010)
8. Mohamed, H.A.E., Elnor, A.E.E.: Assessment of the groundwater industry performance in Sudan. *Sudan J. Sci. Technol.* **2015**(16), 37–42 (2015)
9. Omer, A.: Focus on groundwater in Sudan. *Environ. Geol.* **41**, 972–976 (2002)
10. Thorweihe, U.: Nubian aquifer system. *Geol. Egypt*, 601–614 (1990)

Radar Probing of Subsurface Moisture in Barchan Dunes

Giovanni Scabbia, Essam Heggy, and Abotalib Z. Abotalib

Abstract

Sand sheets and barchan dunes are a dominant landscape feature of the hyper-arid deserts of North Africa and the Arabian Peninsula. The ability to characterize their morphology, moisture content, internal layering and structure provides unique insights into both the local and regional paleoclimatic conditions that prevailed during their formation and development. We constrain the moisture content inside barchan dunes and its association to the dune geomorphology, internal structure and evolution by performing a radar attenuation study at the frequency band from 40 to 150 MHz carried on six barchan dunes in Qatar. Our results suggest that the measured average loss across the dune is $\sim 10\%$ higher than the expected attenuation for dry sand. The inner parts of the dune show higher losses than its outer parts. When compared to laboratory dielectric losses of desiccated sand, our observations suggest that despite the harsh and arid conditions, these aeolian landforms are capable of maintaining a significant amount of moisture arising from the sparse precipitations, several meters deep under their surface. We examine how such moisture content impacts the dunes' dynamics and implications for understanding precipitation variability through the Holocene.

Keywords

GPR • Dunes • Soil moisture • Groundwater and desertification

G. Scabbia
Qatar Environment and Energy Research Institute, Qatar
Foundation, Doha, 34110, Qatar

G. Scabbia · E. Heggy (✉) · A. Z. Abotalib
University of Southern California, Los Angeles, CA 90089-2560,
USA
e-mail: heggy@usc.edu

E. Heggy
NASA Jet Propulsion Laboratory, Pasadena, CA 91109, USA

1 Introduction

Sand dunes cover a large portion of the hyper-arid areas of the Middle East and North Africa (MENA) region. Barchanoid dunes, in particular, are one of the most common surface reliefs in the Great Sahara Desert and in the Rub' al-Khali Desert in the eastern Arabian Peninsula [1]. The internal structure and migration direction and speed are among the most important properties of sand dunes, which are directly related to the climatic and depositional conditions that have formed and continue to shape them [2]. Despite the hot and arid climate, these dunes can trap a relatively high amount of moisture underneath a dry surface layer usually <1 m [3]. The overall moisture content within a dune originates mostly from direct precipitations and air humidity, or could be the trace of the presence of capillary vertical transport of water from a deeper groundwater source. Throughout the MENA region, several shallow aquifer systems occur within unconsolidated Quaternary sands such as the Liwa Aquifer in UAE, the Wahiba Sand Dune Aquifer in Oman, in addition to several small costal sand-dune aquifers along the Mediterranean coast in Morocco, Algeria and Tunisia [4]. These aquifers are often characterized by high productivity and are among the most exploited resources in these arid regions. These groundwater bodies were recharged during wetter climatic periods, while today they rarely receive any significant recharge. Amounts and spatial distribution of the soil moisture that are trapped within the sand dunes profile could be used as a paleoclimatic proxy of the periods of intensified precipitation during the Holocene [1], and hence, could play a significant role in understanding shallow aquifer recharge and the evolution of fresh water lenses in Qatar.

In this study we use a Very High Frequency (VHF) Ground Penetrating Radar (GPR) system to investigate the internal structure of the barchan sand dunes in Qatar and to quantify the additional signal-loss effects due to the moisture within the dunes. The peninsula of Qatar, with its

diverse barchan dune fields that show diverse morphologies and dynamics, represents an ideal case study to understand the characteristics of dune moisture and its effect on their evolutions. Such enhanced understanding of the moisture distribution inside these bodies provides an insight on their potential groundwater dynamics in such area. Moreover, understanding radar characteristics at low frequency for these common desert geomorphological features will also significantly support the ongoing development of airborne and orbital VHF sounders dedicated to large-scale groundwater mapping in hyper-arid areas [5].

2 Site Description and Methodology

Qatar is a hyper-arid region, with a relative atmospheric humidity that can, however, reach up to 90% across the peninsula. The survey sites for this study are located in the Al-Kharrara area, in the central part of the Qatar peninsula (24.91 N, 51.248 E). A full and detailed description of the barchan dunes under study is found in [6], while [7] describes the origin and migration patterns of these landforms.

The GPR data were collected in early November 2016, in the end of the harsh dry season and before the start of the sporadic winter rains. The two closest active meteorological stations are the Al Udeid military base, southwest of Doha (7–15 km from the site), and at the Hamad International Airport of Qatar (30–45 km from the site). While the first station registered only two days with rain (<0.01 inches for less than 6 h) in the period between June and November 2016, the weather station at the Hamad Airport reports a strong thunderstorm cell on the 1st of July, with 2.76 inches of rain over 24 hours [8]. During the summer months, moisture evaporates rapidly due to the average temperature that reaches 34.3 °C and an average maximum daytime temperature up to 41 °C. The average temperature drops to ~20 °C in the winter period, which decreases the potential of moisture evaporation from the inside of the dune.

GPR systems have been widely used to investigate and map the subsurface structure of sedimentary deposits or sand dunes, providing a comprehensive and continuous measurement of the single discrete layers within the ground as well as of the water tables [9]. The main geophysical factors that can limit radar penetration in sand strata are: the moisture variation within the dune, the presence of conductive evaporates, and the lithology of the source rocks [10].

The GPR surveys are conducted with a Cobra Plug-In GPR unit integrated into a SubEcho-70 antenna, both

manufactured by Radarteam Sweden AB. The monostatic antenna is mounted with a broadside direction and the radargram is collected dynamically parallel to the survey line. We collected a total of 15,992 traces over six different profiles of different sand dunes in the same area. We use the same minimal data processing steps for all the GPR profiles to allow for a reliable estimation of the overall loss and to avoid the introduction of processing artifacts in the analysis. The processing steps comprise: (1) dewow filtering, (2) band-pass Butterworth filtering over the 10-dB bandwidth (BW: 40–150 MHz), and (3) average-trace subtraction estimated over the entire GPR profile to remove the direct signal and the ringing effects. Time-depth conversion is approximated by using the average wave speed in the sand dune ($v = 0.169$ m/ns) based on the laboratory dielectric measurement of the samples.

3 Results and Discussion

Among the six different dunes profiled with our VHF GPR system, we present in Fig. 1 an illustrative example of the result obtained in our study. The radargram scan of the windward face of the dune, herein under study, displays a complicated structure of internal layering throughout the whole profile (Fig. 1a). The geophysical interpretation given in Fig. 1b highlights the presence of three different regions: (1) a 1–2-m thick layer of relatively more recent fully-dry sand sheet that covers the dune (yellow area), (2) an area of oblique layering characterized by a non-uniform angle of cross-bedding (green area), and (3) an area of high signal loss (blue area) separated from the upper part by a distinct quasi-horizontal interface. In this inner area reflections from the internal structure are much weaker if compared to the surroundings, which suggests the presence of higher moisture content. The observed complex and inner stratigraphic layering indicates how the wind regimes have mutated in amplitude over the past epoch, as described in [6]. Fig. 1c presents the resulting analysis of the spatial distribution of the overall total attenuation factor inferred from the normalized backscattered signal of the dune-based interface. Finally, Fig. 1d compares the overall inferred signal loss with the average level of dielectric absorption estimated using the results of the laboratory analysis of the dried sand samples. Over most of the dune profile, but in particular in the area 0–70 m, the amount of total loss is above the expected average. Similar results have been obtained for all the other surveyed dunes. This highlights how, even under such arid and harsh climatic conditions, the surveyed dunes capture significant amounts of moisture within them.

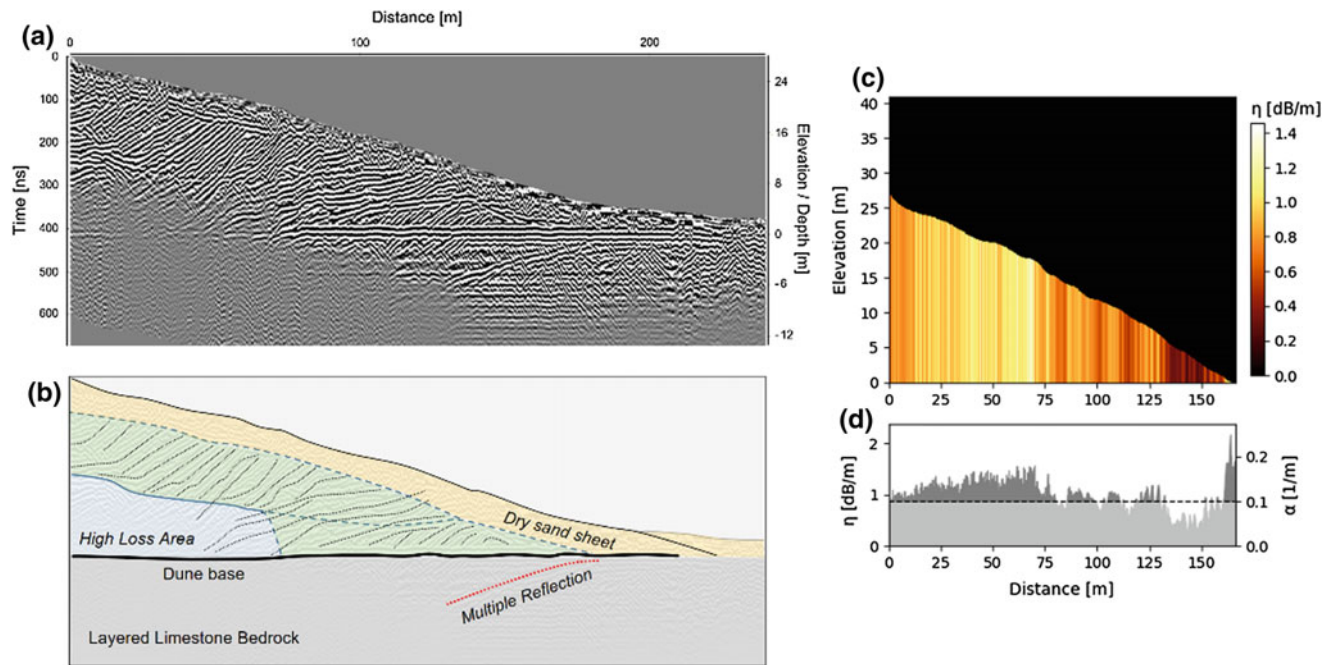


Fig. 1 **a** GPR radargram at 80 MHz (BW: 40–150 MHz) collected over the dune at GPS: 25.037 N, 51.405 E, and graphical interpretation **(b)** showing internal dune layering and areas of low to high signal loss. **c** Overall loss profile inferred from the analysis of the dune-base

backscattered signal for each normalized GPR trace. **d** Comparison between the inferred loss and the average dielectric absorption measured from dried sand samples. The difference is interpreted as increased attenuation due to the dune internal moisture

4 Conclusions

Our results suggest that while the expected attenuation of the measured sand (under dry conditions) should be equal to $\sim 0.863 \text{ dB/m} \pm 0.026$ (at f : 80 MHz), the actual measured average loss results are 0.952 dB/m , with peaks that can reach up to 1.35 dB/m (95th percentile). Our preliminary results indicate that the inner bottom part of the dune forms a vadose zone with an average saturation of $\sim 30\%$, up to a maximum of $\sim 55\%$.

References

- Sharma, P., et al.: Exploring morphology, layering and formation history of linear terrestrial dunes from radar observations: Implications for Titan. *Remote Sens. Environ.* **204**, 296–307 (2018)
- Lancaster, N.: Response of eolian geomorphic systems to minor climate change: examples from the southern Californian deserts. *Geomorphology* **19**(3–4), 333–347 (1997)
- Dincer, T., et al.: Study of the infiltration and recharge through the sand dunes in arid zones with special reference to the stable isotopes and thermonuclear tritium. *J. Hydrol.* **23**(1–2), 79–109 (1974)
- Alsharhan, A.S., et al.: *Hydrogeology of an Arid Region: The Arabian Gulf and Adjoining Areas*. Elsevier, Amsterdam (2001)
- Heggy, E., et al.: Orbiting Arid subsurface and ice sheet sounder (OASIS): exploring desert aquifers and polar ice sheets and their role in current and paleo-climate evolution. In: *IEEE International Geoscience and Remote Sensing Symposium (IGARSS)*, pp. 3483–3486. IEEE (2013)
- Embabi, N.S., Ashour, M.M.: Barchan dunes in Qatar. *J. Arid Environ.* **25**(1), 49–69 (1993)
- Engel, M., et al.: Migration of barchan dunes in Qatar—controls of the 2 Shamal, teleconnections, sea-level changes and 3 human Impact. Preprints (2018)
- NOAA, NNDC Climatic Data OnLine (CDO). Website accessed on May 2018
- Neal, A.: Ground-penetrating radar and its use in sedimentology: principles, problems and progress. *Earth Sci. Rev.* **66**(3), 261–330 (2004). Tatum, D., Francke, J.: Radar suitability in aeolian sand dunes—a global review. In: *2012 14th International Conference on Ground Penetrating Radar (GPR)*, pp. 695–700. IEEE (2012)

2D ERI for Groundwater Exploration in a Crystalline Basement Terrain, Abeokuta, Southwestern Nigeria

Ahzebobor P. Aizebeokhai, Adenifesimi A. Oni, and Kehinde D. Oyeyemi

Abstract

Electrical resistivity imaging (ERI) is widely used for near-surface characterization in geophysical applications for hydrogeological, environmental and engineering investigations. This study involves the application of the two-dimensional (2D) electrical resistivity imaging (ERI) to delineate structures that are suitable for groundwater occurrence in a crystalline basement complex terrain. The dipole-dipole array, which is sensitive to weathered and fractured zones commonly associated with groundwater accumulations in a basement complex, was deployed for the measurements. The survey was conducted to locate possible points for siting productive boreholes in a site at Abeokuta, southwestern Nigeria, as previous boreholes and wells drilled within the study site failed.

Keywords

Near-surface characterization • Groundwater investigations • Basement aquifers • 2D ERI • Southwestern Nigeria

1 Introduction

Groundwater is the main source of water supply in most homes and communities in Nigeria, particularly in rural settlements, as the majority of the surface water sources are polluted due to indiscriminate waste disposal. Most parts of Nigeria are underlain by a crystalline basement complex. Basement aquifers are localized and confined to the weathered and fractured zones and geophysical surveys are conducted to characterise these types of zones. Electrical resistivity is the most common geophysical method for

near-surface characterization in hydrologic investigations [e.g. 1–3], it is traditionally conducted in sounding mode to determine the lithologic layering and/or depth-to-basement based on the assumption that resistivity distribution varies only with depth. Thus, it often produces inaccurate and distorted geologic models in complex geologic environments that are characterised by significant lateral variations [1, 4]. Two-dimensional (2D) and/or three-dimensional (3D) electrical resistivity imaging (ERI) produces more realistic geologic models in such a complex and multi-scale geologic environment. In this study, 2D ERI has been used to delineate the weathered and fractured zones which provide preferential flow paths for groundwater accumulation. Dipole-dipole array, which is one of the most sensitive arrays to such basement features [5, 6], was deployed for the resistivity measurements. The survey was conducted with the aim of locating suitable points for siting productive boreholes and/or wells in a site at Abeokuta, southwestern Nigeria, since the previously drilled ones failed.

2 Site Descriptions and Geological Setting

The study area is located in Abeokuta, southwestern Nigeria. It lies between latitude $7^{\circ}00'–7^{\circ}13'N$ and longitude $3^{\circ}16'–3^{\circ}25'E$. The topography is a lowland and is characterised by sparsely distributed hills and knolls. The mean elevation is about 70 m above mean sea level. The climate is tropical humid, marked by distinct dry (November to March) and rainy (April to October) seasons. The annual mean rainfall is greater than 2300 mm, while monthly temperatures range between $23^{\circ}C$ in July, and $32^{\circ}C$ in February. Abeokuta is drained by the Ogun and Oyan rivers which flow along the strike of the basement rocks. It is underlain by crystalline basement rocks of the Precambrian age. The dominant rocks are biotite garnet gneiss, magmatic augen gneiss and migmatite which are essentially of migmatite-gneiss-granite complex. Figure 1a shows the location and geological map of the study area.

A. P. Aizebeokhai (✉) · A. A. Oni · K. D. Oyeyemi
Applied Geophysics Group, Covenant University, Ota, Nigeria
e-mail: philips.aizebeokhai@covenantuniversity.edu.ng

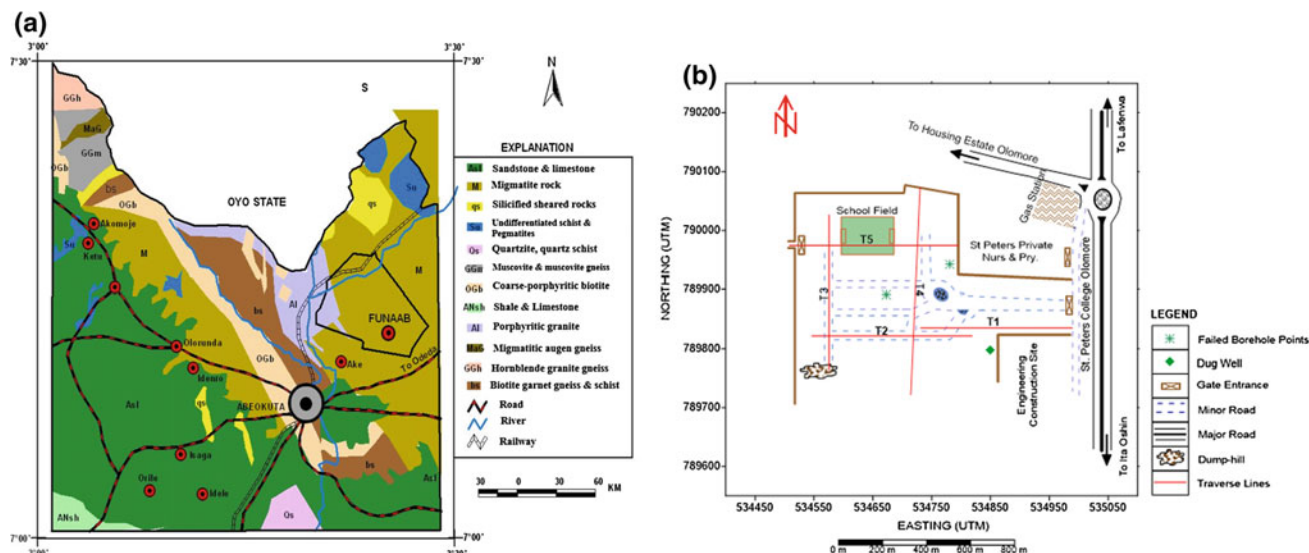


Fig. 1 Study area: **a** location and geological map; **b** base map indicating the 2D ERI traverses

3 Methods

A total of five (5) 2D ERI traverses (Fig. 1b) were conducted in February 2018, with an ABEM (SAS1000/4000) Terrameter, using the dipole-dipole array with a dipole separation factor ranging from 1 to 4. A dipole spacing ranging from 5.0 to 30.0 m was used for the measurements in Traverses 1–3 and 5, while a 10.0 to 50.0 m spacing was used in Traverse 4. Field techniques for the 2D ERI survey have been discussed in several articles [e.g. 7, 8]. The electrode positions were clearly marked and pegged before the commencement of the survey to minimize electrode positioning errors associated with resistivity measurements. Effective contact between the electrodes and ground was ensured while maintaining good connectivity between the electrodes and the connecting cables.

The observed datasets were inverted using RES2DINV inversion code, which uses a nonlinear optimization technique to determine the 2D resistivity distribution [8, 9]. The RES2DINV inversion program subdivides the subsurface into a series of rectangular blocks based on the electrode array and on the spread for the survey. The data sets were inverted using the smoothness constrained least-squares (L_2 -norm) inversion algorithm.

4 Results

The inverse models for the 2D ERI of Traverses 1 and 4 (Fig. 2) are presented as representative resistivity models. Resistivity anomalies that represent the saprolite and the weathered and fractured zones are delineated. The resistivity

inverse models show a general trend in the regolith thickness and basement topography.

5 Discussion

The weathering profile of the crystalline basement rocks consists of the regolith and bedrock. The regolith (collapsed zone and saprolite) is a product of in situ chemical weathering. The bedrock consists of the weathered and fractured basement (saprock), and fresh basement. The saprolite represents decomposed basement rocks with relatively high porosity and permeability that can support groundwater accumulation [10]. These units are identified as distinct resistivity units. Usually, the collapsed zone and bedrock are characterised by high resistivity, while the saprolite (intermediate unit) which forms the main aquifer unit is characterised by relatively low resistivity. In general, storativity of basement aquifers increases with increasing regolith thickness as well as fracture density and connectivity. Thus, groundwater yields increase with increasing regolith thickness, and with higher fracture density and connectivity. The regolith thickness (depth-to-bedrock) delineated is relatively thin, ranging from about 8.0 to 12.0 m. This thickness is inadequate to support sufficient drawdown which allows for moderate-to-high storativity and groundwater yield for productive boreholes and/or wells all year round; however, it can sufficiently support large diameter dug wells. Thus, only zones with significant weathering and fracturing in the saprock should be preferential targets for borehole/well siting, as these zones can potentially support sufficient drawdown for moderate-to-high perennial groundwater yields.

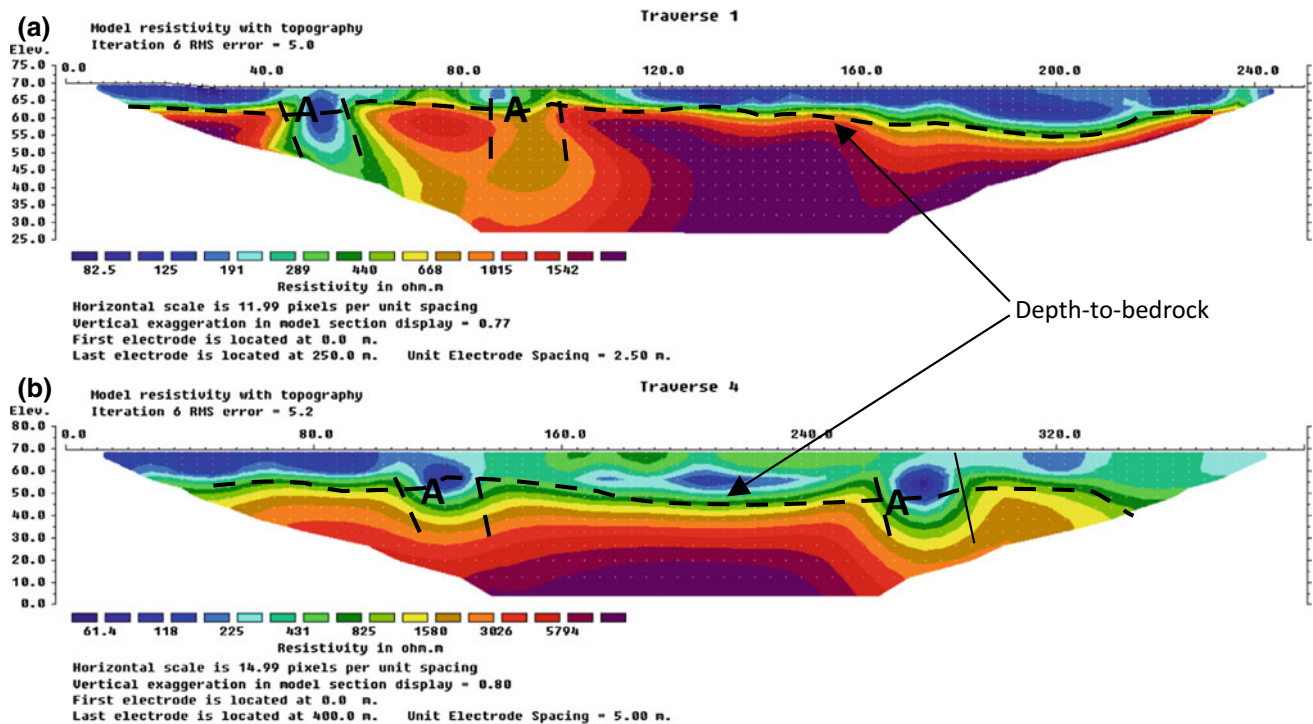


Fig. 2 2D resistivity inverse model for: **a** Traverses 1, and **b** Traverse 4. The regions marked A are weathered and fractured zones

6 Conclusions

The 2D ERI, based on measurements with dipole-dipole array, has been used to characterise the weathering profile developed above crystalline basement rocks in this study. The regolith delineated is relatively thin with a thickness ranging from 8.0 to 12.0 m; this thickness is inadequate to support sufficient drawdown that guarantees moderate-to- high storativity and yield for the development of productive boreholes and/or wells. This may be the reason behind the failure of previous boreholes and wells drilled in the site. Boreholes and/or wells drilled into the weathered and fractured zones would allow for sufficient drawdown that has the potential to support moderate-to- high storativity and yield. Thus, the delineated weathered and fractured zones are recommended for siting borehole and/or well in the site. The dipole-dipole array used for the 2D ERI was able to effectively detect the weathered and fractured zones in the site; hence, the array is effective for characterising near-surface basement structures.

Acknowledgements The authors appreciate Covenant University management for providing conference support for the presentation of this conference paper.

References

1. Aizebeokhai, A.P., Olayinka, A.I., Singh, V.S.: Application of 2D and 3D geoelectrical resistivity imaging for engineering site investigation in a crystalline basement terrain, southwestern Nigeria. *Environ. Earth Sci.* **61**(7), 1481–1492 (2010)
2. Aizebeokhai, A.P., Oyeyemi, K.D.: Geoelectrical characterisation of basement aquifers: the case of Iberekodo, southwestern Nigeria. *Hydrogeol. J.* **26**(2), 651–664 (2018)
3. Loke, M.H., Chambers, J.E., Rucker, D.F., Kuras, O., Wilkinson, P.B.: Recent developments in the direct-current geoelectrical imaging method. *J. Appl. Geophys.* **95**, 135–156 (2013)
4. Pous, J., Queralt, P., Chavez, R.: Lateral and topographic effects in geo-electric soundings. *J. Appl. Geophys.* **35**, 237–248 (1996)
5. Dahlin, T., Zhou, B.: A numerical comparison of 2D resistivity imaging with ten electrode arrays. *Geophys. Prospect.* **52**(5), 379–398 (2004)
6. Wiwattanachang, N., Giao, P.H.: Monitoring crack development in fibre concrete beam by using electrical resistivity imaging. *J. Appl. Geophys.* **75**(2), 294–304 (2011)
7. Aizebeokhai A.P.: 2D and 3D geoelectrical resistivity imaging: theory and field design. *Sci. Res. Essays* **5**(23), 3592–3605 (2010)
8. Loke, M.H., Barker, R.D.: Practical techniques for 3D resistivity surveys and data inversion. *Geophys. Prospect.* **44**, 499–524 (1996)
9. Griffiths, D.H., Barker, R.D.: Two dimensional resistivity imaging and modelling in areas of complex geology. *J. Appl. Geophys.* **29**, 211–226 (1993)
10. Wright, E.P.: The hydrogeology of crystalline basement aquifers in Africa. In: Wright, E.P., Burgess, W.G. (eds.) *Hydrogeology of Crystalline Basement Aquifers in Africa*. Geological Society Special Publications 66, 1–27 (1992)

Geological-Geophysical Investigations for Hydrological Studies in a Basement Complex Terrain, Southwestern Nigeria

Kehinde D. Oyeyemi, Ahzegbobor P. Aizebeokhai, and Oluseun A. Sanuade

Abstract

Geological field mapping and vertical electrical soundings (VES) were conducted in Igbo-Ora, southwestern Nigeria in order to unravel the subsurface structures, as part of the preliminary investigations for groundwater resources assessment, development and management in a crystalline basement terrain, southwestern Nigeria. The geological survey was carried out to produce a local geological map with spatial distributions of different basement rocks and their structural trends. Metamorphic and igneous rocks make up 90 and 10%, respectively, of the rocks in the study area. They include the banded gneiss, biotite granite gneiss, quartzite/quartz-schist and granitic intrusions of varying grain sizes. Twenty-five VES surveys were conducted within the biotite granite gneiss terrain of the area, using Schlumberger array, providing layering and geoelectrical parameters. Three geoelectric layers delineated from the VES 1D inversion models are clayey sand/sandy clay top soil (overburden), partly weathered or fractured basement and fresh basement. The corresponding inverse model resistivity values ranges are: 209.7–2298.0, 45.1–346.2 and 1013.7–33,124.0 Ωm with bottom depths ranges of 0.9–2.9 and 4.6–42.0 m, respectively. The topmost clayey sand/sandy clay layer will serve as the protective layer, while the saturated portion of the partly weathered or fractured basement, at depth, favors groundwater exploration and development in the study area.

Keywords

Geologic field mapping • Basement terrain • Geophysical survey • Groundwater exploration • Southwestern Nigeria

K. D. Oyeyemi (✉) · A. P. Aizebeokhai
Applied Geophysics Unit, College of Science and Technology,
Covenant University, Ota, Nigeria
e-mail: kehinde.oyeyemi@covenantuniversity.edu.ng

O. A. Sanuade
Department of Geosciences, King Fahd University of Petroleum
and Minerals, Dhahran, Saudi Arabia

1 Introduction

The exploration of groundwater is of necessity due to the limitation in the amount of surface water available for domestic, industrial and agricultural use in the face of the continual rise in population and climate change. The successful exploration and exploitation of groundwater within the complex basement aquifers requires a proper understanding of their geohydrological characteristics. Availability of groundwater resources within the complex crystalline basement terrain depends largely on the secondary porosity due to weathering, jointing, and fracturing. Several researches have been carried out on the application of geoelectrical resistivity techniques in the evaluation, exploration and exploitation of groundwater in southwestern Nigeria [1–8]. These geoelectrical resistivity surveys entail the estimation of spatial and/or temporal variability of subsurface electrical properties, which include resistivity, conductivity and dielectric constant [5]. In this research, a geologic constrained geoelectrical method was adopted for subsurface characterization in a crystalline basement terrain for groundwater potential in the study area. The study is directed towards the reduction of the risks associated with dry boreholes drilling as a result of poor groundwater exploitation in a complex basement terrain.

2 Materials and Methods

The location of this study is Temidire village and its environs, Igbo-Ora, Southwestern Nigeria. The area falls within the basement complex of southern Nigeria, which is located in the Dahomeyide section of the pan Africa mobile belt. The geological field mapping involved the systematic study of rock outcrops within the area covering $7^{\circ} 25' - 7^{\circ} 30'$ N latitude and $3^{\circ} 25' - 3^{\circ} 30'$ E longitude within the Abeokuta sheet. The samples of rocks were chipped out for megascopic identification. The orientations (strike and dip) of

various structural features on rock outcrops such as joints, foliations and mineral lineations were measured using compass clinometer and then recorded. Samples of rocks collected from different outcrops were cut into smaller fragments and polished on slides, to make thin sections of rocks that were observed under a petrographic microscope. Twenty-five resistivity soundings were conducted in NS-SW direction (Fig. 1a) with maximum half-current electrode spread (AB/2) of 100 m, sufficient for the anticipated depth of investigation (DOI). The VES points spacing interval is 50 m.

3 Results

The rocks' petrological studies show the outcrops to be banded gneiss, biotite granite gneiss, quartzite and granite in that chronological order (Fig. 1b). Also, the structural features

associated with rocks in the area are joint (trending NE-SW), fault (NEE-SWW), veins and veinlets (NWW-SEE), folds (NWW-SEE) and foliations (NWW-SEE). The geoelectric parameters obtained from the computer iterations of the resistivity soundings are presented in Fig. 1c, d. Three geoelectrical layers were delineated from the iterated curves and presented in Fig. 2. A large consistency of the geoelectric parameters was observed among the VES curves. Based on the local geology of the study area and the available information from the boreholes and hand-dug wells, the delineated layers are: overburden layer (mainly sandy clay units) with model apparent resistivity ranging between 209.7 and 2298.0 Ω m, with a thickness range of 0.9–2.9 m; intercalation of partly weathered and fractured basements with model resistivity range of 45.1–346.2 Ω m, with a thickness range of 4.6–42.0 m; fresh basement with model resistivity ranging from 1013.7 to 33,124.0 Ω m.

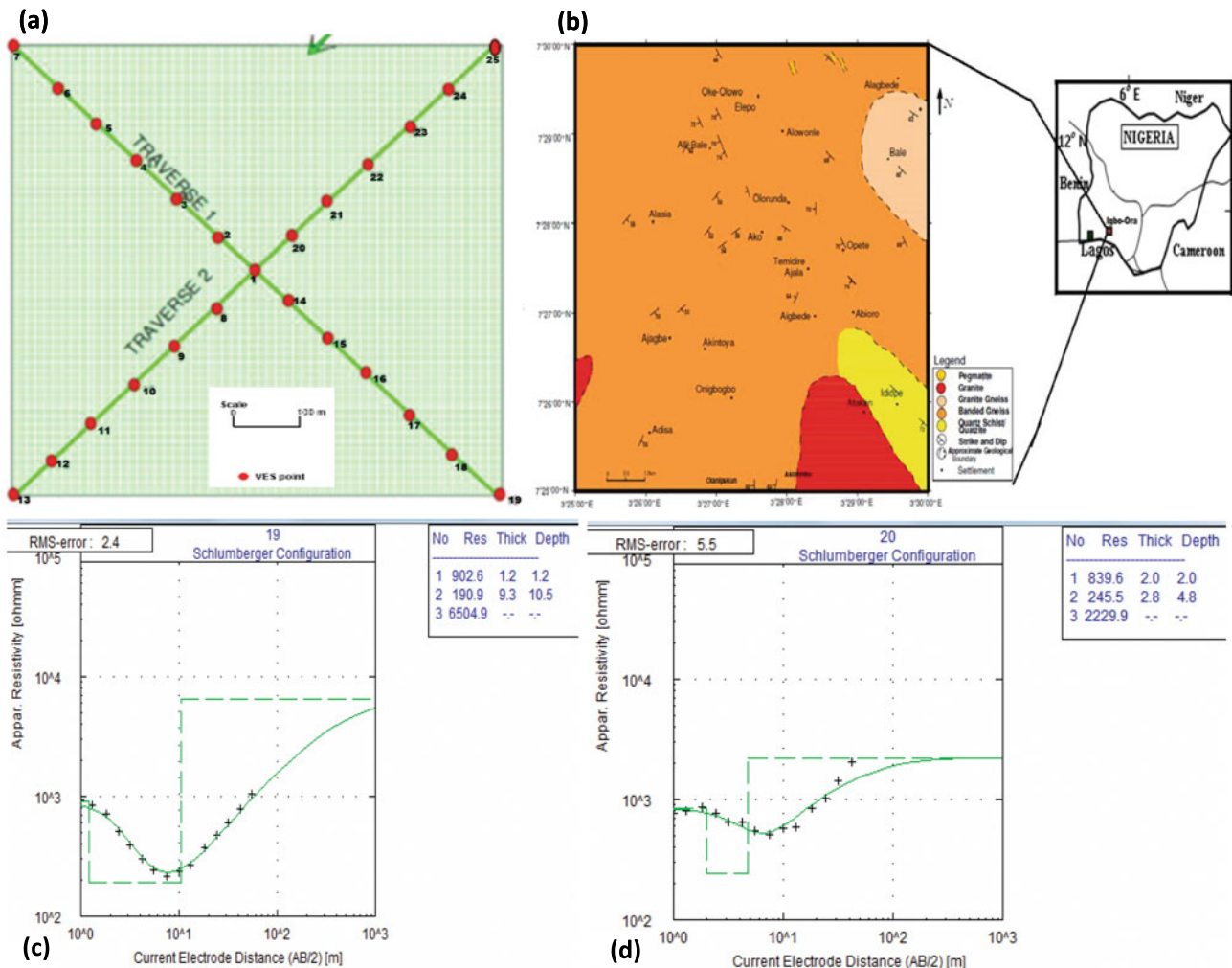
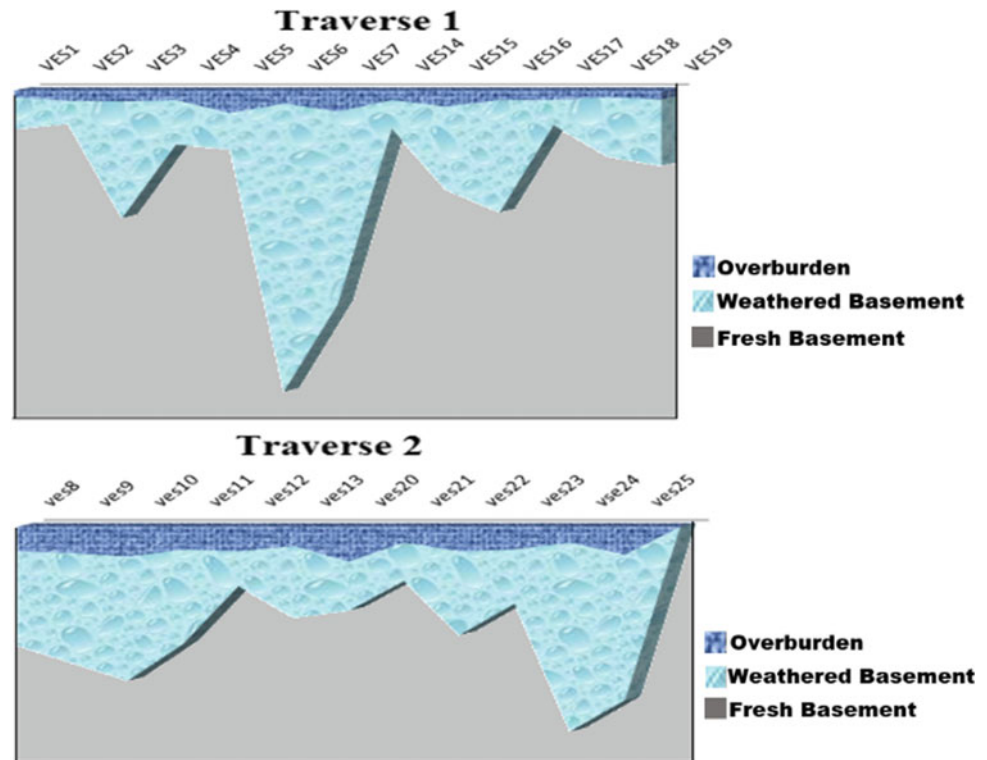


Fig. 1 a Survey basemap b Geologic map of the study area, c and d Representative VES inversion models

Fig. 2 Representative geoelectric section constructed from the VES results



4 Discussion

Considering the groundwater exploration in hard terrain, the essential factors are basement architecture and fracture depths [9]. The variation in the model resistivity values of 1D sounding resistivity models depicts the inhomogeneity of the overburden with clay contents in the study area. The degrees of homogeneity and of thickness of the overburden are important groundwater indices. The thickening of overburden materials in the study area is favorable to the mapping of groundwater aquiferous zones in a basement complex. The second layer is characterized by water-saturated, weathered and fractured basement with model resistivity values of 45.1–346.2 Ωm from the vertical electrical resistivity soundings, which is in agreement with classification of moderately weathered/fractured basement with resistivity ranging from 100 to 800 Ωm as good groundwater aquifer within the Nigerian basement complex [10]. The aquiferous zone is underlain by the fresh basement with very high model resistivity values in the range of 1013.7–33,124.0 Ωm .

5 Conclusions

Geologically constrained vertical electrical soundings have been used to evaluate the groundwater potential in a crystalline basement terrain and to delineate target locations for

sitting boreholes in the study area. The analyses of the sounding resistivity models clearly show three geoelectric layers; top layer, which is inferred to be sandy clayey/clay; water-saturated weathered and fractured basement with clayey materials serving as the aquifer unit; and fresh basement. The electrical soundings delineate higher bottom depth for the water-saturated aquiferous unit. The regoliths (weathered basement) unit within the area with a bottom depth up to 42 m from the VES results. Thus, groundwater exploration and development in the area should target the weathered and fractured basement layer.

Acknowledgements The authors appreciate the Centre for Research, Innovation and Discovery (CUCRID) of Covenant University, Nigeria for conference support.

References

1. Olayinka, A.I., Weller, A.: The inversion of geoelectrical data for estimating aquifer hydrogeological applications in crystalline basement areas of Nigeria. *J. Appl. Geophys.* **37**(2), 103–105 (1997)
2. Adepelumi, A., Ako, B., Ajayi, T.: Groundwater contamination in the basement complex area of Ile-Ife, southwestern Nigeria. *Hydrogeol. J.* **9**(6), 611–622 (2001)
3. Ehinola, O.A., Opoola, A.O., Adesokan, H.A.: Empirical analysis of electromagnetic profiles for groundwater prospecting in rural areas of Ibadan, southwestern Nigeria. *Hydrogeol. J.* **14**(4), 613–624 (2006)

4. Aizebeokhai, A.P., Oyeyemi, K.D.: The use of the multiple gradient array for geoelectrical resistivity and induced polarization imaging. *J. Appl. Geophys.* **111**, 364–375 (2014)
5. Aizebeokhai, A.P., Oyeyemi, K.D.: Application of geoelectrical resistivity imaging and VLF-EM for subsurface characterization in a sedimentary terrain, southwestern Nigeria. *Arab. J. Geosci.* **8**(6), 4083–4099 (2015)
6. Aizebeokhai, A.P., Oyeyemi, K.D., Joel, E.L.: Groundwater potential assessment in a sedimentary terrain southwestern Nigeria. *Arab. J. Geosci.* **9**, 110–117 (2016)
7. Aizebeokhai, A.P., Oyeyemi, K.D., Noiki, F.R., Etete, B.I., Arere, A.U.E., Eyo, U.J., Ogbuehi, V.C.: Geoelectrical resistivity data sets for characterization and aquifer delineation in Iyesi, southwestern Nigeria. *Data. Brief* **15**, 828–832 (2017)
8. Aizebeokhai, A.P., Oyeyemi, K.D.: Geoelectrical characterization of basement aquifers: the case of Iberokodo, southwestern Nigeria. *Hydrogeol. J.* **26**(2), 651–664 (2018)
9. Kumar, D.: Efficacy of electrical resistivity tomography technique in mapping shallow subsurface anomaly. *J. Geol. Soc. India* **80**, 304–307 (2012)
10. Olayinka, A.I., Amidu, S.A., Oladunjoye, M.A.: Use of electromagnetic profiling and resistivity sounding for groundwater exploration in the crystalline basement area of Igbeti, southwestern Nigeria. *Global J. Geol. Sci.* **2**(2), 243–253 (2004)

Hydraulic Parameters Estimation Using 2D Resistivity Technique: A Case Study in Kapas Island, Malaysia

Nura Umar Kura, Mohammad Firuz Ramli, Ahmad Zaharin Aris, and Wan Nor Azmin Sulaiman

Abstract

This work is aimed at generating 2D aquifer porosity and hydraulic conductivity using 2D resistivity techniques. Two resistivity profile lines were measured in an island that is characterized by complex geology. Then, rock and soil samples were collected along the resistivity lines, together with water samples for laboratory analysis which includes determination of the electrical properties of the samples using an inductance-capacitance-resistance (LCR) meter to calibrate the results. Subsequently Bussian equation was employed to determine the aquifer porosity, and then, the hydraulic conductivity of the aquifer via the Kozeny-Carman-Bear equation. Next 2D cross-sections of both porosity and hydraulic conductivity were plotted using surfer software. The result was compared with the pumping test and the results were found to be very close to one another (40 and 38 md^{-1}), respectively. These findings would enhance researchers' understanding of patterns of groundwater flow in an aquifer system.

Keywords

2D • Resistivity • Hydraulic properties • Hydraulic conductivity • Porosity • Aquifer • Small island

N. U. Kura
Department of Environmental Sciences, Faculty of Science,
Federal University Dutse, Dutse, Nigeria

N. U. Kura (✉) · M. F. Ramli (✉) · A. Z. Aris
W. N. A. Sulaiman
Faculty of Environmental Studies, Universiti Putra Malaysia,
43400 UPM Serdang, Selangor, Malaysia
e-mail: nuraumar@gmail.com

M. F. Ramli
e-mail: firuz@upm.edu.my

1 Introduction

Researchers have been working tirelessly to establish a relationship between hydraulic parameters and current flow in a given formation with respect to groundwater studies. The flow of electric current and water in porous media are controlled by the same mechanisms [1]. The groundwater flow follows Darcy's law while electric current flow follows Ohm's law and both are influenced by the same factor, i.e., the aquifer porosity saturated with water. Theoretically, both laws deal with the conservation of mass and charge for water and electric current, respectively [2]. Thus, researchers employ many empirical equations to determine hydraulic parameters from the geophysical measurements [3]. One of the early breakthroughs in this subject matter is the work of Archie (1942), in which he suggested an empirical equation to determine the porosity of a given media [4]:

$$\rho = \alpha \cdot \rho_w \cdot \varphi^{-m} \quad (1)$$

where ρ and ρ_w represent the aquifer's bulk and water resistivity, respectively, φ represents the porosity and α and m are given coefficients, which represent saturation and cementation factors linked to the medium and grain-shape or pore-shape factors, respectively. In the case of m , the more compacted the sediment layers are, the higher the value of m [5]. Archie's equations [4] have set the practical foundation for understanding and calculating liquid saturation in a medium [6]. However, the equation was designed on the assumption that the aquifer in question is clean and clay-free. Should there be any change in respect to that assumption on which the original equation was based, this would render Archie's equation null and void [1, 7]. Researchers use only the one dimension (1D) vertical electric sound (VES) in the determination of hydraulic parameters from electrical resistivity measurement [1–3]. The major limitation of the 1D approach is its disregard for horizontal changes in the resistivity [8]. It will be difficult to satisfy the requirement of real world geological conditions with this

assumption, especially in areas with complex geology as demonstrated by research that 2D and 3D techniques provide more reasonable results [8, 9]. Therefore, this research aims at determining the aquifer's hydraulic parameters on Kapas Island (Malaysia) using 2D resistivity technique.

2 Materials and Methods

It has been established that the hydraulic conductivity and permeability of rocks, as well as the groundwater velocity, strongly depend on porosity [2, 10] while porosity depends on the intrinsic formation factor [4] (Eq. 2).

$$F = \frac{\rho_{sat}}{\rho_w} \quad (2)$$

where the formation factor is represented by F (dimensionless); ρ_{sat} and ρ_w represent the resistivity of aquifer's bulk (Ωm) and the resistivity of water (Ωm), respectively [5]. To reduce the error in porosity estimation, bulk resistivity values that were measured using 2D resistivity were utilized based on Eq. (3) [1]:

$$\rho_w = \frac{10^4}{\sigma_w} \quad (3)$$

where ρ_w represents the resistivity of water (Ωm); while σ_w is the electrical conductivity of water ($\mu mhos/cm$) [15]. The results were then used to calculate the formation factor. The results were then added in the straight line form of a simplified Bussian equation [11] for calibration. These outputs were afterward integrated with the actual resistivity data and the water resistivity both measured from the field to calculate the porosity of the profile area through Eqs. (4)–(6):

$$\sigma_0 \cong \sigma_w \varphi^{m/(1-m)} \quad (4)$$

$$\frac{1}{F} = \sigma_0 / \sigma_w = \varphi^{m/(1-m)} \quad (5)$$

$$F = \frac{1}{\varphi^{m/(1-m)}} \quad (6)$$

Plotting the values of $\log_{10} F$ against $(1/\log_{10} \varphi)$ in a linear coordinate system gives us the relationships shown in Eqs. (7) and (8):

$$\log_{10} F = 0.5626 \left(\frac{1}{\log_{10} \varphi} \right) + 1.8546 \quad (7)$$

$$\log_{10} \varphi = \frac{0.5626}{[\log_{10} F - 1.8546]} \quad (8)$$

where F is the formation factor as above, φ is the porosity, σ_0 and σ_w represent the bulk conductivity of the aquifer and

water conductivity, respectively, and m is the cementation factor, while 0.5626 and 1.8546 are constants derived from soil and rock samples used for calibration. The results were used to calculate the permeability via the Kozeny Eq. (9):

$$k = \left(\frac{d^2}{180} \right) * \left(\frac{\varphi^3}{(1-\varphi)^2} \right) \quad (9)$$

where d is the grain size and φ is the porosity of the aquifer [12]. Subsequently, the hydraulic conductivity values were determined based on Nuttings' equation by [13] and [14] known as the Kozeny-Carman-Bear Eq. (10):

$$K = k \frac{\rho g}{\mu} \quad (10)$$

where k represents the permeability, and fluid dynamic viscosity is represented by μ (kg/ms), while fluid density and gravitation force that influence the movement are represented by ρ (kg/m³) and g (m/s²), respectively [1, 3]. For this research, values of (0.000798 kg/ms) for μ , (995.71 kg/m³) for ρ , and (9.81 m/s²) for g , all at a temperature of 30 °C, were chosen. This is to reflect the actual situation in the field as most of these parameters were believed to be influenced by temperature [15] (Fig. 1).

3 Results

3.1 Results and Discussion

The profile G (Fig. 2 G₁) is oriented east to west towards the sea and it is located at the center of an alluvium deposit with mixtures of sand, coral, shale and a little bit of clay. The resistivity of the line ranges from 4 to 300 Ωm , which is within the acceptable limit of alluvium [16], while the porosity section of the profile line (Fig. 2 G₂), is mostly within the range of 0.38–0.52. The hydraulic conductivity

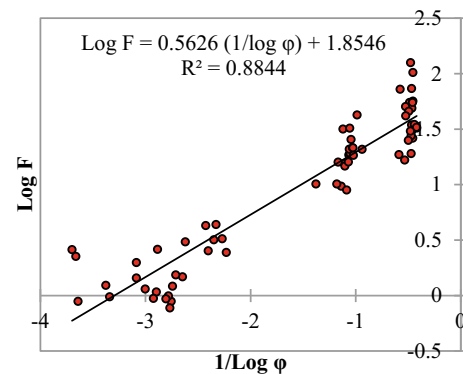


Fig. 1 A straight line graph showing the relationship between the apparent formation factor and fractional porosity based on the Bussian equation

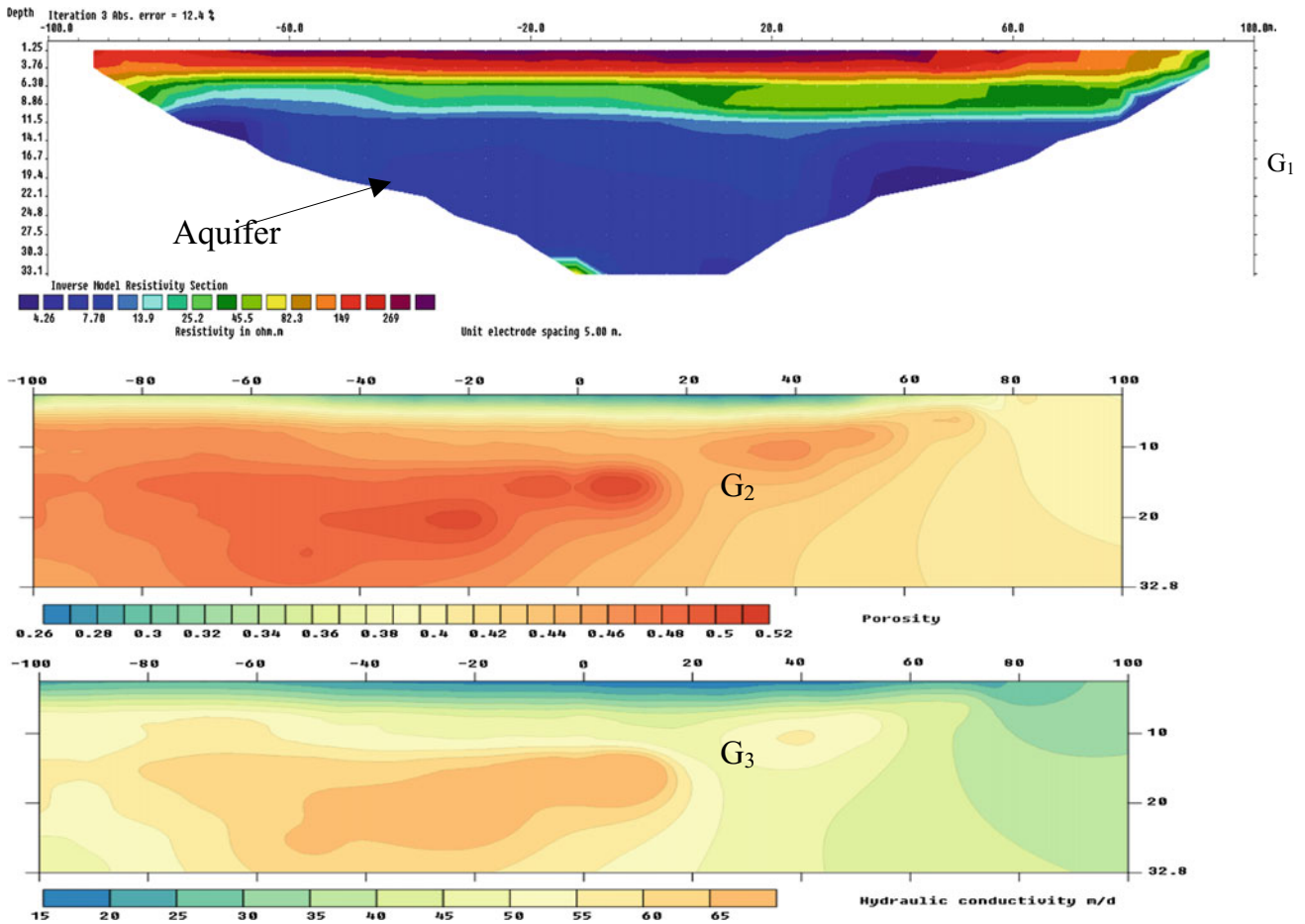


Fig. 2 2D profile lines of A to I (1) resistivity; (2) porosity; (3) hydraulic conductivity

values of the line mostly fall within the range of 30–65 md^{-1} (Fig. 2 G_3). The area shows low resistivity (200–400 Ωm) which corresponds with higher hydraulic conductivities (20–40 md^{-1}). The aquifer’s depth or thickness from the resistivity image was 26 m on average; therefore, the volume is $7.8 \times 10^6 \text{ m}^3$. Thus, the storage capacity was calculated using Eq. (11):

$$V = V_T \theta \tag{11}$$

where V represents the theoretical exploitable volume (m^3); whereas V_T is considered to be the total volume of the aquifer ($7.8 \times 10^6 \text{ m}^3$); and θ reflects the aquifer’s average porosity which is found to be 40% [17]. Thus, the storage capacity of the main aquifer is ($3.12 \times 10^8 \text{ m}^3$).

3.2 Validation

The borehole that was used for the pumping test was 6.4 m deep, and the measured water level before the pumping test was found to be 3.16 m. The transmissivity obtained by the

pumping test was found to be $123 \text{ m}^2\text{d}^{-1}$, and the aquifer thickness is 3.24 m (i.e. thickness of water column). The hydraulic conductivity was calculated using

$$T = Kh \tag{12}$$

where T is the transmissivity; K is the hydraulic conductivity and h is the aquifer thickness [1]. The hydraulic conductivity based on the pumping test is 38 md^{-1} ; while the hydraulic conductivity result based on geophysics and the Bussian equation was found to be 40 md^{-1} , based on the calculation of the average hydraulic conductivity via Eq. (13):

$$K = \frac{ka_1 + ka_2 + ka_3 \dots ka_n}{A} \tag{13}$$

where K is the average hydraulic conductivity, “ k ” is the hydraulic conductivity of area “ $a_1, a_2, a_3 \dots a_n$ ” and “ A ” is the total area of the section. The result was found to be very close to that of the pumping test (just a difference of 2 md^{-1}). This value of hydraulic conductivity is also in agreement with the established values by many researches [5, 9, 18].

4 Conclusions

This research aimed at determining the hydraulic properties of an aquifer using 2D resistivity measurements and has successfully achieved its aim. The Bussian equation was used to determine porosity values. The porosity was then used in the Kozeny-Carman-Bear equation to determine hydraulic conductivity. The hydraulic conductivity that was extracted from resistivity data was compared to the pumping test data and the results demonstrate only a difference of 2 md^{-1} . This suggests that the methodology was successfully executed and the results are believed to be promising. Thus, this technique will open a new research window giving scientists an additional advantage when viewing a complex and true hydrogeological system in a 2D or even 3D mode. In this way, this will help to improve the researchers' ability to come up with a sustainable management plan for any given aquifer system in a way that was not possible before.

Acknowledgements The authors wish to acknowledge the efforts of Late Dr. Shaharin Ibrahim who played a major role in this research. May he rest in peace.

References

- Soupios, P.M., Kouli, M., Vallianatos, F., Vafidis, A., Stavroulakis, G.: Estimation of aquifer hydraulic parameters from surficial geophysical methods: a case study of Keritis Basin in Chania (Crete—Greece). *J. Hydrol.* **338**, 122–131 (2007)
- Chandra, S., Ahmed, S., Ram, A., Dewandel, B.: Estimation of hard rock aquifers hydraulic conductivity from geoelectrical measurements: a theoretical development with field application. *J. Hydrol.* **357**, 218–227 (2008)
- de Lima, O., Niwas, S.: Estimation of hydraulic parameters of shaly sandstone aquifers from geoelectrical measurements. *J. Hydrol.* **235**(1–2), 12–26 (2000)
- Archie, G.: The electrical resistivity log as an aid in determining some reservoir characteristics. *Am. Instit. Min. Metal. Eng. Tech. Publ. Pet. Technol.* **1422**, 8–13 (1942)
- Tizro, T., Voudouris, K., Basami, Y.: Estimation of porosity and specific yield by application of geoelectrical method—a case study in western Iran. *J. Hydrol.* **454–455**, 160–172 (2012)
- Khalil, M.A., Santos, F.A.M.: Hydraulic conductivity estimation from resistivity logs: a case study in Nubian sandstone aquifer. *Arab. J. Geosci.* **6**(1), 205–212 (2013)
- Worthington, P.F.: The uses and abuses of the Archie equations, 1: the formation factor-porosity relationship. *J. Appl. Geophys.* **30**, 215–228 (1993)
- Loke, M., Chambers, J., Rucker, D., Kuras, O., Wilkinson, P.: Recent developments in the direct-current geoelectrical imaging method. *J. Appl. Geophys.* **95**, 135–156 (2013)
- Samouëlian, A., Cousin, I., Tabbagh, A., Bruand, A., Richard, G.: Electrical resistivity survey in soil science: a review. *Soil Tillage Res.* **83**, 173–193 (2005)
- Khalil, M.A., Santos, F.A.M.: 2D resistivity inversion of 1D electrical-sounding measurements in deltaic complex geology: application to the delta Wadi El-Arish, Northern Sinai, Egypt. *J. Geophys. Eng.* **8**, 422–433 (2011)
- Niwas, S., Gupta, P.K., de Lima, O.A.L.: Nonlinear electrical conductivity response of shaly-sand reservoir. *Curr. Sci.* **92**(5), 612–617 (2007)
- Niwas, S., Celik, M.: Equation estimation of porosity and hydraulic conductivity of Ruhrtal aquifer in Germany using near surface geophysics. *J. Appl. Geophys.* **84**, 77–85 (2012)
- Hubbert, M.: The theory of groundwater motions. *J. Geol.* **48**(8), 785–944 (1940)
- Domenico, P.A., Schwartz, F.W.: *Physical and Chemical Hydrogeology*, 2nd edn. Wiley, New York (1998)
- Lide, D.R.: *CRC Handbook of Chemistry and Physics*, 74th edn. Boca Raton, FL. Internet Version 2005. <http://www.hbcpnetbase.com>. CRC Press (2005)
- Loke, M.: Electrical imaging surveys for environmental and engineering studies A practical guide to 2-D and 3-D surveys. 10 2000 [Online]. Available: <http://www.heritagegeophysics.com/>. Accessed 12 11 2012
- Juanah, M.S.E., Ibrahim, S., Sulaiman, W.N.A., Latif, P.A.: Groundwater resources assessment using integrated geophysical techniques in the southwestern region of Peninsular Malaysia. *Arab. J. Geosci.* **6**, 4129–4144 (2013)
- Hördt, A., Blaschek, R., Kemna, A., Zisser, N.: Hydraulic conductivity estimation from induced polarisation data at the field scale—the Krauthausen case history. *J. Appl. Geophys.* **62**, 33–46 (2007)

Numerical Simulation of Groundwater and Surface Water Interaction and Particle Tracking Movement Due to the Effect of Pumping Abstraction of Lower Muda River

Mohd Khairul Nizar Shamsuddin, Wan Nor Azmin Sulaiman, Mohammad Firuz Ramli, Faradiella Mohd Kusin, and Anuar Sefie

Abstract

This study was inspired from the Kedah and Penang water crisis with an objective of solving the problem by applying the conjunctive Riverbank Filtration (RBF) technique. In particular, the RBF technique will improve the water security and sustainability of the water resources. The RBF technique will be exploited in this paper via a case study model, including the evaluations of the effects of groundwater pumping and RBF operation relative to the installation of wells. This study also investigated the impact of pumping rate on flow paths, travel time, the size of the pumping and capture zone delineation, and groundwater mixing within a pumping well. Numerical modeling packages, MODFLOW and MODPATH (particle tracking), were used in these investigations, where the proposed method performed infiltration safely and achieved the ideal pumping rate. The results indicated that the migration of river water into the aquifer is generally slow, which depends on the pumping rate and the distance of the well from the river. The water arrived at the well by the end of the pumping period (1–5 days) at 1054.08, 1238.62, 887.064, 1441.34 m³/day for test wells TW1, TW2, TW3 and TW4, located 5, 10, 15 and 20 m, respectively, from the river. During the 3-day pumping period, 37.5, 23, 21 and 11% of the water pumped from the TW1, TW2, TW3 and TW4 wells was river water, and for pumping periods of 8, 13, 14 and 27 days from TW1, TW2, TW3 and TW4, 100% was river water.

Keywords

Riverbank infiltration • Particle tracking • Groundwater modeling • MODFLOW • MODPATH • Visual modflow flex

1 Introduction

Surface water and groundwater conjunctive use is an important source of freshwater during the water crisis using Riverbank Filtration (RBF) system. Sustainable groundwater resource management through riverbank filtration (RBF) is an alternative surface water treatment method. The RBF system near rivers is utilized in water resource management to increase both water quantity and quality. It is also used to obtain a safe drinking water supply from the river. The RBF method helps prevent problems caused by pollution without the need for additional chemical treatment because some suspended and dissolved contaminants from the surface water are treated or reduced through aquifer materials. Therefore, RBF is an effective, inexpensive, and sustainable means that allows water supply utilities to ensure high water quality. Compared with surface water, groundwater is typically a higher quality source and requires less treatment. However, in many areas, groundwater is insufficient to meet water demand [1]. Therefore, the raw water acquired using the RBF method is a mixture of both surface water and groundwater that contains different chemicals. To manage and protect the water supply, transport processes need to be predicted using the RBF method. To date, the method has mostly been studied using numerical simulations. This study demonstrates a performance simulation of a vertical well using particle tracking with Visual MODFLOW flex and MODPATH for simulating the movement of water particles through the simulated groundwater system. This study aims to identify infiltration-related parameters, such as optimum

M. K. N. Shamsuddin (✉) · A. Sefie
Hydrogeology Research Centre, National Hydraulic Research
Institute of Malaysia, Lot 5377, Jalan Putra Permai,
43300 Seri Kembangan, Selangor, Malaysia
e-mail: nizar@nahrim.gov.my

M. K. N. Shamsuddin · W. N. A. Sulaiman · M. F. Ramli
F. M. Kusin
Faculty of Environmental Studies, University Putra Malaysia,
43400 Serdang, Selangor, Malaysia

pumping rate and distance between the riverbank and the production well. In this study, data on travel time, path lines, and influence zone of river water were determined to characterize the interactions between water in the river and the alluvial aquifer. The applications of particle tracking techniques are important in transportation studies and to predict pathogen attenuation during transportation and artificial recharging. Another goal of the study was to obtain pertinent data regarding RBF implementation and its results, which can be used by water operators. The conjunctive usages of the surface water and the groundwater based on RBF system are important as a source of freshwater during the water crisis. Sustainable groundwater resource management through RBF technique is an alternative method for surface water treatment. Usually, the RBF technique will be applied close to the rivers for water resource management to concurrently increase water quantity with enhanced quality. In addition, the process also enabled the extraction of safe drinking water supplies from the river. The RBF technique is particularly attractive because it helps prevent water pollution without chemical treatment, because some suspended and dissolved contaminants from the surface water will be treated or reduced through aquifer materials. Therefore, RBF is an effective, inexpensive, sustainable, and organic solution that enables water supply utility companies to provide high quality water. Although groundwater is a high-quality water source compared to surface water source, the supply of groundwater is too limited to meet the significant demand [1, 2]. Hence, there is no alternative but to combine surface water and groundwater, which contained varying chemical properties, and processed through RBF technique for safe drinking water. In order to manage and protect the water supply, the integral transport processes need to be predicted using the RBF technique. As a solution to integrate the RBF process into the water transport, many studies had conducted numerical simulations [3, 4]. In the present study, a numerical performance evaluation is conducted for vertical well using the particle tracking method with Visual MODFLOW flex and MODPATH to emulate the movement of water particles through the simulated groundwater system. Particle tracking technique is important in transportation studies, and as well as pathogen attenuation prediction during transportation and artificial recharging. The present study also aims to identify the infiltration-related parameters, such as optimum pumping rate and distance between the riverbank and the production well. The obtained data on travel time, path lines, and influenced zone of river water are applied to characterize the interactions between the river water source and the alluvial aquifer. All of the potential findings above will lead to pertinent data collection on RBF implementation and its viability for water source,

which can be cascaded to water operators for actual implementation.

2 Materials and Methods

2.1 Study Area

The investigation was carried out in Muda River Basin, which is located in the north western part of Peninsular Malaysia. The upper and middle reaches of the basin belonged to the State of Kedah, and the river downstream forms a boundary between the States of Kedah and Penang. The Muda River was particularly chosen because it is one of the most important water resources for agriculture and water supply within Kedah and Penang states. The geographical location of the investigation area lies between 50 31' 30" and 50 35' 30" north latitude, and 1000 29' 0" E and 1000 33' 30" E east longitudes, covering an area of 150 km². The investigation site is located in a Quaternary deposit area. The alluvial layers within the investigation area are composed of upper fine, medium, and lower fine sands, along with a highly conductive sand/gravel layer. These alluvial layers' properties can be confirmed via the sample data obtained from the boreholes MW1-MW22 (riverbank), and further verified with the drill data obtained from the pumping wells TW1 to TW4. The pumping wells were screened from the top of the sand/gravel layer to the bottom layer, while the piezometers were applied to screen from a depth of 1.5 m to the bottom layer. The sand/gravel layer, the main aquifer, has an average thickness of 24 m. The upstream of Muda River was placed on continental deposit, which consisted of clay, silt, sand, and gravels as the parent materials. These unconsolidated sediments can be associated with traces of sand and organic matter, and usually thicken seawards. The downstream area of the Muda River is the northern part of the river, where meta-sedimentary rocks can be observed and reported to be in Ordovician-Silurian age. The rocks consisted of schist, phyllite, and slate with minor intercalation of sandstone. The formations are a thin layer of Sandstone followed by an interbed of schist/phyllite/slate as the main layers (Fig. 1).

2.2 Model Development and Application

The methodologies of the present investigation included collection, analysis, and processing of large amounts of field data. The data include hydrological, hydrogeological, rainfall, and well data. Based on the collected data, a model was developed via Visual Modflow Flex. Upon completing a

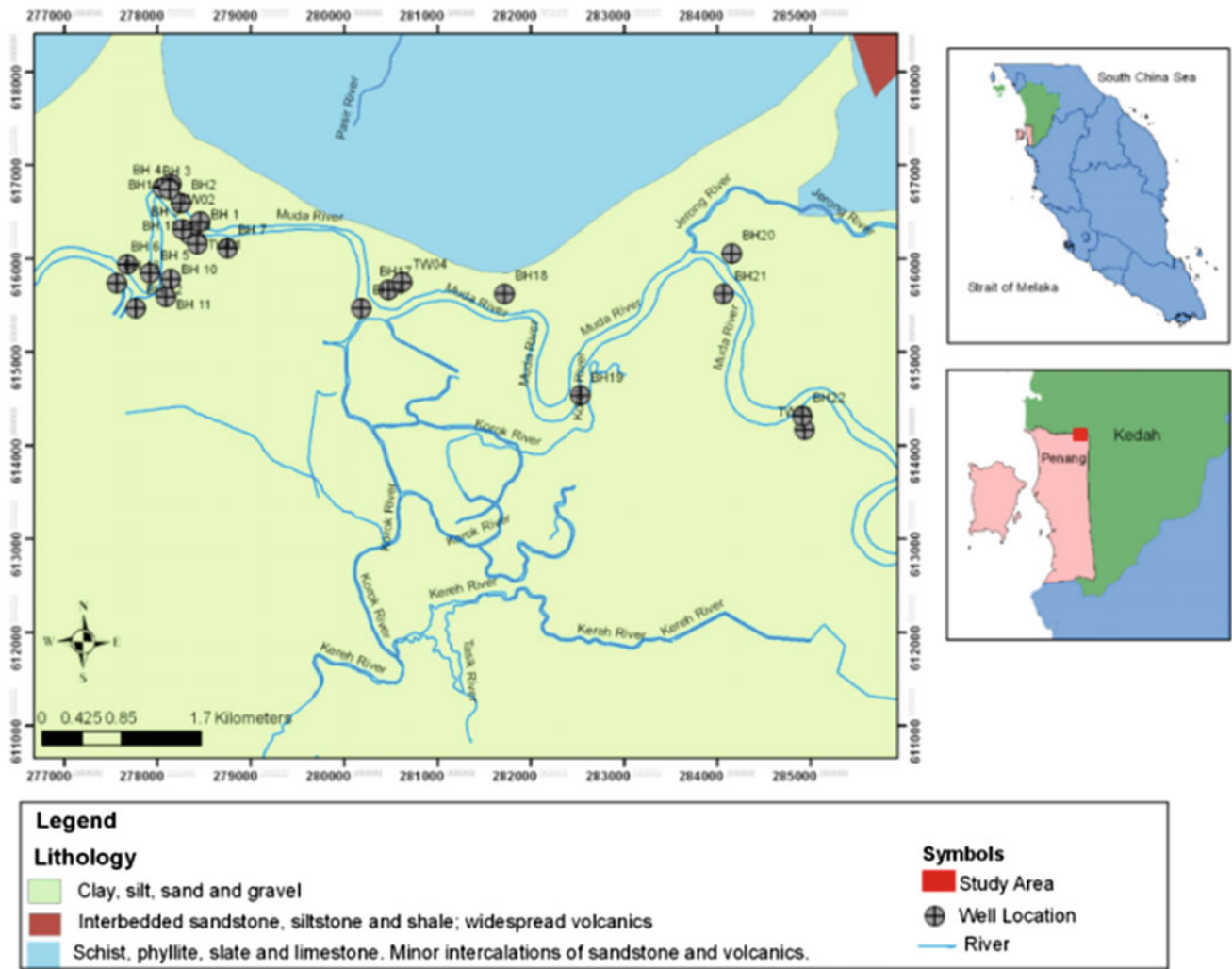


Fig. 1 Location of the study area located at two states Penang and Kedah

thorough study based on the collected and synthesized data, a field reconnaissance was carried out to enable a complete understanding of the site’s hydrogeological aspect and to collect further information on the Lower Muda River basin located between Penang and Kedah. In addition, hydraulic conductivities of the model layers were estimated from the analyzed data of the aquifer test and from the site measurements demarcated according to nine zones. Besides transmissivities, storage coefficients, and leakage rates, the horizontal and vertical hydraulic conductivities, through the confining unit of the aquifer, were estimated from the pump test and the storage coefficients were divided into three zones, that is, one in the first layer and two zones in the second layer. These values were considered as the initial estimates of hydraulic parameters that were applied to the model results.

2.3 Calibration and Validation Results for Groundwater Flow Simulation

The fitted model based on the empirical data was verified by means of simulation, which was computed as the difference between the simulated and the observed hydraulic heads. For the fitted model, the estimated mean absolute error (MAE) value is 0.0045 m, followed by the RMS value at 0.022 m, and the normalized root mean square error (NRMS) value of 8.63%, which collectively indicated that the model was well-calibrated. Furthermore, the calibration statistics coupled with the acceptable model parameters’ values indicated a highly reliable calibration, where the residual mean is close to 10% and the residual standard deviation relative to the overall range is <10%. In the case of transient calibration, the long-term simulated heads (from

Table 1 Scenarios sets of river travel time, pathline determination, pumping rates, and river pumping simulations

Scenarios	Distance from river (m)	Abstraction rate (m ³ day)
Scenario 1 TW1 normal pumping rate	5	1054.0
Scenario 2 TW2 normal pumping rate	10	1238.62
Scenario 3 TW3 normal pumping rate	15	887.064
Scenario 4 TW4 normal pumping rate	20	1441.34
Scenario 5 TW1, TW2, TW3 and TW4 pumping tests concurrently	–	1000
Scenario 6 TW1, TW2, TW3 and TW4 Pumping test concurrently and double pumping rate	–	2000
Scenario 7 TW1, TW2, TW3 and TW4, if half the distance from the river and normal pumping rate	–	–

March 2015 to March 2016) were compared to the measured heads by applying a time series measurement to the observed heads at the 8th observation well. For the stressed model, the estimated MAE, RMS, and NRMS values are 0.005, 0.023 m, and 9.13%, respectively. Based on the overall calibrations, the fitted model will be able to simulate both the water levels and water level fluctuations adequately. As a result, the fitted model can be applied to evaluate the impact of future water resource scenarios with RBF technique, where seven scenarios were considered as part of this investigation; the detailed plans are listed in Table 1.

3 Conclusions

In order to apply the RBF technique, the river-aquifer interactions required to be carefully analyzed due to the rise of groundwater extraction, where some of the important parameters to be considered are particle tracking, pathlines, travel time, and influenced zones. These parameters are essential to study the transport characteristics during the RBF process, which will enable pathogen attenuation prediction during both transport and artificial recharge. The results of the present study indicated that the migration of the river water into the aquifer was generally slow and depended

on the pumping rate and distance from the well to the river. Most of the water arrived at the well by the end of the pumping period (1–5 days), where the measurements were 1054.08, 1238.62, 887.064, 1441.34 m³/day for test wells TW1, TW2, TW3 and TW4, located at 5, 10, 15 and 20 m from riverbank, respectively. During the 3-day pumping period, 37.5, 23, 21 and 11% of the water pumped from the TW1, TW2, TW3 and TW4 wells was river water, while for pumping periods of 8, 13, 14 and 27 days from TW1, TW2, TW3 and TW4, 100% was river water.

References

1. Yusoff, I., Ismail, W.M.Z.W., Rahim, B.E.A.: Simulation of horizontal well performance using Visual MODFLOW. *Environ. Earth Sci.* <https://doi.org/10.1007/s12665-012-1813-x1590> (2012)
2. Shamsuddin, M.K.N., Sulaiman, W.N.A., Suratman, S.: Groundwater and surface-water utilisation using a bank infiltration technique in Malaysia. *Hydrogeol. J.* **22**(3), 543–564 (2014)
3. Chen, X.H.: Migration of induce-infiltrated stream water into nearby aquifer due to seasonal groundwater withdrawal. *Groundwater* **39**(5), 721–728 (2001)
4. Shamsuddin, M.K.N., Suratman, S., Zakaria, M.P., Aris, A. Z., Sulaiman, W.N.A.: Using particle tracking as tool sustainable bank infiltration techniques: a case study in an alluvial area. *Arab. J. Geosci.* **8**(3), 1571–1590 (2015)

Estimating Groundwater Evapotranspiration in Thiaroye Aquifer (Western Senegal)

Ousmane Coly Diouf, Lutz Weihermüller, Mathias Diedhiou, Harry Vereecken, Seynabou Cissé Faye, Sérigne Faye, and Samba Ndao Sylla

Abstract

The use of diurnal or seasonal water table fluctuation (WTF) to estimate groundwater evapotranspiration (ET_G) is increasingly applied in ecohydrological studies. In this study, we applied the WTF method for a shallow aquifer in Senegal over the dry season 2000–2013. To analyze the applicability and validity of the WTF method for this site, the unsaturated/saturated system was first simulated using the 1-D HYDRUS model. The simulated drawdown of the water table over the 14 years ranges from 18.1 to 113.2 cm, and from 10.4 to 101.9 cm for a bare soil and a perennial grass scenario and is highly related to the annual rainfall of the previous rainy season. The results indicate that the estimated actual evapotranspiration (ET_a) from the Hydrus model ranged between 0.22 and 1.11, and between 0.23 and 1.27 mm d^{-1} in bare soil and vegetative condition, respectively. Results indicate that higher ET_a values were observed when the water table is shallow, suggesting that ET_a is driven mainly by the water table depth.

Keywords

Evapotranspiration • Water table fluctuation • Semi-arid regions • Unsaturated zone

O. C. Diouf (✉) · M. Diedhiou · S. C. Faye · S. Faye
Geology Department, Faculty of Sciences and Techniques,
University Cheikh Anta Diop, Dakar, B.P 5005, Dakar-Fann,
Senegal
e-mail: ousmanecoly.diouf@ucad.edu.sn

L. Weihermüller · H. Vereecken
Forschungszentrum Jülich GmbH, Agrosphere Institute IBG-3,
52425 Jülich, Germany

S. N. Sylla
Department of Plant Biology, Faculty of Sciences and Techniques,
University Cheikh Anta Diop, Dakar, B.P 5005, Dakar-Fann,
Senegal

1 Introduction

Sustainable management of groundwater resources requires detailed information of all components of the water budget such as precipitation, storage changes, recharge, as well as actual evapotranspiration (ET_a). Different approaches derived from climatic data are available to estimate potential reference evapotranspiration (ET_0). Unfortunately, ET_a can only be calculated based on ET_0 using physically based models [1]. On the other hand, ET_a can be measured directly using the eddy correlation (EC) method, whereby the EC data have to be often corrected (e.g., [2]) and gap filled (e.g., [3]) resulting in errors in the ET_a estimation. Weighable lysimeters as another direct technique for estimating ET_a are also feasible. In arid and semi-arid regions, groundwater evapotranspiration (ET_G) can be a predominant mechanism of groundwater discharge to infer seasonal fluctuation of it [4].

The objective of this study is to estimate the daily evapotranspiration rates to get knowledge about potential groundwater recharge and extraction capacities. To do so, the ET_G rates from the WTF method were calculated and compared with actual evapotranspiration data (ET_a) calculated by the physically based HYDRUS 1D model for different surface covers, namely bare soil and savanna type grass vegetative in Western Senegal.

2 Materials and Methods

Soil sampling was performed in the Dakar area in May 2015, whereby undisturbed soil cores using Kopecky rings of 250 cm^3 (height = 5 cm, diameter = 8.4 cm) were taken in the uppermost three soil horizons from the sampling depth of 0–25 cm (with $n = 3$), 25–100 cm ($n = 3$), and 100–200 cm ($n = 4$) and transferred to the Forschungszentrum Jülich GmbH, Germany for analysis. For the estimation of the

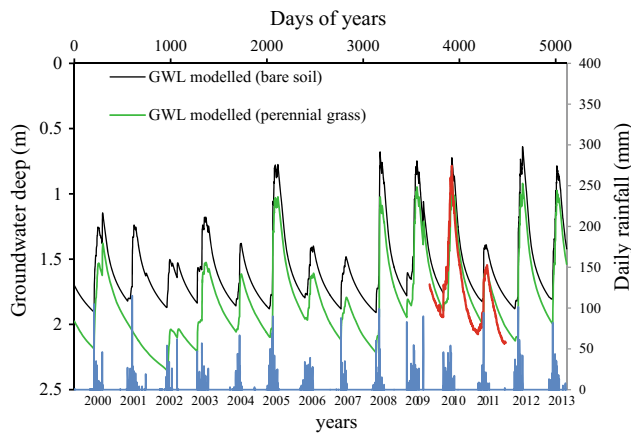


Fig. 1 Daily rainfall and daily groundwater levels monitored (2010–2012) and modeled (2000–2013) for an urbanized (bare soil) and vegetated scenario for piezometer P3-1

hydraulic properties the HYPROP[®](UMS, München, Germany) method as described by [5] was used in combination with the WP4[®]Dewpoint Potentiometer (Decagon Devices, WA, USA).

Groundwater level data in piezometer P3.1 were recorded using Thalimede Orpheus mini recorders (OTT Hydromet GmbH, Germany) during time period 2010–2012 in order to determine groundwater fluctuations over two dry seasons. The vegetation surrounding the groundwater well was grass vegetation but also bare patches were detectable, whereby the vegetation also depends on dry or wet season.

The ET_G derived from the WTF method can be expressed as [6]:

$$ET_G = S_y \frac{\Delta H - \Delta h}{\Delta t} \quad (1)$$

For the HYDRUS simulation of the ET_a in the Dakar region the simulation domain was assumed to be 2300 cm, whereby the largest fraction of the domain was fully water filled (~ 2000 cm) and acts as a groundwater reservoir, which will fluctuate over depth as a system response to infiltration and evapotranspiration.

3 Results

3.1 Seasonal Groundwater level changes

Figure 1 shows the simulated groundwater levels for two different scenarios, where the soil was either assumed to be bare or covered by short perennial grass. Both states (bare and vegetated) are observed in the vicinity of the monitoring piezometer. Additionally, water table fluctuations measured in the piezometer are plotted for the years 2010–2012. Looking at the match between the modelled and measured groundwater tables for the years 2010–2012 indicates that the model results based on the assumption that the soil was bare is less good compared to the vegetated scenario.

3.2 ET_G from piezometer data and HYDRUS 1D simulation

The best parameters of the inversion for the different soil layers are listed in Table 1. Daily ET_G values estimated from measured groundwater levels in the piezometer and the WTF method varies between 0.84 (2012) and 1.34 mm d^{-1} (2011) with a mean of 1.10 mm d^{-1} . ET_G of the year 2011 is in the same range as the ET_a modeled in the vegetated scenario assuming a perennial grass cover (5% mismatch). However, in 2012 the difference between ET_a and ET_G is much larger. The mismatch for the year 2012 can be attributed to the fact that the measured groundwater fluctuations were not recorded for the entire dry season and ended already at April, 7th 2012. Even if only one dry season was covered by the measurements confidence in the WTF method for this study area is given by the synthetic model study using the HYDRUS 1D software.

4 Discussion

The calculated daily ET_a (0.23–1.28 mm d^{-1}) and ET_G (0.17–1.20 mm d^{-1}) values in our study area are comparable with estimated ET_G rates in semi-arid and arid environments,

Table 1 Van Genuchten parameters obtained from HYPROP[®] data for the different soil layers. Note that the tortuosity l [–] was not fitted and set to 0.5

Layers	θ_r ($\text{cm}^3 \text{cm}^{-3}$)	θ_s ($\text{cm}^3 \text{cm}^{-3}$)	α (cm^{-1})	n (–)	Ks (cm d^{-1})
1 (0–25 cm)	0.0062	0.44	0.023	2.6	570
2 (25–100 cm)	0.0011	0.42	0.026	2.8	504
3 (100–200 cm)	0.0011	0.45	0.027	1.8	461

where the groundwater table is in general much deeper. In a hyper-arid environment of northwestern China, [6] obtained similar ET_G values ($0.63\text{--}2.33\text{ mm d}^{-1}$) from 0.5 to 3.5 m water table depth.

5 Conclusions

Daily groundwater level fluctuations were observed during the dry season in Dakar area. In this study, a 13-year modelled time series of measured climatic conditions and soil hydraulic properties from the laboratory was used. Because of the vegetation impact to the actual ET, two different scenarios were included, namely a bare soil and a perennial grass cover. The simulated ET_a model shows that higher and lower ET_a values occurred respectively during the period corresponding to the ends of the rainy and the dry seasons.

References

1. Kollett, S.J., Cvijanovic, I., Schüttemeyer, D., Maxwell, R.M., Moene, A.F., Bayer, P.: The influence of rain sensible heat and subsurface energy transport on the energy balance at the land surface. *Vadose Zone J.* **8**, 846–857 (2009)
2. Wilson, K., Goldstein, A., Falge, E., Aubinet, M., Baldocchi, D., Berbigier, P., Bernhofer, C., Ceulemans, R., Dolman, H., Field, C., Grelle, A., Ibrom, A., Law, B.E., Kowalski, A., Meyers, T., Moncrief, J., Monson, R., Oechel, W., Tenhunen, J., Valentini, R., Verma, S.: Energy balance closure at FLUXNET sites. *Agric. For. Meteorol.* **113**, 223–243 (2002)
3. Moffat, A.M., Papale, D., Reichstein, M., Hollinger, D.Y., Richardson, A.D., Barr, A.G.: Comprehensive comparison of gap-filling techniques for eddy covariance net carbon fluxes. *Agric. For. Meteorol.* **147**, 209–232 (2007)
4. Healy, R.W., Cook, P.G.: Using groundwater levels to estimate recharge. *Hydrogeol. J.* **10**, 91–109 (2002)
5. Schindler, U., Durner, W., von Unold, G., Müller, L.: Evaporation method for measuring unsaturated hydraulic properties of soils: extending the measurement range. *Soil Sci. Soc. Am. J.* **74**(4), 1071–1083 (2010)
6. Wang, P., Grinevsky, S.O., Pozdniakov, S.P., Yu, J., Dautova, D.S., Min, L., Chaoyang, D., Zhang, Y.: Application of the water table fluctuation method for estimating evapotranspiration at two phreatophyte-dominated sites under hyper-arid environments. *J. Hydrol.* **519**, 2289–2300 (2014)
1. Kollett, S.J., Cvijanovic, I., Schüttemeyer, D., Maxwell, R.M., Moene, A.F., Bayer, P.: The influence of rain sensible heat and

Geomorphological Control on Groundwater Occurrence Within the Basement Terrain of Keffi Area, North-Central Nigeria

Ebenezer A. Kudamnya, Aneikan E. Edet, and Azubuike S. Ekwere

Abstract

This research is focused on extracting and evaluating geomorphological features such as slope, elevation, drainage and wetness from remotely sensed data using principal component analysis (PCA). These features are variables and have significantly influenced the geomorphological control on groundwater occurrence. The software ENVI 5.0 was used to extract wetness information by performing a tasselled cap transformation and extraction of slope data, GLOBAL MAPPER 15 was used to extract information on drainage and ARCMAP 10.3 performed the drainage density using the kernel density algorithm (KDA). From the PCA performed, the most suitable principal component was PC3. It was then negated in order to achieve the desired result because it contains the information on the variable that influences the geomorphological control on groundwater. A Multi-fractal analysis (MFA) was performed to identify the threshold or area with high influence of geomorphological factors on groundwater distribution. From the threshold, three classes were identified and thus, areas with low, moderate and high potentials have been delineated corresponding to 199.7834, 501.6503 and 67.0763 km² respectively. It can thus be concluded that other geological, hydrogeological and hydrological factors may have a stronger control on the occurrence and distribution of groundwater within Keffi and its environs than the geomorphology.

Keywords

Geomorphological • Groundwater • Extraction • Software • Threshold

1 Introduction

The study area is Keffi and its environs in north-central Nigeria. It is located on the northern crystalline basement complex and situated within latitudes 8° 45'N to 9° 00'N, and longitudes 7° 45'E to 8° 00'E. There are unique sceneries and this is a reflection of several earth processes the area had undergone in the past. And as such, there is a need to assess the control of some of the geomorphological features on groundwater potential distribution in the area. Conventional methods have been employed to delineate groundwater potential zones [1–5]. However, recent studies have employed remote sensing and geographic information systems (GIS) as a multi-criteria decision tool [6–10].

This research, however, is focused on extracting and evaluating features of geomorphological significance such as slope, elevation, drainage and wetness from remotely sensed data and using principal component analysis (PCA) to establish its influence on the occurrence of groundwater in any given place.

2 Materials and Methods

Landsat imagery was used to extract spatial information, while digital elevation model (DEM) was used to extract information on elevation, drainage and slope. With the aid of ENVI 5.0, a tasselled cap transformation was performed on the satellite imagery and wetness information was extracted. Using DEM and with the aid of GLOBAL MAPPER 15, information on drainage for the study area was extracted. The drainage information was exported into ARCMAP 10.3 as a shape file where the drainage density was performed using the kernel density algorithm (KDA). This, together with the DEM, was imported into the ENVI 5.0 where slope information was extracted, while the DEM was taken to represent the elevation within the study area.

E. A. Kudamnya (✉) · A. E. Edet · A. S. Ekwere
Department of Geology, University of Calabar, Calabar,
Cross River, Nigeria
e-mail: obeydelaw2013@gmail.com

Layer staking was then performed on the slope, DEM, drainage density and wetness information using the layer staking algorithm (LSA). Thematic maps of these features are produced and analysed. On the staked layer, a principal component analysis was performed. The most suitable PCA was extracted and multi-fractal analysis (MFA) was performed to identify the threshold or area with high influence of geomorphological factors on groundwater distribution. From the threshold, areas with low, moderate and high potentials were delineated in both percentage and areal coverage.

3 Results

Thematic layers were produced in map format for slope, elevation, drainage density and wetness. Also, the PCA performed is thus presented below (Table 1).

4 Discussion

The spectral attributes exhibited by each of slope, drainage, elevation and wetness were employed during the extraction process. It is expected that the resultant principal component analysis (PCA) is to have a negative loading on elevation and slope, while a positive loading on drainage density and wetness is expected. Only PC3 contained the highest information and exhibited a close, but inverse, relationship to the expected outcome. Hence, it is the most suitable, while PC1, PC2 and PC4 are not. Also, it was observed that this was not the case because from the values of the obtained Eigen-vector, there was a negative loading on PC3 for drainage density (-0.0118) and wetness (-0.0308), while a positive loading was obtained for elevation (0.0688) and slope (0.9971) against all expectations (Table 1). To correct this, the PCA performed was then negated in order to achieve the expected outcome.

Based on values of the obtained Eigen-vectors after the PC3 band is negated, there is a negative loading for slope (-0.9971) and this shows a very strong negative relationship to the occurrence of groundwater. Elevation (-0.0688), also reveals a negative loading on the PC3, but it has a weak negative correlation. A positive loading was obtained for drainage density (0.0118) and wetness (0.0308). In both

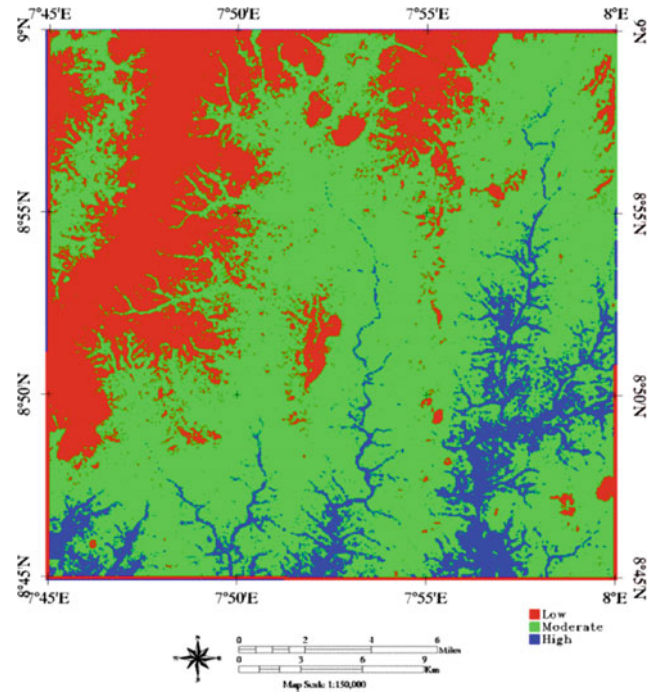


Fig. 1 Groundwater potential map based on the geomorphological factors

cases, they exhibit an influence, though a weak one, on groundwater occurrence. Therefore, the variables that have an influence on geomorphological control on groundwater distribution and occurrence in the study area are drainage density and wetness. Only these two (2) show a positive correlation, although their influence is not very strong. Hence, they both have a low positive correlation on the occurrence of groundwater. This further suggests that other factors, such as lithologies, structural lineaments, soils, rainfall and aquifer properties, may have a stronger control on the occurrence and distribution of groundwater within Keffi and its environs than the geomorphology (Fig. 1).

5 Conclusions

The variables that have an influence on geomorphology in the control of groundwater occurrence in the study area are drainage density and wetness because they show a positive correlation, although their control is a weak one. From the

Table 1 Principal component analysis (PCA) performed on the staked layers for slope, elevation, drainage density and wetness

Eigen-vector	Wetness	Slope	Elevation	Drainage density
PC1	0.1043	0.0717	-0.9920	0.0004
PC2	-0.9941	0.0234	-0.1061	0.0011
PC3	-0.0308	0.9971	0.0688	-0.0118
PC4	-0.0007	-0.0118	-0.0014	-0.9999

threshold, three classes were identified and thus areas with low, moderate and high potentials have been delineated corresponding to 199.7834, 501.6503 and 67.0763 km², respectively. It thus further suggests that other geological, hydrogeological and hydrological factors may have a stronger control on the occurrence and distribution of groundwater within Keffi and its environs.

References

1. Edet, A.E.: Application of photo-geologic and electro-magnetic techniques to groundwater exploration in North-Western Nigeria. *J. Afr. Earth Sci.* **11**(3), 321–328 (1990)
2. Lillesand, T.M., Kiefer, R.W.: *Remote sensing and image interpretation*, 3rd edn. Wiley, New York (1994)
3. Edet, A.E., Okereke, C.S.: Assessment of hydrogeological conditions in basement aquifers of the Precambrian Oban Massif, Southeastern Nigeria. *J. Appl. Geophys.* **36**(4), 195–204 (1997)
4. Srivastava, P.K., Bhattacharya, A.K.: Groundwater assessment through an integrated approach using remote sensing, GIS and resistivity techniques: a case study from hard rock terrain. *Int. J. Remote Sens.* **27**(20), 4599–4620 (2006)
5. Kudamnya, E.A., Osumaje, J.O.: Geo-electric investigation of the groundwater potential distribution within the Northern basement complex of Nigeria. *Int. J. Sci. Eng. Res.* **6**(2), 1152–1160 (2015)
6. Vittala, S.S., Govindaiah, S., Gowda, H.H.: Evaluation of groundwater potential zones in the sub-watersheds of North Pennar River basin around Pavagada, Karnataka-India, using remote sensing and GIS techniques. *J. Indian Soc. Remote Sens.* **33**(4), 483–493 (2005)
7. Mondal, M.D.S., Pandey, A.C., Garg, R.D.: Groundwater prospects evaluation based on hydro-geomorphological mapping using high resolution satellite images: a case study of in Uttarakhand. *J. Indian Soc. Remote Sens.* **36**(1), 69–76 (2008)
8. Fashae, O.A., Tijani, M.N., Talabi, A.O., Adedeji, O.I.: Delineation of groundwater potential zones in the crystalline basement terrain of SW-Nigeria: an integrated remote sensing and GIS approach. *Appl. Water Sci.—Springer* **4**, 19–38 (2014)
9. Rajaveni, S.P., Brindha, K., Elango, L.: Geological and geomorphological control on groundwater occurrence in a hard rock terrain. *Appl. Water Sci.—Springer*, **7**, 1377–1389 (2017)
10. Kudamnya, E.A., Andongma, W.T.: Predictive mapping for groundwater within Sokoto Basin, North-Western Nigeria. *J. Geogr. Environ. Earth Sci. Int.* **10**(2), 1–14 (2017)

Characterization of Superficial Aquifer in Oued M'Zab (Northern Algerian Sahara)

Hadjira Benhedid and Mustapha Daddi Bouhoun

Abstract

Our work focuses on studying the physico-chemical quality of superficial aquifer of Oued M'Zab in order to identify their potability, and their impact on human and the environment. To achieve this goal, we carried out physicochemical measures on forty-five wells aligned along the Oued M'Zab, (that is measuring pH, EC, Ca^{++} , Mg^{++} , Na^+ , K^+ , Cl^- , SO_4^- , HCO_3^- and NO_3^-), allowing the classification of this water according to international standards. The findings in the framework of this work show that the water of the aquifer is close to neutrality and is highly saline. The water facies is variable, of anionic dominance, chlorinated, sulphated or balanced; and of cationic dominance, sodium, calcium, magnesium or balanced. According to WHO standards, the majority of these waters are classified as not drinkable. The location of contaminated wells must be reported and prohibited for human consumption.

Keywords

Characterization • Physico-chemical • Superficial aquifer M'Zab • Algeria

1 Introduction

Groundwater is a strategic water source for human activities. In addition to being often of large volumes, they generally offer better quality water than surface water. These waters account for 23% of the planet's freshwater resources that must be conserved and protected from all kinds of pollution [1].

In Algeria, the main source to satisfy water demand is groundwater. Population growth and the modernization of

agriculture are causing a major problem of deterioration of the quality of this underground source [2].

The physico-chemical study of groundwater plays an important role in defining its quality, and therefore, the possibility to use it for supplying drinking water. As a result, it seems that the purpose of our research is to define the physico-chemical quality of the superficial aquifer of Oued M'Zab, in order to appreciate their potability, and their impact on the human and the environment.

2 Materials and Methods

2.1 Study Area

Our work was carried out in the M'Zab valley, it is located 600 km in the south of the Algeria's capital, in the center of the northern Sahara, located on the western borders of the secondary sedimentary basin of the Sahara and considered as one of the great oases of the Algerian Sahara. Administratively, it is part of the province of Ghardaïa [3, 4].

This research in the M'Zab valley was conducted in four stations: Daya Bendahoua, Ghardaïa, Bounoura and El Atteuf, which spread along Oued M'Zab from upstream to downstream.

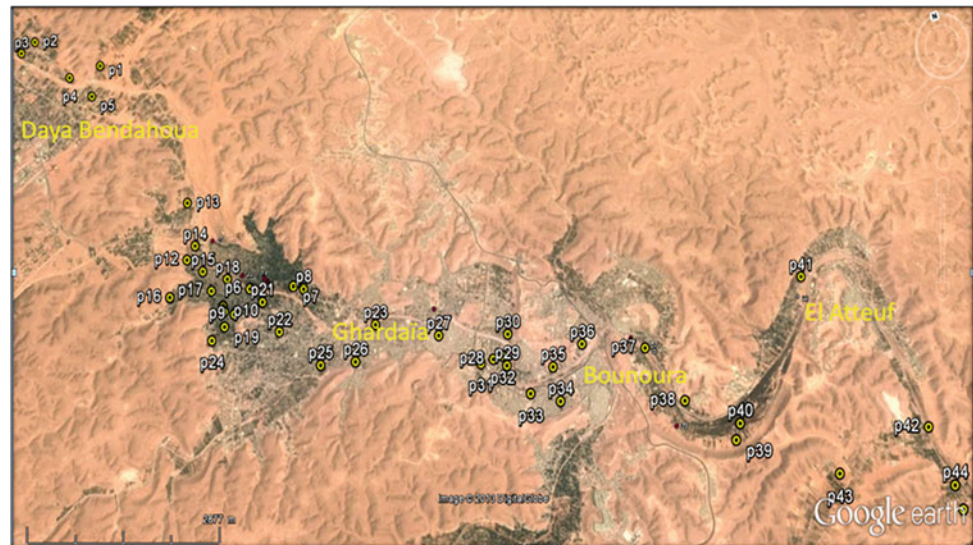
2.2 Study Methods

We performed hydro-chemical measurements for forty-five traditional wells. The sites are spread from upstream to downstream of the valley with a variable number between study stations, in urban and agricultural areas. The numbers of study sites in Daya Bendahoua, Ghardaïa, Bounoura and El Atteuf stations are 5, 29, 6 and 5 respectively (Fig. 1).

Samples of water are taken according to the protocols recommended by Rodier et al. [5]. They lasted in the period of high water, winter period. The parameters studied are

H. Benhedid (✉) · M. Daddi Bouhoun
Laboratory of Ecosystem Protection in Arid and Semi Arid Zones,
University of Ouargla, P. Box 511 30000 Ouargla, Algeria
e-mail: hbenhedid@gmail.com

Fig. 1 Sites and wells location in Oued M'Zab area



(pH, EC, Ca^{++} , Mg^{++} , Na^+ , K^+ , Cl^- , SO_4^- , HCO_3^- and NO_3^-).

3 Results

The results of the physico-chemical analyzes are presented in Figs. 2 and 3.

4 Discussion

1. Hydrogen potential

The pH figure (Fig. 2), shows homogeneity of the spatial variation throughout the Oued M'Zab, the majority of the wells prospected have a pH close to neutrality, being in the pH range of the characteristic drinking water between 5.5 and 8 according to the WHO [5].

2. Electrical conductivity

The figure of the EC (Fig. 2), shows that the waters of the aquifer have a generally very high mineralization, far exceeding the standard value of drinking water set by the WHO (1500 $\mu\text{S}/\text{cm}$) [5].

3. Cation and anion

The examination of the graph (Fig. 2) shows that calcium levels vary from one well to another, but overall are above the WHO water standard (200 mg l^{-1}) [5].

In all the examined wells, the magnesium ion contents are very variable from one well to another. These levels are very high and generally exceed the drinking water standard according to the WHO (150 mg l^{-1}) [5].

An increase in sodium concentrations throughout the valley, exceeding the WHO (200 mg l^{-1}) [5], except Daya Bendahoua's wells P3 and P5, Ghardaia's wells P12, P15 and P18, and Bounoura's well P37, which have substandard levels.

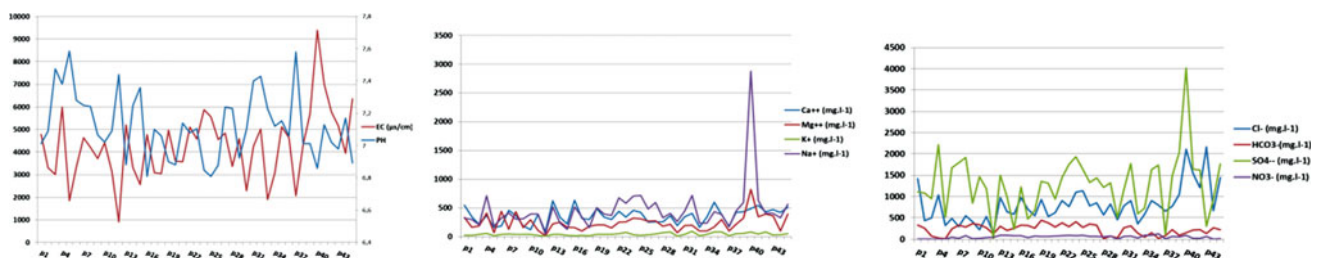
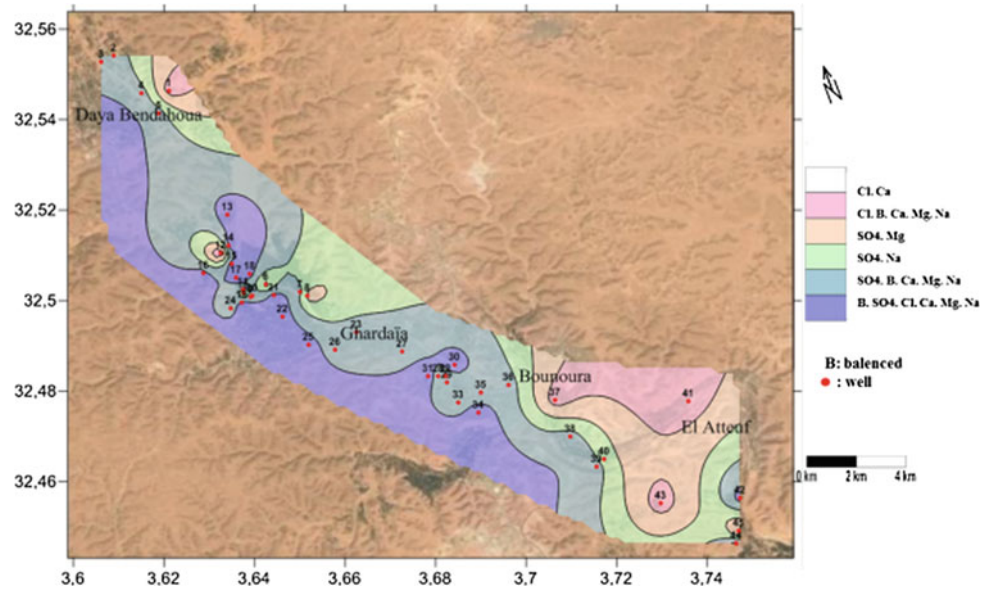


Fig. 2 Physico-chemical analysis of Oued M'Zab aquifer

Fig. 3 Map of distribution of the chemical facies of Oued M'Zab aquifer



Most of the water in this aquifer have a very high potassium content throughout the valley. These concentrations are relatively above the WHO drinking water (12 mg l^{-1}) [5].

The observation of the figure (Fig. 2), shows that chloride contents generally are higher and exceed the standard of drinking water according to the WHO (250 mg l^{-1}) [5].

Most of the wells have very high sulphate levels throughout the valley, especially downstream, where they are above the WHO drinking water standard (250 mg l^{-1}) [5].

In general, the water of this layer is not bicarbonated. These grades are consistent with the WHO (500 mg l^{-1}) [5].

Nineteen wells have concentrations that appear to be well below the WHO drinking water standard (50 mg l^{-1}) [5], while the rest of the wells exceed this standard.

4. Chemical facies of waters

In order to properly identify the hydrochemical facies and to have an indication of the qualitative aspect of the groundwater, we used the Piper diagram, allowing us to have a global approach on the chemical facies of the water and achieve a map of spatial variations of the water facies of the wells (Fig. 3).

The map shows large variations of facies in the M'Zab valley that may be of geological or anthropogenic origin. We generally notice that the cationic facies of the water of the studied aquifer is dominated, either by sodium, calcium or magnesium. But in general, we note a balance between these cations with varying proportions. In the same way, the anionic facies is dominated, either by the sulphates or the

chlorines, but in general, it is balanced, sulphated chlorinated or sulfated chlorinated.

5 Conclusions

The hydrochemical analysis reveals that the Oued M'Zab groundwater is generally close to neutral and highly saline. The water facies is variable, of anionic dominance, chlorinated, sulphated or balanced; and of cationic dominance, sodium, calcium, magnesium or balanced.

The spatial distribution of the chemical elements is high, most likely influenced by the geological nature of the layers crossed by the wells, sometimes rich in evaporites or by anthropogenic agro-urban contamination, favoring the increase of certain elements, such as potassium, chlorides and sulfates.

According to WHO standards, the majority of these waters are classified as not drinkable. The location of contaminated wells must be reported and prohibited for human consumption. It seems that water use regulations are vital, and further developments are needed in the M'Zab Valley.

References

1. Laaouan, M., Aboulhassan, M.A., Bengamra, S., Taleb, A., souabil, S., Tahiri, M.: Etude comparative de la contamination des eaux souterraines des villes de Mohammedia, Temara et Dar Bouazza par les nitrates (Meseta marocaine). *J. Mater. Environ. Sci.* 7(4), 1298–1309 (2016). ISSN: 2028-2508 CODEN: JMESC

2. Abdelbaki, C., Boukli Hacene, F.: Etude du phénomène de dégradation des eaux souterraines du groupement urbain de Tlemcen. *Revue des Energies Renouvelables*. **10**(2), 257–263 (2007)
3. Achour, M., Hassani, M.I. Mansour, H., Hadj Brahim, A.: Apport du SIG à l'établissement de la carte de vulnérabilité intrinsèque de la nappe d'Infero-flux de l'oued M'Zab, Algérie, 1er Séminaire National: Eau et Environnement (– SNEE 01 – Mila, 28–29 Novembre 2016), 7 p (2016)
4. Bnehedid, H.: Etude de l'impact des eaux usées sur la variabilité de la pollution des aquifères superficiels à Oued M'Zab, Mém magister, Université KASDI MERBAH Ouargla, 149 p (2015)
5. Rodier, J. Legube, B., Merlet, N.: *Analyse de l'eau*, 9ème édition (Ed. Dunod, Paris), 1526 p (2009)

Role of Kaolinisation in the Khondalitic Aquifers of Eastern Ghats (India)

Venkateswara Rao Bekkam

Abstract

Khondalitic suite (garneti ferrous Sillimanite gneiss) of rocks occurs extensively in the Eastern Ghats of India. When the khondalite is highly weathered due to the presence of water at low lying areas such as water courses, it becomes kaolinised and acts as a barrier to the lateral movement of groundwater, causing it to be accumulated on either side of the stream, turning the areas adjoining stream courses into non-potential groundwater areas. From electrical resistivity investigations, it has been found that the kaolinised layer is progressively increasing towards the stream, making little to no aquifer thickness near the streams. The resistivity of the kaolinised layer is found to be less than 25 Ω m and that of the weathered and fractured khondalitic aquifer is between 25 and 65 Ω m. Hydrogeomorphological studies have indicated that mostly stream courses are lineaments and between the two lineaments, there is a shallow weathered pediplain where more of high-yielding (>8000 lph) wells are observed. The transmissivity and storage coefficient values of the aquifer has decreased progressively towards the stream conforming the earlier investigations. The hydraulic conductivity of the kaolinised layer varies from 1.6 to 1.9 m/day while that of the fractured layer below varies from 1.6 to 2.3 m/day.

Keywords

Khondalites • Kaolinised layer • Aquifer

1 Introduction

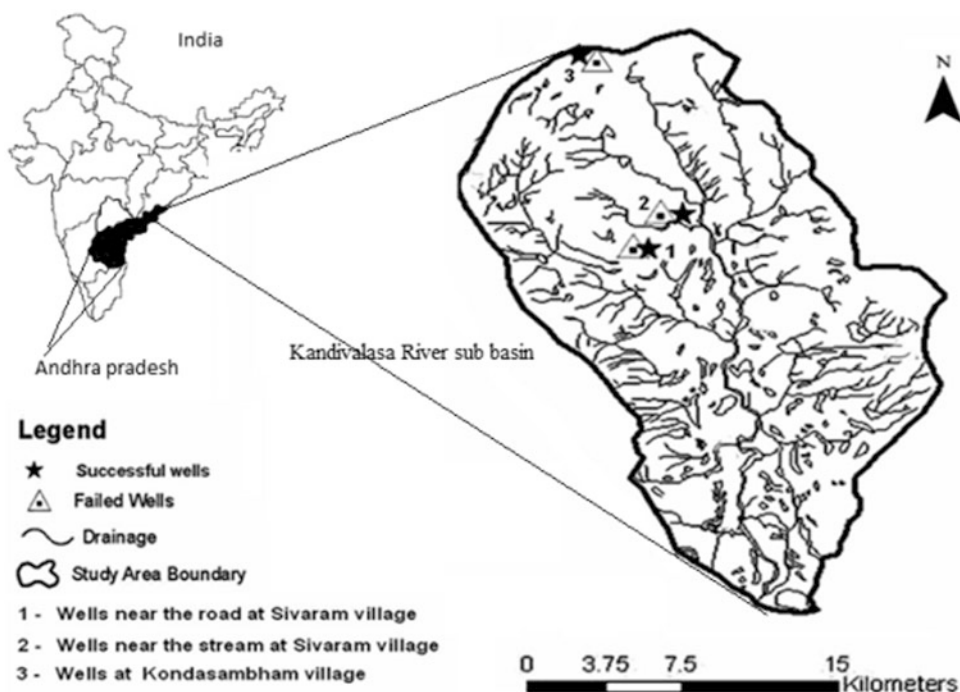
Khondalitic suite (garneti ferrous Sillimanite gneiss) of rocks occurs extensively in the Eastern Ghats of India. Khondalite is basically a sedimentary rock in origin, but it later metamorphosed and became hard rock [1]. However due to folding, faulting, fracturing and weathering of khondalites [3, 4], groundwater has accumulated between 5 and 30 m of depth, forming as a semi-confined aquifer. Groundwater occurs mostly in weathered and fractured formations of the khondalite followed by basement of granitic gneiss. Mahadevan [2] was probably the first scientist to postulate a hydrogeological concept of this region and has pointed out that, due to the action of water, the khondalites are altered into two different forms. On the surface, the rock changes into a lateritic soil and the subsurface formation, when acted upon by water, turns itself into kaolin. Sarma [5] has conceived a four-layer system in the khondalitic terrain i.e., the top soil zone underlain by the talus zone in foot hill areas, which in turn is underlain by a weathered kaolinised portion that merges into a fractured and fissured zone and further followed by basement material. When the khondalite is highly weathered due to the presence of water at low lying areas such as water courses, it becomes kaolinised and acts as a barrier to the lateral movement of groundwater, causing it to be accumulated on either side of the stream, turning the areas adjoining stream courses into non-potential groundwater areas. [6].

To verify these concepts, hydrogeophysical, hydrogeomorphological and geohydrological investigations were carried out in the kandivalasa River sub-basin, having an areal extent of 120 km² and mostly covered with Khondalitic terrain situated at Cheepurupally town of Vizianagaram District, Andhra Pradesh, India (Fig. 1).

V. R. Bekkam (✉)

Centre for Water Resources, Institute of Science and Technology,
Jawaharlal Nehru Technological University, Hyderabad,
Kukatpally, Hyderabad, 500085, India
e-mail: cwr_jntu@yahoo.com

Fig. 1 Location map of the study area



2 Materials and Methods

In the study area, 42 wells were drilled at the recommended vertical electrical sounding (VES) sites. Data such as lithologs and yield logs were available at these places. Lithologic profiles were constructed using the drilled data (Fig. 2). The drilled wells were classified into successful (8000 lph and above) and failed wells based on the yield norms of the irrigation wells for government funding agencies. The successful and failed wells are distributed based on kaolinised layer thickness (Table 1) and aquifer resistivity identified from the VES (Table 2) data. Resistivity imaging profiles were also conducted across and adjacent to the streams (Fig. 3) to determine the progress of kaolinised layer towards the stream. Pumping tests were conducted at 14 places covering the entire basin and the distribution of transmissivity and storage coefficient was mapped (Fig. 4). From the groundwater modeling studies, hydraulic conductivity of the kaolinised layer and the fractured layer was determined.

3 Results

From Table 1, it can be observed that the percentage of successful wells decreases as the kaolinised layer thickness increases. The more the kaolinised layer thickness is, the less yield is obtained from the wells. From Table 2, it can be

observed that, as the aquifer layer resistivity decreases, the success rate also decreases. Aquifer layer (highly weathered, weathered and fractured khondalite) resistivity has been obtained from the vertical electrical soundings data. Layers having a resistivity less than $25 \Omega \text{ m}$ are considered as kaolinised layers and $25\text{--}65 \Omega \text{ m}$ are considered as weathered and fractured layers. Layers having a resistivity greater than $65 \Omega \text{ m}$ represent the basement characteristics. From Fig. 2, it can be seen that the kaolinised layer thickness is maximum near the streams and the weathered and fractured layer is maximum between the two streams. This holds good not only at the smaller streams of the basin, but also at the bigger streams of the basin, as has been shown from the images of Sivaram village near the stream (Fig. 3). From this figure, it can be observed that the kaolinised layer has progressively increased towards the stream from profile 1 (away from the stream) to profile 3 (closer to the stream). The same phenomenon can be more predominantly observed in the case of storage coefficient distribution (Fig. 4). The storage coefficient is low all along the main stream producing low well yields.

4 Discussion

Even hydrogeomorphological investigations were also carried out and found that almost all the stream courses coincided with the fault or fracture zones and considered as lineaments. Between the lineaments, well yields are high due

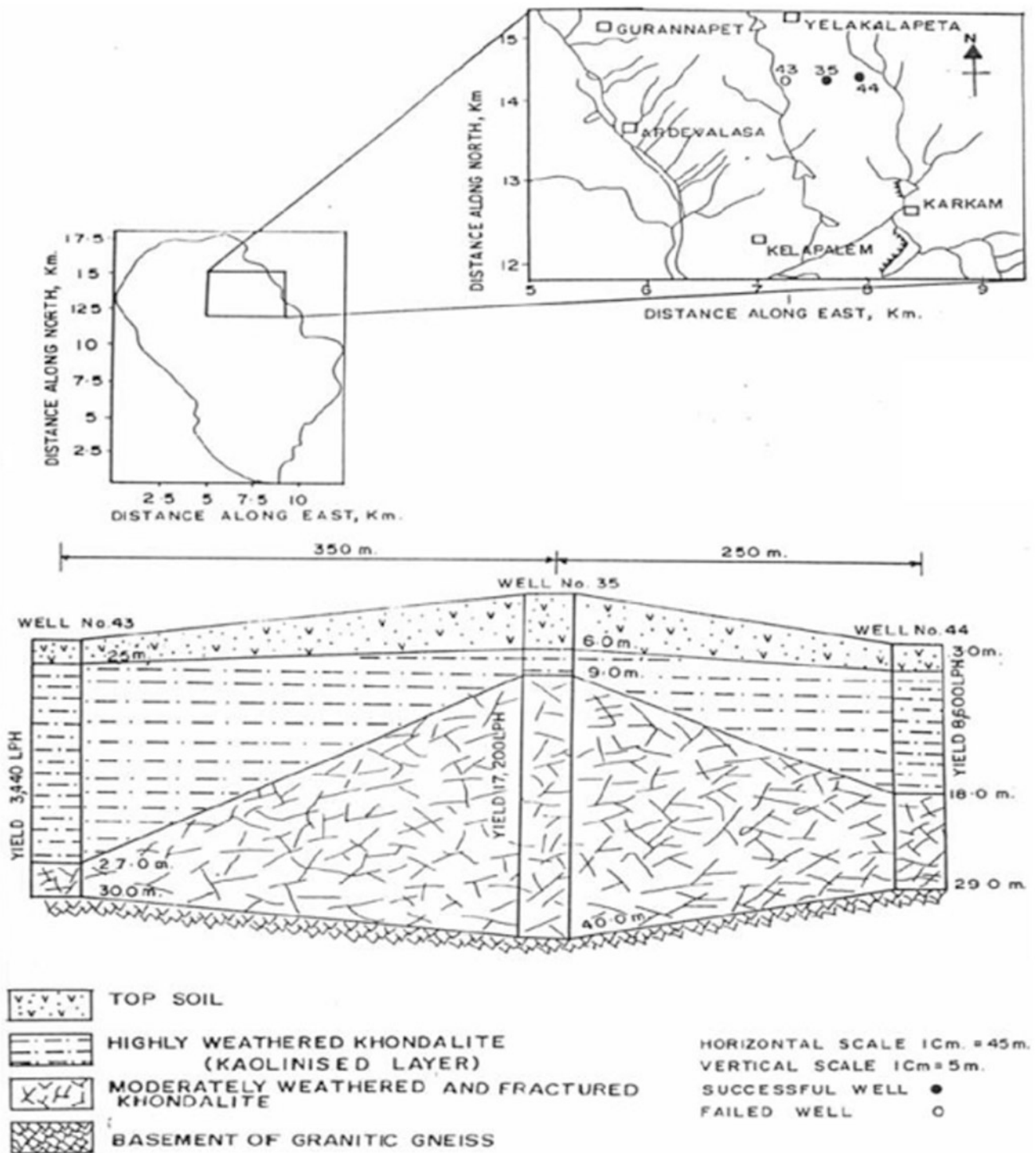


Fig. 2 Lithologic profile across the drainage pattern in the basin

Table 1 Percent success rate of wells in various ranges of thickness of kaolinised layer

Range of kaolinised layer thickness (m)	0-10	10-20	20-30	>30
Number of successful wells	14	8	5	0
Number of failed wells	3	4	4	4
Percent success rate	82.3	66.6	55.5	0

Table 2 Percent success rate of wells in various ranges of aquifer resistivity

Aquifer resistivity range (Ω m)	5–15	15–25	25–35	35–45	45–55	55–65	>65
No. of successful wells	7	7	9	1	0	3	0
No. of failed wells	5	4	4	0	0	0	2
% Success	58.3	63.6	69.2	100	0	100	0

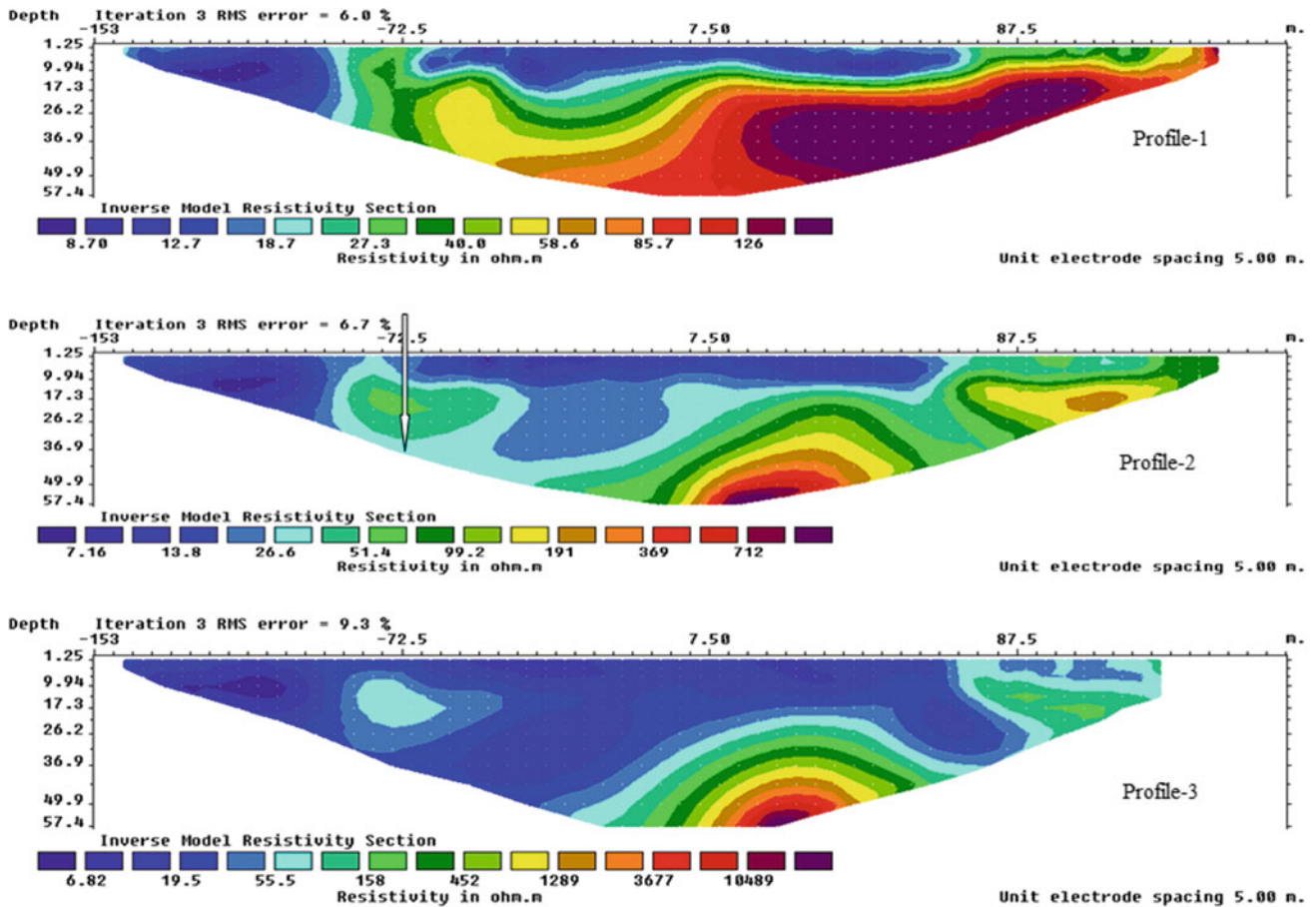


Fig. 3 Resistivity imaging profiles near the stream of Sivaram village

to moderately weathered and fractured formations and considered as shallow weathered pediplains. Nearer to the lineaments, the formation has been deeply weathered and became kaolinised due to the continuous presence of water. Consequently, the areas between the two lineaments or water courses have high groundwater potential zones suitable for high yielding bore wells, whereas areas adjoining the lineaments or stream courses have become low groundwater potential zones suitable only for open wells. These concepts are imbibed into groundwater flow modeling studies with a two-layer conceptual model, in which the kaolinised layer’s hydraulic conductivity varies from 1.6 to 1.9 m per day,

while that of the weathered and fractured layer below it varies from 1.6 to 2.3 m per day.

5 Conclusions

The hydrogeological and hydrogeophysical investigations, in the kandivalasa river sub-basin situated in the khondalitic terrain of the eastern Ghats of India, have converging evidence that the aquifer has become kaolinised beneath the streams with a very low yielding capacity, while aquifer between the streams have moderately weathered and

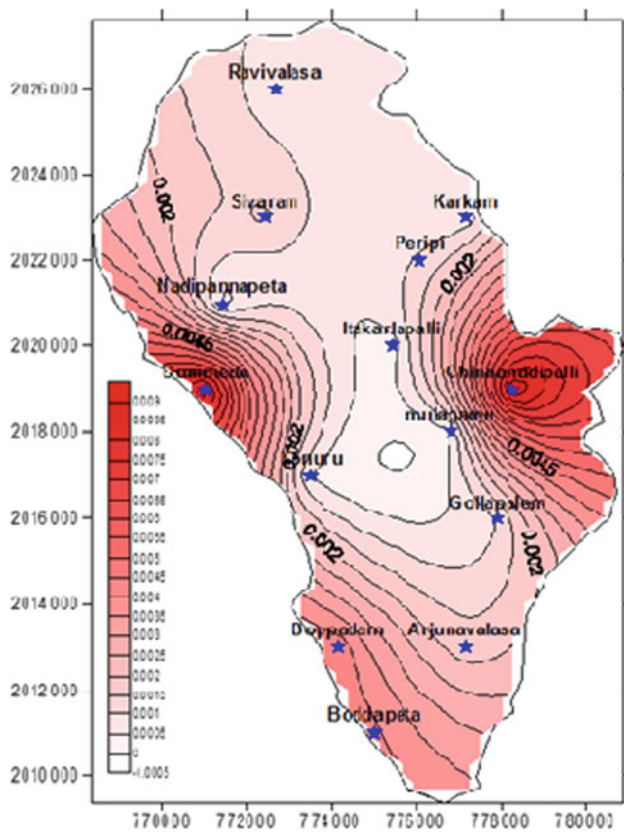


Fig. 4 Storage coefficient distribution over the study area

fractured khondalite, producing good well yield. The kaolinised portion is acting as a barrier to the lateral movement of the groundwater and causing it to be accumulated between the streams. The kaolinised layer resistivity is less than $25 \Omega \text{ m}$, while that of the weathered and fractured layer is $25\text{--}65 \Omega \text{ m}$. Similarly, the hydraulic conductivity of the kaolinised layer is found to be varying between 1.6 and 1.9 m per day and that of the weathered and fractured layer is varying from 1.6 to 2.3 m per day.

References

1. Krishna Rao, J.S.R.: The geology of Chipurupalle area, Visakhapatnam District with special reference to the origin of manganese ores. *Geol. Soc. India* **XXVI**(1), 36–45 (1952)
2. Mahadevan, C.: Geology of Vizag harbour area. *Q. J. Geol. Min. Metal. Soc. India* **2**(4) (1929)
3. Rao, G.V.: Structural control and origin of the manganese ore deposits in Visakhapatnam manganese belt, Andhra Pradesh. In: *International Geological Congress, Part V*, pp. 215–227 (1964)
4. Sriramdas, A., Rao, A.T.: Charnockites of Visakhapatnam A. *P. J. Geol. Soc. India* **20**, 512–517 (1979)
5. Sarma, V.V.J.: Hydrogeology of Visakhapatnam region of Eastern Ghats. *J. Indian Geophys. Union* **4**(2), 422–431 (1967)
6. Venkateswara Rao, B.: Hydromorphogeological investigations in a typical khondalitic terrain using remote sensing data. *J. Indian Soc. Remote Sens.* **26**(1 & 2), 77–93 (1998)

Assessment of Vulnerability and Risk Mapping at Marsaba—Feshcha Catchment

Jawad Shoqeir

Abstract

Water supply entails many activities, among which is to ensure a water supply with a quality that meets the WHO potable water standards. Water resources protection will secure good water quality and quantity in arid and semi-arid regions. Any human activities on the recharge area of a given water resource increase the contamination hazard and vulnerability of the wells and springs that are fed from this resource. This issue becomes problematic in semi-arid and arid zones, where the water resources are quite limited and the effect of dilution of effluents by the rainfall or in the aquifer storage is minimal and rare. Today, the wastewater effluents of the main cities are also discharged into these wadis, which contaminates the environment and the groundwater. The urban sector is growing fast and it produces effluents that are transferred to the wadis flowing into the Jordan Valley. This study focuses on Marsaba-Feshcha (M-F) Basin as one of the most important basins in the Jordan Valley that is connected to the Dead Sea. Rough estimations were provided for the spring annual discharge of water ranging between 30 and 50 MCM/Y. Vulnerability and risk maps were constructed using ArcGIS and My-Observatory software-based PI map. The hazard map shows the localization of potential contamination sources resulting from human activities and evaluates those according to their dangerousness. The risk map for the M-F Basin was thus created by overlaying the hazard and vulnerability maps.

Keywords

Karst • My-observatory software • Intrinsic vulnerability • Risk assessment • Marsaba-Feshcha

1 Introduction

Groundwater is a natural drinking water resource often subjected to severe human impacts, where wastewater and random solid waste dumping sites are considered potential pollution sources in the Karstic aquifers. Strategies are required to preserve optimum groundwater quality, and so, the management of this vital natural resource has become a worldwide priority. In the last years, the international scientific community has shown a great interest in this topic, and thus, many works focused on the environmental management for groundwater protection. Groundwater from karst aquifers is among the most important resources of drinking water supply of the worldwide population, in some countries, karst water contributes by 50% to the total drinking water supply, and in some regions, it is the only available freshwater resource. At the same time, karst aquifers are particularly vulnerable to contamination. Indeed, due to the thin soil cover and to the flow concentration in the epikarst, contaminants can easily reach the groundwater, where they may be transported rapidly in karst conduits over large distances.

This study focuses on a small area in Marsaba-Feshcha (M-F) since it is considered as one of the few places in the West Bank where additional limited amounts of groundwater can be exploited. This area, the Eastern Basin (Jerusalem-Dead Sea sub-basin), as well as the other parts of the whole semi-arid eastern slope of the West Bank mountains, is arid and suffers from an acute shortage and quality deterioration for the available replenished fresh water resources; the outlet of this basin is the Ein Feshcha spring group which is located in the upper North-Western shore of the Dead Sea, and whose discharge amounts to about 50–80 MCM/Y of fresh/saline to brackish water [1].

More than 15,000 MCM/Y of untreated wastewater flows through the catchment, which may infiltrate into the aquifer and contaminate the groundwater of the M-F basin. The M-F basin is considered as one of the most important future

J. Shoqeir (✉)

Soil and Hydrology Research, Al-Quds University, Abu Dis 89, Palestine

e-mail: jhassan.aqu@gmail.com

resources to be developed for the Palestinians in the EAB, therefore, risk maps and vulnerability maps should be used as a tool for stakeholders in planning and management options, as well as in identifying the point and non point pollution sources [2].

2 Materials and Methods

The study area covers a surface of approximately 800 km² (Fig. 1), extending from the eastern slopes of Jerusalem anticlinorium, through the Marsaba anticline in the West, to the Jordan Valley and the Dead Sea in the East, including the spring complex of Ein Feshcha (Fig. 1). This catchment area is considered as a part of the eastern drainage basin of the Jerusalem hills, and the outlet of this basin is Ein Feshcha spring group which is located in the upper North-Western shore of the Dead Sea at an elevation of approximately 413 m below sea level, that is, ahead of 860 m over a lateral distance of about 20–25 km [3].

To develop the risk mapping and vulnerability mapping, a field survey, field observations and data collection were the tools to identify the potential source of pollution.

Different software programs were used for factors identification (soil cover, runoff, permeability). The WinLoG version 5 extension module and WinFence version 3 of Strata Explorer have been used to create a full-color cross-section, depending on types of strata that have been used, including layers and faults. The PI method, using My-Observatory, is a GIS method based on an origin pathway target model [4].

3 Results

3.1 Prediction of Vulnerability Map

The protection factor (π) (Fig. 2) was calculated by multiplying the P and I factors. The range of values for (π) was subdivided into five classes of natural protection and

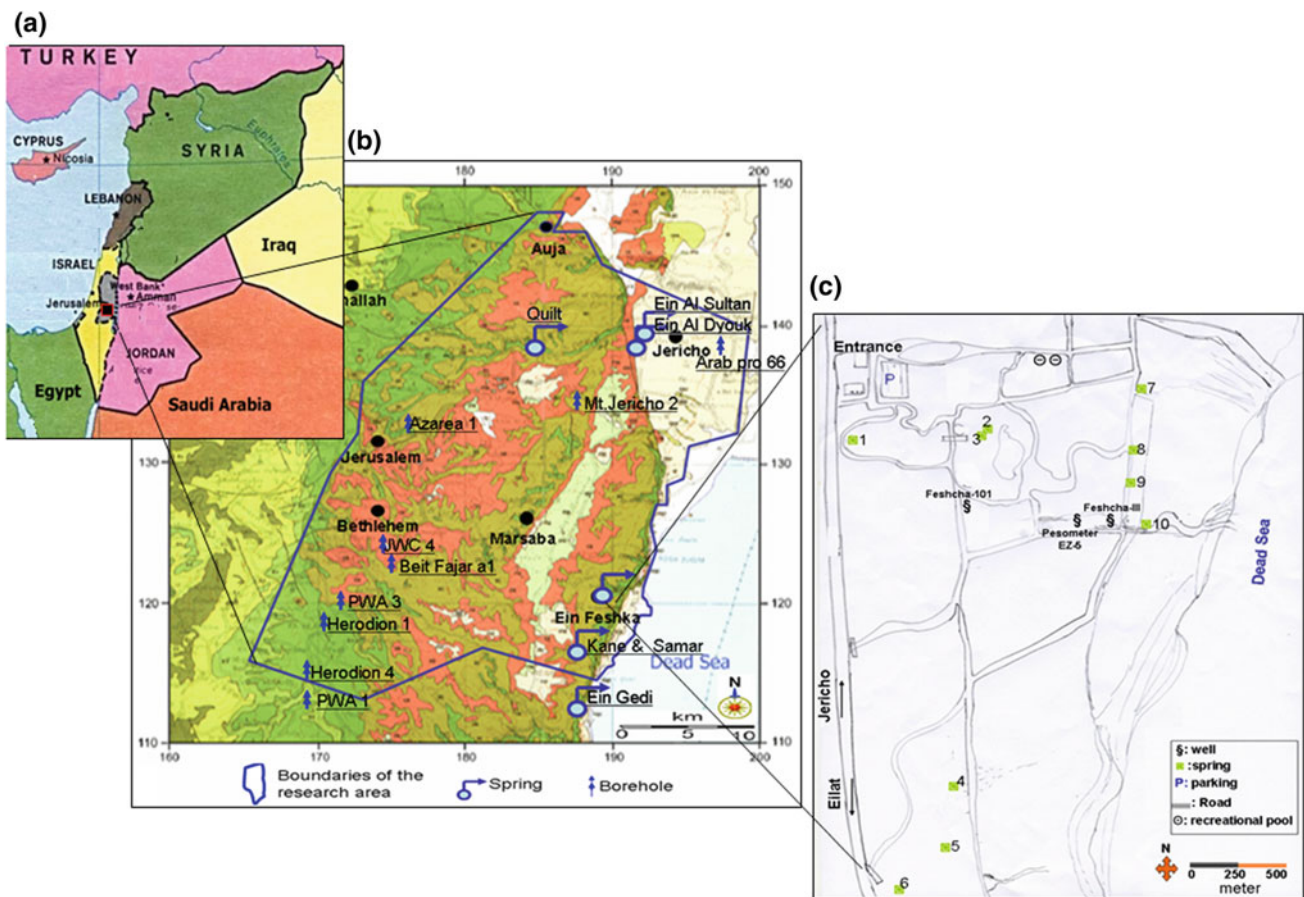


Fig. 1 Location map of the study area in the West Bank, Palestine. **a** The location on the background of the Near East countries. **b** A geological map showing the locations of wells and springs in the

catchment area. **c** Ein Feshcha springs group map showing the locations of wells and springs in the study area [3]

vulnerability respectively. According to land use activities it can be, clearly seen that most areas under irrigated vegetables farming are of a low vulnerability, while those under permanent cropping, i.e. grapes, olives, citrus and fruits, are of a moderate to low vulnerability. Most of the groundwater vulnerability of the study area ranges from moderate to very low.

3.2 Prediction of Pollution Risk Map

The PI map from ArcGIS has been uploaded to My-Observatory and the hazard index shape file. Then, the calculation of the risk has been applied in My-Observatory. The produced Risk Map shows that the study area can be classified as a low or very low-risk area corresponding to the pollution source, but its majority can be classified as an area with a low risk level of groundwater contamination (Fig. 3).

4 Discussion

The use of the PI method to produce the risk map was challenging, therefore, this study focused on using two methods (PI method and My-Observatory software) to develop the vulnerability map and risk map respectively. Several Geological Cross Sections have been studied and are very significant in developing an overview of the hydro-stratigraphy related to Marsaba-Feshcha basin. These cross-sections are essential to evaluate the characteristics of the groundwater movement and aquifer recharge. The vulnerability map, obtained by using the PI method, shows the intrinsic vulnerability and the natural protection of the uppermost aquifer. Most of the study area ranges from moderate to very low groundwater vulnerability.

The conducted analysis in this research identified as well as classified the hazards and their sources, the highly-vulnerable areas to contamination and the high-risk areas

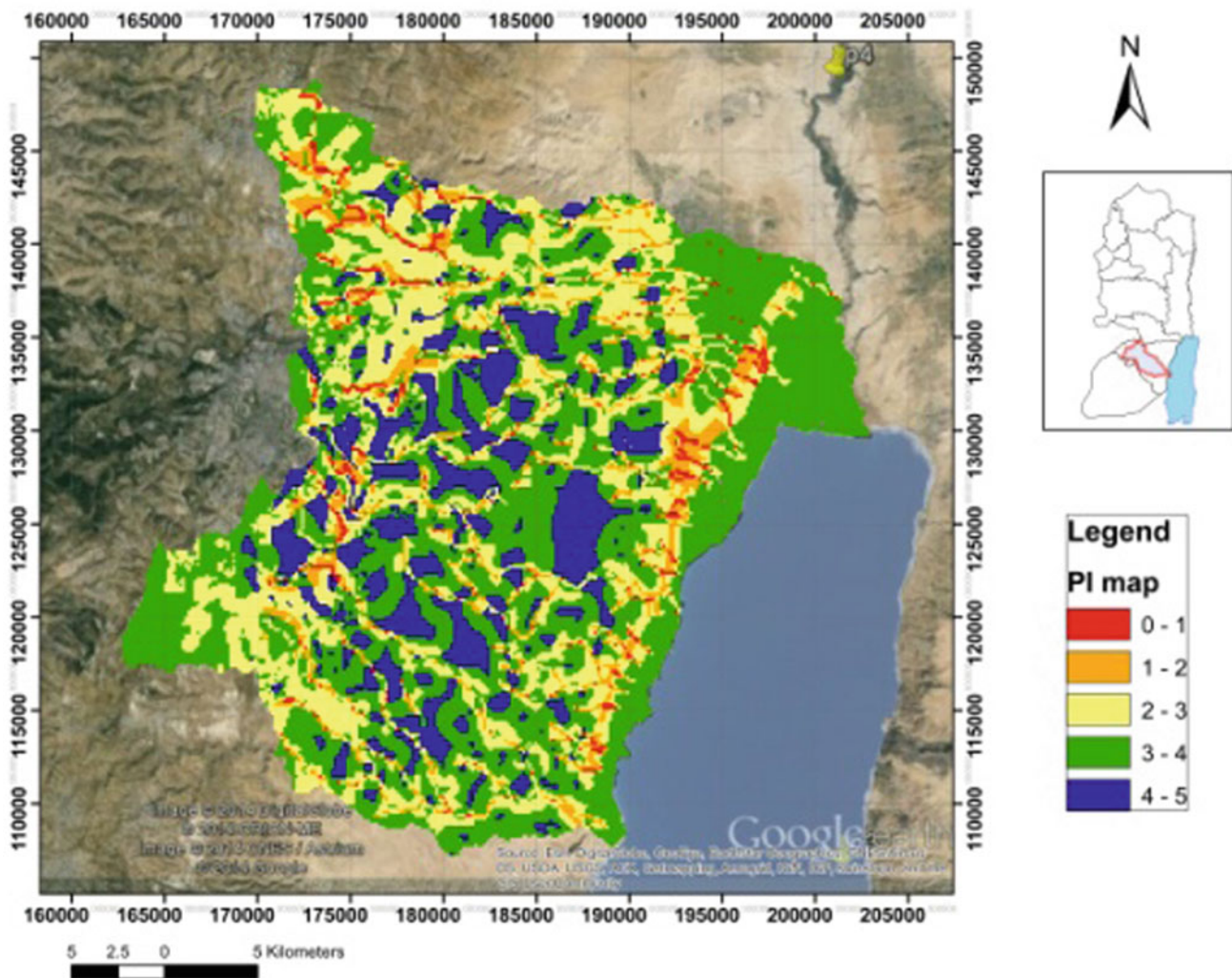


Fig. 2 Vulnerability map according to the PI method

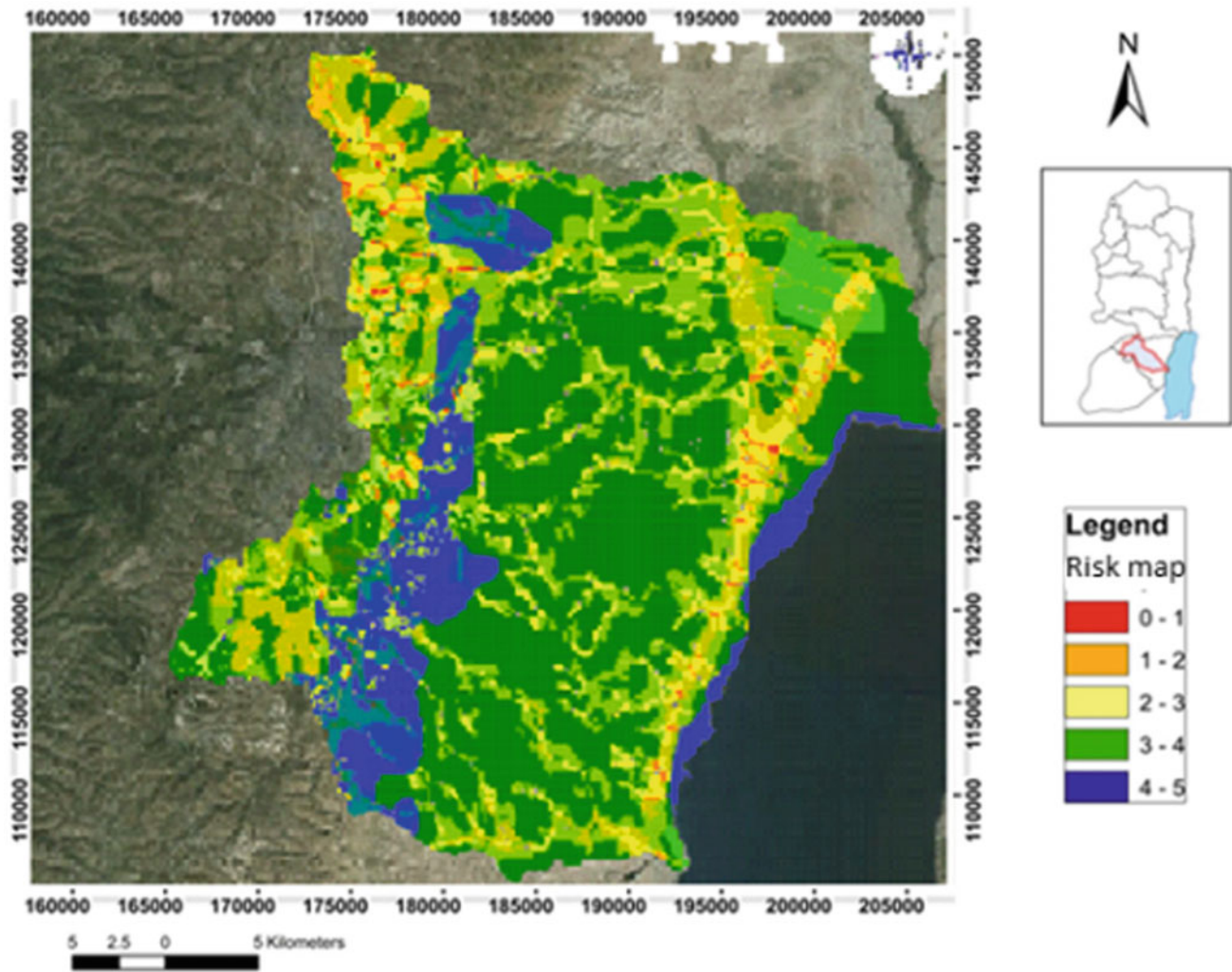


Fig. 3 Risk map of M-F basin using My-observatory

regarding groundwater contamination. According to the analysis, the sensitive risks resulted from the wastewater which was generated from the urban and agricultural areas. The risk assessment scheme used for risk map of M-F basin is based on the intrinsic vulnerability map constructed using the PI method and the hazard map and focuses on risk assessment for the groundwater resources. The first part used ArcGIS and Risk Map of the study area that can be classified as low or very low, the second part used My-Observatory and it showed a Risk Map of the study area that can be classified as a low or very low risk.

5 Conclusions

The vulnerability assessment is recommended to be applied on other basins with high potential for specific contamination, and this can be implemented via My-Observatory

platform to assess the risk map of M-F Basin, using mapping and GIS-centric features to produce visual illustrations of contaminants. The PI method uses one type of file formats which did not show much flexibility as the My-Observatory method did. The My-Observatory method uses multiple data sources and it is connected to Google Earth, which makes the used data dynamic. This means that any new data entry from the field by the researchers will be uploaded automatically into My-Observatory website. This will ensure the dynamics of the produced maps to be updated with minor efforts.

References

1. Shoqeir, J.: Tracing Groundwater in Karstic Aquifer: IWRM Components Implications and Challenges, 1st edn. Lambert academic Publishing. ISBN: 978-3-659-27211-0 (2014)

2. Palestinian Water Authority: Annual Status Report on Water Resources, Water Supply, and Wastewater in the Occupied State of Palestine (2011)
3. Hassan, J.: Nature and the origin of Ein Feshcha springs. A thesis for the degree of Doctor of Natural Sciences submitted to the Faculty of Civil Engineering, Geosciences and Environmental Sciences, University of Karlsruhe, Germany (2009)
4. Zwahlen, F.: Vulnerability and risk mapping for the protection of carbonate (karst) aquifers. Final Report (COST Action 620), 297p. European Commission, Brussels (2003)

Comparison of Two Methods for Groundwater Pollution Intrinsic Vulnerability Mapping in Wadi Nil (Jijel, North-East Algeria)

Abdelmadjid Boufekane, Hakim Saibi, and Omar Saighi

Abstract

The excessive use of fertilizers in agriculture led to the increase of the nitrates pollution of wadi Nil groundwater (Jijel, North-East Algeria). The use of fertilizers in high quantities with respect to the plants' needs will lead to the leaching and infiltration of the excess fertilizers towards groundwater by increasing the nitrate percentage, which ultimately leads the contaminant's level to exceed the allowed norms of water consumption (50 mg/l). The aims of this work were to assess the aquifer's vulnerability caused by pollution using DRASTIC and GOD methods. The study is based on the obtained measurements during the field surveys conducted during the hydrological year 2010–2011 and supplemented by the compilation of the information collected from various technical services of Jijel city. The comparison of nitrate-concentration distribution map and that of vulnerability levels obtained by each approach, showed that the DRASTIC method was the most appropriate in this case with a percentage of 71.4% versus 47.2% for GOD method. It was found that the studied water was characterized by a medium to high degree of vulnerability, which requires finding solutions to protect and preserve the water of this area.

Keywords

Nitrate • Vulnerability • Agriculture • Groundwater • Algeria

A. Boufekane (✉)

GEE Research Laboratory, Ecole Nationale Supérieure d'Hydraulique de Blida, Blida, Algeria
e-mail: boufekane_ab@yahoo.fr

H. Saibi

Department of Geology, United Arab Emirates University, Al-Ain, United Arab Emirates

O. Saighi

Department of Geology, FSTGAT/USTHB, Algiers, Algeria

1 Introduction

The prevention of aquifers' pollution is considered as an important factor in the management of groundwater resources. Also, the assessment of aquifer vulnerability by scientists is an essential factor which gives us solutions to protect groundwater resources. The Nil valley groundwater (Jijel, Algeria) which is characterized by a favorable vegetables and greenhouse gardening activity undergo a contamination by nitrates due to the use of fertilizers in agriculture. In order to prevent groundwater resources pollution, the present work studies the aquifer by using two parametric methods, DRASTIC and GOD, and by examining the surface activities which characterize the aquifer. The obtained vulnerability maps via the three methods are validated by comparison with the observed nitrates in the groundwater.

2 Materials and Methods

2.1 Study Area

The studied area is located in the north-east of Algeria. The alluvial aquifer of this area forms part of the coastal plains region of Jijel (Fig. 1). It covers an area of 83 km² and opens to the north of the Mediterranean Sea. The maritime location of this region gives it a mild and damp climate. The average temperature is 17 °C/year, while rainfall, relatively high, reaches 900 mm/year. In addition, the geological substratum of the area consists of gneiss, schist and mica-schist [2]. However, the parts of swallow, sedimentary formations are mainly Oligocene, Miocene and Pliocene marly. Finally, the depressions and valleys are filled with quaternary alluvial deposits which are interstation terraces aquifers.

The groundwater recharge is mainly done by infiltration of rainfall and the low water seepage from the various rivers which cross the plain. The aquifer forms part of the socio-economic development of the region by the



Fig. 1 Location map of the study area

exploitation of the domestic wells and boreholes (36 million m^3 /year) [2].

2.2 Working Environment and Data Preparation

The study is based on the measurements obtained from the field surveys that were conducted during the hydrological year 2010–2011 and supplemented by the compilation of the information collected from various technical services of the city of Jijel (National Agency Resources Water, Direction of the Water Resources, Direction of the Agricultural Services). The documents of the different parameters allowing the development of the vulnerability map to groundwater pollution have been created according to grid values by using a regular grid of 25×25 m and by dividing the 83 km^2 of the study area (elementary units of this size).

Table 1 Weight settings of DRASTIC [1]

Symbol	Parameter	Weight
D	Water depth	5
R	Effective recharge	4
A	Middle aquifer	3
S	Soil type	2
T	Topography	1
I	Impact of the vadose zone	5
C	Hydraulic conductivity	3

2.3 Presentation of the Methods Used for Vulnerability Assessment

DRASTIC method: was developed by the staff of the U.S. Agency for Environmental Protection, USEPA [1]. It allows the assessment of vulnerability of the vertical aquifer pollution caused by parametric systems. It is based on the estimation of 7 parameters, (Table 1) such as the percentage of the effective recharge, the soil type and the characteristics of the saturated and unsaturated zones of the aquifer. Each parameter, divided into intervals of significant values, is assigned by a numerical rating based on its growing importance in the vulnerability [3].

The DRASTIC vulnerability index was calculated by the addition of the different products (score \times weight of the corresponding parameter):

$$\text{DRASTIC Index} = D_w D_r + R_w R_r + A_w A_r + S_w S_r + T_w T_r + I_w I_r + C_w C_r.$$

where: D, R, A, S, T, I and C are the seven parameters and the subscripts r and w are the corresponding rating and weights, respectively.

GOD method: This method is characterized by a rapid assessment of the aquifer vulnerability [4]. It was developed by Foster in 1987 for studying the vulnerability of the aquifer against the vertical percolation of pollutants through the unsaturated zone, without considering their lateral migration in the saturated zone.

The GOD index which is used to evaluate and map the aquifer vulnerability caused by the pollution, was calculated by the multiplication of the influence of the three parameters using the following equation:

$$\text{GOD Index} = C_l \times C_a \times C_d,$$

where: C_a is the type of aquifer, C_l is the lithology of the unsaturated zone and C_d is the depth on the water surface.

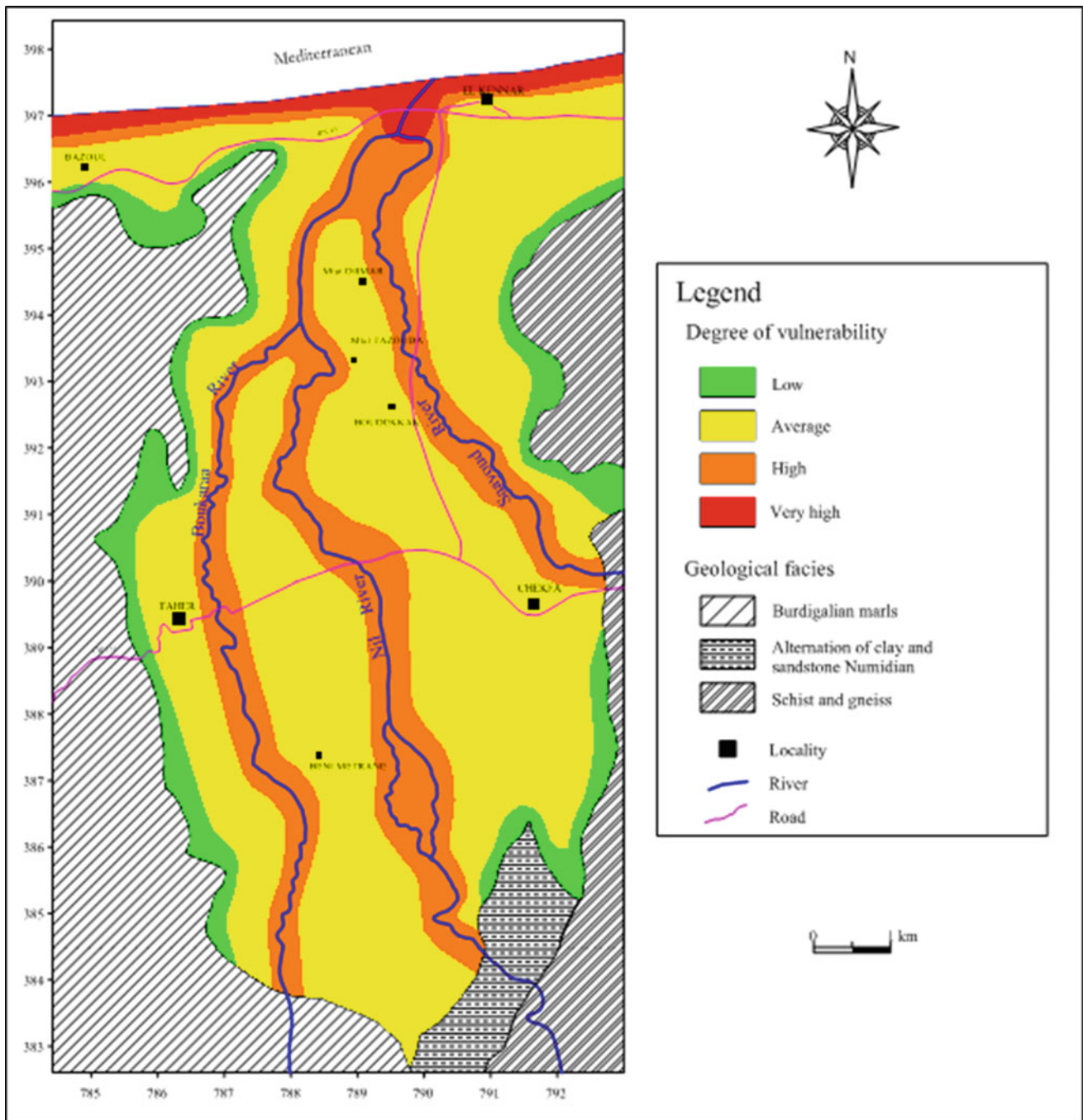


Fig. 2 Aquifer vulnerability map (DRASTIC method)

3 Results

3.1 DRASTIC Method

The obtained values of the DRASTIC index vulnerability by this method vary from 85 to 210. Their spatial distribution allows distinguishing, within the studied area, four zones

with different degrees of vulnerability (Fig. 2), closely related to the hydrographic network.

- (a) The zone with very high vulnerability at the coast affects more particularly the mouth of the Nil valley. It occupies around 3% of the studied plain. This high degree of vulnerability can be explained by the shallow aquifer as well as by the existence of a permeable

massif of dunes, allowing the infiltration of pollutants present at the surface.

- (b) The zone with high vulnerability encompasses the previous one and penetrates inside the land along the topographic drains of the Nil valley and its two tributaries, Saayoud and Boukaraa. This second zone represents 26% of the plain surface area, and juxtaposes the extended areas of the major waterways, where the major sediments composing the alluvial terraces are

dominant, and the piezometric level varies between 1.5 and 5 m. Such characteristics favor the penetration of pollutants into the aquifer, particularly in the depressed parts.

- (c) The zone with an average vulnerability covers about two-thirds (2/3) upstream the plain, where, despite the importance of the gravelly and sandy section of the aquifer, it is less protected from pollution because of its shallow depth (generally not more than 5 m).

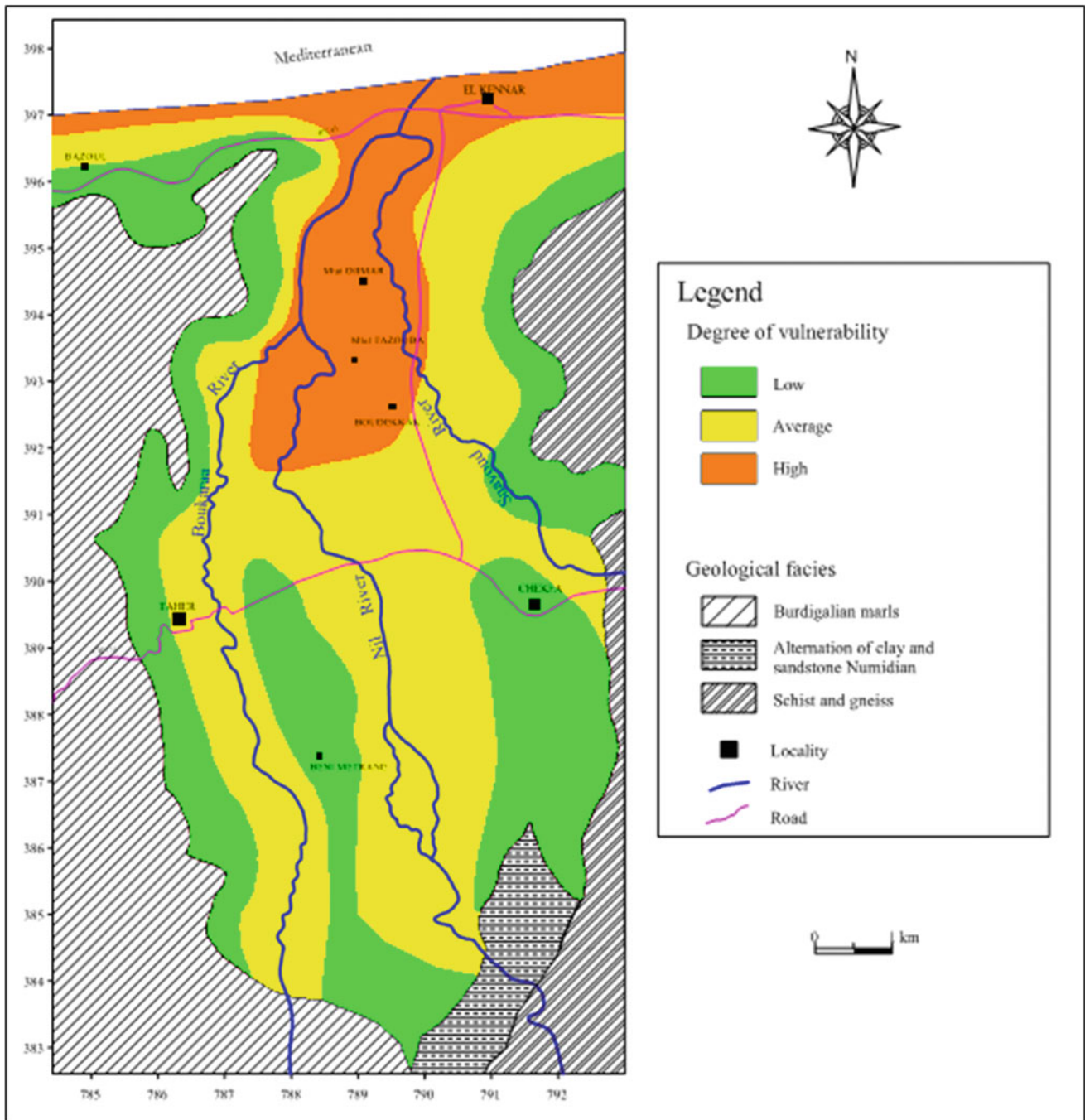


Fig. 3 Aquifer vulnerability map (GOD method)

Table 2 Spatial distribution of nitrate in groundwater, with respect to vulnerability classes

Vulnerability	DRASTIC method				GOD method			
	Samples number per nitrate content class (mg/l)							
	0–15	15–30	30–45	>45	0–15	15–30	30–45	>45
Low	1	0	0	0	5	3	0	0
Average	15	2	1	3	8	3	1	3
High	6	7	0	0	9	3	0	0
Very high	0	0	0	0	0	0	0	0
Total	22	9	1	3	22	9	1	3

- (d) The zone which is a bit vulnerable corresponds to the edges of the plain and covers 10% of the area. Its low vulnerability is due first to the depth of the aquifer (about 10 m) and secondly, to the low permeable covering soil and the unsaturated zone.

3.2 GOD Method

GOD indices show values ranging from 0.16 to 0.54. Their low dispersion allows differentiating just three zones of vulnerability (Fig. 3), whose spatial distribution, somewhat different from the DRASTIC case, is as follows:

- (a) The highest degrees of vulnerability are located in coastal areas, especially at the Nil river. However, they remarkably invade inland up along Boukraa and Saayoud valley, around 4 km. This area covers 18% of the plain area and, as already mentioned, corresponds to shallow-aquifer areas (1.5–5 m), associated with highly permeable sediments at the surface (dune, sandy and gravelly aquifer, etc.).
- (b) Moderate vulnerability zones contain the previous one and go up further along the valley, until covering 47% of the plain surface area. The aquifer is situated between 5 and 9 m deep and consists of gravel and sand that promote the spread of pollutants, despite the sporadic presence, in the airy area, of clay and marly intercalations.
- (c) Regarding DRASTIC case, though somewhat wider, low-vulnerability band surrounds the plain. On the other hand, the valley intervals also indicate low vulnerability levels because the underground water there is more than 12 m deep, and saturated and unsaturated zones are a bit permeable. The cumulative surface area of low vulnerability areas reaches 35%.

3.3 Spatial Distribution of Nitrate in Groundwater

Nitrate concentrations' spatial variation in groundwater depends on agricultural activities, covering soil lithology and thickness of the vadose zone. Recorded contents in 35 samples (19 drillings and 16 wells) were collected in September 2010. Comparing the nitrate concentration distribution map and that of vulnerability levels obtained by each approach [the results (Table 2)] reveals that the DRASTIC method seems to be the most reliable in reflecting reality on the ground, with a coincidence rate of 71% (25 out of 35 values), against 54% for the GOD method (19 values out of 35).

4 Discussion

This study has been applied to an area clearly defined by natural conditions and hydrogeological limitations. The combined use of three approaches allows a better understanding of the mechanism and representativeness of pollution vulnerability in the examined area. In the case of the Nil valley groundwater, DRASTIC method proves to be the one that best reflects reality on the ground. However, it takes into account seven parameters including reliability that depends on data used for their implementation. Many of them such as recharge, hydraulic conductivity and vadose zone impact, are either approximate or produced via scaling-up.

5 Conclusion

Vulnerability study results of the Nil valley groundwater show that the vulnerability degree increases upstream and downstream due to the rising of the aquifer and the important sandy fraction in the vadose zone. In addition, this

relates to intensive anthropogenic soil activity. The high index areas are on the coast where groundwater is shallow and agricultural activity is dense. DRASTIC approach is more reliable in representing nitrate distribution into water, with a matching rate of 71%, against 54% for GOD. Nevertheless, whatever the method used is, results reveal that the Nil valley groundwater, mainly downstream, is highly vulnerable.

References

1. Aller, L., Bennet, T., Lehr, J.H., Petty, R.: DRASTIC: A standardised system for evaluating groundwater pollution potential using hydrogeologic settings. EPA 600/2-87. U.S. Environmental Protection Agency Report. Environmental Research Laboratory, Office of Research and Development, Worthington, Ohio, 622p (1987)
2. Boufekane, A., Saighi, O.: Assessment of groundwater pollution by nitrates using intrinsic vulnerability methods: a case study of the Nil valley groundwater (Jijel, North-East Algeria). *Afr. J. Environ. Sci. Technol.* **7**(10), 949–960 (2013)
3. Engel, B.A., Navulur, K.C.S., Cooper, B.S., Hahn, L.: Estimating groundwater vulnerability to non point source pollution from nitrates and pesticides on a regional scale. *Int. Assoc. Hydrol. Sci.* **235**, 521–526 (1996)
4. Foster, S.S.D.: Groundwater recharge and pollution vulnerability of British aquifers: a critical review. In: Robins, N.S. (ed.) *Groundwater Pollution, Aquifer Recharge and Vulnerability*, Geological Society, vol. 130, pp. 7–22. Special Publications, Nottingham, UK (1998)

Groundwater Risk Assessment for Shallow Aquifers within the Atankwidi Basin of (Ghana)

Maxwell Anim-Gyampo, Geoffrey K. Anornu, Sampson K. Agodzo, and Emmanuel K. Appiah-Adjei

Abstract

This study reveals the potential risk to the quality of shallow groundwater aquifers from the application of agro-chemicals in upscaling crop production to ensure food security within the Atankwidi basin of Ghana, using the combination of DRASTIC and Arc GIS methods. The DRASTIC indices ranged from 41 to 117, representing the lowest to highest vulnerable areas. 34.4, 93.3 and 63.9 km² representing 20, 48.8 and 33.2% of the area had low, moderate and high vulnerabilities with indices ranging between 41–71, 71–88 and 88–117, respectively. The moderate and high vulnerable areas, which constituted approximately 80% of the area, were underlain by clay-loam and sandy-loam soils, respectively, where major farming takes place. The most vulnerable areas were in the highest elevated areas (recharge), with the shallowest depth to water-table and the highest permeability values. Sensitivity analysis using a map removal approach revealed influential parameters in the order of Hydraulic conductivity (C) > Soil type (S) > Depth to water table (D) > Net Recharge (R) > Influence of vadose zone (I) > Topography (T) > Aquifer material (A). The validation of the model using heavy metals measured in shallow aquifers showed the highest values within the most vulnerable areas and the lowest values in the least vulnerable ones.

M. Anim-Gyampo (✉)

Earth Science Department, University for Development Studies, Box 24 Navrongo, Ghana
e-mail: gyampom@gmail.com

M. Anim-Gyampo · G. K. Anornu

Civil Engineering Department, College of Engineering, KNUST, PMB, Kumasi, Ghana

S. K. Agodzo

Department of Agricultural Engineering, College of Engineering, KNUST, PMB, Kumasi, Ghana

E. K. Appiah-Adjei

Geological Engineering, College of Engineering, KNUST, PMB, Kumasi, Ghana

Keywords

Atankwidi • DRASTIC index • Ghana • Groundwater risk assessment • Shallow aquifers

1 Introduction

Groundwater, especially in arid and semi-arid regions, remains the most and sometimes the only reliable source of water to meet the domestic, agricultural and industrial demands of inhabitants [1] due to its quality and quantity, compared with surficial waters. However, anthropogenic activities [2] could result in a deterioration in the quality of groundwater [3] due to the leaching of heavy metals (e.g. Pb, Cd, As, Hg, Ni etc.) through the soil into the saturated zone underground.

To improve food security and lower poverty levels, the Atankwidi basin in Ghana had been earmarked for the upscaling of irrigational farming by the government of Ghana [4], with an anticipated utilization of groundwater [5] and large quantities of agrochemicals, since previous hydrological studies revealed surface water as very unreliable.

Thus, a potential risk to groundwater contamination, and consequently, potential health implications to human health and aspects of the ecosystem are envisaged. This study evaluates the intrinsic vulnerability of shallow aquifers within the Atankwidi basin of Ghana to assess their potential resilience to contamination from leachates from agricultural fields by mapping out the most vulnerable area(s).

2 Materials and Methods

The area (Fig. 1) is located between Lon 0°, 50'–1°, 10' W and Lat: 10°, 45'–11°, 00' N, with an area of 286 km². It is endowed with large tracks of fertile soils that can support

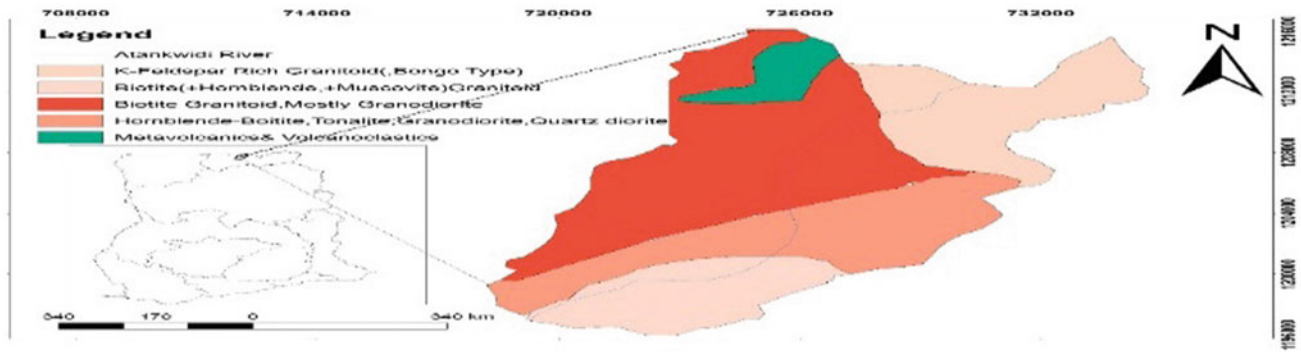


Fig. 1 The study area

large scale irrigational farming of which approximately 80% are uncultivated [4].

2.1 Determination of Intrinsic Vulnerability Shallow Aquifers

The Groundwater risk was assessed using a combination DRASTIC index (DI) and GIS tools. According to [6], DRASTIC is an acronym which incorporates seven parameters of the hydrogeological and physical characteristics of an area, namely depth to water table (D), net recharge (R), aquifer media (A), soil type (S), topography (T), influence of vadose zone (I) and hydraulic conductivity (C). $DI = \sum (\text{weight} * \text{Rating of each of parameter in DRASTIC})$. Weights (between 1 and 5) reflecting the relative influence on the rate of infiltrating groundwater were assigned to each parameter with the most influential assigned 5 and vice versa [6]. Thus, in this study, the assigned weights are D-5; R-3; A-2; S-4; T-1; I-4 and C-3. The product (i.e. W*R) of the

assigned weights and ratings based on variations in hydro-geological and geographical conditions were utilized by the Geostatistical Analyst and Spatial Analyst Tools in the GIS to create classified raster layer (index layer) for each parameter. Overlay analysis (summation of all index layers) using Spatial Analyst Tools under “Overlay” in Arc-GIS was carried out to produce a single composite layer (Risk map or DRASTIC model). The Scores (DRASTIC Indices) obtained from the DRASTIC model were reclassified into three categories as low; moderate and high vulnerable zones.

3 Results and Discussion

3.1 Groundwater Vulnerability Map

The final vulnerability map using the seven hydro-geological data layers showed in Fig. 2a–g is as depicted in Fig. 3.

The vulnerability map (Fig. 3) revealed that: out of 191.27 km², about 34.48 km² (20%) had low risk with a DI

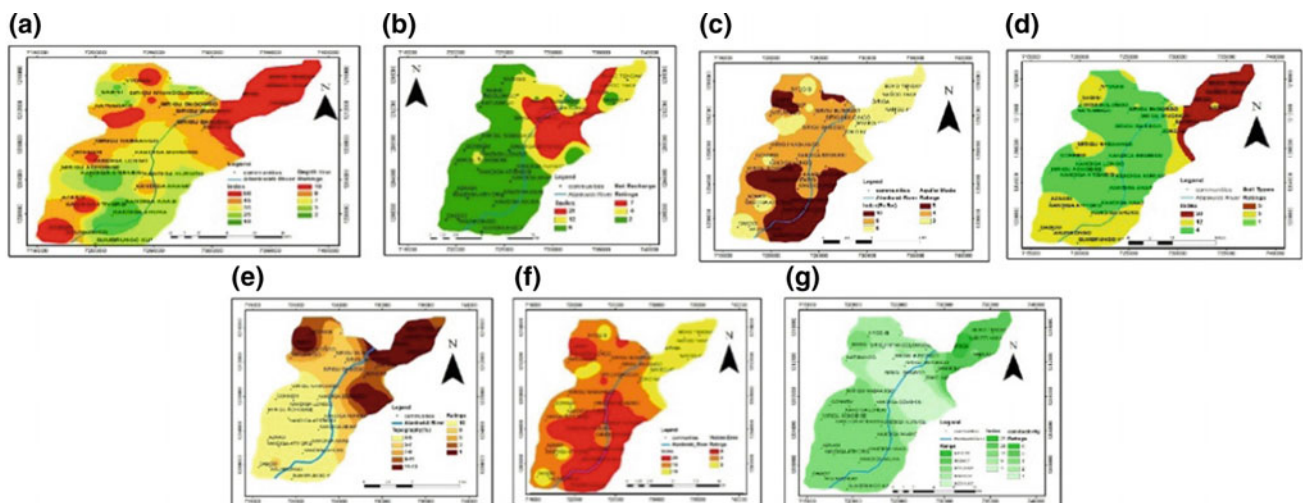


Fig. 2 a Depth to aquifer media (D). b Net recharge (R). c Aquifer media (A). d Soil media (S). e Topography (T); f Impact of the vadose zone (I). g Hydraulic conductivity (C)

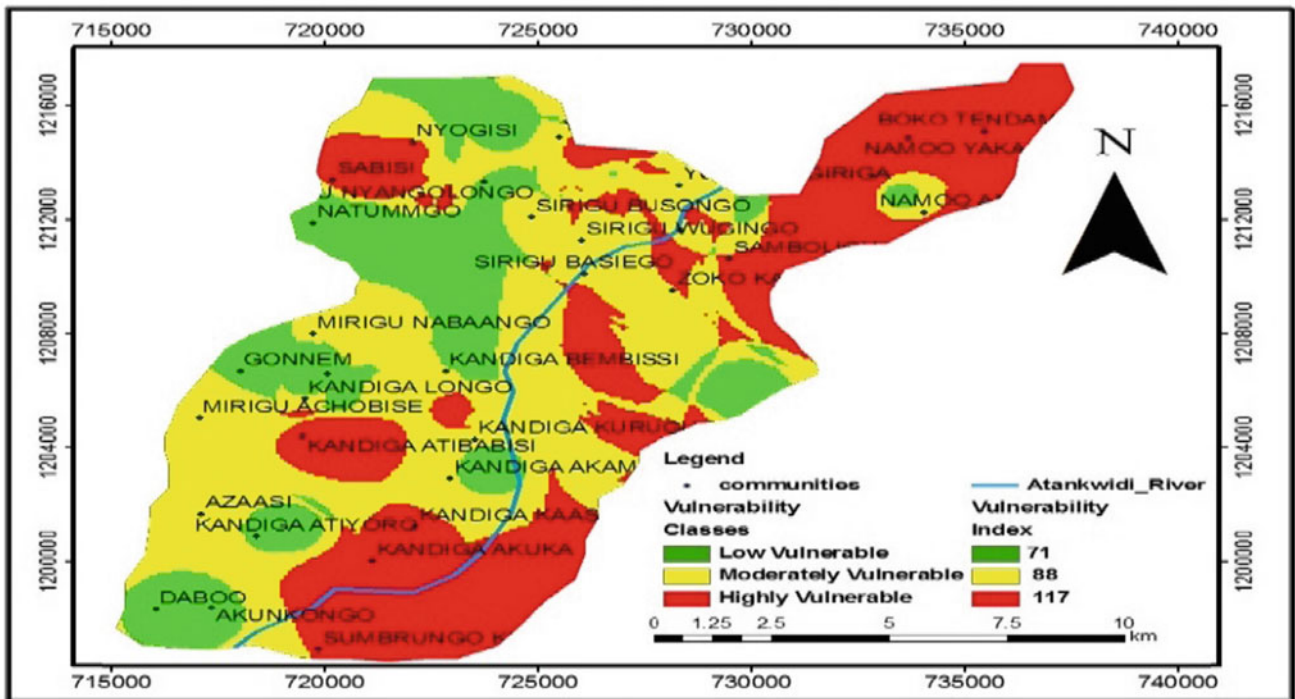


Fig. 3 Groundwater vulnerability zones of Atankwidi catchment

range of 40–71, about 93.31 km² (48.8%) were under a moderately vulnerable zone with a DI between 71 and 88, while about 63.48 km² (33.2%) were under the highly vulnerable zone with a DI ranging from 88 to 117. The moderate to highly vulnerable areas constitute about 80% of the entire Atankwidi catchment, signifying that a greater part of the area could be at risk in terms of aquifer pollution potential. Moderate and highly vulnerable zones are incidentally located in areas known for intensive modern irrigation farming involving the use of agro-chemicals (e.g.

fertilizers, weedicides, pesticides etc.). Areas under the high vulnerability zones have a low depth to water-table and coarse sandy-loam soils.

3.2 Sensitivity Analyses

The map removal analysis [7] indicated the order of influence of the parameters based on mean variation index as C > S > D > R > I > T > A.

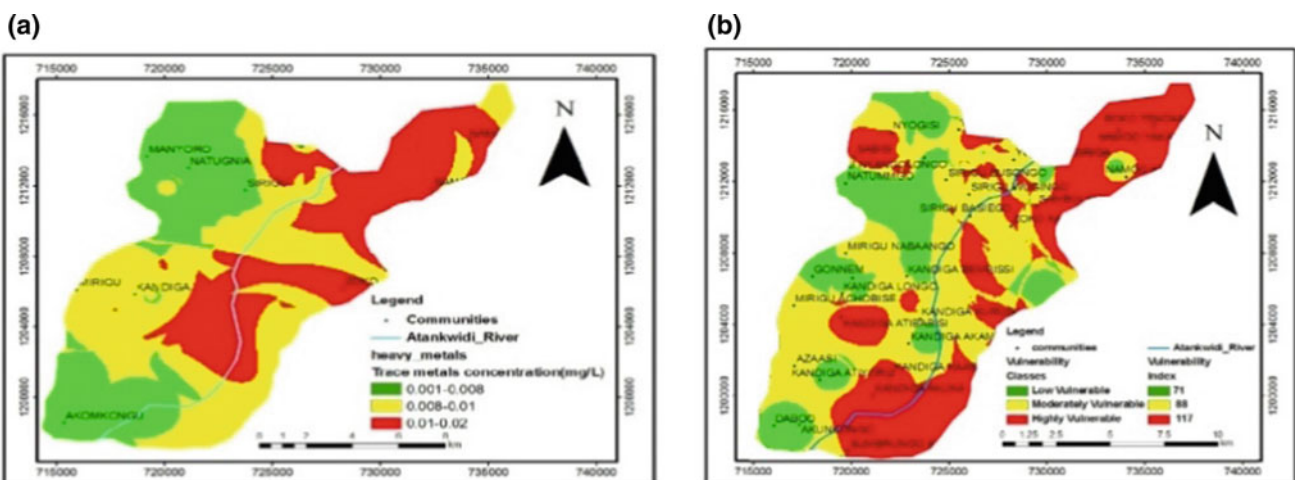


Fig. 4 a Composite thematic map of heavy metals, b vulnerability model of basin

3.3 Validation of DRASTIC Model

Analysis of measured concentrations of some heavy metals (Zn, Cu, Cr, As, Pb, Cd and Ni) of health significance [8] in 30 groundwater samples (Fig. 4a) revealed that the moderate to high risk zones contained elevated concentrations of heavy metals compared to low vulnerability zones.

4 Conclusions

About 33.2, 48.8 and 20% of the area had high, moderate and low risk potentials to contamination, respectively, with about 80% of the area having moderate to high risks. Moderate to high risk areas coincided with elevated areas (recharge) and intense farming areas (sandy-loam soils). Low risk areas were localized in low-lying, clay-rich areas. Validation using heavy metals from groundwater samples indicates that moderate to high risk areas had elevated concentrations of heavy metals and vice versa.

References

1. Gupta, S., Mahato, A., Roy, P., Datta, J.K., Saha, R.N.: Geochem of groundwater, Burdwan district, W. Bengal, India. *Env. Geol.* **53**, 1271–1282 (2008)
2. Wang, Y., Ma, T., Luo, Z.: Geostatistical and geochemical analysis of surface water leakage into groundwater on a regional scale: a case study in the Liulin karst system, NW China. *J. Hydrol* **246**, 223–234 (2001)
3. Lindström, R.: Groundwater vulnerability assessment using process-based models. *Trita-Lwr Ph.D. Thesis 1022*, Stockholm, Sweden, 36p (2005)
4. Ofosu, E., van der Zaag, A., P., van de Giesen, N., Odai, S.N., Amanor, R.: Analysis of Upscaling of Irrig Dev't in the W. Volta sub-Basin. *JENRM I(1)*, 36–43 (2014)
5. Barry, B., Forkuor, G., Gumma, M.K., Namara, R., Rebelo, L.-M., van den Berg, J., Laube, W.: *Shallow Groundwater in the Atankwidi Catch of the W. Volta Basin: Current Status and Future Sustainability*. Colombo, Sri Lanka (2010)
6. Anornu, G.K., Kabobah, A.T., Anim-Gyampo, M.: Evaluation of groundwater vulnerability in the Densu Basin of Ghana. *Am. J. Hum.* **3(1)** (2012)
7. Dixon, B.: Groundwater vulnerability mapping: a GIS and fuzzy rule based integrated tool. *Appl. Geogr.* **25**, 327–347 (2005)
8. World health Organisation: *Guidelines for Drinking Water Quality*, 3rd edn. World Health Organization, Geneva, Switzerland (2008)

Groundwater Flow Modelling of a Multilayer Aquifer in Semi-arid Context

Nesrine Ghouili, Mounira Zammouri, Faten Jarraya-Horriche, Fadoua Hamzaoui-Azzaza, and José Joel Carrillo-Rivera

Abstract

The Takelsa multilayer aquifer system, located in north-eastern Tunisia, contains important groundwater resources that have mainly been used for agricultural purposes. To ensure a solid base for the sustainable management of this aquifer system, an adequate comprehensive hydrogeologic investigation was undertaken. A sampling campaign of stable isotopes was carried out in 2016 to identify groundwater recharge and related processes. A groundwater flow model was implemented. The model calibration was performed during a steady state, based on the average state of the period 1980–1984, using Modflow. Modelling results have been determined by a least squares fit of observed heads. The groundwater model was coupled with a physically based model (WetSpas model) used to quantify groundwater recharge and discharge of the Takelsa multilayer aquifer.

Keywords

Groundwater flow • Modelling • Recharge • Isotopes • Takelsa

1 Introduction

As is the case in all developing countries, the freshwater requirements in Tunisia have strongly increased, resulting in a prevailing agricultural activity expansion, population growth and economic development. The population rose

N. Ghouili · M. Zammouri (✉) · F. Hamzaoui-Azzaza
Tunis El Manar University, Faculty of Sciences of Tunis,
Campus Universitaire, 2092 Tunis, Tunisia
e-mail: mounira.zammouri@fst.utm.tn

N. Ghouili · F. Jarraya-Horriche
Centre de Recherches et des Technologies des Eaux,
BP 273-8020, Soliman, Tunisia

J. J. Carrillo-Rivera
Institute of Geography, UNAM, CP 04510, México City, Mexico

from 3.45 million in 1956 to 11.27 million in 2015. The agricultural policy in Tunisia, in the last 50 years, is governed by key considerations of food security and self-sufficiency. As a result, the amount of irrigated land has increased fourfold over the same period.

The Takelsa multilayer aquifer system is an important aquifer in the northeast of Tunisia; the knowledge of its hydrogeological functioning is insufficient, even though groundwater has been extracted since the 1980's, because of its complex structure which is affected by several fractures and faults. Total extraction increased from 8.5×10^6 m³ in 1980 to 22.21×10^6 m³ in 2015. Appropriate groundwater management in the semi-arid regions is one of the pillars of sustainable development. The aim of this paper is to briefly describe surface water, groundwater flow, and isotopes modelling studies, which constitute together adequate tools to propose sustainable management policies for the Takelsa multilayer aquifer system.

2 Materials and Methods

2.1 Study Area Description

The Takelsa basin, covering a surface of about 300 km², is located between the longitudes 10° 30' 0" and 10° 50' 0" east, and the latitudes 36° 40' 0" and 36° 55' 0" north. It is characterized by a semi-arid Mediterranean climate, a mean annual precipitation of 518 mm, a mean annual potential evapotranspiration of 880.5 mm and a dense hydrographic network. This basin encompasses a multilayer aquifer system formed mainly by sandstone and clay series, dated from Oligocene to Quaternary ages. The Miocene levels are constituted by two formations, locally called by Saouaf (Serravalien–Tortonian) and Beglia (Serravalien).

From the top to the bottom, a phreatic aquifer unit is contained in the Quaternary deposits and in the shallow sandstone level of the Saouaf formation, followed by three additional deep aquifer units contained in a sandstone

formation of the Miocene (Saouaf and Beglia) plus an Oligocene aquifer unit (Fortuna). Groundwater recharge is provided mainly by infiltration of rainwater through the Quaternary deposits and the sandstone outcrops of Beglia and Saouaf formations. The discharge zone is the Mediterranean Sea and by the drainage as a base flow of surface streams.

2.2 Methods

A water sampling campaign was carried out in December 2016, comprising 32 wells tapping the Takelsa phreatic aquifer. Stable isotopes were analyzed in the “Integrated Water Sciences Laboratory” of the “Higher Institute of Sciences and Techniques of Water of Gabes” of the University of Gabes. The sample collection and preservation followed the standard methods of APHA [1]. Analyzed oxygen and hydrogen isotopes were reported to “ δ ” notation relative to Vienna-Standard Mean Oceanic Water.

In order to assess the water balance components of the Takelsa multilayer aquifer system, a quasi-three-dimensional finite-difference flow model was implemented using MODFLOW-2000, a modular finite difference groundwater model code [2]. For modelling pre- and post-processing, Processing MODFLOW was utilized [3].

When a groundwater flow model calibration is based on hydraulic head data only, the problem is considered ill-posed because of the lack of a unique solution. However, by coupling the groundwater flow model with a surface water model, the number of plausible flow models is greatly reduced. WetSpas, a physically based model, is used to quantify groundwater recharge of the Takelsa multilayer aquifer. Groundwater recharge is calculated based on a seasonal water balance equation, which is obtained by the difference between the precipitation and the surface runoff, the actual evapotranspiration and the interception fraction [4]. The WetSpas inputs include data on groundwater depth, topography, slope, land use, soil type and the meteorological data (precipitation, wind-speed, temperature and the potential evapotranspiration).

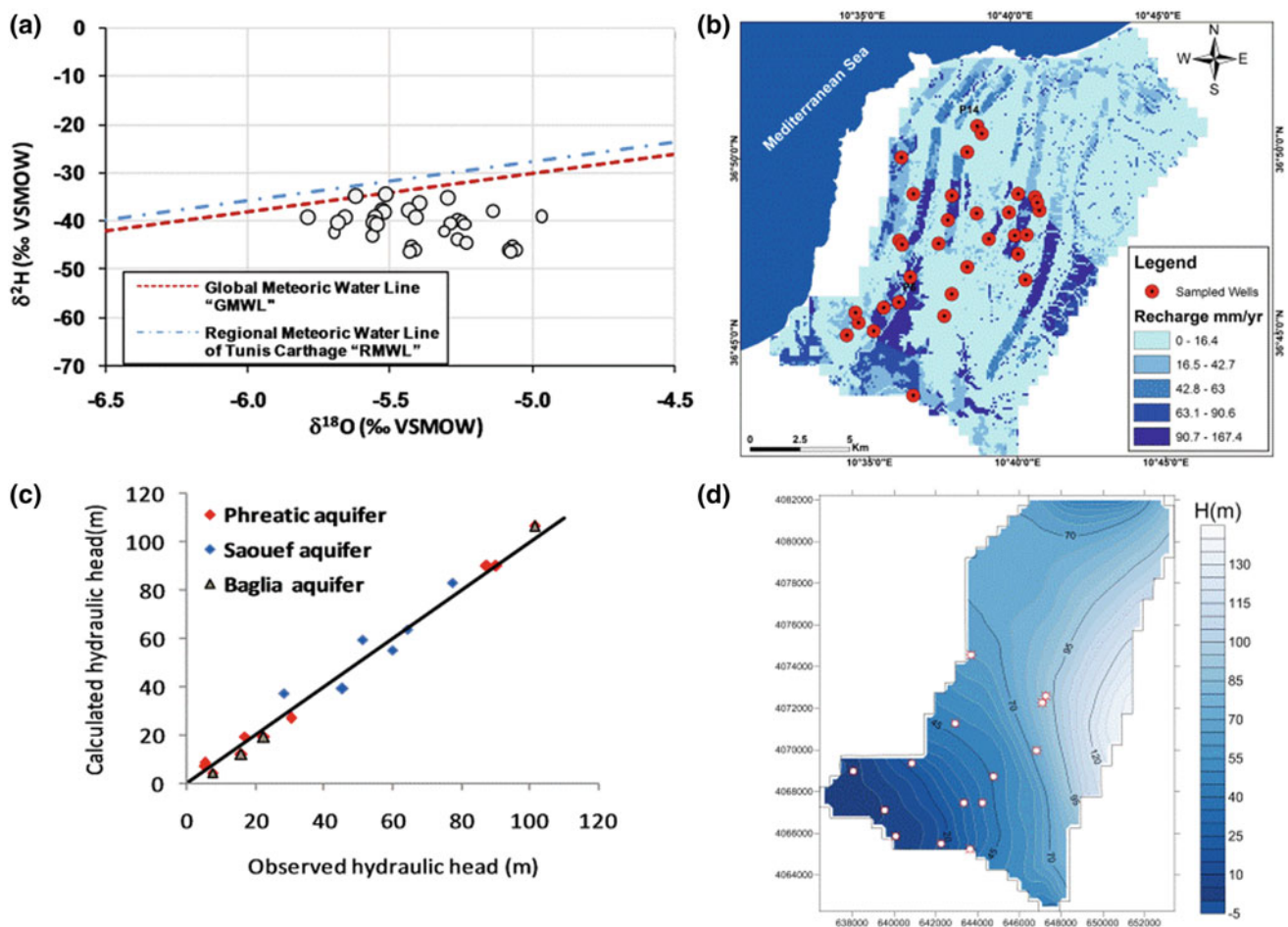


Fig. 1 a $\delta^{18}\text{O}$ - $\delta^2\text{H}$ stable isotope diagram of analyzed groundwater samples. b Calculated groundwater recharge rate. c Scatter plot of steady-state hydraulic head calibration. d Simulated piezometric of phreatic aquifer in steady state

3 Results and Discussion

The values of the oxygen-18 isotope ($\delta^{18}\text{O}$) range between -5.79 and -4.97‰ with a mean value of -5.38‰ . The values of the hydrogen isotope ($\delta^2\text{H}$) vary from -46.66 to -34.29‰ with an average value of -40.93‰ . The data are plotted with the Global Meteoric Water Line "GMWL" and the Regional Meteoric Water Line of Tunis Carthage "RMWL", which are expressed by $\delta^2\text{H} = 8 \times \delta^{18}\text{O} + 10$ [5] and $\delta^2\text{H} = 8 \times \delta^{18}\text{O} + 12.4$ [6], respectively. All groundwater samples are scattered below the RMWL and around the GMWL (Fig. 1a) suggesting that most samples have been subject to evaporation processes before recharge took place.

The groundwater recharge modelling indicates a rate from 0 to 168 mm/year (Fig. 1b) with a mean value of 22 mm/year and a standard deviation of 32.12 mm [7]. High values were observed in zones characterized by sandy loam and loamy sand soils, a low slope and with an intense vegetation cover. The computed infiltration coefficient ranges from 0 to 32% with a mean value of 4% of the yearly rainfall.

The Takelsa multilayer aquifer system model is formed by three main layers, represented from top to bottom by the phreatic aquifer unit and the two deep aquifer units of Saouaf and Beglia. All aquifer units are connected by a leakage term. Dirichlet boundary condition is imposed in the discharges zone. Recharge is represented by Neumann boundary condition according the WetSpas model results. Cauchy boundary conditions represent the drainage of groundwater (base-flow) by wadis. The isotopes results helped correct the first comprehensive attempts to model the groundwater flow by revising the boundary conditions according to these results.

The model calibration in steady state for each of the three main components of the aquifer system is based on the average state of the period 1980–1984. The comparison of the available observed and calculated piezometric values of the aquifers in steady state indicates a satisfactory model calibration with a correlation coefficient of 0.989 and a root mean squared error of 5.0 m. Calculated piezometry (Fig. 1c) compares well to observed values lacking any systematic deviation. The piezometric distribution calculated for the aquifer units allows to understand groundwater flow dynamics. The groundwater flow from the eastern border is then directed to the basin center and outflows to the discharges zones in the north and in the southwest (Fig. 1d). According to the calculated water balance, groundwater recharge is $13 \times 10^6 \text{ m}^3$, of which 46% are infiltrated in the

Beglia outcrops. A large part of this fraction flows within this aquifer, percolates towards the Saouaf aquifer and then towards the phreatic aquifer. The flow to the Mediterranean Sea is 10^6 m^3 , while the drainage by wadis is $3.5 \times 10^6 \text{ m}^3$.

4 Conclusions

The stable isotopes results confirm the evaporation processes in groundwater recharge. The physically based modelling of surface water allows assessing groundwater discharge and recharge rates, which were introduced in the groundwater flow model. The availability of groundwater recharge makes the calibration process in steady state a well-posed problem. The water balance calculated by the groundwater flow model indicates that the current extraction ($22.21 \times 10^6 \text{ m}^3/\text{year}$) largely exceeds groundwater renewable inflows ($13 \times 10^6 \text{ m}^3/\text{year}$) confirming the ongoing aquifer intensive extraction. A sustainable management is required for the Takelsa multilayer aquifer system to avoid the saline water inflows that may be induced by current and future intensive extraction.

References

1. APHA: Standard Methods for the Examination of Water and Wastewater, 19th edn. American public Health Association, Washington, DC (1995)
2. Harbaugh, A.W., Banta, E.R., Hill, M.C., McDonald, M.G.: Modflow-2000, the U.S. Geological Survey Modular Groundwater Model: User Guide to Modularization Concepts and the Groundwater flow Process. US Geological Survey, Reston, VA, USA (2000)
3. Chiang, W.H., Kinzelbach, W.: 3D-Groundwater Modeling with PMWIN a Simulation System for Modeling Groundwater Flow and Pollution. Springer, Berlin (2001)
4. Batelaan, O., De Smedt, F.: GIS-based recharge estimation by coupling surface- subsurface water balances. *J. Hydrol.* **337**, 337–355 (2007)
5. Craig, H.: Isotopic variation in meteoric waters. *Science* **133**, 1702–1703 (1961)
6. Zouari, K., Aranyosy, J.F., Mamou, A., Fontes, J.C.: Etude isotopique et géochimique des mouvements et de l'évolution des solutions de la zone aérée des sols sous climat semi-aride (Sud tunisien). In: the final meeting of the joint IAEA/GSF coordinated research program Proceedings on Stable and Radioactive Isotopes in the Study of the Unsaturated Soil Zone, pp. 121–144. IAEA, Vienna (1985)
7. Ghouili, N., Jarraya Horriche, F., Zammouri, M., Benabdallah, S., Farhat, B.: Coupling WetSpas and MODFLOW for groundwater recharge assessment: case study of the Takelsa multilayer aquifer (Northeastern Tunisia). *Geosci. J.* (2017). <http://dx.doi.org/10.1007/s12303-016-0070-5>, pISSN 1226-4806 eISSN 1598-7477

Statistical Analysis of Groundwater Level Variation in Semi-arid Upper Godavari Basin

Pallavi Kulkarni, Sudhakar Pardeshi, and Suchitra Pardeshi

Abstract

Groundwater supports the economy of semi-arid parts of India during the non-monsoon season. However, in the era of climate change and increased water demand, the groundwater supply is at risk. In the current study, the variation in the groundwater levels in the semi-arid upper Godavari basin is examined for pre- and post-monsoon seasons using the Mann-Kendall trend test. The trend in the difference between the groundwater levels during these seasons is also analyzed. Breaks in the groundwater level time series in both seasons are identified using the Pettitt test. The study revealed that, the groundwater levels are mostly increasing in the post-monsoon season. However, more than 60% of wells depict the declining trend of groundwater level in the pre-monsoon season. The gap between the groundwater levels measured during the pre- and post-monsoon seasons is widening throughout the upper Godavari basin. Though the breaks in the pre- and post-monsoon groundwater levels coincide with the major drought year, the negative change in the mean value after the break year cannot be attributed only to climatic variation. Hence, the current study highlights the immediate need for water conservation and water demand management, in the upper Godavari basin.

Keywords

Groundwater level • Mann-Kendall trend test • Pettitt test • Semi-arid upper Godavari basin

1 Introduction

Besides rainfall, groundwater is the prominent source of water to the agricultural sector in India. More than 65% of irrigation is dependent on groundwater [7]. However, the studies have shown that groundwater level is declining in many parts of India [4, 9] which might affect the overall availability of groundwater in the regions of shallow aquifers [1], especially ones with the semi-arid climate. Hence, timely understanding of variation in groundwater level is vital for better irrigational water management. In the current article, an attempt is made to examine the trend and break in the pre- and post-monsoon groundwater levels in the semi-arid Upper Godavari basin, India.

2 Data and Methodology

A total of 172 and 152 wells representing the pre- and post-monsoon season, respectively, were selected. There are only 140 wells which have the continuous data of both seasons. Hence, only these wells are considered while examining the changes in the difference between the groundwater levels of these two seasons. The data for both seasons are available for two time periods ranging from 1980 to 2015 (36 years) and from 1989 to 2015 (27 years). The existence of a trend in groundwater level and its magnitude of change are estimated using the Mann-Kendall test [2, 3] and the Sen's Slope estimator method [6, 10]. For the autocorrelated data, the Trend Free Whitening Approach (TFPW) suggested by Yue et al. [12] was adopted. The same methodology was employed to check how the difference between the pre- and post-monsoon groundwater level is varying. The significance of the trend was tested at the confidence level of 0.05, and the null hypothesis stands for 'no trend' in the data. The trend analysis was followed by examining the presence of breaks in the groundwater levels using the non-parametric Pettitt test [5]. The test finds the

P. Kulkarni · S. Pardeshi (✉)
Department of Geography, Savitribai Phule Pune University,
Pune, India
e-mail: spardeshi@rediffmail.com

S. Pardeshi
Prof. Ramkrishna More ACS College, Akurdi, Pune, 411044, India

breaks in the middle of the time series and does not assume the normal distribution of the observations [11].

3 Results

3.1 Groundwater Level Trend

The application of Mann-Kendall test reveals that around 60% of the wells are experiencing a decrease in groundwater level in the pre-monsoon season (Fig. 1). This declining trend is significant for 53% of the wells. As per Sens's slope estimator, the rate of groundwater level variation during this season ranges between -0.35 and 0.23 m/year. The majority of the wells (around 40%) exhibits a magnitude of change varying from -0.001 to -0.1 m/year. In the post-monsoon season, around 58% of wells are experiencing increasing groundwater level (significant for 34% of wells). In this season, the rate of change varies between -0.21 and 0.32 m/year. For more than 67% of the wells, the gap between the pre- and post-monsoon season is widening, i.e. they are depicting an upward trend of the calculated difference.

3.2 Identification of break

Around 47% of the wells in the study area have experienced the statistically significant break in the groundwater level (confidence level—0.05) during the pre-monsoon season. In the decade starting from 1996 to 2005, a maximum number of wells has witnessed this break. In case of a post-monsoon season, around 33% of the wells indicate the existence of a break. The breaks in this season have occurred mainly between the years 2000 and 2005. Many wells represent the falling mean groundwater level after the break in both seasons (Fig. 2).

4 Discussion

A falling and rising groundwater level in the pre- and post-monsoon seasons, respectively, is a usual phenomenon in the semi-arid upper Godavari basin. However, identified long-term declining trend of groundwater level indicates the overexploitation of groundwater in major parts of the basin. Though the groundwater level is mostly increasing in the post-monsoon season, probably due to recharge from the rainfall during the monsoon season, the gap between the pre- and post-monsoon groundwater levels is increasing for more than 3/4th of area of the basin. This is alarming because it indicates that, even though more groundwater is available in the post-monsoon season, it is exploited to a great extent during the following pre-monsoon season (considering the water year starting from June). This exploitation of groundwater makes the upper Godavari basin vulnerable to water scarcity during the pre-monsoon season if the monsoon is delayed or if less-than-normal rainfall occurs.

Another interesting fact about the long-term groundwater level variation is that, many of the wells indicate the statistically significant break in the time series during 2000 to 2005 for the pre- and post-monsoon season. However, the break in the time series cannot be only attributed to the meteorological drought which occurred in 2002, since after this period, many wells showed a reduction in mean groundwater level. A study carried out by Sishodia et al. [8] in the semi-arid districts of Telangana State has confirmed that, the groundwater levels there are falling mainly after the subsidization of the electricity. Hence, it becomes necessary to check whether the declining trend and the reduced mean after the break year is in response to climatic variations or if they are the results of anthropogenic activities and government policies.

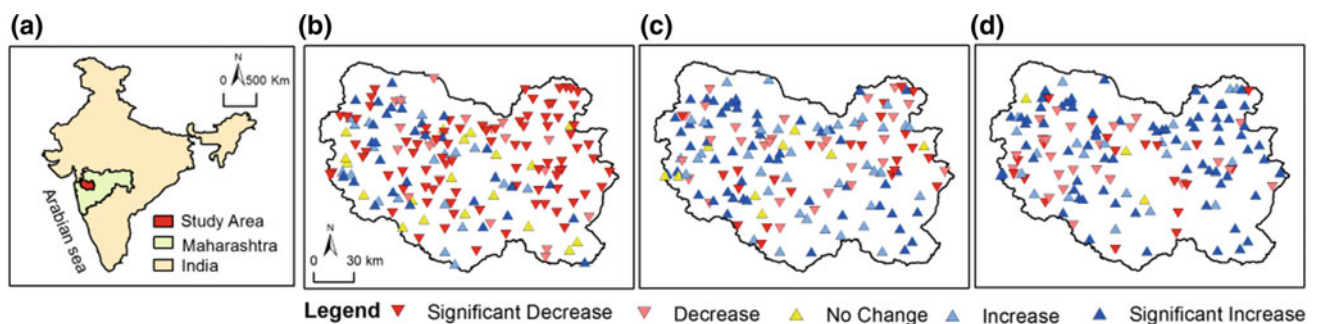


Fig. 1 a Location of upper Godavari basin in Maharashtra State, India. Maps b and c represent the trends in groundwater level in pre- and post-monsoon seasons, respectively. The trends in the difference between pre- and post-monsoon groundwater levels are depicted in map d

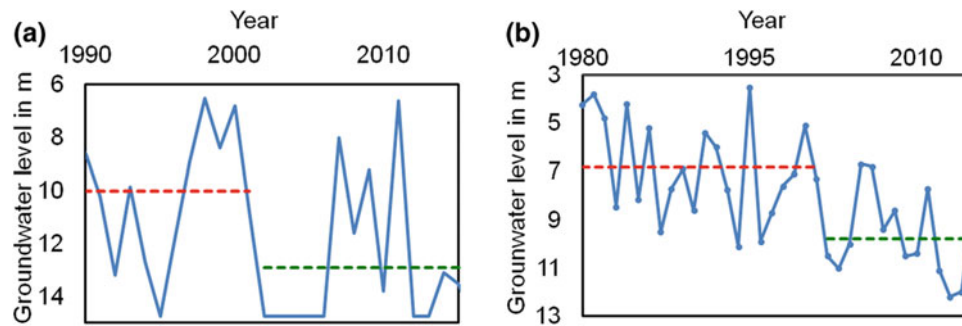


Fig. 2 The graphs represent the groundwater level time series and average mean before and after the break year in the pre-monsoon season for two selected wells (a) Ranjangaon Deshmukh and b

Telwadi). The blue continuous line represents the groundwater level while the red and green lines stand for the average mean before and after the break year

5 Conclusions

An immediate action for water conservation is required in the upper Godavari basin as the groundwater levels are declining for more than 60% of the wells in the pre-monsoon season, though they are increasing for more than 58% of the wells in the post-monsoon. Besides, the difference between the pre- and post-monsoon groundwater levels is also increasing over the same period of time. Although the break in the groundwater level coincides with the drought year, the afterward reduction of groundwater level cannot be attributed only to climatic variations. Hence, a detailed study of factors causing groundwater levels to decline, besides climate variations, like agricultural patterns and related government policies, should be examined carefully.

References

1. Fishman, R., Siegfried, T., Raj, P., Modi, V., Lall, U.: Over-extraction from shallow bedrock versus deep alluvial aquifers: reliability versus sustainability considerations for India's groundwater irrigation. *Water Resour. Res.* (2011). doi:<http://dx.doi.org/10.1029/2011WR010617>
2. Kendall, M.: *Rank Correlation Methods*. Charles Griffin, London (1975)
3. Mann, H.: Nonparametric tests against trend. *Econometrica* **13**, 245–259 (1945)
4. Panda, D., Mishra, A., Kumar, A.: Quantification of trends in groundwater levels of Gujrat in western India. *Hydrol. Sci. J.* **57**(7), 1325–1336 (2012)
5. Pettitt, A.: A non-parametric approach to the changing point problem. *J. Appl. Stat.* **28**, 126–135 (1979)
6. Sen, P.: Estimates of the regression coefficient based on Kendall's tau. *J. Am. Stat. Assoc.* **63**, 1379–1389 (1968)
7. Siebert, S., Burke, J., Faures, J., Frenken, K., Hoogeveen, J., Döll, P., Portmann, F.: Groundwater use for irrigation: a global inventory. *Hydrol. Earth Syst. Sci. Discuss.* **7**, 3977–4021 (2010)
8. Sishodia, R., Shukla, S., Graham, W., Wani, S., Garg, K.: Bi-decadal groundwater level trends in a semi-arid south Indian region: declines, causes and management. *J. Hydrol. Reg. Stud.* (2016). doi:<http://dx.doi.org/10.1016/j.ejrh.2016.09.005>
9. Somashekhara Reddy, S.: Declining groundwater levels in India. *Int. J. Water Resour. Dev.* **5**(3), 183–190 (1989)
10. Theil, H.: A rank-invariant method of linear and polynomial regression analysis III. *Proc. K. Ned. Akad. Wet.* **53**, 1397–1412 (1950)
11. Wijngaard, J., Klein, Tank A., Koemmen, G.: Homogeneity of 20th century European daily temperature and precipitation series. *Int. J. Climatol.* **23**, 679–692 (2003)
12. Yue, S., Pilon, P., Phinney, B., Cavadias, G.: The influence of autocorrelation on the ability to detect trend in hydrological times series. *Hydrol. Process.* (2002). <https://doi.org/10.1002/hyp.1095>

Groundwater Pollution Index Evaluation Test Using Electrical Conductivity in a Semi-arid Quaternary Aquifer (Kousseri-Cameroon, Lake Chad Basin): Multivariate Statistical Analysis Approach

André Firmin Bon, Sylvain Doua Aoudou,
Arouna Mbouombouo Ndam, Etienne Ambomo Bineli,
and Elisabeth Dassou Fita

Abstract

The shallow quaternary aquifer of the Lake Chad Basin is an important source of drinking water supply and irrigation in the city of Kousseri. Electrical Conductivity (EC), Total Dissolved Solids (TDS) and pH were measured in situ in samples from 161 boreholes, while 8 boreholes selected based on EC spatial variation—were used to determine the concentrations of major cations and anions in groundwater. The pH values ranged between 6.94 and 9.97 with an average of 7.74 ± 0.45 which indicates that the groundwater of the study area is acidic to alkaline. TDS, representing the hydrochemical properties of groundwater, ranges from 45 to 144 mg/L with an average of 76.52 ± 20.16 mg/L. These values indicate that the groundwater of the study area is fresh (TDS < 1000 mg/L). EC of groundwater ranges from 94 to 296 $\mu\text{S}/\text{cm}$ with an average of 151.32 ± 40.54 $\mu\text{S}/\text{cm}$. The Pollution Index (PI) determined on 8 points varies between 2.96 and 4.67. This index presents a relationship according to a polynomial model with the corresponding EC values. Substantial differences in EC and PI values are observed in the groundwater of boreholes, which may indicate local contamination.

Keywords

Pollution index • Electrical conductivity • Polynomial model • Kousseri • Lake Chad basin

1 Introduction

In areas with a dry tropical climate, groundwater is of paramount importance as it is often the only source of water supply. Water quality management mainly involves the identification and analysis of the contaminants, the identification of their sources and the possible implementation of remedial measures [5]. Studies conducted in this perspective have shown that the shallow aquifer in the Lake Chad basin is highly vulnerable to pollution and the contamination of the groundwater resource by nitrate NO_3^- is of much concern in this basin [5]. This knowledge is interesting, but studies are generally conducted at the regional level without working in peri-urban environments. In addition, physico-chemical studies are numerous, however, they do not relate to the groundwater Pollution Index (PI).

The objective of this study is to evaluate, using a representative polynomial model, the pollution index of the quaternary aquifer of Kousseri.

2 Methods

The study zone covers approximately 2 km² and is located between 12° 3' 00" and 12° 5' 00" of latitude North and 15° 2' 00" and 15° 3' 00" west longitude (Fig. 1). The Lake Chad basin is characterized by a thick sequence of cretaceous, tertiary and quaternary sediments. The most important regional aquifer is the quaternary aquifer. It is formed by alluvial deposits which range from 15 to 70 m in thickness [5].

The boreholes used for physico-chemical monitoring have a depth of 40–70 m. EC, pH, TDS, and temperature were determined in situ using a Hanna multiparameter (HI 98429). These parameters were measured from December 2016 to August 2017. The spatial distribution of the EC data was done using QGIS 2.10.1 software. The Inverse Distance Weighting (IDW) model was chosen to construct the

A. F. Bon (✉) · S. D. Aoudou · A. M. Ndam
E. A. Bineli · E. D. Fita
National Advanced School of Engineering of Maroua,
University of Maroua, Maroua, Cameroon
e-mail: bon_andr@yahoo.com

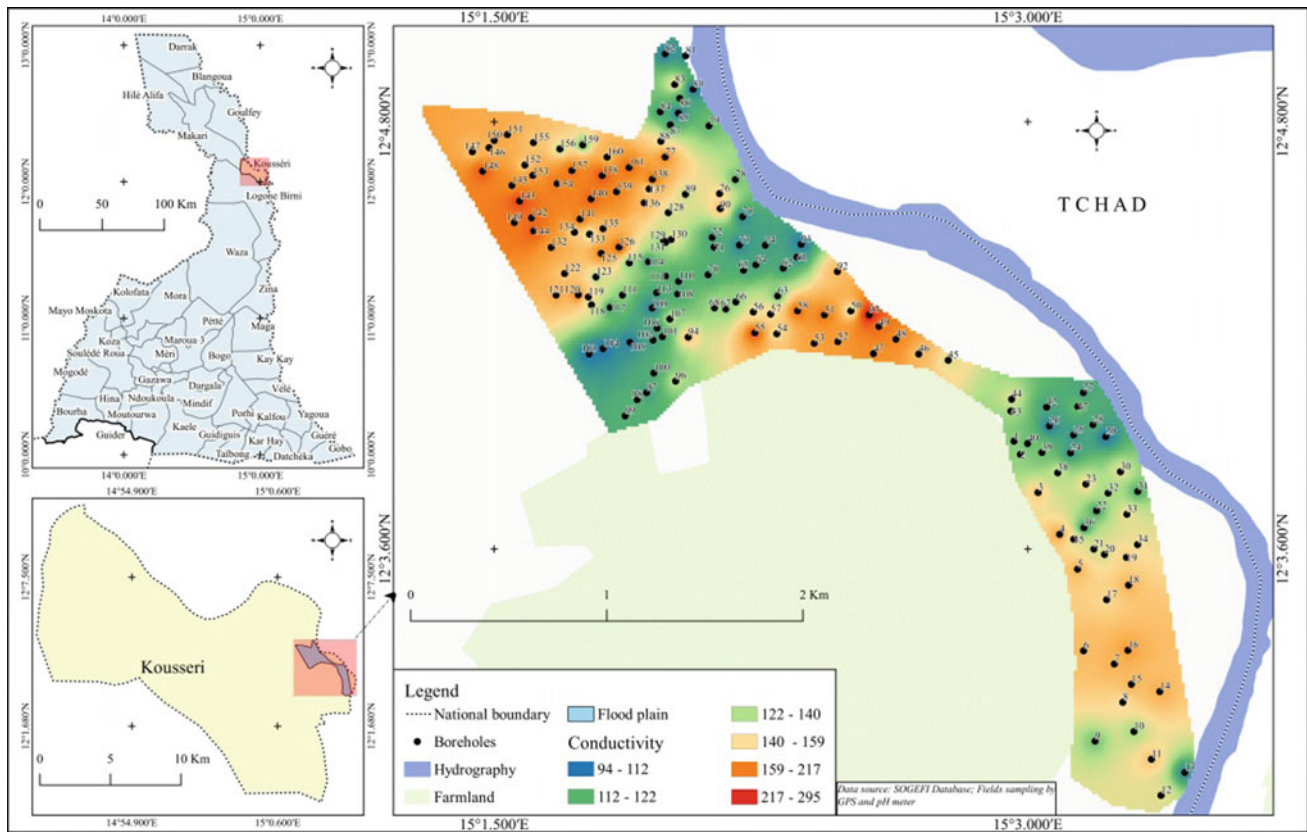


Fig. 1 Spatial distribution of mean EC

thematic maps. This method is widely used in hydrochemistry [4]. The sampling, in August 2017, of the 8 boreholes used for cation and anion analysis was done according to the variation ranges of the EC. The pollution index (PI) was calculated based on the concentration of nitrate and sulfate anions using the following formula [6]:

$$PI = (1.33 \times \text{ABS}(\text{pH} - 7) + \text{LN}(10 \times (\text{SO}_4 + \text{NO}_3)))/1.7 \quad (1)$$

The different PI values were correlated with those of EC to calculate at the scale of the whole PI zone.

3 Results

3.1 Hydrogeochemistry

The pH values are in the range of 6.94–9.97 with an average of 7.74 ± 0.45 which indicates that the groundwater of the study area is acidic to alkaline. TDS ranges from 45 to

144 mg/L with an average of 76.52 ± 20.16 mg/L. These values indicate that the groundwater of the study area is fresh (TDS < 1000 mg/L). EC of groundwater ranges from 94 to 296 $\mu\text{S}/\text{cm}$ with an average of 151.32 ± 40.54 $\mu\text{S}/\text{cm}$. The lower values are overall close to the Logone river (Fig. 1). Cl–Na–K, SO_4 –Na–K and Cl– SO_4 hydrogeochemical facies would dominate in this zone.

3.2 Pollution Index and Its Relationship with EC

PI values for the 8 boreholes vary between 2.96 and 4.67 with an average of 3.34 ± 0.68 . This index is correlated with EC according to a polynomial model of equation

$$PI = -0.0003 \text{ Cnd}^2 + 0.0827 \text{ Cnd} - 2.2036 \quad (2)$$

The PI calculated on the basis of this equation vary from -4.00 (≈ 0.00) to 3.50 with an average of 2.88 ± 0.99 . They indicate that the strong EC corresponds to the weak PI (Fig. 2).

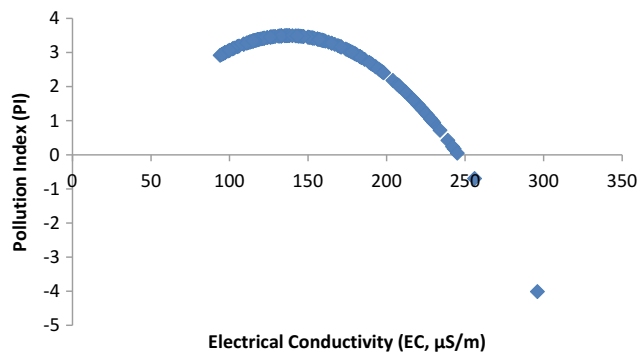


Fig. 2 Correlation between PI and EC

4 Discussion

Groundwaters are naturally of very good quality, but this quality can be affected by several factors such as industrial development, agricultural activity and wastewater production [2]. In fact the distribution of PI, as shown in Fig. 2, indicates a compartmentalization of this parameter. The low values of EC correspond to the strong values of PI and vice versa. The high values would be derived from the high concentration of sulphate caused by the dissolution of gypsum or a particular source of pollution, namely the existence of a septic tank. According to Liu et al. [3], these high sulphate concentrations can significantly speed up groundwater salinization. Moreover, the high value of this factor could be due to a high concentration of nitrates which results mainly from the use of fertilizers [5]. The low EC observed near the Logone river seems to highlight the possible exchanges between groundwater and surface water. This type of interaction is characteristic of alluvial environments [1].

Effective control and management of groundwater contamination requires a good identification of the specific source(s). With regard to sulphate for example, stable sulphate isotope [3], trace elements and Sr/ca ratio [1] should

be used in future research to identify the sources and processes that control its concentration in groundwater.

5 Conclusions

The groundwater of the quaternary aquifer of the city of Kousseri is sweet, acid to alkaline. The distribution of PI based on the analysis of a representative polynomial model seems to compartmentalize them into two groups: low EC (<150 $\mu\text{S}/\text{cm}$) and high EC (>150 $\mu\text{S}/\text{cm}$). However, further analyses are needed to better understand the hydrochemical properties of this peri-urban environment in the Lake Chad Basin.

References

1. Abderamane, H., Razack, M., Vassolo, S.: Hydrogeochemical and isotopic characterization of the groundwater in the Chari-Baguirmi depression, Republic of Chad. *Environ. Earth Sci.* **69**, 2337–2350 (2013)
2. Asmael, N.M., Huneau, F., Garel, E., Celle-Jeanton, H., Le Coustumer, P., Dupuy, A., Hamid, S.: Origin and recharge mechanisms of groundwater in the upper part of the Awaj river (Syria) based on hydrochemistry and environmental isotope techniques. *Arab. J. Geosci.* (2015). <https://doi.org/10.1007/s12517-015-1953-x>
3. Liu, X., Simunek, J., Li, L., He, J.: Identification of sulfate sources in groundwater using isotope analysis and modeling of flood irrigation with waters of different quality in the Jinghuiqu district of China. *Environ. Earth Sci.* **69**, 1589–1600 (2013)
4. Mir, A., Piri, J., Kisi, O.: Spatial monitoring and zoning water quality of Sistan river in the wet and dry years using GIS and geostatistics. *Comput. Electron. Agric.* **135**, 38–50 (2017)
5. Ngatcha, B.N., Djoret, D.: Nitrate pollution in groundwater in two selected areas from Cameroon and Chad in the Lake Chad basin. *Water Policy* **12**, 722–733 (2010)
6. Stuyfzand, P.J.: A new hydrochemical classification of water type. *IAHS Red Books* **182**, 89–98 (1989)

Part V

**Water Resources Sustainability
and Climate Change**

Hydrological Impacts of Climate Change in Northern Tunisia

Hamouda Dakhlaoui, Jan Seibert, and Kirsti Hakala

Abstract

Tunisia is a water-stressed country, which derives most of its surface water from its northern regions. Given Northern Tunisia's role as a water provider, this study investigated the hydrological impacts of climate change on five catchments located in this region. Three hydrological models are considered: HBV, GR4, and IHACRES. Climate projections were derived from eleven high-resolution EURO-CORDEX regional climate models (forced by general circulation models; GCM-RCMs). A quantile mapping (QM) bias correction method was applied to correct the climate simulations. Historical streamflow simulations (1970–2000), achieved by forcing the hydrological models with GCM-RCM precipitation and temperature, were first assessed in order to select the most realistic GCM-RCMs for future projections. The remaining bias corrected GCM-RCMs were then used to force the hydrological models in order to achieve projections of streamflow. The evaluation of the streamflow projections was conducted over two time periods (i) mid-term: 2040–2070 and (ii) long-term: 2070–2100 to identify the magnitude of the projected change of streamflow under the climate scenarios RCP 4.5 and RCP 8.5. The hydrological projections were analyzed according to several metrics commonly used by water managers.

Keywords

Rainfall-runoff modelling • Hydrological projections • EURO-CORDEX • Climate change • Tunisia

1 Introduction

The Mediterranean region has been identified as a hot spot of climate change, especially Tunisia, which has already undergone marked climate shifts during the 1950–1999 period [8]. Recent climate change scenarios project a 20% decrease in total precipitation and a +1 °C to +3 °C increase in mean annual temperature by the 2050 horizon compared with the 1971–1990 period [7]. This could result in critical water stress in the future, given that Tunisia already suffers from water paucity. However, only a few studies have considered the hydrological impacts of climate change in Tunisia. Sellami et al. [6] applied the SWAT model to a small catchment, located in eastern Tunisia, and provided future hydrological scenarios based on a climate model ensemble. Their projections point towards drier and hotter climatic conditions leading to more severe hydrological droughts in the future. Northern Tunisia provides the majority of the surface water for the country, with also the highest water quality. Given the importance of this region as a lifeline for the rest of the country, this study aims to assess the impact of climate change on surface water in Northern Tunisia with the most recent high-resolution EURO-CORDEX climate projections.

2 Data and Models

2.1 Study Catchments and Observational Data

Five catchments located in Northern Tunisia were selected for this study (Fig. 1). All basins are located upstream from major hydraulic installations.

H. Dakhlaoui (✉)
LMHE, Ecole Nationale d'Ingénieurs de Tunis, Université Tunis
El Manar, Tunis, Tunisia
e-mail: hammouda.dakhlaoui@laposte.net

H. Dakhlaoui
Ecole Nationale d'Architecture et d'Urbanisme, Université de
Carthage, Sidi Bou Said, Tunisia

H. Dakhlaoui · J. Seibert · K. Hakala
Department of Geography, University of Zurich, Zurich,
Switzerland

J. Seibert
Department of Earth Sciences, Uppsala University, Uppsala,
Sweden

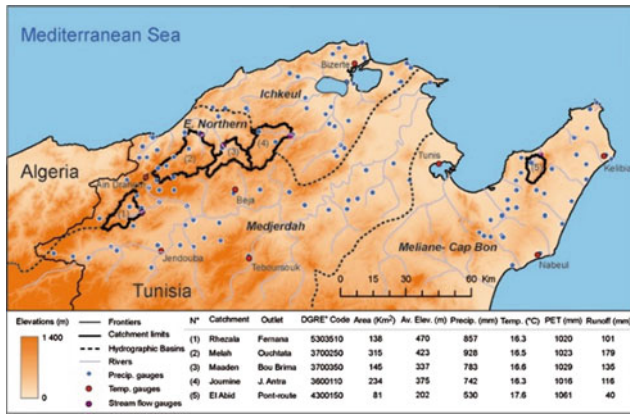


Fig. 1 Location of study basins, with precipitation, stream flow and climate (temperature) stations plotted. The main hydro-climatic characteristics are averaged over 1970–2000

2.2 Hydrological Models

Three conceptual lumped rainfall runoff models (RRM) were used in this study: GR4J, HBV, and IHACRES. The recent successful applications of these models in Tunisia [1–4] were the basis for their inclusion in this study. The model parameters were calibrated using the Kling-Gupta Efficiency (KGE, [5]).

2.3 High-Resolution Climate Models and Bias Correction of Climate Variables

Projections of daily mean temperature and precipitation were extracted from 11 regional climate models forced by general circulation models (GCM-RCMs) issued from the EURO-CORDEX project (<http://www.euro-cordex.net/>). EURO-CORDEX provides the most recent, high-resolution climate projections for the European domain with a 0.11° resolution (horizontal grid spacing of ~ 12.5 km). The period 1970–2000 corresponds to the historical model simulation. Streamflow projections were evaluated over two future time periods (i) mid-term: 2040–2070 and (ii) long-term: 2070–2100. Two radiative concentration pathway scenarios (RCP 4.5 and RCP 8.5) were used for the future projections. Quantile mapping

(QM) was used to bias correct the daily precipitation and temperature of the GCM-RCMs. The aim of QM is to correct the distribution of the climate model data, so that it matches the distribution of the observational data.

2.4 Evaluation of Performance of GCM-RCMs in Reference Historical Period

The hydrological simulations were used as a tool to evaluate the EURO-CORDEX climate projections and bias correction methods. The hydrological metrics adopted in this paper include: low flow (Q5), high flow (Q95), annual mean maximum, half flow date, mean flow and Nash Sutcliffe Efficiency (NSE).

3 Results

3.1 Efficiency of the RCM-GCMs Over the Control Period

In Fig. 2, we present the RRM performance forced by bias corrected GCM-RCMs outputs (P and T) over the reference period 1970–2000. The hydrological metrics were normalized (transformed to the range 0–1, with 0 as the best performance and 1 as the worst). As Fig. 2 shows, GCM-RCM 4, 11 and 1 perform the best over the reference period, while GCM-RCM 7 performs the worst. Given the poor performance of the GCM-RCM 7 across multiple metrics, it was decided to remove it from further analysis.

3.2 Hydrological Projection

The projected changes in precipitation and temperature result in the following:

Mid-term (2040–2070)

- 10–30% decrease of runoff under scenario RCP 4.5.
- 25–38% decrease of runoff under scenario RCP 8.5.

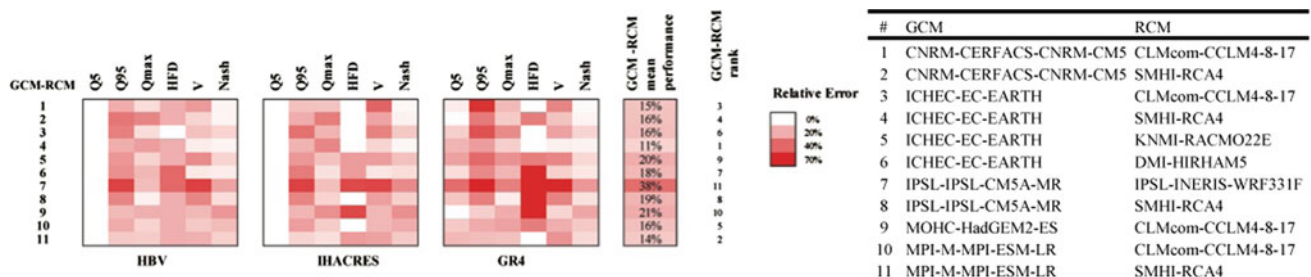


Fig. 2 Evaluating the performance of the hydrological simulations achieved when forced with bias corrected GCM-RCMs over the historical period 1970–2000 (mean results from 3 RRM). Performance is displayed in relative error with the exception of Q5 which is shown in absolute error

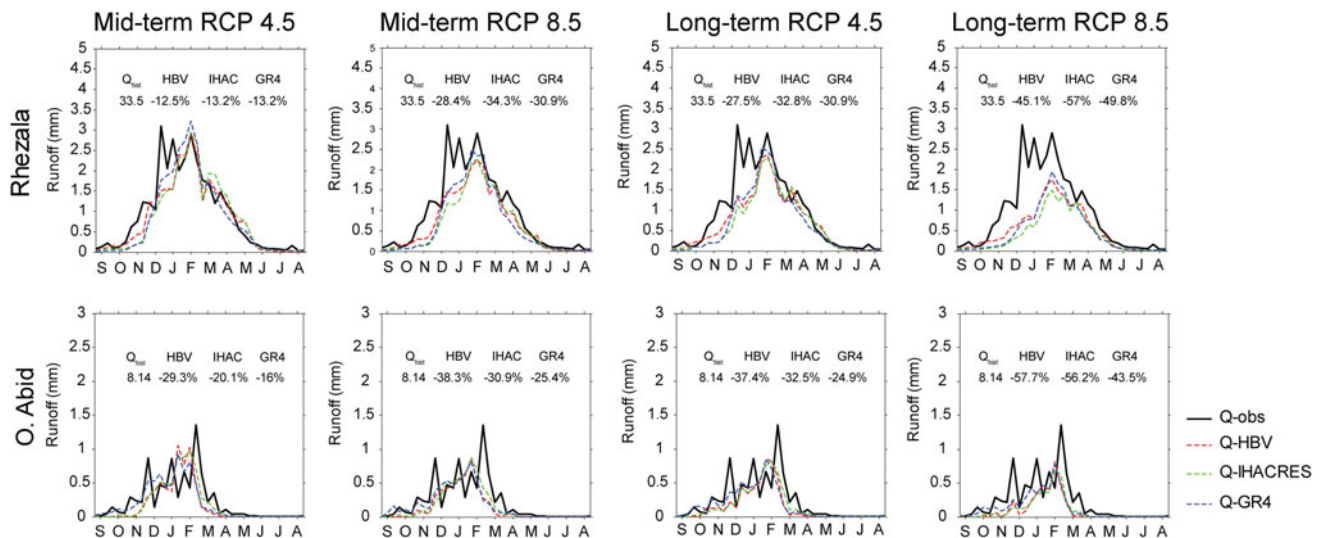


Fig. 3 Hydrological projections for Rhezala and O. Abid catchments

Long-term (2070–2100)

- 20–37% decrease of runoff under scenario RCP 4.5.
- 41–58% decrease of runoff under scenario RCP 8.5.

The different scenarios indicate a large decrease in surface water resources, mostly during the wet season (Fig. 3). Our results illustrate a similarity between the different studied catchments in terms of hydrological projections.

4 Conclusion

The hydrological projections show a marked decrease of surface water, especially for the most pessimistic climate scenario (RCP 8.5) towards the end of the century, reaching a loss of 58%. Our results illustrate a significant similarity between the different RRM in terms of hydrological projections, despite their different structures.

References

1. Abbaris, A., Dakhlaoui, H., Thiria, S., Bargaoui, Z.: Variational data assimilation with the YAO platform for hydrological forecasting evolving water resources systems. In: Understanding, Predicting and Managing Water-Society Interactions. IAHS Publ., vol. 364, pp. 1–6 (2014)
2. Bargaoui, Z., Dakhlaoui, H., Houcine, A.: Modélisation pluie-débit et classification hydroclimatique. Rev. Sci. Eau **21**, 233–245 (2008)
3. Dakhlaoui, H., Bargaoui, Z., Bárdossy, A.: Comparaison de trois méthodes d'usage de la technique des voisins les plus proches en vue d'amélioration de la performance de l'algorithme SCE-UA appliqué pour le calage du modèle pluie-débit HBV. In: Hydroinformatics in Hydrology, Hydrogeology and Water Resources, IAHS Publ., vol. 331, pp. 139–153 (2009)
4. Dakhlaoui H., Ruelland D., Trambaly Y., Bargaoui Z.: Robustness of conceptual rainfall-runoff models to high-resolution climate projections in Northern Tunisia. J. Hydrol. (2017). <https://doi.org/10.1016/j.jhydrol.2017.04.032>
5. Gupta, H.V., Kling, H., Yilmaz, K.K., Martinez, G.F.: Decomposition of the mean squared error and NSE performance criteria Implications for improving hydrological modelling. J. Hydrol. **377**, 80–91 (2009)
6. Sellami, H., Benabdallah, S., La Jeunesse, I., Vanclooster, M.: Quantifying hydrological responses of small Mediterranean catchments under climate change projections. Sci. Total Environ. **543**, 924–936 (2015)
7. Terink, W., Immerzeel, W.W., Droogers, P.: Climate change projections of precipitation and reference evapotranspiration for the Middle East and Northern Africa until 2050. Int. J. Climatol. **33**, 3055–3072 (2013). <https://doi.org/10.1002/joc.3650>
8. Xoplaki, E., González-Rouco, J.F., Luterbacher, J., Wanner, H.: Wet season Mediterranean precipitation variability: influence of large-scale dynamics and predictability. Clim. Dyn. **23**, 63–78 (2004)

Climate Change Impact on Future Flows in Semi-arid Environment, Case of Essaouira Basin (Morocco)

Salah Ouhamdouch, Mohammed Bahir, Paula M. Carreira, and Kamel Zouari

Abstract

The objective of this study was to simulate future flows in Essaouira basin (Morocco) by 2050, using the two-variable Rural Engineering model at the monthly time step (GR2M). The quality criteria revealed very interesting values obtained from the model on the Igrounzar and Zelten stations of the Essaouira basin with Nash higher than 70% and R^2 higher than 0.70. The results obtained by the GR2M model under Representative Concentration Pathway (RCP) 2.6 and 8.5 scenarios of the fifth phase of the Coupled Model Intercomparison Project (CMIP5) predict that future flows will show an upward trend of 19 and 43%, respectively. However, under the RCP 4.5 scenario, future flows show a downward trend of 38%. Nevertheless, planning for future uses of water resources in the Essaouira basin should take this situation into account.

Keywords

Climate change • Essaouira basin • Flow • GR2M • Semi-arid area

1 Introduction

Predicting and characterizing the climate change impact on water availability in space and time becomes an essential step in proposing solutions adapted to development projects

S. Ouhamdouch (✉) · M. Bahir
LGE-ENS, ENS, Université Cadi Ayyad, 40000 Marrakech,
Morocco
e-mail: salah.ouhamdouch@edu.uca.ma

P. M. Carreira
Campus Tecnológico e Nuclear, Instituto Superior Técnico,
Universidade Técnica de Lisboa, Lisbon, Portugal

K. Zouari
LRAE, Ecole Nationale d'Ingénieurs de Sfax, Université de Sfax,
BP W3038, Sfax, Tunisia

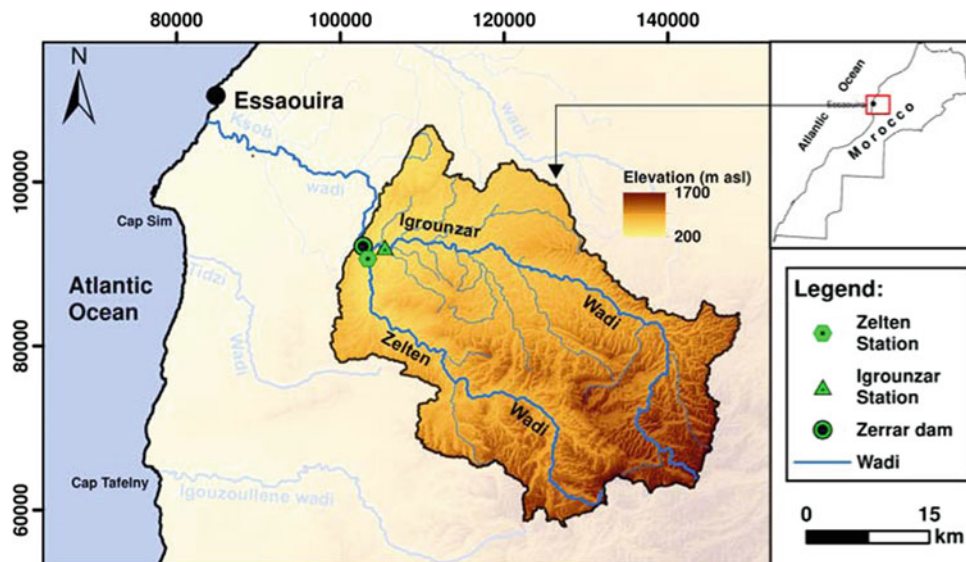
and sustainable environmental management. In arid and semi-arid environments, the main aquifers recharge sources are rainfall and surface runoff. However, good management and exploitation of this water feature with the scarcity of rainfall, which characterizes the arid and semi-arid zones, is a very important action to enhance aquifers' recharge and management. The Essaouira basin (Morocco) is used as an example in this study (Fig. 1). It is characterized by a semi-arid climate with an average annual rainfall of 300 mm and a temperature of 20 °C [1]. The objective of this study is to evaluate the impact of climate change on future flows in the Essaouira basin. The methodological approach consists in applying the Rural Engineering model, in two variables, at the monthly time step (GR2M). This model has been used in several studies and has yielded satisfactory results [2, 3].

2 Methods

Due to the limited availability of climatic and hydrometric data, only Igrounzar and Zeltten station data were used (see Fig. 1). Data were obtained from the Tensift Basin Hydraulic Agency (ABHT). The assessment of the climate change impact on flows within Essaouira basin was made based on the GR2M model and the climate projection under scenarios RCPs 2.6, 4.5, and 8.5. After calibration and validation of the GR2M, the parameters X1 and X2 obtained were applied to simulate future flows under the new climatic conditions.

3 Results and Discussion

The GR2M model evaluation is based on the examination of the performance of Nash and R^2 parameters during the calibration and validation phase. GR2M was calibrated and

Fig. 1 Location of the study area**Table 1** Calibration and validation results for Igrounzar and Zelten stations

Station	Parameter	Calibration	Validation
Igrounzar	X1 (mm)	772.78	772.78
	X2 (mm)	1.03	1.03
	Nash (%)	81	77
	R ²	0.88	0.70
Zelten	X1 (mm)	127.74	127.74
	X2 (mm)	0.95	0.95
	Nash (%)	88	62
	R ²	0.70	0.75

validated on the basis of the observation period (1991–2001) of the flows of the Igrounzar and Zelten wadis. The results obtained are grouped in Table 1. The values obtained from Nash (greater than 70%) and the significant positive correlations between observed and simulated flow rates (Table 1; Fig. 2) make it possible to accept the simulation. Consequently, the GR2M model used is powerful for modeling data collected at Igrounzar and Zelten stations. Simulation of future flows using the RG2M model requires the use of future precipitation and future evaporation data. The future values of these two parameters were obtained from [4]. The results of the future flow simulation for the period 2020–2050 under RCPs 2.6, 4.5, and 8.5 scenarios of CMIP5 are grouped in Fig. 3. Under RCP 2.6 and 8.5 scenarios, future

flows show an upward trend in the order of 19 and of 43%, respectively. Nevertheless, under the RCP 4.5 scenario, future flows show a downward trend during the study period of around 38%.

4 Conclusions

The objective of this study was to evaluate the climate change impact on the future evolution of the hydrological regime of the Igrounzar and Zelten wadi in Essaouira basin (Morocco), by 2050. The use of the future precipitation and evaporations values, as inputs to the previously well-calibrated and validated GR2M model, allowed the

Fig. 2 Correlation between observed and simulated flows
a calibration phase and
b validation phase

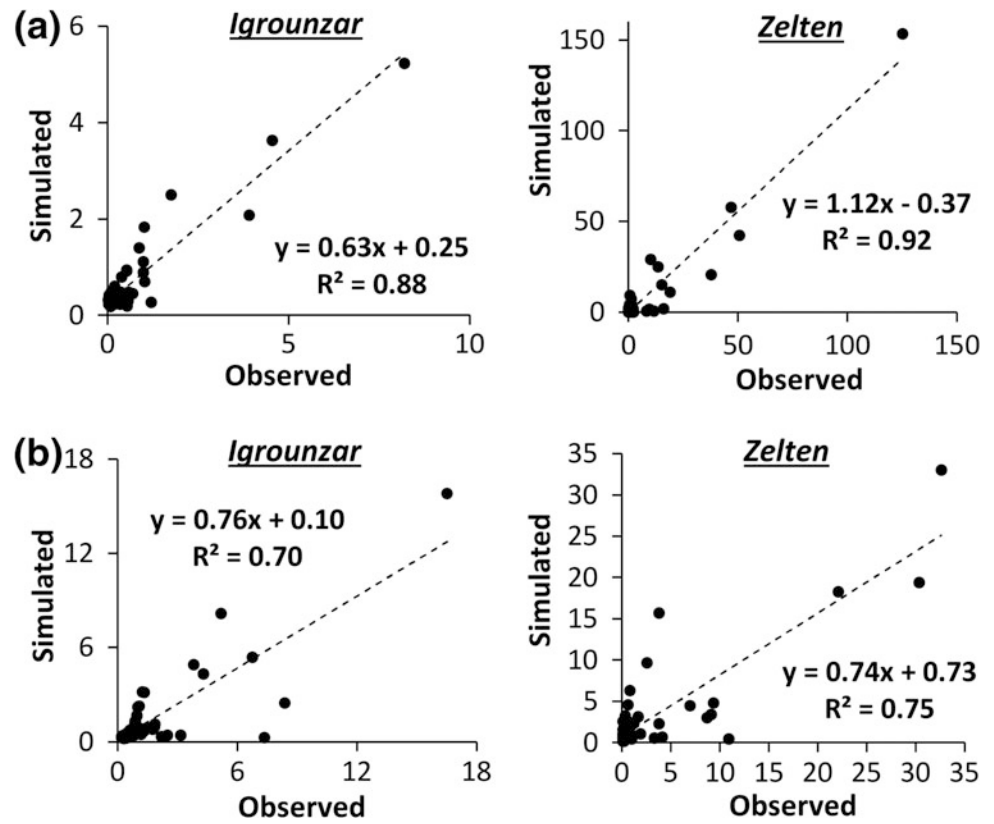
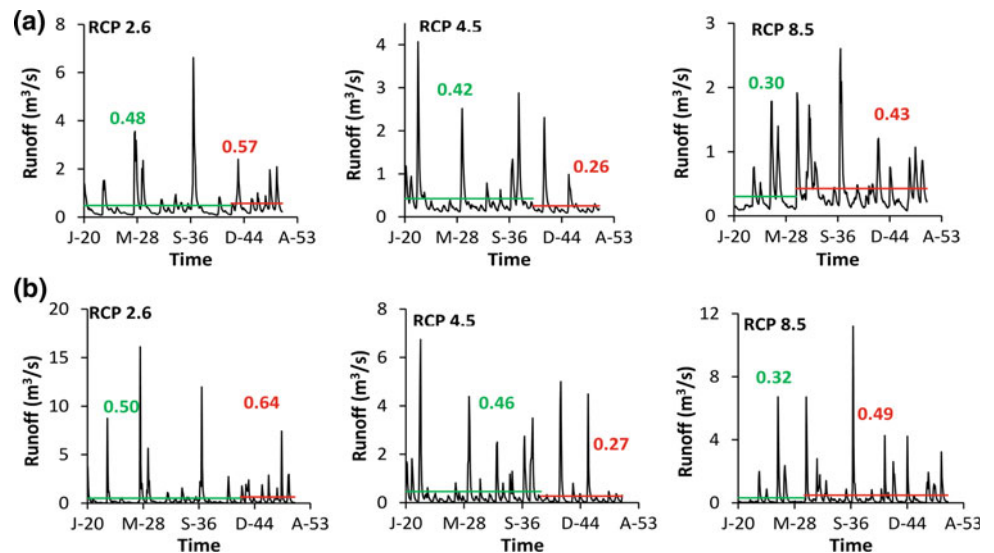


Fig. 3 Future flows under RCPs 2.6, 4.5, and 8.5 scenarios of CMIP5 in Essaouira basin
a Igrounzar station and **b** Zelten station



simulation of future flows for the period 2020–2050. The simulation of future flows based on the GR2M model under RCPs 2.6 and 8.5 scenarios of CMIP5 showed an upward trend of 19 and 43%, respectively, and a downward trend of 38% under RCP 4.5 scenario of CMIP5. Nevertheless, the results of this document can serve as a basis for the

management of the water resources in the Essaouira basin by constructing hill dams along Igrounzar and Zelten wadis. This makes it possible to mitigate the water flows speed during floods, and therefore, to store a portion of water that supplies the groundwater.

References

1. Bahir, M.: La ressource en eau au Maroc face aux changements climatiques; cas de la nappe Plio-Quaternaire du bassin synclinale d'Essaouira. *Comunicações Geológicas* **103**(1), 35–44 (2016)
2. Mouelhi, S.: Stepwise development of a two-parameter monthly water balance model. *J. Hydrol.* **318**, 200–214 (2006)
3. Meddi, M.: Impact des changements climatiques sur les débits dans le bassin du Chéllif (Algérie). In: Eric Servat et al.: 6th World FRIEND Conference, IAHS Publ., pp. 95–102 (2010)
4. Ouhamdouch, S.: Climate change impact on future rainfall and temperature in semi-arid areas (Essaouira Basin, Morocco). *Environ. Process.* **4**(4), 975–990 (2017)

Climate Change Effects on Groundwater Recharge in Some Sub-Saharan Areas

Maurizio Barbieri, Stefania Vitale, and Giuseppe Sappa

Abstract

Groundwater is a key element for people living in the Sub-Saharan region because it is the primary source of water, covering a crucial role in supplying water for multiple purposes. Water scarcity is becoming a limiting factor for economic development in these basins, as it is in many other basins located in developing countries with arid climates, lagging water infrastructure development, and rapidly increasing populations. Groundwater and climate change make a linked system. Climate change has a huge impact on groundwater, considering the fact that it is one of the main drivers which stresses the resilience of people living in these areas and makes groundwater resource highly sensitive to it. The goal of this paper is to give an integrated view of two focus themes, groundwater and climate change, inside two areas: the first is Dar es Salaam Coastal plain, in the eastern part of the United Republic of Tanzania; the second one is the area of Limpopo National Park, in the Mozambican part of the Limpopo River Basin.

Keywords

Groundwater recharge • Climate change • Mozambique • Tanzania

1 Introduction

Groundwater is the key source for water supply, but it is a poorly known resource which interacts with other systems and which is stressed by several impacts, such as the effects

M. Barbieri · S. Vitale (✉)
Department of Earth Science, Sapienza University, Piazzale Aldo Moro 5, 00185 Rome, Italy
e-mail: stefania.vitale@uniroma1.it

G. Sappa
Department of Civil Building and Environmental Engineering,
Sapienza University, Via Eudossiana 18, 00184 Rome, Italy

of climate changes. In the aim to harmonize the management of this natural resource, the water cycle assessment is important to place a priority on strategies for a sound water resources planning. A great part of the sub-Saharan region has limited surface and groundwater resources, and many people still do not have access to the accepted minimum supply of water. Most rural communities in SADC (Southern African Development Community) are served by groundwater resources. Accessing these resources is one of the important and critical factors. The lack of management of groundwater resources is also evident in community water supplies, where in some cases groundwater resources are developed in an unsustainable way.

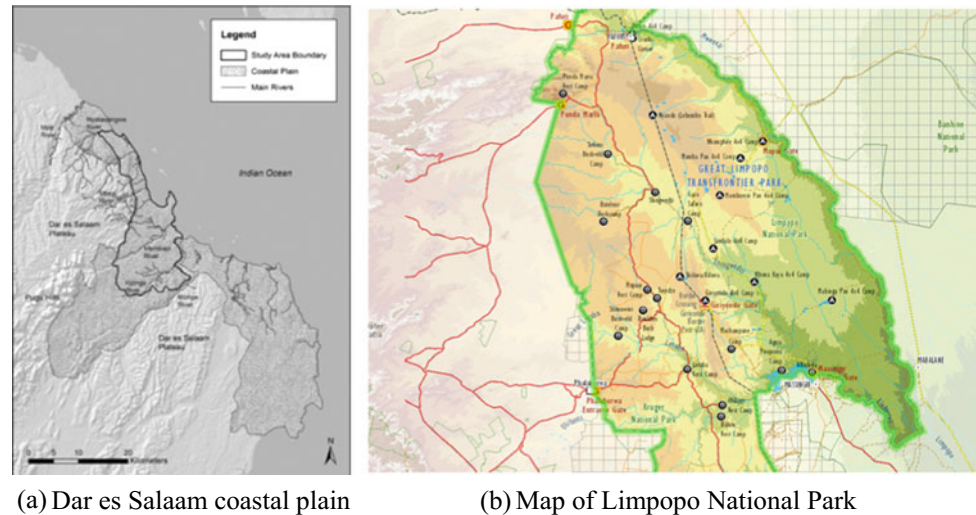
The main purpose of this paper is to advance understanding of the effects of climate change on groundwater, in two specific sites included in the Sub-Saharan region: Dar es Salaam Coastal plain located in the eastern part of the United Republic of Tanzania and Limpopo National Park, in the Mozambican part of the Limpopo River Basin (Fig. 1).

In both cases, the inverse budget method [1] has been applied to evaluate groundwater recharge, as this methodology gives us a general assessment of potential water resources in areas with scarcity data conditions.

2 The Dar es Salaam Coastal Plan and the Limpopo National Park in Mozambique Case Histories

This first study shows some results coming from the activities of the ACC Dar Project, which aims to improve the effectiveness of municipal initiatives for supporting the coastal peri-urban population in their efforts to adapt to the Climate Change (CC) impacts, in the United Republic of Tanzania.

The second study presented has been carried out in the framework of the SECOSUD Phase II project, funded by the Italian Ministry of Foreign Affairs in the SADC (South African Department of Environmental Affairs, DEA, 2015).

Fig. 1 The areas under study

(a) Dar es Salaam coastal plain

(b) Map of Limpopo National Park

The Limpopo National Park, in the Limpopo Basin, is the area of interest in the Mozambican part of Limpopo River Basin [2]. It is an important agricultural area, rich from a biodiversity point of view and with extraordinary mineral resources [3].

3 Materials and Methods

The first study focused on the impact of Climate Change on groundwater active recharge in the Dar es Salaam's coastal aquifer, due to two main factors: the decrease of precipitations, registered in the last ten years, and the change in the land's covering which happened in the same period. The first mentioned factor has an indirect effect on the second one, due to the decrease of precipitation in the last decade, all over the Tanzanian territory, where more and more people have come from villages to Dar es Salam, giving their contribution to land cover modifications and groundwater exploitation increase. In the second case study, the only data available were the precipitations and temperature historical series, collected in 53 years of measurements, all over Mozambique. The main goals of the present study are to evaluate the total rainfall dropped on Mozambique territory and to understand rainfall variability in time, in the aim of addressing a correct management of water resources in the area of Limpopo National Park, because of the lack of meteorological data about the Limpopo National Park area. In both cases, the hydrogeological inverse budget has been applied by the elaboration of available precipitation measurements.

4 Results

In the aim of analyzing the climate change impact on groundwater active recharge in Dar es Salaam's area [4], we first considered the average precipitation data which referred to all the 50 years of measurements. Secondly, the meteorological data have been divided in sets of 5 years measurements in order to compare different ranges of annual precipitation rates. To evaluate the impact of climate change on groundwater recharge [5], different conditions of land cover have been considered, which referred to 5 different years, as this is the second most important factor affecting the infiltration and, as a consequence of it, the precipitation. As a matter of fact, the land cover evolution, in the five years considered, changes the infiltration capacity of the soil and is a consequence of the adaptation of people to climate change. In the last 10 years, the soil in this area, which is the kind of land covering with the maximum value of PIF (Potential Infiltration Factor), has decreased from 46.7% in 2002 to 26.7% in 2012 of the area under study. As a consequence of the combined effects of climate change and land cover evolution in the range of 10 years, between 2002 and 2012, about 25% of groundwater recharge has been lost, while groundwater demand is increasing due to population increase (Fig. 2).

In the second study area, monthly precipitations historical series, which referred to 53 years of observations, have been compared to the monthly precipitations historical series which referred to 23 years of observations. The Mozambique rainfall data have been applied to the focus area. The

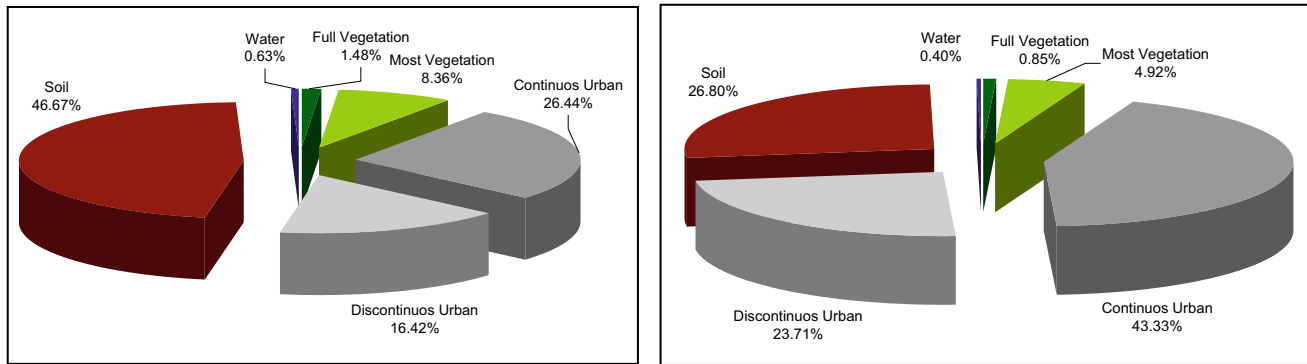


Fig. 2 Land cover distribution in 2002 and 2012

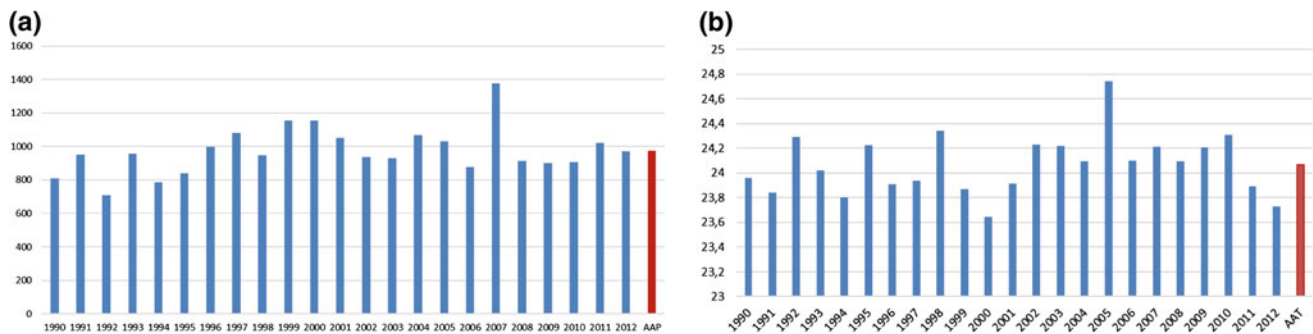


Fig. 3 a Precipitations (mm) and b temperature (°C) in Mozambique from 1990 to 2012

hydrogeological inverse budget [1] was applied for the assessment of potential infiltration, taking into consideration the conditions of outcropping rocks, from the Soil and Terrain database (SOTER) for Southern Africa [6] occurring in the area of Limpopo National Park.

The results suggest that there aren't sensitive modifications in precipitation trends, while the increase in Annual Average Temperature seems to be sensitive, as it is of 0.5 °C (Fig. 3). The study is aimed to estimate the Infiltration, evaluating the precipitation and temperature historical series referred to the period 1990–2012, ranging from the regional scale of Mozambique to the local scale of Limpopo National Park.

References

1. Civita, M., et al.: Una metodologia per la valutazione della ricarica attiva degli acquiferi. quaderni di Geologia Applicata- vol I. Pitagora editrice Bologna (1999)
2. Vitale, S., Barbieri, M., Sappa, G.: Groundwater management strategy in Limpopo national park (Mozambico) aimed to preserve biodiversity. International multidisciplinary scientific geoconference surveying geology and mining ecology management, SGEM, vol. 1, pp. 815–822 (2016)
3. Vitale, S., Barbieri, M., Sappa, G.: Groundwater quality characterization to protect biodiversity in SADC region (Southern African Development Community). *Senses Sci.* **3**(2), 184–189 (2016)
4. Sappa, G., Trotta, A., Vitale, S.: Climate change impacts on groundwater active recharge in coastal plain of Dar es Salaam (Tanzania). In: *Engineering Geology for Society and Territory—Volume 1: Climate Change and Engineering Geology*, pp. 177–180 (2015a)
5. Sappa, G., Ergul, S., Ferranti, F., Sweya, L.N., Luciani, G.: Effects of seasonal change and seawater intrusion on water quality for drinking and irrigation purposes, in coastal aquifers of Dar es Salaam, Tanzania. *J. Afr. Earth Sci.* **105**, 64–84. Elsevier, (2015b)
6. ISRIC.: *The Soter Manual Procedure for small scale digital map and database compilation of soil and terrain conditions* (1991)

Recharge Estimation of Hardrock-Alluvium Al-Fara Aquifer, Oman Using Multiple Methods

Azizallah Izady, Osman Abdalla, Mansoor Amerjeed, Mingjie Chen, Ali Al-Maktoumi, Anvar Kacimov, and Hilal Al-Mamari

Abstract

Groundwater resources have been extensively explored in Wadi Al-Fara coastal catchment, located at the northwest of Oman, to supply agricultural, industrial and domestic demands. Consequently, groundwater level has declined, which calls for urgent mitigation strategies to sustain the groundwater resources. Reasonable knowledge of natural recharge to a groundwater basin is fundamental for its sustainability and management. Thus, recharge was estimated using different methods including chloride mass balance (CMB), water table fluctuation (WTF) and groundwater modeling methods in Wadi Al-Fara catchment. Based on the CMB method, the recharge is respectively estimated at about 45 and 8 mm/year for the highland and coastal zones. According to the WTF method, the recharge is estimated as 10–22 mm/year and 6–14 mm/year in the plain and coastal zones, respectively. Modeling showed that a long-term regional groundwater recharge is about 31 Mm³/year (26 mm/year) for the whole study area, and the long-term lateral flux from the highland to the coastal zone (12 Mm³/year) is a major contributor to water resources in the coastal plain.

Keywords

Recharge • WTF • CMB • Modelling • Hardrock-alluvium aquifer

A. Izady (✉) · O. Abdalla · M. Chen · A. Al-Maktoumi
A. Kacimov · H. Al-Mamari
Water Research Center, Sultan Qaboos University, Muscat, Oman
e-mail: az.izady@gmail.com

A. Izady
Department of Hydroinformatics, East Water and Environmental
Research Institute (EWERI), Mashhad, Iran

M. Amerjeed
Ministry of Regional Municipalities and Water Resources
(MRMWR), Salahlah, Oman

1 Introduction

Sustainable development in any region depends on the availability and renewability of fresh water resources. Groundwater resources provide the main supply in arid and semi-arid regions due to the lack of surface water. Therefore, the sustainable developments in these arid regions demand a proper estimate of natural groundwater recharge to ensure its renewability [5]. However, recharge rates are one of the most challenging hydrological parameters to estimate in almost all of the groundwater flow models [2]. This is largely because of the significant spatial and temporal variations of recharge rates [4]. Therefore, it is recommended by several authors to use multiple methods to complement and ascertain the recharge estimate (e.g. [3]). The objective of this study was to estimate recharge in Wadi Al-Fara coastal catchment, Oman, using CMB, WTF and groundwater modeling methods.

2 Materials and Methods

2.1 Study Area and Geology

The study area of Wadi Al-Fara catchment is located in northwest Oman, and covers a total surface area of 1172 km². The climate is characterized by its hot summer with a temperature that may reach 40 °C, whereas the average temperature during winter ranges between 20 and 28 °C. The average annual rainfall is between 73 mm/year at the coast and 270 mm/year at the mountain zone. The potential evapotranspiration may reach 2300 mm/year in this area. The geologic units of the area are divided into six principal zones that include the Wadi Alluvium, Plain Alluvium, Upper and Lower Fars, Hajar Super Group, and Ophiolite units (Fig. 1).

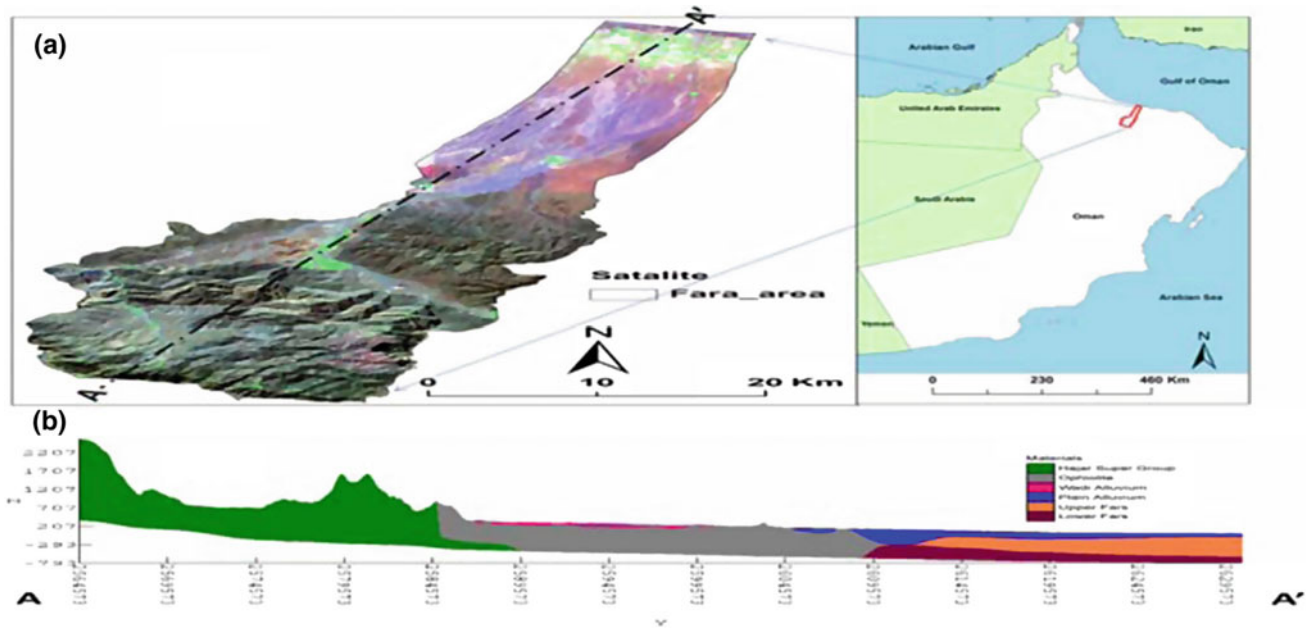


Fig. 1 a Location of study area in Oman. b Vertical cross-section. Adapted from [1]

2.2 Dataset and Methodology

Groundwater recharge was investigated in the Wadi Al-Fara coastal catchment using three methods: (1) the CMB [6], (2) the WTF [3] and (3) groundwater modeling methods. All required data were collected from the Ministry of Regional Municipalities and Water Resources (MRMWR) database and the Directorate General of Meteorology. The chloride concentrations were measured from the 15 and 39 collected rainfall and groundwater samples in order to estimate groundwater recharge using the CMB method for the highland and coastal zones. It is worth noting that the rainfall events were sampled from January to April 2013. All monitoring wells have been categorized into coastal, plain, and highland zones to estimate groundwater recharge using the WTF method. A fully transient groundwater flow model was developed for the 1993–2013 period and groundwater model calibration and validation were respectively performed for the period of Oct. 1993 to Sep. 2008 and Oct. 2008 to Sep. 2013. Six principal hydrogeological units were considered to generate a 3D stratigraphic model of the study area, using collected data from hundreds of borehole logs. Materials and layer elevations for the numerical model grid were directly obtained from the stratigraphic model. The time unit, time step and stress period were respectively specified as daily, monthly and monthly. Six layers, with a regular mesh and a block centered finite difference grid (500×500 m) with 150 rows and 97 columns, were considered in the model. After that, the developed groundwater conceptual model was assigned into the numerical model.

Different performance criteria, consisting of Root Mean Square Error (RMSE), Mean Absolute Error (MAE) and Mean Error (ME), were used to evaluate the accuracy of the model (Fig. 2).

3 Results and Discussion

According to the CMB method, the recharge is respectively estimated at about 45 and 8 mm/year for the highland and coastal zones. The estimated annual recharge ranges from 6 to 14 mm for the coastal area, while it varies from 10 to 22 mm for the plain area based on the WTF method. The Wadi Al-Fara study area is recognized for its substantial hydrogeological and geological diversity. Therefore, a root mean square error of 3.39 m is considered quite reasonable regarding the model resolution and the scale of the study area. Using the validated model, the groundwater budget components were calculated for the study area. It showed a long-term water balance deficit as the abstraction ($51 \text{ Mm}^3/\text{year}$) exceeds natural recharge ($31 \text{ Mm}^3/\text{year}$). The system is balanced by an inflow from the aquifer storage and the sea, leading to an advanced seawater intrusion, and consequently increasing salinity at the coastal areas. Recharge flux from the upper catchment (highland) to the coastal zone is a major contributor ($12 \text{ Mm}^3/\text{year}$) to water resources in the coastal plain, sustaining the hydrological system along the southern margin, by a flow from the storage in the adjoining highland-fractured aquifers. Direct recharge from precipitation over the plain is comparatively small.

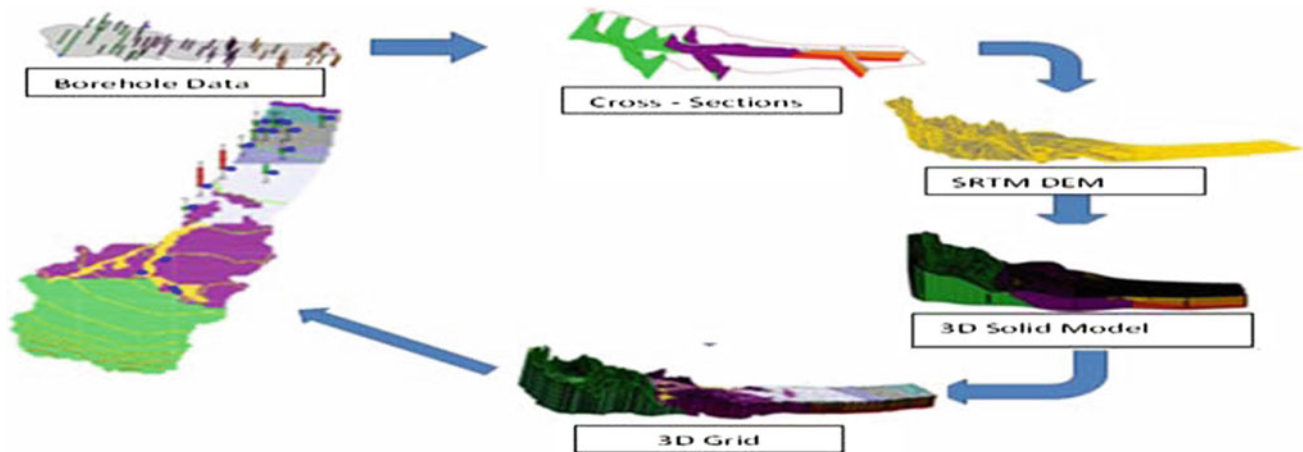


Fig. 2 Steps to develop groundwater model to estimate recharge (after [1])

Table 1 Estimated recharge using different methods for the whole study area

Method	Recharge (mm/year)
CMB	22
WTF	13
Groundwater modeling	26

The estimated recharge rates for each method is shown in Table 1. As the actual annual recharge is not known previously, it is difficult to ascertain the accuracy of one of the three methods. Though none of the used methods can be called the “best”, all methods provide more or less similar results and the variation is not significant. However, various conclusions can be drawn from this study about the limitations, advantages and disadvantages of the approaches employed.

4 Conclusion

Groundwater recharge estimation during this study was accomplished by implementing three methods: CMB, WTF and groundwater modeling. The adopted methods complement one another and provide reliable results for estimating

groundwater recharge in the Wadi Al-Fara coastal catchment. Thus, using multiple methods is valuable to constrain recharge rates estimate and limit its uncertainty.

Acknowledgements We would like to express our gratitude to the Sultan Qaboos University for providing financial support under the project # IG/DVC/WRC/18/01.

References

1. Amerjeed, M.: Groundwater modeling with emphasis on recharge estimation in hardrock-alluvium Al-Fara catchment, Oman: comparison of methods. PhD Thesis, Sultan Qaboos University, Oman (2016)
2. Anderson, M.P., Woessner, W.W.: Applied groundwater modeling: simulation of flow and advective transport, 1st edn. Academic Press, San Diego (1992)
3. Healy, R.W., Cook, P.G.: Using groundwater levels to estimate recharge. *J. Hydrol.* **10**, 91–109 (2002)
4. Healy, R.W.: Estimating groundwater recharge, 1st edn. Cambridge University Press, Cambridge (2010)
5. Izady, A., Abdalla, O., Joodavi, A., Karimi, A., Chen, M., Tompson, A.F.B.: Groundwater recharge estimation in arid hardrock-alluvium aquifers using combined water-table fluctuation and groundwater balance methods. *Hydrol. Process.* **31**(19), 3437–3451 (2017)
6. Wood, W.W., Sanford, W.E.: Chemical and isotopic method for quantifying ground-water recharge in a regional, semiarid environment. *Ground Water* **33**(3), 458–486 (1995)



Groundwater Favourable Infiltration Zones on Granitic Areas (Central Portugal)

José Martins Carvalho, Maria José Afonso, José Teixeira, Liliana Freitas, Ana Rita Lopes, Rosário Jesus, Sofia Batista, Rosário Carvalho, and Helder I. Chaminé

Abstract

The Infiltration Potential Index (IPI) was used at Castelo Novo (Fundão, Central Portugal) to delineate favourable infiltration zones. The Infiltration Potential Index is a valuable tool to include in integrated water resources management in crystalline fractured rocks. An integrated approach combining hydrogeomorphology and GIS was developed applying multiple layers of information (tectonic lineaments, hydrogeological units, slope, drainage, land use, and precipitation). Different ranks were assigned to thematic layers and different weights were given to classes according to their contribution for groundwater using the Analytical Hierarchical Process (AHP) methodology. Almost 80% of the area is covered by slightly to moderately weathered (W_{1-2} – W_3) granite, having slopes of 5–15° and 15–25°, tectonic lineaments densities of 6–12 km/km² and 12–18 km/km² and drainage densities of 6–9 km/km² and >9 km/km². Scrub and/or herbaceous vegetation associations and bare rocks dominate. A moderate to high Infiltration Potential Index (IPI) is dominant in the area.

Keywords

Groundwater • Infiltration potential index (IPI) • GIS mapping

1 Introduction

There has been a world rising demand for groundwater for various purposes, such as domestic, agricultural and industrial use. Digital techniques, such as the Infiltration Potential Index (IPI), emerge as a rapid and cost-effective tool to delineate favourable infiltration zones to contribute to estimate recharge (e.g., [4, 8]).

The challenge of this study is to identify favourable infiltration zones using the integrated use of hydrogeology, hydrogeomorphology and Geographic Information Systems (GIS) at a small-scale area (about 100 hectares) in Castelo Novo (Fundão, Central Portugal).

2 Castelo Novo Site: Regional Framework

Castelo Novo is a well-known historical location: its hydrogeological and economic importance is given by the thermal spa open since the middle of XIX century till 1945 [1] and by a prestigious water bottling production plant. Castelo Novo area is located near the *Gardunha* mountain system (Fig. 1), in Central Portugal, within the Iberian Massif [5]. The mountainous ridge system trends NE-SW and is part of an extensive tardy- to post-Variscan granitic batholith [5]. Quartz, aplite and pegmatite veins outcrop in this area following the regional fault trends. Granitoids are surrounded by metasedimentary rocks, namely the schist-greywacke complex. Sedimentary deposits have a very low extension and thicknesses and are related to the Holocene water stream dynamics. Locally, the bedrock is mainly composed of moderately to slightly weathered (W_3 – W_{1-2}) granite, medium to coarse grained. The highly

J. M. Carvalho · M. J. Afonso (✉) · J. Teixeira · L. Freitas

H. I. Chaminé

Laboratory of Cartography and Applied Geology (LABCARGA),
Department of Geotechnical Engineering, School of Engineering
(ISEP), Polytechnic of Porto, Porto, Portugal
e-mail: mja@isep.ipp.pt

J. M. Carvalho · M. J. Afonso · H. I. Chaminé

Centre GeoBioTec, UA, Aveiro, Portugal

J. Teixeira

CEGOT and Department of Geography, Faculty of Arts,
University of Porto, Porto, Portugal

A. R. Lopes · R. Jesus · S. Batista

APA—Portuguese Environment Agency, Lisbon, Portugal

R. Carvalho

IDL and Department of Geology, Faculty of Sciences, University
of Lisbon, Lisbon, Portugal

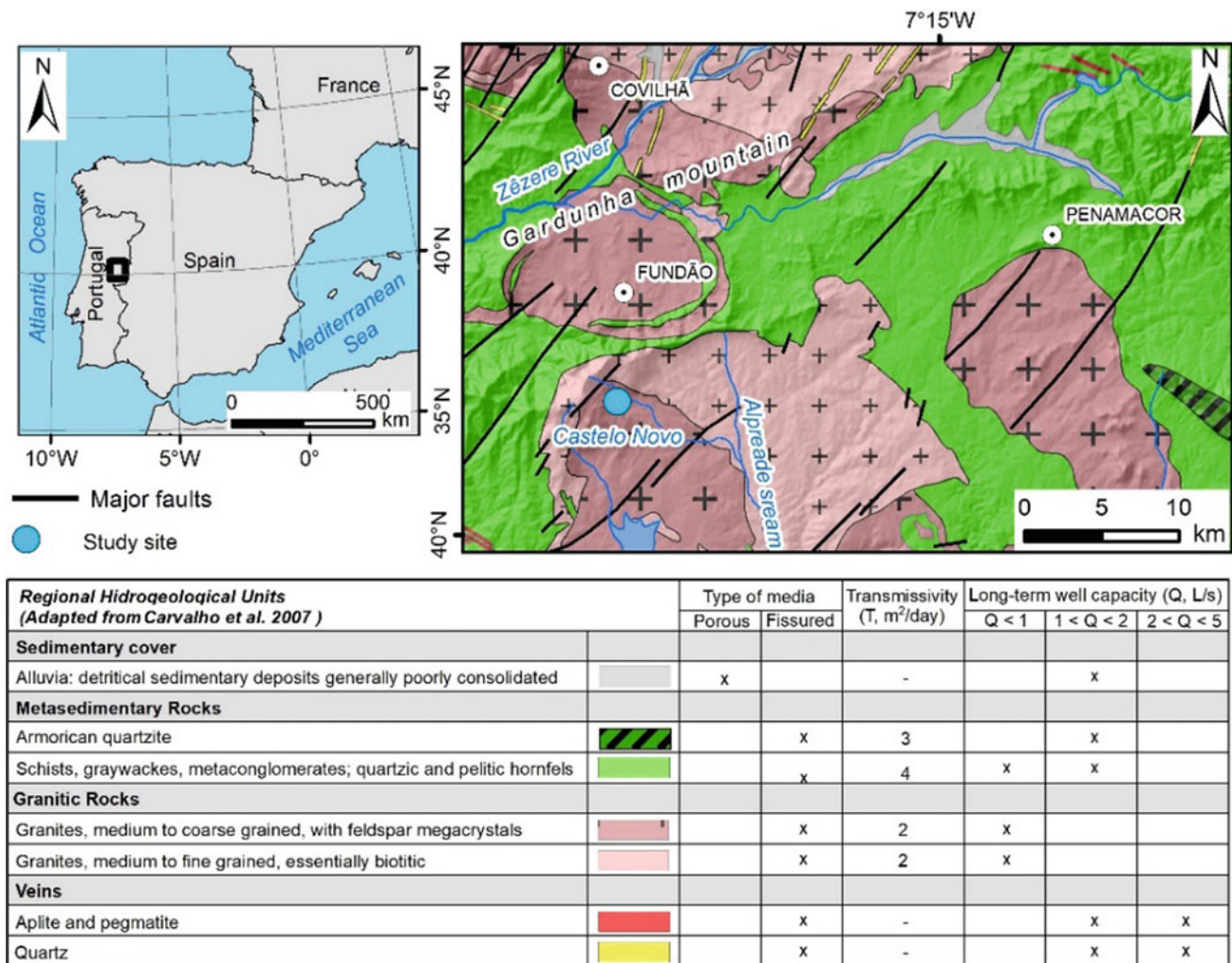


Fig. 1 Hydrogeological setting of Castelo Novo site. Adapted from [2, 8]. Geological background: [5]

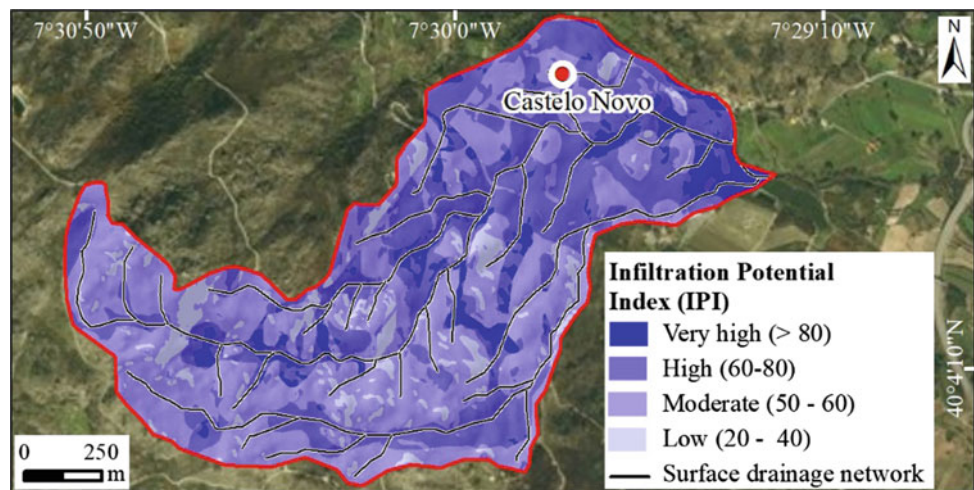
weathered (W_{4-5}) granite outcrops are observed in sloped areas. Also, a granitic sandy-clayey regolith was identified, and a slightly to moderately weathered (W_{1-2} – W_3) granite also outcrops [3].

3 Materials and Methods

Geology, morphotectonics and hydrogeology basic techniques have been applied in this study. A geodatabase was created in a GIS environment to organise the input data, including geological and hydrogeological features, like lithology, tectonic lineaments density and weathering grade, land use, drainage density, slope and precipitation. Data were weighted and overlay operations completed, which permitted the conception of several derivative map themes, to assess the spatial distribution and controls on groundwater infiltration. The identification of the explaining factors for

the calculation of the infiltration zoning index followed the methodology proposed by Teixeira et al. [8]. The Analytical Hierarchical Process (AHP) was used as a multicriteria decision-making technique to normalize the weights of various thematic layers and their classes for delineating the groundwater favourable infiltration zoning, and the inner scores were mainly assessed from fieldwork data (e.g. [6–8]). The adopted grid data structure consisted of a pixel of $1 \times 1 \text{ m}^2$. This GIS analysis resulted in a map of the Infiltration Potential Index (IPI) which represents the combination of all factors, ranging from 0 to 100, where the higher values represent better conditions for water infiltration, according to all factors. The ranking of the explaining factors was the following: lithology, considering weathering grade, 39%, slope 32%, land use 14%, tectonic lineaments density 10% and drainage density 5%. Thematic layers were integrated using weighted overlay to produce the groundwater infiltration map.

Fig. 2 Infiltration Potential Index (IPI) for Castelo Novo site (Fundão, Central Portugal)



4 Results and Discussion

Figure 2 shows the Infiltration Potential Index (IPI) for Castelo Novo site (Central Portugal).

Considering the lithology factor, slightly to moderately weathered (W_{1-2} - W_3) granite is prevalent (77%) in the area. For the Slope factor, the most representative classes are 5–15° (45%) and 15–25° (34%). For the Land use factor, the classes scrub and/or herbaceous vegetation associations and bare rocks represent, respectively, 43 and 40% of the area. For the tectonic lineaments density factor, classes 6–12 km/km² and 12–18 km/km² are the most representative, corresponding, respectively, to 38 and 36% of the area. For the drainage density factor, the more representative classes are 6–9 km/km² (40%) and > 9 km/km² (33%). The prevalent Infiltration Potential Index (IPI), corresponding to 84% of the area, is moderate (40–60) to high (60–80) (Fig. 2). The highest IPI arises mainly in areas with gentle gradients (<15°), occupied by the highly to moderately weathered granite, and with scrub and/or herbaceous vegetation. The groundwater favourable infiltration zones follow the Infiltration Potential Index (IPI).

5 Final Remarks

Wherever meteorological, reservoir and hydrodynamical data are available, it is possible to turn IPI and groundwater favourable infiltration zones into a groundwater resources

assessment. This study can be applicable as a guideline to other aquifer settings and is a valued tool for the water authorities to manage sustainable groundwater resources.

References

1. Acciaiuoli, L.M.C.: Le Portugal hydromineral. Direction Générale des Mines et des Services Géologiques. 2 vols. I vol., 1952, 284p.; II Vol., 1953, 574 p., Lisbonne (1952/53)
2. Carvalho, J.M.: Prospecção e pesquisa de recursos hídricos subterrâneos no Maciço Antigo Português: linhas metodológicas. Universidade de Aveiro, Ph.D. Thesis (2006)
3. LABARGA: Estudo hidrogeológico da área de concessão hidromineral HM51 Águas do Alardo (Castelo Novo, Fundão). Laboratório de Cartografia e Geologia Aplicada, ISEP, Porto (unpublished report) (2009)
4. Nag, S.K., Kundu, A.: Application of remote sensing, GIS and MCA techniques for delineating groundwater prospect zones in Kashipur block, Purulia district, West Bengal. *Appl. Water Sci.* **8**, 38 (2018)
5. Oliveira, J.T., Pereira, E., Ramalho, M., Antunes, M.T., Monteiro, J. H.: Carta geológica de Portugal, escala 1/500000. Serviços Geológicos de Portugal, Lisboa (1992)
6. Saaty, T.L.: Decision making with the analytic hierarchy process. *Int. J. Serv. Sci. Manag. Eng. Technol.* **1**(1), 83–98 (2008)
7. Şener, E., Şener, Ş., Davraz, A.: Groundwater potential mapping by combining fuzzy-analytic hierarchy process and GIS in Beyşehir Lake Basin, Turkey. *Arab. J. Geosci.* **11**, 187 (2018)
8. Teixeira, J., Chaminé, H.I., Carvalho, J.M., Pérez-Alberti, A., Rocha, F.: Hydrogeomorphological mapping as a tool in groundwater exploration. *J. Maps* **9**(2), 263–273 (2013)

Assessment of Groundwater Potential in the Upper Tigris/Turkey Plain

Recep Celik

Abstract

The Upper Tigris Basin lays in the part of the upper historic Mesopotamian Basin, where agricultural activities have been carried out since civilization has passed through settled life. Products such as grain and cotton are grown in this region providing resources not only for Turkey, but also for other Middle Eastern countries. In recent years, irrigation agriculture has started to get more value-added products. However, the national dam for irrigation projects has not yet been completed in this basin, and groundwater is mostly for irrigation. For this purpose, the determination of the basin's groundwater potential is enormously significant for sustainable irrigation. In this study, groundwater potential of the basin was assessed by handling data of opened water wells. The study shows the groundwater potential is high in the southern, southeastern and eastern parts of the Basin. While the groundwater potential in the western and southwestern parts of the Basin is normal, it has been found to be low in the Northern part.

Keywords

Groundwater • Upper Tigris basin • Diyarbakır • GIS • Static water level

1 Introduction

Historically the Upper Tigris Basin had a priority for agricultural activities. Between the Tigris River and the southeastern Taurus Mountains, remains a broad area called the Diyarbakir Basin. Extending from northwest to south, the altitude of Karacadağ separates the Diyarbakir Basin from Sanliurfa Plateau. The Euphrates River forms the western

region boundary. In the east, the Ambar and Göksu streams blend into the Tigris River [1].

The average annual precipitation in the basin is 814 mm [2], which is equal to 12 billion m³ of annual water volume in the basin. 6.5 bm³ of water volume evaporate from the mass of water, of which 3.65 bm³ infiltrate into the groundwater, and 1.85 bm³ contribute to surface water [3]. However, Turkey's water potential has been calculated as 224 bm³ (surface and groundwater) [4].

Around the world, GIS methods are considered to be a popular technique for mapping groundwater, and many authors have used remote sensing and GIS techniques for groundwater searches [5, 6].

In this study, the Upper Tigris Basin static water level, dynamic water level and well flow yield maps were obtained using Arc Map 10.2.1 program Spatial Analyze method. The groundwater potential of the basin was assessed taking into account the topographic (drainage, slope), meteorological and geological characteristics of the plain.

2 Materials and Methods

The Upper Tigris Basin is located between lines 40–44° east and 37–55° north, in the province of Diyarbakır, Turkey. This basin is surrounded by mountains in the north. Diyarbakir belongs to the southeastern Anatolian Province [7]. The study area is 12,655 km². Farming in the province is mostly rain-fed and fallowing is a common practice there. Diyarbakır Plain is surrounded by the Taurus Mountains in the north and north-east, Mardin-Midyat brink in the south, and Karacadağ volcanic massif in the west (Fig. 1). In the basin, a mixed agricultural cultivation (dry and wet) is practiced.

About 180 water wells were examined (Fig. 2) for obtaining groundwater properties. ESRI ArcGIS Desktop/ArcInfo 10.2.1 software, Spatial Analyses extension IDW method was used in this study to process and create map layers. A common reference system familiar to

R. Celik (✉)

Dicle University, 21128 Sur/Diyarbakır, Turkey
e-mail: recep.celik@dicle.edu.tr

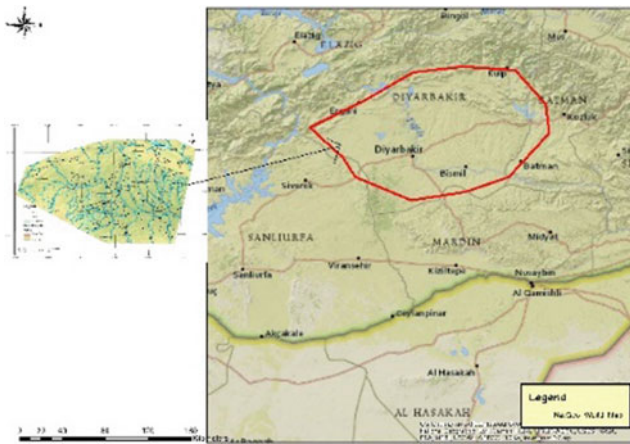


Fig. 1 Study area

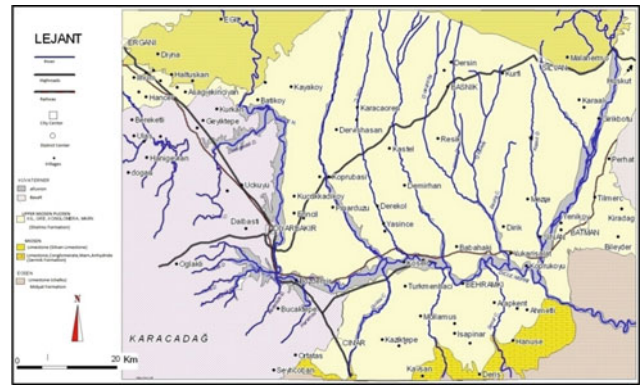


Fig. 3 Upper Tigris Basin

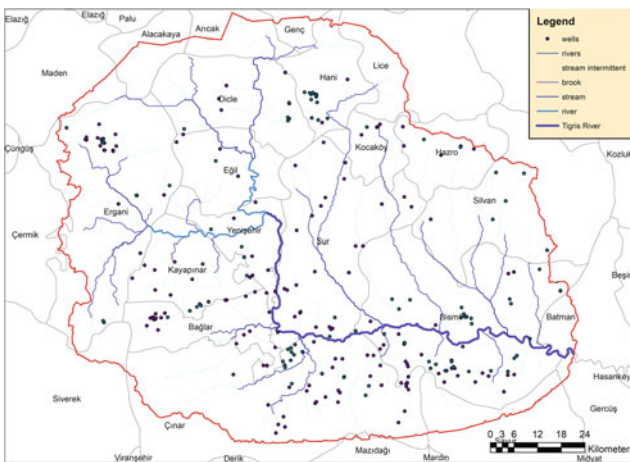


Fig. 2 Well location

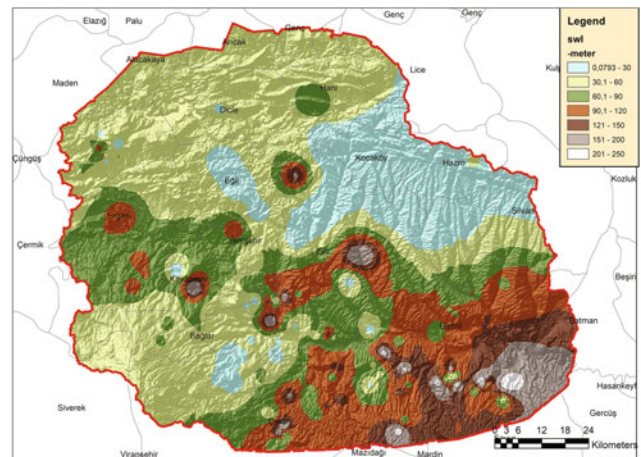


Fig. 4 Static water level map

national mapping standards, UTM (Universal Transverse Mercator) with European Mean Datum 1950, was used to produce all of the maps. The geological map was digitalized from DSI 1979 [8] 1/100 000 map (Fig. 3).

Geological Map (obtained from DSI 1979)

Data pertaining to these water wells were converted into digital map layers using GIS together with geological maps to obtain common ground formation maps and well drilling data. The result was a map used especially for hydrogeological studies which became a useful source of information about the infrastructure and properties of water aquifers and their ability to hold water.

3 Results and Discussion

In this study, the final thematic map production began using data from boring wells. First, the static water level depth map was issued (Fig. 4). Static Water Level maps are prepared using the available wells' data obtained from the static water levels using Geographic Information Systems (GISs), which are modeled for the whole Diyarbakir Plain region.

Similarly, this method was used for obtaining a Dynamic Water Level thematic map (Fig. 5). The Dynamic Water Level Map prevents unnecessary well drilling. Figure 6 also uses the same map logs to locate wells that would produce efficient groundwater pump flow.

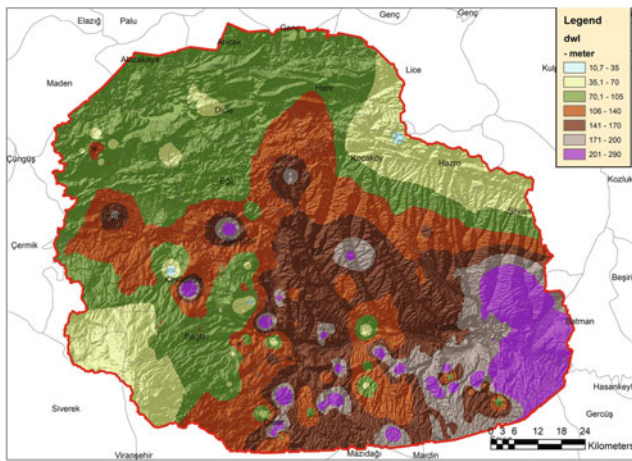


Fig. 5 Dynamic water level map

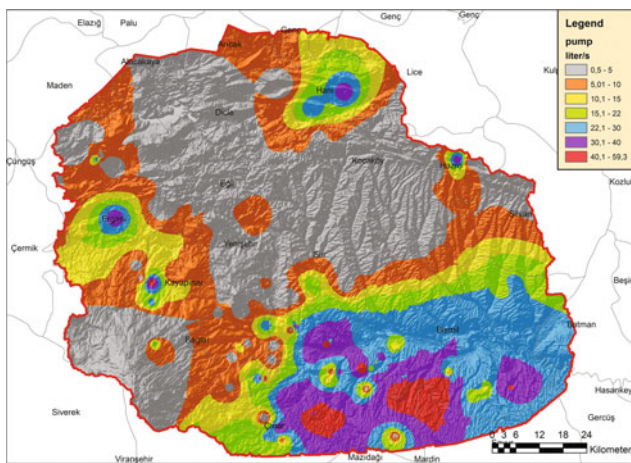


Fig. 6 Pump yield map

Hydrogeological data were collected from field observations and records of previously drilled wells. The upper units and the bedrock are semi-permeable and impermeable, respectively. The top units and the bedrock floor are semi-permeable and impermeable, respectively. The depth of groundwater level ranges from 6 to 10 m, approximately 585 m above the average sea level, similarly to the water level of the Tigris River in the alluvial regions of Bismil. The static level of the basin observes a static level of groundwater at high locations, increasing up to 65 m and up to 100 m, respectively, for the lower and the higher sections of Tigris. The depth exceeds 100 m at some locations.

Artesian fed by Midyat formation, having a flow capacity of 3–10 L/s, is possible in the area between the Bozdemir and Ambar villages. This amount is too small for irrigation. It can though be used for small scale irrigation or drinking water

supply. Obtaining an artesian flow rate of 10–20 L/s from Midyat formation in the field between the Ambar and Korukçu villages is possible. It is possible to obtain a flow of 40–50 L/s just in and around the river bed of the Tigris (lower than the altitude of 600 m) for a drilling depth of 30–40 m. As the water level of wells drilled at higher elevations decreases, going forward toward the south of the Tigris yields relatively less capacity. There, a flow of 20–40 L/s can be obtained.

Projection delays for irrigation in GAP regions have concluded in a wide usage of underground resources. It is observed that activities for well digging are increasing. This huge amount of water discharging will result in diminishing the seasonally static water level, so exploiting groundwater resources for new applications must be strictly controlled.

4 Conclusions

The morphologic outlook of the area is defined by a wide valley which connects parallel hills. The sections located in the middle part of the study area are mostly impermeable. Groundwater is recharged from the valleys in the west and seeps through an open deduction in the basalt mass. Leakages are also determined across the edges, between the basalts and the tertiary deposits.

Alluviums in the water beds of the Tigris are generally suitable for groundwater retention, and at most groundwater locations, resources come from big river alluviums. The conglomerate and sandstone layers within the bedrock result in a noticeable increase in the overall permeability.

When the geological nature of the region is examined, it should be noted that fountains are fed by the basalt formation in Karacadag. The basalt formation does not have a normal groundwater level. However, depending on the joints and cracks in the basalt formations, there exists a groundwater resource fed by local resources in shallow lowlands.

Selmo formation is usually composed of dried clayey, silty sandstone and marly with gravel stone levels. The dominant lithology is clay that forms an impermeable unit.

References

1. DPES Report (2011): http://www.csb.gov.tr/db/ced/editordosya/diyarbakir_icdr2011.pdf
2. DMI: Actual average values in long period for Diyarbakir city (1970–2011). (DMI; Turkish) (2018). Available from: <https://www.mgm.gov.tr/veridegerlendirme/il-ve-ilceler-istatistik.aspx?k=A&m=DIYARBAKIR>. Accessed 27 April 2018
3. Çelik, R.: Temporal changes in the groundwater level in the Upper Tigris Basin, Turkey, determined by a GIS technique. *J. Afr. Earth Sci.* **107**, 134–143 (2015)

4. Nalbantođlu, U.: Water resources in Turkey. DSI-State Hydraulic Works and Implementation of Water Database at DSI. Report: Country about Turkey (2006). pp. 1–11. Available from: http://www.minenv.gr/medeuwi/meetings/conference.of.the.water.directors.athens.6&7-11-06_en/00/dsi-turkey.pdf
5. Çelik R (2014) Mapping of groundwater potential zones in the Diyarbakir city center using GIS. Arab. J. Geosci. <https://doi.org/10.1007/s12517-014-1485-9>
6. Abdalla, F.: Mapping of groundwater prospective zones using remote sensing and GIS techniques: a case study from the Central Eastern Desert, Egypt. J. Afr. Earth Sci. **70**, 8–17 (2012)
7. GAP BÖLGE KALKINMA PLANI 2002 (Turkish); Güneydođu Anadolu Projesi Bölge Kalkınma İdaresi. Ankara
8. DSI: Yukarı Dicle Havzası Hidrojeolojik Etüt Raporu. p. 113, Ankara, Turkey (1979)

Assessment of Turkey-Harran Basin's Groundwater Potential and Hydrogeological Properties

Veysel Aslan and Recep Celik

Abstract

The Harran Plain is located in the region of Upper Mesopotamia where agricultural activities have been carried out for 4000 years. This region has a very fertile soil for agricultural activities. Its agricultural and socio-economic values have increased since this area was subjected to irrigated agriculture within the scope of Southeastern Anatolian Irrigation Project. Hence, the determination of the hydrogeological properties and alternative groundwater potential of this basin is vital for sustainability. For this study, hydrogeological data belonging to Sanliurfa-Harran plain and general information about natural water resources were used. Using the DEM data of Sanliurfa province, river basins and geomorphological surfaces were formed. Hydrogeological and geomorphological thematic maps were produced. With the help of thematic maps showing the geomorphological structure, the groundwater potential of Harran Basin was revealed. Besides, groundwater layer levels and aquifer layer thicknesses of the basin have been determined.

Keywords

Harran basin • Water resources • Groundwater • GIS • Hydrogeology

1 Introduction

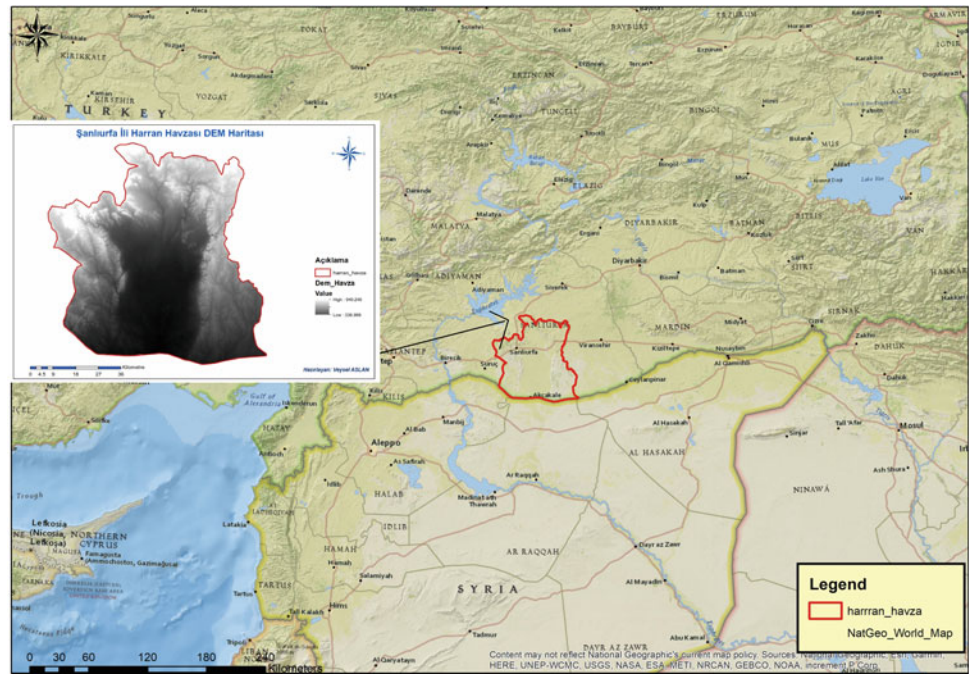
Harran Plain is located in the province of Sanliurfa, on the territory of Upper Mesopotamia, between 36 ° 43'–37 ° 08 'N parallels, 38 ° 57'–39 ° 55' eastern meridians in Turkey [1]. Harran Plain is a region extending from the southern part of the city of Sanliurfa to the border of Syria. The land is one of the most fertile plains in Turkey. After the construction of Atatürk Dam, Urfa Tunnels were giving water to the plains and watery agriculture started. It was opened in 1995 as the first irrigation in the Southeastern Anatolia, in which 140.000 km² of irrigation systems were installed. Mainly cotton is cultivated.

The climate of Harran is influenced by the Mediterranean climate, the terrestrial climate is dominant. Winters are cold and rainy, summers are too hot and dry. Annual mean precipitation is 365 mm, annual evaporation is 1848 mm, and average annual temperature is 17.2 °C [3]. On the south-western side of the plain, pumped irrigation is done using groundwater where the irrigation system is inadequate.

There are many studies that have been done in the Harran Plain, especially regarding the agricultural activities of agriculturists [4–7]. Groundwater studies were mostly done on groundwater pollution vulnerability [8, 9]. While hydrogeological studies were carried out by State Hydraulic Works (SHW) [10] in 1972, there is a need for more current studies. In this study, the hydrological characteristics and hydrogeological maps of Harran Plain were prepared using GIS, taking into account the groundwater potential, precipitation nutrition, basin condition and the geological structure of Harran Ovasi by using data of selected wells pre-determined in the basin fed with groundwater flow. For this, ArcGIS 10.2.1 software programme was used.

V. Aslan
Harran University, Hilvan Vocational High School, Dep. of Const.
Tech, S.Urfa, Turkey
e-mail: vaslan@harran.edu.tr

R. Celik (✉)
Department of Civil Engineering, Dicle University, 21100
Diyarbakır, Turkey
e-mail: recep.celik@dicle.edu.tr

Fig. 1 Harran Basin study area

2 Materials and Methods

2.1 Study Area

The investigation area is located in Southeastern Anatolia and south of Urfa Province of Turkey. It spreads from north to south in eastern Syria. Studies pitch $37^{\circ} 20'$ latitude, Turkey-Syria border in the south, $39^{\circ} 30'$ longitude in the

east and $38^{\circ} 30'$ in the west is bordered by east longitude. The average height is 500 m in the north, near the Turkish Syrian border and it drops up to 350 m in the south (Fig. 1).

2.2 Method

In order to obtain DEM map, in the 1/25.000 scale, topographic maps of the study area with a 5-meter contour in the

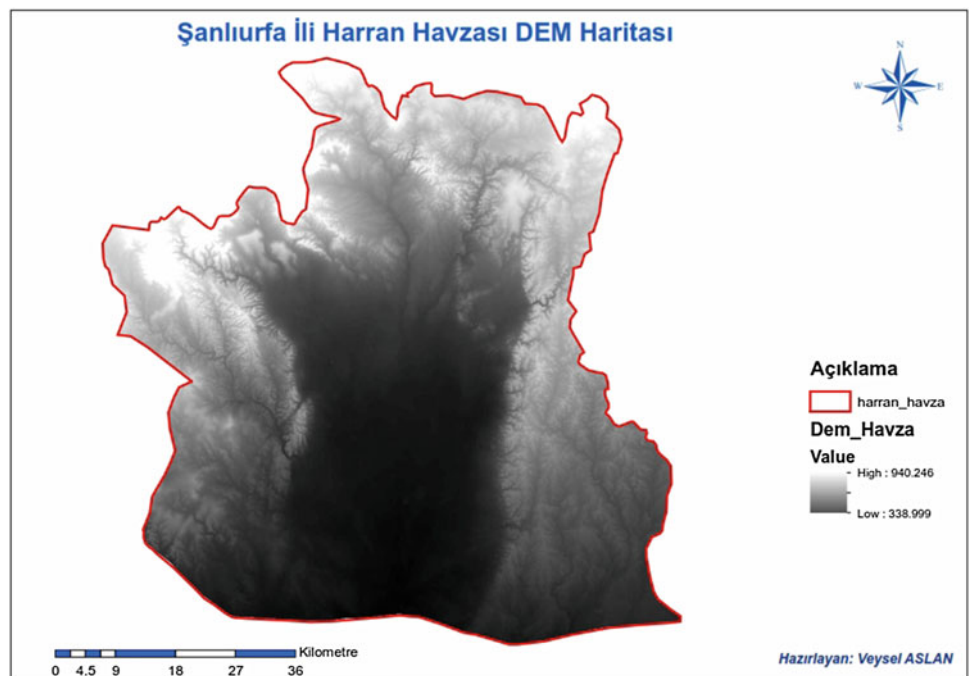
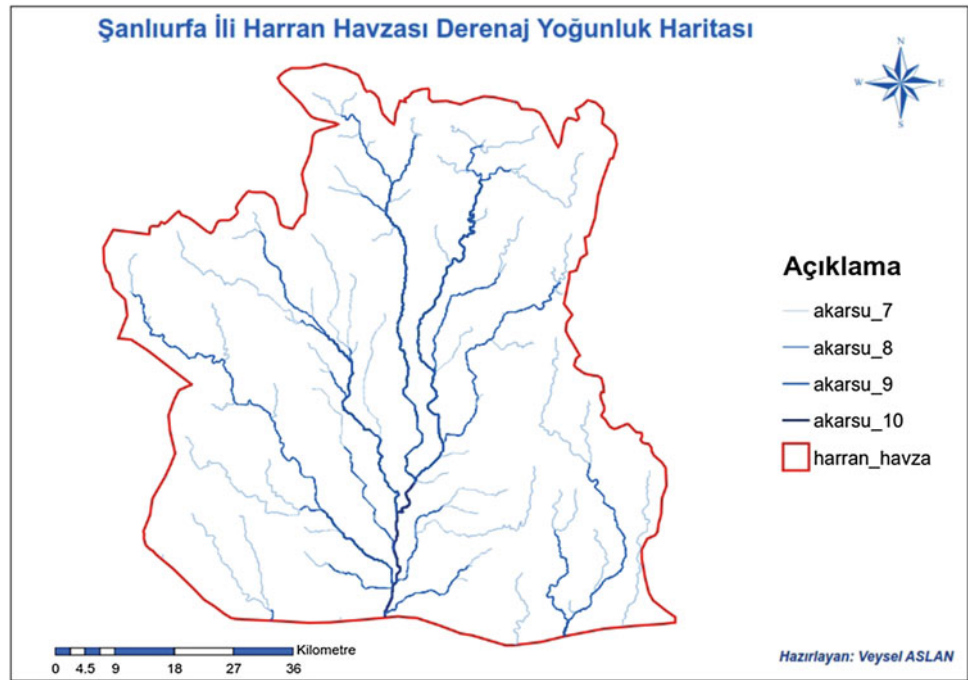
Fig. 2 Harran Basin DEM map

Fig. 3 Harran Drainage Density map



isohips were digitized (Fig. 2). For Flow Direction Calculation operations; Flow Direction, Flow Accumulation commands from Arctoolbox/Spatial Analyst Tools/Hydrology commands were used to calculate the cumulative flow direction. With this method, the number of cells in a cell's water collection area is calculated. Thus, water collection area and river branches were identified. Stream Order, Stream to Feature operations were used to define the

river. A Drainage Density map was created while recording with the vector name (Fig. 3).

The geomorphological map was obtained by classifying the heights with Arctoolbox/3D Analyst Tools/Raster Surface/Contour List with DEM map (Fig. 4). A slope map of the basin was also obtained from the DEM map (Fig. 5).

The geological map was digitized from the General Directorate of State Hydraulic Works (GDSHW) geological

Fig. 4 Harran Basin Geomorphology map

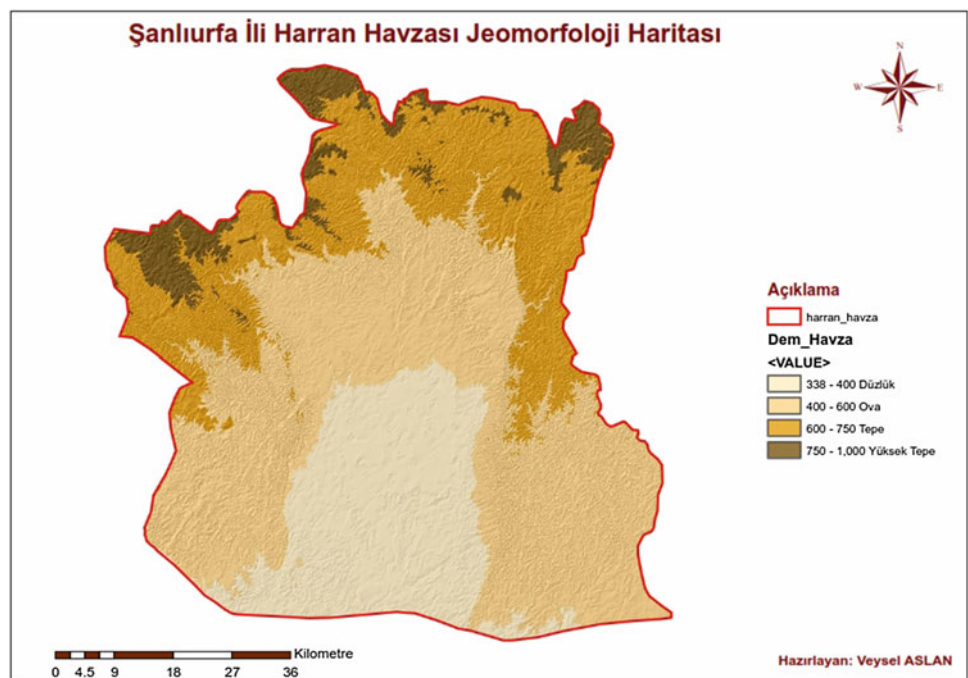
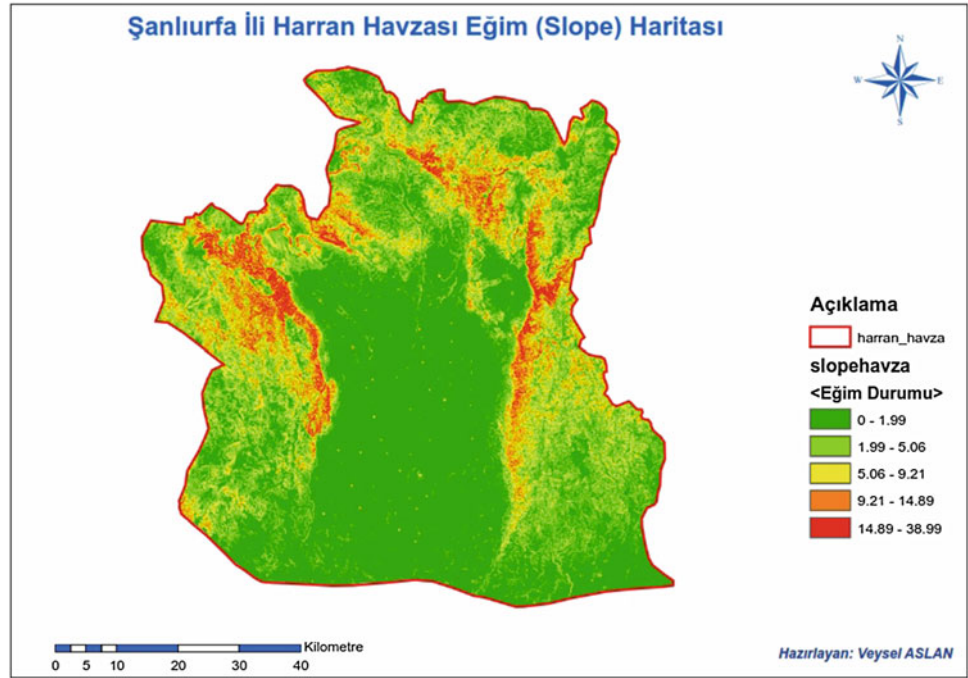


Fig. 5 Harran slope map

survey report (Fig. 6). Basin precipitation maps (Fig. 7) were generated considering the average rainfall data of 1967-2013 [11]. GDSHW Hydrogeology [9] map was digitized and a total of 185 well points were identified, and coordinates were obtained in the ArcGIS program that entered the basin. Static water levels belonging to the

coordinates and wells are added to the Excel table and the well data are added to the ArcGIS environment. The file has been created.

First, the groundwater static level map (Fig. 8) was created. When the DEM data opened in the ArcGIS program, the altitude values of the good points were obtained by

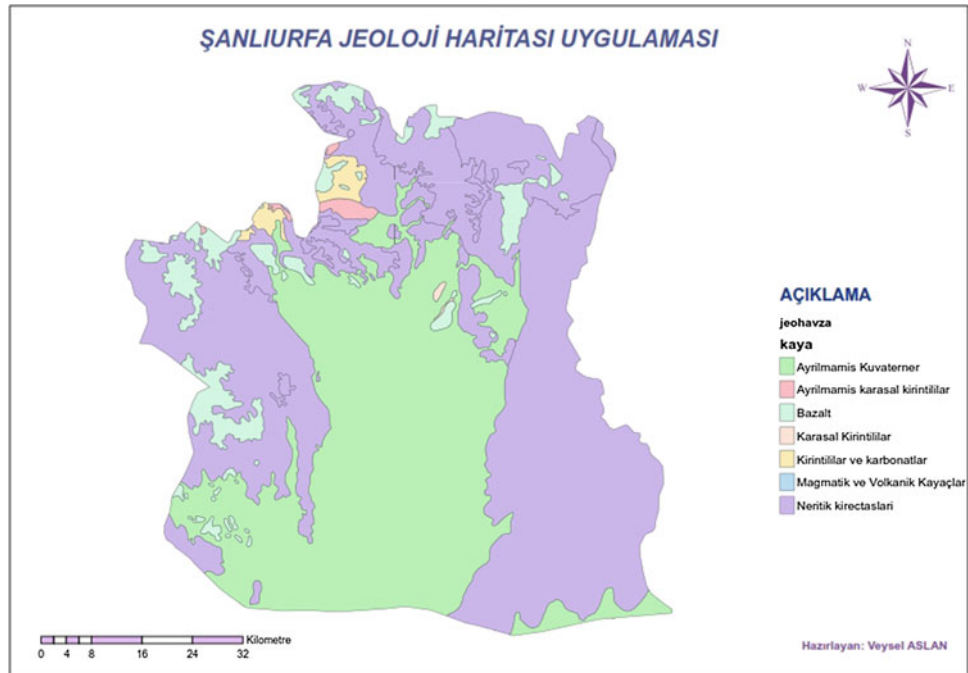
Fig. 6 Harran Geology map

Fig. 7 Harran Rainfall map

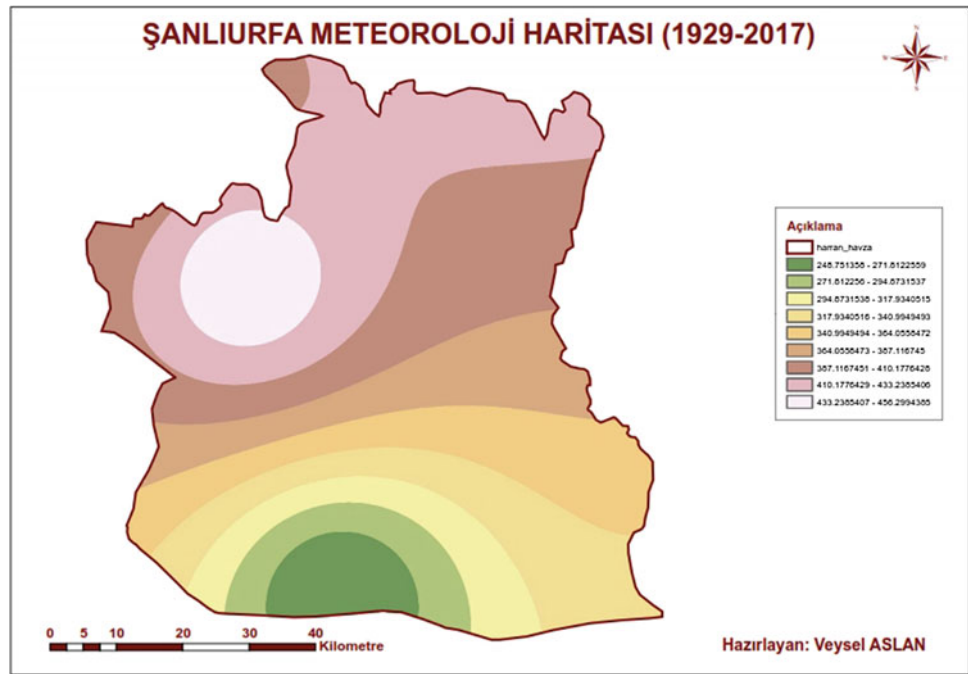
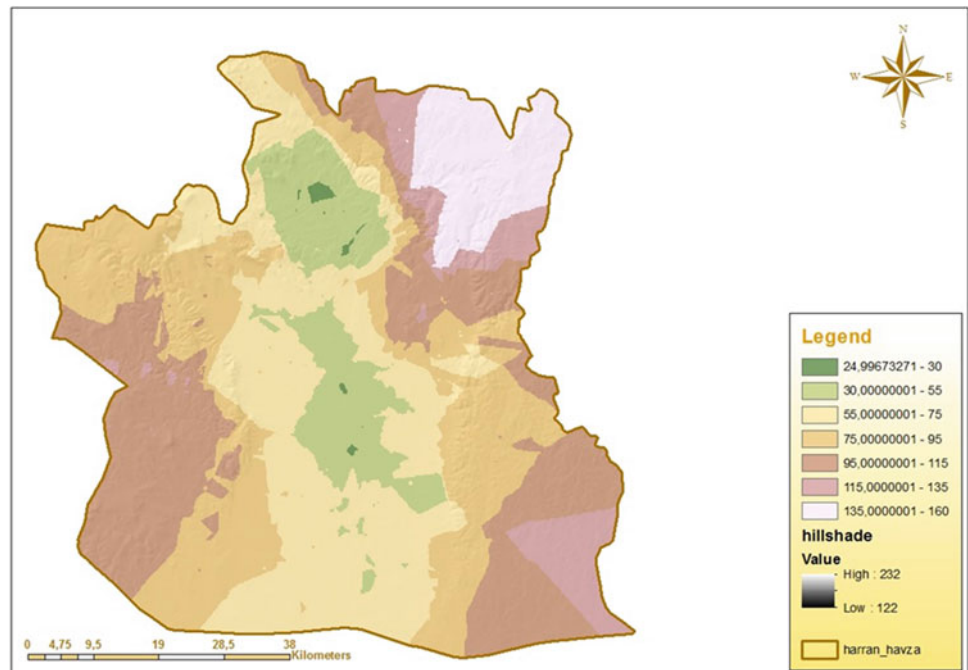


Fig. 8 Harran Basin groundwater table map

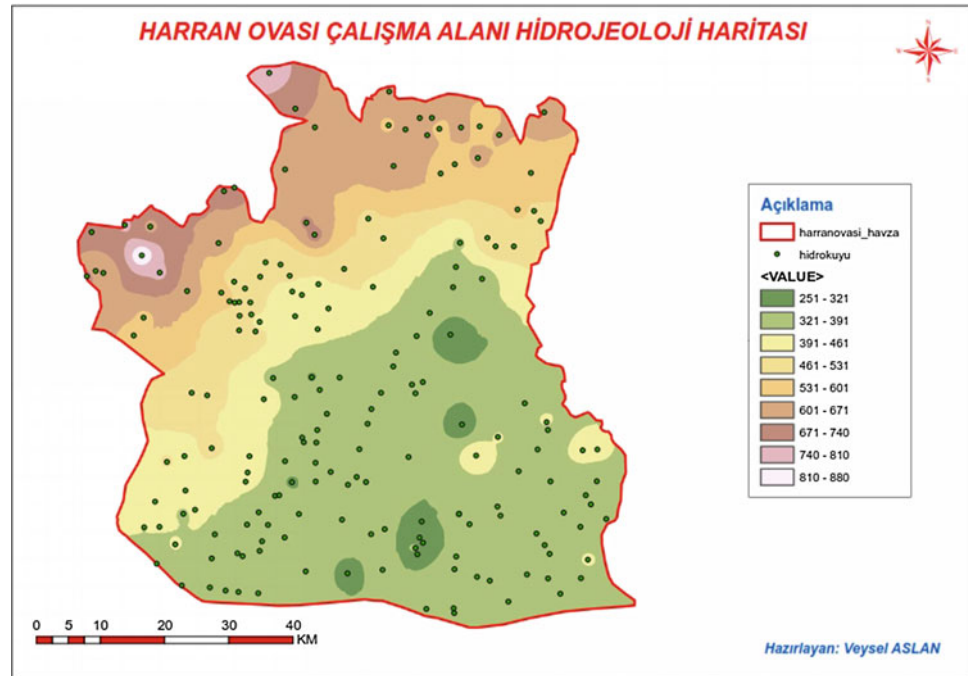


Spatial Analyst tools/Extract Multi Values to Point method. Altitude values are processed in the Excel table and the level of the aquifer was obtained by subtracting the Static Water Level value of the altitude value. An aquifer map was created with Spatial Analyst Tools/Interpolation/IDW methods (Fig. 9).

3 Results

The maps of hydrological characteristics of the Harran Basin are shown in Figs. 2-9.

Fig. 9 Harran Basin hydrogeology map



4 Conclusion

In geomorphological maps; zones between 312 and 400 m elevations are said to be “flat”, areas between 400 and 600 m elevations are “plain”, areas between 600 and 750 m are “sloppy”, and areas between 750 and 1000 m are seen as “hills”. Hence, the majority of the basin is defined as flat and plain. Likewise, a very large part of the slope of the basin is between 0 and 2% in slope maps. In the north and west, except in hilly places, the slope is between 5 and 9%.

Geological maps show that the central and southern parts of the basin are composed of unconquered terrestrial detritus in a significant part of the unqualified quaternary, north-western and eastern parts of the basin. In some regions in the north, basalt and limestones also show up.

In the precipitation maps; in the north of the basin, the average annual rainfall is between 370 and 450 mm/year, and in the southern part, it is between 270-330 mm/year. Therefore, the average basin precipitation is about 365 mm.

The static level maps show that the groundwater level of most of the basins ranges between 30 and 60 m. Considering the hydrological map; it is seen that the majority of the basin is at the lowest position as the basin code and the streams are inclined towards the basin.

In the case of precipitation, surface waters are seen to flow down to the Harran Basin, which is the lowest level of

the basin, and the thesis is confirmed from the aquifer layer obtained from GDSHW (the General Directorate of State Hydraulic Works) data.

References

1. Delgado, C., Pacheco, J., Cabrera, A., Batllori, E., Orellana, R., Bautista, F.: Quality of groundwaters for irrigation in tropical karst environment: The case of Yucatan, Mexico. *Agricultural Water Manag* **97**, 1423–1433 (2010)
2. Kanber, R., Çullu, M. A., Kendirli, B., Antepli, S., & Yılmaz, N.: Sulama, drenaj ve tuzluluk. *Türkiye Ziraat Mühendisliği VI. Teknik Kongresi*, 3–7 (2005)
3. ÇELİK, R., ASLAN, V., & Akyıldız, M.H.: Harran Ovası'nın Yeraltısuyu Potansiyelinin Coğrafi Bilgi Sistemi İle Modellenmesi (2017)
4. Bilgili, A. V., Çullu, M. A., Aydemir, S., Aydemir, A., & Almaca, A.: Probability mapping of saline and sodic soils in the Harran plain using a non-linear kriging technique. *Eurasian Journal Of Soil Science (EJSS)*, **2**(2), 76–81 (2013)
5. Bilgiç, C., Bahçeci, İ.: Harran Ovası Serbest Akışlı Drenaj Sistemlerinde Bazı Bitki Besin Elementleri İle Sediment Yükünün Belirlenmesi. *Harran Tarım Ve Gıda Bilimleri Dergisi* **18**(4), 1–9 (2014)
6. Aktaş, Y., Öcal Kara, F.: Şanlıurfa Harran Ovası Sulama Projesi'nde Aşırı Sulamanın Sosyo-Ekonomik Nedenleri. *Küresel İklim Değişimi ve Su Sorunları Çözümünde Ormanlar Semp. Ü. Akkemik (Editör)*, İstanbul S, 223–228 (2007)
7. Kirnak, H., DOĞAN, E., Demir, S., Yalçın, S.: Determination of hydraulic performance of trickle irrigation emitters used in

- irrigation systems in the Harran Plain. *Turkish Journal of Agriculture and Forestry*, 28(4), 223–230 (2004)
8. Yesilnacar, M.I., Sahinkaya, E., Naz, M., Ozkaya, B.: Neural network prediction of nitrate in groundwater of Harran Plain. Turkey. *Environmental Geology* **56**(1), 19–25 (2008)
 9. Yesilnacar, M.I., Gulluoglu, M.S.: Hydrochemical characteristics and the effects of irrigation on groundwater quality in Harran Plain, GAP Project. Turkey. *Environmental Geology* **54**(1), 183–196 (2008)
 10. DSİ (Devlet Su İşleri): “Harran Ovası Hidrojeolojik Etüdü”, pp. 49, DSI printing office, Ankara (1972)
 11. <https://www.mgm.gov.tr/veridegerlendirme/il-ve-ilceler-istatistik.aspx?k=A&m=SANLIURFA>

Evaluation of the Potential for Artificial Groundwater Recharge of Crystalline Rocks Aquifer, Nuba Mountains (Sudan)

Dafalla Wadi, Wenbing Wu, and Abuzar Fuad

Abstract

Biteira district lies in southern Sudan, underlain by deformed basement rocks. The geological setting of this area, with its position in the heavy savannah region, has produced water scarcity in the dry season. Also, the steady population growth and the expansion of agricultural activities, coupled with desertification and climate issues, have further augmented the stress on the resources of water. To overcome such a problem, we proposed the artificial recharging of groundwater at a specific location as a justified solution. Detailed geological, hydrometeorological, hydrological, and drainage pattern studies—along with an analysis of soil grain size and tests of infiltration—have been taken into consideration in this investigation. In addition, a Landsat image covering the area was analysed to obtain data bearing of regional features and structures. The results show that the selected area is suitable for groundwater recharge, the proposed dam is capable of storing water with a capacity of $20.73 \times 10^6 \text{ m}^3$, the infiltration average rate is $1.23 \text{ m}^3/\text{day}$, and groundwater flow estimated towards NW direction (approximately 285°). The proper position of the potential water wells has been determined. The proposed approach proved to be the most rapid and reliable method to investigate the basement-dominant region for artificial groundwater recharge.

Keywords

Crystalline rocks • Artificial recharge • Site selection
Check dam • Sudan

1 Introduction

This study is intended to show how rainwater can be caught and stored, and then recovered to supply domestic and livestock needs. Since the climate of the investigated area is scorching and the long summer is the primary water-loss factor, the artificial groundwater recharge has been taken into account as a solution.

The techniques of rainwater harvesting (RWH) have attracted attention as another source of essential drinking water [1–6]. Rainfall can be infiltrated to the subsurface formation or behind manufactured structures or stored in tanks [7, 8].

The topography of the district has been analyzed using satellite images to ensure the water storage. The soil grain size analysis and the infiltration test have been done to confirm the infiltration. The rocks' deformations have been analyzed to define the groundwater flow direction. Referring to these points, an appropriate site of a retention dam has been selected for water retention. A 10-metre-high check dam was proposed to store runoff in order to increase the infiltration process.

2 Materials and Methods

The following data types and methods were used: Remotely sensed data of Landsat ETM+ 7 imageries, Shuttle Radar Topographic Mission (SRTM) data, Survey of Sudan topographic maps and Meteorological data of Rashad Meteorological Station. Field data: rocks' structures and fracture measurements, soil samples, and infiltration tests. Laboratory analysis of soil: grain size analysis.

D. Wadi (✉) · W. Wu

Engineering Research Center of Rock—Soil Drilling Excavation and Protection, Ministry of Education, China University of Geosciences, Wuhan, 430074 Hubei, China
e-mail: wadiadam@cug.edu.cn

A. Fuad

Department of Chemistry and Earth Science, College of Arts and Science, Qatar University, Doha, Qatar

3 Results

3.1 Watershed Characteristics

The highest elevation in the watershed is 1041 m above sea level, while the lowest is 670 m—in the district of the Nuba Mountains in Sudan. The shape of the watershed becomes narrow towards the end of the upstream. It consists of several micro-watersheds adjacent to each other, covering an area of 78.7 km². The watershed is defined by a gentle to moderate slope (1–9%).

3.2 Geological Structures

A folded ridge of quartzite defines the area with an axis trending to 30°. This fold axis is plunging 70°. The dip amounts of limbs are ranged between 55° and 75° westward (Fig. 1). Release fractures at right angles with the direction of folding force were formed and denoted as lineaments.

Lineaments are varying in their frequency, orientation, size, density, and degree of intersection.

3.3 Infiltration

In this investigation, some tests were implemented to assess the rates of infiltration for unlike geomorphological and soil parameters. The checks were distributed to cover stream-filled sediments, floodplain sediments and peneplain sediments within the potential reservoir area. Table 1 shows the test results.

4 Discussion

The results of infiltration tests showed that the rate of infiltration of the floodplain soil is the least, among other soils within the proposed area. The reduction of infiltration was interpreted as the result of the sedimentation of fine-grained

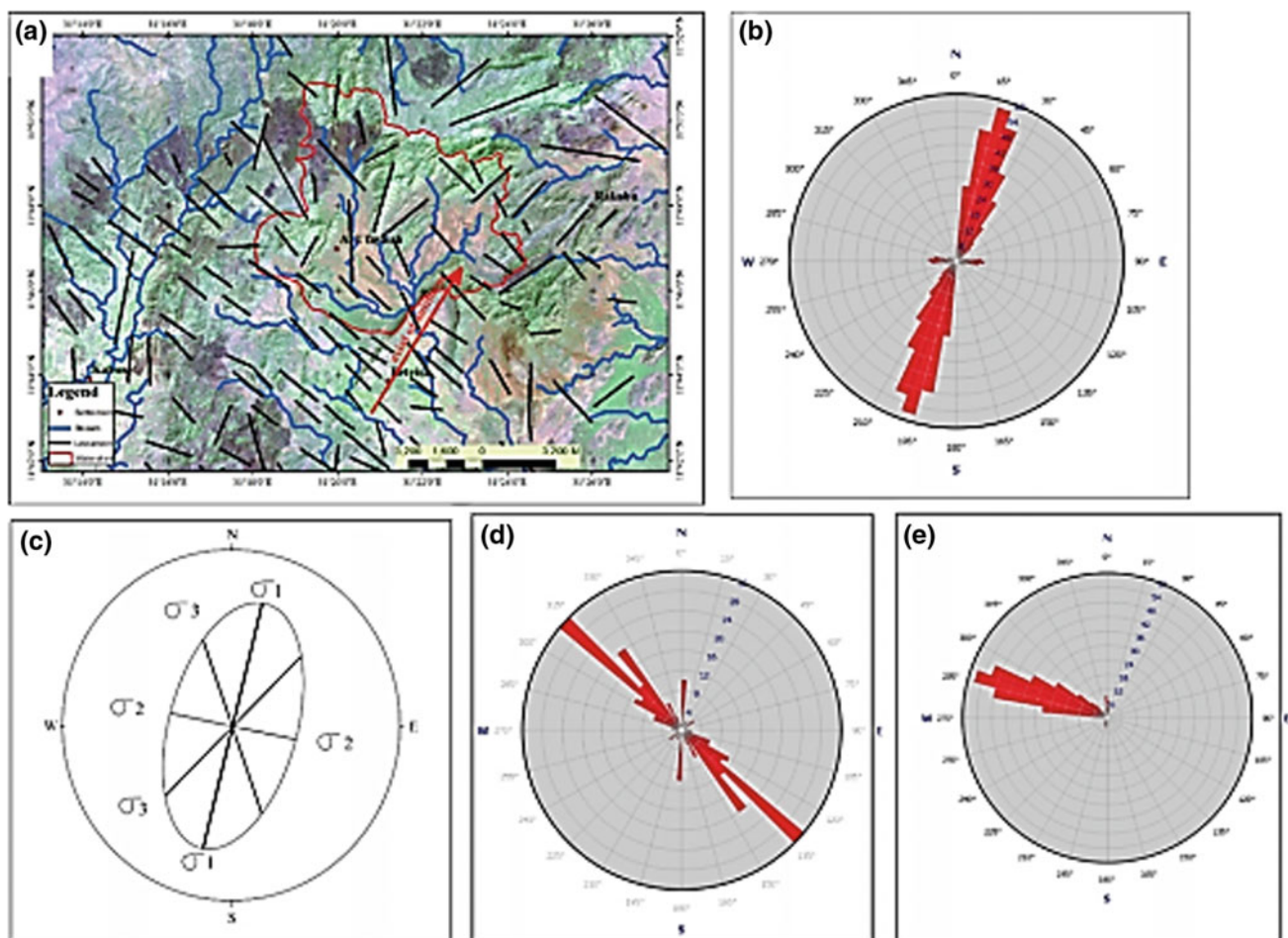


Fig. 1 Foliation and lineament models **a** lineaments superimposed on the satellite image, **b** rose diagram of foliation trend, **c** strain ellipsoid of the deformation, **d** rose diagram of the direction of lineament **e** rose diagram of foliation dip

Table 1 Summary of infiltration test results

Test bit No.	Test site	Infiltration rate (m ³ /day)
1	Floodplain	0.6888
2		0.6120
3		0.5664
4		0.4800
5		0.4272
6	Stream bed	2.1480
7		2.3712
8		2.2896
9		2.3352

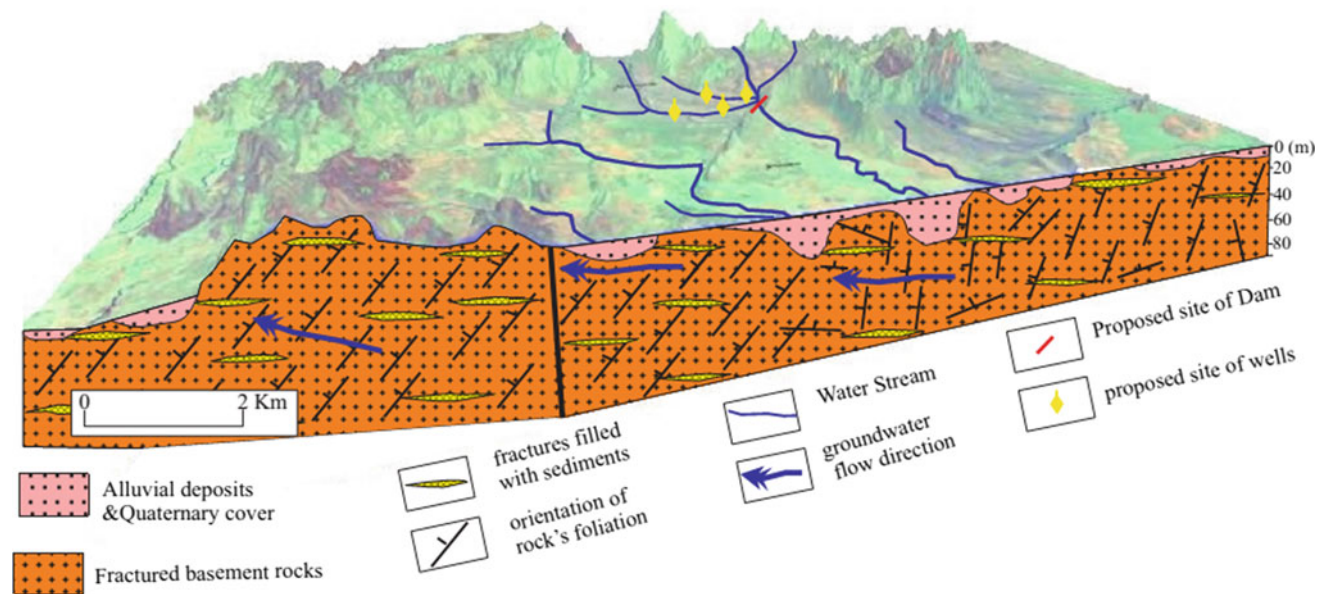


Fig. 2 A Schematic conceptual groundwater flow model at the watershed-scale as a function of foliations and lineaments conditions

soil as the flood speed reduced. The sedimentation area will increase to cover stream bed and the peneplain which is included within the potential reservoir area when the proposed dam is constructed. Therefore, the infiltration rates showed by these tests will decline gradually over time, which means decreasing the percentage of water recharge to groundwater. Regarding this issue, recharge wells in the stream bed have been suggested. These wells are proposed to be located in the stream bed. They should be deep enough (3 m), elevated at least one meter above the earth's surface and filled with layers of gravel. The well tops must be covered with a fence to prevent cobbles and rubbish from falling in. The gravel filled in the wells can be frequently checked and cleaned yearly during the dry season and whenever the water table gets lower in the reservoir. The results of structural analysis showed that the rock's foliations are dipping to the west direction while the Lineaments are

trending to WNW direction (Fig. 1). In that way, the groundwater of these rocks will flow in the same direction as its movement is controlled by the formation's structures. This point is very useful for the location of the potential boreholes. Locally weathered zones below the lineaments will facilitate the recharge process.

5 Conclusions

This study illustrates the application of engineering geology, techniques of remote sensing, and GIS in site investigation for the enhancement of the groundwater recharge potentiality in an area underlined by crystalline rocks. Topographically, the site is very satisfying for surface storage capacity. Gravelly and/or sandy soils underlying the stream bed help the water seep in with an average infiltration rate of

>1.22 m³/day. The rock's foliations are dipping to the west direction. Lineaments of the district are trending more or less in a WNW direction. A schematic conceptual model of groundwater flow has been built (Fig. 2) to emphasize the general groundwater flow direction. However, the locations of the water recovery wells were sited. A 10-meter-high check dam has been proposed to store surface runoff for infiltration purposes. The recharge holes have been recommended to reduce the adverse effect of the sedimentation.

References

1. Kim, Y., Han, M., Kabubi, J., Sohn, H.-G., Nguyen, D.-C.: Community-based rainwater harvesting (CB-RWH) to supply drinking water in developing countries: lessons learned from case studies in Africa and Asia. *Water Sci. Technol. Water Supply* **16**(4), 1110–1121 (2016)
2. Nguyen, D.C., Han, M.Y.: Proposal of simple and reasonable method for design of rainwater harvesting system from limited rainfall data. *Resour. Conserv. Recycl.* **126**, 219–227 (2017)
3. Mwamila, T.B., Han, M.Y., Kim, T., Ndomba, P.M.: Tackling rainwater shortages during dry seasons using a socio-technical operational strategy. *Water Sci Technol. Water Supply* **15**(5), 974–980 (2015)
4. Temesgen, T., Han, M., Park, H., Kim, T.: Design and technical evaluation of improved rainwater harvesting system on a university building in Ethiopia. *Water Sci. Technol. Water Supply* **15**(6), 1220–1227 (2015)
5. Nguyen, D.C., Dao, A.D., Kim, T., Han, M.: A sustainability assessment of the rainwater harvesting system for drinking water supply: a case study of Cukhe village, Hanoi, Vietnam. *Environ. Eng. Res.* **18**(2), 109–114(2013)
6. Ahammed, M.M., Meera, V.: Iron hydroxide-coated sand filter for household drinking water from roof-harvested rainwater. *J. Water Supply Res. Technol. AQUA* **55**(7–8), 493–498 (2006)
7. Terêncio, D., Fernandes, L.S., Cortes, R., Moura, J., Pacheco, F.: Rainwater harvesting in catchments for agro-forestry uses: a study focused on the balance between sustainability values and storage capacity. *Sci. Total Environ.* **613**, 1079–1092 (2018)
8. Isioye, O.A.: A multi criteria decision support system (MDSS) for identifying rainwater harvesting site (S) in Zaria, Kaduna state, Nigeria. *Int. J. Adv. Sci. Eng. Technol. Res.* **1**(1) (2012)

The Impact of Urbanization Versus the Impact of the Change in Climatic Conditions on Groundwater Recharge from Precipitations: Case Study Algiers

Mohamed Amine Boukhemacha

Abstract

A comparative quantitative study on the impact of two of the most important factors threatening fresh water resources (urbanization and climate change) is presented. Using the Soil Conservation Service-Curve Number (SCS-CN) model, the individual impacts of the development of urban areas and the changes in the climatic conditions on several components of the urban hydrological cycle (runoff, initial abstraction with a focus on groundwater recharge from precipitations) are assessed with a daily time step at the scale of Algiers during the period 1987–2016. For the presented case study, it was found that the changes in the climatic conditions impacted all three components of the hydrological cycle with a higher magnitude than the development of the urban area. A strong correlation between groundwater recharge (and runoff) and the climatic conditions is observed. Moreover, it is estimated that potential natural groundwater recharge in constructed areas can be higher than that in non-constructed ones; an aspect that can shift with changes in the climatic conditions (particularly the changes in rainfall intensity and frequency).

Keywords

Urban area development • Climatic conditions change • Groundwater recharge • Runoff • Algiers

1 Introduction

Managing water resources, and particularly groundwater (the largest available freshwater resource [1]), has become a must under the now-widely recognized threats of scarcity and quality degradation that are mainly related, directly or

M. A. Boukhemacha (✉)
National Polytechnic School, 10 Avenue Hassen Badi BP 182 El Harrach, 16200 Algiers, Algeria
e-mail: boukhemacha-amine@hotmail.com

indirectly (through climate change), to human activities (e.g. [2, 3]). The magnitude of these threats is particularly accentuated in urban areas [4, 5]. Since modern cities are under continuous horizontal and vertical expansion, it was considered necessary to investigate the individual magnitudes of the impacts associated with two continuously changing factors (i.e. climatic conditions and urbanization) threatening groundwater resources and challenging the establishing of adequate management practices.

2 Data and Methods

2.1 Study Zone

Algiers, the largest urban agglomeration in Algeria, is located in the north of the country, on its Mediterranean coast. The city covers an area of about 774 km² and hosts about 3 million inhabitants (according to the 2008 census). With its Mediterranean climate, the city receives 600 mm/year of rain on average. From a hydrogeological perspective, Algiers lays on a shallow semi-confined Quaternary aquifer made of sand and gravels (transmissivity up to 0.1 m²/s) and a main flow direction toward the N.

2.2 Approach

Assuming the water balance equation of Eq. 1, the Soil Conservation Service-Curve Number (SCS-CN) model [6] was used to quantify the key components of the hydrological cycle, with a daily time step and under different urban settings and climatic conditions.

$$P = I_a + Q + F \wedge Q = \frac{(P - I_a)^2}{(P - I_a) + S} \wedge I_a$$

$$= \min(P, \lambda S) \wedge S = \frac{25,400}{CN} - 254 \quad (1)$$

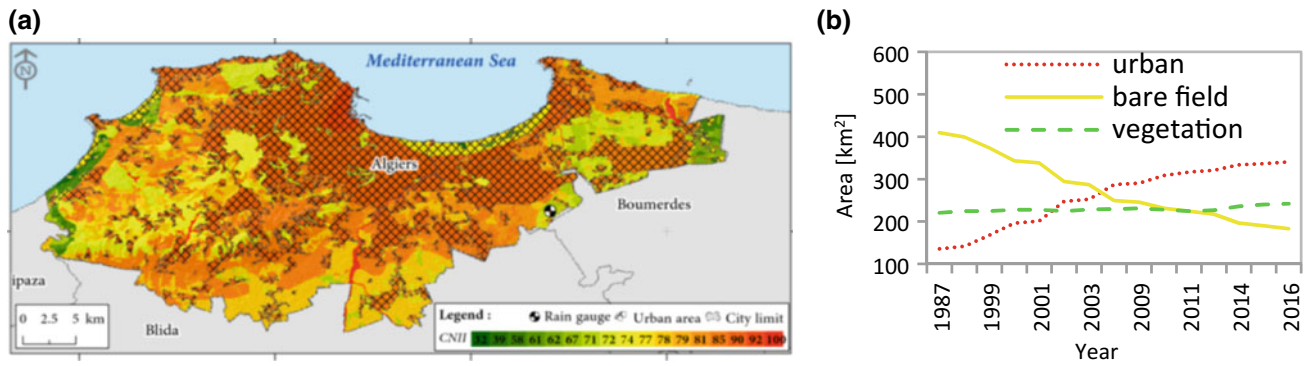


Fig. 1 The study zone: **a** settings in 2011: urban area and computed CN (based on data from [7, 8]); **b** land-use development during 1987–2016 (adapted from [9])

where, P [mm/day]: the precipitation, F [mm/day]: the infiltration, I_a [mm/day]: the initial abstraction and Q [mm/day]: the runoff. In the SCS-CN, λ a coefficient (equal to 0.2) and S [mm/day]: the potential maximum retention that depends on the hydrological conditions, soil type, land cover and the water content (these conditions are incorporated into the dimensionless parameter CN).

Using a detailed mapping of the land-use corresponding to the urban configuration of the city in 2011 [7] and Algiers' soil map [8], a reference CN map was derived (Fig. 1a). This map was then extrapolated to account for the development of the urban area during the period 1987–2016, using a less detailed mapping of the land-use change (Fig. 1b) in the city from [9]. As for the climatic data, a time series with daily precipitations from the Dar El-Beida rain gauge (Fig. 1a) was used (data from [10]).

Three analyses were conducted: (1) **combined effects**: both effects (climate change and urbanization) were considered simultaneously allowing for an assessment of the system's response (described by Q , F and I_a) under actual state conditions; (2) **climate effect**: to provide an assessment of the system's response while taking into consideration only one changing factor, the urban configuration was fixed to that of

1987 when accounting for the changes in the climatic conditions; (3) **urban effect**: similarly, here the climatic conditions were fixed to those of 1987 when accounting for the changes in the urban settings during the studied period, in order to isolate the effects of this latter factor.

3 Results and Discussion

3.1 Natural Aquifer Recharge in Constructed Versus Non-constructed Areas

For individual CN classes, computed potential groundwater recharge rates (F) in constructed areas (high CN values) are higher (Fig. 2a) than those computed for non-constructed areas (low to average CN values); this aspect is caused by I_a patterns (I_a is higher for low CN values). Though one may expect to find less infiltration in impervious surfaces than in permeable ones, the obtained results are in agreement with previous findings (e.g. [11]) that relate the ceiling of land surface (urbanization) to a decrease in evapotranspiration (accounting for the largest part in I_a) that exceeds the increase in the runoff in constructed areas.

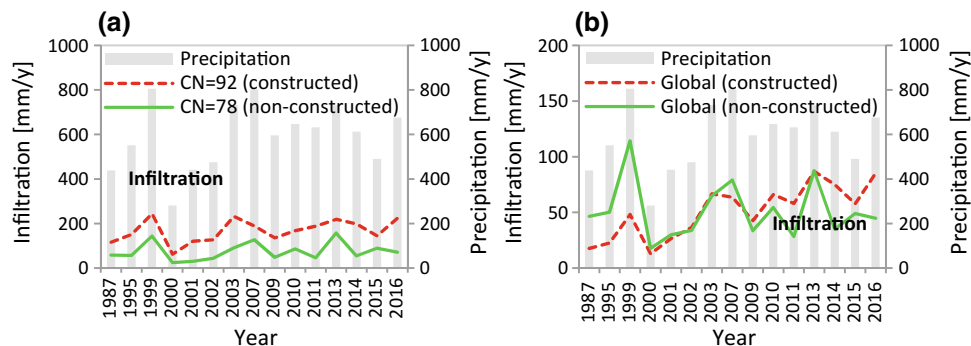
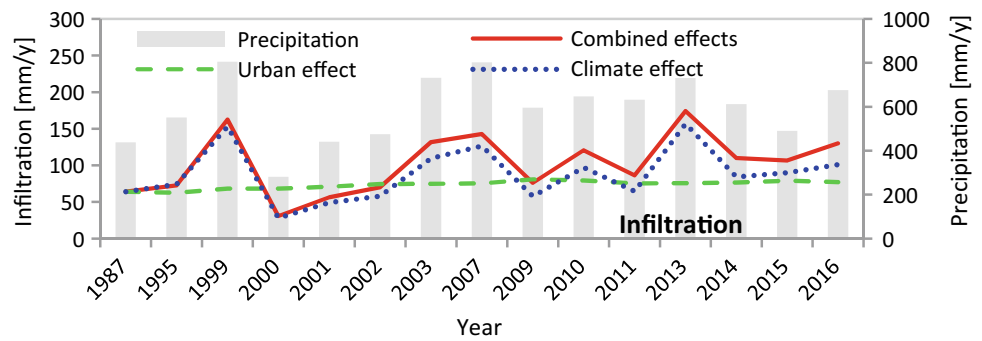


Fig. 2 Comparison between constructed and non-constructed settings under actual state conditions (combined effects) in terms of: **a** F for $CN = 78$ and $CN = 92$ and **b** F for all constructed and non-constructed areas

Fig. 3 City scale infiltration for all three analyses



Nevertheless, the results of the 1st analysis (actual state conditions) show that, at the global scale (area-proportional averaging the infiltration rates of all CN classes in each type of land surface), the above behavior is not consistent during the entire period (see Fig. 2b). The shift between $F_{\text{constructed}} < F_{\text{non-constructed}}$ and $F_{\text{constructed}} > F_{\text{non-constructed}}$ is found to be related to the changes in the climatic conditions (changes in rainfall intensity and frequency—precipitation events with high intensity and low duration are becoming more and more frequent).

3.2 Urbanization Versus the Change in Climatic Conditions

Even though the relative changes (relatively to 1987) in the urban area (max. change of +151% observed in 2016) are much higher than those observed in the climatic conditions (max. change of +83% in 2007), the results indicate that the changes in climatic conditions produced a higher impact on all three components of the hydrological cycle (I_a , Q and F) assessed at the scale of Algiers city than urbanization did (Fig. 3). Furthermore, a strong correlation between F (potential aquifer recharge) and the climatic conditions can be observed for the 1st (actual state) and 2nd (climate effect) analyses. Similar trends were found for Q .

4 Conclusions

Aquifers' recharge in urban areas is strongly affected by human activities and their direct and indirect consequences. The natural recharge from precipitation in such areas is particularly influenced by the ceiling of land surface and climate change. In the presented case study, it is estimated

that the magnitude of the effects of the last factor can be higher than of those related to urbanization. Nevertheless, an adequate management of this water resource and a suitable city development will require integrated actions.

References

- Shiklomanov, I.: World fresh water resources. In: Gleick, H. (ed.) *Water in Crisis: A Guide to the World's Fresh Water Resources*, pp. 13–14. Oxford University Press, New York (1993)
- Cooley, H., Christian-Smith, J., et al.: Climate change and transboundary waters. In: Gleick, H. (ed.) *The World's Water*, vol. 7, pp. 1–22. Island Press, Washington (2012)
- Trenberth, K.: Changes in precipitation with climate change. *Clim. Res.* **47**, 123–138 (2011)
- Boukhemacha, M.A., Gogu, C.R., Serpescu, I., Gaitanaru, D., Bica, I.: A hydrogeological conceptual approach to study urban groundwater flow in Bucharest city, Romania. *Hydrogeology J.* **23** (3), 437–450 (2015)
- Boukhemacha, M.A., Gogu, C.R., Serpescu, I., Gaitanaru, D., Bica, I.: General aspects on urban hydrogeology and highlights from Bucharest (Romania). *Environ. Eng. Manage. J.* **14**(6), 1279–1285 (2015)
- USDA: *National Engineering Handbook*. US Department of Agriculture, Washington (1954)
- INSID: Institut National des Sols, de l'Irrigation et Drainage data base (2011)
- Selvaradjou, S.K., Montanarella, L., et al.: *EuDASM—Soil Maps of Africa*. Office for Official Publications of the European Communities, Luxembourg (2005)
- Bouchachi, B., Zhong, Y.: Monitoring urban land cover/land use change in Algiers city using landsat images (1987–2016). In: *The International Archives of the Photogrammetry, Remote Sensing and Spatial Information Sciences*, vol. XLII-2/W7, pp. 1083–1090 (2017)
- Tutiempo Climate Webpage. <http://www.tutiempo.net>. Last accessed 27 April 2018
- Minnig, M., Moeck, C., Radny, D., Schirmer, M.: Impact of urbanization on groundwater recharge rates in Dübendorf, Switzerland. *J. Hydrol.* (2017)

Frequency Ratio Model for Mapping Groundwater Potential Zones Using GIS and Remote Sensing; Medjerda Watershed Tunisia

Fatma Trabelsi, Saro Lee, Slaheddine Khelifi, and Achouak Arfaoui

Abstract

Groundwater potential mapping and its sustainable development are an important aspect in the Lower Valley of Medjerda (LVM) river sub-basin due to increased water demand for irrigation and domestic use. The main goal of this study is to investigate the application of the probabilistic-based frequency ratio (FR) model in groundwater potential mapping at LVM river in Tunisia using GIS. This study includes the analysis of the spatial relationships between Transmissivity and various hydrological conditioning factors such as elevation, slope, curvature, river, lineament, geology, soil, rainfall, and land use. Eighteen groundwater-related factors were collected and extracted from topographic data, geological data, satellite imagery, and published maps. About 60 groundwater data of transmissivity were randomly split into a training dataset, 70% was used for training the model and the remaining 30% for validation purposes. Finally, the FR coefficients of the hydrological factors were used to generate the groundwater potential map. It was classified into five zones as very high, high, moderate, low, and very low. This information could be used by water decision makers as a guide for groundwater exploration and assessment in the LVM River.

Keywords

Groundwater potential map • Frequency ratio • GIS • Medjerda • Tunisia

F. Trabelsi (✉) · S. Khelifi · A. Arfaoui
 RU-Sustainable Management of Water and Soil Resources, Higher School of Engineers of Medjez El Bab (ESIM)_University of Jendouba, Medjez El Bab, Tunisia
 e-mail: trabelsifatma@gmail.com

S. Lee
 Geological Research Division, Korea Institutes of Geoscience & Mineral Resources (KIGAM), Daejeon, Republic of Korea

1 Introduction

In Tunisia, water resources are already limited in space and time. Their sustainable management is a national priority for ensuring water security and development of the country. The Medjerda basin, subject of this study, is the largest watershed in Tunisia, where groundwater resources are used in conjunction with surface water. While local surface water resources are relatively well managed, groundwater resources are hidden and more difficult to conceptualize, in addition to the lack of groundwater data. Hence, it is necessary to recognize the methods used to approach groundwater management and to predict the groundwater potential at the regional scale. Therefore, groundwater potential mapping (GPM) is essential, and constitutes an effective way to explore these invaluable natural resources [1, 4].

Recently, GIS and Remote Sensing techniques have also provided other cost- and time-effective approaches for the spatial prediction of groundwater productivity [3].

The aim of this study is to evaluate the efficiency of the Frequency Ratio (FR) model for groundwater potential mapping from aquifers of the Lower Valley of Medjerda (LVM) river basin.

2 Setting & Methods

2.1 Study Area

The study area is the Lower Valley of Medjerda (LVM) sub-basin; its reach extends from the dam of Laaroussia to the outlet of the river in the Mediterranean Sea, with a catchment covering approximately 1656 km². The climate is Mediterranean, characterized by mild, rainy winters and hot, dry summers with no marked prevailing seasons.

In the study area, the sources of water supply are mainly the surface water of the Medjerda River, and to a lesser

extent, groundwater. The groundwater is mainly utilized for irrigation purposes via pumping wells. The most common land use within this plain is irrigated agriculture. From a geological point view, the LVM represents a region of subsidence and collapse whose Mio-Pliocene and Quaternary formations cover the major downstream part of the watershed. Hydrogeologically, the LVM aquifers are mainly lying in alluvial deposits of the river, sometimes in sandstone and calcareous deposits. These aquifers are considered as unconfined in nature and are recharged across their entire surface by rainfall infiltration and Medjerda streams.

2.2 Methodology

To carry out the GPM, various data sets were used in the study via satellite images, toposheets, field data, hydrogeological data which were collected from three Regional Commissioner for Agricultural Development (CRDA of Ariana, Bizerte and Manouba), and Rainfall data collected from the National Institute of Meteorology (INM). Sentinel-2A data, from the Copernicus Sentinels Scientific Data Hub, were used to interpret the various groundwater influencing factors such as land use, lineament and drainage. Airborne LIDAR satellite Digital Elevation Model (DEM), with 28 m resolution, has been used for preparing morphometric maps such as slope, TWI, Curvature, aspect, etc. Figure 1 summarizes the adopted methodology.

2.2.1 Groundwater Occurrence Characteristics

In order to prepare a groundwater database, hydrodynamic data (Groundwater Level, Transmissivity, Groundwater Specific Capacity: SPC) of 60 pumping tests were collected from drilling wells (CRDA of Ariana, Bizerte and Manouba). Transmissivity is determined based on actual pumping test analysis of groundwater well. Out of these, 42 (70%) groundwater data were randomly selected for training the models and the remaining 18 (30%) were used for the validation purposes.

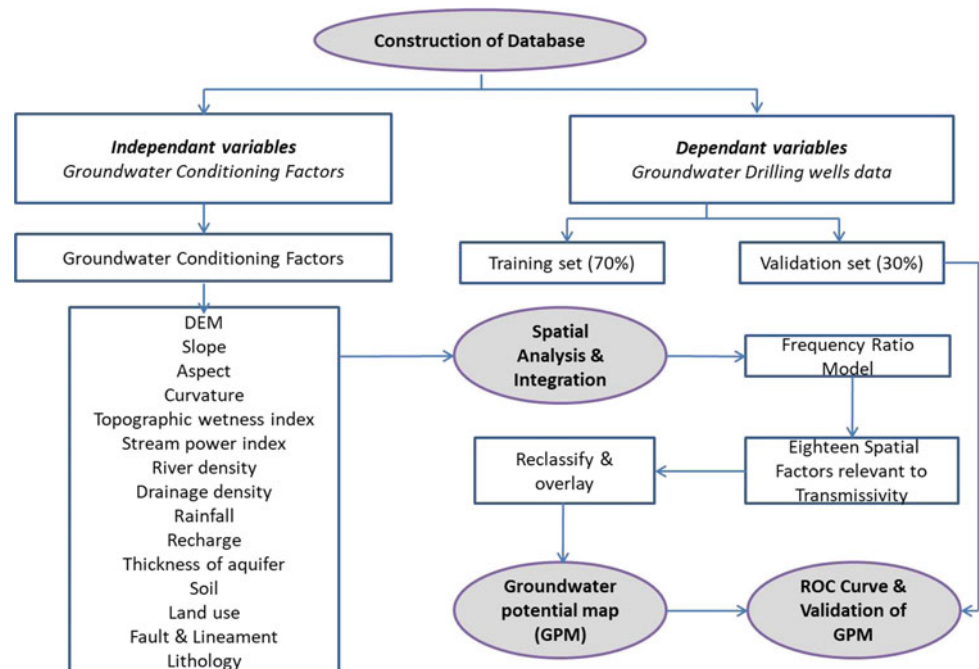
2.2.2 Groundwater Conditioning Factors

Generally, the occurrence and productivity of groundwater in a given aquifer is affected by various conditioning factors. The number of conditioning factors used depends on the data availability in the study area. Fifteen thematic layers were chosen as conditioning factors. They provide a reliable data base for an effective groundwater potential prediction of the study area in GIS framework.

2.2.3 Frequency Ratio (FR) Model

Frequency ratio (FR) model is a bivariate statistical approach which can be used as a useful geospatial assessment tool to determine the probabilistic relationship between dependent and independent variables, including multi-classified maps [5]. In fact, the FR is defined as the ratio of the area where groundwater wells (high groundwater productivity) occurred in the total study area. FR model structure is based on the

Fig. 1 Flow chart of methodology



correlation and observed relationships between each groundwater conditioning factor and distribution of groundwater well locations. FR value in each class of the groundwater-related factor can be expressed based on Eq. (1) [6]:

$$FR = \frac{W/G}{M/T} \quad (1)$$

where, **W** is the number of pixels with groundwater well for each conditioning factor; **G** is the number of total groundwater wells in study area; **M** is the number of pixels in the class area of the factor; **T** is the number of total pixels in the study area.

In the FR model, the FR value of each class in a thematic layer was considered as the weight of that particular class in thematic parameters to determine groundwater potentiality.

The FR value was derived from each thematic layer on the basis of a relationship with the Transmissivity values of training data set using Eq. (1). The accuracy of the FR model was validated using receiver operating characteristic (ROC) curve in the form of a success rate curve and a prediction rate curve. The area under the curve (AUC) value indicates the prediction accuracy [4].

In a given pixel, groundwater potential can be determined by summation of pixel values according to Eq. (2) [6]:

$$GWPI = \sum_{R=1}^{R=N} FR \quad (2)$$

where, GWPI and FR are groundwater potential index and the final weight for the FR model, respectively.

The groundwater potential zone indicates the groundwater potentiality Index in quantitative form, i.e. high GWPI indicates high groundwater potentiality whereas low GWPI indicates low groundwater potentiality. In this study the GWPI were derived by integration of all thematic data layer using raster calculator tool in Arc GIS 10.4.

3 Results and Discussion

The probability of GW occurrence is usually reduced with the value of altitude. A high slope angle leads to surface runoff increase, and hence the infiltration process will be decreased [6]. In case of slope, the FR ratio is >1 for the first slope range (0°–3°) indicating a high correlation between this slope range and the GW productivity. However, with a high slope range, the ratio suddenly increases along with the slope increase, and then it decreases. To interpret this, it is

important to relate this range with other used factors such as geology. The aerial extension of this range is mainly associated with the extension of flood deposits. These deposits consist mainly of sand and gravel and have higher values of hydraulic conductivity. The higher values of FR for flood deposits support this conclusion. In case of geology, the Quaternary lithological layers have relatively higher values of FR for flood deposits and alluvium. The FRs for the rest of the lithological layers were zero indicating the low probability of groundwater occurrence.

A high slope generates high TWI. There is a good connection between TWI and the occurrence of GW, where the increase in TWI value will result in a higher potential of GW. For the land use, the vegetation indicates a low probability of GW occurrence, while bare soil indicates higher values. The regions that are distant from faults have high FR and vice versa. For rainfall, the high class shows high correlation. Concerning the relationship between groundwater potential and the soil factor, it can be seen that FRs are high for the calcareous soil and low for other groups. The higher infiltration rates of this soil support the resultant higher FR values. As the infiltration rate increases, the groundwater recharge increases as well, leading to more productivity conditions. For the distance-to-river factor, the FR value decreases in relation to the distance to the river.

The final groundwater productivity index for the study area was calculated using Eq. (2) and demonstrated in a map in Fig. 2. The FR model provides values of GWPI ranging from 260 to 3098. The mean value was 68,312 and the standard deviation was 95,337. It was classified into five potential classes based on value intervals given by the natural breaks (Jenks) classification method [2], i.e., very low, low, moderate, high and very high (Fig. 2). It is notable that most of the high and very high potential zones are located in the central part of this study area due to the presence of high lineament density, high river density, lower slope, and porous nature of surface and subsurface which was mainly composed of alluvium, gravel and sandy clay deposits. The high lineament density and low slope categories influence the infiltration of water into the ground in the presence of old and recent alluvium deposits containing sands, clay sands, and gravels in the study area [5, 6].

The low and very low potential zones are found in the surroundings of this central part, where a higher slope and the presence of lower drainage density made the region unfavourable for groundwater potentiality. The integration was taken up both with all thematic data layers and also with its different combinations to evaluate the influence of different causative factors on groundwater potentiality index of the study area.

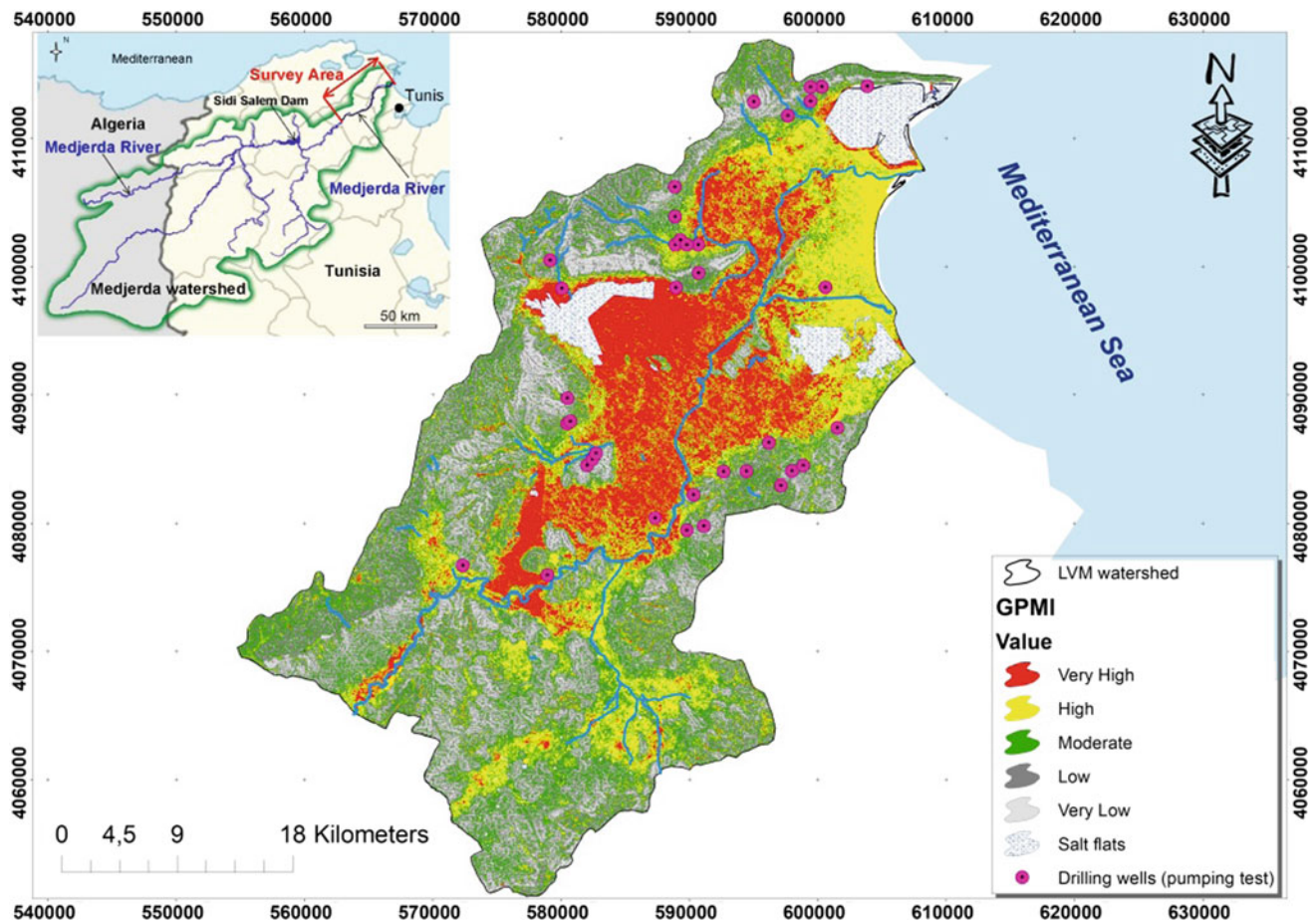


Fig. 2 Groundwater potential map

4 Conclusions

The FR results showed a high-frequency ratio in areas with slopes 0° – 3° ; lithology of alluvium, sandy clay, sand, and gravel; soil type of calcareous; and high density of river. The high-FR indicates a high groundwater occurrence probability. The validation of a map that used fifteen factors showed an accuracy of 86%. The validation results indicate a viable application of the FR model in groundwater potential mapping. The selection of groundwater factors was based on the availability of the data in the study area. For future research, it is suggested to include many available hydrological factors to improve the prediction accuracy of groundwater potential map. The GPM will be helpful to the decision makers in groundwater management and in identifying suitable locations for drilling production wells.

Acknowledgments This research (NRF-2016K1A3A1A09915721) was supported by Science and Technology Internationalization Project through National Research Foundation of Korea (NRF) grant funded by the Korean Ministry of Science and ICT and Tunisian Ministry of Higher Education and Scientific Research.

References

1. Adiat, K., Nawawi, M., Abdullah, K.: Assessing the accuracy of GIS-based elementary multi criteria decision analysis as a spatial prediction tool—a case of predicting potential zones of sustainable groundwater resources. *J. Hydrol.* **440**, 75–89 (2012)
2. Jenks, G.F.: The data model concept in statistical mapping. *Int. Yearb. Cartography* **7**, 186–190 (1967)
3. Lee, S., Kim, Y.S., Oh, H.J.: Application of a weights-of-evidence method and GIS to regional groundwater productivity potential mapping. *Environ. Manage.* **96**(1), 91–105 (2012)

4. Lee, S., Pradhan, B.: Landslide hazard mapping at Selangor, Malaysia using frequency ratio and logistic regression models. *Landslides* **4**, 33–41 (2007)
5. Manap, M.A., Nampak, H., Pradhan, B., Lee, S., Sulaiman, W.N. A., Ramli, M.F.: Application of probabilistic-based frequency ratio model in groundwater potential mapping using remote sensing data and GIS. *Arab. J. Geosci.* **7**, 711–724 (2014)
6. Oh, H.J., Kim, Y.S., Choi, J.K., Park, E., Lee, S.: GIS mapping of regional probabilistic groundwater potential in the area of Pohang City, Korea. *J. Hydrol.* **399**, 158–172 (2011)

Multivariate Statistical Evaluation of Groundwater Recharge Potential in Arid Region, Southern Tunisia

Mohamed Haythem Msaddek, Dhekra Souissi, Yahya Moumni, Ismail Chenini, and Mahmoud Dlala

Abstract

The purpose of this work is to evaluate the groundwater recharge using multivariate statistical evaluation and AHP (analytic hierarchy process) as an additional method to the hydrogeological research. This technique was utilized to establish a map that represents the groundwater recharge potentiality. The map extraction is founded on the investigation of multi-criteria input data such as lineaments, land use, lithology, drainage, slope, soil, rainfall and geomorphology. Weights were assigned using the AHP method to all these multi-influencing factors according to their influence on groundwater recharge. Sensitivity analyses were calculated to validate AHP weight results. The presented methodology has been applied to Belkhir region in southwestern Tunisia, which has an arid climate. Agriculture is the main activity in the plains and the use of groundwater has been raised for both irrigation and drinking purposes. This technique revealed the very good, good, moderate, and poor groundwater recharge potential zones. Furthermore, the impact of each influencing factor on groundwater ability was calculated. The results provide significant information that can be useful to ameliorate groundwater development. The approach may also help improve plans for sustainable groundwater resources exploitation.

Keywords

Multivariate evaluation • Statistical assessment • Groundwater recharge • Arid region • Tunisia

1 Introduction

Groundwater is considered to be the largest freshwater source in arid regions. It should be studied more closely given its potentiality and its evaluation. To ensure a sustainable management of water resources, the identification of groundwater recharge area is important and essential [4]. Remote Sensing and Geographic Information Systems (GIS), combined with multi-criteria evaluation, can reveal useful tools in groundwater survey mapping.

Many researchers around the world have proposed several methods and approaches in the last years. These methods aim to delineate the groundwater recharge using spatial analysis and multi-criteria evaluation [1, 2].

This work presents the inquiry and delineation of groundwater recharge of the Belkhir region, which is located in southwestern Tunisia and which has an arid climate. It employs an integration of further influencing factors and multivariate statistical evaluation to the previously applied methodology [4], with the contribution of weighted linear combination method (WLC) and the analytic hierarchy process (AHP) [5]. Therefore, the recognition of potential groundwater recharge zones will be performed by the combination of GIS and remote sensing to prepare various influencing layers of lineaments, land use, lithology, drainage, slope, soil, rainfall and geomorphology with assigned weightage, rate and score.

2 Methods

To identify the groundwater recharge zone of the region, a weighted spatial analysis method was applied. The relative importance of the factors influencing groundwater recharge, are collected according to previous literature and only representative factors were extracted [3].

Eight-significant factors influencing groundwater recharge were used in this study. The factors are lineaments,

M. H. Msaddek (✉) · D. Souissi · Y. Moumni · I. Chenini
M. Dlala
UR13ES26, Paléoenvironnement, Géomatériaux et Risques
Géologiques, Faculté Des Sciences de Tunis, Université de Tunis
El Manar, 2092 Tunis, Tunisie
e-mail: mmhaythem@gmail.com

land use, lithology, drainage, slope, soil, rainfall and geomorphology. Eventually, a groundwater recharge map was created (using layer reclassification and weighted overlay of spatial analysis by ArcGIS software), including four classes of potentiality, ranked from poor to very good (see Fig. 1).

To delineate the groundwater recharge map, the mathematical method of weighted linear combination method (WLC) [5] was used. It also helped in the calculation of the groundwater recharge index in accordance with Eq. (1):

$$I_r = \sum I_{x_w} \times I_{x_r} \tag{1}$$

(x: influencing factors).

The subscripts w and r indicate, respectively, weights and rates.

$$I_r = I_{lnw}I_{lnr} + I_{usw}I_{usr} + I_{liw}I_{lir} + I_{drw}I_{drr} + I_{slw}I_{slr} + I_{sow}I_{sor} + I_{rfw}I_{rfr} + I_{gmw}I_{gmr}$$

where I_r : groundwater recharge index is the value for each pixel of the final groundwater recharge map. I_{ln} : lineaments index; I_{us} : land use index; I_{li} : lithology index; I_{dr} : drainage index; I_{sl} : slope index; I_{so} : soil index; I_{rf} : rainfall index; I_{gm} : geomorphology index.

An appropriate weight was assigned to the multi-influencing factors for groundwater recharge zones. The impact of each influencing factor may involve the delineation of groundwater recharge areas. According to Shaban et al. [7], each of the contributing factors has a degree of influence and effect on the others. It can be a major effect, a minor effect or no effect at all. Furthermore, these influencing factors are interrelated. The impact of each major factor was assigned a weight of 1.0, and a weight of 0.5 was assigned for each minor factor.

The combined weights of both major and minor factors were used to compute the relative rates. The assigned score for each factor was computed using the following mathematical Eq. (2):

$$Score\ assigned = \frac{(Major\ effect + Minor\ effect)}{\sum(Major\ effects + Minor\ effects)} \times 100 \tag{2}$$

Analytical Hierarchy Process (AHP) is an organized strategy utilized for investigating complex issues, where an extensive number of interrelated targets or criteria are included [5]. The weight of each factor is defined using the AHP. The weights of these criteria are characterized after they are positioned by their relative significance. In this way, when all variables are arranged in a multi-leveled way, a pairwise examination grid for each factor is set up to empower a significance correlation. The relative significance between the criteria is assessed from 1 to 9 demonstrating “less imperative” to “substantially more vital” criteria [6].

To evaluate the matrix of the AHP, we computed the consistency ratio (CR) using the Eq. (3):

$$CR = CI/RI \tag{3}$$

where, RI is the random index whose value depends on the order of the matrix; and CI is the consistency index which can be obtained as (4):

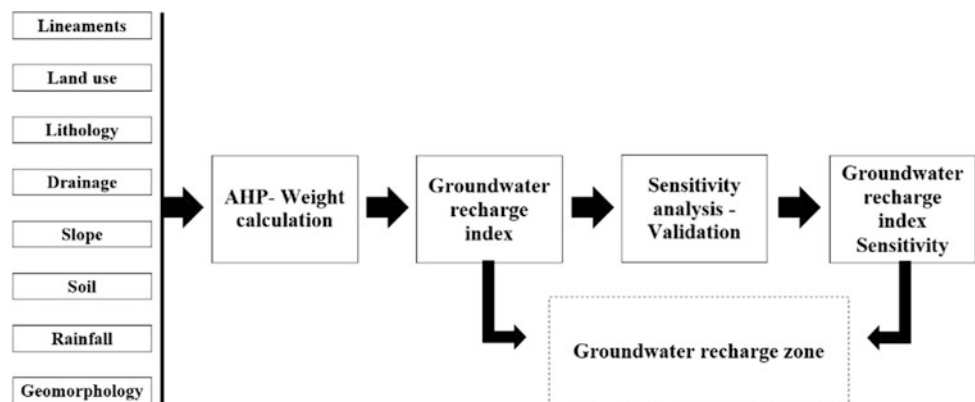
$$CI = \frac{\lambda_{max} - n}{n - 1} \tag{4}$$

where, λ is the largest eigenvalue of the matrix and can be easily determined from the mentioned matrix, and n is the number of groundwater conditioning factors. According to Saaty [5], the consistency ratio (CR) must be <0.1.

Consequently, all the conditioning factors are compared against each other in a pairwise comparison matrix.

To determinate the assigned rank of different features of influencing factors, we classified them into ten classes according to the description of each factor based on literature review [7].

Fig. 1 Flowchart of the used methods



3 Results and Discussion

To determine the relative importance values, authors used Saaty's AHP process with a scale from 1 to 9. The score of 1 shows an equal importance between the two factors. The score of 9 denotes the extreme importance of one factor compared to the other.

The authors used Eq. (3) for the measurement of Consistency Ratio (CR) to calculate the consistency of the pairwise comparison matrix. Since CR's value is lower than the threshold (0.1), the weights' consistency is affirmed.

To proceed with the classification of various factors for groundwater recharge zones, each factor was divided within its domain of effect and a weighted rating was assigned for each domain based on weightage calculation of factors. All factors have groundwater recharge potential classification from poor to very good within their domain of effect. To determine the sensitivity of factors to the weights changing,

the authors have coupled the AHP with a sensitivity analysis process that evaluates the impact of each factor. In the sensitivity analysis the former AHP random rates of the indices are substituted with some derivative indices.

Figure 2 represents the map of groundwater recharge potential zones. It shows that the best potential zone located basically in the eastern and central part of the Belkhir region by dint of high infiltration capacity of wide lowlands. It shows that more than 70% have a "good" to "very good" recharge potential.

The total of weighted ratings of each factor was used in the mathematical Eq. (1) of the weighted linear combination method (WLC) to calculate the groundwater recharge index. It allowed computing the impact of factors on the groundwater recharge ability.

However, when comparing our results to those of older studies, in different regions and different case studies from the world, it is worth noting that the impact of factors on

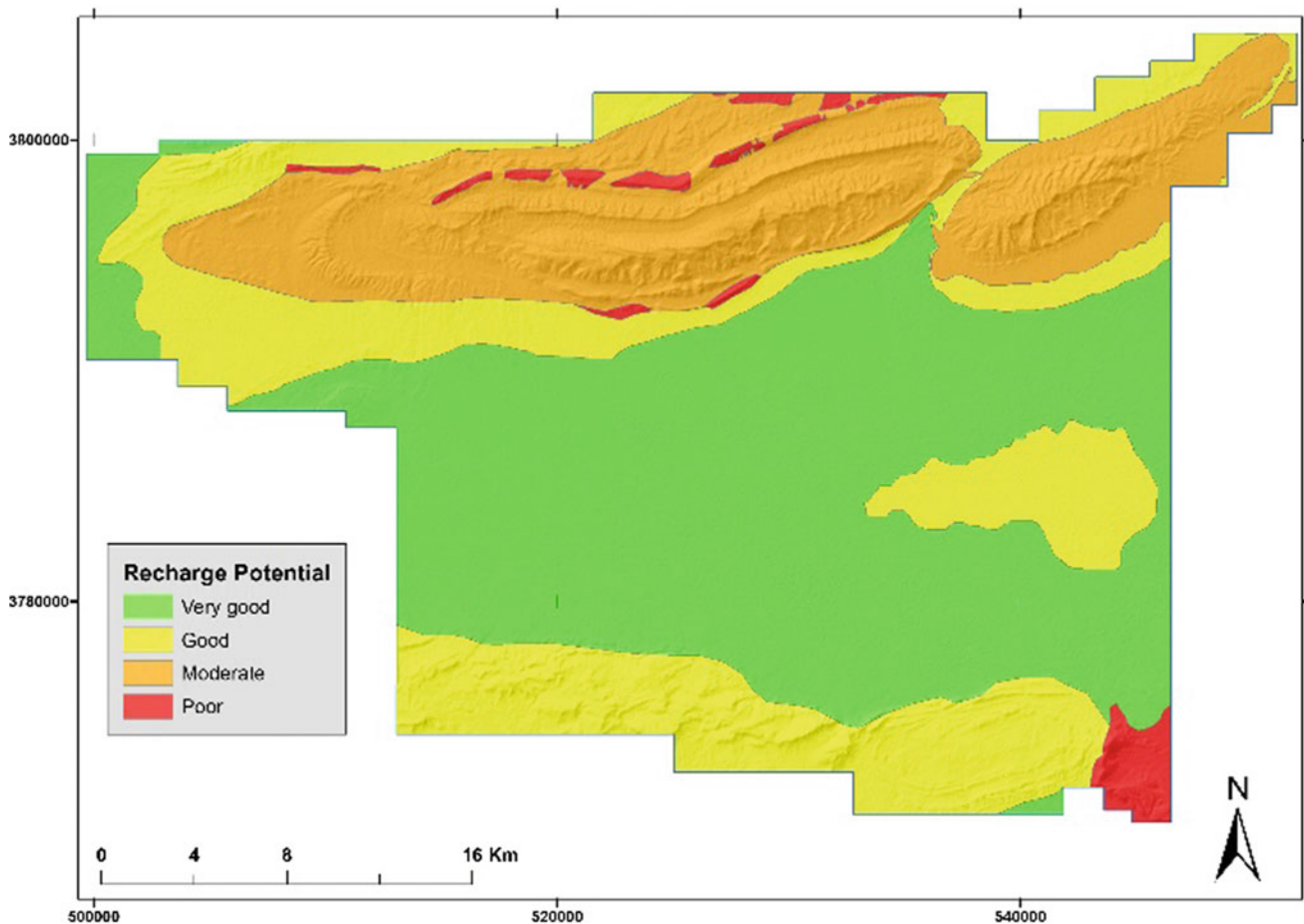


Fig. 2 Map of groundwater recharge potential of Belkhir region

groundwater potential may depend on site specificities and user's definitions of weights and rates.

4 Conclusions

In summary, this paper applied a specific technique to assess the groundwater recharge in the Belkhir region, in southwestern Tunisia, based on a multivariate statistical assessment and Analytic Hierarchy Process (AHP). Eight parameters with different weights were used, resulting in a final map based on a weighted linear combination. To validate the effectiveness of the used methods, authors employed a statistical sensitivity analysis on the values assigned to the different criteria. The Belkhir area was split into four potential zones, namely; very good, good, moderate, and poor. Results reveal a high groundwater recharge potential (good to very good) in more than 70% of the region. The impact of each influencing factor on groundwater ability was calculated.

The approach may help improve plans for sustainable groundwater resources exploitation if it is combined with a complementary hydrogeological study, such as aquifer geometry, piezometry and groundwater geochemistry. This method is applicable in any other semi-arid and wetland basins.

References

1. Fenta, A.A., Kifle, A., Gebreyohannes, T., Hailu, G.: Spatial analysis of groundwater potential using remote sensing and GIS-based multi-criteria evaluation in Raya Valley, northern Ethiopia. *Hydrogeol. J.* **23**(1), 195–206 (2015)
2. Magesh, N.S., Chandrasekar, N., Soundranayagam, J.P.: Delineation of groundwater potential zones in Theni district, Tamil Nadu, using remote sensing, GIS and MIF techniques. *Geosci. Front.* **3**(2), 189–196 (2012)
3. Msaddek, M.H., Souissi, D., Moumni, Y., Chenini, I., Dlala, M.: Integrated multi-criteria evaluation and weighted overlay analysis in assessment of groundwater potentiality in Segui Region, Southern Tunisia. In: Kallel, A., Ksibi, M., Ben D.H., Khélifi, N. (eds.) *Recent Advances in Environmental Science from the Euro-Mediterranean and Surrounding Regions. EMCEI 2017. Advances in Science, Technology & Innovation (IEREK Interdisciplinary Series for Sustainable Development)*, pp. 631–632. Springer, Cham (2018)
4. Oikonomidis, D., Dimogianni, S., Kazakis, N., Voudouris, K.: A GIS/remote sensing-based methodology for groundwater potentiality assessment in Tirnavos area, Greece. *J. Hydrol.* **525**, 197–208 (2015)
5. Saaty, T.L.: *The analytic hierarchy process: planning, priority setting, resources allocation*, p. 281. McGraw, New York (1980)
6. Saaty, T.L.: How to make a decision: the analytic hierarchy process. *Eur. J. Oper. Res.* **48**(1), 9–26 (1990)
7. Shaban, A., Khawlie, M., Abdallah, C.: Use of remote sensing and GIS to determine recharge potential zones: the case of Occidental Lebanon. *Hydrogeol. J.* **14**(4), 433–443 (2006)

Water Balance Estimation Under Wildfire and Restoration Scenarios in Semiarid Areas: Effects on Aquifer Recharge

Hassane Moutahir, Issam Touhami, Aymen Moghli, and Juan Bellot

Abstract

In semiarid areas, water is a crucial and limited resource and its management is a challenge. Hydrological models allow the estimation of water balance under different land cover and climate scenarios which can help improve the management of water resources. In this study, we used the “DISRUM” model (a Distributed Eco Hydrological Model) to estimate the water balance and aquifer recharge according to different scenarios of vegetation cover changes induced by wildfire and restoration during two hydrological years (wet and dry year) and determine the best scenarios that can substitute the current vegetation cover of a small aquifer in the semiarid area of Southeastern Spain. The main results of the preliminary work show that the vegetation cover has a significant impact on aquifer recharge. Furthermore, reducing the vegetation cover or substituting pine by shrub gave positive results for the aquifer recharge.

Keywords

Water balance • Aquifer recharge • Vegetation cover scenario • DISRUM model • Ventós

1 Introduction

The scarcity of surface water resources in the semiarid areas of SE Spain has made of groundwater the main freshwater source. The major part of the economy and development of this region is based on water-demanding activities which has led to an overexploitation of groundwater [4]. This resource is facing a great challenge in the future because of the likely effects of climate change. Several studies indicated an increase of temperatures and a decrease of precipitation in this region [6, 7]. These trends are expected to continue in the same way in the future [6, 7]. Such changes are expected to affect the water balance. In addition, changes in vegetation cover can affect the water balance in quantitative terms [8]. The simulation of water balance under different land cover and climate scenarios can help improve the management of water resources. The main objective of this work is to determine how changes in the vegetation cover affect the water balance and aquifer recharge estimation using an eco-Hydrological model in Ventós aquifer, SE of Spain, during two hydrological years (wet year 2012–2013 and dry year 2013–2014).

2 Materials and Methods

2.1 Study Area

The aquifer of Ventós Castellar is located approximately 20 km northwest of Alicante SE Spain. The climate in the area is characterized by high variability and scarcity of precipitation (Annual precipitation = 275 mm/year). The vegetation cover that dominates in the area is summarized in Table 1.

2.2 DISRUM Model

A Distributed Eco-Hydrological Model using global equations as approximations of HYDROBAL model [1] allows (using the advantages of this last one) to apply it on large

H. Moutahir (✉) · A. Moghli · J. Bellot
The Multidisciplinary Institute for Environmental Studies
“Ramon Margalef” (IMEM) and the department of Ecology,
University of Alicante, Carretera San Vicente del Raspeig s/n,
03690 Alicante, Spain
e-mail: hassane.moutahir@ua.es

I. Touhami
The National Research Institute of Rural Engineering,
Water and Forestry (INRGREF). Laboratory of Management
and Valorization of Forest Resources, University of Carthage,
BP 10, 2080 Ariana, Tunisia

A. Moghli
IAMZ-CIHEAM, Av. Montañana 1005 50059 Zaragoza, Spain

Table 1 Summary of inputs data for DISRUM model

	Cover (%)	CN		Depth (cm)	Porosity (%)	Wilting point (%)	Field capacity (%)
		Dry	Wet				
Pine	0.6	36	46	30	42	7	32
Shrub	6.5	30	35	30	42	7	32
Alpha grass	53.6	46	58	30	42	7	30
Bare	19.3	77	80	30	42	11	21
Rock	20.0	80	85	–	1	–	–

areas with inhomogeneous distribution of hydrological variables [5]. To execute the DISRUM model, the software requires: daily climatic data of (precipitation, air temperature, radiation), the characteristics of the soil of each vegetation community and the structure of the vegetation by strata, along with the vegetation, elevation, slopes and flow direction maps. In addition, the curve number for each vegetation type is needed to estimate the surface runoff. The calibration and validation of the model for the study area were done in a previous work [5].

2.3 Climate Data, Vegetation Structure and Soil Parameters

Observed data of precipitation (Pr), maximum and minimum temperatures from a local meteorological station during two wet (406.9 mm, 2012/2013) and dry (111.9 mm, 2013/2014) hydrological years were used. Spatial distribution and structure of vegetation cover and the physical properties of the soil for each vegetation type were determined from the work of Chirino [3] and Gonzalez [5] and are summarized in Table 1.

2.4 Scenarios of Vegetation Cover Change

Estimation of the water balance during the two hydrological years for the following scenarios:

The scenario of control “C”: without changes

1. Wildfire scenario: the wildfire affects 100% of vegetation cover
2. Wildfire scenario that burnt 50% of vegetation cover in two origins: (a) upstream and (b) downstream
3. Substitution of Shrub by Pine
4. Substitution of bare soil by Pine
5. Substitution of bare soil by Shrub
6. Substitution of Pine by Shrub.

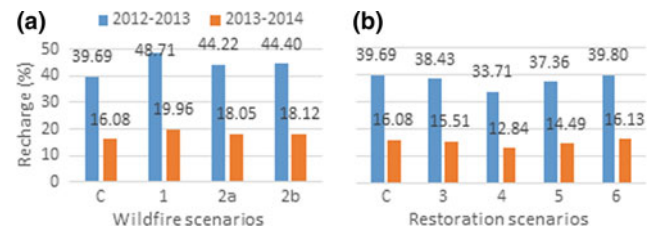


Fig. 1 The aquifer recharge (% of Pr) for the wildfire scenario (a) and for the restoration scenario (b) during two hydrological years (2012–13/2013–14)

3 Results and Discussion

3.1 Wildfire Scenarios

In all scenarios, less vegetation generates more aquifer recharge (Fig. 1a). Furthermore, the proportions of recharge during the dry year are lower than the wet year. This can be explained by the fact that small amounts of rainfall, which reach the ground, are used by vegetation and are then lost by evapotranspiration. The results of the simulations show that reducing the vegetation cover decreases the interception and evapotranspiration, which explains the increase of recharge, and as a consequence, the soil water content showed higher values. Similar results were obtained by Bellot et al. [2]. The small difference between aquifer recharge observed in the two wildfire (50%) scenarios is due to runoff effects.

3.2 Restoration Scenarios

Figure 1b shows that increasing the vegetation cover lowers the aquifer recharge. The substitution of bare soil by pine reduces the recharge more than by shrub due to the interception capacity of vegetation canopy and evapotranspiration of each vegetation type. The substitution of pine by

shrub gives a higher result for aquifer recharge which means that pine generates more water loss (Interception and Evapotranspiration) than shrub.

4 Conclusions

The main focus of this work was the impact that the vegetation cover change has on the aquifer recharge during the two years of study. The increase of the vegetation, especially of pine, has a negative effect on the recharge of the aquifer. The results show a decrease of the aquifer recharge when the pine and shrub was introduced instead of bare soil due to the interception and evapotranspiration. The decrease of the vegetation cover (wildfires) generates more recharge (water available for human), but we should consider that the runoff and erosion effects will increase. For that reason, the substitution of pine by shrub, which gave positive results for aquifer recharge, seems to be the best scenario that can substitute the current vegetation cover. However, a multi-year study is required to better understand the effects of vegetation changes on aquifer recharge.

Acknowledgements This research is part of the project: ALTER-ACLIM (CGL2015-69773-C2-1-P) funded by the Spanish Ministry of Economy and Competitiveness.

References

1. Bellot, J., Chirino, E.: Hydrobal: an eco-hydrological modelling approach for assessing water balances in different vegetation types in semi-arid areas. *Ecol. Model.* **266**, 30–41 (2013)
2. Bellot, J., Sanchez, J.R., Chirino, E., Hernandez, N., Abdelli, F., Martinez, J.M.: Effect of different vegetation type cover on the soil water balance in semi-arid areas of south eastern Spain. *Phys. Chem. Earth* **24**(4), 353–357 (1999). [https://doi.org/10.1016/S1464-1909\(99\)00013-1](https://doi.org/10.1016/S1464-1909(99)00013-1)
3. Chirino, E.: Influencia de las precipitaciones y de la cubierta vegetal en el balance hídrico superficial y en la recarga de acuíferos en clima semiárido. Tesis doctoral. Universidad de Alicante. 408pp (2003)
4. Custodio, E., Andreu-Rodes, J.M., Aragón, R., Estrela, T., Ferrer, J., García-Aróstegui, J.L., Manzano, M., Rodríguez-Hernández, L., Sahuquillo, A., Villar, A.: Groundwater intensive use and mining in south-eastern peninsular Spain: hydrogeological, economic and social aspects. *Sci. Total Environ.* **559**, 302–316 (2016)
5. Gonzalez, C.: Aplicación de los modelos HIDROBAL y DISRUM para estimar el balance hídrico en diferentes escenarios de cubierta vegetal y cambio climático. Tesis Master. Universidad de Alicante (2012)
6. IPCC.: Summary for Policymakers. *Climate Change 2014: Synthesis Report. Contribution of Working Groups I, II and III to the Fifth Assessment Report of the Intergovernmental Panel on Climate Change* (2014)
7. Moutahir, H.: Likely effects of climate change on water resources and vegetation growth period in the province of Alicante, south-eastern Spain. Tesis doctoral. Universidad de Alicante, 206p (2016)
8. Touhami, I.: Estimación del balance hídrico y de la recarga en el acuífero ventós-castellar (SE España). Efectos del cambio climático. Tesis doctoral. Universidad de Alicante. 238pp (2014)

The Impact of the Mobilization of Water Resources in Semi-Arid Areas on Sustainable Development: The Case of Timgad Basin, Northeastern of Algeria

Athamena Ali, Menani Mohamed Redha, Djaiz Fouad, and Belalite Halima

Abstract

A hill reservoir research project aims, among other perspectives, to improve the regional agriculture potential through irrigation of small areas. For such a project, the feasibility study for a given area is fundamental before the establishment of any related applied research works. This paper is of a socio-economic relevance for the Timgad region (NE Algeria) as the presented results consist of a contribution of both socio-economic operators and policy makers. In the study area, water resources are closely related to the regional geology and the main objectives of the establishment of the Foum-Toub hill reservoir is to promote the irrigation of its plain, regulate the flow of the Foum-Toub creek and minimize the silting of the Koudiet Lemdaour dam. The selected sites for the construction of this work are characterized by an impermeable bedrock. Loose material, favorable to serve as borrow areas, can be supplied from the surrounding depressions where sandstone can also be used for the dike construction.

Keywords

Feasibility • Hill reservoir • Foum-Toub • Timgad NE Algeria

1 Introduction

The construction of dams is one of the solutions adopted by decision makers, when reducing the deficit in water is their primary strategy, regarding crucial water needs during drought events. As for similar heavy projects, geomorphological and geological data, as well as geotechnical tests, are

of a particular relevance for the feasibility study and necessary precautions. In NE Algeria, the Timgad basin is one of the water-in-need areas with a dry continental climate. Regional decision makers opted for the realization of a dam in suitable sites for agricultural and citizen water supply purposes. This contribution proposes geomorphological and sedimentometric studies, reinforced by geotechnical analyses on which may lie the suitable decision for a dam realization in the study area.

2 Materials and Methods

2.1 The Study Area: Climatology, Geomorphology and Geology

The study sites are located 2 km to the South of Timgad; GPS coordinates being: 6° 30'–6° 35' East, and 35° 20'–35° 25' North. These proposed sites belong to a small depression encased between two mountain ranges, where sandstone layer peaks are trending NE-SW. These peaks cover a narrow depression filled by recent continental formations, mainly polygenic glaciers and debris in the center, and clayey facies at the periphery. Further to the South, the formations become mainly carbonated with marly intercalations, forming the Chelia massif and extending to Khenchela, after a small depression with quaternary fillings [2]. The altitudes peak at 1331 m in the Tizagrout relief and at 1606 m in the Jebel Aslaf. This altitude difference is accompanied by a climatic diversity, corresponding to tough and typically continental-type climate in the area. In the plain, the total rainfall does not exceed 400 mm. However, mountains may receive up to 800 mm of water, mainly as snowfalls. The climate is semi-arid, dry and hot in summer with 26 °C as an average temperature with an average humidity of 36%. In winter, the climate is cold and humid with an average temperature of 4 °C and a humidity of 79%. Hydrography is characterized by a set of unimportant-flow wadis, whose irregular diets do not allow the actual rate

A. Ali (✉) · M. M. Redha · D. Fouad · B. Halima
Mobilization and Water Resources Management Laboratory,
University of Batna 2, Batna, Algeria
e-mail: aliaures68@gmail.com

determination. Thus, all surface waters flowing from the northern Chélia massif hills head south, through Seba and Reboa wadis, to reach the Koudiat-El-Medouar dam.

The region of Fom-Toub is situated to the South of Timgad Basin and in the northern part of the Chelia mountain. This is a depression filled by marine Miocene clastic deposits (Fig. 1) [1], with wide anticlines and synclines axes which are trending NE-SW. These structures are affected by NE-SW and NW-SE faults, responsible for the formation of the grooves. The bedrock is of Cretaceous limestone/marl alternations topped by sandstone formations dated as Miocene. The surface is formed by quaternary deposits (Glacis—Eboulies—Stringers). The geological accidents are NS trending faults, NNW-SSE, NNE-SSW and EW.

2.2 Geotechnical Framework

For the geotechnical research program, focused on the dam feasibility study including borrow required material, six samples (for dike and basin) and six others for material borrow areas are wisely collected. These samples were the object of physical and mechanical laboratory tests at the dam, bowl and borrow areas.

3 Results and Discussion

3.1 Foundation Tests and Interpretations

The particle size tests show that formations encountered at a depth of 1–2 m are, from top to bottom:

- fine silty clay soil with a CaCO_3 content of 29–30%;
- compact waterproof marls.

Shear test values fit the standard and are in line with the implementation of this restraint. The bearing capacity,

calculated from these data, indicates that the chosen ground is rather good for such a work (10–12 m high). The bearing capacity of the substratum is much higher than that of the soil cover. The tests show that the compressibility oedometric curve shows a non-compressible soil with a satisfactory oedometric module. However, the underlying formations, which consist mainly of compact non-compressible marls, often have better mechanical properties. Analyses show a mild soil, containing only traces of insignificant gypsum. Therefore, the substratum is safe for foundations and requires no special hardware for complex calculations and related adjustments.

3.1.1 Borrow Required Material Tests and Interpretations

The sedimentometry analysis shows a distribution curve spanning from gravel to clay, with a high percentage of fine clay, limon and sand elements. Percentages are around 72%, with a diameter between 0.2 and 2 mm. Small percentages (8%) characterize coarse material of sandy and gravel petrography with a diameter ranging between 2.00 and 20 mm.

The wet and dry densities ($\gamma_h = 1.58$ and $\gamma_d = 1.51$, respectively) indicate a moderately dense and unsaturated soil. Chemical analyses show a moderately aggressive ground. The sand equivalent is of 35.77%, indicating plastic soil and sandy clay sensitive to water, ($d_{\max} = 1.67 \text{ t/m}^3$). The proctor test indicates a water content $W_{\text{opt}} = 12.74$ and a dry density $\gamma_{d_{\max}} = 1.67 \text{ t/m}^3$, [1].

3.2 Study of Watershed Flows

See Table 1.

3.3 Evaluation of Inter-Annual Liquid Intake

See Table 2.

Fig. 1 Geological section in the study area

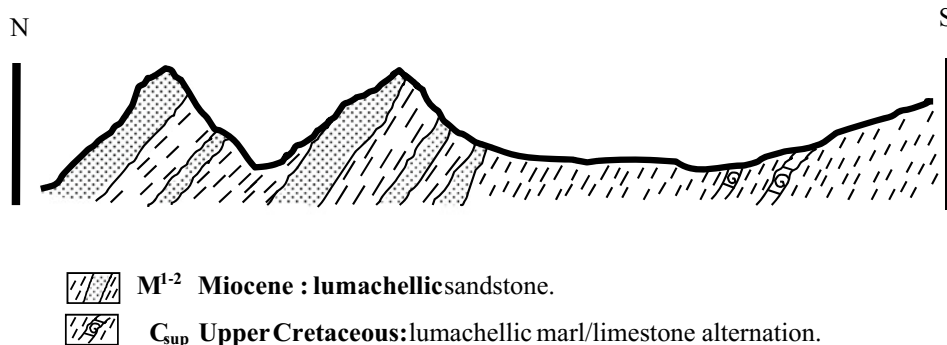


Table 1 Flows watershed

Parameter	Symbol	Value	Unit
Inter-annual rain	\bar{R}	484	mm
Average annual daily maxima rains	R_d	44.0	mm
Rain maximum day rainfall	$\bar{P}_{24\max}$	49.73	mm
Coefficient of variation	C_v	0.35	–
Climatic exhibitor	b	0.33	–

Table 2 Study of inter-annual liquid

Formula	Run of wave L_e (mm)	Inter-annual average contribution \bar{A} (Hm ³)
Cordonna	20	0.832
Sami	65.31	2.70
Mallet and Gouthier	51.25	2.13
ANRH (Algeria)	72.28	3.01
Formula called Algerian	40.92	1.7 (seems the most reliable)

4 Conclusion

The watershed of the Foug Toub hill reservoir is elongate, with a fairly low slope and a dense hydrographic network; morphologically, the proposed sites are suitable for the realization of a small hill reservoir. For water supply, the fluid intake is eligible for a small work, but it must take into account the rate of abrasion which is quite important. The volume of solid contribution during the project work life is higher than that of potential water intake to be stored in the reservoir. Hence, this work is hydrologically and economically impracticable when taking into account the height limits. If the same site is maintained for such a realization, it is recommended to perform solutions upstream the edifice,

aiming to reduce the rate of solids leading to a small dam, considering the importance of fluid intake. Geotechnical results plead in favor of satisfactory soil characteristics for a dam realization at the dike level.

References

1. Athamena, M., Athamena, A.: Etude de la retenue collinaire à vieux Foug Toub. DHW de Batna, p. 21 (2006)
2. Laffitte, R.: Etude de la géologie de l'Aurès. Doctorat ès Sciences Paris, Bulletin Service Carte Géol. Algérie, série 1, n° 15, 484 p (1939)
3. Tixeront, J.: Les débits solides des cours d'eau d'Algérie et de Tunisie. Etude hydrologique. Série II, Secrétariat agricole, Tunis, pp. 117–121 (1960)



Groundwater Mounding in Fractured Fossil Aquifers in the Saharan-Arabian Desert

Abotalib Z. Abotalib and Essam Heggy

Abstract

Understanding the role of geological structures in controlling groundwater flow in fossil aquifers is central for proper assessment of groundwater dynamics and aquifer connections. In such settings, connections between deep and shallow aquifers could potentially affect groundwater quality and availability as well as karst formation and landscape evolution. Herein, we integrate available hydrological and isotopic datasets with remote sensing data covering two aquifer units in Sinai and Qatar to indicate the occurrence of significant recharge of gaseous-rich groundwater from deep to shallow aquifers under upward hydraulic gradients along vertical/subvertical faults. Evidence include: (1) the presence of localized recharge mounds ranging from 7 to 50 m in height, in Qatar and Sinai; (2) the recharge mounds are correlated with the locations of mapped strike-slip and oblique-slip faults; and (3) isotopic composition of the groundwater in these locations indicate significant depletion ($\delta^{18}\text{O}$: -9.53% to -8.4% ; $\delta^{18}\text{O}$: -5.2 to -2.6%) compared to modern precipitation ($\delta^{18}\text{O}$: -3.43% ; $\delta^{18}\text{O}$: -0.68%) in Sinai and Qatar, respectively, which implies limited surface recharge. The mechanism of formation of these groundwater mounds and the amount of upward recharge from the deep aquifers need further investigations to be addressed.

Keywords

Groundwater mounding • Fossil aquifers • Arid environments

1 Introduction

Though numerous studies throughout the last 40 years have investigated the hydrologic settings and aquifer characterizations of the Nubian Sandstone Aquifer System (NSAS) in Sinai and the Umm er Radhuma and Rus aquifer system (hereafter referred to as the main aquifer unit) in Qatar [1, 2], the role of geological structures in connecting aquifer units, and consequently affecting water quality and landscape evolution, is poorly constrained.

Recent studies on major aquifers in the Saharan-Arabian desert suggest significant artesian upward leakage from deep to shallow aquifers leading to a substantial change in water characteristics and evolution of the landscape [3]. In this study, we integrate remote sensing data with available hydrological and isotopic datasets in a GIS environment to: (1) map the main faults, (2) conduct spatial analysis between the hydrological, isotopic and mapped faults and (3) develop a conceptual model to interpret the results.

2 Materials and Methods

We co-register all data layers to a unified geographic projection (Datum: WGS-84; UTM Zones: N36 and N39 for Sinai and Qatar, respectively) in a GIS environment. First, we regenerate geocoded, geographically corrected potentiometric head maps for the two study areas from previously published data [1, 2]. Second, we use remote sensing datasets including Landsat 8 and Sentinel-2 mosaics to derive Principal Component Analysis (PCA) images for fault mapping. Third, we conduct spatial analysis of mapped faults and potentiometric head maps of different aquifers'

A. Z. Abotalib · E. Heggy (✉)
Viterbi School of Engineering, University of Southern California,
Los Angeles, CA 90089, USA
e-mail: heggy@usc.edu

A. Z. Abotalib
Department of Physical Geology, National Authority for Remote
Sensing and Space Sciences (NARSS), Cairo, 1564, Egypt

E. Heggy
Jet Propulsion Laboratory, Caltech, 4800 Oak Grove Drive,
Pasadena, CA 91109-8001, USA

units to examine whether the mapped faults have significant control on the groundwater flow in the studied aquifers. Fourth, we use isotopic data of the groundwater isotopes (^2H and ^{18}O) [2, 4] and precipitation data from the IAEA isotope monitoring stations in Bahrain and Rafah to validate the role of faults in the formation of the identified groundwater mounds.

3 Results

3.1 Inspection of Potentiometric Head Maps

We regenerated geocoded thematic maps for the potentiometric head data in Sinai and Qatar. The new maps show localized groundwater mounds that anomalously rise from the average groundwater elevation in the two aquifers and against the regional groundwater gradient, which implies the presence of recharge either from the surface or the subsurface. The groundwater mound in the NSAS is reported from two wells that are 40 km apart and it attains an average elevation of 50 meters above the normal head in the surrounding wells (Fig. 1). Nevertheless, the limited number of

wells and the data interpolation impede the proper characterization of the geometry of the mound.

In the main aquifer unit in Qatar, two mounds are reported (M1 and M2; Fig. 2). M1 occurs in central-south Qatar and occupies an area of about 1000 km². The water table abruptly increases from 3 to 10 m amsl at the center of the mound and creates a local groundwater divide within the aquifer. M2 occurs to the north of M1 and occupies a larger area (~1750 km²) but attains only an elevation of 7 m amsl along its central axis.

3.2 Spatial Correlation Between Groundwater Mounds and Faults

NE-SW dextral faults are the predominant structural patterns in the two studied areas (Figs. 1 and 2). Superimposing major faults over the potentiometric head maps shows high spatial correlation between the faults and the groundwater mounds. In the NSAS (Fig. 1), Minsherah shear zone perfectly aligns with the groundwater mound. Moreover, in the main aquifer unit, M1 occurs along the newly identified NE-SW fault which laterally displaces the Mio-Pliocene

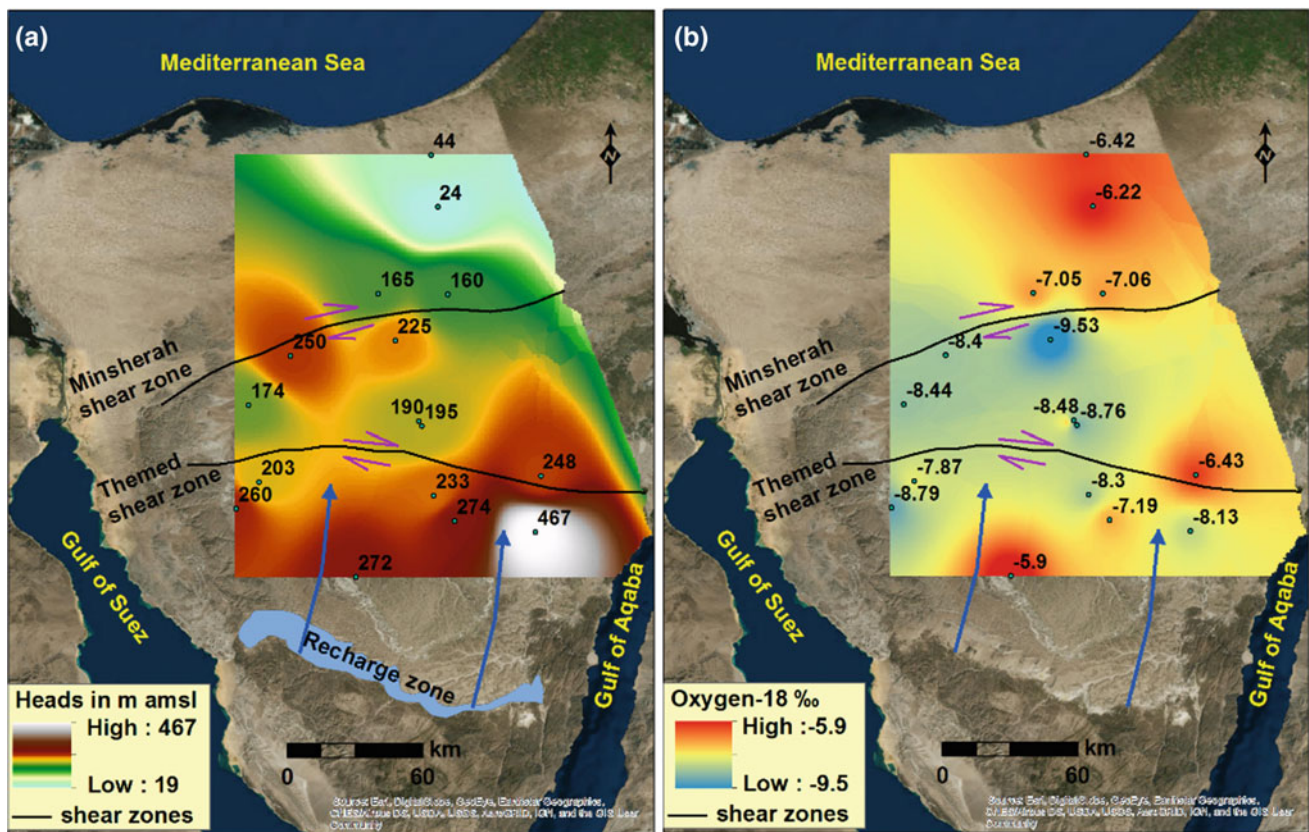


Fig. 1 Groundwater mound in the NSAS, Sinai. **a** Head map showing the anomalous groundwater mounding along the mapped Minsherah shear zone and far away from the recharge zone. **b** ^{18}O distribution in

Sinai showing depleted isotopic composition in the groundwater mounding area compared to compositions near the recharge zone. Solid green circles refer to observation wells

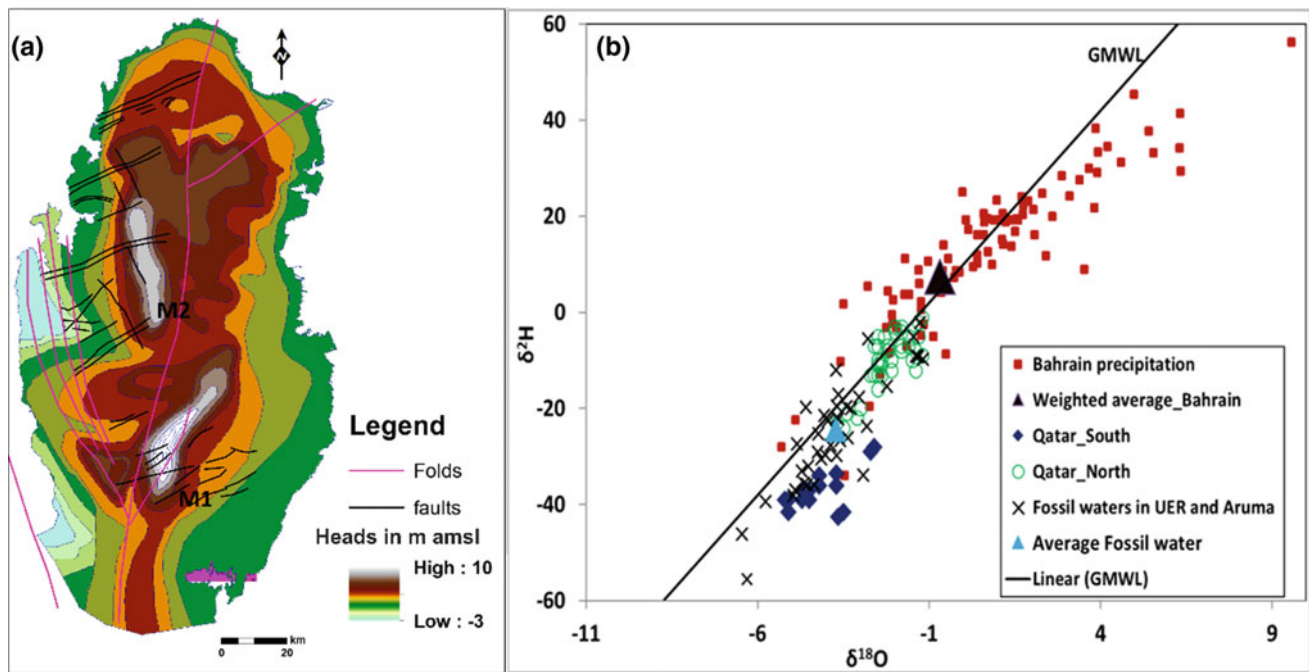


Fig. 2 Groundwater mound in the main aquifer unit, Qatar. **a** Head map showing the anomalous groundwater mounding (M1 and M2) above the average head elevation within highly faulted areas. **b** δD

versus $\delta^{18}\text{O}$ plot for groundwater samples from north and south Qatar, fossil waters from Eastern Saudi Arabia and modern precipitation over the IAEA Bahrain station

sediments along the two sides of the fault. On the other hand, M2 has little correlation with the mapped faults along the northwestern coast of Qatar.

3.3 Isotopic Composition of the Groundwater Mounds

The isotopic composition of the groundwater in the NSAS (Fig. 1) shows that the isotopic composition in the recharge mounds is highly depleted ($\delta^{18}\text{O}$: -9.53% to -8.4%) compared to the recent precipitation (weighted average $\delta^{18}\text{O}$: -3.43%), as well as the case in M1 in Qatar (Fig. 2) that has depleted isotopic composition ($\delta^{18}\text{O}$: -5.2 to -2.6%) compared to the modern precipitation (weighted average $\delta^{18}\text{O}$: -0.68%). On the other hand, M2 in north Qatar show isotopic composition that is mixed between modern precipitation and fossil groundwater composition.

4 Discussion

The spatial correlation between major faults and groundwater mounds in the two studied areas and the depleted isotopic composition of these mounds compared to modern precipitation support an artesian upward recharge origin of these mounds from deeper aquifers along the faults. In Sinai,

the saline Jurassic aquifer underlying the NSAS has higher hydraulic heads [5], as well as in Qatar where Aruma Aquifer that underlies the main aquifer unit has hydraulic heads up to 50 m higher than those in the main aquifer unit [6]. In the two areas, deep aquifers have gaseous-rich fossil groundwater [5, 6]

5 Conclusions

Integration of remote sensing data with hydrological and isotopic datasets is crucial for the identification of groundwater mounds in fractured aquifers, as in Sinai and Qatar. These mounds are attributed to artesian upward leakage from deeper aquifers along vertical/subvertical faults. Further investigations are necessary to evaluate the effects of these upward leakages from saline/brackish gaseous-rich aquifers on the water quality and karst development in the two study areas, where both have strategic groundwater reserves and are covered with highly soluble carbonate rocks.

References

1. Al-Hajari, S.: Geology of the Tertiary and its influence on the aquifer system of Qatar and Eastern Arabia. Ph.D. thesis, University of South Carolina. pp. 1–219 (1990)

2. Rosenthal, E., et al.: The hydrochemical evolution of brackish groundwater in central and northern Sinai and in the western Negev. *J. hydrol.* **337**(3–4), 294–314 (2007)
3. Abotalib, A., Sultan, M., Elkadiri, R.: Groundwater processes in Saharan Africa: implications for landscape evolution in arid environments. *Earth-Sci. Rev.* **156**, 108–136 (2016)
4. Yurtsever, Y., Payne, B.: Application of environmental isotopes to groundwater investigations in Qatar. In: *Anonymous Isotope Hydrology* (1979)
5. Vengosh, A., et al.: New isotopic evidence for the origin of groundwater from the Nubian Sandstone Aquifer in the Negev. *Isr. Appl Geochem* **22**(5), 1052–1073 (2007)
6. Shamruk, M., Al-Muraikhi, A., Al-Hamar, Y.: Exploring of deep groundwater in the southwest aquifer of Qatar. In: *The 10th Gulf Water Conference*, pp. 1–13 (2012)

A Coupled Hydrogeophysical Approach to Enhance Groundwater Resources Management in Developing Countries

Zakari Arétouyap, Dieudonné Bisso, Philippe Njandjock Nouck, and Jamal Asfahani

Abstract

The present paper aims mainly at promoting an environment-friendly method to detect and locate aquifers in a context of effective and sustainable groundwater resources management. Concretely, it is a matter of illustrating how traditional hydrological and modern geophysical methods can be used conjointly to characterize aquifers. Main hydrodynamic characteristics of the Pan-African aquifer obtained in this survey could be observed in all regions worldwide where the Pan-African geological setting is extended. And this environment-friendly approach, using conjointly geophysical and hydrological methods, can be used to explore aquifers elsewhere in the context of sustainable management of groundwater resources.

Keywords

Developing countries • Groundwater • Hydrodynamic parameter • Sustainable management • VES

1 Introduction

Nowadays, water scarcity is a serious concern throughout the globe and especially in developing countries. Vörösmarty et al. [1] established that more than a third of humanity lives with less than 1.7 m³ of water per year. In the area including more than 20 countries in North Africa and the Middle East, there is a situation of chronic shortage where each person must settle for less than 3 l of water per day. According to the same authors, 4 million people die every year in developing

Z. Arétouyap (✉) · D. Bisso · P. Njandjock Nouck
Faculty of Science, University of Yaounde I,
P.O. Box 812 Yaounde, Cameroon
e-mail: aretouyap@gmail.com

J. Asfahani
Applied Geophysics Division, Atomic Energy Commission,
P.O. Box 6091 Damascus, Syria

countries from diseases caused by the lack of good quality water, and 6000 children die every day for drinking unsafe water. In such a context, groundwater, because of its better quality compared to surface water, is a resource which is highly valued by humans. In fact, in addition to its potential availability, regardless of the spatial distribution of population, its relatively better physicochemical quality [2] may help reduce water scarcity that billions of people are experiencing worldwide. Hence, the present paper aims at promoting an environment-friendly method to detect and locate aquifers in a context of effective and sustainable groundwater resources management. Concretely, it is a matter of illustrating how traditional hydrological and modern geophysical methods can be used conjointly to characterize aquifers. The effective and sustainable management of groundwater resources also involves the method used for at least two reasons, namely the accuracy and the way (environment-friendly or not) aquifers are located.

2 Materials and Methods

2.1 Gathering and Processing of VES

Local aquifer systems have been located thanks to 50 VESs carried out in the study area using the Schlumberger configuration. The Terrameter (ABEM SAS-1000) was used with a spacing of current electrodes ranging from 1 to 300 m to directly measure the resistance $\Delta U_{MN}/I$. Then, the latter parameter enabled us to compute the apparent resistivity of the rock using Ohm's law expressed by Eq. 1, taking into account the geometric factor of the quadrupole device expressed in Eq. 2.

$$\rho_a = k \frac{U_{MN}}{I} \quad (1)$$

where

$$k = \frac{2\pi}{\left(\frac{1}{AM} - \frac{1}{BM} - \frac{1}{AN} + \frac{1}{BN}\right)} \quad (2)$$

The resistivity curves are interpreted using the reference curves derived from the VES conducted close to the 14 control-boreholes. Then, these reference curves are used to calibrate the inversion software IPI2Win [3]. In a more quantitative interpretation of the VES curves. The quantitative interpretation of the VES curves is conducted on the basis of a double assumption: the earth is horizontally stratified with the last layer, having infinite thickness, and each layer is electrically homogeneous and isotropic [3].

2.2 Pumping Tests

Fourteen out of 50 VESs are carried out near the reference boreholes where pumping tests were performed in order to experimentally determine the values of the flow rate Q and the transmissivity T (Eq. 3) for each point. The hydraulic conductivity K is computed as shown in Eq. 4, then the calibration method developed by Asfahani [4] is applied to analytically determine K values for the remaining VES points.

$$T = \frac{0.183Q}{\Delta s} \quad (3)$$

$$K = \frac{T}{h} \quad (4)$$

Q , h and Δs represent respectively the flow rate, the aquifer thickness and the drawdown difference according to Jacob [5].

The methodology consists in three major steps:

- (1) Establishing an empirical relationship between R values obtained by interpreting the 14 reference VES, and $K\sigma$. In this relation, K is the hydraulic conductivity obtained by pumping tests and σ is the aquifer electrical conductivity.
- (2) Using Eqs. 5 and 6 to determine the transverse resistance R and the longitudinal conductance S for the other 36 VES points where no borehole exists.

$$R = \sum_{i=1}^n h_i \rho_i \quad (5)$$

$$S = \sum_{i=1}^n \frac{h_i}{\rho_i} \quad (6)$$

h_i and ρ_i are respectively the thickness and the resistivity of the i th layer.

- (3) computing $K\sigma$ and, therefore, K for all VES locations from the empirical equation obtained in step 1.

3 Results and Discussion

3.1 From Pumping Tests

Pumping tests were carried out from 25th June to 19th August, 2016, in the Pan-African context of the Adamawa-Cameroon region by making flow levels, with constant flow for a short period of 1 to 8 h. Three parameters (time, drawdown and flow) are measured. Each flow level is followed by a pumping break for a period at least equal to the rise of water level, and by measuring the residual drawdown. 14 pumping tests were performed and pumping curves were plotted. These pumping tests enabled us to directly measure the flow rate, transmissivity and hydraulic conductivity values of the 14 experimental boreholes presented in Table 1. Note that this is an unconfined aquifer since water seeps from the ground surface directly above the aquifer.

3.2 Calibration Line

Hydrodynamic parameters have been deduced from the relationship established between R and $K\sigma$ and summarized in Table 2.

3.3 Contribution to the Sustainable Management of Groundwater Resources

Actually, an efficient and sustainable management of groundwater resources involves mainly the use and conservation of this resource, and the protection and the control of the environment and populations from hazards associated with it. This involves further care and precaution to conserve groundwater quality and quantity for a long-lasting use [6]. This paper contributes upstream to the efficient and sustainable management of groundwater resources. Indeed, before launching any action or investigation regarding the physico-chemical analysis, productivity, vulnerability, pollution and contamination, environmental impacts or sustainability and management improvement of groundwater resources, aquifers should first be detected and located accurately and then evaluated. Geophysical methods, such as VES, can contribute significantly to the precision in the location of aquifers and pumping tests to the determination of their hydrodynamic parameters. It's worth mentioning

Table 1 Parameters obtained from 14 experimental boreholes by pumping tests

VES N°	Q (m ³ h ⁻¹)	σ (Ω^{-1})	T (m ² day ⁻¹)	K ($\times 10^{-6}$ m/day)	$K\sigma$ ($\times 10^{-4}$)
1	0.2	20	0.46	14.06	2.78
3	1.8	41	2.73	7.23	3.00
12	8.1	40	7.48	6.36	2.52
13	0.9	101	8.21	2.35	2.38
16	2.1	5	9.25	3.70	0.20
17	3.0	67	9.54	2.67	1.78
21	0.4	12	12.5	11.05	1.39
22	3.2	70	12.85	2.20	1.53
27	0.8	22	15.37	10.02	2.85
28	4.2	8	15.65	2.52	2.20
34	2.3	96	18.54	1.04	1.00
38	4.1	57	21.03	0.88	0.50
42	1.8	18	23.7	6.44	1.99
50	12.0	3	46.01	0.99	0.03

Table 2 Summary of Pan-African aquifers' characteristics

	σ ($\times 10^{-4}/\Omega$)	ρ (Ω .m)	T (m ² day ⁻¹)	K (mday ⁻¹)	S (Ω^{-1})	$K\sigma$ ($\times 10^{-4}$)
Min	1.60	3	0.46	0.01	0.004	1.5
Max	122.15	825	46.02	1.68	5.25	428.5
Mean	17.29	228	15.46	0.46	0.61	28.5
SD	18.61	215	10.33	0.40	0.9	99.0

that the VES technique introduced and used in this study is “very” environment-friendly as it doesn't require any ground drilling.

4 Conclusions

In this study, the conjoint use of both hydrological and geophysical (VES in this case) methods is presented as a proficient approach for the efficient and sustainable management of groundwater resources. VES, which is environment-friendly, can contribute significantly to the precision in the location of aquifers, and hydrology (pumping tests in this case) helps in the determination of their hydrodynamic parameters. The present paper has clearly illustrated how hydrological and geophysical methods can be used conjointly to characterize aquifers. This ecological approach can be used to explore aquifers elsewhere in the context of a sustainable management of groundwater resources.

References

- Vörösmarty, C.J., Green, P., Salisbury, J., Lammers, R.: Global water resources, vulnerability from climate change and population growth. *Science* **289**, 284–288 (2000)
- Nshagali, B.G., Njandjock Nouck, P., Meli'i, J.L., Arétouyap, Z., Manguelle-Dicoum, E.: High iron concentration and pH change detected using statistics and geostatistics in crystalline basement equatorial region. *Environ. Earth Sci.* **73**, 7135–7145 (2014)
- Zohdy, A.A.R.: A new method for the automatic interpretation of Schlumberger and Wenner sounding curves. *Geophysics* **54**, 245–253 (1989)
- Asfahani, J.: Electrical earth resistivity surveying for delineating the characteristics of groundwater in semi-arid region in Northern Syria. *Hydrol. Process.* **21**, 1085–1097 (2007)
- Jacob, C.E.: Draw-down test to determine effective radius of artesian well. *Trans. Am. Soc. civ. Eng.* **112**, 1047–1070 (1947)
- Gupta, A.D., Onta, P.R.: Sustainable groundwater resources development. *Hydrol. Sci. J.* **42**(4), 565–582 (1997)

Characterization and Origin of Some North-Eastern Algeria Thermal Waters

Yasmina Bouroubi-Ouadfel, Abdelkader Khiari, Corinne Le Gal La Salle, Mounira Djebbar, and Mahmoud Khaska

Abstract

Northeastern Algeria has been known, since ancient times, by the presence of thermo-mineral springs emerging from different geological formations, especially in the vicinity of the Tunisian borderline. These hot waters circulate along the fractured system and the main thermal spring emerges from a Neogene graben. Each of the four inventoried hot springs has at least three griffins. These thermal waters are found to be saline and carbo-gaseous. The geochemical facies are of the Cl–HCO₃–Na type. Stable isotopes contents ($\delta^2\text{H}$, $\delta^{18}\text{O}$) showed that the waters are of meteoric origin. Strontium isotopic ratios $^{87}\text{Sr}/^{86}\text{Sr}$ indicated the presence of a mixture of thermal fluids with infiltrated meteoric waters at shallow depths as well as strong water-rock interactions. The combined use of geochemical and isotopic tracers highlights the existence of a hydrothermal alteration and a saline fluid circulation.

Keywords

North-Eastern Algeria • Graben • Thermal waters • Strontium isotopic ratios • Saline fluid circulation

1 Introduction

In northern Algeria, an update of the hot springs inventory showed the existence of more than 240 sites [1]. The largest number is located in northeastern Algeria [2, 3]. That region is individualized by the presence of one of the most

radioactive springs in the world (in Setif with 155 $\mu\text{Ci/L}$) [4] and the hottest water worldwide (98 °C in Guelma) [2, 3], [1], when Icelandic geysers are not taken into account. The geothermal gradient (5–7 °C/100 m) [3] and the average geothermal heat flux (more than 90 mW m^{-2}) [5] are related to the active tectonics of Northern Algeria [6]. This vast region is part of the Maghrebides' alpine chain, known for its complex tectonic structures. Mesozoic karstified carbonate formations are the main geothermal reservoirs [3]. The study area concerns the hydrothermal karsts located near to the Tunisian borderline. Our objective in this work is to determine the origin of the thermal waters and the origin of their mineralization. Thus, a combined geochemical and isotopic tracing approach was implemented in order to determine the origin and the circulation modes of the thermal saline fluid within the aquifer.

2 Geological Setting and Methods

The study area is part of the thermo-seismic axis “Constantine El Kef Maktar” [7]. Spring S2 (T = 40 °C) emerges from the Neogene graben of the Taoura (Fig. 1) of the pull-apart basin type. Hydrothermal activities are found in areas of high tectonic activity and have a very close relationship with faulted zones [8]. The litho-structural disposition and the seismo-tectonic activity of northern Algeria have both favored the development of hydrothermal complexes.

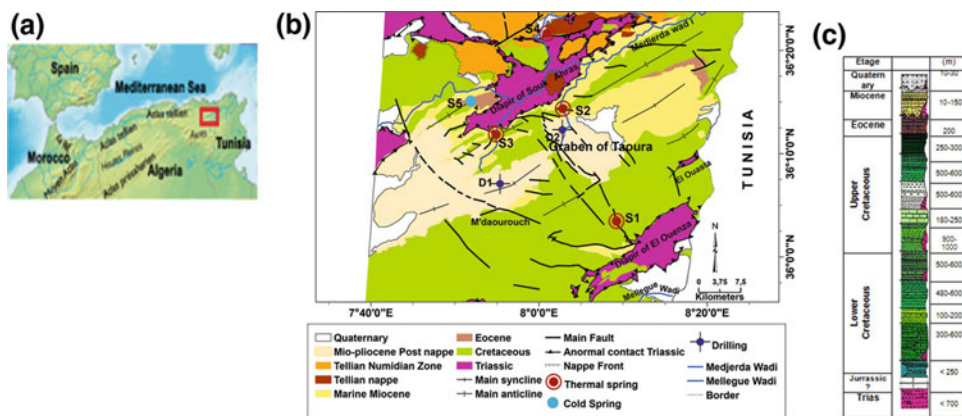
The collected water samples, (2011–2014) were analyzed respectively for major ions (Ca, Mg, Na, K, HCO₃, Cl, SO₄, NO₃), traces (Sr) and isotopes ($\delta^2\text{H}$, $\delta^{18}\text{O}$ & $^{87}\text{Sr}/^{86}\text{Sr}$). T (°C), pH and EC were measured in situ. Cations and anions were analyzed at the National Agency for Water Resources (Algiers). Analyses for stable isotopes of water were performed at the Algiers Nuclear Research Centre on a Picaro-2110i. ($^{87}\text{Sr}/^{86}\text{Sr}$) ratio was determined by mass spectrometry at the “GIS” laboratory in Nîmes. P_{CO₂} (Partial pressure of carbone dioxide) values were calculated using the free software “Phreeqci-3.1.4-8929”.

Y. Bouroubi-Ouadfel (✉) · A. Khiari
Larbi Ben M'hidi University, 04000 Oum El Bouaghi, Algeria
e-mail: yasmina.bouroubi@univ-ueb.dz

C. Le Gal La Salle · M. Khaska
GIS Laboratory, Nîmes University, 130035 Cedex, France

M. Djebbar
Mentouri University, Constantine, Algeria

Fig. 1 a Location of the study area. b Simplified geological map with location of sampled springs and boreholes. c Synthetic stratigraphic column [9]



3 Results

3.1 Physico-Chemical Parameters

See Table 1.

Piper classification shows different types of water, Cl–HCO₃–Na for S1, S2 and S3, HCO₃–Ca to HCO₃–Na for S4, HCO₃–Ca for D1 and S5 and HCO₃–Na D2, respectively. On the binary diagrams (Fig. 2), major ions selected were plotted against Cl. Calculated P_{CO2} for S1 and S2 are abnormally high, and gas bubbling were clearly visible at emergence points.

3.2 Isotopes

All the waters are found to lay near the Algerian Local Meteoric Line (ALML) as defined by [11] ($\delta^2\text{H} = 7.5 \delta^{18}\text{O} + 7.92$) and the Western Mediterranean Meteoric Line (OMML) whose equation is: $\delta^2\text{H} = 7.23 \delta^{18}\text{O} + 6.07$

[12] (Fig. 3). S1 and D1 waters exhibit enrichment in ¹⁸O. ⁸⁷Sr/⁸⁶Sr ratios range from 0.707881 to 0.709007 ± 5 (±2σ). S2 sample shows the highest ⁸⁷Sr/⁸⁶Sr ratio (Fig. 4).

4 Discussion

Correlation (a) (Fig. 2) shows the dissolution of NaCl and the contribution of saline fluids in S2 waters. The high K⁺ contents of S1 and S2 indicate either dissolution of Sylvine or hydrolysis of micas and/or K–feldspar. Low levels of SO₄²⁻ indicate a biochemical reduction of dissolved sulfates. The sulfur odor released by S1, S2 and S4 indicates the presence of H₂S. In addition, and according to Guigue [2], the waters of S2 and S4 are sulfurous. The very low NO₃⁻ concentrations of S2 and S4 indicate a long water circulation and residence times. The very high P_{CO2} of S1 and S2, highlights a deep origin for CO₂. Stable isotopes unveil the meteoric origin of water. The enrichment in ¹⁸O in S1 and D1 is due to the evaporation of water before infiltration. The

Table 1 Physical parameters and P_{CO2}

Sampling site	Type	Flow rate (L s ⁻¹)	T (°C)	pH	EC (ms cm ⁻¹)	P _{CO2} (Atm)
S1	Thermal spring	2	27	5.65	7.00	3.54
S2	Thermal spring	4	40	5.65	3.52	2.09
S3	Thermal spring	8–16	27	6.65	1.80	0.20
S4	Thermal spring	6.5	39	6.14	2.04	0.50
D1	Borehole (146 m)	100	22.5	6.20	1.38	0.33
D2	Borehole (150 m)	4	24	6.75	1.10	0.07
S5	Cold spring	0.2	17	6.47	0.46	0.07

Fig. 2 Chemical binary diagrams (SWML = 0.856; Current sea water mixing line [10] and (Na/Cl = 1; HDL Halite Dissolution Line)

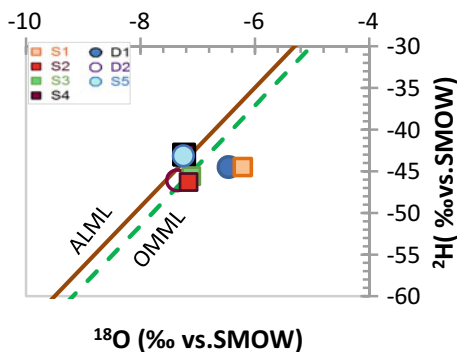
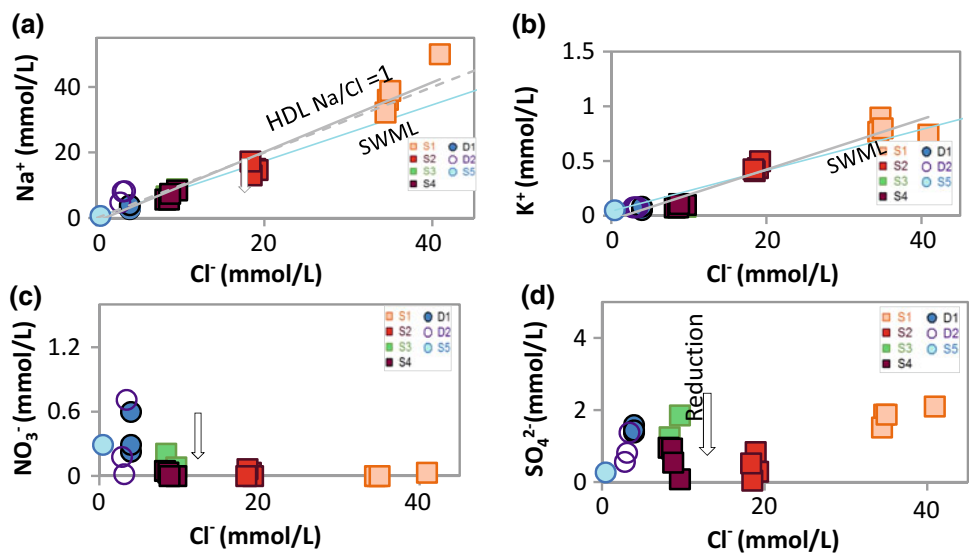


Fig. 3 Stable isotope compositions

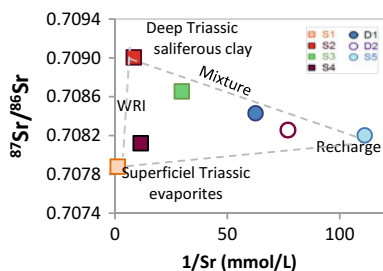


Fig. 4 ⁸⁷Sr/⁸⁶Sr versus 1/Sr

high value of the ⁸⁷Sr/⁸⁶Sr ratio in S2 derives from strong water-rock interaction with deep triassic saliferous clay. S1 and S4 are affected by water-rock interaction with superficial triassic evaporites. Waters of S3, D1 and D2 originate from a

mixture in varying proportions, of the deep thermal saline fluid and the recharge water.

5 Conclusions

The north-eastern Algeria hydrothermal complex that is present in the vicinity of Tunisian boundary emerged mainly in the Cretaceous carbonates. It is the seat of a mixing of a deep thermal saline fluid and meteoric waters from the shallow layers. The Neogene graben of Taoura allows the ascension of a thermal saline fluid which is sought to originate from an alteration of the saliferous clays of the basal Triassic formations.

References

1. Saibi, H.: Geothermal resources in Algeria. *Renew. Sustain. Energy* **13**, 2544–2552 (2009)
2. Guigue, S., Betier, G.: Les sources thermominérales de l'Algérie-Étude géochimique. *Bull. Serv. Carte Géol. Algérie*, 117–120 (1947)
3. Kedaid, F.: Database on the geothermal resources of Algeria. *Geothermics* **36**, 265–275 (2007)
4. Pouget, I., Chouchak, D.: Radioactivité des eaux minérales d'Algérie. *Acad. Sci.* **177**, 1112–1114 (1925)
5. Takherist, D., Lesquer, A.: Detection of significant regional variations in heat-flow in Algeria. *Earth Sci.* **26**, 615–626 (1989)
6. Yelles-Chaouche, A., Boudiaf, A., Djellit, H., Bracene, R.: La tectonique active de la région nord algérienne. *C. R. Geoscience* **338**, 126–139 (2006)

7. Verdeil, P.: Algerian thermalism in its geosstructural setting. *J. Hydrol.* **56**, 107–117 (1982)
8. Khaska, M., Le Gal La Salle, C., Videau, G., Flinois, J., Frappe, S., Teamb, A.: Deep water circulation at the northern Pyrenean thrust. *Chem. Geol.* (419), 114–131 (2015)
9. Haddouche, O., Boutaleb A., Hebert R., Picard D. et Sami L.: Les minéralisations à Pb- Zn, Fe, Ba (Sr) d'El Ouasta (Algérie Nord orientale): typologie et apport des études d'inclusions fluides. *Bulletins A.N.G.C.M- Algérie* (15) (2004)
10. Wilson, T.: Salinity and major elements of sea water. In: Riley, P., Skirrow, G. (eds.) *Chemical Oceanography*, 2nd edn. Academic Press, New York (1975)
11. Saighi, O.: Isotopic composition of precipitation in the Mediterranean Basin in relation to air circulation patterns and climate. In: IAEA-TECDOC-1453, pp. 5–18 (2005)
12. Celle-jeanton, H., Zouari, K., Travi, Y., Daoud, A.: Caractérisation isotopique des pluies en Tunisie. *Earth Planet. Sci.* **333**, 625–631 (2001)

Water Footprint and Governance Assessment for Sustainable Water Resource Management in Drought-Prone Barind Area, NW Bangladesh

Razzaqul Islam, Chowdhury S. Jahan, Quamrul H. Mazumder, Suman Miah, and Ferozur Rahaman

Abstract

Livelihood in agro-based Barind area in northwest Bangladesh is at risk due to moderate-extreme drought impacts. Assessment of water governance status is carried out considering the blue water footprint (WF). Here, the cropping pattern is dominated by rice and the majority of the farmers use groundwater for irrigation. Among crop varieties, *Boro* rice accounts for the highest WF (3109 l/kg) consuming 70% of water with little economic return, and all crops exceed global WF standards. The performance indicators like transparency, accountability, participation, social equity, environmental integrity, efficiency and effectiveness of government organizations (BMDA, BWDB, DPHE and LGED) and NGOs (DASCOH Foundation) show that the performance of DASCOH Foundation was ‘good’; BMDA and LGED ‘moderate’; while BWDB and DPHE ‘bad’, and should take rigorous action plans for scaling up in these issues. DASCOH Foundation has started to institutionalize IWRM, updating water laws etc. So, appropriate strategies for governance performance due to sustainable resource management should be given priority with enabling environment, institutions, and instruments.

Keywords

Water footprint • Governance assessment • Drought • Barind area • Bangladesh

1 Introduction

In Bangladesh, water governance conflict is seldom practiced, but it is a very much burning tool for policy makers, particularly for the drought-prone Barind area where unsustainable groundwater development and governance failures have affected the availability of water resources with social equity and economic justice. The study area covers two *Upazilas* of Rajshahi District (Godagari and Tanore), and two of Chapai Nawabganj District (Nachole and Gomastapur) (Lat: 24° 26' 45"N–24° 26' 45"N and Lon: 88° 13' 00"E–88° 33' 10"E) (*Upazila and District*—the second and third lowest tiers, respectively, of administrative units in Bangladesh), covering 1942 km² area with a population of 1.5 million. Here, the meagre surface water resources have made the crop production mostly irrigation-based, creating pressure on groundwater resources due to over-exploitation. Knowledge gaps related to sustainable resource management exist here alone with enforcement of water laws, policies and regulations also exist. So, the aims of the present study are to calculate WF to know the potentiality of water resources that may help future efficient use of resources; and to assess the status of water governance using quantitative and qualitative data.

The study area enjoys a sub-tropical monsoon climate, but due to its landscape nature, most of the rain water is lost as runoff and ultimately the area cannot retain adequate rain water quantities. The area has suitability mostly for domestic water supply and for irrigation needs to some extent. Here, the groundwater table goes down to its maximum depth in the dry season and the situation is reversed in the rainy season due to accretion of rainwater. After 2004, GWT did not return to its original position in the rainy season indicating a “not fully” replenishment of resources due to over-exploitation. This worsens the water crisis scenario of the drought-prone area and jeopardizes food security in the country.

R. Islam · C. S. Jahan (✉)

Department of Geology and Mining, University of Rajshahi, Rajshahi, 6205, Bangladesh
e-mail: sarwar_geology@yahoo.com

Q. H. Mazumder · S. Miah

DASCOH Foundation, Dingadoba, Rajshahi, 6201, Bangladesh

F. Rahaman

Institute of Environmental Science, University of Rajshahi
Institute of Bangladesh Studies, University of Rajshahi, Rajshahi, 6205, Bangladesh

2 Materials and Methods

The present study deals with blue WF impedibility within only the domestic and agricultural sectors. It has been calculated after [1]. For agriculture and domestic WF accounting, both primary and secondary data are collected from a field survey and a secondary source like household (HH) water consumption; source; HH number; distribution of ethnic minority; average size; number of cattle; point of waste water discharge; area of cropping agricultural land; crop types; evaporation rate; number of irrigation operations; and pump capacity and operation time of Deep Tubewell (DTW). For agricultural information, *Union* wise focus group discussions (FGD) with at least 10 farmers are conducted.

In this study, water governance assessment framework [2] deals with solid quantitative and indicative measures based on perception of stakeholders. Four government organizations, like the Department of Public Health Engineering (DPHE)—drinking water supply agency; Barind Multipurpose Development Authority (BMDA)—irrigation agency; Bangladesh Water Development Board (BWDB)—flood and drainage control agency; and Local Government Engineering Department (LGED)—small scale surface water irrigation agency; and NGO like the Development Association for Self-Reliance, Communication and Health (DASCOH) Foundation, are selected; knowing that they have been working in the water sector here for long time. The water decision-making stakeholders (like household, agricultural, fishery, commercial, industrial etc.) are part of the governance analysis in the present study where the total number of water users is 80, among whom 50% are female respondents. The water-related schemes such as drinking water supply, irrigation, rain water harvesting, flood control and drainage that have been implemented within the last five years were considered. Teachers, elected public representatives in the local government institute (LGI), religious leaders, political leaders, women organizers, business men, and members of the water users association were selected as civil society representatives. Considering relevancy with the water sector, officials from government organizations were selected. 64 of total Water Resource Management Organizations (WRMOs), which were randomly selected from 864 organizations are working with LGIs, were assessed through quantitative methods. Accordingly, the overall and individual governance performance was ranked into categories as: very bad (<20%); bad (21–40%); moderate (41–60%); good (61–80%); and very good (81–100%). The water governance (WG) is categorized into grades (very bad = <20%; bad = 21–40%; 41–60% = moderate; 61–80% = good and 81–100% = very good) for the general understanding of the governance status. The findings from quantitative

(assessment questionnaire survey) and qualitative (experts' opinions on the national level) data were validated to check the assessment results and to provide concerned stakeholders with an opportunity to react with the findings related to their institutions.

The sustainability wheel is used to assess the status having broader components such as economic efficiency, environmental integrity and social equity, and is categorized as: non-existent (0), very poor ($\leq 20\%$), poor ($\leq 40\%$), moderate ($\leq 60\%$), good (80%) and very good ($\leq 100\%$). Moreover, the existing legal instruments such as acts/ordinances, rules, policies etc. are also reviewed to find out potentials and lacunae for sustainable resource development and management.

3 Results and Discussion

In the study area, each HH uses 267 L water/day for drinking, cooking and other HH purposes which vary significantly *Upazila* wise. Rice production consumes around 65% of water where *Boro* rice requires maximum (45% or 3109 l/day), followed by *Aman* rice (1103 l/kg), potato and rain-fed *Aus* rice (1079 l/kg), mustard (1075 l/kg), lentil (895 l/kg), wheat (863 l/kg) and potato (156 l/kg), while wheat, lentil and mustard with substantially lower amounts of water. *Boro* rice accounts for the highest WF, whereas potato is considered as the most water efficient crop, but all crops exceed (by up to nine times) the global WF standard. The maximum amount of water is used by *Boro* rice with net amount of loss of (18 US\$/ha). In terms of water use efficiency, lentil, mustard and wheat are water efficient crops (use only 4–7% of water to produce 12–29% of economic return).

In the present study, the institutional capacity has been assessed based on the perception of the key stakeholders with regard to the level of commitment of the leadership towards good water administration; vertical and horizontal coordination; post-maintenance and follow up; decentralization; and capacity of the organization. The average score of studied organizations shows 'moderate' capacity in terms of governance rank. The level of transparency and integrity is almost similar whereas accountability seems to be 'very poor' for LGED, but DASCOH Foundation with apparently a participatory role. In terms of economic efficiency and effectiveness, BMDA has shown the best performance with a 'good' category, whereas DASCOH Foundation and LGED were ranked as 'moderate', while BWDB and DPHE exhibited a 'bad' performance. However, the average score of all organizations indicates a 'moderate' performance. In the context of social equity, DASCOH Foundation performed better in comparison to other public sector

organizations with a 'bad' to 'good' performance. Accordingly, DASCOH Foundation's approach is more inclusive, gender sensitive or mainstreaming to improve the access and control of women and socially-marginalized people below the poverty level and ethnic minorities; and has started to work with the concept of the Integrated Water Resource Management (IWRM) as a noble and conflict-sensitive approach. The environmental integrity of BWDB exhibited the worst performance, and DASCOH Foundation showed 'good'. From FGD, it is observed that BMDA is performing very well in agricultural productivity, but their indiscriminate groundwater exploitation for irrigation results in a negative impact from a couple of years back, and people are not even able to get drinking water during the dry season which is mainly due to the failure of engineering solutions and outlooks in predicting environmental and social impacts in general.

The overall water governance situation belongs to the 'moderate' category, where DASCOH Foundation's performance was 'good'; BMDA and LGED were 'moderate'; while BWDB and DPHE were 'bad'. The lack of governance parameters like transparency, accountability and participation of BWDB impedes its good practice with a lack of effective participation in management activities. DPHE has success in ensuring supply coverage of safe drinking water and the project implementation system includes sharing mostly with the public representatives. The IWRM project of DASCOH is working although in limited scale but in dimensions like citizen mobilization through water resource organization; strengthening LGIs for institutionalization; and creating an enabling environment through formulating necessary rules and regulations through multifaceted intervention in cooperation with its national counterpart like the Water Resource Planning Organization (WARPO), Ministry of Water Resource (MoWR), Bangladesh. The sustainability

wheel shows moderate category of overall sustainability of studied organisations.

4 Conclusions

The rice-dominated cropping pattern, climate variability and excessive dependence on groundwater for irrigation practices are making the scenario of the area worse day by day. Here, WF of all crops have a higher value than that of the global standard. The water governance performance of almost all public sector organizations is very poor in terms of transparency, accountability, participation, efficiency and environmental equity, and these issues should be considered seriously with a rigorous action plan in order to scale up the water governance performance. The significant gaps in terms of transparency prevailing in the public sector agencies need to be improved. The IWRM model as a noble concept should be generalized not only to the community and LGIs but also to other government sectors. Finally, to meet the challenges for implementing the IWRM model, changes are required to enable environmental and institutional functions and instruments in this drought-prone area, in particular, and Bangladesh, in general.

References

1. Mekonnen, M.M., Hoekstra, A.Y.: National Water Footprint Accounts: The Green, Blue and Grey Water Footprint of Production and Consumption, Volume 1: Main Report, UNESCO-IHE, Institute for Water Education, Delft, The Netherlands (2011)
2. UNDP (United Nations Development Programme): Fostering Social Accountability: From Principle to Practice, UNDP Oslo Governance Centre, Oslo (2010)

Part VI

**Hydrologic Engineering and Urban
Groundwater**

Water Quality for Irrigation Purposes in the Middle Tafna Watershed (NW, Algeria)

Lamia Yebdri, Fatiha Hadji, Yahia Harek, and Abbas Marok

Abstract

Irrigation water quality in semiarid areas of North Algeria is degrading because of contaminants originating from anthropogenic sources. Among these harmful contaminants, nitrate and phosphate ions are the most common. In this context, this study was carried out to assess the contamination degree of irrigation water, with a particular emphasis on nitrate and phosphate enrichment in the groundwater of Hennaya alluvial aquifer and surface water of Sikkak wadi. Surface and groundwater samples were collected, during April and November in 2017 and analyzed. The concerned physicochemical parameters were pH, Temperature (T), Electrical conductivity (EC), Total Dissolved Solids (TDS), Chloride (Cl^-), Nitrate (NO_3^-) and Phosphate (PO_4^{3-}). The obtained results were compared to irrigation water quality guidelines. All groundwater samples showed that nitrate concentrations were distinctly higher (up to 98 mg/L) than the guideline values of irrigation water quality (30 mg/L). Phosphate contents were observed in 3 wells in which they attained the maximal value of 0.42 mg/L. These high concentrations in nutrients (Nitrate and phosphate) originated from an excessive use of agrochemicals, when penetrating the soil and reaching the groundwater.

Keywords

Water • Irrigation quality • Nitrate • Alluvial aquifer • Sikkak wadi

1 Introduction

Tafna watershed is a semi-arid zone with intense agricultural activity (herbaceous crops, vineyards, fruit tree plantations), in which water resources and water quality for irrigation purposes are facing a great pressure. In order to maintain healthy growth and sustainable crop yields, water for irrigation must meet quality standards [3, 5]. This watershed has important sources of pollution contaminating water whose deterioration of quality is a direct consequence of the agricultural practices and discharges of the waste effluents in surface water. This water is used for human consumption and for agricultural and industrial practices. In this study, the evaluation of the water quality of the Middle Tafna watershed (NW, Algeria) and of its suitability for agricultural purposes has been attempted.

2 Materials and Methods

The study area is located in the middle of Tafna watershed, on the extreme northwest of Algeria. It comprises the Sikkak wadi with a length of 28 km, that feeds the Sikkak dam, and the Hennaya alluvial aquifer with a total surface of about 22 km². Hennaya aquifer corresponds to a basin filled with Mio-plio-quaternary age, consisting of tortonian sandstone, conglomerates, travertine and clayey gravels, with an average permeability of about 13 m/day, resting on a substratum constituted by Helvetian marls.

Forty-five water samples were collected during April and November 2017 and analyzed (Fig. 1). Measurements were based on seven physical and chemical parameters (Temperature, pH, Electrical conductivity, total dissolved solids, chloride, nitrate, and phosphate). The obtained results were compared to the FAO guidelines (Table 1) published in the Food and Agriculture Organization of the United Nations (FAO) [1].

L. Yebdri (✉) · F. Hadji · A. Marok
Department of Earth and Universe Sciences, University of Tlemcen, P.O. BOX 119 Tlemcen, Algeria
e-mail: lamia.yebdri@gmail.com

L. Yebdri · Y. Harek
Laboratory of Analytical Chemistry and Electrochemistry,
University of Tlemcen, P.O. BOX 119 Tlemcen, Algeria

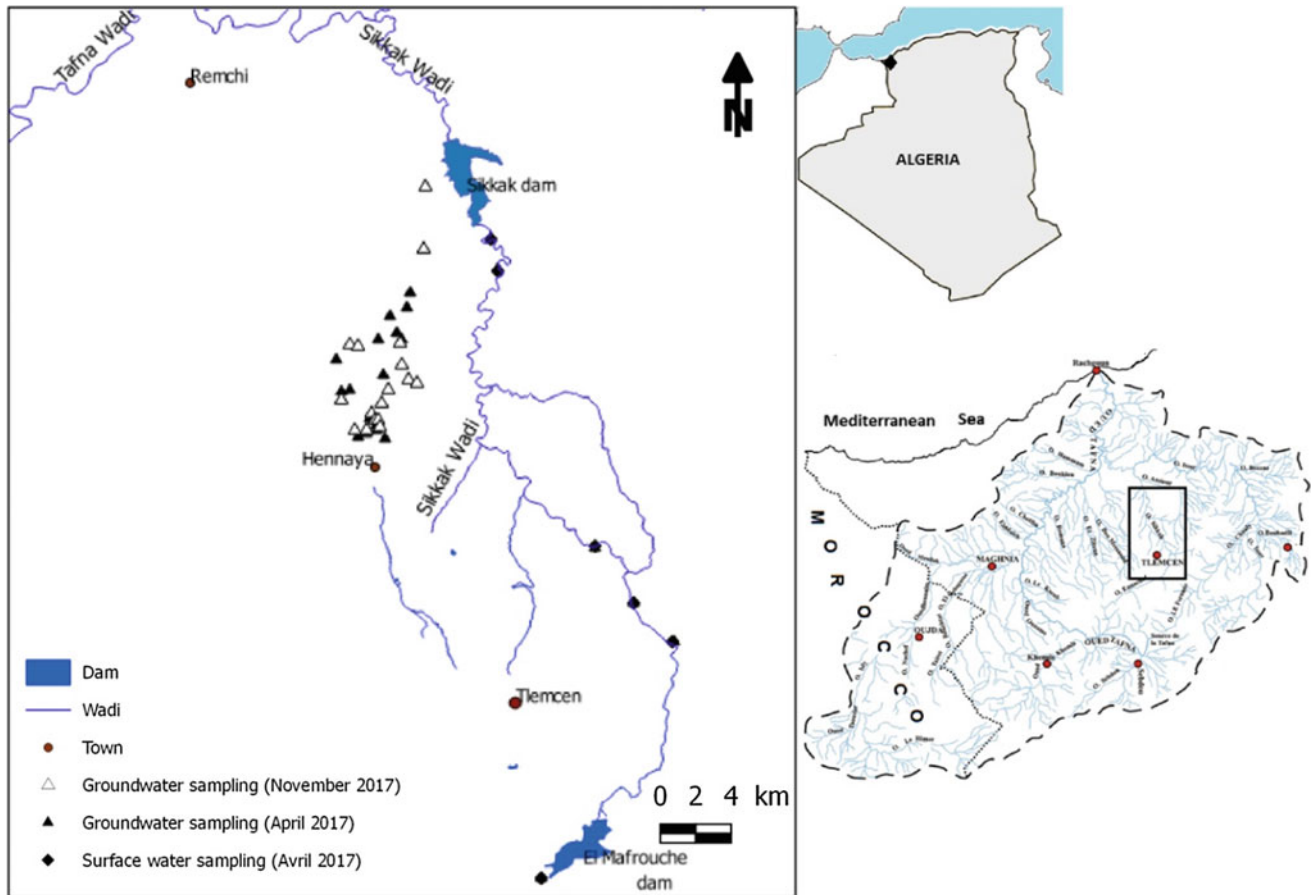


Fig. 1 Study area and sampling points locations

Table 1 Guidelines for interpretation of water quality for irrigation [1]

Potential irrigation problems		Units	None	Slight to moderate	Severe
Salinity	EC	$\mu\text{S}/\text{cm}$	<700	700–3000	>3000
	TDS	mg/L	<450	450–2000	>2000
Specific ion toxicity	Chloride	mg/L	<140	140–350	>350
Miscellaneous effects	Nitrate	mg/L	<5	5–30	>30
	pH		Normal range 6.5–8.5		

3 Results

3.1 Physicochemical Characteristics

Table 2 resumes statistics of the analyzed parameters of the 45 water samples of the two periods. The wadi was dry in November 2017.

In general, minimal values of the measured parameters were observed in surface water and the maximal values in groundwater.

Concerning the groundwater of the aforementioned alluvial aquifer, water was acidic during April. Values of pH varied between 5.87 and 6.42 (Avg. = 6.29). As for EC, values varied from 405 to 1383 $\mu\text{S}/\text{cm}$ in April and from 1365 to 2130 $\mu\text{S}/\text{cm}$ in November with averages of 1493.8 and 1613.6 $\mu\text{S}/\text{cm}$, respectively. Chloride and nitrate contents varied widely in surface water and groundwater during April and November (Table 2). Phosphate ions were observed only in three wells during the second sampling period where they attained a maximum value of 0.42 mg/L.

Table 2 Descriptive statistics of physicochemical parameters of surface water and groundwater of Middle Tafna watershed

Parameters	T (°C)	pH	EC ($\mu\text{S}/\text{cm}$)	TDS (mg/L)	Cl^- (mg/L)	NO_3^- (mg/L)	PO_4^{3-} (mg/L)
<i>Period 1—April 2017 (8 Surface water samples)</i>							
Min	14	7	405	162	17.48	0	0
Max	19	7.65	1383	566	353.69	47.5	0
Mean	17.3	7.27	844.5	338.8	129.1	28.7	0
SD	1.8	0.22	396.1	164.6	131.1	17.3	0
<i>(20 Groundwater samples)</i>							
Min	18.3	5.87	1365	530	185.47	97.99	0
Max	24	6.42	2130	840	545.6	217.26	0
Mean	21.78	6.29	1493.76	595.41	318.55	151.91	0
SD	1.59	0.14	188.14	73.25	91.95	31.98	0
<i>Period 2—November 2017 (17 Groundwater samples)</i>							
Min	14.2	7.14	1314	531	263.37	64.06	0
Max	22.7	8.06	3310	1300	879.1	218.58	0.42
Mean	19.9	7.37	1613.56	675.12	397.42	130.10	0.07
SD	2.18	0.25	496.1	193.18	171.95	43.95	0.15

4 Discussion

Except for the pH values of groundwater analyzed during the first period, which were below the lower limit of the normal range (6.5–8.4), pH values of the second-period sampled groundwater and surface water are within the aforementioned range. For all other parameters of groundwater samples EC, TDS, and Cl^- , were in classes of moderate to severe. Nitrate concentrations were distinctly higher compared to the limit value of guidelines for water quality for irrigation (30 mg/L) [1].

Chloride concentrations, which constitute the common toxicity of water, are present in surface water and groundwater with generally large quantities. They indicate a good to harmful quality for irrigation use.

Nitrate contents in sampling groundwater were found to be higher when compared to that of surface water in all samples showing high nitrate concentration (i.e. above 30 mg/L). This can be justified by an excessive use of agrochemicals (nitrogen fertilizers), when penetrating the soil and reaching groundwater [4].

The presence of phosphate ions in some wells during April 2017 is also justified by agricultural use, but they are mainly retained by soils [2].

contents are somewhat important in the majority of the sampling sites. The use of such water can lead to plant injury which can cause early leaf drop or defoliation. Nitrate levels were high in groundwater. This is due mainly to the excessive use of fertilizers.

References

1. Ayers, R.S., Westcot, D.W.: Water quality for agriculture, FAO irrigation and drainage. Rev I, Paper 29. UN Food and Agriculture Organisation, Rome (1985)
2. Di, H.J., Harrison, R., Campbell, A.S.: Assessment of methods for studying the dissolution of phosphate fertilizers of differing solubility in soil. *Fertil. Res.* **38**, 1–9 (1994)
3. Islam, M.A., Rahman, M.M., Bodrud-Doza, M., Muhib, M.I., Shammi, M., Zahid, A., Akter, Y., Kurasaki, M.: A study of groundwater irrigation water quality in south-central Bangladesh: a geo-statistical model approach using GIS and multivariate statistics. *Acta Geochim.* **37**, 193–214 (2017)
4. Rezaei, M., Nikbakht, M., Shakeri, A.: Geochemistry and sources of fluoride and nitrate contamination of groundwater in Lar area, south Iran. *Environ. Sci. Pollut. Res.* **24**, 15471–15487 (2017)
5. Vyas, A., Jethoo, A.S.: Diversification in measurement methods for determination of irrigation water quality parameters. *Aquat. Proc.* **4**, 1220–1226 (2015)

5 Conclusions

The hydrochemical analyses provided significant information on groundwater and surface water qualities for irrigation purposes in the Tafna middle watershed. The chloride

Statistical Multivariate Analysis Assessment of Dams' Water Quality in the North-Central Algeria

Somia Hamil, Djaouida Bouchelouche, Siham Arab, Nassima Doukhandji, Ghiles Smaoune, Monia Baha, and Abdeslem Arab

Abstract

The aim of this study is to evaluate the dam's water quality of North-Central Algeria. The water quality data was monitored at twenty different dams, between January and December of 2017, using 9 water quality parameters and a multivariate analysis such as Cluster Analysis (CA). The CA allowed the formation of five clusters between the sampling sites, reflecting differences between the water quality at different locations. The Ghrib and Herraiza Dams were characterized by a strong mineralization with a concentration of total solids of more than 1600 mg L^{-1} , reflecting the geological nature of the watershed.

Keywords

Cluster analysis • Mineralization • Water quality • Dams • Algeria

1 Introduction

The water quality of these sources is considered to be a key contributor to both health and disease states of humans [1, 2]. The water quality of the Algerian dams in recent years has been degraded due to their over-exploitation by a rapidly growing population and affected by different sources of pollution [3, 4]. Multivariate analysis methods are widely used for physicochemical data-sets, these analyses give a general idea about the sources of pollution. During four

sampling campaigns, many hydro-chemical data were acquired on surface waters from the twenty dam lakes in central and north-central Algeria. A series of samples was conducted in order to monitor the water quality in the dams, and to study the temporal variation of chemical parameters from these waters, with the application of certain multivariate analyses to find the relations that exist between them.

2 Materials and Methods

A total of 80 representative water samples were collected between January and December 2017 at the different dams located in north Algeria, illustrated in Fig. 1. The following physicochemical and organic data: pH, water temperature (WT), Total solids (RS), nitrate (NO_3^-), ammoniac (NH_4^+), phosphate (PO_4^{3-}), oxygen concentration level (DO), chemical oxygen demand (COD), biochemical oxygen demand after 5 days (BOD_5), and organic matter (OM) were analyzed in the national agency of water resources (NAWR) according to the standard methods as suggested by Rodier [5].

Cluster analysis was used to explore the similarities between water samples and to group each similar site in the cluster with respect to a predetermined selection criterion.

3 Results and Discussion

3.1 Water Quality Evaluation

The results of the average concentration of physicochemical parameters in the studied dams are shown in Fig. 2. Fluctuations in dissolved oxygen values are noted throughout the period. The super-saturations are recorded in the Kaddera and Ladrat Dams (104 and 103% respectively), pH values range from a minimum of 7.6 at Harreza Dam to a maximum of 8.3 at Hamiz Dam. The Rs concentration shows a significant variation between study sites, and varied between 1752 and 353 mg L^{-1} . The average nutrient concentrations

S. Hamil (✉) · M. Baha
L.E.B.A., ENS, Kouba, Algeria
e-mail: dj.soumia@hotmail.fr

S. Hamil · D. Bouchelouche · S. Arab · N. Doukhandji ·
G. Smaoune · A. Arab
LaDyBio; FSB, USTHB, Bab Ezzouar, Algeria

S. Arab
FST/GAT, USTHB, Bab Ezzouar, Algeria



Fig. 1 Location of the study sites; Tich (Tichy haf), Tile (Tilesdite), Tak (Taksebt), Lakh (Lakhel), BniA (Bni Amran), K.Ase (Kodiat Aserdoun), Ham (Hamiz), Kadd (Keddara), Lad (Ladrat), Ghr (Ghrib),

Bour (Bouromi), Bouk (Boukerdan), Deur (Deurdeur), Harr (Harraza), O.mel (Oued Mlouk), S.ahm (Sidi m'ahmed bentiba), Fod (Fouda), Tekz (Tekzal), S.yak (Sidi Yakoub), Mer (Merad)

in the waters of the different study sites show an instability of concentrations, which indicates the presence of pollution. A peak of NO_3^- concentration is observed at the Bouroumi Dam (9.7 mg L^{-1}). The high concentrations of phosphorus are recorded at the Sidi Yakoub and Harraza Dam with 0.31 and 0.306 mg L^{-1} , respectively. The chemical oxygen demand varies considerably between the studied dams (between 5 and 25 mg L^{-1}), while the biological demand has a “not significant” variation.

3.2 Multivariate Analysis

Cluster analysis was used to detect the similarity groups between the sampling sites. It yielded a dendrogram, grouping the sampling sites on the basis of percentage of similarity and dissimilarity of water quality parameters. Figure 3, showing the results of the CA, indicates that the sampling sites are similar and clustered into five distinct regions as follows: The first cluster includes two reservoirs: Ghrib and Herraza Dams. This group is characterized by a strong mineralization whose concentration of SR is more than 1600 mg L^{-1} .

The second cluster includes six dams (Tichy-hef, Sidi yakoub, Oued melouk, Deurdeur, and Koudiat Aserdoun) which are characterized by an average mineralization above 1000 mg L^{-1} , and a high concentration of organic matter.

The third cluster includes the dam lakes which are characterized by a low level of mineralization (R_s is less than 500 mg L^{-1}). The Bni Amran, Bouroumi, Lakhel, Keddara, Fouda and Merad dams are grouped in the same cluster, which presents well-oxygenated waters. The last cluster includes the dam lakes of Hemiz, Tekzel, Boukerdan and Ladrat, characterized by high concentrations of nitrate and phosphorus, and also a large biological oxygen demand. The elevated concentration of total solids may not explain the presence of ions (cations and anions) leading to a high degree of mineralization [6]. These research results suggest that the strong mineralization of the dam waters of the first cluster can be associated mainly with the geological nature of the lands crossed by the wadi which are alimending these dams' water. The presence of PO_4^{3-} and NO_3^- in water generally originates from fertilizer application on farms. Agricultural land use strongly influences stream phosphorus and nitrate nitrogen.

4 Conclusions

In this study, we monitored the water quality of the surface in twenty dams in Algeria. The majority of the studied parameters indicated a significant spatial variability. The water quality of the dams generally reflects the quality of the water in their watersheds. The strong mineralization in the

Fig. 2 Spatial variation of the average concentrations of some physicochemical parameter in study sites

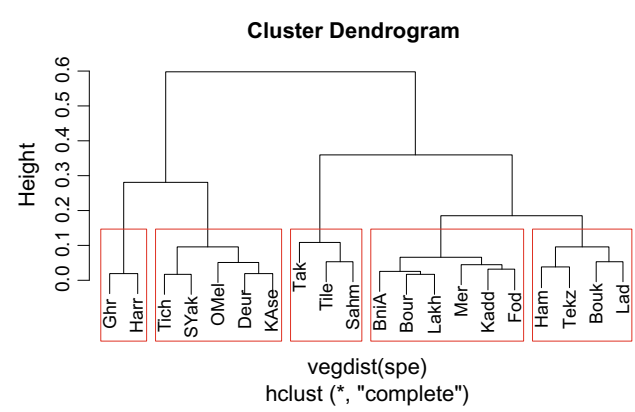
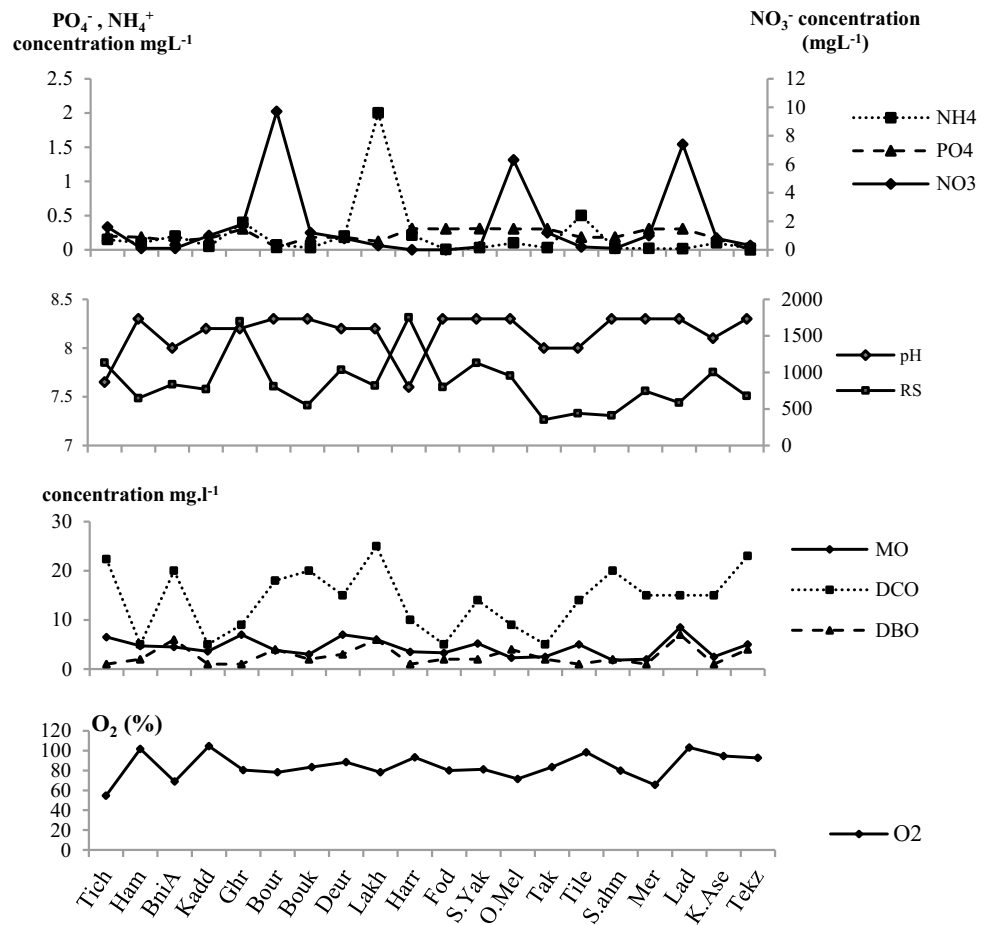


Fig. 3 Dendrogram showing clustering of sampling stations according to surface water quality characteristics of some lakes Dam in Algeria

Ghrif and Herraza dams is relatively associated with the geological nature of the wadis flowing into the dam. Also, the increase in the nutrient concentration in some dams is due to the excessive use of agricultural fertilizers for fields located near the dam or its sedimentary basin.

References

1. Zhao, A.Y., Xia, X.H., Yang, Z.F., Wang, F.: Assessment of water quality in Baiyangdian Lake using multivariate statistical techniques. *Proc. Environ. Sci.* **13**, 1213–1226 (2012)
2. Barakat, A., El Baghdadi, M., Rais, J., Aghezzaf, B., Slassi, M.: Assessment of spatial and seasonal water quality variation of Oum Er Rbia River (Morocco) using multivariate statistical techniques. *J. Soil Water Conserv.* **4**, 284–292 (2016)
3. Hamil, S., Baha, M., Arab, S., Doukhandji, N., Arab, A.: A multivariate analysis of water quality in Lake Ghrif, Algeria. In: Kallel, A., Ksibi, M., Ben Dhia, H., Khélifi, N. (eds.) *Recent Advances in Environmental Science from the Euro-Mediterranean and Surrounding Regions. EMCEI 2017. Advances in Science, Technology & Innovation*, pp. 805–807. Springer, Cham (2017)
4. Arab, S., Arab, A.: Effect of the physico-chemical parameters on the distribution of the fecal flora in a dam reservoir (Algeria). *Rev. Écol. Terre Vie* **72**, 269 (2017)
5. Rodier, J.: *L'analyse de l'eau: Eaux naturelles, Eaux résiduaires, Eaux de mer*, 9th edn. Dunod, Paris (2009)
6. Gumbo, J.R., Dzaga, R.A., Nethengwe, N.S.: Impact on water quality of Nandoni water reservoir downstream of municipal sewage plants in Vhembe district, South Africa. *Sustainability* **8**, 597 (2016)

Application of Water Quality Index for Surface Water Quality Assessment Boukourdane Dam, Algeria

Siham Arab, Djaouida Bouchelouche, Somia Hamil, and Abdeslam Arab

Abstract

Boukourdane dam in Northern Algeria plays a fundamental role in the local society as a source of irrigation and drinking water. In order to characterize the temporal variability of water quality in the dam lake, monthly monitoring was conducted for a period of 2 years (January 2013–January 2015) at four sites. The water in the dam tended to be alkaline, with the highest pH = 9.95 recorded in the spring of 2013. The highest value of temperature was recorded in summer (37.6 °C). The dissolved oxygen levels varied between 2.58 and 11.61 mg L⁻¹. Nitrates were low and the fecal coliform ranged between 85.60 and 1099.67 UFC mL⁻¹. The overall water quality in the Boukourdane dam is medium to good according to SEQ-EAU (Normes de qualité des eaux des masses d'eau naturelles [4]). To confirm these results, we calculated the water quality index (WQI); during the study period, the WQI varied between 60 and 72. The water quality is frequently impaired; conditions often depart from desirable levels which classified the water quality as medium. There was a general trend of decrease in the summer and autumn of 2014 and this is the result of natural processes (degradation of organic matter as well as the concentration of nutrients in those seasons).

Keywords

Water quality • WQI • Physico-chemical parameters • Boukourdane dam • Algeria

S. Arab (✉) · D. Bouchelouche · S. Hamil · A. Arab
Laboratory of Dynamics and Biodiversity, FSB, USTHB,
LP 32 El Alia, Bab Ezzouar, Algiers, Algeria
e-mail: sihemarab@gmail.com

S. Arab
FSTGAT—USTHB, LP 32 Alia Bab Ezzouar, Algiers, Algeria

S. Hamil
L.E.B.A., ENS, Kouba, Algeria

1 Introduction

The quality of surface water depends primarily on the geological formation of a particular region, and other factors such as leachate from solid waste dumping sites, municipal solid waste, etc. This latter may have a direct effect on the surface water quality, and directly threaten the integrity of the aquatic ecosystems. Recognizing and understanding the relative influence of natural and human-induced processes on hydrological and biochemical functioning are prerequisites for improved water resources management. Therefore, in this study, the water quality index was monitored for 2 years (January 2013–January 2015) at four different stations.

2 Materials and Methods

Boukourdane dam is located on the bed of wadi El Hachem, at the juncture of two principal intermittent wadis, Menacer and Fedjana. The site is 11 km from the Mediterranean Sea in a catchment area of over 177 km². The climate is typically Mediterranean, with a dry and hot period of 5 months, stretching from mid-May to mid-October.

Six parameters were measured, three of them were measured in situ which are water temperature, pH and dissolved oxygen, determined using a Multi 340i/SET WTW analyzer, and two physicochemical parameters, nitrate and phosphate—analyzed in the laboratory using the colorimetric method with a continuous flow on an automated chain (SKALAR). Samples were also analyzed for fecal coliforms according to the protocol described by [3].

National Sanitation Foundation Water Quality Index (NSF-WQI) is used to determine the level of water quality, based on physico-chemical parameters such as: Dissolved oxygen, nitrate, phosphate, temperature, pH, and Fecal Coliform. This technique, developed by [1] using the Delphi method, was done by selecting parameters rigorously,

Table 1 Seasonally environmental variables and fecal coliform summarized with their means (\pm SD), for the Boukourdane lake dataset

Obs		WT ($^{\circ}$ C)	pH	O ₂ d (mg L ⁻¹)	NO ₃ (mg L ⁻¹)	PO ₄ (mg L ⁻¹)	CF (UFC/100 ml)
Winter.13	Moy \pm SD	13.05 \pm 0.65	7.95 \pm 0.28	7.450.34	0.017 \pm 0.007	0.137 \pm 0.008	85.60 \pm 91.16
Spring.13	Moy \pm SD	17.56 \pm 1.85	8.32 \pm 0.69	6.56 \pm 1.09	0.170 \pm 0.179	0.680 \pm 0.677	283.11 \pm 535.86
Summer.13	Moy \pm SD	23.79 \pm 3.30	7.71 \pm 0.32	5.88 \pm 1.65	0.045 \pm 0.031	0.286 \pm 0.545	313.11 \pm 512.55
Autumn.13	Moy \pm SD	20.53 \pm 3.98	7.98 \pm 0.29	6.85 \pm 1.22	0.053 \pm 0.030	0.038 \pm 0.023	1061.59 \pm 1100.98
Winter.14	Moy \pm SD	13.26 \pm 0.63	8.54 \pm 0.29	6.81 \pm 2.10	0.084 \pm 0.049	0.019 \pm 0.018	1099.67 \pm 1086.11
Spring.14	Moy \pm SD	18.02 \pm 3.24	7.96 \pm 0.62	6.00 \pm 1.37	0.452 \pm 0.789	0.086 \pm 0.218	314.00 \pm 579.16
Summer.14	Moy \pm SD	24.46 \pm 3.62	7.83 \pm 0.34	5.13 \pm 1.42	0.047 \pm 0.027	0.037 \pm 0.025	751.33 \pm 975.81
Autumn.14	Moy \pm SD	20.90 \pm 3.45	8.05 \pm 0.32	5.86 \pm 1.15	0.017 \pm 0.010	0.041 \pm 0.008	289.28 \pm 568.85
Winter.15	Moy \pm SD	13.23 \pm 1.67	8.09 \pm 0.10	7.58 \pm 1.13	0.073 \pm 0.014	0.036 \pm 0.010	1426.00 \pm 1123.34

developing a common scale and assigning weights to the parameters.

$$WQI = \sum_{i=1}^n WiQi$$

$$I = \sum_{i=1}^n IiWi$$

where, $\sum_{i=1}^n Wi = 1$, Ii = Sub-index of each parameter, Wi = Weighting factor, Qi = is the rating value of parameter i and n = Number of sub-indices.

3 Results

The water in the dam tended to be alkaline, with the highest pH = 9.95 recorded in the spring of 2013. The highest value of temperature was recorded in summer (37.6 $^{\circ}$ C). The dissolved oxygen levels varied between 2.58 and 11.61 mg L⁻¹. The nitrates were low (Table 1).

We calculated the water quality index (WQI) during the study period, the WQI varied between 60 and 72 (Table 2).

4 Discussion

The overall water quality in the Boukourdane dam is medium to good according to [4]. The water quality is frequently impaired; conditions often depart from desirable levels which classified the water quality as medium. There was a general trend of decrease in the summer and autumn of 2014 and this is the result of natural processes (degradation of organic matter as well as the concentration of nutrients in those seasons) [2].

Table 2 Water quality index values

Season	WQI
Winter 2013	72
Spring 2013	65
Summer 2013	66
Autumn 2013	64
Winter 2014	64
Spring 2014	66
Summer 2014	60
Autumn 2014	61
Winter 2015	66

5 Conclusion

Establishing a network to monitor the water quantity and quality provides the basis for characterizing the lacustrine system as well as the impacts of the domestic discharges on the site and surrounding environment. The data can be used for assessing impacts on downstream aquatic ecosystems, as well as to limit risks of pollution. The 2015–2017 rainfall was relatively low compared to our study period, so there is no significant amount of run-off, which means that the water quality has not significantly changed.

The results of this study could help in pollution management and in projects for the preservation of this Wetland. The use of micro-organisms for their rapid response and evolution related to the environmental changes increases the interest of their ecological follow-up and can be a good method to support the results of WQI for the water quality determination.

References

1. Brown, R.M., McClelland, N.I., Deininger, R.A., Tozer, R.: A Water Quality Index. Do we dare? Water and Sewage Works (1970)
2. Hamil, S., Baha, M., Arab, S., Doukhandji, N., ARAB, A.: A multivariate analysis of water quality in lake Ghrib, Algeria. In: Kallel, A., Ksibi, M., Ben Dhia, H., Khélifi, N. (eds.) Recent Advances in Environmental Science from the Euro-Mediterranean and Surrounding Regions. EMCEI 2017. Advances in Science, Technology & Innovation, pp. 805–807. Springer, Cham (2017)
3. Rodier, J., Legube, B., Merlet, N., et al.: L'Analyse de l'eau. 9emeEd. Dunod, Paris (2009)
4. Systeme d'évaluation de la qualite de l'eau (SEQ-Eau). Normes de qualité des eaux des masses d'eau naturelles. Directive cadre eau européenne MEED et agence de l'eau (2014)

Cumulative Probability and Water Quality Index (WQI) for Finding Drinking Water Suitability in a Tannery Belt (Southern India)

Nepal Mondal

Abstract

Groundwater quality is continuously getting polluted due to the increasing human activities and the rapid growth of urbanization in and around a tannery belt of Southern India, where around 80 functioning tanneries are discharging untreated effluents into open land and channels. Detecting and evaluating the effects of industrial and human activities are keys to finding the hydrochemical backgrounds and drinking water suitability. Thus, this paper deals with the cumulative probability distribution of analytical hydrochemical data, which was adopted to estimate the backgrounds on groundwater quality as well as quantify its abnormality. Results show two types of threshold values. The first threshold values of TDS, Ca^{2+} , Mg^{2+} , Na^+ and K^+ ions are estimated at about 906, 182, 60, 160 and 5 mg/l, respectively, whereas 191, 280, 109 and 12 mg/l for Cl^- , HCO_3^- , SO_4^{2-} and NO_3^- ions. They directly indicate the background levels of these ions. The second threshold values indicate the strong influence areas, mainly distributed in and around the tannery clusters. Furthermore, Water Quality Index (WQI) shows that there is no excellent groundwater type but about 59% of the samples are of poor quality for drinking water use.

Keywords

Groundwater pollution • Cumulative probability • Water quality index (WQI) • Drinking water • Tannery industry

1 Introduction

Nowadays, groundwater is being deteriorated progressively due to the human activities [1, 2]. In addition to these activities, groundwater quality is also changed by the impacts of natural factors [3, 4]. Therefore, it is not so easy to determine the backgrounds of groundwater quality in the presence of industrial and human activities on a large scale [5]. There are several approaches utilized to derive natural backgrounds [6]. Some parametric approaches use the statistics via a normal or log-normal distribution, mode analysis, component separation method, pre-selection approach and relative cumulative probability distribution. Of course, the cumulative probability distribution approach based on the knowledge about geochemical processes and abundance of monitoring data has also been used [7]. Apart from this, if the values of hydrochemical parameters are more than the permissible limits/maximum acceptable ranges, the water could be considered as unfit for drinking purposes, which leads to harming human health. Therefore, the Water Quality Index (WQI), one of the most important hydrochemical indicators, has been used to describe the water suitability for drinking purposes [8]. Nowadays, groundwater and eco-systems are continuously being polluted by the tannery industries which are located in many parts of the world and also in India [9, 10]—like the tannery cluster located at Dindigul town in Southern India, which was established in 1939. These industries have since then been spreading and more than 80 tanneries are now well-established. These industries are the major source of groundwater contamination, which leads to health problems of the human beings [9]. Therefore, the main objectives of this research paper are to (1) undertake a hydrochemical analysis, (2) estimate backgrounds using cumulative probability for demarcating the occurrence of pollutants, and (3) assess the drinking water suitability.

N. Mondal (✉)

Earth Process Modeling Group, CSIR-National Geophysical Research Institute & Academy of Scientific & Innovative Research (AcSIR, CSIR-NGRI), Hyderabad, Telangana, India
e-mail: mondal@ngri.res.in

2 Materials and Methods

For assessing background and drinking water suitability, 29 groundwater samples were collected from dug wells, bore wells and hand pumps (depth range: 5.0–65.0 m, bgl). Methods of the sample collection and analysis were followed as given by APHA [11]. The precise sample locations were taken using a handled Global Position System (GPS) during the field work. The Cumulative probability distribution of hydrochemical parameters was adopted to separate the anomalous features from the backgrounds which were affected locally by salinization and/or anthropogenic pollution [12] and also to observe its distribution. These plots and distributions were considered to interpret hydrochemical levels of individual parameters. The Water Quality Index (WQI) is defined as a rating reflecting the composite influence of different water quality parameters on the overall quality of water [13]. It had been calculated to evaluate the drinking water suitability. The computed WQI values were utilized to classify groundwater into five types from “excellent water” to “unsuitable” for drinking water.

3 Results and Discussion

Total Dissolved Solids (TDSs), chloride (Cl^-), sodium (Na^+), sulphate (SO_4^{2-}) and nitrate (NO_3^-) concentrations as per the guide line of World Health Organization for drinking water are 500, 200, 200, 200 and 45 mg/l, respectively. When the hydrochemical parameters of the study area were compared with these standards, it was shown that about 96, 72, 62, 52 and 3% of the samples exceeded the limits for the TDS, chloride, sodium, sulphate and nitrate values, respectively. This indicates that the groundwater quality had significantly deteriorated. Types of water were mainly in NaCl , CaCl_2 , Ca-HCO_3 , mixed, and Na-HCO_3 types. The degree of salinization at the monitoring well was indicated by enhancing the TDS values, which possibly increases all the major ions. Most of the solute concentrators having wide ranges and high standard deviations suggest that several sources and/or complex hydrochemical processes acted in accord to make the hydrochemical composition.

The cumulative probability distributions of TDS, Ca^{2+} , Mg^{2+} and Na^+ had three individual intersections with two distinct inflection points on the cumulative plots. It had been presumed that the regional threshold values as well as the highly impacted threshold values had differentiated the analysed samples. These samples were perhaps affected by the geogenic and anthropogenic activities, and the saline water mixing in this area. The first threshold values obtained were 906 mg/l for TDS, 182 mg/l for Ca^{2+} , 60 mg/l for

Mg^{2+} , and 160 mg/l for Na^+ . Similarly, the first threshold values obtained were 191 mg/l for Cl^- and 109 mg/l for SO_4^{2-} corresponding to the second values, which were 390 and 310 mg/l, respectively. The samples having more than the first threshold values in groundwater were highly affected by anthropogenic activities and other processes in the several folds. The spatial distribution of plume, along with the backgrounds, had been plotted as individual constituents on the same plate. This information helps to demarcate the occurrence of pollutants and assign a background level for the preparation of mass transport modelling. For example, except for a small part in the south-east of the site, the background level of TDS value was more than the limit of drinking water (TDS = 500 mg/l [14]). But its estimated value was more than the background level in almost the entire study area, and particularly, the impact was more in the tannery clusters. The chloride concentration at all the sampling locations, as well as their backgrounds, was more than the permissible limit [14] and the maximum occurrence was obtained in the middle part of the study area, where the tannery clusters occur.

The WQI is one of the cumulative indices for evaluating groundwater quality and its suitability for the society [15, 16]. In the study area, the WQI values were calculated and varied from 92 to 349. In this tannery belt, about 59% of groundwater samples were of poor quality and only 3% of the samples were found to be of good quality for drinking purposes. About 31 and 7% of the samples had very poor and unsuitable water quality, respectively. There was no sample found in the excellent for drinking water category during the experimental period.

4 Conclusions

The objectives of this paper were to assess groundwater quality for drinking purposes and identify the hydrogeochemical backgrounds of the analytical data, using the cumulative probability distribution in a tannery belt, Southern India, an area continuously affected by the untreated tannery effluents. The results show that there are several degrees of abnormality in hydrochemical data estimated by the threshold values. The threshold values are of two types which indicate three main processes. The first threshold values of TDS, Ca^{2+} , Mg^{2+} , Na^+ , K^+ , Cl^- , HCO_3^- , SO_4^{2-} and NO_3^- ions are about 906, 182, 60, 160, 5, 191, 280, 109 and 12 mg/l, respectively, indicating the backgrounds in the tannery belt. However, the second threshold values are about 2896, 442, 136, 424, 12, 390, 360 and 310 mg/l, respectively, for these ions except for the NO_3^- indicating the resilient environmental influence areas which are located in and around the industrial clusters. The Water Quality Index

(WQI) shows that there is no excellent water type to be used as drinking water, but about 59% of the water samples are of poor quality. This information helps initially to demarcate the occurrence of pollutants and to attribute the backgrounds for mass transport modelling, which will serve as support for the judicial use of drinking water.

References

1. Mondal, N.C., Singh, V.P.: Hydrochemical analysis of salinization for a tannery belt in Southern India. *J. Hydrol.* **405**(2–3), 235–247 (2011)
2. Li, J., et al.: Method for screening prevention and control measures and technologies based on groundwater pollution intensity assessment. *Sci. Total Environ.* **143**, 551–552 (2016)
3. Guo, H.M., et al.: Contrasting distributions of groundwater arsenic and uranium in the western Hetao basin, Inner Mongolia: implication for origins and fate controls. *Sci. Total Environ.* **541**, 1172–1190 (2015)
4. Mondal, N.C., et al.: A diagnosis of groundwater quality from a semiarid region in Rajasthan, India. *Arab. J. Geosci.* **9**(12), 602, 1–22 (2016)
5. Peng, C., et al.: Identifying and assessing human activity impacts on groundwater quality through hydrogeochemical anomalies and NO_3^- , NH_4^+ , and COD contamination: a case study of the Liujiang River Basin, Hebei Province, P.R. China. *Environ Sci Pollut Res* **25**, 3539–3556 (2018)
6. Matschullat, J., et al.: Geochemical background—can we calculate it? *Environ. Geol.* **39**, 990–1000 (2000)
7. Caro, M.D., et al.: Hydrogeochemical characterization and Natural Background Levels in urbanized areas: Milan Metropolitan area (Northern Italy). *J. Hydrol.* **547**, 455–473 (2017)
8. Singh, A.N., et al.: Assessment of groundwater quality using GIS—a case study of the Churu District of Rajasthan. *Water Res. Manag.* **5**(4), 35–43 (2015)
9. Mondal, N.C., Singh, V.P.: Need of groundwater management in tannery belt: a scenario about Dindigul town, Tamil Nadu. *J. Geol. Soc. India* **76**(3), 303–309 (2010)
10. Hassen, A.S., Woldeamanuale, T.B.: Evaluation and characterization of tannery waste water in each process at Batu and Modjo Tannery, Ethiopia. *Int. J. Environ. Sci. Nat. Res.* **8**(2), 555732, 1–9 (2018)
11. American Public Health Association (APHA): Standard methods for the examination of water & waste. 16th edn. Am. Public Health Assoc. (1985)
12. Sinclair, A.J.: Selection of thresholds in geochemical data using probability graphs. *J. Geochem. Explor.* **3**, 129–149 (1974)
13. Horton, R.K.: An index number system for rating water quality. *J. Water Pollut. Cont. Fed.* **37**(3), 300–305 (1965)
14. World Health Organization (WHO): Guideline of drinking quality. Washington, DC, World Health Organization (1984)
15. Gorde, S.P., Jadhav, M.V.: Assessment of water quality parameters: a review. *Int. J. Eng. Res. Appl.* **3**(6), 2029–2035 (2013)
16. Mondal, N.C.: Reconnoitering hydrochemical background using log-probability distribution in a Channel Island, Andhra Pradesh. In: 5th National Conference Proceeding on Water, Environment & Society, pp. 271–277, BSP Books Pvt. Ltd., Hyderabad (2018)

Bio-Evaluation of Water Quality in an Algerian Dam by the Application of Biotic Indices; Case of Ghrib Dam

Somia Hamil, Siham Arab, Djaouida Bouchelouche, Mounia Baha, and Abdeslem Arab

Abstract

The watershed Cheliff-Ghrib undergoes important anthropogenic pressures which mainly affect the river of Cheliff and the Ghrib reservoir. Dammed water is used, without preliminary treatment, for farm irrigation. This work is a biological characterization of the quality of water of the Ghrib Dam. Surface water samples were taken monthly (2014–2016) from 3 sites from the dam. We determined Species Richness (Margalef's diversity index) as well as biological quality using saprobity index. By qualitative and quantitative analysis of the zooplankton community, 51 bio-indicator species were recorded from 3 groups in the dam. The results of the saprobity index show that the water quality is between Oligo to Beta Mesosaprobic (very slight pollution to moderate pollution). Thus, any change or altering in the water body due to anthropogenic activities, agricultural runoff and various other factors, accounts for the increase or decrease in physi-chemical parameters, which in turn results in the change of the zooplankton composition in the Ghrib Dam.

Keywords

Pollution • Saprobity index • Bio-evaluation • Rotifera • Algeria

1 Introduction

Water pollution is one of the most common problems in the world. Continuous monitoring is required for the sustainability of water resources and registered changes [1]. The use of zooplankton as indicators of subtle changes in water quality is highly efficient due to their rapid reproduction and responsiveness to environmental changes [2]. They may be useful as easily identified bioindicators of undisturbed and semi-natural conditions [3]. Recently, the saprobic system was used to assess water quality by zooplankton. This study aims to determine the zooplankton structure and to assess the water quality of Ghrib Dam using zooplankton as a tool of the saprobity index.

2 Materials and Methods

Ghrib Dam was implanted on the wadi Chélif in the northwestern part of Algeria and it is located between 36° 12'–36° 16'N and 2° 55'–2° 60'E (Fig. 1). To obtain significant results, the sampling of waters has been carried out monthly from 2014 to 2016 in three stations; 5 L were taken from surface water at each sampling site by filtering through a zooplankton net of 50 µm mesh diameter. The collected samples were preserved by 5% formalin. In laboratory, the samples were studied under the compound microscope and specimens identified at the species level when possible.

2.1 Data Analysis

Species Richness Index or Margalef's diversity index (d), commonly varies between 1 and 5, where a larger index indicates a healthier water body and when the index tends towards 1, pollution is thought to increase [4]. It is expressed by $d = S - 1/\log N$ where (S) is the total number of species and (N) is the total number of individuals.

S. Hamil (✉) · M. Baha
L.E.B.A., ENS-Kouba, Algiers, Algeria
e-mail: dj.soumia@hotmail.fr

S. Hamil · S. Arab · D. Bouchelouche · A. Arab
LaDyBio, FSB, USTHB Bab-Ezzouar, Algiers, Algeria

S. Arab
FST/GAT, USTHB Bab-Ezzouar, Algiers, Algeria

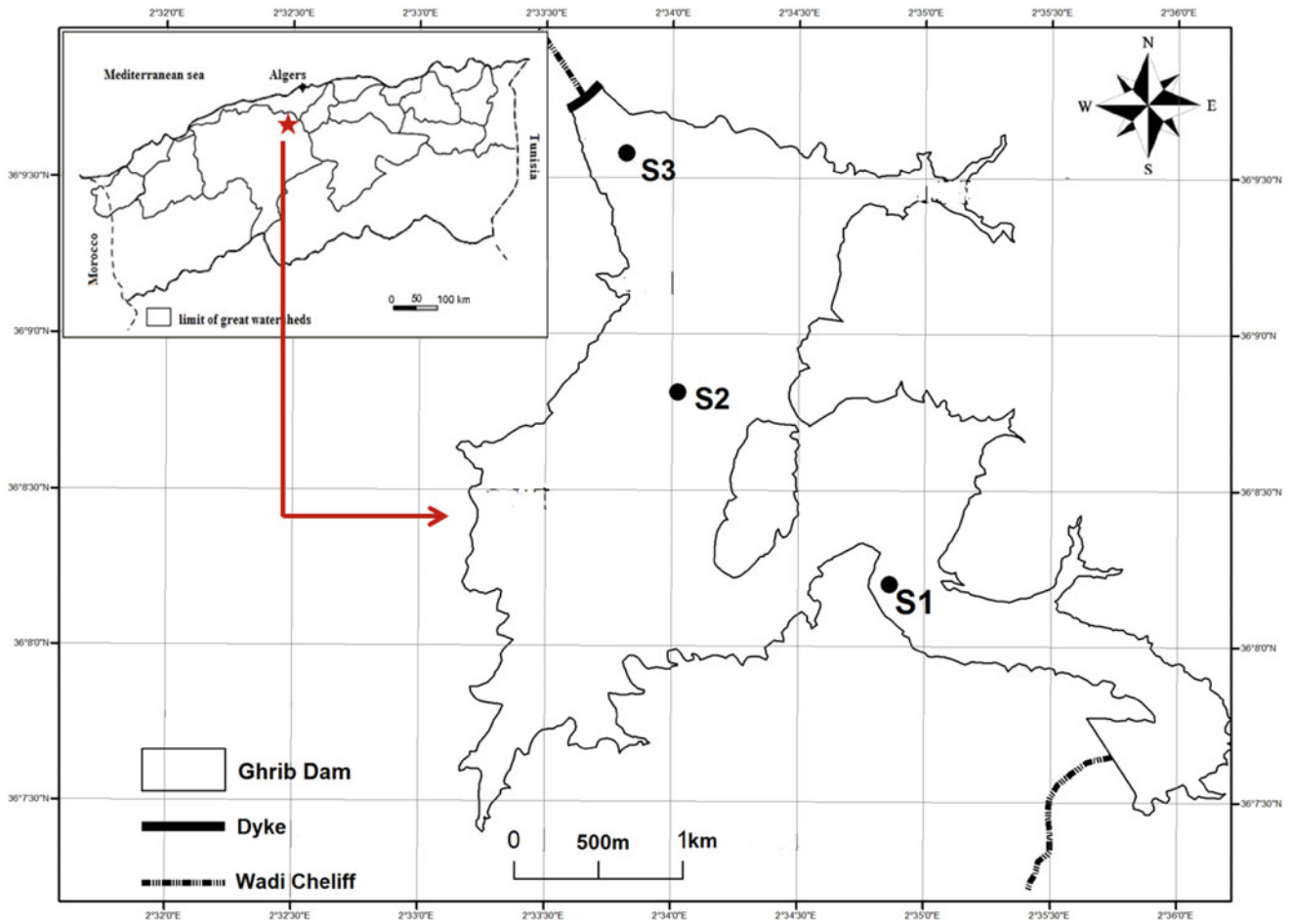


Fig. 1 Location of the study area

The saprobity index (SI) of water was evaluated after Sládeček [5], employing the equation of Zelinka and Marvan [6].

3 Results

3.1 Zooplankton Structure

During this study, we observed 63 taxa of zooplankton (3 Copepoda, 15 Cladocera, and 45 Rotifera). Rotifers were the

most diverse and dominant group in the three localities, including several indicator species of eutrophication; *Keratella quadrata*, *Diaphanosoma brachyurum*. The most species-rich family was Brachionidae with 15 species. The rest of the families were represented by just a few species. *Keratella quadrata* was present during most of the study period with important densities.

At the three studied localities, the highest value of richness index D_{mg} (5.7) was detected in January (Fig. 2), while the lowest one (1.33) was recorded in November and December 2015.

Fig. 2 Temporal changes of richness index D_{mg} in Ghib Dam

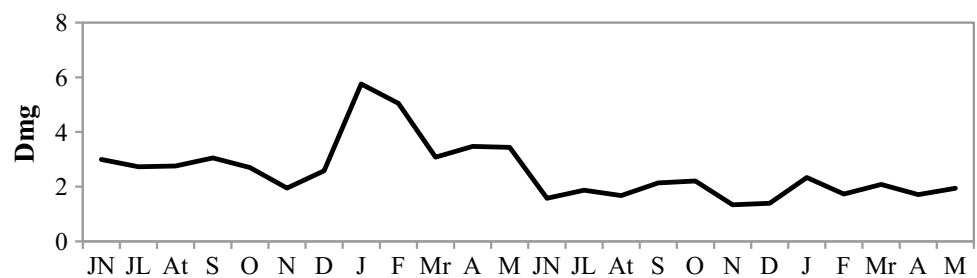
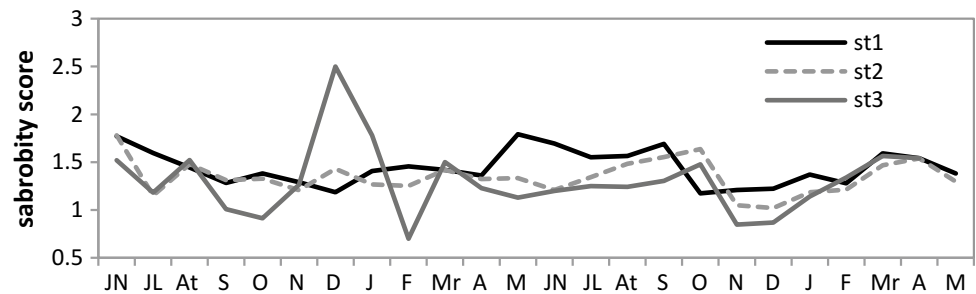


Fig. 3 Temporal changes of saprobity index scores at different sites of Ghrib Dam



3.2 Bio-Evaluation of Water Quality

The composition of zooplankton communities clearly reflects values of saprobity index. Out of 63 species that were harvested in the Ghrib, 51 species were bio-indicators. Mean values of the saprobity index along the stations ranged between 0.7 and 2.5. The highest values were recorded at station (St3), particularly in December 2014 (1.79) (Fig. 3). Significant differences in the value of the saprobity index were recorded at the three stations ($p < 0.05$), i.e., its values clearly indicate a change in the water quality. The results of the saprobity index show that the water quality along the investigated localities is between the first and second class, i.e., from oligo to beta mesosaprobic. There was a general trend of decrease in the saprobity index from the beginning to the end of the seasons. This is a result of natural processes (terminated degradation of introduced organic matter as well as settlement of suspended matter introduced with the water supply).

4 Discussion

Zooplankton can be used as “bioindicators” of water pollution, because their occurrence, vitality and responses, change under adverse environmental conditions [7]. Rotifers are one of the sensitive indicators but pose difficulties in acquiring adequate taxonomic skills to identify them. Nevertheless, it has been well documented that Brachionids are indicators of eutrophic waters [5]. During this study this group was dominant in both localities. Their dominance in Lake Ghrib is due to the abundance of *Keratella quadrata* which mainly characterized the eutrophic system [8, 9]. Saprobiological analysis at the localities showed that is ranged from oligo and β -mesosaprobic, i.e., from very slight pollution to moderate pollution. Oligo- β mesosaprobic and β -mesosaprobic rotifers account for the major fraction of the zooplankton (*Asplanchna* sp, *Cephalodella* sp, *Hexarthra* sp, *Keratella* sp, *Lecane* sp, *Polyarthra* sp and *Trichocerca* sp). However, just some inventory species are alpha-mesosaprobic and polysaprobic (*Epiphanes santa*, *Rotaria rotatoria* and *Brachionus rubens*, respectively). Admittedly, rotifers are good

indicators of saprobity [5], but this does not exclude the importance of the cladocerans as indicators of water quality. Many researchers [10] [11] determined the quality of several lakes based on the presence of some cladocerans (e.g. daphniidae, bosminidae, sididae, chydoridae, llyocryptidae), known for their bacterivore activity, namely phytophagous and detritivores.

5 Conclusions

This study concludes that, the saprobity index somewhat gives a good indication to assess the water quality of Lake Ghrib, and there are some developments that are needed according to the nature of the lake and their dominant zooplankton indicator species.

References

- Giardino, C., Brando, V.E., Dekker, A.G., Strombeck, N., Candiani, G.: Assessment 299 of water quality in Lake Gorda (Italy) using hyperion. *Remote Sens. 300 Environ.* **109**:183–195 (2007)
- Khalifa, N., El-Damhogy, K.A., Fishar, R.M., Nasef, A.M., Hegab, M.H.: Using zooplankton in some environmental biotic indices to assess water quality of Lake Nasser, Egypt. *Int. J. Fish. Aquat. Stud.* **2**(4), 281–289 (2015)
- Souty-Grosset, C., Badenhausser, I., Reynolds, J.D., Morel, A.: Investigations on the potential of woodlice as bioindicators of grassland habitat quality. *Eur. J. Soil Biol.* **41**, 109–116 (2005)
- Margalef, R.: Information theory in Ecology. *Int. J. Gen Syst.* **3**, 36–71 (1958)
- Sládeček, V.: Rotifers as indicators of water quality. *Hydrobiologia* **100**, 169–201 (1983)
- Zelinka, M., Marvan, P.: Zur Präzisierung der biologischen Klassifikation der Reinheit fließender Gewässer. *Arch. Hydrobiol.* **57**, 389–407 (1961)
- Oliver, J. Hao.: Bioindicators for water quality evaluation—a review. *J. Chin. Inst. Environ. Eng.* **6**(1):1–19 (1996)
- Geng, H., Xie, P., Deng, D., Zhou, Q.: The rotifer assemblage in a shallow, eutrophic Chinese lake and its relationships with cyanobacterial blooms and crustacean zooplankton. *J. Fresh Eco.* **20**, 93–100 (2005)
- Bozkurt, A., Tepe, Y.: Zooplankton composition and water quality of Lake Gölbasi (Hatay-Turkey). *Fresenius Environ. Bull.* **20**, 166–174 (2011)

-
10. Gannon, J.E., Stemberger, R.S.: Zooplankton (especially crustaceans and rotifers) as indicators of water quality. *Trans. Am. Microsc. Soc.* **97**(1), 16–35 (1978)
 11. Thouvenot, A., Richardot, M., Debroas, D., Devaux, J.: Bacterivory of metazooplankton, ciliates and flagellates in a newly flooded reservoir. *J. Plankton Res.* **21**(9), 1659–1679 (1999)

2D Water Quality Modeling of Dam Reservoir (Case Study: Doosti Dam)

Saeed Reza Khodashenas, Arezoo Hasibi, Kamran Davary,
and Bahman Yargholi

Abstract

Due to the developments in the field of computer sciences, numerous models have recently been developed for hydrodynamic and water quality assessment in water-bodies. Among these models, the two-dimensional laterally averaged CE-QUAL-W2 has received considerable attention worldwide and has become a commercial model in the recent decade. Considering the model's abilities and the need to study the Doosti dam, the present study examines the water quality parameters of the Doosti dam Reservoir, such as phosphorus, Nitrate, etc., over a year-long period. The model was calibrated and yielded satisfying results, especially in the case of water temperature. Here, the results for the period from 2013 to 2014 have been presented. The results showed a three-month thermal stratification in the reservoir. Also, results of quality parameters showed that the Doosti dam reservoir is in danger of eutrophication.

Keywords

Water quality • Modeling • Thermal stratification • CE-QUAL-W2 • Eutrophication

1 Introduction

Dams are one of the most important water-bodies that supply water for agriculture, irrigation, human consumption, and industrial use. They act as barriers which hold back the water, and by blocking the rivers which they are built upon, they turn them into lakes with stagnant water. Establishing a

dam means water availability to certain regions and drought to others. Stratification and the duration over which the water stays in the reservoir are two significant factors in changing the quality of the river waters before and after the dam.

Many reservoirs show a vertical stratification of their water masses, at least for some extended time periods. Stratification refers to a change in the water density at different depths in the reservoir, caused by temperature, salinity, and suspended solids. Recent progress in the field of reservoir water quality studies has led to the development of various hydrodynamic and water quality models for simulating water-bodies. Water quality modeling involves the prediction of physical, chemical, and biological changes in water bodies using mathematical simulation techniques. One of these models is CE-QUAL-W2 (W2), which is a two-dimensional, laterally averaged, hydrodynamic and water-quality model. It is capable of modeling basic eutrophication processes and is best suited for long, narrow water bodies [1]. In the last decades, W2 has been applied to hundreds of studies on various types of water bodies (rivers, reservoirs, lakes, and estuaries) all over the world [2]. Here, the results for the period 2013 to 2014 have been presented. This period was selected due to the complete setup data available relative to more recent years.

2 Approaches and Methods

2.1 Study Site

Doosti dam is built on the Harirood River, which is located 75 km south of the border city of Sarakhs, northeast of the Khorasan province, upstream of the Polkhatun Hydrometric station—longitude 14° 61', latitude 35° 54' (Fig. 1). This dam was built through a collaboration between Iran and Turkmenistan. The construction of the dam began in 2000 and was officially opened on 12 April, 2005, by both the president of Iran and the president of Turkmenistan.

S. R. Khodashenas (✉) · A. Hasibi · K. Davary
Water Engineering Department, Ferdowsi University of Mashhad,
Mashhad, Iran
e-mail: khodashenas@ferdowsi.um.ac.ir

B. Yargholi
Agricultural Engineering Research Institute, Karaj, Iran

Fig. 1 Doosti Dam location (Between Iran and Turkmenistan)



2.2 Geometry

The geometry data will be used to define the finite difference in the representation of the water-body. They quantify the height, length, width and the orientation of each cell used in a grid to describe the reservoir geometry. As shown in Fig. 2, the Doosti reservoir is simulated with one branch and divided into 41 segments in length, and 49 layers down to its deepest segment.

the temperature of the top layers of the water which are in contact with the cool air. The density of the cold water is higher than that of the warm water in the lower layers, which pushes the cold water down, thus replacing the warm water, and this mixing process occurs with the help of the wind. All of these changes occur under the withdrawal level of 455 m, that is the metalimnion layer. The other months do not show any significant changes in water temperature.

3 Results

3.1 Temperature (T)

According to Fig. 3, the maximum layering occurred during the summer, (i.e. in June 2014), when a difference of 20 °C between the top and the bottom layers of the reservoir was recorded. This severe layering lasted for 3 months, until September 2014—when it started to mix and became stable. This happens because when the weather gets colder, and the wind which starts blowing in this month causes a decrease in

3.2 Nitrate (NO₃)

Nitrate layering in the reservoir began in May 2014. When mountain snow begins to melt, the volume of water entering the reservoir increases. Severe Nitrate layering occurred in August 2014 and the metalimnion thickened. The other months of the year did not show any signs of Nitrate layering, there were just some changes in the length of the reservoir because of the temporary entrance of the polluting sediments into the reservoir. As depicted in Fig. 4, the high level of nitrate concentration exposes the reservoir to the danger of eutrophication.

Fig. 2 Finite difference grids representing the bathymetry of the Doosti reservoir, **a** top view (segments), **b** end view (layers), **c** side view (layers)

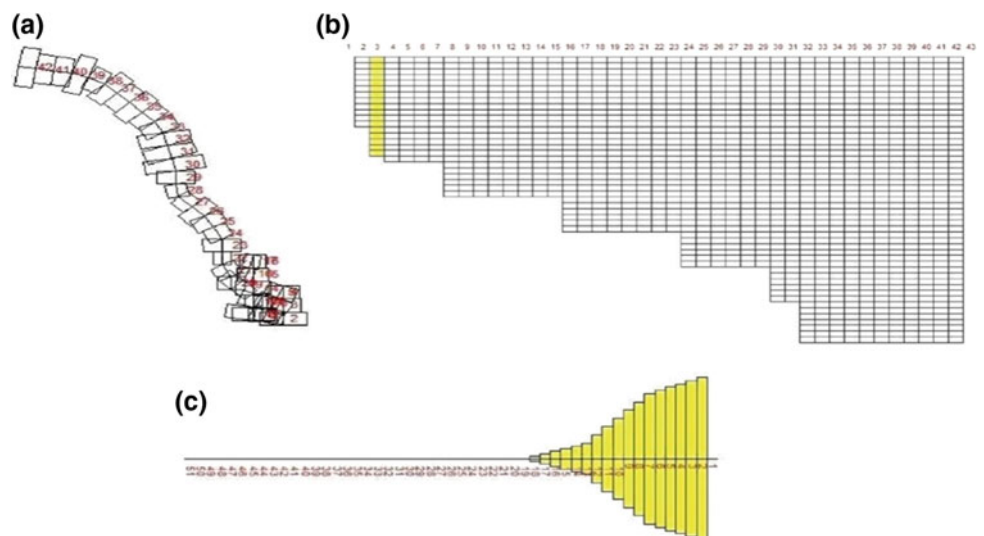


Fig. 3 Results of thermal stratification in Doosti Dam reservoir

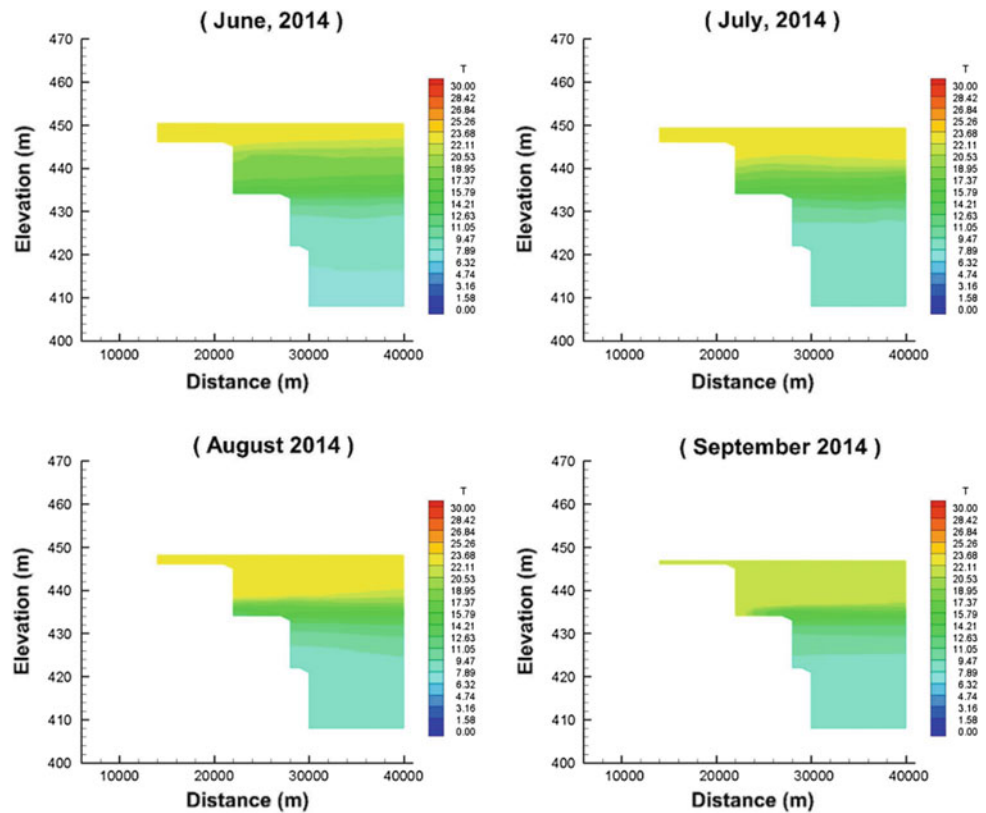
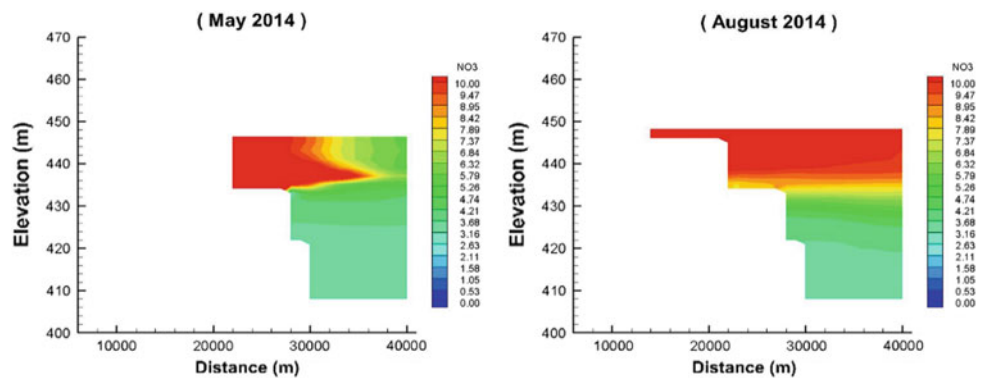


Fig. 4 Results of thermal stratification in Doosti Dam reservoir



4 Conclusions

The Doosti dam reservoir has a three-month thermal layering period, that starts from May 2014 and lasts until August 2014, with a temperature difference between Epilimnion and Hypolimnion of approximately 20 degrees centigrade. In the summer period, and as the air temperature increases, the water elevation in the reservoir reduces and the salinity level increases, which affects the reservoir performance.

Also, the reservoir is in danger of eutrophication because of the high level of nitrate concentration. This problem results in water with odor and a bad taste that affects the reservoir's performance as a municipal water

supply. Unlike the study of Khajepour et al. [3], the WSC coefficient had a negligible effect on the results of the model. It has been found that the W2 model can be calibrated with geometry elements and water elevation. In conclusion, this model was able to simulate the Doosti dam reservoir successfully, and we suggest to study this reservoir with different scenarios and water budgeting using this model.

References

1. Cole, T.M., Wells, S.A: CE-QUAL-W2: A Two-dimensional, laterally averaged, hydrodynamic and water quality model, Version

- 3.6 Instruction Report EL-06-1, U.S. Army Corps of Engineers, Washington (2014)
2. Razdar, B., Mohammadi, K., Samani, J., Pirooz, B.: Determining the best water quality model for the rivers in north of Iran (Case study: Pasikhan River). *J. Comput. Models Eng.* **2**(1), 109–121 (2011)
3. Khajepour, E., Eftekhari, M., Eghbal, A., Javan, M.: Calibration of numerical model CE-QUAL-W2 (Case study: 15-Khordad reservoir). In: *First National Conference on Water Flow and Pollution*, Tehran University, Tehran, Iran (2012)

Efficiency of a Neuro-Fuzzy Model Based on the Hilbert-Huang Transform for Flood Prediction

Zaki Abda, Mohamed Chettih, and Bilel Zerouali

Abstract

Flooding is a natural phenomenon, which constitutes a threat that could lead to loss of human life and material property. It constitutes the first major risk. During the last years, artificial intelligence has been widely applied in the field of hydrology and in many other fields of hydraulic engineering. The Hilbert-Huang Transform (HHT) is a new signal processing technique in the analysis of non-stationary time series, particularly effective for hydrological series. Currently, the application of intelligent hybrid systems in different areas has shown a good performance and an unequalled efficiency. As such, the hybrid technique of an adaptive neuro-fuzzy inference system (ANFIS) coupled to the Hilbert-Huang transform (HHT-ANFIS), was used in this study to estimate daily flow rates in Algiers' coastal basin. The results obtained are very encouraging and more efficient than those obtained by the neuro-fuzzy inference model and the classical multiple linear regression (MLR) model.

Keywords

Prediction • Flow • Intelligent hybrid model • Hilbert-Huang transform • Neuro-Fuzzy system

1 Introduction

In hydrology, a simplified mathematical representation of all or part of the processes of the hydrological cycle is indispensable. So, the hydrological concepts are expressed in mathematical language to represent the corresponding behaviour observed in nature. Floods are one of the most important natural risks. The damage they cause, the lives

they take, and the fear they generate have led researchers to prevent them from occurring by different techniques. The hydrological forecasting plays an important role in risk reduction and prevention against the water-related disasters. Modelling the hydrological behaviour of the watershed is essential to reduce the damage caused by the floods. The rainfall-runoff models are essential tools for calculating the project of flood or forecasting short-term flood. Although a lot of research has been done on them, the models remain difficult and uncertain [1, 2].

In hydrology, intelligent hybrid models have been widely applied in several highly different regions and at different scales. Numerous works were realized and proved the efficiency of these models, even if they remain pragmatic, their performances remain superior to the other models. Among these works, we can cite, among others, the works of [3–6].

In this work, we propose an intelligent hybrid model by combining the HHT technique with ANFIS (HHT-ANFIS) for forecasting the daily flow of the Oued Hachem basin situated in coastal Algiers. The results obtained will be compared with the results obtained by the neuro-fuzzy model (ANFIS) and with the results obtained by the classical multiple linear regression (MLR) model.

2 Materials and Methods

2.1 The Hilbert-Huang Transform

The Hilbert-Huang Transform (HHT) is a method of signal processing introduced by Norden Huang in 1998 [7]. This method seeks to decompose any oscillating signal into a finite number of parts, with the increasingly slow oscillations. The originality of the method is not based on a choice of fixed frequency filters a priori, but to be directly controlled by the data, the identification of the fast component is done locally and relative to a time scale determined by the interval between successive extrema. It is used more

Z. Abda (✉) · M. Chettih · B. Zerouali
Research Laboratory of Water Resources, Soil and Environment,
Department of Civil Engineering, Amar Telidji University,
Laghouat, Algeria
e-mail: z.abda@lagh-univ.dz

Table 1 The combinations of the input vectors proposed for HHT-ANFIS

Model input	Model input	Output
1: $P_{C1}(t + 1)$ and $Q_{C1}(t)$.	4: $P_{C1}(t + 1)$, $P_R(t + 1)$ and $Q_{C1}(t)$	$Q_{t + 1}$
2: $P_{C1}(t + 1)$, $Q_{C1}(t)$ and $Q_{C2}(t)$	5: $P_{C1}(t + 1)$, $P_R(t + 1)$, $Q_{C1}(t)$ and $Q_{C2}(t)$	$Q_{t + 1}$
3: $P_{C1}(t + 1)$, $Q_{C1}(t)$, $Q_{C2}(t)$ and $Q_R(t)$	6: $P_{C1}(t + 1)$, $P_R(t + 1)$, $Q_{C1}(t)$, $Q_{C2}(t)$ and $Q_R(t)$	$Q_{t + 1}$

particularly in the analysis of non-stationary and nonlinear time series data [7].

2.2 The Adaptive Neuro-Fuzzy Inference System

Neuro-fuzzy hybrid systems are non-linear mathematical models of the “black box” type, able to establish relations between the inputs and the outputs of a system.

An adaptive neuro-fuzzy inference system (ANFIS) is a fuzzy inference system implemented in the framework of adaptive networks, first introduced by Jang [8], which consists in using a neuron network of the multilayer perceptron type. It is a network of a Sugeno-type fuzzy system [9, 10] endowed by the learning capacities of neurons.

2.3 Prevision of Daily Flow Rates

The data used in this study come from the National Agency of Water Resources. The database contains rainfall and flows data for the Oued Hachem basin, located in the region of Cherrhell, in Wilaya of Tipaza. It is part of the Mediterranean coastal basins of Algiers. The data correspond to a period of 7 years of daily observations of precipitation and flow from 1 September, 1983, to 31 August, 1989.

The database was divided into three sets to adjust the parameters of the model and obtain the optimal performances; a set of 70% of the data for the learning phase, a set of 30% of the data for the validation phase, and the set that contains all the series was used for the test phase.

For the development of the HHT-ANFIS model, we have decomposed the predicted rainfall ($P_{t + 1}$) and the previous day's flow (Q_t) by HHT into Intrinsic Mode Functions (IMF's). We take all IMF's of $P_{t + 1}$ ($P_{C1}(t + 1)$ and $P_R(t + 1)$) and Q_t ($Q_{C1}(t)$, $Q_{C2}(t)$, and $Q_R(t)$), in order to form input vectors of ANFIS (Table 1).

Table 2 Statistical data of HHT-ANFIS for the Oued Hachem basin

Criteria	Learning	Validation	Test
MSE (m^3/s)	3.4185	8.1284	4.8309
E	0.8872	0.5009	0.8152

2.4 Choice of Performance Criteria

The performance of HHT-ANFIS and ANFIS models was evaluated by the statistical parameters in learning, validation and testing phases. The statistical parameters used in this work are: The Mean Squared Error (MSE) and the coefficient of Nash-Sutcliffe efficiency (E).

3 Results

According to the development of the input vector combinations proposed in Table 1, the HHT-ANFIS model gave us better performance in the input vector model (4) with a membership function number of Gaussian type equal to 2. The results obtained for the learning, validation and testing phases for the HHT-ANFIS model are summarized in Table 2.

Figure 1 shows the comparison between the observed and simulated flow rates by the HHT-ANFIS model for the learning, validation, and test phases.

To evaluate the performances of the HHT-ANFIS model, a comparison was made on the test phase with the ANFIS model and the traditional Multiple Linear Regression (MLR) model (Table 3 and Fig. 2).

4 Discussion

The results obtained in this study indicate that the HHT-ANFIS model is much better than both the ANFIS model and the traditional statistical model, MLR. Its high performance is well-illustrated by the performance criteria indicated in Table 3, as well as the values of the simulated flow rates obtained. These criteria can be further improved by a metaheuristic optimisation technique if we would couple this model with one of these techniques.

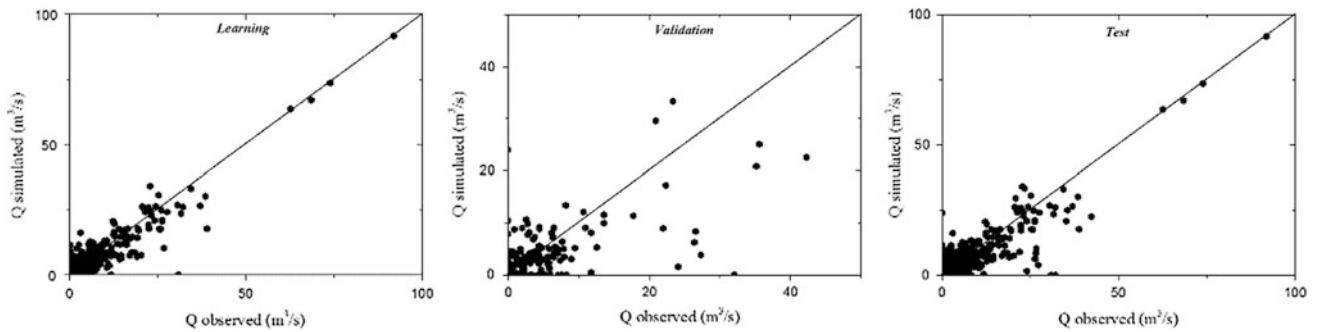


Fig. 1 Comparison between simulated and observed flow values at learning, validation, and testing phases

Table 3 Comparison of the results obtained by the HHT-ANFIS, ANFIS, and MLR in the test

Criteria	HHT-ANFIS	ANFIS	MLR
MSE (m ³ /s)	4.8309	5.0171	6.9701
E	0.8152	0.8081	0.7334

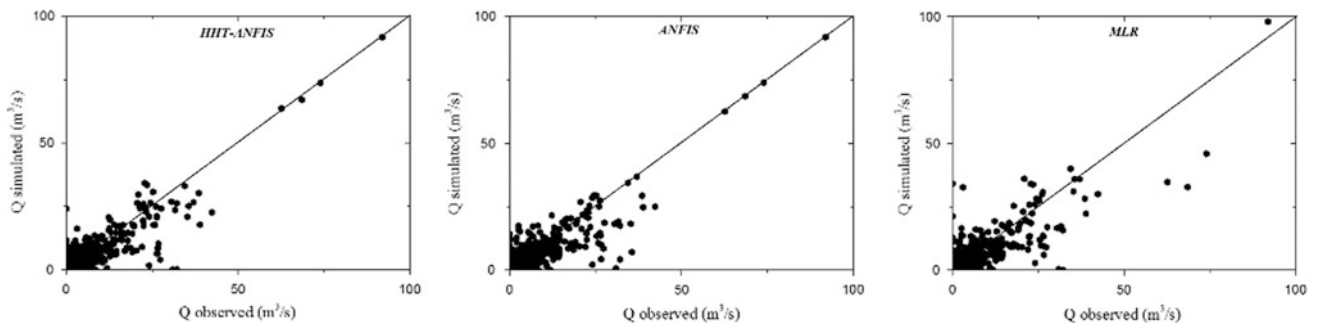


Fig. 2 Comparison between simulated and observed flow values obtained by HHT-ANFIS, ANFIS, and MLR in the testing phase

5 Conclusions

This study highlighted the effectiveness of intelligent hybrid models in the field of flood predictions. The rainfall-runoff transformation is known by its non-linearity and by the non-stationarity of its hydrological series. The decomposition of these series by HHT, which is well-adapted to non-stationary time series and combined with the neuro-fuzzy inference system, has significantly increased the efficiency of flow rates prediction. The role of HHT in this combination is crucial, because it has allowed decomposing the original signal into several resolutions at different levels, which in turn allowed having more detailed information than the original data.

On a practical plan, this study also indicated that the HHT-ANFIS model has allowed a better estimate of floods in order to take the necessary protective measures and reduce the risk of flooding. In order to increase the performance of

this model, we plan to associate it with other optimization techniques such as Genetic Algorithms.

References

1. Kuczera, G., Franks, S.W.: Testing hydrologic models: fortification or falsification? In: Singh, V.P., Frevert, D.K. (eds.) *Mathematical Modelling of Large Watershed Hydrology*. Water Resources Publications, Littleton (2002)
2. Vrugt, J.A., Diks, C.G.H., Gupta, H.V., Bouten W., Verstraten, J. M.: Improved treatment of uncertainty in hydrological modelling: combining the strengths of global optimization and data assimilation. *Water Resour. Res.* **41** (2005)
3. Rajurkar, M.P., Kothari, U.C., Chaube, U.C.: Artificial neural networks for daily rainfall-runoff modelling. *Hydrol. Sci. J.* **47**, 865–877 (2002)
4. Kisi, O., Shiri, J.: Precipitation forecasting using wavelet-genetic programming and wavelet-neuro-fuzzy conjunction models. *Water Resour. Manag.* **25**, 3135–3152 (2011)

5. Parmar, K.S., Bhardwaj, R.: Water quality management using statistical and time series prediction model. *App. Water Sci.* **4**(4), 425–434 (2014)
6. Parmar, K.S., Bhardwaj, R.: River water prediction modeling using neural networks, fuzzy and wavelet coupled model. *Water Resour. Manag.* **29**(1), 17–33 (2015)
7. Huang, N.E., Shen, Z., Long, S.R., Wu M.C., Shih, H.H., Zheng, Q., Yen, N.C., Tung, C.C., Liu, H.H.: The empirical mode decomposition and the Hilbert spectrum for nonlinear and non-stationary time series analysis. *Proc. Roy. Soc. London A: Math., Phys. Eng. Sci.* (1998)
8. Jang, J.S.: ANFIS: adaptive-network-based fuzzy inference system. *IEEE Trans. Syst. Man Cyber.* **23**, 665–685 (1993)
9. Takagi, T., Sugeno, M.: Fuzzy identification of systems and its applications to modeling and control. *IEEE Trans. Syst. Man Cyber.* **1**, 116–132 (1985)
10. Sugeno, M., Kang, G.: Fuzzy modelling and control of multilayer incinerator. *Fuzzy Sets Syst.* **18**, 329–345 (1986)

Floodline Delineation for Brandfort Area of South Africa: An Integrated Approach

Saheed Adeyinka Oke[✉] and George Ndhlovu

Abstract

Floodline estimation was approached from an integrated developmental view-point in this study. The objective was to determine areas prone to flooding. This was done to serve as an early warning mechanism to support planning and development. The paper estimates the design flood with various return periods for the sub-catchment. Investigations integrated together to derive the floodline areas were the geographical information system (GIS), extraction of catchment properties from Google earth maps, digital elevation models (DEM), modelling using hydrological engineering center and river analysis system (HEC RAS). Delineated catchment parameters show that the Brandfort sub-catchment area covers 48.63 km², while the channel length is 7.124 km. The channel slope is 0.489% indicating a flat and flood-prone region. 1:50 years and 1:100 years floodline modelling shows that larger areas of the catchment have the potential of being flooded. The significance of the study suggests that by using an integrated approach, floodline delineation can serve as an early warning tool for proper flood management in order to prevent future disasters.

Keywords

HEC RAS • GIS • Floodline • Brandfort • Sub-catchment

1 Introduction

Floodline can be described as lines on a map depicting the water level reached by floods with a recurrence interval. The rise in the numbers of flooded areas, in recent years, has led

S. A. Oke (✉) · G. Ndhlovu
Unit for Sustainable Water and Environment, Civil Engineering
Department, Central University of Technology Free State,
Bloemfontein, 9301, South Africa
e-mail: soke@cut.ac.za; okesaheed@gmail.com

to loss of human life and economic damages. Flooding which results from a catchment receiving more water than the catchment can process, has impacted human life adversely. This phenomenon is aggravated by the unpredictable climatic changes. It is important to study the flood risk and characteristics of areas like Brandfort due to its semi-arid location, flat topographical landscape and the originating presence of two streams which are tributaries of the Modder River. These two streams confluence within the study area. Therefore, the study aimed to delineate 1:50 years and 1:100 years floodline.

2 Materials and Methods

The study approach to floodline delineation was to use multi-dimensional methods. The first exercise involved sub-catchment delineation with digital elevation model (DEM) and Google earth. The delineation was done at a resolution of 30 m covering the entire sub-catchment. Estimations of the flood return periods were calculated using the standard flood design method (SDM). Rainfall and flow gauges data for the evaluation of peak discharges were sourced from the hydrological unit of Water Affairs, Republic of South Africa. This was followed by the extraction of the catchment properties which included: size, channel length characteristics, slopes and total area covered. These data were sourced from the United State Geological Survey (USGS) earth explorer.

Extracted properties were validated with field physical measurements. Generated hydrological data with the catchment properties served as floodline delineation input parameters modelled using HEC-GEO RAS and HEC RAS [1] tool. Final floodline delineations showing spatial distributions of flood risk areas were presented in a GIS based map.

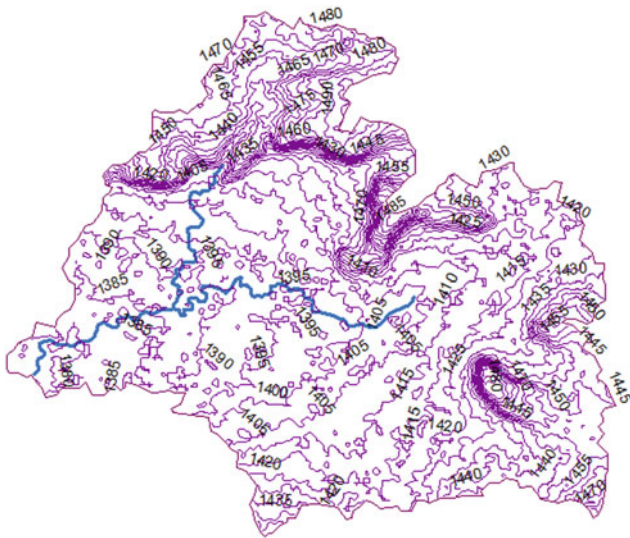


Fig. 1 DEM derived contour map of Brandfort sub-catchment with an overlaid river system

3 Results

3.1 Catchment Delineation

The site falls under the C54G sub-catchment of the water management area (WMA) of South Africa. The major river system in this sub-catchment is the Modder River. The Modder River receives the majority of the flow from adjoining rivers and streams. Therefore, the stream is a tertiary tributary of the Modder River catchment. Delineation of the sub-catchment was based on the topography of the Modder River catchment using the digital elevation model (DEM) of 30 m resolution in GIS. The contour map derived

from DEM was sourced from USGS earth explorer for the entire Brandfort area but clipped to the study area (Fig. 1).

3.2 Extraction of Catchment Parameters

Parameters were extracted using GIS Arc tool box procedures under hydrology. Table 1 presents the major parameters extracted for the sub-catchment.

The results from the standard design method (SDM) are derived using the Eq. 1.

$$Q = 0.278CIA \quad (1)$$

The design flood method is based on a rational method described in flood frequency estimation methods [2].

3.3 Modelling with HEC RAS

The generated geometric data from HEC GEO RAS were then imported to HEC RAS and further adjustments on X-sections data were done. More entries were made for Mannings values, in boundary conditions to facilitate hydraulic simulations. Figure 2 indicates the river's geometric data in HEC RAS.

4 Discussion

Results showed that the design flood magnitude with a return period of 1:50 years has the potential of inundating a smaller study area while the design flood magnitude with a return period of 1:100 years would potentially inundate a larger study area (Fig. 3). These should be considered in the design of structures for the area.

Table 1 Extracted sub-catchment parameters

S/N	Parameters	Units	Comments
1	Catchment area	Km ²	48.63
2	Average slope	Percentage	0.489
3	Main channel length	Km	7.124
4	Drainage density	Km/Km ²	0.23
5	Contours	M	5 m contour interval

Fig. 2 River geometric data in HEC RAS

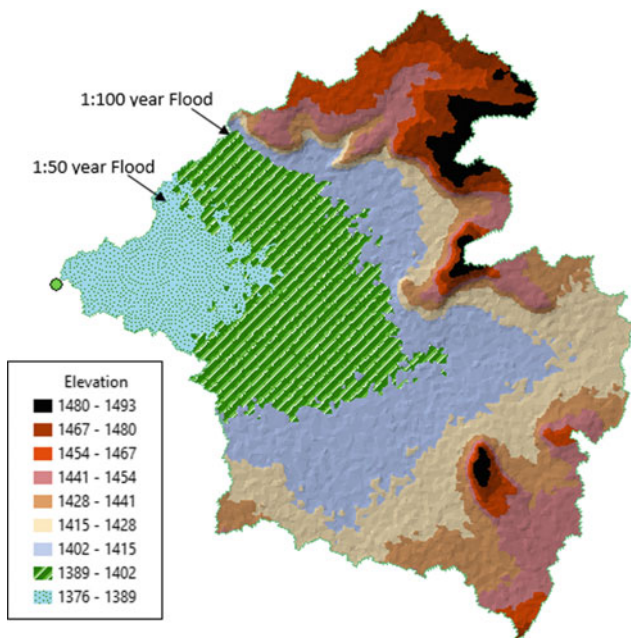
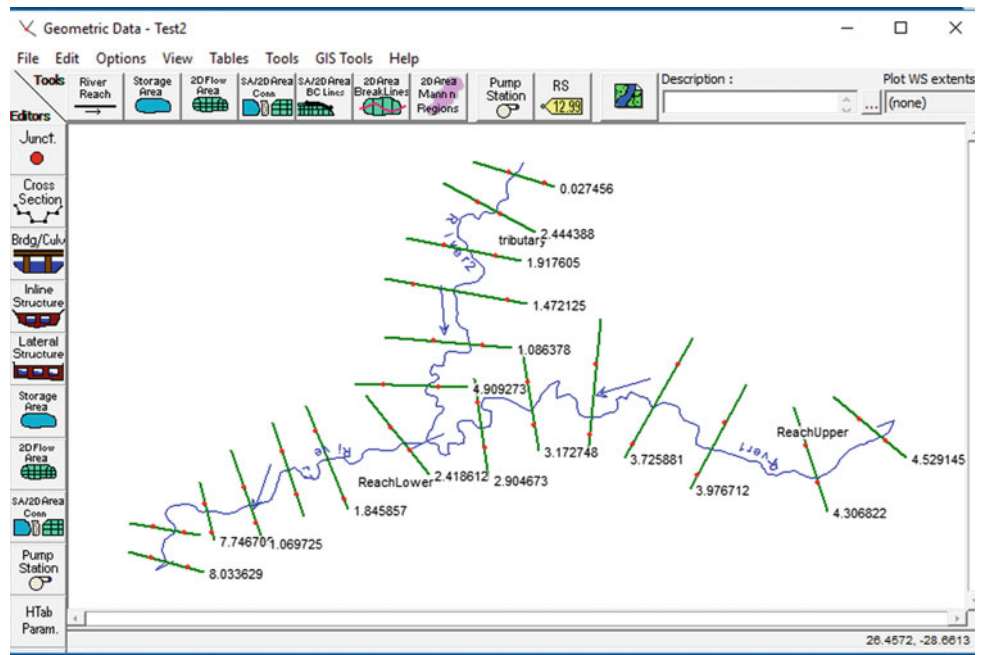


Fig. 3 1:50 years and 1:100 years flood delineation of the Brandfort sub-catchment

5 Conclusions

The use of an integrated approach i.e. GIS, HEC RAS, HEC GEO RAS, Google Earth Map, DEM and site reconnaissance survey to delineate the flood line has proved to be more effective, as it is less time-consuming and the results are more reliable.

References

1. HEC: HEC-RAS River Analysis System User's Manual. US Army Corps of Engineers Institute for Water Resources, Davis, CA (2010)
2. Van Der Spuy, D., Rademeyer, P.F.: Flood Frequency Estimation Methods as Applied in the Department of Water Affairs. Department of Water Affairs, Pretoria, South Africa (2010)

The Effect of Urban Development on Urban Flood Runoff (Case Study: Mashhad, Iran)

Saeed Reza Khodashenas and Javad Azizi

Abstract

In this research, the effects of the development of Mashhad city (in Iran) on the amount of runoff generated were investigated. The urban catchment of this city with a total area of 328 km² was divided into 288 sub-catchments, 399 waterways, 398 nodes, and 5 outlets using GIS software. The pervious, impervious, residential, agricultural and street areas were then determined using the GIS software and Google Earth. The Curve Number (CN) was calculated for each sub-catchment. Three different methods of periodic block, uniform distribution and SCS (CN) II were used for selection of the storm discharges. Finally, the SCS (CN) II method was selected. The results of the modelling showed that the peak of flood in 2016 was 307, 259 and 177% greater than the years 1941, 1976 and 1986, respectively. In addition, the results showed that the central, northern, and northeastern regions (downstream of the city) were flooded due to the increase of the impervious surfaces and the insufficient capacity of the channels.

Keywords

Mashhad • Runoff • Urban flood • SWMM

1 Introduction

Europe has experienced a series of severe floods in the recent years, such as the floods in central Europe in August 2002 in England in the summer of 2007 [4], in Italy in the fall of 2011 [1], and again, in central Europe in June

2013 [2]. These frequent events show that human actions can play a key role in the occurrence of these floods. The researches show that the climate changes led to an increase in flood peaks in the Rhine catchment [3, 6]. The annual peak discharges are expected to increase by 3–19% in the year 2050, due to the climate changes [5, 7].

In this research, the impacts of the urban development of Mashhad between the years 1941–2015 on downstream runoff were investigated using SWMM model. For the modeling, the SCS (CN) method was used for infiltration and runoff estimation. The Arc GIS software was used for catchment zoning and determination of catchment physiological properties, including the area and length of the river.

2 Methods and Materials

2.1 Study Area

Mashhad is located in northeastern Iran. Figure 1 shows population and area growth of the city between 1941 and 2016. For the modeling of this city, a network of 398 nodes, 399 runoff canals, and 5 main outlet points were used (Fig. 2).

In this study, the cumulative method was used for the rainfall data and the interval of 30 min was selected as a rainfall interval. For selecting a precipitation pattern, the SCS (CN) II method was used. This method has a non-uniform distribution. For rainfall Intensity–duration–frequency (IDF), a rainfall with duration of 360-minute was used as a 25-year return period.

In addition to calculating the discharge of the catchment using the SCS (CN) method, the discharge was also investigated using the Horton equation. The maximum and minimum infiltration rates and the constant decrease of infiltration rate were as follows: 150, 40 mm/h and 0.025 1/s, respectively. Figure 3 shows the precipitation pattern obtained by the SCS (CN) II method.

S. R. Khodashenas (✉)
Water Engineering Department, Ferdowsi University of Mashhad,
Mashhad, Iran
e-mail: khodashenas@ferdowsi.um.ac.ir

J. Azizi
Islamic Azad University-Mashhad Branch, Mashhad, Iran

Fig. 1 Area and population changes

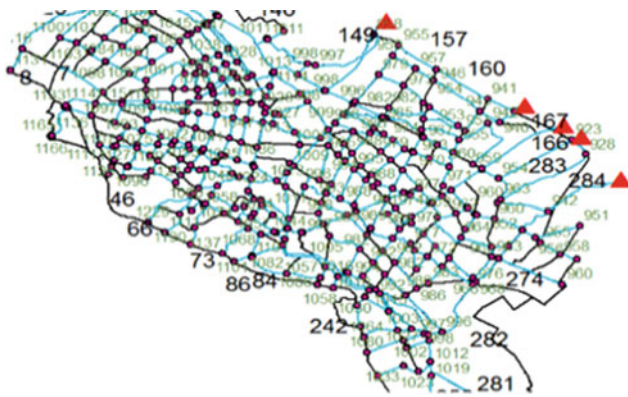
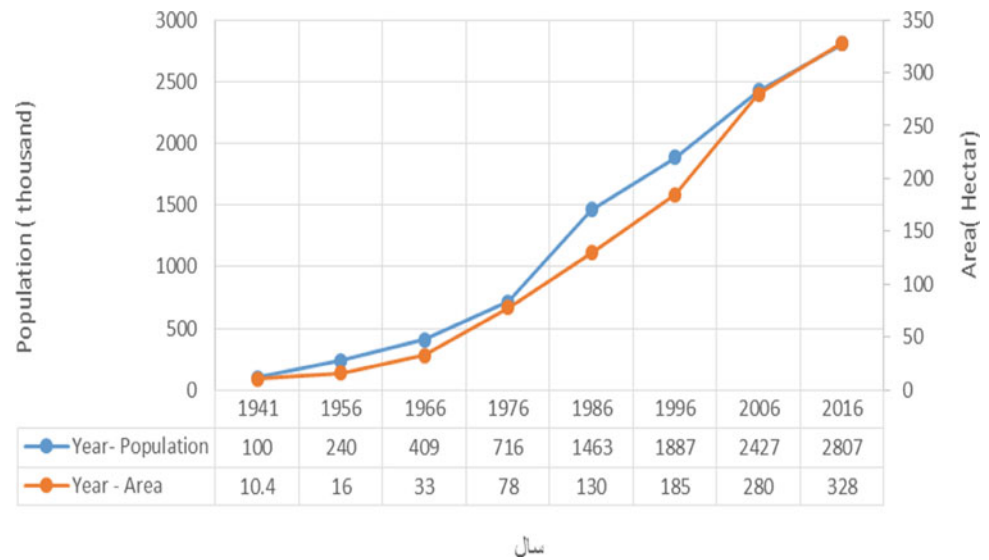


Fig. 2 Study Area and the outlets points

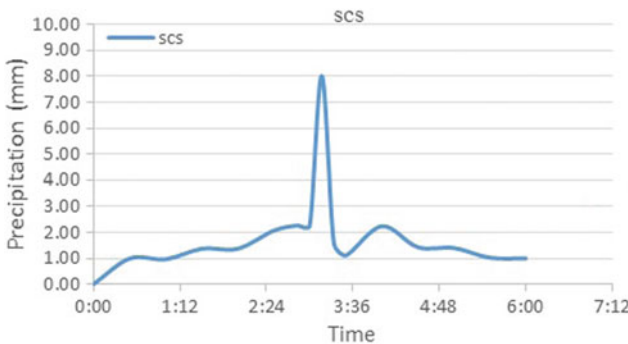


Fig. 3 Precipitation pattern obtained by the SCS (CN) II method

3 Results

After determining the appropriate precipitation pattern, the model was run for the years 1941–2016. For this purpose, two approaches were considered: (1) Real mode: in this

approach, the real dimensions of the existing waterways were considered. The modelling results showed that in this case, due to the insufficient capacity of the waterways and drainages, several points were overtopped and some regions were flooded. (2) Free mode: in the second approach, virtual dimensions were estimated for waterways in order to allow the entire flood to pass without overtopping. Table 1 shows the exiting of flood waters through 5 outlets out of the city, calculated by two approaches in 2016. Q1–Q5 are the outlets showed in Fig. 1. In Fig. 4, the flood-sensitive points of the city are shown. These regions have the highest volumes of flooding in the city. Maximum flooded regions have volumes in the ranges of 60,000–115,000 m³, Medium flooded regions have volumes in the ranges of 40,000–60,000 m³, and Minimum flooded regions have volumes in the ranges of 20,000–40,000 m³. There were many flooded regions, however, these points are the most critical points in the city. Figure 5 shows the effect of the city development on the peak discharge. The results show that, from 1941 to 2016, the city area increased about 31.5 times, however, the discharge increased 3.08 times.

4 Conclusion

The results of this study showed that the peak discharge in 2016 was 308 percent higher than in 1941. The effect of the city development trend was clearly evident on increasing the discharge. The peak discharge in 2016, with a higher summit and a shorter time, indicated that by increasing the impervious surfaces and the urban development, the peak discharge increased, and the time to reach the peak discharge was reduced up to 1 h and 30 min. The results suggested that, due to the low slope and insufficient capacity of the

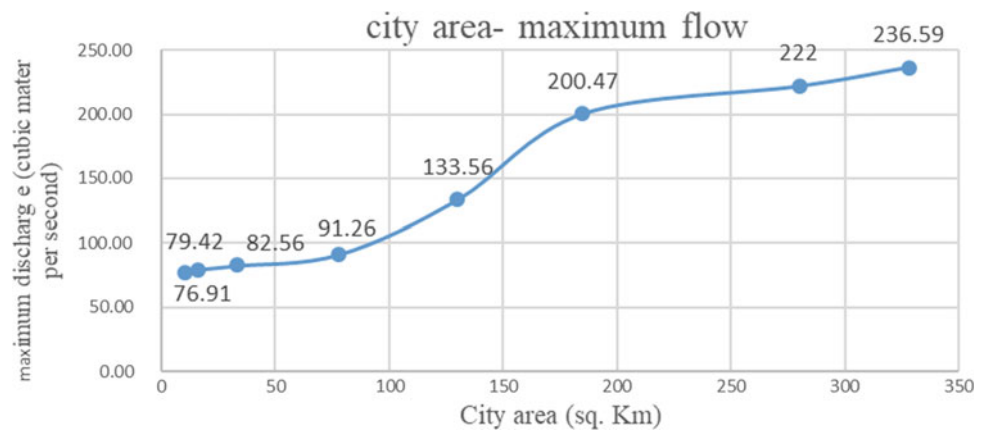
Table 1 Flood Estimation in 2016

2016	Max flow (m ³ /s)		Total volume (m ³)	
	Real	Free	Real	Free
Q1	35.82	133.02	1,231,500	1,234,800
Q2	105.27	246.21	1,960,600	1,998,300
Q3	6.89	15.18	137,400	138,800
Q4	7.97	19.10	196,300	196,800
Q5	88.12	205.19	1,725,300	1,780,700



Fig. 4 Flood-sensitive points of the city

Fig. 5 Outflow discharge and the city development of Mashhad for 1941 and 2016



waterways at the central, northern, and north-eastern parts of the city, Mashhad experienced flooding episodes after 4 h of rainfall, the first of which occurred at 2 h and 45 min after the beginning of the rainfall. After 4 h and 15 min of rainfall, the whole city was flooded and 215 points were affected by flooding. The peak of flood was 35 m³/s and the peak of runoff produced by the system was 795 m³/s.

References

- Amponsah, W., Borga, M., Marchi, L., Boni, G., Cavalli, M., Comiti, F., Crema, S., Ana, L., Marra, F., Zoccatelli, D.: The flash flood of October 2011 in the Magra River basin (Italy): rainstorm characterisation and flood response analysis. *J. Hydrometeorol.* (2014)

2. Blöschl, G., Nester, T., Komma, J., Parajka, J., Perdigão R.A.P.: The June 2013 flood in the Upper Danube Basin and comparisons with the 2002, 1954 and 1899 floods. *Hydrol. Earth. Syst. Sci.* **17**, 5197–5212 (2013). <https://doi.org/10.5194/hess-17-5197-2013>
3. Hooijer, A., Klijn, F., Pedroli, G.B.M., Van Os, A.G.: Towards sustainable flood risk management in the Rhine and Meuse basins: synopsis of the findings of IRMA-SPONGE. *River Res. Appl.* **20**, 343–357 (2004). <https://doi.org/10.1002/rra.781>
4. Marsh, T.: A hydrological overview of the summer 2007 floods in England and Wales. *Weather* **63**, 274–279 (2008). <https://doi.org/10.1002/wea.305>
5. Middelkoop, H., Daamen, K., Gellens, D., Grabs, W., Kwadijk, J.C.J., Lang, H., Parmet, B.W.A.H., Schadler, B., Schulla, J., Wilke, K.: Impact of climate change on hydrological regimes and water resources management in the Rhine basin. *Climatic Change* **49**, 105–128 (2001). <https://doi.org/10.1023/a:1010784727448>
6. Pinter, N., Van der Ploeg, R.R., Schweigert, P., Hofer, G.: Flood magnification on the River Rhine. *Hydrol. Process.* **20**, 147–164 (2006). <https://doi.org/10.1002/hyp.5908>
7. Vellinga, P., Mills, E., Berz, G., Bouwer, L., Huq, S., Kozak, L., Palutikof, J., Schanzenbacher, B., Soler, G.: Insurance and other financial services. In: *Climate Change 2001: Impacts, Adaptation, and Vulnerability* (2001)

Integrated Approach to Assess the Urban Green Infrastructure Priorities (Alexandria, Egypt)

Mona G. Ibrahim, Bahaa Elboshy, and Wael Elham Mahmod

Abstract

Extreme rainfall and pluvial flood hazard has recently occurred in Alexandria and caused large human and economic losses. In this regard, the urban green infrastructure (UGI) is considered as a sustainable alternative to urban water management with different applications to reduce water accumulation in the streets caused by the inadequate drainage network capacity. This paper aims at demonstrating an assessment approach to prioritizing urban areas where UGI should be applied. The proposed method integrates flood modeling and land use classification into an assessment index called the UGI Priority Index. This index can help determine the neediest areas for UGI implementation alternatives to reduce the amount of accumulated rain. The introduced priority map can help the decision makers to direct the development plans to the priority areas and reduce the pluvial flood risk level using environmentally-friendly options.

Keywords

Urban green infrastructure • Remote sensing • Pluvial flood • GIS

1 Introduction

Green infrastructure as a concept has been developed within the last two decades. It commonly refers to the connective matrices of green spaces that can be found in and around urban and urban-fringe landscapes. Green infrastructure could be simply defined as urban green space systems [1]. The green infrastructure is considered as a sustainable alternative to urban water management and it includes bioretention systems, green roofs, rain gardens, permeable pavement, bioswales and rain barrels as defined in Table 1 [2].

In order to effectively design and plan the green infrastructure, two main factors should be taken into account; the pluvial flood level based on accumulated water height in the streets, and the existing green/vegetation areas [3].

Alexandria is one of the most susceptible Egyptian cities to the pluvial flood, where the lack of vegetation and green area increases the exposure to flood hazards. In this paper, Almontaza district is investigated, as a case study, to prioritize its urban areas to apply the UGI alternatives. Almontaza district is located in the north of the city and it is considered as the most vulnerable area to the pluvial flood, due to the low drainage network capacity and to the spread of informal areas and slums [4] (see Fig. 1). The aim of this study is to develop an index, namely the UGI Priority Index, to evaluate the urban green infrastructure (UGI) priorities. This index is expected to help determine the neediest areas for implementing the UGI alternatives to reduce the amount of accumulated rain.

2 Methods

In order to prioritize the urban areas to develop the UGI, this research introduces an integrated approach using the flood modeling and land use classification to identify the green and vegetation areas. The flood hazard modeling HEC-RAS

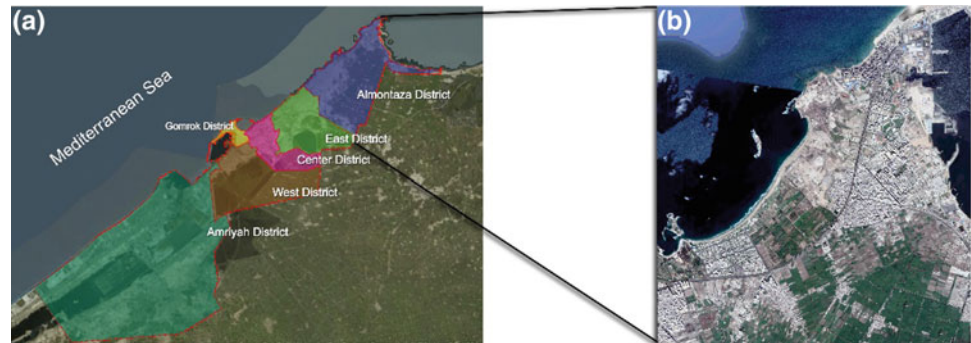
M. G. Ibrahim (✉) · B. Elboshy · W. E. Mahmod
Environmental Engineering Department, Egypt-Japan University
of Science and Technology, E-JUST, Alexandria, Egypt
e-mail: mona.gamal@ejust.edu.eg

M. G. Ibrahim
Environmental Health Department, High Institute of Public
Health, Alexandria University, Alexandria, Egypt

W. E. Mahmod
Civil Engineering Department, Faculty of Engineering, Assiut
University, 71515 Assiut, Egypt

Table 1 Urban Green infrastructure alternatives

Bioretention systems	Small depressional areas with soil filter media and native plants to promote soil infiltration and decrease rapid runoff
Rain gardens	Lightweight vegetation at the rooftops that enable rainfall infiltration
Green roofs	Shallow and smaller vegetated areas that collect and infiltrate runoff
Permeable pavements	Porous material that allows rainfall to gradually infiltrate into soils
Bioswales	Vegetated channels that infiltrate rainfall and runoff
Rain barrels	Containers that collect and store rainfall

Fig. 1 a Alexandria map, b Almontaza district map (Google Maps 2018)

software has been used in order to determine the flood levels in the urban area (<https://www.usgs.gov/software/hec-ras>). The flood has been divided into four levels depending on the water height. The data used in this step (using the Digital Elevation Model (DEM)) are produced through contour maps obtained from the General Organization for Physical Planning (GOPP) in Egypt. Also, the rainfall rate has been assumed according to the most aggressive event of November 2015, which was about 200 mm [5]. In order to classify land-use into urban and green areas, remote sensing was used. The data used in this step was obtained through Google Satellite Maps. This step has been accomplished using the image classification tool in ArcMap software.

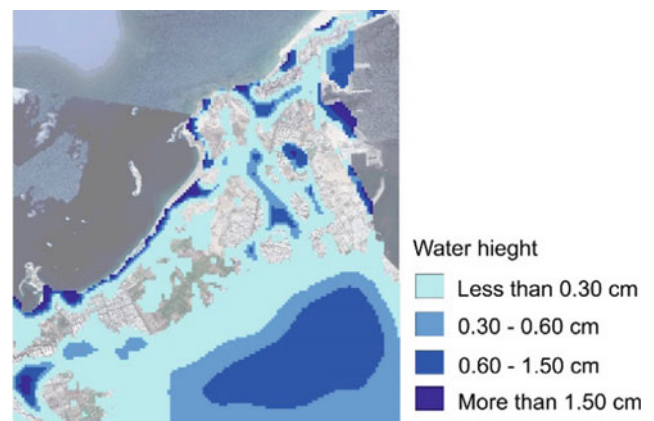
While flood management is a complex issue and contains several factors [6], the UGI Priority Index has been formed by integrating the flood levels and land use classifications to estimate the priority to implement UGI in each urban area. The urban area map has been divided into a grid cell with size 50 m × 50 m and the built/green ratio has been estimated by dividing the built area by the total area (green areas + built area) in each cell, then by multiplying by the flood level as shown in Eq. 1. The index score ranges from 0 to 1.

$$UGI \text{ Priority Index} = \frac{\text{Built Area}}{\text{Green Area} + \text{Built Area}} \times \frac{\text{Flood Level}}{4} \quad (1)$$

3 Results and Discussion

The flood level exposure map has been introduced by using HEC-RAS software as shown in Fig. 2. The map reveals that the expected flood water level ranges from 0 to 1.5 m. The flood was divided into four levels as shown in Fig. 2.

Also, the land-use classification has been done for the district to identify the built area and the green and vegetation areas using the image classification tool in ArcMap software. Google Satellite Map has been used to accomplish this step as shown in Fig. 3.

**Fig. 2** Flood level exposure map for Almontaza district

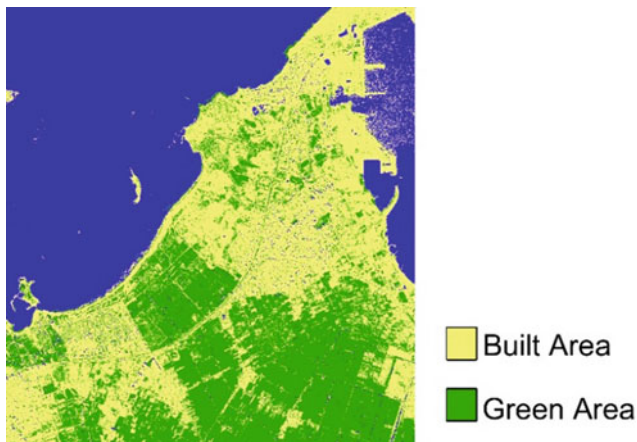


Fig. 3 Land-use classification for Almontaza district

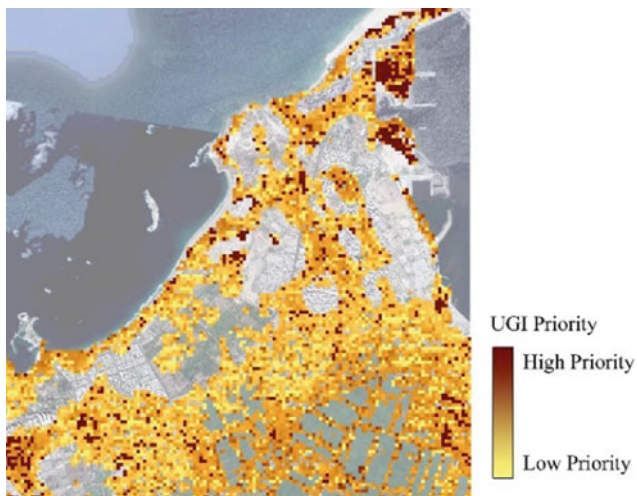


Fig. 4 UGI priority map for Almontaza district (cell size 50 m × 50 m)

After that, the UGI index has been estimated for each cell in the map based on two factors; the flood levels and the built/green area ratio. A UGI priority map has been introduced as shown in Fig. 4. The introduced map can help in

flood management and risk mitigation by implementing the UGI in the neediest areas.

4 Conclusions

In order to help decision-makers achieve sustainable development and reduce the pluvial flood hazard, this paper introduced an assessment tool to prioritize the urban area regarding the need to implement the urban green infrastructure (UGI) alternatives. In this research, a UGI priority index has been developed. This index integrates the flood level, depending on the accumulated water in the streets, and the built/green area ratio. The introduced map reveals the levels of priority to implement the UGI. The introduced map can help decision makers and urban planners to reduce the pluvial flood risk level using an environmentally-friendly option, which can also reduce the needed resources to improve the drainage network capacity.

References

1. Breuste, J., Artmann, M., Li, J., Xie, M.: Special issue on green infrastructure for urban sustainability. *J. Urban Plan. Dev.* **141**(3), A2015001 (2015)
2. Golden HE, Hoghooghi N (eds) Green infrastructure and its catchment-scale effects: an emerging science. Wiley Interdiscip. Rev. Water, e1254 (2017)
3. Mguni, P., Herslund, L., Jensen, M.B.: Sustainable urban drainage systems: examining the potential for green infrastructure-based stormwater management for Sub-Saharan cities. *Nat. Hazards* **82**, 241–257 (2016)
4. Elboshy, B.M., et al.: A framework for pluvial flood risk assessment in Alexandria considering the coping capacity. *Environ. Syst. Decis.* (2018)
5. Zevenbergen, C., Bhattacharya, B., Wahaab, R.A., Elbarki, W.A.I., Busker, T., Salinas Rodriguez, C.N.A.: In the aftermath of the October 2015 Alexandria Flood Challenges of an Arab city to deal with extreme rainfall storms. *Nat. Hazards* **86**(2), 901–917 (2017)
6. Cançado, V., Brasil, L., Nascimento, N., Guerra, A.: Flood risk assessment in an urban area: measuring hazard and vulnerability. In: 11th International Conference on Urban Drainage, Edinburgh, Scotland, UK, 2008 Flood, no. Equation 1, pp. 1–10 (2008)

Urbanization Growth Effect on Hydrological Parameters in Mega Cities

Case Study: 5th Settlement—Cairo—Egypt

Ahmed Mohamed Helmi, Ahmed Mahrous, and Ashraf El. Mustafa

Abstract

Rapid urbanization in the 5th settlement—Cairo, Egypt, led to a dramatic impact on the hydrological parameters within the area, due to a reduction in the soil infiltration, and consequently increased runoff volumes. Many researches were conducted for similar cases throughout the world to assess the urbanization hydrological impact. In the current study, remote sensing raster classification is utilized to assess the land use and associated Curve Number (CN) variation within the study area, and the SCS method was used to estimate the runoff volume. A Long-Term Hydrologic Impact Assessment (LTHIA) GIS tool has been developed to assess the temporal variation of hydrological parameters through different stages of development from 2006 to 2016 in the study area. It was concluded that during 10 years of development, the impervious areas increased and covered 30% of the study catchment area, the runoff volume increased by about 800% more than the 2006 base line runoff. This study clearly shows the excessive increase in runoff due to urban development and raises the flag for the urban planners at this area, particularly the New Administrative Capital in Egypt which lies along the extent of the 5th district to take necessary flood mitigation measures into account.

Keywords

Storm water management • Remote sensing • GIS • SCS

1 Introduction

The rapid urbanization in the 5th settlement—Cairo, Egypt, led to a dramatic impact on the hydrological parameters resulting into an increase in the runoff volume, and a reduction in soil infiltration. During the last rain event in April-2018 (about 30 mm), a severe runoff negatively impacted the properties and caused road blockages for a long time as shown in Fig. 1. No available studies investigated the variation of the urbanization impact of the hydrological parameters in this area. The Land-Sat images processing for land cover changes assessment to evaluate its impact on the Curve Number (CN), and the application of SCS method to calculate the corresponding runoff volume under GIS environment have been utilized to develop The Long-Term Hydrologic Impact Assessment (LTHIA) GIS tool used in this study. The integration between remote sensing and GIS has been used for modeling urban growth effects on surface runoff [1]. The assessment of the urbanization impact on hydrological parameters has been extensively studied along different locations in the world, [2–4]. Each area has its own characteristics regarding the future urbanization plan, and building regulations concerned with the built-up area percentage, and the minimum required greeneries. Generally, urbanization will lead to an increase in runoff which should be taken into account in the urban planning stage and in building regulations, in order to apply appropriate measures and/or use low impact urbanization [5] to avoid the flooding's negative impacts. The urban development spreading in the 5th Settlement in Cairo during the period from 2006 to 2016 is shown in Fig. 2.

The land use can be defined based on the satellite image classification into color bands. Under ARC-GIS, the raster classification can be either supervised or unsupervised classification. The unsupervised classifications split the colors in the satellite image into ranges with unique IDs, leading to some uncertainties in the archived results especially when the raster image has the same color bands for

A. M. Helmi (✉)
Faculty of Engineering, Cairo University, Cairo, Egypt
e-mail: Ahmed.Helmi@eng.cu.edu.eg

A. Mahrous
Jacobs International, Dubai, UAE

A. El.Mustafa
Faculty of Engineering, Ain Shams University, Cairo, Egypt



Fig. 1 Fifth settlement flooding, April 2018 [6]



Fig. 3 Image key signature

different land use. The supervised raster classification depends on human judgment by picking specific sample pixels and assigning reference ID known as image key signature as shown in Fig. 3. A comparison between the supervised and unsupervised methods' outcome is shown in Fig. 4. The supervised raster classification is selected to be adopted in the current study.

For each classified pixel, an ID and associated curve number are assigned to be stored in the data base attribute table, [Roads (CN = 90), Buildings (CN = 80), Green areas (CN = 65), Natural Sandy Soil (CN = 75)].

The excess runoff depth is calculated based on the SCS method

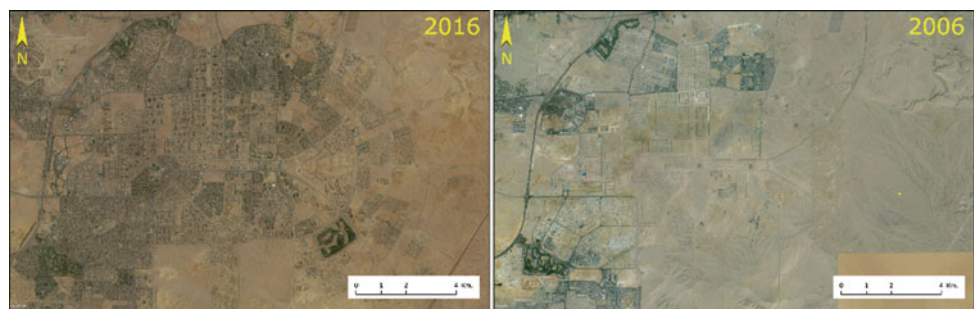
$$S = 25.4 \left(\frac{1000}{CN} - 10 \right) \quad (1)$$

$$I_a = 0.2S \quad (2)$$

$$R = \frac{(P - I_a)^2}{(P + 0.8S)} \quad (3)$$

where S: is the maximum soil potential storage (mm.), I_a : initial storm abstraction (mm.), and R: excess runoff depth (mm.)

Fig. 2 Urban development spreading from 2006 to 2016



2 Results and Discussion

A 2.2 m. pixel size raster classification within the drainage catchment has been achieved for both years, 2006 and 2016, by applying the proposed methodology as shown in Fig. 5. The 1 in 50-year storm based on the available meteorological data frequency analysis is 23.5 mm which is used in the calculation of excess runoff depth for each classified raster pixel, using the SCS method. The runoff volume had been increased from 60,000 cubic meters in 2006 to 465,000 cubic meters in 2016 with an increased percentage of about 700%.

3 Conclusions

The developed Long-Term Hydrologic Impact Assessment model GIS tools showed good matches between the raster classification and the satellite image and can be easily adopted with high confidence in assessing the urban development impact on the hydrologic parameters. The rapid growth of the urbanized areas in the 5th settlement during the period from 2006 to 2016 has severely impacted the hydrologic parameters and led to a 700% increase in the

Fig. 4 Comparison between supervised, and unsupervised raster image

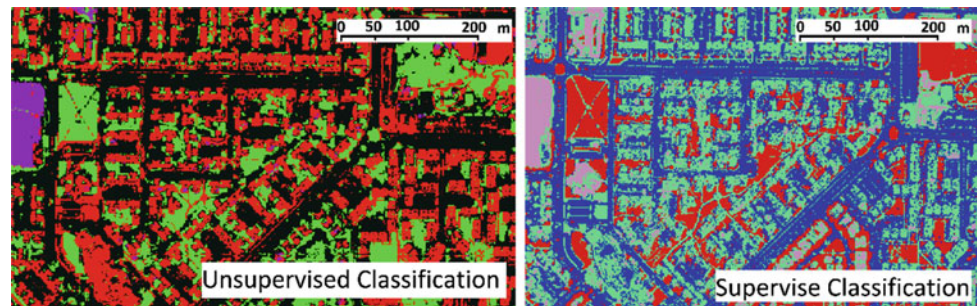
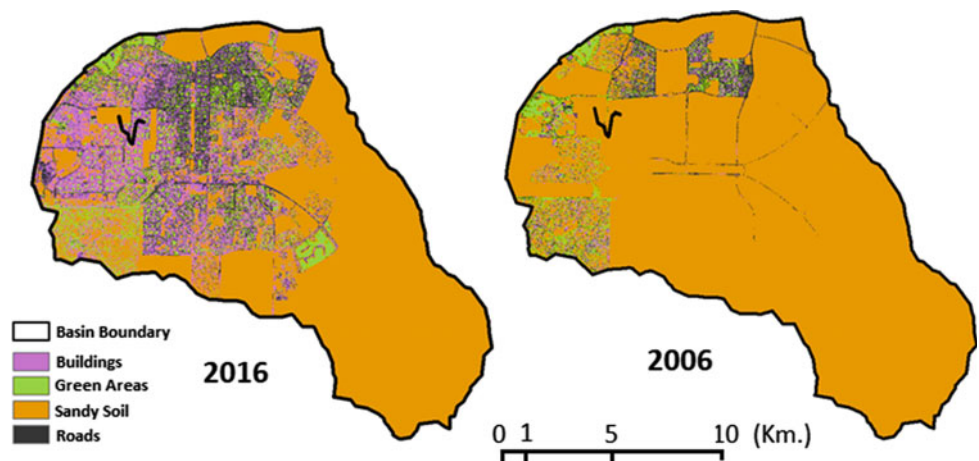


Fig. 5 Classified roasters within the catchment boundaries




runoff volume base line values in 2006, which in turn led to the aggressive impacts of 30 mm. storm of April, 2018. The urbanization rate in the area and its extent to the new Administrative Capital in Egypt is going faster than the previous decade and flood mitigation measures should be carefully considered.

References

1. Weng, Q.: Modeling urban growth effects on surface runoff with the integration of remote sensing and GIS. *Environ. Manage.* **28**, 737–748 (2001)
2. Ali, M., Khan, S.J., Aslam, I., Khan, Z.: Simulation of the impacts of land-use change on surface runoff of Lai Nullah Basin in Islamabad, Pakistan. *Landscape Urban Plan.* **102**(4), 271–279 (2011)
3. Olivera, F., DeFee, B.B.: Urbanization and its effect on runoff in the Whiteoak Bayou watershed, Texas. *Am. Water Resour. Assoc.* **43** (1), 170–182 (2007)
4. Hejazi, M.I., Markus, M.: Impacts of urbanization and climate variability on floods in Northeastern Illinois. *Hydrol. Eng.* **44**(6), 606–616 (2009)
5. Ahiablame, L.M., Engel, B.A., Chaubey, I.: Effectiveness of low impact development practices in two urbanized watersheds: Retrofitting with rain barrel/cistern and porous pavement. *Environ. Manage.* **119**, 151–161(2013)
6. Sharkiatoday Home Page, <http://www.sharkiatoday.com/wp-content/uploads/2018/04/التجمع-الخامس-سيول.jpg>. Last accessed 28 April 2018

Urban Hydrogeological Studies of Groundwater in Central University of Technology Bloemfontein Campus

Saheed Adeyinka Oke  and Mpho Aloysius Matobo

Abstract

Groundwater within the Central University of Technology (CUT), Bloemfontein, was investigated in order to determine its hydraulic and hydrochemical characteristics with potentials for urban water supply. The investigations involved carrying out pump yield tests on three boreholes on the CUT campus. Further examination involved laboratory testing of the groundwater for chemical signature, and geophysical investigation to determine the geological and aquifer target of the boreholes using an electrical resistivity tomography (ERT). Additionally, electrical conductivity profiling (EC Profiling) was used to detect the fracture positions within the boreholes. Pumped test results monitored from the three boreholes were interpreted using FC (flow characteristics) software program. Cooper-Jacobs and Basic FC methods from this software recommend a sustainable yield of 7.83–9.34 l/s, respectively, while storativity values are 7.93×100 for Cooper Jacobs and 2.2×10^{-3} for Basic FC method. Hydrochemical analysis shows Mg-HCO₃ water type from Stiff diagram. This shows dissolved solutes from rainfall and the host rocks, but not from urban activities. The results of the fracture positions at an ambient state in the wells were 5, 6 and 9.5 mbgl in boreholes 1, 2 and 3, respectively. The hydrogeological characteristics displayed by the groundwater of the CUT campus relate to the general characteristics of the Karoo aquifers.

Keywords

Groundwater • Pump test • FC method • CUT • Aquifers

1 Introduction

Rapid increase in urban population growth in central South Africa has negatively impacted water resources of the Bloemfontein areas of South Africa. Urbanization and previous droughts have worsened the scarcity of surface-water [1]. This is putting pressure on urban water supplies. Future urban water demand is gradually increasing towards groundwater resources [2]. Thus, it is important to supplement the supply of Bloemfontein urban areas with urban groundwater resources. However, previous studies [3–5] have shown that the quantity and quality of groundwater systems in urban areas have become endangered due to, amongst others, the population as well as physico-chemical and biochemical interaction between groundwater and anthropogenic contaminants associated with urban settings.

Therefore, this research aims to monitor the quality of groundwater in the area of study and uses conventional methods of hydrogeology investigation on CUT boreholes to assess the potential yield and aquifer characteristics beneath the area of study for urban supply purposes. This research is important because, no data exist for the boreholes used for this investigation. Few studies have been conducted in similar settings in and around Bloemfontein. On a regional scale, Mbinze [5] dealt specifically with the contamination of groundwater by nitrate, on the other end, Molaba [2] focused mainly on detecting the lineaments beneath the central city.

1.1 Site Description

The focused area of study for this paper is situated within the central business district (CBD) of Bloemfontein, and is

S. A. Oke (✉)

Unit for Sustainable Water and Environment, Civil Engineering Department, Central University of Technology, Bloemfontein, Free State, 9301, South Africa
e-mail: soke@cut.ac.za; okesaheed@gmail.com

M. A. Matobo

Department of Environmental Health, Central University of Technology, Bloemfontein, Free State 9301, South Africa

characterized by paved areas, high buildings and a few open sports fields. Geologically, Bloemfontein lies within the Adelaide subgroup of the Karoo supergroup rock formations. This formation is characterized by sandstone, shale and mudstone rocks. These sedimentary rocks of the hosts have been intensively intruded by magmatic dolerite intrusive, such as sills and dykes of Jurassic aged Drakensberg Group [6]. The contact between dolerite dykes and the host rock, within the weathered zone, remains therefore the most important target for groundwater exploration [1]. All targeted boreholes are found within the CUT campus and are less than 420 m away from each other, Fig. 1.

2 Materials and Methods

The geological logs and blow yields' information for all existing boreholes within the campus were not available to determine the exact position of fractures or the main water strikes. So the electrical conductivity profiling (EC Profiling) was used as an alternative method to detect the fracture positions within the boreholes. For EC profiling, an EC probe was advanced from the surface throughout the column of the borehole and the values were taken on 1 m intervals starting at static water level (SWL) to the bottom of the borehole. The profiling was done on all boreholes at an ambient state, before the commencement of the constant rate test.

The constant discharge test of borehole involves pumping boreholes at a constant discharge rate over a period of time. Constant discharge rate testing was conducted to estimate

sustainable yields of the boreholes, and other aquifer parameters were estimated using this test. The constant rate test was conducted on borehole BH1, while BH2 and BH3 were set as the monitoring wells. As it is recommended, the test was conducted for a period of 8 h, followed by a recovery test [7]. FC computer software was used to interpret the hydraulic property of the aquifer. During the yield test, two water samples from the boreholes were collected (from BH1 and BH2). Using sterilized metal bailer, the first sample was collected from BH2 before the constant rate test on BH1 can commence. The sample collected from pumping well BH1 was taken from the discharge point of the test, after pumping out the water for about 2 h to obtain a representative sample of the aquifer. A physico-chemical and bacteriological test was carried out on the water.

3 Results

3.1 EC Profile

The EC profiles recorded in the boreholes are shown in Fig. 2. For pumping well BH1, the profile shows that the water in the well has low EC values from SWL at 4 mbgl to the depth of 5 mbgl (ranging between 150 and 233 $\mu\text{S}/\text{cm}$, respectively).

However, from that level and below, there is a sudden increase in the EC values from 233 to 633 $\mu\text{S}/\text{cm}$ and above, as the profile goes deeper. This buoyant fresh water at the top is a result of the density difference between water that comes from fractures and ambient water in the borehole.

3.2 Aquifer Flow Characteristics

The FC program provides the diagnostic plots (Fig. 3a, b in order to determine the aquifer flow characteristics from the pump test results. According to Van Tonder et al. [7], these results suggest that the bilinear flow occurs mainly in reservoirs that have a continuous fracture network embedded in porous media.

3.3 Hydrochemical Quality

The results of physico-chemical properties of the two samples from BH1 and BH2 show that they are potable enough for human consumption. The micro and macro elements found in both samples met the requirement of South African National Standard (SANS 241) for drinking purposes, except for the high heterotrophic bacteria content.

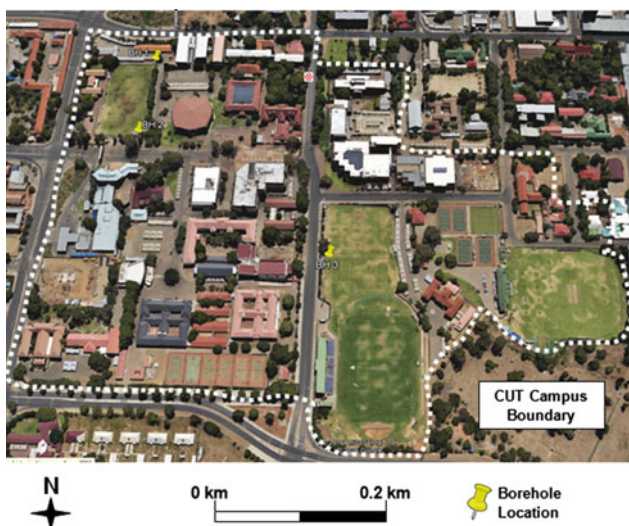


Fig. 1 Map showing the location of the boreholes within the Central University of Technology, Bloemfontein

Fig. 2 EC profile from CUT campus boreholes

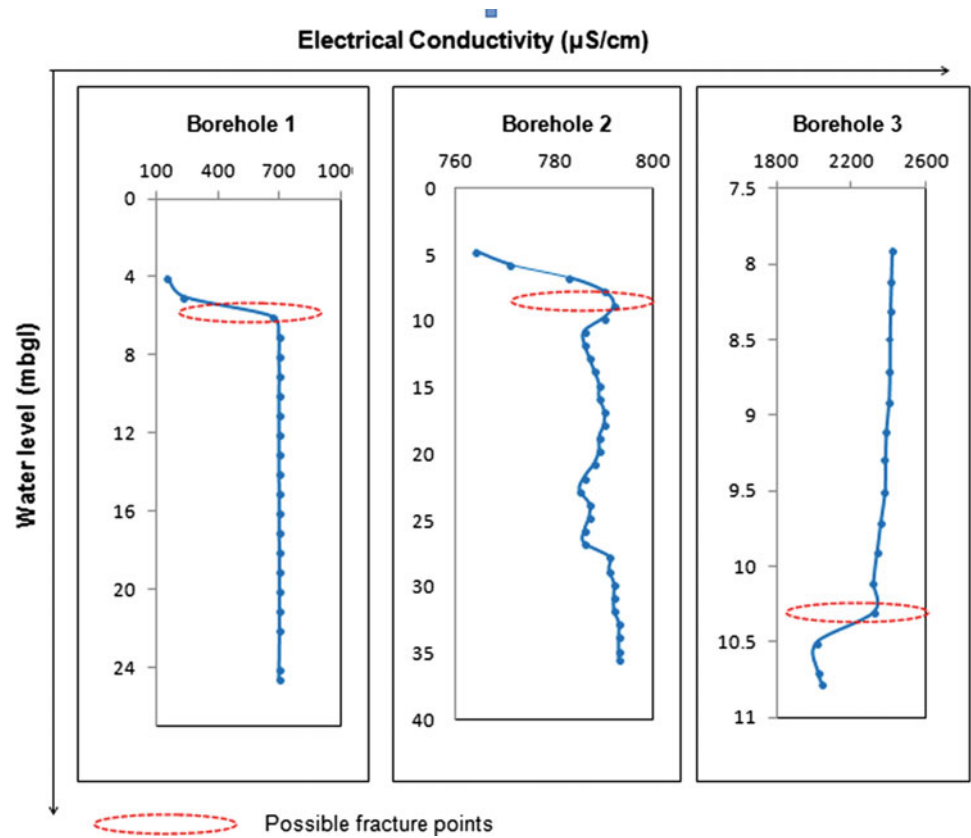
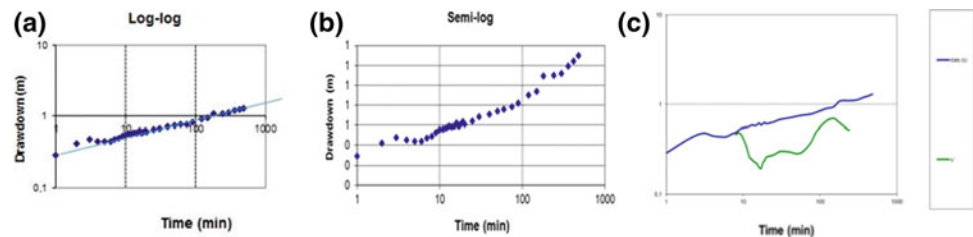


Fig. 3 Plot of hydraulic derivations from FC method



4 Discussion

The summary of the estimated hydraulic parameters results is shown in Table 1. According to Wei et al. [8], the long bilinear flow phase similar to the one observed in plot 3(a) came as a result of a low conductivity contrast between fracture (K_f) and matrix (K) conductivities ($K_f/K = 100$). This suggests that the setting of this aquifer is of a very porous media with a continuous fracture network. Therefore, the aquifer multi-porous media has the potential for urban supply. However, the available drawdown (AD) used in the FC is not the actual AD, but the geometric mean between the rest water level and position of main water strike. Therefore, the sustainable yields recommended from FC on this paper are based on conservative AD. The hydrochemical analysis

shows a $Mg-HCO_3$ water type from Stiff diagram. This suggests dissolved solutes from rainfall and the host rocks, particularly fractures associated with dolerite dykes structures [9] and not that of anthropogenic sources which might have originated from the urban setting of the study area. Geophysical results show that the boreholes were constructed targeting contact zones between dolerite dyke positions within the campus.

5 Conclusions

The study investigated hydrogeological properties of groundwater at CUT campus, which is located in the CBD of Bloemfontein. Results of groundwater hydraulics and hydrochemical properties show no contaminations from

Table 1 Summarized hydraulic parameters from CUT boreholes

Method	Sustainable yield (l/s)	Std. Dev	Late T (m ² /d)	S	AD used
Basic FC	9.34	5.86	301.6	2.20E-03	5.2
Cooper-Jacob	7.76	5.02	212.0	7.79E+00	5.2

activities in the urban areas and highlighted a good sustainable yield and a water quality good for urban water consumption purposes.

References

1. DWA: Water Quality Assessment Study for the Large Bulk Water Supply Systems of the Greater Bloemfontein Area. DWA, Pretoria (2012)
2. Molaba, G.L.: Investigating the possibility of targeting major dolerite intrusives to supplement municipal water supply in Bloemfontein: a geophysical approach. University of the Free State, Institute for Groundwater Studies, Bloemfontein, South Africa (2017)
3. Tijani, M.N., Oke, S.A., Olowookere, A.T.: Hydrogeochemical characterization of shallow groundwater system in the weathered basement aquifer of Ilesha Area, South-western Nigeria. In: Evolving Water Resources Systems: Understanding, Predicting and Managing Water-Society Interactions, Proceedings of ICWRS2014. IAHS Press, Bologna Italy (2014)
4. Van Rooyen, J.M.: A methodology to quantify the risks of urbanisation on groundwater systems in South Africa. North-West University, Department of Hydrology and Hydrogeology, Potchefstroom (2014)
5. Mbinze, A.: The influence of anthropogenic nitrate on groundwater quality in the Thaba Nchu area. University of the Free State, Institute for Groundwater Studies, Bloemfontein, South Africa (2012)
6. McCarthy, T., Rubidge, B.: The Story of Earth & Life. Struik Publishers, Netherlands (2005)
7. Van Tonder, G.V., Bardenhagen, I., Riemann, K., Bosch, J.V., Dzanga, P., Xu, Y.: Manual on Pumping Test Analysis in Fractured Rock Aquifers. Water Research Commission, Pretoria (2001)
8. Wei, L., Hadwin, J., Chaput, E., Rawnsley, K., Swaby, P.: Discriminating fracture patterns in fractured reservoirs by pressure transient tests. Society of Petroleum Engineers, SPE paper 49233 (1998)
9. Woodford, A.C., Chevallier, J.: The influences of dolerite sill and ring complexes on the occurrence of groundwater in Karoo fractured aquifers: a morpho-tectonic approach. Water Research Commission Report, 937/1/01, 146 (2002)

Assessment and Mapping of Proposed Dam Sites in North West Bank, Palestine Using GIS

Radwan El-Kelani and Abdelhaleem Khader

Abstract

Most of the countries in the eastern Mediterranean region, including Palestine, are characterized by arid to semi-arid climatic conditions and have limited water resources. This work aims at applying the Geographical Information Systems (GIS) to assess the suitability of proposed dam sites for the construction of earth dams to mitigate flood flows in the Sanour area in Jenin district, north of the West Bank, Palestine. The GIS techniques were utilized in site mapping and characterization to assess different criteria including delineation of drainage network and watershed boundaries, geology, soil, topography, and land use. ArcHydro tools, ArcGIS and SCS-CN methods were employed to model rainfall-runoff on a sub-catchment basis. For the rainy season of 2009/2010, the total runoff of stream network was estimated at about 1.57 million m³. Eventually, two selected dam locations were suggested for flash flood controls. Total rainwater harvesting of about 270,000 m³ is estimated from the two proposed dam sites. This water will also be of great importance to meet the rising demand for agriculture uses and expansion in reclamation.

Keywords

Dams • Flood control • Geographical information systems (GIS) • West Bank • Palestine

1 Introduction

Flash floods affect both civilian and agricultural activities as the negative impact of flooding lasts a long time after the event [1, 2]. In order to minimize and remediate this negative impact, different solutions are proposed such as dams,

tracking canals, or storm drainage systems [3–5]. In the context of research program activities to develop the rural regions in the West Bank, Palestine, sites have been proposed for the construction of dams, as earth-fill, to temporarily impound flood flows in the Sanour area in Jenin district, north of the West Bank (see Fig. 1). Sanour watershed forms a unique closed watershed of a catchment area that covers about 59 km²; out of which, 16000 m² form a basin called Marj Sanour Lake (MSL) which is considered one of the fertile agricultural areas in the West Bank [6]. Nevertheless, MSL is flooded by rainwater as a result of its geomorphologic feature causing direct and indirect harmful impacts. This work aims at applying the GIS techniques in site mapping and characterization to assess the suitability of proposed dam sites in the Sanour area for flood mitigation and water harvesting.

2 Settings

The study area is located in the northern part of the West Bank between Nablus and Jenin districts (Fig. 1). Sanour watershed has a nearly rectangular shape with northwest-southeast elongation; it reaches 5–8 km in length, and 2–4 km in width (Fig. 1). The watershed is one of the close karst plains in the northern part of the West Bank which spread within the mountains [6].

The geology is characterized mostly by carbonate rocks crop out in the surrounded mountainous area overlain by a thick mantle of soil that reaches more than 30 meters in some places beneath the MSL basin. The area is dominated by a clay texture soil of a Terra Rossas type [7]. The soil is reddish brown, composed of clay, silt, sand, and gravel, and characterized by its low permeability and high ability to store water.

R. El-Kelani (✉) · A. Khader
An-Najah National University, Nablus, Palestine
e-mail: radwan@najah.edu

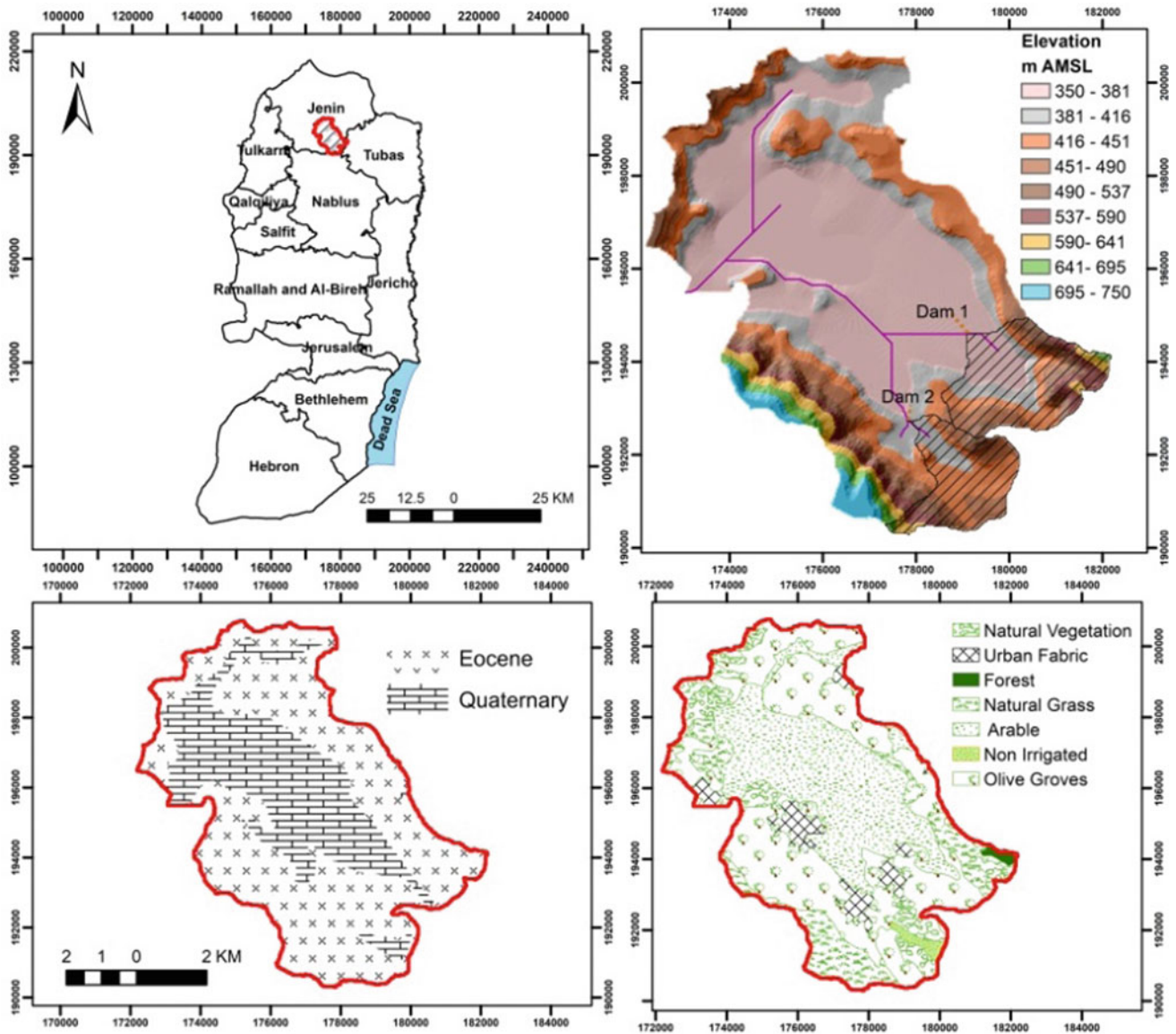


Fig. 1 Location map of the study area, also shown the geology, topography, and land use maps of Sanour watershed, and the proposed dam sites

3 Results

Before conducting any hydrological study on the catchment basis, the catchment first needs to be delineated. The availability of a digital elevation model (DEM) with adequate spatial resolution covering the whole area of interest is a basic requirement to achieve the delineation [8]. The hydrological modeling is applied to estimate the surface water runoff from each sub-catchment. SCS-CN method is used as one of the most popular methods for computing the volume of surface runoff in catchments for a given rainfall event [9]. The standard SCS-CN method is based on the following relationship between rainfall, P (mm), and runoff, Q (mm):

$$Q = \begin{cases} \frac{(P-I_a)}{P-I_a+S} & P > I_a \\ 0 & P \leq I_a \end{cases} \quad (1)$$

where S (mm) is the potential maximum retention after runoff begins. Through studies of many small agricultural catchments, I_a was found to be approximated by empirical equations such as $I_a = 0.2S$.

The variable S , which varies with antecedent soil moisture and other variables, can be estimated as:

$$S = \frac{25,400}{CN} - 254 \quad (2)$$

where CN is a dimensionless catchment parameter ranging from 0 to 100. The value 68 of the CN s was used for the

three sub-catchments. Daily rainfall values are needed to apply the SCS-CN method in order to estimate surface water runoff for the entire area and for the proposed dam sites. After investigating the rainfall data of the Mythaloon station, it was found that the annual average is about 536 mm. In the rainy season of 2009/2010, the annual rainfall was about 508 mm, which is close to the average value. And so, the daily rainfall values of 2009/2010 season were used in this study. The total runoff of the stream network was estimated at about 1.57 Million m³. Two proposed dam sites have been suggested for flash flood controls (Fig. 1). A total rainwater harvesting of about 270,000 m³ is estimated from the two proposed dam sites.

4 Discussion

In addition to the flow of flood in MSL, Sanour area suffers from water scarcity that yields a double-sided problem. The increasing demand of groundwater, over the recent years, to meet the rising need for rural supplies and the expansion in reclamation makes Palestine suffer from limited water resources [10]. In arid and semi-arid regions of the world, the shortage of water is a major limiting factor in the development of sound economic and social structures. Therefore, in such regions, including Palestine, a good and comprehensive management of the water system should be applied in order to ensure an adequate water supply [11, 12]. The land use map of the Sanour area is divided mainly into residential, agricultural and forest lands. The selected locations for dams must be based on land use plans and topographic restrictions. Consequently, the dam sites were proposed in areas of less land-use value, and according to the topographic constraints (Fig. 1).

5 Conclusions

Two sites have been proposed for the construction of dams to minimize flood flows in the Sanour area in Jenin district, north of the West Bank, Palestine. GIS techniques were utilized to assess different criteria, including delineation of drainage network and watershed boundaries, geology, soil, topography, and land use (Fig. 1). The hydrological modeling is applied to estimate the surface water runoff from

each sub-catchment using the SCS-CN method. A total runoff of about 1.57 million m³ of drainage network was estimated. Out of which, a total rainwater harvesting of about 270,000 m³ was estimated for two dam locations proposed for flash flood controls. This water will also be of great importance to meet the rising demand for agriculture uses and expansion in reclamation, so we can maximize water storage and minimize flood flows.

References

1. Garbero, A., Muttarak, R.: Impacts of the 2010 droughts and floods on community welfare in rural Thailand: differential effects of village educational attainment. *Ecol. Soc.* **18**(4), 1–18 (2013)
2. Abushandi, E., Alatawi, S.: 2015. Dam site selection using remote sensing techniques and geographical information system to control flood events in Tabuk City. *Hydrol. Current Res.* **6**(1), 1–13 (2015)
3. El-Behiry, M.G., Shedid, A., Abu-Khadra A., El-Huseiny M.: Integrated GIS and remote sensing for runoff hazard analysis in Ain Sukhna Industrial Area, Egypt. *Earth Sci.* **17**, 19–42 (2006)
4. Thilagavathi, G., Tamilenth, S., Ramu, C., Baskaran, R.: Application of GIS in flood hazard zonation studies in Papanasam Taluk, Thanjavur District, Tamilnadu. *Adv. Appl. Sci. Res.* **2**(3), 574–585 (2011)
5. Zaid, S., Zaghloul, E., Ghanem, F.: Flashflood impact analysis of Wadi Abu-Hasah on Tell El-Amarna archaeological area using GIS and Remote Sensing. *Aust. J. Basic Appl. Sci.* **7**(2), 865–881 (2013)
6. Abu Safat, M.: Geomorphology and the possibilities of resolving sinking problem in MarjSanour. *An-Najah Univ. J. Res. Human.* **6**(1), 7–48 (1992)
7. Abed, A., Wishahi, S.: *Geology of Palestine: The West Bank Gaza Strip, Palestine*, 1st edn. Palestine Hydrology Group (PHG), Ramallah (1999)
8. Hammouri, N., El-Naqa, A.: Hydrological modeling of ungauged wadis in arid environments using GIS: a case study of Wadi Madoneh in Jordan. *Revista Mexicana de Ciencias Geológicas* **24**(2), 185–196 (2007)
9. Ramakrishnan, D., Bandyopadhyay, A., Kusuma, K.N.: SCS-CN and GIS based approach for identifying potential water harvesting sites in the Kali Watershed, Mahi River Basin. *India J. Earth Syst. Sci.* **118**, 355–368 (2009)
10. Shadeed, S.: Spatio-temporal drought analysis in arid and semi-arid regions: A case study from Palestine. *Arab. J. Sci. Eng.* **38**, 2303–2313 (2012)
11. Dhawale, A.W.: Runoff estimation for Darewadi watershed using RS and GIS. *Int. J. Recent Technol. Eng.* **1**(6), 46–50 (2013)
12. Abushandi, E., Merkel, B.: Rainfall estimation over the Wadi Dhuliel arid catchment, Jordan from GSMaP-MVK + Hydrol. and Earth Syst Sci **8**, 1665–1704 (2011)

Reduction in the Storage Capacity of Dokan Dam Reservoir

Rebwar Hasan, Ammar Ali, Anwer Hazim, Nadhir Al-Ansari, and Sven Knutsson

Abstract

Dokan reservoir is located on the Lesser Zab River NE Iraq. Its drainage area is 11,690 km² with a storage capacity of 6.87×10^9 m³. Calculation of the volume of the reservoir before the construction of the dam and from the bathymetric survey conducted in 2014 indicates that an annual average of 7 million cubic meters of sediments are deposited within the reservoir. This reduced the storage capacity of the reservoir by 28%.

Keywords

Dokan reservoir • Lesser Zab river • Siltation of reservoirs • Iraq

1 Introduction

Dokan dam and its reservoir are located on the Lesser Zab River, one of the important tributaries of Tigris River in the northeast of Iraq (Fig. 1). The dam is a multipurpose (flood control, storage, hydropower and irrigation) concrete arch dam. It is the oldest dam in Iraq and it started operating since 1959. The catchment area is 11,690 km². The surface area of the reservoir is 270 km² and its storage capacity at the normal operation level (511 m.a.s.l.) is 6.87×10^9 m³ [1]. The geology of the area is mainly limestone rocks [2].

The actual storage capacity of the reservoir now is not known. Hassan et al. [1] conducted a bathymetric survey in

2014. This survey was compared with the stage-volume curve of the dam. In this research, the designed volume of the reservoir was calculated and compared with that of 2014 bathymetric survey to find out the exact rate of siltation within the reservoir.

A topographical map of the reservoir before the construction of the dam was prepared for the reservoir area. The maps had a scale of 1:20000 and a contour interval of 20 m. These topographic maps were drawn by Hunting Aerosurveys LTD in 1951–1952 [3]. The contours between 420 and 520 m.a.s.l. were digitized, and a Digital Elevation Model (DEM) was prepared using ArcGIS (Fig. 2).

2 Methodology

2.1 Bathymetric Survey

A bathymetric survey for Dokan Dam Reservoir was conducted using a single beam echo sounder in November 2014. Details of the transect lines of the bathymetric survey are shown in Fig. (3a). The bathymetric survey was conducted in a calm environment to avoid water surface fluctuation due to wind waves. The water surface elevations varied between 482.47 and 482.85 m.a.s.l during the surveying days. The error in depth measurement was estimated for the echo sounder, and it has been of a small value of ± 4 cm [1, 4].

2.2 Data Processing

The outputs of the echo sounder were converted to spot the points of water depth of (E, N, D) format in an Excel file. These depth points were transformed to elevation points of the reservoir bed, according to the water surface elevations of the reservoir for that day. A DEM of the reservoir bed was created using the extracted 65,416 elevation points from the bathymetric survey using ArcGIS software (Fig. 3b).

R. Hasan · N. Al-Ansari (✉) · S. Knutsson
Lulea University of Technology, 97187 Lulea, Sweden
e-mail: nadhir.alansari@ltu.se

A. Ali
University of Baghdad, Baghdad, 10071, Iraq

A. Hazim
Koya University, Koya, 46017, Iraq

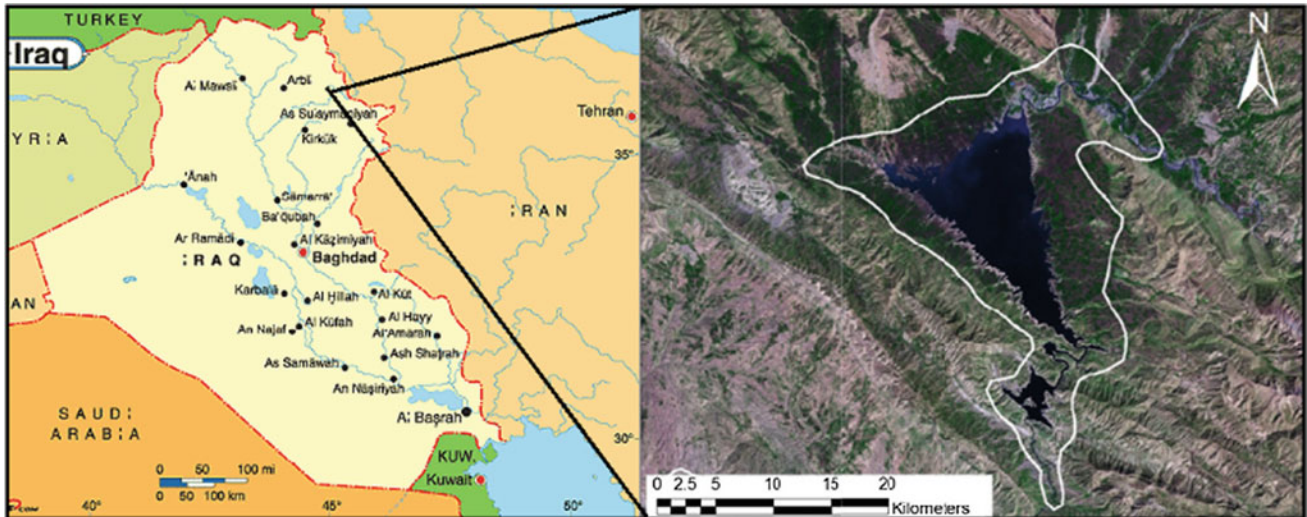
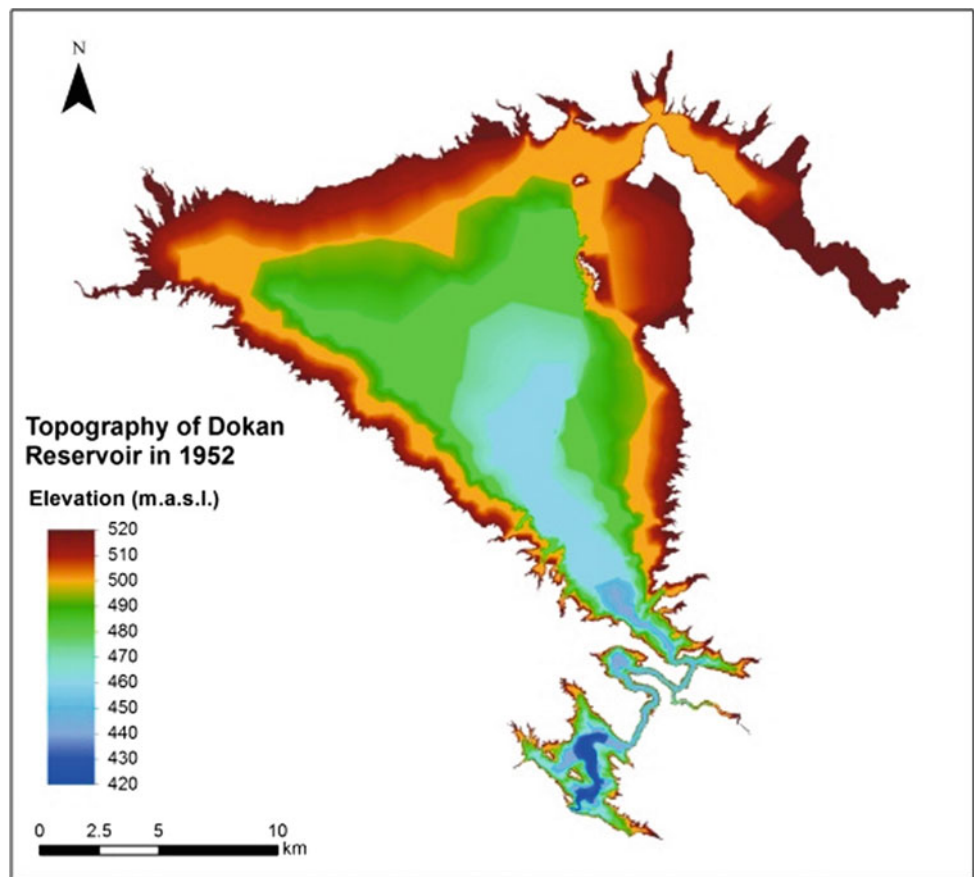


Fig. 1 Location map of Dokan Dam and its reservoir

Fig. 2 Topographical map of Dokan reservoir in 1952 (prior to dam construction)



2.3 Storage-Elevation Curves

Two sets of storage-elevation curves were prepared depending on the DEMs of the reservoir. The first set is

related to the topography of the reservoir in 1952 (Fig. 4), before constructing the dam. The second set is corresponding to the bathymetric survey in 2014 (Fig. 4).

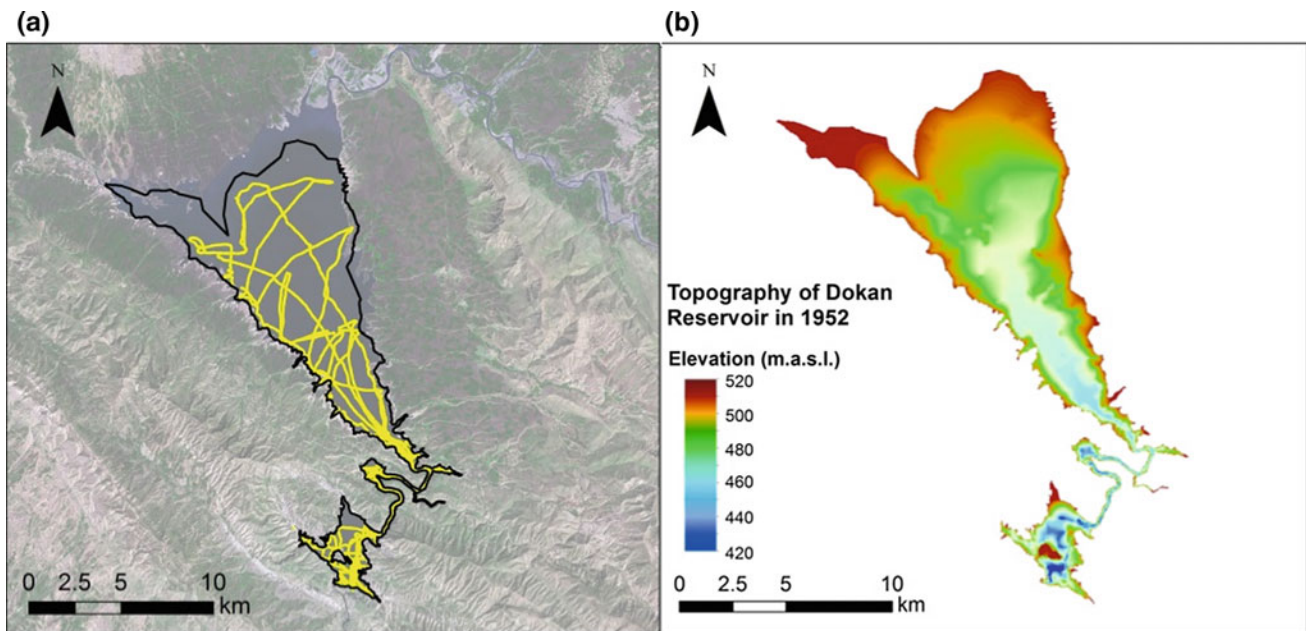


Fig. 3 a Transect lines of the bathymetric survey in 2014. b Topographical map of Dokan reservoir in 2014

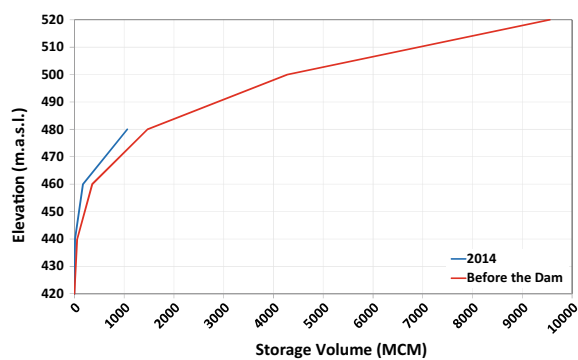


Fig. 4 Storage-elevation curve of Dokan reservoir

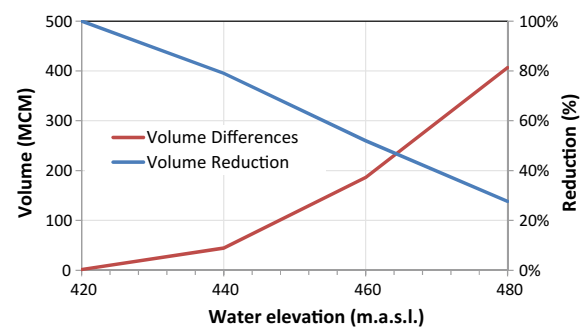


Fig. 5 Differences of storage volume in Dokan reservoir with storage reduction percentage for the period 1952–2014

3 Results and Discussion

3.1 Storage Reduction

Comparing these two sets of curves leads to determining the changes in the storage volume at each contour line during the period of 1952–2014. The accumulated sediment in the reservoir at the level of 480 m.a.s.l. was determined at about 407 million m^3 (0.4 km^3) according to the difference in the storage volume at that elevation (Fig. 5). This amount of sediment deposition has reduced the storage capacity of the reservoir by 28% of the design capacity at the level of 480 m.a.s.l. The annually averaged deposition is about 7 million m^3 .

According to Figs. 4 and 5, the storage volume at contour 420 has been fully in aggradation, which is the only

occupied part of the southern reservoir. Contour 440, which extends from the southern reservoir to the south of the northern reservoir, has been occupied by 78% by sediment. While 47% of the contour 460 and 20% of contour 480 have been filled by sediment.

4 Conclusions

The volume of the Dokan Reservoir was calculated at the start of the dam operation in 1959 using topographic maps of scale 1:20000. The result was compared with the volume calculated for the same reservoir using the bathymetric data collected in 2014. Comparison of the results indicates that an annual average of 7 million cubic meters is deposited in Dokan Reservoir. Siltation of the reservoir decreased its storage capacity by 28%.

References

1. Hassan, R., Al-Ansari, N.A., Ali, A.A., Ali, S.S., Knutsson, S.: Bathymetry and siltation rate for Dokan Reservoir, Iraq. *J. Lakes Reserv.: Res. Manag.* **20**(2), 1–11 (2017)
2. Sissakian, V., Abdulhad, A., Al-Ansari, N.A., Hassan, R., Knutsson, S.: The regional Geology of Dokan Area, NE Iraq. *J. Earth Sci. Geotech. Eng.* **6**(3), 35–63 (2016)
3. Directorate General of Surveys-Iraq (DGoS): Contour Maps of Sulimaniay and Erbil Provinces, Iraq (1956)
4. Issa, I.E.: Sedimentological and hydrological investigation of Mosul Dam reservoir. Doctoral thesis, Lulea University of Technology, Sweden (2015)

Impact of Landfill Leachate Organics on the Behavior of Heavy Metals in Groundwater

Irina Galitskaya, Vera Putilina, Irina Kostikova, and Tatiana Yuganova

Abstract

This paper describes the research example of the impact of organics on the behavior of heavy metals in the aquifers in the zone of the influence of the municipal solid waste landfill in the Moscow region. The aim of the study is to clarify the factors of groundwater contamination by heavy metals after recultivation in order to develop environmental protection measures. The obtained results allowed to identify the hazard of landfill as a source of contamination by heavy metals, to clarify the main stage of organic decomposition (in the top part—active stable methanogenesis and in the lower part—stable methanogenesis), and to determine the present stage of redox zoning development (the formation of the reduction zone of iron compounds contained in the solid phase water-bearing rocks, accompanied by the release of nickel and cobalt, previously adsorbed on iron and magnesium oxides and hydroxides).

Keywords

Heavy metals • Organics • Landfill • Groundwater contamination • Hydrogeological conditions • Municipal solid wastes

1 Introduction

Due to the fact that the municipal waste storage in the landfills remains one of the main ways of their utilization, the task of minimizing the damage for the environment and public health under the impact of existing and projected landfills is very relevant. The groundwater contamination by the different substances, including heavy metals, in the territories of the municipal solid waste landfill (MSWL) has become one of the major ecological concerns. The choice of

efficient managerial decisions is largely dependent on the results of forecasting the effect of the landfill on the groundwater quality by these contaminants, that is, in turn, dependent on the knowledge of the metals' behavior taking place in the aquifers at the sites under consideration.

This paper describes the example of researching the impact of organic matter on the behavior of heavy metals in the aquifers in the zone of the influence of MSWL in the Moscow region. The landfill arose in the sand quarries located at a distance of 400–600 m from the Pakhra River. Waste storage was carried out without a preliminary preparation of the base and sides of the quarries. The waste included brick, glass, plastic, rubber, metal, textile waste, paper, etc., interspersed with sand and loam. The maximum thickness of the technogenic sediments reached 25–30 m. The impact of MSWL led to a change in the groundwater chemistry in all aquifers, from Alluvial to Kashirskii aquifer in the Carboniferous deposits. In different periods, the concentrations of chloride, sodium, ammonium, nitrate, iron, manganese, nickel, cobalt, barium, mercury and the other components in groundwater exceeded the maximum permissible concentrations.

The remediation measures contributed to the reduction of the amount of the atmospheric water infiltrating through the landfill body, and also the contaminants entering the aquifers. However, despite the general positive effect on the groundwater quality, the tendency of increasing the groundwater contamination by iron, manganese and other metals was detected in Alluvial and Jurassic aquifers. In this regard, there was a need to clarify the causes of groundwater contamination after reclamation in order to develop the needed environmental protection measures.

2 Materials and Methods

To achieve the goal, the following tasks were set: (1) to identify the landfill as a source of groundwater contamination by heavy metals, including the study of the chemical

I. Galitskaya (✉) · V. Putilina · I. Kostikova · T. Yuganova
Sergeev Institute of Environmental Geoscience Russian Academy
of Science (IEG RAS), Moscow, 101000, Russia
e-mail: galgeoenv@mail.ru

composition of the leachate and the determination of the stage of the organic decomposition in the landfill; (2) to study the hydrogeochemical situation in the area of the MSWL and the adjacent territories from the moment of introduction of the landfill into operation to the current moment.

The chemical composition of the leachate was studied based on the chemistry of the technogenic aquifer. Identification of the current stage of organic matter decomposition in a landfill is necessary for the assessment of the activity of heavy metals release from the bound state and their entry to the aquifers. We established [2] that the most active period is determined by the aerobic phase and the anaerobic phase of acetogenesis and that situation is due to the formation of carboxylic acids and pH decrease. In the process of the “aging” of the landfill, the pH of the leachate increases while the content of dissolved organic matter decreases. The stage of decomposition of organics in the landfill can be determined as the ratio of BOD/COD, where BOD is biochemical oxygen demand, COD is chemical oxygen demand.

The identification of the hydrogeochemical situation in the study area was performed on the basis of the results of monitoring conducted from 1985 to 2006. The complex of studies included the determination of pH, chlorides, sulfates, hydrocarbonates, calcium, magnesium, nitrates, nitrites, ammonium, sodium, potassium, oil products, iron, manganese, lead, copper, zinc, nickel, cobalt, chromium, cadmium. Monitoring was carried out in all aquifers, but in this paper, while taking into account the limited volume, we consider only alluvial and Jurassic aquifers, where the impact of MSWL was the most significant.

3 Results and Discussion

The technogenic aquifer that we used for the study of chemical composition of the landfill leachate has formed due to the atmospheric precipitation seeping through the wastes, as well as the moisture coming from the wastes. It is substantially contaminated with various organic and inorganic compounds. The technogenic aquifer was discharged into the underlying aquifer. The mineralization of water varied in a significant range, from 411 to 19490 mg/l, BOD was 7.95–9.3, COD was 9.09, and pH was 6.6–10.62. The ranges of heavy metal concentrations over the period 1985–2006 are presented in Table 1. There were no tendencies in the heavy metal concentration changes.

The results of identification of the present stage of organics decomposition showed that at the time of research the landfill was in the stage of stable methanogenesis, which was confirmed by the low (BOD/COD = 0.01) ratio in the

groundwater under the landfill. At the methanogenic stage, the content of organics, iron, manganese, zinc, magnesium and a number of other pollutants in the leachate is substantially reduced.

The ranges of heavy metal concentrations in 1985–2006 are presented in Table 1. After closure of the landfill, the tendency of increase of the concentration of iron, manganese, cobalt and nickel was noted. The most significant values were fixed in the end of the monitoring research. We proposed that the concentration changes of iron, manganese, nickel and cobalt in groundwater were largely governed by the formation of redox zones in the aquifers around the landfill. As is known [1], when organics enter the groundwater, aerobic degradation takes place first and then anaerobic degradation occurs in the following order: nitrate reduction, manganese reduction, iron reduction, sulfate reduction, and finally methanogenesis. Formation of oxidation-reduction zones is due to the presence of oxidizing components: free oxygen, nitrates in groundwater and iron (III) and manganese (IV) compounds in the solid phase.

The reduction of iron (III) compounds (either of natural genesis or, possibly, precipitated earlier on the oxidation barrier) caused an abrupt increase in iron (II) concentration in groundwater. In the period under consideration, the leaching of iron and manganese from the landfill body was not the main process for the high concentrations of those elements in groundwater. Iron came mostly from water-bearing rocks as the result of reduction. In this context, we can conclude that the high concentrations in groundwater are mostly due to the reduction of natural or natural–technogenic iron contained in the solid phase of water-bearing rocks during oxidation transformations of organics of landfill leachate. To a lesser extent, the mobilization process is typical of manganese as well, which is likely due to its lower concentration in the solid phase.

The major factors of the increase of nickel and cobalt concentrations at the stage of iron and manganese reduction could be the release of these elements earlier sorbed by oxides and hydroxides of iron and manganese. The absence of concentration peaks of other heavy metals may be due to the specifics of their geochemical behavior. For instance, for cadmium and zinc, the sorption on surface areas of silicates and AlOH, associated with either kaolinite edges or Al oxides, is more significant than that on the crystalline phase of Fe oxide.

So, the main factor of groundwater contamination by heavy metals after the recultivation of MSWL was not these elements entering from the landfill body, but physicochemical and biochemical processes in the aquifers, mainly the reduction of oxides and hydroxides of iron and manganese, accompanied by the release of the other previously desorbed heavy metals.

Table 1 Concentration ranges of heavy metals in the aquifers (mg/L)

Element	Technogenic aquifer	Alluvial aquifer	Jurassic aquifer
Iron	0.92–140.0	0.01–654.0	0.01–2226.0
Manganese	0.002–0.08	0.004–4.12	0.02–13.1
Cobalt	0.001–0.09	0.0001–0.2	0.0001–0.18
Chromium	0.02–0.53 s	0.0005–1.99	0.0008–1.32
Nickel	0.0001–0.35	0.0001–0.36	0.0001–0.62
Cadmium	0.001–0.07	0.001–0.07	0.001–0.08
Lead	0.001–0.15	0.001–0.41	0.001–0.33
Copper	0.0002–0.4	0.0002–0.41	0.0002–27.0
Zinc	0.05–0.78	0.0008–1.53	0.001–4.0

4 Conclusions

Analysis of heavy metal concentration changes in the aquifers from the beginning of landfill operation allowed: (1) to identify the hazard of landfill as a source of heavy metal contamination, (2) to clarify the main stage of organic matter decomposition (in the top part–active stable methanogenesis, in the lower part–stable methanogenesis), (3) to determine the present stage of redox zoning development (the formation of the reduction zone of iron compounds contained in the solid phase water-bearing rocks, accompanied by the

release of nickel and cobalt, previously adsorbed on iron and magnesium hydroxides).

References

1. Heron, G., Crouzet, C., Bourg, A.C.M., Christensen, T.H.: Speciation of Fe (II) and Fe (III) in contaminated aquifer sediments using chemical extraction techniques. *Environ. Sci. Technol.* **28**(9), 1698–1705 (1994)
2. Putilina, V.S., Galitskaya, I.V., Yuganova, T.I.: Effect of organic matter on the migration of heavy metals at SMW disposal sites: analytical review, GPNTB SO RAN; IGE RAN, Novosibirsk, (Ser. Ecology, no. 76) (2005)

Modeling of Toluene and Benzene Concentrations in the Groundwater of Tanjero Waste Dump Area, Kurdistan Region, Iraq

Aras Kareem and Omed Mustafa

Abstract

Wastes are dumped in the main Tanjero landfill site from different sources, such as domestic waste and uncontrolled waste dumping from the refineries in the area. The BTEX complex has been recognized in the analyses of the groundwater sample in some wells around the Tanjero waste dump site. Benzene and toluene were the two main components with significant concentrations compared with the other components of BTEX. In this study, the variation in the concentration of benzene and toluene was simulated in different depths for 25 years. The modeling of the benzene and toluene scenario is correlated with regard to the climate conditions as well as physical and chemical conditions of the soil in the waste dump site. The contamination can reach the groundwater but in low concentration and inversely with the depth. Different phases of contaminants in the unsaturated zone in the subsoil show different rates of contamination, depending on the phase type (gas, liquid and solid). The contamination potentials of benzene and toluene are different in the rates, and toluene has more concentration in the liquid phase than benzene in the unsaturated and saturated zones. Benzene is attenuated more rapidly than toluene in this area. The current study aims to evaluate the potential impact of BTEX contamination on the groundwater.

Keywords

BTEX • Toluene • Benzene • Waste • Tanjero area • VLEACH

1 Introduction

BTEX complex is composed of benzene, toluene, ethylbenzene and three xylenes. These components make up a large harmful group to human health. Studies on drinking water show the neurological effects of toluene when it is found in drinking water [1]. The presence of benzene in drinking water could be a reason for the decrease of blood platelets with the risk of getting cancer, and according to the EPA standards, 0.005 mg/L of benzene in the drinking water is considered the minimum harmful level on human health of this contaminant in drinking water [2]. The Tanjero landfill site (Kurdistan region, northern Iraq) has many dumping sources, such as domestic sources (more than 1000 tons per day), industrial sources and illegal oil refineries' wastes and remains. All these materials are dumped uncontrollably in a fenced, unsupervised and unconstructed landfill site on 50 ha of land [3]. The local authorities are planning to discontinue the dumping process of waste landfill site in the present way and they are establishing a recycling factory for the dumped wastes [4]. The aim of this study is to simulate the transport of volatile organic contaminants—namely toluene and benzene, which are the highest concentrated components of BTEX compared with the rest of the BTEX components in this case study, in the unsaturated zone of the dump site soil, which is composed of clay, sand and silt—by using commercially available transport models.

2 Materials and Methods

This study depends on BTEX data of the closest water well (well No. 3) to the Tanjero dump site and the leachate BTEX concentration of the same dump site in the Tanjero area, southeast of Sulaimani City, Fig. 1. These concentrations got after the analysis of the water samples collected during the summer of 2013. Well No. 3 has the highest values of BTEX components compared with the other wells around the dump

A. Kareem (✉)
Sulaimani Polytechnic University, 46024 Sulaimaniyah, Iraq
e-mail: aras.omer@spu.edu.iq

O. Mustafa
Charmo University, 46023 Chamchamal, Iraq

site. BTEX components' concentrations were analyzed by a headspace technique with gas chromatography, and detection was made by mass spectrometry (Thermo Scientific Ultra-ISQ GC-MS) [5]. The soil texture is silty clay loam and this depends on the percentages of sand, silt and clay, which are 17.87, 53.32 and 28.81%, respectively [6].

To calculate the vertical direction of water leaching through the soil, which is named 'percolation' in the study area, the HELP3 model was used [7]. The data of meteorological station in Sulaimani City were used in this model to predict the percolation in the soil column. The annual percolation through the model column representing the waste dump site was calculated using HELP3, Table 1. The determined total percolation was 8.2 m [4] (Fig. 2).

The VLEACH model simulated the sink flow movement of BTEX components, which is represented by benzene and toluene in this study, through the soil column, which is 8.5 m in depth. The first concentration was from the leachate in the waste dump site. The leachate flowed with 14.2549 and 23.93099 mg/L concentration for benzene and toluene, respectively. The concentrations of benzene and toluene in well No. 3 are 0.09 and 1.4 mg/L, respectively. The water table in well No. 3 was 8 m deep during the water sample collection in summer 2013. Table 2 shows the input parameters of the soil in VLEACH model.

3 Results and Discussion

In Figs. 3 and 4 the results show the toluene and benzene concentrations at several depths of the soil during the 25 years. The depths are 0.49 ft (0.15 m), 3.44 ft (1.0485 m), 13.29 ft (4.051 m) and 28.05 ft (8.51 m). The concentrations of toluene and benzene in the first 0.15 m of the soil column from the surface are the highest concentrations compared with the concentrations at the other mentioned depths. The concentrations at 8.51 m are the lowest. In Fig. 3a, b, the concentration of toluene is still above zero at all the mentioned depths and it ranged between zero to 0.0075 mg/L after 25 years, with regard to a certain expansion in the 4.051 and 8.51 m depths as the volatilization rate decreases with depth of the soil because the soil particles decrease and the hydraulic conductivity decreases while the organic matter increases [8]. The expansion of hydrocarbon plume in the soil has been demonstrated to reduce more rapidly in concentration of the hydrocarbons with time than the dimensions of the plume in the soil [9].

In Fig. 4a, b, there is a demonstration of the concentration of benzene during 25 years. These figures show that the concentrations of benzene in the different mentioned depths become zero after approximately 22 years. As in the toluene case, there is a certain expansion in the depths 4.051 and

Fig. 1 Geological profile of the case study determining the contaminated, saturated and unsaturated zones

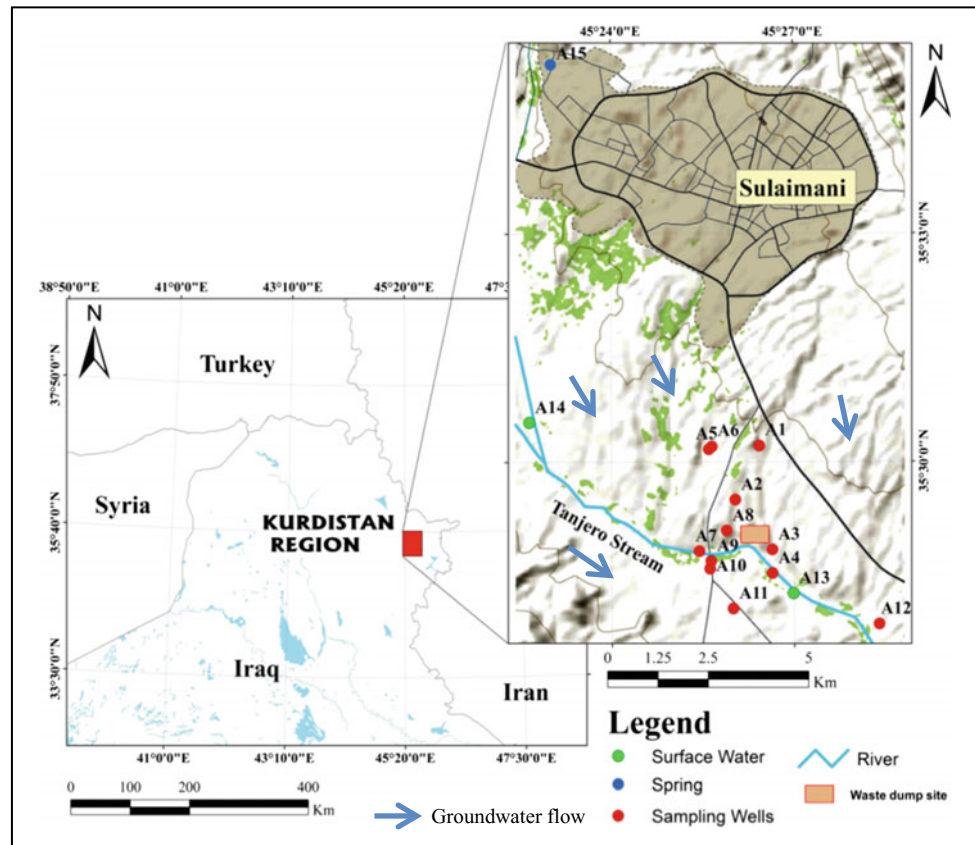


Table 1 Soil input parameters to HELP3

Parameter	Value	Unit	Source
Thickness of the polluted zone	1	meter	Field survey and assumption
Total porosity	0.478	– (vol/vol)	Najmadeen et al. [6]
Field capacity	0.353	– (vol/vol)	Abdulla [10]
Wilting point	18.4	%	Abdulla [10]
Initial moisture content	0.09	– (vol/vol)	Calculated by HELP3
Saturated hydraulic conductivity	0.00019	cm/sec	Najmadeen et al. [6]
Surface slope	5	%	Assumption
Area from where runoff is allowed	90	%	Assumption
Vegetation class	Bare soil	–	Assumption
Evaporative zone depth	12	inch	Assumption

Fig. 2 Geological profile of the study case determining the contaminated, saturated and unsaturated zones

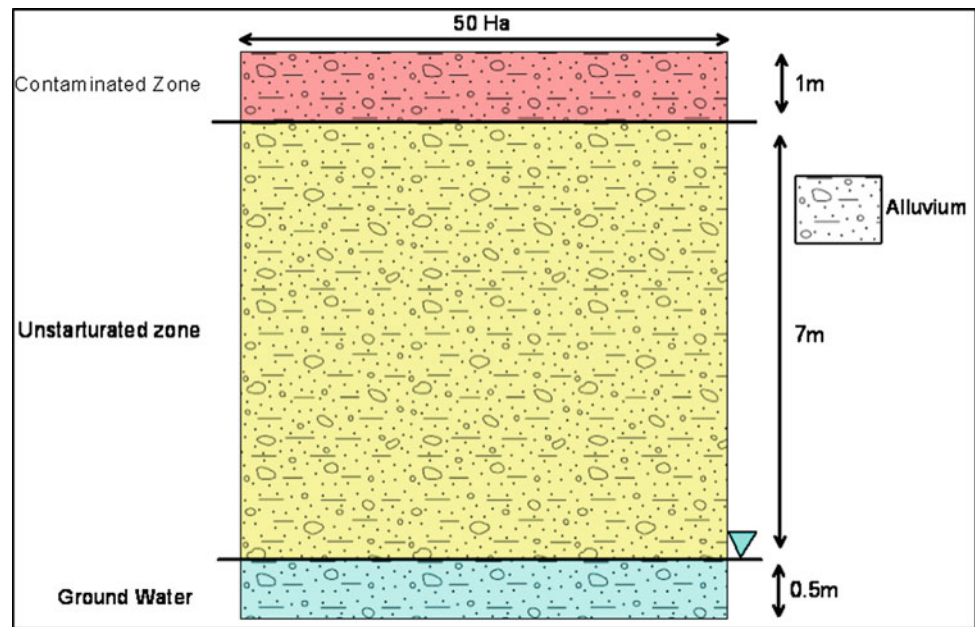


Table 2 The input parameters for the soil to the VLEACH model

Parameter	Value	Unit	Source
Bulk density	1.3	(g/cm) ³	Rashid [3]
Effective porosity	0.14	(vol/vol)	Najmadeen et al. [6]
Water content	0.019	(vol/vol)	Rashid [3]
Fraction organic content	0.28	(%)	Najmadeen et al. [6]

8.51 m with the same scenario of interpretation. The concentration of the toluene is greater than the concentration of benzene in the leachate of the dump site and the groundwater of well No. 3. This indicates that the toluene requires more time, temperature and moisture in the soil with biological remains and biodegradable materials to dissolve and absorb in the soil. By comparing the results of the modeling of toluene and benzene, we find that the benzene is more

dissolved and volatilized than toluene in this study. This is because of the comparatively high water-solubility with low octanol–water partition coefficient (K_{ow}) values, these compounds will tend to be dissolved in the water phase or evaporate into the air spaces of the soil, and relatively more than toluene. This made benzene highly mobile in the soil and groundwater environment [4].

Fig. 3 a, b The Toluene concentration in different depths during 25 years

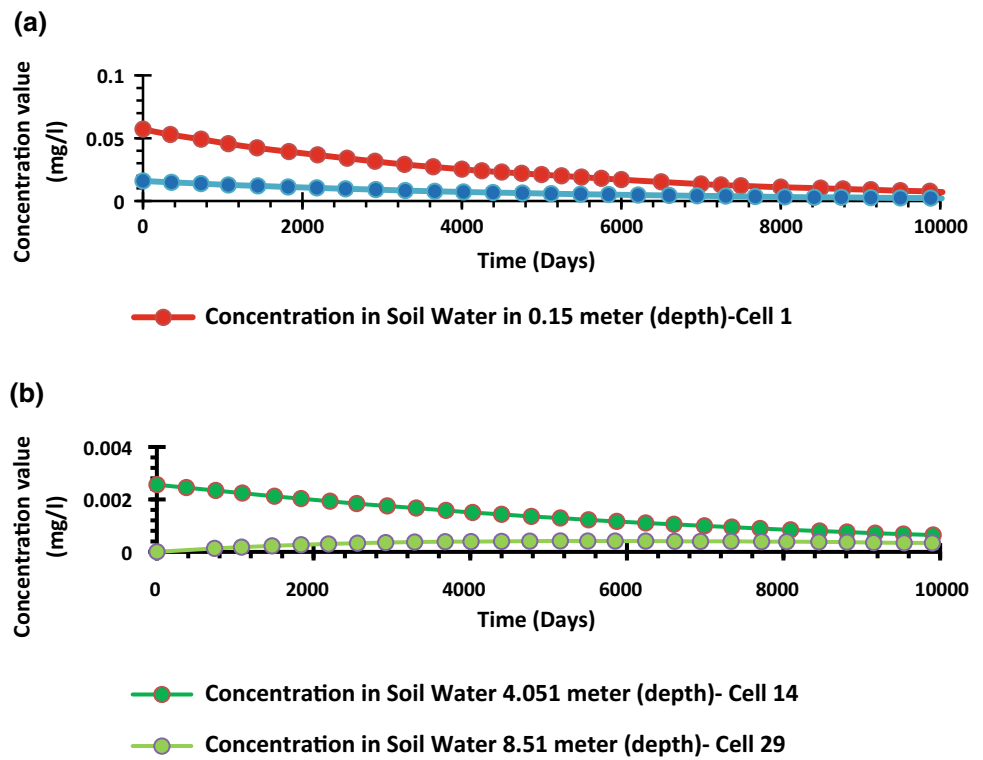
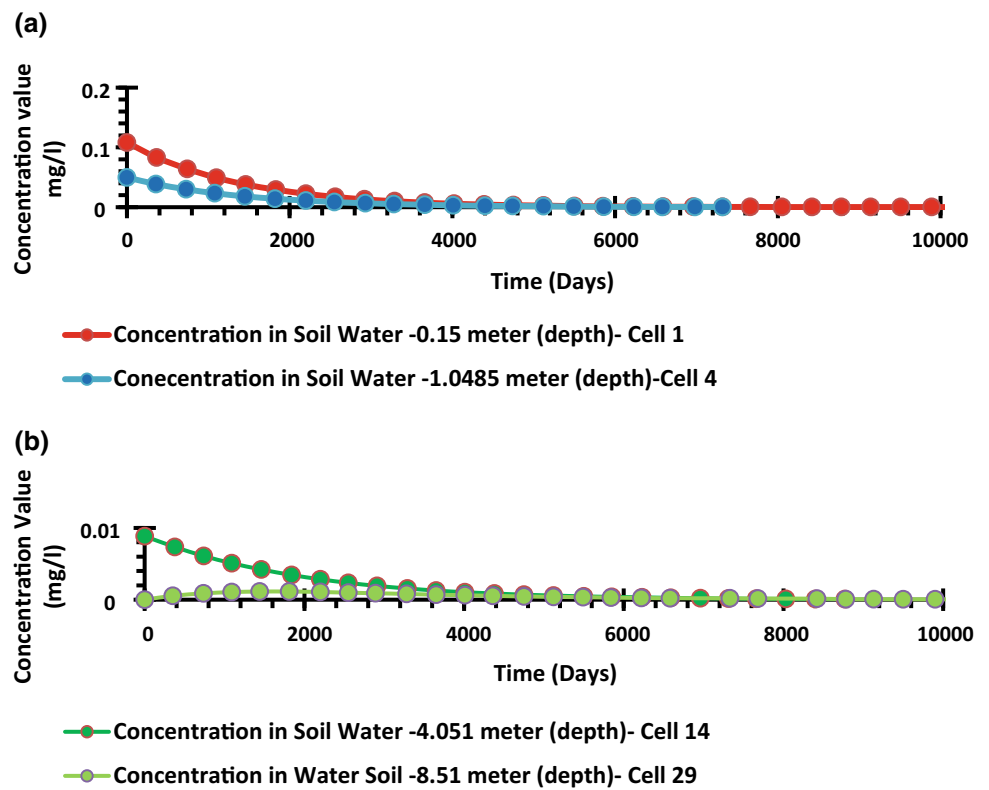


Fig. 4 a, b Benzene concentration in different depths during 25 years



4 Conclusions

The effects of benzene and toluene in the saturated and unsaturated zones of the dump site in the Tanjero area will remain for more than 25 years for toluene and 22 years for benzene. Toluene approached zero concentration at deeper depths than benzene. The physicochemical properties acted as the main factors to create chronic differences in the rate of volatilization, absorption, dissolution and biodegradation between toluene and benzene. Benzene is more volatilized, dissolved and absorbed than toluene in this area. The groundwater in this dump site area will need remediation from the hydrocarbon contaminants even after the waste dumping process stops or a recycling process is established there.

References

1. The Federal-Provincial-Territorial Committee on Drinking Water, Toluene, Ethylbenzene and Xylenes in Drinking Water, Health Canada consultation document, (2013). http://www.hc-sc.gc.ca/ewh-semt/consult/_2014/tex/consultation-eng.php#s2.1
2. US Environmental Protection Agency: Drinking Water Contaminants—Standards and Regulations, (2016). <http://water.epa.gov/drink/contaminants/basicinformation/benzene.cfm>
3. Rashid K.: Environmental impalication of Tanjero waste disposal site of Sulaimani, unpublished Ph.D. student thesis, Sulaimani University (2010)
4. Aras, Kareem, Rudy, Abo, Broder, Merkel: Modeling the Fate of Toluene and Benzene at the Tanjero Waste Dump Site. Sulaimani, North Iraq (2016)
5. Butler, J., Steiniger, D., Robarge, T., Phillips, E.: Combining Hardware, Software, and Chromatography to Improve the GC/MS Analysis of Semi-Volatile Compounds. Thermo Fisher Scientific, Austin, TX, USA (2010)
6. Najmadeen, H., Mohammad, A.O., Mohamed-Amin, H.: Effects of Soil Texture on Chemical Compositions, Microbial Populations and Carbon Mineralization in Soil. The Egyptian Society of Experimental Biology (2010)
7. Singh, V.P.: Elementary Hydrology, p. 973. Prentice-Hall, Englewood Cliffs (1992)
8. Arthurs, P., Stiver, W.H., Zytner, R.G.: Passive volatilization of gasoline from soil. *J. Soil Contam.* **4**(2), (1995)
9. Newell C.J., Connor, J.A.: Characteristics of Dissolved Petroleum Hydrocarbon Plumes, Groundwater Services, Inc., API Soil/Groundwater Technical Task Force, American Petroleum Institute, Vers. 1.1, December (1998)
10. Abdulla, Z.O.: Characterization and Classification of Soils and Land Use Suitability in Some Selected Areas from Iraqi Kurdistan Region. University of Sulaimani, Iraqi Kurdistan Region (2015)

Using Chance Constrained Programming Approach for Optimal Crops Selection and Economic Profitability of Irrigation Under Hydrological Risk: The Case Study of Small Dams in Tunisia

Hacib El Amami, Jean R. Kompany, Taoufik Hermassi, and Nada Lellia

Abstract

This study aimed to analyze the economic profitability of irrigation under hydrological risk. Towards this end, two hill lakes located in different climatic conditions (sub-humid and semi-arid climates) were selected and a chance constraint linear programming model was used. The model incorporated the uncertainty of water supply at exceedance probability of 80, 90, 95 and 99%. The results showed that in a sub-humid climate, there are 100 and 95% chances to meet monthly water requirements for winter and summer crops, respectively. The impact of a small dam on local farming economic profitability was highly significant. Both environmental and socio-economic objectives can be achieved. In a semi-arid climate, results showed that, at the 90% water supply reliability, only winter crops and olive trees were included in the optimal cropping pattern under deficit irrigation and on a limited area. Summer crops were not recommended. The economic profitability of irrigation around the small dam would be strongly reduced. Therefore, the objective to improve the population well-being in arid and semi-arid regions assigned to these structures is not likely to be achieved. As the public budget allocated to environment protection becomes more and more restraint, this study suggests implementing hill lakes first in areas where their economic and environmental efficiency is proven.

Keywords

Small dam • Sub-humid • Semi-arid • Profitability
Water supply • Probability

1 Introduction

Small dams (or hill lakes) have constituted an important component in the “national strategy of surface runoff mobilization” in Tunisia since the early 1990s. Today, more than 900 hill lakes have already been constructed in the central and northern parts of the country within the sub-humid and semi-arid climate regions. It is argued that small dams ensure the mobilization of a non-negligible amount of water in areas where the heavy hydraulic infrastructure cannot be installed because of physical and economic constraints [1, 2]. From this point of view, they are considered as ensuring better equity of water resources allocation through increasing water supply in remote mountainous areas where the poor live.

By collecting surface runoff from the catchment and storing it in small surface reservoirs, these structures give the opportunity for farmers to access water and to develop irrigated cropping, thus, raising their income and the well-being of the overall area, in general. However, achieving this goal is complicated by the uncertainties that exist over the availability of water, which depends on rainfall and the water stored in the reservoirs.

These uncertainties could weaken the farmers’ incentive to invest in irrigation. Many authors argued that the uncertainty about surface water availability deters irrigators from making long-term investments [3]. This is especially the case with the small hill dams in Tunisia, where reports showed limited use. The overall objectives of this study were to (a) identify the optimum planning crops suitable to water supply uncertainty in various climatic regions (b) analyze the economic profitability of irrigation and (c) investigate how supply uncertainty would affect the optimal irrigated area and expected economic profit.

H. El Amami (✉) · T. Hermassi
National Institute for Research in Rural Engineering, Water and
Forests, 2080 Ariana, Tunisia
e-mail: hacib.amami@gmail.com

J. R. Kompany · N. Lellia
National Agronomic Institute of Tunisia, Tunis, Tunisia

2 Methodological Approach

The conceptual framework is based on chance constrained programming developed by Charnes and Cooper [4]. It was applied in this study in order to account for the risk associated with water availability in two studied hill lakes. The first one called “El Kamech” is localized at Houwaria region (Governorate of Nabeul) with rainfall ranging between 650 and 700 mm per year. The dominant farming system is based on rainfed agriculture (wheat, barley, oat, spices) and livestock (fattening and dairy cows). The second one is localized at Haffouz (Governorate of Kairouan) where the average rainfall doesn't exceed 350 mm per year with a high variability from year to year. The dominant farming system is based on rainfed agriculture (wheat, barley, olive tree) and livestock (sheep). The model is designed to maximize a farmer's expected net profit from alternative crops subject to hydrological risk and a set of constraints that define the physical and economic environment of each study area.

3 Results

3.1 Optimum Crop Planning in Deterministic and Probabilistic Scenarios

Compared to deterministic scenario, our results showed that in the case of El Kamech hill lake, the optimal cropping patterns under probabilistic scenario remains unchanged for winter and autumn crops. As shown in Table 1, there is 100% reliability to meet monthly water requirement of crops cultivated through the period from September to March.

Regarding to summer season, the empirical results reveal that requiring a high reliability of water supply, exceeding 95%, to satisfy the monthly water requirements leads to cultivate short season crops that mature by the end of July. The selected crops include industrial tomatoes and water melon. However, fodder crops, like sorghum, can be also cultivated but under deficit irrigation particularly since August.

Crops with long growth cycles, like pepper, are not included in the optimal plan. As shown by Table 1, the cultivated area of pepper decreases as the probability level is raised. This is due to the low reliability of water availability in August.

Unlike El Kamech, the gap between deterministic and probabilistic optimal cropping patterns increases when considering water supply uncertainty in the case of Dekikira hill lake. Results in Table 2, indicated that, at 90% of water supply reliability, no land and irrigation water were allocated to summer crops (vegetables and fodder). Only olive trees and winter wheat, as well as winter fodder crops, were proposed for the optimal solution. At the other two levels of certainty, i.e. 95 and 99%, these same crops appear, on a reduced area relative to the baseline scenario and under severe deficit irrigation.

Requiring high reliability of water supply (risk reduction) in Dekikira case, leads to a significant reduction in cultivated land, and therefore, to a fall in the farmers' income. For example, achieving a 90% probability level will reduce both the irrigated area and the expected economic profit by 65 and 86%, respectively, relative to baseline scenario. Whereas achieving the same probability level will decrease profit and cultivated area only by 8 and 9%, respectively, in the case of El Kamech hill lake.

Table 1 Optimum crop planning and cropped area in deterministic and probabilistic scenario (area unit: ha; income unit: TND)

Season irrigation	Selected crops	Deterministic scenario	Probabilistic scenario			
			Water supply reliability			
			80%	90%	95%	99%
Autumn-winter	Peas	1.5	1.5	1.5	1.5	1.5
	Spices	2	2	2	2	2
	Bean	2	2	2	2	2
Summer	Tomatoes	4	4	4	4	4
	Peppers	2.5	2	0	0	0
	Water melon	1.5	1.5	1.5	1.5	1.5
	Sorghum	1.5	1.5	1	0.5	0
Total cropped area		15	15	14.5	14	13.5
Aggregate income		100	100	91.6	86.4	77.6
Net farm income		12.5	12.5	11.45	10.8	9.7

Table 2 Optimum crop planning and cropped area in deterministic and probabilistic scenario for Dekikira hill lake (area unit: ha, income unit: TND)

Season irrigation	Selected crops	Deterministic scenario	Probabilistic scenario			
			Water supply reliability			
			80%	90%	95%	99%
Autumn-Winter	Wheat	4	1.5	1.5	1.5	1.5
	Fodder	2	2	2	2	1
	Bean	2	1.5	1	0.5	0.5
Summer	Tomatoes	2	0.25	0	0	0
	Peppers	2	0.25	0	0	0
	Sorghum	1.5	1	0.5	0	0
Olive trees		4	4	4	2	2
Total cropped area		15	10.5	9	6	5
Aggregate income		75.2	46.4	33.6	28	9.6
Net farm income		9.4	5.8	4.2	3.5	1.2

4 Discussion

As the economic profitability depends strongly on rainfall, hill lakes would be effective in regions where rainfall is regular and sufficiently high to store the large amounts of water received. This makes these structures particularly suitable for sub-humid areas where both the economic and environmental objectives can be achieved. In semi-arid regions, the small dams have the capacity to store water during the wet season, which be useful to cultivate winter crops like wheat, oat, barley as well as olive trees under supplementary irrigation, but they are not able to provide water to irrigate crops during the dry season (summer crops). Therefore, the economic profitability of irrigation around the lake and the amplitude of its impact on the local economy would be strongly reduced. However, in some cases and when geological conditions are suitable for deep percolation, hill lakes might contribute to local economy development by increasing groundwater supply.

5 Conclusions

The study aimed to analyze the economic profitability of irrigation around small dams (hill lakes) under different climatic conditions (sub-humid and semi-arid). The results showed that the impacts on local farming economics and the

profitability of irrigation were largely related to the amount of rainfall received. In a sub-humid climate, the impact on irrigated agriculture development and farmers' income was highly significant. Both environmental (soil erosion reduction) and socio-economic objectives can be simultaneously achieved. In a semi-arid climate, results showed that, the economic impact was limited given the high uncertainties about water stored. Only the environmental objective is likely to be achieved. Based on these results, this study suggests to rethink the implementation of hill lakes in semi-arid conditions because, to protect the environment, other structures are more effective in controlling soil erosion and are perhaps less costly.

References

1. Ben Mechlia N., Oweis, T., Masmoudi, M., Mekki, I., Ouessar, M., Zante, P., Zekri, S.: Conjunctive Use of Rain and Irrigation Water from Hill Reservoirs for Agriculture in Tunisia. 40p, ICARDA (2009)
2. Boufarwa, M., Slimani, M., Oweis, T., Albergel, J.: Hill lakes: innovative approach for sustainable rural management in semi-arid regions in Tunisia. *Glob. NEST J.* **15**(3), 366–373 (2013)
3. Dwyer, G., Loke, P., Appels, D., Stone, S., Peterson, D.: Integrating rural and urban water markets in south east Australia: preliminary analysis. In: *OECD Workshop on Agriculture and Water: Sustainability, Markets and Policies* (2005)
4. Charnes, A., Cooper, W.W.: Chance-constrained programming. *Manage. Sci.* **6**(1), 73–79 (1959)

Farmers' Adaptive Strategies in Face to Groundwater Depletion: A Short-Term Panacea or a Sustainable Solution? Evidences from the Center of Tunisia

Hacib El Amami, Taoufik Hermassi, and Nada Lellia

Abstract

In a virtual absence of effective regulation, the large scale adoption of surface wells in the Center of Tunisia have led to enormous extraction rates of groundwater, often exceeding natural recharge rates. To overcome the negative impact of groundwater depletion, farmers adopt in general several coping strategies. This study aimed to identify the type of strategies adopted and to quantify their potential to mitigate the negative impact on farmers' income. To this end a survey was undertaken over 95 small farmers, owning less than 5 ha and using surface well for irrigation. A linear programming model was applied to a representative farm. Results showed that as a first step, farmers act on crops selection and agriculture practices so to minimize the impact of water shortage. However, this implies losses in farmer's income. This study suggests that, even though there are some successes, adaptive strategies should be considered as "short-term panaceas" and not a sustainable solution, as they are not able to prevent further losses in farmer's income directly resulting from overexploitation and increasing pumping cost.

Keywords

Groundwater • Depletion • Adaptive strategies
Short term panaceas • Sustainable

1 Introduction

In the central parts of Tunisia, where surface water is both scarce and random, groundwater is the only source of irrigation. Favorable marketing opportunities for various crops

H. El Amami (✉) · T. Hermassi
National Institute for Research in Rural Engineering,
Water and Forests, 2080 Ariana, Tunisia
e-mail: hacib.amami@gmail.com

N. Lellia
National Agronomic Institute, Ariana, Tunisia

and the easy and heavily subsidized availability of water lifting technology launched in the arid and semi-arid regions have led to a real intensive groundwater withdrawal, tapping reserves which could not be reached with older technologies. Such rapid growth, however, is not without serious environmental implications. In a virtually absence of effective regulation, the large scale adoption of surface wells have led to overexploitation: the rate of groundwater currently extracted is far exceeds the natural recharge rates; which is the amount of water that should be extracted for promoting sustainable use of groundwater [1].

This is due because groundwater is classified as common-pool resource with the two characteristics: subtractability and low excludability [2]. When it is exploited under open access regime, two externalities occur and prevent the efficient exploitation of the resource: stock externality and cost externality.

The stock externality arises when extraction rate exceeds natural recharge rate which is the case of the center of Tunisia. Pumping cost externalities arise because the cost of pumping groundwater depends on the groundwater stock. As water table drops with every unit of water extracted the cost of pumping the next unit increases as a consequence of increasing lift and additional invest cost to capture deeper water. In general, farmers adopt several coping strategies to overcome the negative externalities of groundwater.

There are two main strategies adopted by farmers to cope with groundwater scarcity in the region. These strategies appear to vary across farms groups and closely follow the structure of land ownership. In general, large farmers, owning more than 15–20 ha, adopt a strategy based on 'chasing' groundwater, by drilling boreholes, so as to maintain a water intensive farming system and maximize farm profit. This strategy requires intensive capital which explains that is mostly adopted by rich farmers who can afford such actions. The second strategy, called "adaptive strategy" is mainly adopted by small farmers, owning less than 5 ha and lack financial capital to invest in bore wells.

This study focuses on this category of farmers which represents approximately more than 92% of farmers in the region and covers near 80% of the cultivated area.

The objectives of this paper were to (a) identify the type of strategies adopted, (b) to quantify their potential impact and (c) how these strategies might mitigate the impact of groundwater depletion on farmers' income. The obtained results will provide indicators on how farmers should adjust their irrigated agriculture in face to groundwater depletion in order to minimize risk and attenuate the impact of water scarcity, at least in short term.

2 Methodological Approach

The study was conducted in three perimeters located in different climatic and socio-economic context in Tunisia: Kasserine, Sidi Bouzid and Kairouan. In a first step, farm level survey was conducted during 2016–2017 covering 95 farmers mainly to get the details on frequency and cost of deepening the existing wells, crop production, coping strategies and other socio-economic parameters that influenced the development of irrigated agriculture. In a second step, the analysis was performed using the mathematical programming method [3]. Specifically, in this study, this method was used to identify crops selection as well as irrigation strategies that could be adopted to maximize farmers' incomes under conditions of increasing pumping depth and additional energy requirement. It was also used to simulate the potential impact of adaptive strategies to attenuate the negative externalities of groundwater over-exploitation. An optimization model was constructed for representative farm.

3 Results

Results showed that as a first step in adapting to groundwater drop consists to act on farming systems and agriculture practices so to minimize the impact of water shortage. More than 43% of interviewed farmers reported that they maintain the same grown crops but they reduce the cropped area (Fig. 1).

Other farmers reported adjusting crops choices to water availability by selecting less water sensitive crops (36%) or clearly shifting from summer to winter crops (14%). Overall, it was found that 50% of surveyed farmers react to water shortage by introduce change in cropping pattern or in agricultural practices or in both.

Deficit irrigation is adopted only by 7% of farmers, although it has mentioned by many empirical research as suitable strategy in a context of water shortage particularly for cereals, fodder crops and olive trees.

Under adaptive scenario, model results showed a significant change in optimal cropping pattern compared to the one obtained in the initial situation where groundwater is assumed to be no constraining. High-value crops, but requiring more much water like tomatoes, peppers and water melon, were substituted by less-remunerative crop, but requiring less water, like peas, bean, winter wheat and fodder (winter crops). With regard to groundwater resources, the adaptive strategy may be considered sustainable. However, it introduces loss in farmer's income compared to baseline situation, as shown by Table 1.

Simulation results showed also that an additional depletion of groundwater by 5 m would result in an increase of pumping cost by 17% and a decrease of farmer's income by 23%, relative to baseline scenario (Table 2).

Fig. 1 Actions adopted by farmers to cope with groundwater depletion

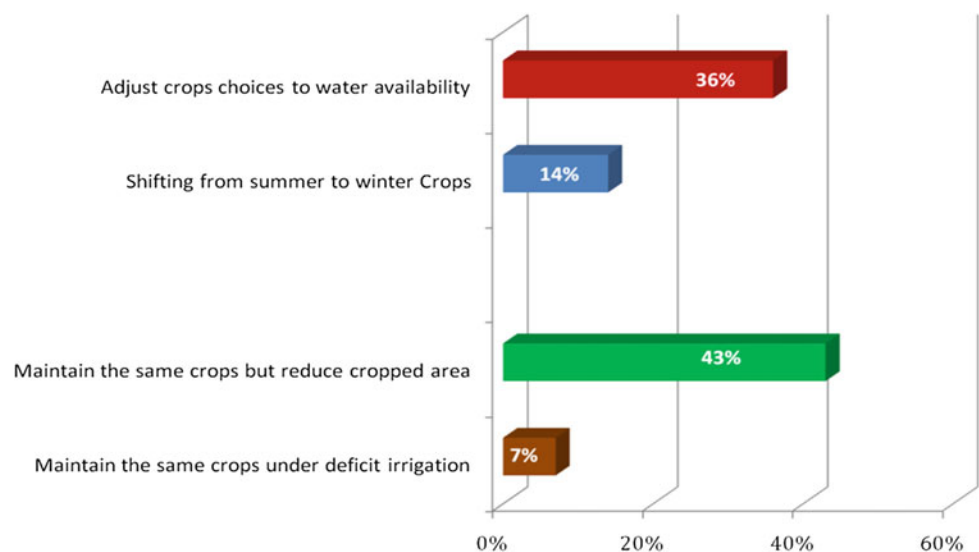


Table 1 Farmers' income in baseline scenario and in adaptive context (unit: TND)

Farmer's income in baseline scenario (water availability)	Farmer's income in adaptive strategy context	Evolution relative to baseline scenario
12,500	10,625	-15%

Table 2 Impact of additional groundwater depletion on pumping cost and farmers' income

Additional groundwater depletion	Evolution relative to initial situation	
	Groundwater pumping cost	Farmers' income
5 m	+17.5%	-23%

4 Discussion

Results showed that there are opportunities and limitations in adopting adaptive strategies. Even though there are some successes in overcoming the negative externalities of groundwater depletion, these strategies should be considered as "short-term panaceas" and not as sustainable solution for the problem of groundwater over-exploitation. Significant agricultural policy reform is therefore necessary if we are to prevent further degradation of our groundwater. Among robust policies, this study suggests the involvement of local users, with the assistance of regional department of agriculture, to ensure effective control on groundwater withdrawal.

5 Conclusions

This study aimed to identify the type of strategies adopted by small farmers to cope with groundwater depletion and to quantify their potential to mitigate the negative impact of

this depletion on farmers' income. Results showed that there are opportunities and limitations in adopting adaptive strategies. Even though there are some successes in overcoming the negative externalities of groundwater depletion, these strategies should be considered as "short-term panaceas". Since the regulatory instruments adopted until now have had little success, this study suggests the involvement of local users, with the assistance of regional department of agriculture, to ensure effective control on groundwater withdrawal.

References

1. Ben Guessim, A.: For a new vision of the underground water management. In: Workshop "Valorization of Scientific Research in Water Sector", 17–18 March, Gammart, Tunisia (2015)
2. Ostrom, E.: *Governing the Commons: The Evolution of Institutions for Collective Action*. 271p. Cambridge University Press (1990)
3. Hazell, P.B.R., Norton, R.D.: *Mathematical Programming For Economic Analysis in Agriculture*. 399p. MacMillan Publishing Company, New York (1986)